Contemporary Cardiology
Series Editor: Christopher P. Cannon

Stephen J. Nicholls
Tim Crowe *Editors*

Imaging Coronary Atherosclerosis

Humana Press

Contemporary Cardiology

Christopher P. Cannon, MD
Series Editor

For further volumes:
http://www.springer.com/series/7677

Stephen J. Nicholls • Tim Crowe
Editors

Imaging Coronary Atherosclerosis

Humana Press

Editors
Stephen J. Nicholls, MBBS, PhD, FRACP, FACC, FESC, FAHA, FCSANZ
South Australian Health and Medical Research Institute
Royal Adelaide Hospital
University of Adelaide
Adelaide, SA, Australia

Tim Crowe, BS
C5Research
Cleveland Clinic
Cleveland, OH, USA

ISSN 2196-8969
ISBN 978-1-4939-0571-3
DOI 10.1007/978-1-4939-0572-0
Springer New York Heidelberg Dordrecht London

ISSN 2196-8977 (electronic)
ISBN 978-1-4939-0572-0 (eBook)

Library of Congress Control Number: 2014926606

Printed on acid-free paper

Humana Press is a brand of Springer
Springer is part of Springer Science+Business Media (www.springer.com)

To Kathy, Emily, Oliver, and Angus
&
Connie, Justin, and Sean

Preface

For more than 50 years, we have used coronary angiography to diagnose and quantify the extent of obstructive disease due to atherosclerosis. This has provided an important tool for the cardiologist in the evaluation and management of the patient with coronary artery disease. In more recent years, major technological advances in arterial wall imaging enable more precise visualization of the atherosclerotic plaque. These developments have expanded beyond traditional angiographic techniques, which simply visualize the arterial narrowings that develop as a complication of vascular disease. Rather, the ability to use a range of intravascular and noninvasive imaging techniques permits direct visualization of the full thickness of the artery wall and the whole burden of disease within. As a result, we now have the opportunity to image the amount of plaque, distinguish its individual components, and potentially evaluate the functionality of the disease. The latter will be further enhanced by advances in molecular imaging, which in combination with the invasive and noninvasive approaches described in this book, have the ability to translate the vascular biological insights from the experimental setting to the daily management of patients. This has important implications for the risk prediction, management, and evaluation of novel anti-atherosclerotic therapies. In this book, we focus on each of the major approaches to imaging of the coronary arteries. In particular, our authors have highlighted how each of these modalities has enhanced our understanding of the disease process and propose challenges that need to be overcome for their increasing integration into clinical practice.

Adelaide, SA, Australia — Stephen J. Nicholls
Cleveland, OH, USA — Tim Crowe

Contents

Contributors

Takashi Akasaka, MD, PhD Department of Cardiovascular Medicine, Wakayama Medical University, Wakayama, Japan

Olcay Aksoy, MD Department of Cardiovascular Medicine, Cleveland Clinic, Cleveland, OH, USA

Christie M. Ballantyne, MD Department of Medicine, Baylor College of Medicine, Methodist DeBakey Heart and Vascular Center, Houston, TX, USA

Subhash Banerjee, MD Department of Cardiovascular Diseases, VA North Texas Health Care System, University of Texas Southwestern Medical School, Dallas, TX, USA

Sorin J. Brener, MD Department of Medicine, New York Methodist Hospital, Brooklyn, NY, USA

Emmanouil S. Brilakis, MD, PhD Department of Cardiovascular Diseases, VA North Texas Health Care System, University of Texas Southwestern Medical School, Dallas, TX, USA

Salvatore Brugaletta, MD, PhD Department of Cardiology, Hospital Clinic, Thorax Institute, Barcelona, Spain

Matthew J. Budoff, MD, FACC, FAHA Los Angeles Biomedical Research Institute at Harbor-UCLA Medical Center, Torrance, CA, USA

Razvan T. Dadu, MD Department of Cardiovascular Research, Baylor College of Medicine and Methodist DeBakey Heart and Vascular Center, Houston, TX, USA

Maria Drakopoulou, MD First Department of Cardiology, Athens Medical School, Hippokration Hospital, Halandri, Greece

Hector M. Garcia-Garcia, MD, PhD Department of Interventional Cardiology, Thoraxcenter—Erasmus University, Rotterdam, The Netherlands

Zhihua He, PhD Infraredx, Inc., Burlington, MA, USA

Farouc A. Jaffer, MD, PhD Cardiology Division, Department of Medicine, Massachusetts General Hospital, Harvard Medical School, Boston, MA, USA

Samir R. Kapadia, MD Department of Cardiovascular Medicine, Cleveland Clinic, Cleveland, OH, USA

Manabu Kashiwagi, MD Wellman Center for Photomedicine, Massachusetts General Hospital, Boston, MA, USA

Yu Kataoka, MD Heart Health Theme, South Australian Health and Medical Research Institute, Adelaide, SA, Australia

Hironori Kitabata, MD, PhD Department of Cardiovascular Medicine, Wakayama Medical University, Wakayama, Japan

Brian S.H. Ko, BSc, (Med), MBBS (Hons), PhD, FRACP Monash Cardiovascular Research Centre, Department of Medicine, Monash University and Monash Heart, Southern Health, Clayton, VIC, Australia

Peter Libby, MD Department of Cardiovascular Medicine, Brigham and Women's Hospital, Harvard Medical School, Boston, MA, USA

Sean Madden, PhD Infraredx, Inc., Burlington, MA, USA

Archontoula Michelongona, MD First Department of Cardiology, Athens Medical School, Hippokration Hospital, Peiraeus, Greece

James Muller, MD Infraredx, Inc., Burlington, MA, USA

Vijay Nambi, MD, PhD Department of Internal Medicine, Staff Cardiologist Michael E DeBakey Veterans Affairs Hospital, Ben Taub General Hospital, Baylor College of Medicine, Center for Cardiovascular Prevention, Methodist DeBakey Heart and Vascular Center, Houston, TX, USA

Stephen J. Nicholls, MBBS, PhD, FRACP, FACC, FESC, FAHA, FCSANZ South Australian Health and Medical Research Institute, Adelaide, SA, Australia

University of Adelaide, Adelaide, SA, Australia

Royal Adelaide Hospital, Adelaide, SA, Australia

Femi Philip, MD Department of Cardiovascular Medicine, Cleveland Clinic, Cleveland, OH, USA

Rishi Puri, MBBS, FRACP Department of Cardiovascular Medicine, CS Research Cleveland Clinic, Cleveland, OH, USA

University of Adelaide, Adelaide, SA, Australia

Joseph B. Selvanayagam, MBBS (Hons), FCACP, DPhil, FCSANZ, FESC Department of Cardiovascular Medicine, Flinders University, Flinders Medical Centre, Adelaide, SA, Australia

Sujith K. Seneviratne, MBBS, FRACP Monash Cardiovascular Research Centre, Department of Medicine, Monash University and Monash Heart, Southern Health, Clayton, VIC, Australia

Samuel L. Sidharta, MBBS, BMedSc Department of Medicine, Cardiovascular Research Centre, University of Adelaide, Adelaide, SA, Australia

Govind Srinivasan, MBBS, FRACP Department of Medicine, Flinders University, Flinders Medical Centre, Adelaide, SA, Australia

Christodoulos Stefanadis, MD First Department of Cardiology, Athens Medical School, Hippokration Hospital, Paleo Psychico, Greece

Stephen T. Sum, PhD Infraredx, Inc., Burlington, MA, USA

Guillermo J. Tearney, MD, PhD Department of Pathology, Massachusetts General Hospital, Boston, MA, USA

Konstantinos Toutouzas, MD First Department of Cardiology, Athens Medical School, Hippokration Hospital, Holargos, Greece

E. Murat Tuzcu, MD Department of Cardiovascular Medicine, Cleveland Clinic, Cleveland, OH, USA

Dennis T.L. Wong, BSc (Med), MBBS (Hons), PhD, FRACP Monash Cardiovascular Research Centre, Department of Medicine, Monash University, Monash Heart, South Australian Health & Medical Research Institute (SAHMRI), Clayton, VIC, Australia

Discipline of Medicine, University of Adelaide, Adelaide, SA, Australia

Matthew Worthley, MBBS, PhD, FRACP, FCSANZ, FACC Department of Cardiology, Royal Adelaide Hospital, Adelaide, SA, Australia

Stephen Worthley, MBBS, PhD Department of Cardiology, Royal Adelaide Hospital, Adelaide, SA, Australia

Irfan Zeb, MD Department of Medicine/Cardiology, Los Angeles Biomedical Research Institute at Harbor-UCLA Medical Center, Torrance, CA, USA

Residual Risk and Biology of the Disease: Implications for Plaque Imaging

1

Yu Kataoka and Stephen J. Nicholls

The Mechanism of Atherosclerosis

Atherosclerotic cardiovascular disease is the leading cause of morbidity and mortality in the Western world [1]. Due to the gradual increase in abdominal obesity and diabetes, cardiovascular disease has been considered to become the leading cause of mortality all over the world. This underscores the elucidation of factors associated with atherogenesis to prevent cardiovascular diseases through the best therapeutic approach.

Biochemistry Pathway for the Development of Atherosclerosis

The underlying pathology of atherosclerosis is characterized by a chronic inflammatory process of the arterial wall that occurs at predilection sites with disturbed laminar flow such as branch points [2–4] (Fig. 1.1). It is initiated by endothelial dysfunction and structural alterations, including the absence of a confluent luminal elastin layer and the exposure of proteoglycans, which permit subendothelial accumulation of low-density lipoprotein (LDL) [5, 6]. The retention of LDL in the vessel wall seems to involve interactions between the LDL constituent apolipoprotein B and matrix proteoglycans [7, 8]. In addition to LDL, other apolipoprotein B-containing lipoproteins, namely lipoprotein (a) (Lp (a)) and remnants, can accumulate in the intima and promote atherosclerosis [9, 10]. After the modification of LDL such as oxidation, lipolysis, proteolysis, and aggregation, LDL is taken up by macrophages [11, 12].

The recruitment of monocytes and lymphocytes to the artery wall also contribute to the atherogenesis [11]. A triggering event for this process is the accumulation of minimally oxidized LDL, which stimulates the overlying endothelial cells to produce a number of pro-inflammatory molecules, including adhesion molecules and growth factors [12]. Oxidized LDL can also inhibit the production of nitric oxide, a chemical mediator with multiple anti-atherogenic properties including vasorelaxation [13]. The entry of specific types of leukocytes into the artery wall is mediated by adhesion molecules and chemotactic factors including P- and E-selectin, intercellular adhesion molecule 1 and vascular cell adhesion molecule 1 [14, 15].

Through reactive oxygen species (ROS) and enzymes including myeloperoxidase (MPO), sphingomyelinase, and secretory phospholipase [16, 17],

Y. Kataoka, MD
Heart Health Theme, South Australian Health and Medical Research Institute, Level 9, 121 King William Street, Adelaide, SA 5001, Australia
e-mail: yu.kataoka@sahmri.com

S.J. Nicholls, MBBS, PhD, FRACP, FACC, FESC, FAHA, FCSANZ (✉)
South Australian Health and Medical Research Institute, Adelaide, SA, Australia

University of Adelaide, Adelaide, SA, Australia

Royal Adelaide Hospital, Adelaide, SA, Australia
e-mail: stephen.nicholls@sahmri.com

S.J. Nicholls and T. Crowe (eds.), *Imaging Coronary Atherosclerosis*, Contemporary Cardiology,
DOI 10.1007/978-1-4939-0572-0_1,

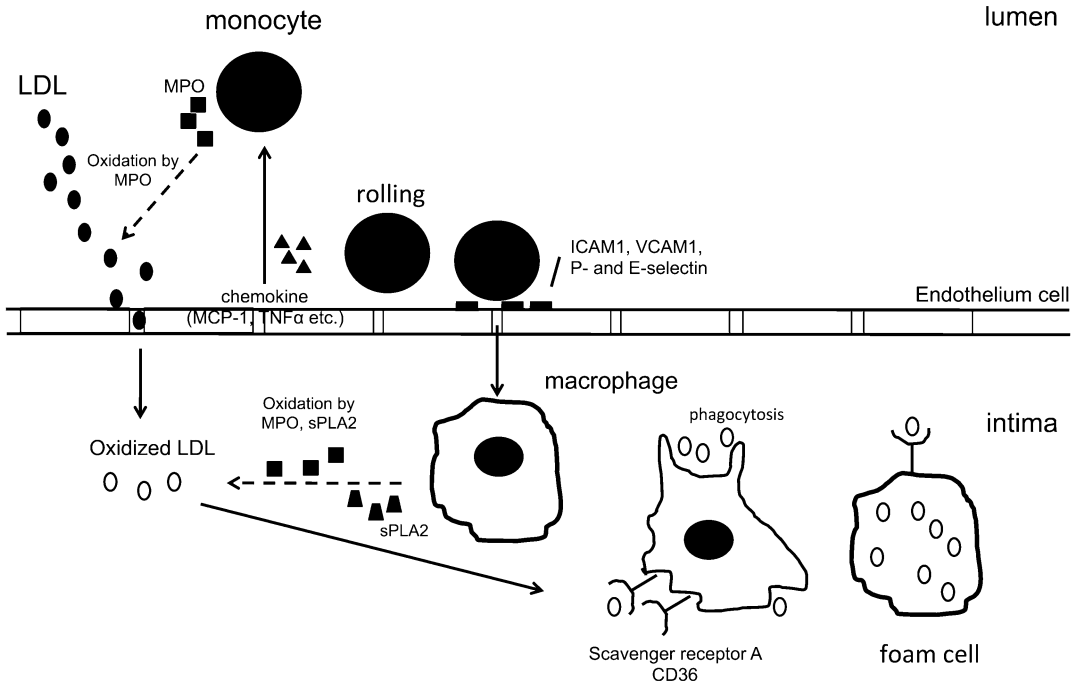

Fig. 1.1 Role of LDL, monocyte, macrophage, and chemokines for atherogenesis. *ICAM* intercellular adhesion molecule, *LDL* low-density lipoprotein, *MCP* monocyte chemoattractant protein, *MPO* myeloperoxidase, *sPLA2* secretory phospholipase A2, *TNF* tumor necrosis factor, *VCAM* vascular cell adhesion molecule

LDL is extensively modified in atherosclerotic lesions. The rapid uptake of highly oxidized LDL particles by macrophages leads to foam-cell formation which is derived by a group of receptors such as scavenger receptors, scavenger receptor A and CD36 [18, 19]. The expression of scavenger receptors is regulated by peroxisome proliferator-activated receptor-γ, a transcription factor whose ligands include oxidized fatty acids, and by cytokines such as tumor necrosis factor-α and interferon-γ [20, 21].

Any process that decreases the synthesis of fibrous cap collagen by intimal fibromyoblast-like smooth muscle cells (SMCs) and/or contributes to cap collagen degradation would be expected to promote the formation of plaques prone to rupture [22]. Vulnerable plaques show evidence of SMC death and decreased numbers of SMCs, and in vitro data show that macrophages can trigger apoptosis in SMCs by activating their Fas apoptotic pathway and by secreting proapoptotic tumor necrosis factor-α and nitric oxide [23, 24]. Macrophages may also decrease collagen synthesis in intimal SMCs without actually killing the cells. Macrophage-derived matrix metalloproteinases (MMP), which are a family of protease-activated enzymes, can degrade various types of extracellular matrix proteins and may also be involved in thinning of the fibrous cap [25, 26].

Residual Risk Factors: Potential New Targets

Over the course of the last two decades, large randomized controlled trials have consistently demonstrated that lowering levels of LDL cholesterol reduce cardiovascular event rates across the full spectrum of risk [27–30]. As a result, LDL-C lowering has become an integral component of therapeutic strategies in the prevention of cardiovascular diseases. However, despite statins therapy, substantial amount of cardiovascular events is

still observed (Table 1.1). The Scandinavian Simvastatin Survival Study (4S) reported a 20 % cardiovascular events occurring in statin-treated patients although statin treatment was associated with a significant reduction of cardiovascular events compared to placebo [27]. The presence of residual cardiovascular risk was similarly observed in other major trials of statin therapy, which prompted the focus on optimal statin use [31, 32]. Even in three landmark trials focusing on the effect of high-dose statins, residual cardiovascular risk was still apparent in the intensive statin arms [33–35]. Thus, analyses of clinical trial data indicate the need to retool our cardiovascular risk reduction algorithms beyond the focus on LDL cholesterol levels.

Atherogenic Lipoproteins

The deposition of atherogenic lipoproteins in the vessel wall is the major driver for atherosclerosis (Table 1.2). In the recent years, there has been increased recognition of the relationship between cardiovascular risk and other lipid parameters, most notably high-density lipoprotein (HDL) cholesterol and triglycerides (TG).

HDL Cholesterol

Epidemiological studies have shown that, in addition to elevated LDL cholesterol levels, low levels of HDL cholesterol are an independent predictor of the risk of coronary heart disease [36, 37]. Furthermore, the ability of a low level of HDL cholesterol to predict an adverse clinical risk persists in patients who achieve very low levels of LDL cholesterol on statin therapy [38, 39]. As HDL contains the potential atheroprotective properties such cholesterol mobilization, promotion of nitric oxide bioavailability, and inhibition of inflammatory activity [40], lower level of HDL has been considered to induce and progress atherosclerosis.

Triglycerides

Numerous studies have demonstrated an association between high TG level and cardiovascular risks [41–43]. The meta-analyses of data in 29 prospective studies have demonstrated that the TG level is a strong and independent predictor of cardiovascular events [41]. In addition, the PRavastatin Or atorVastatin Evaluation and Infection Therapy-Thrombolysis In Myocardial Infarction (PROVE IT-TIMI) 22 trial revealed that TG levels, independent of LDL cholesterol levels, had a substantial impact on the cardiovascular outcomes in patients with acute coronary syndromes [42]. Notably, among statin-treated patients, on-treatment TG level <150 mg/dL was associated with reduced cardiovascular risk. These findings underscore the optimal control of TG level for the prevention of future cardiac events.

Non-HDL Cholesterol

Non-HDL cholesterol has been shown to predict cardiovascular events as well as correlate with most lipid parameters associated with future outcomes [43, 44]. Evidence for the association between non-HDL cholesterol and cardiovascular risk has also come from epidemiologic data reported by Liu et al. [45]. In their analyses of the Framingham study cohort, a strong association between non-HDL cholesterol and cardiovascular risk was noted within all strata of LDL cholesterol values. In this study, non-HDL cholesterol was apparently a stronger predictor of cardiovascular events than LDL cholesterol, and this finding was independent of whether the TG level was <200 or >200 mg/dL.

Lipoprotein (a)

Lp (a) is a unique lipoprotein particle consisting of a moiety identical to LDL to which the glycoprotein apolipoprotein (a) that is homologous to plasminogen is covalently attached [46, 47]. Lp (a) has been considered to promote atherosclerosis through an increased Lp (a)-associated cholesterol entrapment in the arterial intima, inflammatory cell recruitment, carrying of proinflammatory oxidized phospholipids, impairing fibrinolysis by inhibition of plasminogen activation, and enhancing coagulation by inhibition of the tissue factor pathway inhibitor [48, 49]. Evidence from epidemiological studies continues to accumulate that elevated plasma concentrations

Table 1.1 Residual risks observed in clinical trials under statins therapy

Trials	Subjects	Therapy	Follow-up period (years)	Outcome after therapy	Annual residual risks[a]
Statin vs. placebo					
4S [27]	4,444 patients with CAD or previous MI	Simvastatin vs. placebo	5.4	33 % reduction of CV events	3.5 %
AFCAPS/ TexCAPS [28]	6,605 patients without CAD	Lovastatin 20–40 mg vs. placebo	5.2	25 % reduction in CV events (MI, cardiac cause death, revascularization, unstable angina)	2.2 %
CARE trial [29]	4,159 patients with MI	Pravastatin 40 mg vs. placebo	5	24 % reduction in CV events (MI, cardiac-cause death)	1.5 %
CARDS trial [30]	2,838 diabetic patients without CAD	Atrovastatin 10 mg vs. placebo	3.9	37 % reduction in CV events (MI, cardiac-cause death, revascularization, arrest, unstable angina, stroke)	1.5 %
LIPID Study [31]	9,014 patients with CAD	Pravastatin 40 mg vs. placebo	6.1	29 % reduction in CV events (MI, cardiac-cause death, revascularization, stroke)	2 %
PROSPER trial [32]	5,804 elderly patients with cardiovascular risk factors	Pravastatin 40 mg vs. placebo	3.2	13 % reduction in CV events (MI, cardiac-cause death, stroke)	4.4 %
High-dose statin					
PROVE IT-TIMI 22 trial [33]	4,162 patients with ACS	Pravastatin 40 mg vs. atorvastatin 80 mg	2	16 % reduction in CV events (MI, any-cause death, revascularization, unstable angina, stroke)	11.2 % (atrovastatin) 13.2 % (pravastatin)
IDEAL study [34]	8,888 patients with MI	Atrovastatin 80 mg vs. simvastatin 20 mg	4.8	12 % reduction in CV events (MI, cardiac-cause death, revascularization, arrest, unstable angina, stroke)	2.5 % (atrovastatin) 2.9 % (simvastatin)
TNT study [35]	10,001 patients without CAD	Atrovastatin 10 mg vs. 80 mg	4.9	22 % reduction in CV events (MI, cardiac-cause death, arrest, stroke)	1.8 % (80 mg) 2.2 % (10 mg)

ACS acute coronary syndrome, *ASPEN* The Atorvastatin Study for Prevention of Coronary Heart Disease Endpoints in Non-Insulin-Dependent Diabetes Mellitus, *CAD* coronary artery disease, *CARDS* Collaborative Atorvastatin Diabetes Study, *CARE* Cholesterol and Recurrent Events, *CV* cardiovascular, *IDEAL* Incremental Decrease in End points Through Aggressive Lipid Lowering Trial, *LIPID* Long-term Intervention with Pravastatin in Ischaemic Disease, *MI* myocardial infarction, *PROSPER* PROspective Study of Pravastatin in the Elderly at Risk, *PROVE IT-TIMI* Pravastatin Or atorVastatin Evaluation and Infection Trial-Thrombolysis in Myocardial Infarction, *TNT* Treating to New Targets, *WOSCOPS* West of Scotland Coronary Prevention Study

[a] Calculated by the cumulative event rate divided by duration of study

Table 1.2 Lipid markers for the Prediction of Residual Risks

	Study population	Outcome	Follow-up periods (years)	Findings
HDL-C				
Gordon et al. [36]	15,252 patients without CAD	CAD	2	Each 1 mg/dL increase in HDL-C is associated with a 2 % decrease in CAD risk in men and a 3 % decrease in women
Castelli et al. [37]	1,605 patients without CAD	CHD	12	HDL-C <40 mg/dL exhibits the highest risk of developing CHD
Barter et al. [38]	9,770 patients with CAD	CHD	5	Patients with HDL-C <38 mg/dL had a highest incidence of CHD despite low LDL-C level
Jafri et al. [39]	543,210 patients	MI	3.9	10 mg/dL increase in HDL-C was associated with higher incidence of MI under statin therapy
TG				
Sarwar et al. [41]	9,757 men with CHD	CHD	12	Odds ratio: 1.7 (1.5–1.9) for CHD under an increase in triglyceride
Miller et al. [42]	4,162 patients with ACS	CHD	2	10 mg/dL decrease in triglyceride reduces the incidence of CHD by 1.6 % under statin therapy
Assmann et al. [43]	4,849 men without CAD	CHD	8	Patients with TG <200 mg/dL exhibited the lowest incidence of CAD
Non-HDL-C				
Cui et al. [43]	4,462 patients without CHD	CHD	19	Non-HDL-C >220 mg/dL was associated with high mortality
Boekholdt et al. [44]	38,153 patients	CAD	4.6	The adjusted HR for CVD per 1-SD increase was 1.16 (1.12–1.19) for non-HDL-C. This HR was significantly higher than LDL-C and apoB
Liu et al. [45]	19,381 patients without CAD	CAD	13	Each increase by 1 mg/dL of non-HDL cholesterol was associated with a 5 % increased risk for cardiac-cause death
Lp (a)				
Danesh et al. [50]	5,436 patients with CHD	CAD	10	The adjusted HR for CHD was 1.7 (1.4–1.9) for Lp (a)
The Emerging Risk Factors Collaboration [51]	126,634 patients without CHD	CHD	10.2	The adjusted risk ratio for CHD was 1.2 (1.1–1.2) for Lp (a)
Nicholls et al. [52]	2,769 patients with CAD	CHD	3	Lp(a) ≥ 30 mg/dL was associated with a greater rate of MACE in patients with LDL-C > 70 mg/dL
Oxidized LDL				
Melsinger et al. [55]	346 patients without CAD	CVD	5.6	Plasma oxLDL was the strongest predictor of CHD events compared with a conventional lipoprotein profile and other traditional risk factors for CHD
Shimada et al. [56]	246 patients with CVD	CVD	3	The adjusted hazard ratios for CVD were 3.15 (95 % CI 1.47–6.76, $P = 0.003$) in patients with the highest quartile of oxLDL levels than in those within the lowest quartile

ACS acute coronary syndrome, *BNP* B-type natriuretic peptide, *CAD* coronary artery disease, *CHD* coronary heart disease, *CVD* cardiovascular disease, *hs-CRP* high-sensitivity c-reactive protein, *Lp (a)* lipoprotein (a), *Lp-PLA2* lipoprotein-associated phospholipase A2, *MPO* myeloperoxidase, *sPLA2* secretory phospholipase A2

of Lp (a) are a risk factor for a variety of atherosclerotic and thrombotic disorders. Recent data from genetic and epidemiological studies strongly support a causal relationship between elevated Lp (a) concentrations and the development of atherosclerosis and cardiovascular disease [50–52]. This relationship is independent of LDL cholesterol and HDL cholesterol levels.

Oxidized LDL

Oxidized LDL is generated during lipid peroxidation when oxygen-free radicals abstract a hydrogen atom from a methylene carbon on polyunsaturated fatty acids. It results in generation of reactive species that modify both the lipid and protein components of LDL [53, 54]. Oxidation of LDL occurs primarily in the vessel wall, activating many inflammatory and atherogenic pathways. The data from two population-based MONICA/KORA Augsburg surveys showed that plasma-oxidized LDL was the strongest predictor of cardiovascular events compared with a conventional lipoprotein profile, and other traditional risk factors [55]. Similar result was observed in another study of patients with CAD [56].

Biomarkers for the Prediction of Residual Risks

The need to improve the risk prediction has prompted the search for novel markers of cardiovascular risk (Table 1.3). The clinical utility of these biomarkers will depend on their ability to provide a reflection of the underlying atherosclerotic burden or activity and the ability to predict future events. Several emerging plasma biomarkers may ultimately prove useful in risk stratification and prognosis of cardiovascular disease.

High-Sensitivity C-Reactive Protein

High-sensitivity c-reactive protein (hs-CRP) provides a stable plasma biomarker for low-grade systemic inflammation. Recent evidence suggests

Table 1.3 Nontraditional biomarkers for the prediction of residual risks

Biomarkers	Study population	Outcome	Follow-up periods	Risk estimates (95 % CI)
hs-CRP				
Ridker et al. [57]	27,939 women without CAD	CVD	8 years	2.3 (1.6–3.4)
Haverkate et al. [58]	2,121 patients with angina pectoris	CVD	2 years	1.4 (1.1–1.8)
Rutter et al. [59]	3,037 patients without CAD	CVD	7 years	1.9 (1.2–2.9)
Ridker et al. [60]	3,745 patients with acute coronary syndrome	MI or death	2 years	1.7 (1.1–2.5)
Lp-PLA2				
Koenig et al. [66]	934 men without CAD	CHD	14 years	1.2 (1.0–1.5)
Oei et al. [67]	2,199 elderly patients without CAD	CHD	10 years	1.8 (1.1–2.9)
sPLA2				
Mallat et al. [74]	25,663 patients with CAD	CAD	6 years	1.6 (1.2–2.0)
Kugiyama et al. [75]	142 patients with CAD	CAD	2 years	3.5 (1.4–8.3)
MPO				
Baldus et al. [79]	1,090 patients with ACS	CAD	6 months	2.1 (1.2–3.7)
Meuwese et al. [80]	1,138 patients without CAD	CAD	8 years	1.4 (1.1-1.7)
Tang et al. [81]	1,895 patients with suspected CAD	CVD	3 years	1.7 (1.3–2.3)

ACS acute coronary syndrome, *BNP* B-type natriuretic peptide, *CAD* coronary artery disease, *CHD* coronary heart disease, *CVD* cardiovascular disease, *hs-CRP* high-sensitivity c-reactive protein, *Lp (a)* lipoprotein (a), *Lp-PLA2* lipoprotein-associated phospholipase A2, *MPO* myeloperoxidase, *sPLA2* secretory phospholipase A2

that hs-CRP may have direct proinflammatory effects, and contribute to the initiation, and progression of atherosclerotic lesions. Epidemiological studies have provided strong evidence for CRP to predict future cardiovascular risks in a variety of clinical settings [57–59]. Moreover, recent studies reported that an elevated hs-CRP level is associated with clinical events under optimal LDL-C control [60]. Thus, to date, of all biomarkers investigated in cardiovascular disease, the most extensive and robust database exists for hs-CRP. Still, its incremental predictive value above and beyond traditional risk factors, based on any of the available scores has not been definitely proven.

Lipoprotein-Associated Phospholipase A2

Lipoprotein-associated phospholipase represents another emerging biomarker for atherosclerotic disease. Lipoprotein-associated phospholipase A2 (Lp-PLA2) hydrolyzes sn-2 side chains of oxidized phospholipids to yield a free oxidized fatty acid and lysophosphatidylcholine [61]. It is produced mainly by monocytes, macrophages, T-lymphocytes, and mast cells and has been found to be upregulated in atherosclerotic lesions, especially in complex plaque, as well as in thin cap coronary lesions prone to rupture [62]. The weight of evidence suggests that this biomarker promotes vascular inflammation [63–65]. In recent studies of dyslipidemic patients, healthy people and patients with stroke, elevated baseline Lp-PLA2 levels were found to be associated with death, myocardial infarction and revascularization, independent of a variety of potential confounders [66–68]. Thus, measurement of Lp-PLA2 may have a potential to identify people at increased risk for cardiovascular disease. However, the sub-analysis of PROVE IT-TIMI 22 trial showed that measurement of Lp-PLA2 in the early phase of the acute coronary syndrome was not associated with increased risk for recurrent events [68]. Currently, no clear recommendation on its clinical usefulness can be given until further data document its incremental value in addition to traditional risk factors.

Secretory Phospholipase A2

Secretory phospholipase A2 (sPLA2) is another well-studied member of the phospholipase 2 family and is widely expressed in hepatocytes, macrophages, platelets, and vascular SMCs. It has been found to be involved in a range of pathways related to the development of atherosclerosis and cardiovascular disease [69]. The action of sPLA2 on LDL results in smaller particles that are more susceptible to oxidative modification and to uptake by macrophages, the seminal events in foam cell formation [70, 71]. Moreover, the hydrolysis of lipoprotein phospholipid by sPLA2 generates free fatty acids and lysophospholipid products that may independently promote inflammation and oxidative stress within the arterial wall [72, 73]. The potential role of sPLA2 in cardiovascular disease is supported by consistent demonstration of the direct relationship between sPLA2 mass or activity and prospective cardiovascular risk in a broad range of clinical settings. Case–control studies have demonstrated that sPLA2 levels predict cardiovascular risk in asymptomatic subjects and patients with stable or unstable angina pectoris [74, 75]. Although consistent, study population in all of the above studies was relatively small and results in healthy subjects have to be replicated in other cohorts until the clinical usefulness of sPLA2 in the prediction of CHD may be established.

Myeloperoxidase

MPO, a member of the heme peroxidase superfamily, is a leukocyte-derived enzyme that generates reactive intermediates, leading to oxidative damage of host lipids and proteins [16, 76]. MPO could also be involved in the development of endothelial dysfunction because MPO uses the atheroprotective endothelial-derived nitric oxide as a substrate [77]. It has been shown that MPO is present within atherosclerotic plaque in human arteries [78]. From the results of two prospective studies in patients with chest pain or acute coronary syndrome, increasing systemic levels of MPO predicted the presence of CAD and risks of subsequent major adverse cardiac events [79–81]. In addition, this relationship remained significant

after statistical adjustments for Framingham risk score and hs-CRP. Thus, MPO might be a promising prognostic marker for cardiovascular events. However, further studies are needed to replicate these findings and to establish a potential role for MPO as a predictor of incident CHD in initially healthy subjects.

Plaque Imaging Modalities for the Assessment of Residual Risks

Over the past few years, considerable advances have been made in imaging techniques for the assessment of atherosclerotic changes. Recently, various noninvasive and invasive imaging modalities enable us to not only evaluate the natural history of atheroma burden but also refine cardiovascular risk assessment. These abilities will contribute to the assessment of residual risk and the identification of patients who need more intensive therapies.

Noninvasive Imaging

Carotid Ultrasound

Noninvasive B-mode ultrasonic imaging of the carotid arteries visualizes the artery wall with resolution to detect very early thickening of the intimal–medial layer that precedes the appearance of macroscopic atherosclerosis. Multiple studies have demonstrated that carotid intima-media thickness (CIMT) predicts future cardiovascular events in diabetic patients, asymptomatic patients, and patients with CAD [82, 83] (Table 1.4). As a result, measurement of CIMT of the carotid artery can serve as a useful method for cardiovascular risk assessment.

Computed Tomography

Coronary Artery Calcification

Coronary artery calcification (CAC) is a characteristic of atherosclerosis and readily identified by computed tomography (CT). Multiple studies have demonstrated that CAC is an independent

Table 1.4 Anatomical plaque imaging modalities

Imaging modalities	Physical basis	Spatial resolution	Luminal stenosis	Plaque area	Plaque composition	Limitation
A. noninvasive						
Carotid ultrasound	reflection of high-frequency sound	>400 μm	○	○	Δ	Interobserver variability
Computed tomography						
1. Coronary artery calcification	X-ray	400–600 μm	X	X	Calcium	Radiation exposure
2. Multidetector-computed tomography	X-ray	400–600 μm	○	○	○	Radiation exposure, contrast use
Magnetic resonance imaging	Radiowaves	150–200 μm	○	○	○	Unsuitable for the assessment of small arteries
B. Invasive						
Intravascular ultrasound (IVUS)	Reflection of high-frequency sound	100 μm (40 MHz)	○	○	Δ	A suboptimal characterization of plaque composition
Virtual histology-IVUS	Reflection of high-frequency sound	200 μm (20 MHz)	○	○	○	Only R wave gated images, no algorithm for thrombus
Optical coherence tomography	Near-infrared light	10 μm	○	X	○	Limited penetration
Near-infrared spectroscopy	Near-infrared light	N/A	X	X	Lipid	Not structural information

predictor of cardiovascular events including myocardial infarction and sudden death [84, 85]. Recent studies reported that CAC scanning improves risk stratification for coronary heart disease in the elderly patients [86] and in asymptomatic healthy subjects independent of standard risk factors [87]. Additionally, risk assessment through CAC is more accurate than standard risk factors and CRP, and refines Framingham risk stratification. It remains to be determined, however, to what degree its measurement provides an incremental benefit in risk prediction with clinical use of calcium scoring and whether its use ultimately changes the treatment strategy or outcome for individual patients.

Atherosclerotic Plaque in Coronary Arteries and Aorta

Multidetector-computed tomography (MDCT) has recently emerged as a useful imaging modality for the assessment of vessel anatomy and atherosclerotic plaque morphology in arterial beds. Recent studies using MDCT have demonstrated that plaque characteristics within coronary artery such as positive remodeling, spotty calcification, and napkin-ring enhancement are associated with a higher risk of acute coronary syndrome [88, 89]. In addition, the assessment of aortic plaque burden in thoracic aorta has been shown to be associated with increased long-term mortality in patients following cardiac surgery [90]. These data indicate that coronary and thoracic aortic atherosclerosis is a marker of cardiovascular events including all-cause death and myocardial infarction.

Magnetic Resonance Imaging

Due to recent improvements in magnetic resonance imaging (MRI) techniques, this modality can provide information on both plaque volume and composition in multiple arterial territories [91, 92]. The composition of plaque within the carotid artery on MRI has been reported to correlate with likelihood of cerebrovascular events [93]. Also, a number of studies have revealed that MRI could document a marked reduction in atherosclerotic lesion size induced by statin therapy [94, 95]. However, the data of MRI for risk assessment is still limited. Further investigation will be required.

Positron Emission Tomography

Nuclear imaging techniques such as positron emission tomography (PET) can target distinct mediators and regulators involved in the cascade of atherosclerosis. PET imaging with F18-fluorodeoxyglucose (FDG) is currently considered to be one of the most promising imaging modalities for the identification of inflammation. Preliminary studies have demonstrated greater uptake in plaques containing a large proportion of macrophages, suggesting that this approach may be used to evaluate the inflammatory composition of atherosclerotic plaque [96, 97]. There is some evidence that arterial FDG uptake is related to subsequent risk of both plaque rupture and clinical events. In a study of patients with cancer, patients with the highest FDG uptake were more likely to have a vascular event during the 6 months after PET imaging [98]. In another study focusing on patients with symptomatic carotid artery disease, those in the high FDG group had poorer outcomes over the next 6 months than subjects with initially lower FDG levels [99].

Invasive Imaging

Intravascular Ultrasound

Intravascular ultrasound (IVUS) allows robust quantitative measurements, including lumen, vessel, and plaque area, and provides information on vessel remodeling and, to a lesser extent, on its composition [100] (Table 1.4). Recently, IVUS has been increasingly used as the gold standard in trials evaluating progression or regression of plaque in the coronary arteries [101–108]. Post hoc analysis from pooled data of seven clinical IVUS trials has demonstrated the importance of control for residual risks for the prevention of ongoing disease progression [109]. In addition, IVUS-measured progression of coronary plaque has been shown to serve as a

marker for future cardiovascular events [110]. Thus, monitoring atherosclerosis by IVUS enables us to reveal residual risks related to plaque progression and predict cardiovascular events.

Virtual Histology-IVUS

Virtual histology-IVUS (VH-IVUS) technique displays a reconstructed color-coded tissue map of plaque composition (fibrous, fibrofatty, necrotic core, and dense calcium) superimposed on cross-sectional images of the coronary artery obtained by grayscale IVUS [111]. The VH-IVUS map successfully predicted the histology of these with a high accuracy in detecting fibrous, fibrofatty, necrotic cores, and calcium [112]. Recently, the Providing Regional Observations to Study Predictors of Events in the Coronary Tree (PROSPECT) trial has reported that plaque composition assessed by VH-IVUS is associated with future cardiovascular events [113]. The detection of high-risk plaques may contribute to the improvement of patients care and prognosis.

Optical Coherence Tomography

Optical coherence tomography (OCT) is a recently developed intravascular imaging modality using near-infrared light (1,300 nm) to create images. Compared with various other coronary imaging modalities, the greatest advantages of OCT are its high resolution of up to 10 μm in an axial resolution and to 20 μm in a lateral resolution, which is approximately ten times higher than that of IVUS and its accuracy of tissue characterization [114–116]. Given that the increase in imaging resolution is accompanied by poor tissue penetration, coronary OCT imaging produces high-quality imaging for fibrous cap, microchannel, accumulation of lipid and macrophages below the endothelial surface [117, 118]. As a result, OCT has been proposed to have a potential role in the assessment of factors that increase the vulnerability of atherosclerotic plaque. However, it remains unknown whether OCT findings could correlate with future cardiovascular events. Limitation of OCT is poor tissue penetration. Due to this limited penetration, it is difficult to image atherosclerotic plaques in large arteries.

Near-Infrared Spectroscopy

Near-infrared spectroscopy (NIRS) is based on the absorbance of light by organic molecules. Because different molecules absorb and scatter near-infrared light differently, NIRS allows for the chemical characterization of biological tissues and can be used to assess lipid and protein content in atherosclerotic plaques [119, 120]. The probability of high lipid content at the interrogation site is displayed on a color scale and is termed a chemogram. The ability to visualize lipid cores has been validated in autopsy specimens and in vivo [121]. In these validation studies, NIRS identifies the histological hallmarks of plaque vulnerability, such as a lipid pool, a thin cap, and inflammatory cells. Further clinical studies to reveal the usefulness of NIRS for the risk assessment will be required. The major limitation of NIRS is that it only detects one characteristic of vulnerable plaque and is unable to determine depth, superficial versus deep, of the lipid core. Further advances may permit detection of other plaque features implicated in future cardiovascular events.

Functional Imaging

Molecular imaging technology can elucidate the biology of relevant cellular and molecular targets, and serve to complement current anatomic and physiologic imaging (Table 1.5). Cardiovascular molecular imaging studies utilize MRI, CT, nuclear, ultrasound, and optical imaging in stand-alone or integrated/hybrid systems. Through noninvasive assessment of important disease-specific markers, molecular imaging has the great potential to stratify residual risks for primary and secondary prevention in the future.

Adhesion Molecules

The recruitment process for leukocytes, predominantly monocytes is one of the attractive targets for imaging because atherosclerotic plaque begins to evolve under recruiting leukocytes [11, 12]. Adhesion molecules that are expressed by endothelial cells play an important role in this process. Although sensitive endothelial targeting

Table 1.5 Functional Plaque Imaging Modalities

Molecular target	Contrast agents	Imaging	Subjects	Results
VCAM-1				
Kaufmann et al. [122]	VCAM1-targeted microbubbles	Contrast-enhanced ultrasound	ApoE knockout mice	VCAM-1 targeted microbubbles detect inflammatory processes in atherosclerosis
Nahrendorf et al. [123]	VCAM1-targeted nanoparticles (VINP-28)	MRI	ApoE knockout mice	VINP-28 visualized VCAM-1 expressing EC and macrophage
Macrophage				
Kooi et al. [130]	Ultrasmall superparamagnetic particles of iron oxide (USPIOs)	MRI	Patients with TIA	USPIOs accumulate in macrophages in ruptured and rupture-prone plaque
Nahrendorf et al. [131]	Superparamagnetic and fluorescent nanoparticle with the PET tracer 64Cu	PET and MR	ApoE knockout mice	The novel nanoagent directly detects macrophages in atherosclerotic plaques
Amirbekian et al. [132]	Macrophage scavenger receptor-targeted immunomicelles	MRI	ApoE knockout mice	Immunomicelles-enhanced atherosclerotic plaques containing macrophage
Mulder et al. [133]	Macrophage scavenger receptor-targeted pegylated micelles	MRI	ApoE knockout mice	Macropage can be detected by molecular MRI with pegylated micelles
Cathepsins				
Jaffer et al. [134]	Cathepsin K-sensitive NIR fluorescence imaging agents	Near-infrared fluorescence probe	ApoE knockout mice	This system detects localization of enzymatically active cathepsin K to macrophages
MMP				
Wagner et al. [136]	Radiolabelled MMP inhibitor [123I]I-HO–CGS 27023A	Scintigraphy	ApoE knockout mice	MMP activity was imaged in vivo in the MMP-rich vascular lesions
Breyholz et al. [138]	Radioligand HO-[123I]I-HO-CGS 27023A	PET	ApoE knockout mice	This agents specifically visualized activated MMPs in vascular lesions
Lancelot et al. [139]	Gadolinium-based MRI contrast agent P947	MRI	Rabbit, ApoE knockout mice	P947 detects the MMP-rich atherosclerotic plaques
Annexin V				
Johnson et al. [140]	Tc-99m Annexin A5	SPECT	Swine	Uptake of Tc-99m Annexin A5 corresponded to plaque apoptosis
Kietselaer et al. [141]	Tc-99m Annexin A5	SPECT	Patients with transient ischemic attack	Annexin A5 uptake in carotid artery lesion

(continued)

Table 1.5 (continued)

Molecular target	Contrast agents	Imaging	Subjects	Results
Integrin				
Winter et al. [142]	Alpha(v)beta3-integrin-targeted nanoparticles	MRI	Rabbit	Increased alpha(v)beta3-integrin distribution within the atherosclerotic wall
Waldeck et al. [143]	falphagvfbetag3 integrin-targeted fluorochrome	Fluorescence reflectance imaging	Apolipoprotein E-deficient mice	A significant fluorochrome accumulation in atherosclerotic plaques
MPO				
Ronald et al. [146]	Myeloperoxidase sensor bis-5HT-DTPA(Gd)	MRI	Rabbit	Active inflammation within the plaques can be detected by this agent
Shepherd et al. [147]	Sulfonaphthoaminophenyl fluorescein	Fluorescence reflectance imaging		This imaging detects HOCl production by MPO

LDL low-density lipoprotein, *MMP* matrix metalloproteinase, *MPO* myeloperoxidase, *MRI* magnetic resonance imaging, *PET* positron emission tomography, *SPECT* single photon emission-computed tomography, *VCAM-1* vascular adhesion molecule-1

is challenging given the thin monolayer and high shear stress environment, several innovative strategies have been developed to overcome these difficulties. In particular, targeted microbubbles and magnetofluorescent nanoparticles have allowed visualization of adhesion molecule expression in experimental mouse models of atherosclerosis by ultrasound and MRI [122, 123].

Macrophage

Macrophages are critically involved in atheroma initiation, propagation, and rupture, and demarcate high-risk plaques [124–126]. Therefore, specific of plaque macrophages may have crucial implications for the risk assessment of cardiovascular disease. Uptake of ^{18}FDG-PET has been demonstrated in the aorta, carotid artery atherosclerotic plaques of patients with ischemic symptoms, and peripheral atherosclerotic arteries [96, 127–129]. Histological analysis demonstrates that its accumulation in atherosclerotic lesions is associated with the degree of macrophage infiltration [96, 97]. A promising approach for imaging macrophages involves the use of small iron oxide particles that are efficiently phagocytosed by macrophages. In some groups, magnetic nanoparticles or ultra small superparamagnetic iron oxide particles show clinical utility for detecting plaque macrophages in atherosclerosis [130, 131]. Other groups introduced macrophage scavenger receptor targeted micelle for imaging macrophages in atherosclerotic mice with the use of MRI [132, 133]. These imaging tools could potentially present an adjunct to the clinical evaluation of patients with atherosclerotic disease.

Proteases

Inflammatory proteases promote extracellular matrix protein digestion, plaque remodeling, and fibrous cap weakening and are implicated in plaque destabilization and rupture [11]. Proteases thus represent attractive targets for molecular imaging.

Cathepsin is a potent cysteine protease that localized to the shoulders of ruptured atherosclerotic plaques. Jaffer et al. imaged cathepsin activity in vivo in mice and ex vivo in human carotid endatherectomy specimens through near-infrared fluorescence imaging approach [134].

MMPs produced by macrophages, SMCs, and endothelial cells in atherosclerotic plaque proteolyze components of the extracellular matrix and contribute to plaque instability [135]. Radiolabelled molecules designed to specifically target proteolytic activity have been developed for SPECT and PET. For example, radiolabelled MMP inhibitors showed a higher uptake in carotid artery stenosis of mice model [136, 137]. Histological analysis showed co-localization of the specific tracer and MMP-9. In rabbit models, MMP activity detected by SPECT imaging correlated well with the presence of MMP-2 and MMP-9 in the atherosclerotic plaque [138]. Lancelot et al. developed a novel gadolinium-based agent (P947) to visualize MMP presence using in vivo MRI [139]. In human carotid endarterectomy specimens, P947 delineated MMP-rich complex internal carotid atheroma. On in vivo testing, ApoE$^{-/-}$ mice injected with P947 showed strong and heterogeneous signal uptake in aortic plaques.

Apoptosis

Dying cells within atheroma may structurally weaken the protective fibrous cap and expand the underlying necrotic core, facilitating plaque rupture [10, 11]. Imaging of apoptotic cells in atheroma may be useful to evaluate plaques at risk for future complications. Imaging of apoptosis in carotid artery plaques has mainly been studied in animal models by targeting markers of apoptosis such as annexin A5. In a swine model, Technetium-99m labelled annexin A5 showed a higher uptake in unstable carotid atherosclerotic lesions, corresponding to apoptosis using noninvasive SPECT imaging [140]. In a clinical pilot study in four patients with a history of TIA caused by symptomatic carotid artery stenosis, annexin A5 uptake corresponded well with histopathological characterization of vulnerability of the endarterectomy specimens [141]. Unstable plaques showed a higher uptake of annexin A5 while in stable plaques no uptake of annexin A5 was seen after SPECT imaging.

Angiogenesis

Intraplaque angiogenesis by proliferation of medial vasa vasorum has been implicated in rapid plaque growth, intra-plaque hemorrhage, and plaque rupture [10, 13, 99, 100]. A potential marker of inflammation and angiogenesis in atherosclerotic lesions is avb3 integrin, a cell surface glycoprotein receptor highly expressed by macrophages and endothelial cells [142, 143]. MRI of aVb3 integrin-targeted paramagnetic nanoparticles demonstrated signal enhancement in the rabbit aorta with early atherosclerotic changes including expansion of the adventitial vasa vasorum [142]. More recently, cyclic peptides that contain the Arg–Gly–Asp (RGD) attachment site labelled for optical imaging or PET have demonstrated focally increased uptake in advanced, macrophage-rich atherosclerotic lesions of hypercholesterolaemic mice [143, 144].

Oxidative Stress

Oxidative stress has been considered as contributing to atherosclerosis by promoting further lipid oxidation and cell death and by sustaining the inflammatory response [145]. ROS mediate oxidative stress. ROS in atheroma originates predominantly from macrophages and SMCs. In particular, plaques contain MPO, an enzyme that generates hypochlorous acid [145]. MPO can therefore serve as a marker of inflammatory cells and an indirect marker of ROS production. Recent studies demonstrated that MRI using a specialized probe for MPO and the fluorescence reflectance imaging could identify inflammation in rabbit atherosclerotic plaques [146, 147].

Future Perspectives

Findings from numerous clinical studies stimulate attention on the importance of residual risks for the further reduction of cardiovascular events [31–35]. Given that the various biological pathways contribute to the development and progression of atherosclerosis, it is likely that risk stratification through not only LDL cholesterol but also other atherogenic lipid targets and novel biomarkers will be incorporated into the clinical assessment for high-risk patients. To assist this process, it will be necessary to identify reliable biomarkers reflecting the underlying atheroma burden and predicting future events.

Ongoing technological advances in imaging modalities enable us to visualize natural history of atherosclerosis and evaluate factors driving disease progression. Recently, the imaging of atherosclerosis has reached beyond anatomy to encompass the assessment of plaque biology related to the pathogenesis and complication of the disease. This technological advancement may permit us to correctly evaluate residual risks in each individual through noninvasive fashion.

Novel molecular imaging agents are illuminating critical molecular and cellular aspects of atherosclerosis biology in vivo and show utility for all major clinical cardiovascular imaging modalities. However, imaging of coronary arteries is technically challenging. Moreover, the clinical data about the utility of molecular imaging is still limited. Therefore, in addition to further improvement in contrast-to-noise ratios and motion correction of the signals for coronary artery imaging, it is necessary to investigate safety, diagnostic and prognostic values of molecular imaging in the clinical settings.

Considering that biomarkers and plaque imaging have complementary functions to assess the atherosclerotic disease, the use of sophisticated imaging modalities in conjunction with biomarkers will be useful in refining risk assessment, individualizing therapy, and monitoring the response to therapy. Further investigation will be expected to establish more powerful predictive stratification for patients with residual risks associated with the occurrence of future cardiovascular events.

References

1. Lloyd-Jones D, Adams R, Carnethon M, De Simone G, Ferguson TB, Flegal K, Ford E, Furie K, Go A, Greenlund K, Haase N, Hailpern S, Ho M, Howard V, Kissela B, Kittner S, Lackland D, Lisabeth L, Marelli A, McDermott M, Meigs J, Mozaffarian D, Nichol G, O'Donnell C, Roger V, Rosamond W, Sacco R, Sorlie P, Stafford R, Steinberger J, Thom T, Wasserthiel-

Smoller S, Wong N, Wylie-Rosett J, Hong Y. American Heart Association Statistics Committee and Stroke Statistics Subcommittee. Heart disease and stroke statistics—2009 update: a report from the American Heart Association Statistics Committee and Stroke Statistics Subcommittee. Circulation. 2009;119:e21–181.
2. Rocha VZ, Libby P. Obesity, inflammation, and atherosclerosis. Nat Rev Cardiol. 2009;6:399–409.
3. Malek AM, et al. Hemodynamic shear stress and its role in atherosclerosis. JAMA. 1999;282:2035–42.
4. Widlansky ME, Gokce N, Keaney Jr JF, Vita JA. The clinical implications of endothelial dysfunction. J Am Coll Cardiol. 2003;42:1149–60.
5. Williams KJ, Tabas I. The response-to-retention hypothesis of early atherogenesis. Arterioscler Thromb Vasc Biol. 1995;15:551–61.
6. Borén J, Gustafsson M, Skålén K, Flood C, Innerarity TL. Role of extracellular retention of low density lipoproteins in atherosclerosis. Curr Opin Lipidol. 2000;11:451–6.
7. Devlin CM, Lee SJ, Kuriakose G, Spencer C, Becker L, Grosskopf I, Ko C, Huang LS, Koschinsky ML, Cooper AD, Tabas I. An apolipoprotein(a) peptide delays chylomicron remnant clearance and increases plasma remnant lipoproteins and atherosclerosis in vivo. Arterioscler Thromb Vasc Biol. 2005;25:1704–10.
8. Ehnholm C, Jauhiainen M, Metso J. Interaction of lipoprotein(a) with fibronectin and its potential role in atherogenesis. Eur Heart J. 1990;11(Suppl E):190–5.
9. Steinberg D. The LDL, modification hypothesis of atherogenesis: an update. J Lipid Res. 2009; 50(Suppl):S376–81.
10. Ghosh S. Macrophage cholesterol homeostasis and metabolic diseases: critical role of cholesteryl ester mobilization. Expert Rev Cardiovasc Ther. 2011;9:329–40.
11. Libby P, Okamoto Y, Rocha VZ, Folco E. Inflammation in atherosclerosis: transition from theory to practice. Circ J. 2010;74:213–20.
12. Tsimikas S, Miller YI. Oxidative modification of lipoproteins: mechanisms, role in inflammation and potential clinical applications in cardiovascular disease. Curr Pharm Des. 2011;17:27–37.
13. Chikani G, Zhu W, Smart EJ. Lipids: potential regulators of nitric oxide generation. Am J Physiol Endocrinol Metab. 2004;287:E386–9.
14. Huo Y, Xia L. P-selectin glycoprotein ligand-1 plays a crucial role in the selective recruitment of leukocytes into the atherosclerotic arterial wall. Trends Cardiovasc Med. 2009;19:140–5.
15. Eriksson EE. Mechanisms of leukocyte recruitment to atherosclerotic lesions: future prospects. Curr Opin Lipidol. 2004;15:553–8.
16. Nicholls SJ, Hazen SL. Myeloperoxidase, modified lipoproteins, and atherogenesis. J Lipid Res. 2009;50(Suppl):S346–51.
17. Devlin CM, Leventhal AR, Kuriakose G, Schuchman EH, Williams KJ, Tabas I. Acid sphingomyelinase promotes lipoprotein retention within early atheromata and accelerates lesion progression. Arterioscler Thromb Vasc Biol. 2008;28:1723–30.
18. de Winther MP, van Dijk KW, Havekes LM, Hofker MH. Macrophage scavenger receptor class a: a multifunctional receptor in atherosclerosis. Arterioscler Thromb Vasc Biol. 2000;20:290–7.
19. Nakata A, Nakagawa Y, Nishida M, Nozaki S, Miyagawa J, Nakagawa T, Tamura R, Matsumoto K, Kameda-Takemura K, Yamashita S, Matsuzawa Y. CD36, a novel receptor for oxidized low-density lipoproteins, is highly expressed on lipid-laden macrophages in human atherosclerotic aorta. Arterioscler Thromb Vasc Biol. 1999;19:1333–9.
20. Duan SZ, Usher MG, Mortensen RM. Peroxisome proliferator-activated receptor-gamma-mediated effects in the vasculature. Circ Res. 2008;102: 283–94.
21. Li N, Salter RC, Ramji DP. Molecular mechanisms underlying the inhibition of IFN-γ-induced, STAT1-mediated gene transcription in human macrophages by simvastatin and agonists of PPARs and LXRs. J Cell Biochem. 2011;112:675–83.
22. Leskinen MJ, Kovanen PT, Lindstedt KA. Regulation of smooth muscle cell growth, function and death in vitro by activated mast cells—a potential mechanism for the weakening and rupture of atherosclerotic plaques. Biochem Pharmacol. 2003;66:1493–8.
23. Tan NY, Li JM, Stocker R, Khachigian LM. Angiotensin II-inducible smooth muscle cell apoptosis involves the angiotensin II type 2 receptor, GATA-6 activation, and FasL-Fas engagement. Circ Res. 2009;105:422–30.
24. Geng YJ, Henderson LE, Levesque EB, Muszynski M, Libby P. Fas is expressed in human atherosclerotic intima and promotes apoptosis of cytokine-primed human vascular smooth muscle cells. Arterioscler Thromb Vasc Biol. 1997;17:2200–8.
25. Lee E, Grodzinsky AJ, Libby P, Clinton SK, Lark MW, Lee RT. Human vascular smooth muscle cell-monocyte interactions and metalloproteinase secretion in culture. Arterioscler Thromb Vasc Biol. 1995;15:2284–9.
26. Kodali R, Hajjou M, Berman AB, Bansal MB, Zhang S, Pan JJ, Schecter AD. Chemokines induce matrix metalloproteinase-2 through activation of epidermal growth factor receptor in arterial smooth muscle cells. Cardiovasc Res. 2006;69:706–15.
27. Randomised trial of cholesterol lowering in 4444 patients with coronary heart disease: the Scandinavian Simvastatin Survival Study (4S). Lancet 1994, 344:1381–1389.
28. Downs JR, Clearfield M, Weis S, Whitney E, Shapiro DR, Beere PA, Langendorfer A, Stein EA, Kruyer W, Gotto Jr AM. Primary prevention of acute coronary events with lovastatin in men and women with average cholesterol levels: results of AFcaps/Texcaps. AirForce/Texas Coronary Atherosclerosis Prevention Study. JAMA. 1998;279:1615–22.
29. Sacks FM, Pfeffer MA, Moye LA, Rouleau JL, Rutherford JD, Cole TG, Brown L, Warnica JW,

Arnold JM, Wun CC, Davis BR, Braunwald E. The effect of pravastatin on coronary events after myocardial infarction in patients with average cholesterol levels. N Engl J Med. 1996;335:1001–9.
30. Colhoun HM, Betteridge DJ, Durrington PN, Hitman GA, Neil HA, Livingstone SJ, Thomason MJ, Mackness MI, Charlton-Menys V, Fuller JH. CARDS investigators. Primary prevention of cardiovascular disease with atorvastatin in type 2 diabetes in the Collaborative Atorvastatin Diabetes Study (CARDS): multicentre randomised placebo-controlled trial. Lancet. 2004;364:685–96.
31. Prevention of cardiovascular events and death with pravastatin in patients with coronary heart disease and a broad range of initial cholesterol levels. The Long-Term Intervention with Pravastatin in Ischemic Disease (LIPID) Study Group. N Engl J Med. 1998;339:1349–57.
32. Shepherd J, Blauw GJ, Murphy MB, Bollen EL, Buckley BM, Cobbe SM, et al; PROSPER study group. PROspective Study of Pravastatin in the Elderly at Risk. Pravastatin in elderly individuals at risk of vascular disease (PROSPER): a randomised controlled trial. Lancet. 2002;360:1623–30.
33. Cannon CP, Braunwald E, McCabe CH, Rader DJ, Rouleau JL, Belder R, et al; Pravastatin or Atorvastatin Evaluation and Infection Therapy-Thrombolysis in Myocardial Infarction 22 Investigators. Intensive versus moderate lipid lowering with statins after acute coronary syndromes. N Engl J Med. 2004;35:1495–504.
34. Pedersen TR, Faergeman O, Kastelein JJ, Olsson AG, Tikkanen MJ, Holme I, Larsen ML, Bendiksen FS, Lindahl C, Palmer G. Incremental decrease in end points through aggressive lipid lowering study group. High-dose atorvastatin vs usual-dose simvastatin for secondary prevention after myocardial infarction: the IDEAL study: a randomized controlled trial. JAMA. 2005;294:2437–45.
35. LaRosa JC, Grundy SM, Waters DD, Shear C, Barter P, Fruchart JC, Gotto AM, Greten H, Kastelein JJ, Shepherd J, Wenger NK, Treating to New Targets (TNT) Investigators. Intensive lipid lowering with atorvastatin in patients with stable coronary disease. N Engl J Med. 2005;352:1425–35.
36. Gordon DJ, Probstfield JL, Garrison RJ, Neaton JD, Castelli WP, Knoke JD, Jacobs Jr DR, Bangdiwala S, Tyroler HA. High-density lipoprotein cholesterol and cardiovascular disease: four prospective American studies. Circulation. 1989;79:8–15.
37. Castelli WP, Garrison RJ, Wilson PWF, Abbott RD, Kalousdian S, Kannel WB. Incidence of coronary heart disease and lipoprotein cholesterol levels: the Framingham Study. JAMA. 1986;256:2835–8.
38. Barter P, Gotto AM, LaRosa JC, Maroni J, Szarek M, Grundy SM, Kastelein JJ, Bittner V, Fruchart JC. Treating to New Targets Investigators. HDL cholesterol, very low levels of LDL cholesterol, and cardiovascular events. N Engl J Med. 2007;357:1301–10.
39. Jafri H, Alsheikh-Ali AA, Karas RH. Meta-analysis: statin therapy does not alter the association between low levels of high-density lipoprotein cholesterol and increased cardiovascular risk. Ann Intern Med. 2010;153:800–8.
40. Barter PJ, Nicholls S, Rye KA, Anantharamaiah GM, Navab M, Fogelman AM. Antiinflammatory properties of HDL. Circ Res. 2004;95:764–72.
41. Sarwar N, Danesh J, Eiriksdottir G, Sigurdsson G, Wareham N, Bingham S, Boekholdt SM, Khaw KT, Gudnason V. Triglycerides and the risk of coronary heart disease: 10,158 incident cases among 262,525 participants in 29 Western prospective studies. Circulation. 2007;115:450–8.
42. Miller M, Cannon CP, Murphy SA, Qin J, Ray KK, Braunwald E, PROVE IT-TIMI 22 Investigators. Impact of triglyceride levels beyond low-density lipoprotein cholesterol after acute coronary syndrome in the PROVE IT-TIMI 22 trial. J Am Coll Cardiol. 2008;51:724–30.
43. Cui Y, Blumenthal RS, Flaws JA, Whiteman MK, Langenberg P, Bachorik PS, Bush TL. Non-high-density lipoprotein cholesterol level as a predictor of cardiovascular disease mortality. Arch Intern Med. 2001;161:1413–9.
44. Boekholdt SM, Arsenault BJ, Mora S, Pedersen TR, LaRosa JC, Nestel PJ, Simes RJ, Durrington P, Hitman GA, Welch KM, DeMicco DA, Zwinderman AH, Clearfield MB, Downs JR, Tonkin AM, Colhoun HM, Gotto Jr AM, Ridker PM, Kastelein JJ. Association of LDL cholesterol, non-HDL cholesterol, and apolipoprotein B levels with risk of cardiovascular events among patients treated with statins: a meta-analysis. JAMA. 2012;307:1302–9.
45. Liu J, Sempos C, Donahue RP, Dorn J, Trevisan M, Grundy SM. Joint distribution of non-HDL and LDL cholesterol and coronary heart disease risk prediction among individuals with and without diabetes. Diabetes Care. 2005;28:1916–21.
46. Anuurad E, Boffa MB, Koschinsky ML, Berglund L. Lipoprotein(a): a unique risk factor for cardiovascular disease. Clin Lab Med. 2006;26:751–72.
47. Berglund L, Ramakrishnan R. Lipoprotein(a): an elusive cardiovascular risk factor. Arterioscler Thromb Vasc Biol. 2004;24:2219–26.
48. Boffa MB, Marcovina SM, Koschinsky ML. Lipoprotein(a) as a risk factor for atherosclerosis and thrombosis: mechanistic insights from animal models. Clin Biochem. 2004;37:333–43.
49. Koschinsky ML. Lipoprotein(a) and atherosclerosis: new perspectives on the mechanism of action of an enigmatic lipoprotein. Curr Atheroscler Rep. 2005;7:389–95.
50. Danesh J, Collins R, Peto R. Lipoprotein(a) and coronary heart disease. Meta-analysis of prospective studies. Circulation. 2000;102:1082–5.
51. Emerging Risk Factors Collaboration, Erqou S, Kaptoge S, Perry PL, Di Angelantonio E, Thompson A, White IR, Marcovina SM, Collins R, Thompson

SG, Danesh J. Lipoprotein(a) concentration and the risk of coronary heart disease, stroke, and nonvascular mortality. JAMA. 2009;302:412–23.
52. Nicholls SJ, Tang WH, Scoffone H, Brennan DM, Hartiala J, Allayee H, Hazen SL. Lipoprotein(a) levels and long-term cardiovascular risk in the contemporary era of statin therapy. J Lipid Res. 2010;51:3055–61.
53. Mehta A, Yang B, Khan S, Hendricks JB, Stephen C, Mehta JL. Oxidized low-density lipoproteins facilitate leukocyte adhesion to aortic intima without affecting endothelium-dependent relaxation. Role of P-selectin. Arterioscler Thromb Vasc Biol. 1995;15:2076–83.
54. Liao L, Starzyk RM, Granger DN. Molecular determinants of oxidized low-density lipoprotein-induced leukocyte adhesion and microvascular dysfunction. Arterioscler Thromb Vasc Biol. 1997;17:437–44.
55. Meisinger C, Baumert J, Khuseyinova N, Loewel H, Koening W. Plasma oxidized low-density lipoprotein, a strong predictor for acute coronary heart disease events in apparently healthy, middle-aged men from the general population. Circulation. 2005;112:651–7.
56. Shimada K, Mokuno H, Matsunaga E, Miyazaki T, Sumiyoshi K, Miyauchi K, Daida H. Circulating oxidized low-density lipoprotein is an independent predictor for cardiac event in patients with coronary artery disease. Atherosclerosis. 2004;174:343–7.
57. Ridker PM, Cook N. Clinical usefulness of very high and very low levels of C-reactive protein across the full range of Framingham Risk Scores. Circulation. 2004;109:1955–9.
58. Haverkate F, Thompson SG, Pyke SD, Gallimore JR, Pepys MB. Production of C-reactive protein and risk of coronary events in stable and unstable angina. European Concerted Action on Thrombosis and Disabilities Angina Pectoris Study Group. Lancet. 1997;349:462–6.
59. Rutter MK, Meigs JB, Sullivan LM, D'Agostino Sr RB, Wilson PW. C-reactive protein, the metabolic syndrome, and prediction of cardiovascular events in the Framingham Offspring Study. Circulation. 2004;110:380–5.
60. Ridker PM, Cannon CP, Morrow D, Rifai N, Rose LM, McCabe CH, Pfeffer MA, Braunwald E. Pravastatin or atorvastatin evaluation and infection therapy-thrombolysis in myocardial infarction 22 (PROVE IT-TIMI 22) Investigators. C-reactive protein levels and outcomes after statin therapy. N Engl J Med. 2005;352:20–8.
61. Vittos O, Toana B, Vittos A, Moldoveanu E. Lipoprotein-associated phospholipase A2 (Lp-PLA2): a review of its role and significance as a cardiovascular biomarker. Biomarkers. 2012;17:289–302.
62. Rosenson RS, Stafforini DM. Modulation of oxidative stress, inflammation, and atherosclerosis by lipoprotein-associated phospholipase A2. J Lipid Res. 2012;53:1767–82.
63. Gonçalves I, Edsfeldt A, Ko NY, Grufman H, Berg K, Björkbacka H, Nitulescu M, Persson A, Nilsson M, Prehn C, Adamski J, Nilsson J. Evidence supporting a key role of Lp-PLA2-generated lysophosphatidylcholine in human atherosclerotic plaque inflammation. Arterioscler Thromb Vasc Biol. 2012;32:1505–12.
64. Münzel T, Gori T. Lipoprotein-associated phospholipase A(2), a marker of vascular inflammation and systemic vulnerability. Eur Heart J. 2009;30:2829–31.
65. Packard CJ, O'Reilly DS, Caslake MJ, McMahon AD, Ford I, Cooney J, Macphee CH, Suckling KE, Krishna M, Wilkinson FE, Rumley A, Lowe GD. Lipoprotein-associated phospholipase A2 as an independent predictor of coronary heart disease. West of Scotland Coronary Prevention Study Group. N Engl J Med. 2000;343:1148–55.
66. Koenig W, Khuseyinova N, Löwel H, Trischler G, Meisinger C. Lipoprotein-associated phospholipase A2 adds to risk prediction of incident coronary events by C-reactive protein in apparently healthy middle-aged men from the general population: results from the 14-year follow-up of a large cohort from southern Germany. Circulation. 2004;110:1903–8.
67. Oei HH, van der Meer IM, Hofman A, Koudstaal PJ, Stijnen T, Breteler MM, Witteman JC. Lipoprotein-associated phospholipase A2 activity is associated with risk of coronary heart disease and ischemic stroke: the Rotterdam Study. Circulation. 2005;111:570–5.
68. O'Donoghue M, Morrow DA, Sabatine MS, Murphy SA, McCabe CH, Cannon CP, Braunwald E. Lipoprotein-associated phospholipase A2 and its association with cardiovascular outcomes in patients with acute coronary syndromes in the PROVE IT-TIMI 22 (PRavastatin Or ator-Vastatin Evaluation and Infection Therapy-Thrombolysis In Myocardial Infarction) Trial. Circulation. 2006;113:1745–52.
69. Rosenson RS. Phospholipase A2 inhibition and atherosclerotic vascular disease: prospects for targeting secretory and lipoprotein-associated phospholipase A2 enzymes. Curr Opin Lipidol. 2010;21:473–80.
70. Blache D, Gautier T, Tietge UJ, Lagrost L. Activated platelets contribute to oxidized low-density lipoproteins and dysfunctional high-density lipoproteins through a phospholipase A2-dependent mechanism. FASEB J. 2012;26:927–37.
71. Boyanovsky BB, van der Westhuyzen DR, Webb NR. Group V secretory phospholipase A2-modified low density lipoprotein promotes foam cell formation by a SR-A- and CD36-independent process that involves cellular proteoglycans. J Biol Chem. 2005;280:32746–52.
72. Yamamoto K, Isogai Y, Sato H, Taketomi Y, Murakami M. Secreted phospholipase A2, lipoprotein hydrolysis, and atherosclerosis: integration with lipidomics. Anal Bioanal Chem. 2011;400:1829–42.
73. Leitinger N, Watson AD, Hama SY, Ivandic B, Qiao JH, Huber J, Faull KF, Grass DS, Navab M, Fogelman AM, de Beer FC, Lusis AJ, Berliner JA. Role of group II secretory phospholipase A2 in atherosclerosis: 2. Potential involvement of biologically active oxidized phospholipids. Arterioscler Thromb Vasc Biol. 1999;19:1291–8.

74. Mallat Z, Steg PG, Benessiano J, Tanguy ML, Fox KA, Collet JP, Dabbous OH, Henry P, Carruthers KF, Dauphin A, Arguelles CS, Masliah J, Hugel B, Montalescot G, Freyssinet JM, Asselain B, Tedgui A. Circulating secretory phospholipase A2 activity predicts recurrent events in patients with severe acute coronary syndromes. J Am Coll Cardiol. 2005;46:1249–57.
75. Kugiyama K, Ota Y, Takazoe K, Moriyama Y, Kawano H, Miyao Y, Sakamoto T, Soejima H, Ogawa H, Doi H, Sugiyama S, Yasue H. Circulating levels of secretory type II phospholipase A(2) predict coronary events in patients with coronary artery disease. Circulation. 1999;100:1280–4.
76. Nicholls SJ, Hazen SL. Myeloperoxidase and cardiovascular disease. Arterioscler Thromb Vasc Biol. 2005;25:1102–11.
77. Daugherty A, Dunn JL, Rateri DL, Heinecke JW. Myeloperoxidase, a catalyst for lipoprotein oxidation, is expressed in human atherosclerotic lesions. J Clin Invest. 1994;94:437–44.
78. Sugiyama S, Okada Y, Sukhova GK, Virmani R, Heinecke JW, Libby P. Macrophage myeloperoxidase regulation by granulocyte macrophage colony-stimulating factor in human atherosclerosis and implications in acute coronary syndromes. Am J Pathol. 2001;158:879–91.
79. Baldus S, Heeschen C, Meinertz T, Zeiher AM, Eiserich JP, Münzel T, Simoons ML, Hamm CW, CAPTURE Investigators. Myeloperoxidase serum levels predict risk in patients with acute coronary syndromes. Circulation. 2003;108:1440–5.
80. Meuwese MC, Stroes ES, Hazen SL, van Miert JN, Kuivenhoven JA, Schaub RG, Wareham NJ, Luben R, Kastelein JJ, Khaw KT, Boekholdt SM. Serum myeloperoxidase levels are associated with the future risk of coronary artery disease in apparently healthy individuals: the EPIC-Norfolk Prospective Population Study. J Am Coll Cardiol. 2007; 50:159–65.
81. Tang WH, Wu Y, Nicholls SJ, Hazen SL. Plasma myeloperoxidase predicts incident cardiovascular risks in stable patients undergoing medical management for coronary artery disease. Clin Chem. 2011;57:33–9.
82. Belhassen L, Carville C, Pelle G, Monin JL, Teiger E, Duval-Moulin AM, Dupouy P, Dubois Rande JL, Gueret P. Evaluation of carotid artery and aortic intima-media thickness measurements for exclusion of significant coronary atherosclerosis in patients scheduled for heart valve surgery. J Am Coll Cardiol. 2002;39:1139–44.
83. Bots ML, Hoes AW, Koudstaal PJ, Hofman A, Grobbee DE. Common carotid intima-media thickness and risk of stroke and myocardial infarction: the Rotterdam Study. Circulation. 1997;96:1432–7.
84. Arad Y, Spadaro LA, Goodman K, Newstein D, Guerci AD. Prediction of coronary events with electron beam computed tomography. J Am Coll Cardiol. 2000;36:1253–60.
85. Raggi P, Callister TQ, Cooil B, He ZX, Lippolis NJ, Russo DJ, Zelinger A, Mahmarian JJ. Identification of patients at increased risk of first unheralded acute myocardial infarction by electron-beam computed tomography. Circulation. 2000;101:850–5.
86. Elias-Smale SE, Proença RV, Koller MT, Kavousi M, van Rooij FJ, Hunink MG, Steyerberg EW, Hofman A, Oudkerk M, Witteman JC. Coronary calcium score improves classification of coronary heart disease risk in the elderly: the Rotterdam study. J Am Coll Cardiol. 2010;56:1407–14.
87. Arad Y, Goodman KJ, Roth M, Newstein D, Guerci AD. Coronary calcification, coronary disease risk factors, C-reactive protein, and atherosclerotic cardiovascular disease events: the St. Francis Heart Study. J Am Coll Cardiol. 2005;46:158–65.
88. Motoyama S, Sarai M, Harigaya H, Anno H, Inoue K, Hara T, Naruse H, Ishii J, Hishida H, Wong ND, Virmani R, Kondo T, Ozaki Y, Narula J. Computed tomographic angiography characteristics of atherosclerotic plaques subsequently resulting in acute coronary syndrome. J Am Coll Cardiol. 2009; 54:49–57.
89. Otsuka K, Fukuda S, Tanaka A, Nakanishi K, TaguchiH YJ, Shimada K, Yoshiyama M. Napkin-ring sign on coronary CT angiography for the prediction of acute coronary syndrome. J Am Coll Cardiol Img. 2013;6:448–57.
90. Kurra V, Lieber ML, Sola S, Kalahasti V, Hammer D, Gimple S, Flamm SD, Bolen MA, Halliburton SS, Mihaljevic T, Desai MY, Schoenhagen P. Extent of thoracic aortic atheroma burden and long-term mortality after cardiothoracic surgery: a computed tomography study. JACC Cardiovasc Imaging. 2010;3:1020–9.
91. Cai JM, Hatsukami TS, Ferguson MS, Small R, Polissar NL, Yuan C. Classification of human carotid atherosclerotic lesions with in vivo multicontrast magnetic resonance imaging. Circulation. 2002; 106:1368–73.
92. Chu B, Phan BA, Balu N, Yuan C, Brown BG, Zhao XQ. Reproducibility of carotid atherosclerotic lesion type characterization using high resolution multicontrast weighted cardiovascular magnetic resonance. J Cardiovasc Magn Reson. 2006;8:793–9.
93. Yuan C, Zhang SX, Polissar NL, Echelard D, Ortiz G, Davis JW, Ellington E, Ferguson MS, Hatsukami TS. Identification of fibrous cap rupture with magnetic resonance imaging is highly associated with recent transient ischemic attack or stroke. Circulation. 2002;105:181–5.
94. Corti R, Fayad ZA, Fuster V, Worthley SG, Helft G, Chesebro J, Mercuri M, Badimon JJ. Effects of lipid-lowering by simvastatin on human atherosclerotic lesions: a longitudinal study by high-resolution, noninvasive magnetic resonance imaging. Circulation. 2001;104:249–52.
95. Corti R, Fuster V, Fayad ZA, Worthley SG, Helft G, Chaplin WF, Muntwyler J, Viles-Gonzalez JF, Weinberger J, Smith DA, Mizsei G, Badimon JJ.

Effects of aggressive versus conventional lipid-lowering therapy by simvastatin on human atherosclerotic lesions: a prospective, randomized, double-blind trial with high-resolution magnetic resonance imaging. J Am Coll Cardiol. 2005;46:106–12.
96. Rudd JH, Warburton EA, Fryer TD, Jones HA, Clark JC, Antoun N, Johnström P, Davenport AP, Kirkpatrick PJ, Arch BN, Pickard JD, Weissberg PL. Imaging atherosclerotic plaque inflammation with [18F]-fluorodeoxyglucose positron emission tomography. Circulation. 2002;105:2708–11.
97. Worthley SG, Zhang ZY, Machac J, Helft G, Tang C, Liew GY, Zaman AG, Worthley MI, Fayad ZA, Buchsbaum MS, Fuster V, Badimon JJ. In vivo noninvasive serial monitoring of FDG-PET progression and regression in a rabbit model of atherosclerosis. Int J Cardiovasc Imaging. 2009;25:251–7.
98. Marnane M, Merwick A, Sheehan OC, Hannon N, Foran P, Grant T, Dolan E, Moroney J, Murphy S, O'Rourke K, O'Malley K, O'Donohoe M, McDonnell C, Noone I, Barry M, Crowe M, Kavanagh E, O'Connell M, Kelly PJ. Carotid plaque inflammation on 18F-fluorodeoxyglucose positron emission tomography predicts early stroke recurrence. Ann Neurol. 2012;71:709–18.
99. Paulmier B, Duet M, Khayat R, Pierquet-Ghazzar N, Laissy JP, Maunoury C, Hugonnet F, Sauvaget E, Trinquart L, Faraggi M. Arterial wall uptake of fluorodeoxyglucose on PET imaging in stable cancer disease patients indicates higher risk for cardiovascular events. J Nucl Cardiol. 2008;15:209–17.
100. Mintz GS, Nissen SE, Anderson WD, Bailey SR, Erbel R, Fitzgerald PJ, Pinto FJ, Rosenfield K, Siegel RJ, Tuzcu EM, Yock PG. American College of Cardiology Clinical Expert Consensus Document on Standards for Acquisition, Measurement and Reporting of Intravascular Ultrasound Studies (IVUS). A report of the American College of Cardiology Task Force on Clinical Expert Consensus Documents. J Am Coll Cardiol. 2001;37:1478–92.
101. Nissen SE, Tuzcu EM, Schoenhagen P, Brown BG, Ganz P, Vogel RA, Crowe T, Howard G, Cooper CJ, Brodie B, Grines CL, DeMaria AN, REVERSAL Investigators. Effect of intensive compared with moderate lipid-lowering therapy on progression of coronary atherosclerosis: a randomized controlled trial. JAMA. 2004;291:1071–80.
102. Nissen SE, Tuzcu EM, Libby P, Thompson PD, Ghali M, Garza D, Berman L, Shi H, Buebendorf E, Topol EJ, CAMELOT Investigators. Effect of antihypertensive agents on cardiovascular events in patients with coronary disease and normal blood pressure: the CAMELOT study: a randomized controlled trial. JAMA. 2004;292:2217–25.
103. Nissen SE, Tuzcu EM, Brewer HB, Sipahi I, Nicholls SJ, Ganz P, Schoenhagen P, Waters DD, Pepine CJ, Crowe TD, Davidson MH, Deanfield JE, Wisniewski LM, Hanyok JJ, Kassalow LM, ACAT Intravascular Atherosclerosis Treatment Evaluation (ACTIVATE) Investigators. Effect of ACAT inhibition on the progression of coronary atherosclerosis. N Engl J Med. 2006;354:1253–63.
104. Nissen SE, Nicholls SJ, Sipahi I, Libby P, Raichlen JS, Ballantyne CM, Davignon J, Erbel R, Fruchart JC, Tardif JC, Schoenhagen P, Crowe T, Cain V, Wolski K, Goormastic M, Tuzcu EM, ASTEROID Investigators. Effect of very high-intensity statin therapy on regression of coronary atherosclerosis: the ASTEROID trial. JAMA. 2006;295:1556–65.
105. Nissen SE, Tardif JC, Nicholls SJ, Revkin JH, Shear CL, Duggan WT, Ruzyllo W, Bachinsky WB, Lasala GP, Tuzcu EM, ILLUSTRATE Investigators. Effect of torcetrapib on the progression of coronary atherosclerosis. N Engl J Med. 2007;356:1304–16.
106. Nissen SE, Nicholls SJ, Wolski K, Nesto R, Kupfer S, Perez A, Jure H, De Larochellière R, Staniloae CS, Mavromatis K, Saw J, Hu B, Lincoff AM, Tuzcu EM, PERISCOPE Investigators. Comparison of pioglitazone vs glimepiride on progression of coronary atherosclerosis in patients with type 2 diabetes: the PERISCOPE randomized controlled trial. JAMA. 2008;299:1561–73.
107. Nissen SE, Nicholls SJ, Wolski K, Rodés-Cabau J, Cannon CP, Deanfield JE, Kastelein JJ, Steinhubl SR, Kapadia S, Yasin M, Ruzyllo W, Gaudin C, Job B, Hu B, Bhatt DL, Lincoff AM, Tuzcu EM, STRADIVARIUS Investigators. Effect of rimonabant on progression of atherosclerosis in patients with abdominal obesity and coronary artery disease: the STRADIVARIUS randomized controlled trial. JAMA. 2008;299:1547–60.
108. Nicholls SJ, Ballantyne CM, Barter PJ, Chapman MJ, Erbel RM, Libby P, Raichlen JS, Uno K, Borgman M, Wolski K, Nissen SE. Effect of two intensive statin regimens on progression of coronary disease. N Engl J Med. 2011;365:2078–87.
109. Bayturan O, Kapadia S, Nicholls SJ, Tuzcu EM, Shao M, Uno K, Shreevatsa A, Lavoie AJ, Wolski K, Schoenhagen P, Nissen SE. Clinical predictors of plaque progression despite very low levels of low-density lipoprotein cholesterol. J Am Coll Cardiol. 2010;55:2736–42.
110. Nicholls SJ, Hsu A, Wolski K, Hu B, Bayturan O, Lavoie A, Uno K, Tuzcu EM, Nissen SE. Intravascular ultrasound-derived measures of coronary atherosclerotic plaque burden and clinical outcome. J Am Coll Cardiol. 2010;55:2399–407.
111. Nair A, Kuban BD, Tuzcu EM, Schoenhagen P, Nissen SE, Vince DG. Coronary plaque classification with intravascular ultrasound radiofrequency data analysis. Circulation. 2002;106:2200–6.
112. Nasu K, Tsuchikane E, Katoh O, Vince DG, Virmani R, Surmely JF, Murata A, Takeda Y, Ito T, Ehara M, Matsubara T, Terashima M, Suzuki T. Accuracy of in vivo coronary plaque morphology assessment: a validation study of in vivo virtual histology compared with in vitro histopathology. J Am Coll Cardiol. 2006;47:2405–12.

113. Stone GW, Maehara A, Lansky AJ, de Bruyne B, Cristea E, Mintz GS, Mehran R, McPherson J, Farhat N, Marso SP, Parise H, Templin B, White R, Zhang Z, Serruys PW, PROSPECT Investigators. A prospective natural-history study of coronary atherosclerosis. N Engl J Med. 2011;364:226–35.
114. Low AF, Teaney GJ, Bouma BE, Jang IK. Technology insight: optical coherence tomography-current status and future development. Nat Clin Pract Cardiovasc Med. 2006;3:154–62.
115. Jang IK, Bouma BE, Kang DH, Park SJ, Park SW, Seung KB, Choi KB, Shishkov M, Schlendorf K, Pomerantsev E, Houser SL, Aretz HT, Tearney GJ. Visualization of coronary atherosclerotic plaques in patients using optical coherence tomography: comparison with intravascular ultrasound. J Am Coll Cardiol. 2002;39:604–9.
116. Jang IK, Tearney GJ, MacNeill B, Takano M, Moselewski F, Iftima N, Shishkov M, Houser S, Aretz HT, Halpern EF, Bouma BE. In vivo characterization of coronary atherosclerotic plaque by use of optical coherence tomography. Circulation. 2005;111:1551–5.
117. Kume T, Akasaka T, Kawamoto T, Okura H, Watanabe N, Toyota E, Neishi Y, Sukmawan R, Sadahira Y, Yoshida K. Measurement of the thickness of the fibrous cap by optical coherence tomography. Am Heart J. 2006;152:e1–4.
118. Yabushita H, Bouma BE, Houser SL, Aretz HT, Jang IK, Schlendorf KH, Kauffman CR, Shishkov M, Kang DH, Halpern EF, Tearney GJ. Characterization of human atherosclerosis by optical coherence tomography. Circulation. 2002;106:1640–5.
119. Cassis LA, Lodder RA. Near-IR imaging of atheromas in living arterial tissue. Anal Chem. 1993;65:1247–56.
120. Jaross W, Neumeister V, Lattke P, Schuh D. Determination of cholesterol in atherosclerotic plaques using near infrared diffuse reflection spectroscopy. Atherosclerosis. 1999;147:327–37.
121. Gardner CM, Tan H, Hull E, Lisauskas JB, Sum ST, Meese TM, Jiang C, Madden SP, Caplan JD, Burke AP, Virmani R, Goldstein J, Muller JE. Detection of lipid core coronary plaques in autopsy specimens with a novel catheter-based near-infrared spectroscopy system. JACC Cardiovasc Imaging. 2008;1:638–48.
122. Kaufmann BA, Sanders JM, Davis C, Xie A, Aldred P, Sarembock IJ, Lindner JR. Molecular imaging of inflammation in atherosclerosis with targeted ultrasound detection of vascular cell adhesion molecule-1. Circulation. 2007;116:276–84.
123. Nahrendorf M, Jaffer FA, Kelly KA, Sosnovik DE, Aikawa E, Libby P, Weissleder R. Noninvasive vascular cell adhesion molecule-1 imaging identifies inflammatory activation of cells in atherosclerosis. Circulation. 2006;114:1504–11.
124. Libby P. Inflammation in atherosclerosis. Nature. 2002;420:868–74.
125. Naghavi M, Libby P, Falk E, Casscells SW, Litovsky S, Rumberger J, Badimon JJ, Stefanadis C, Moreno P, Pasterkamp G, Fayad Z, Stone PH, Waxman S, Raggi P, Madjid M, Zarrabi A, Burke A, Yuan C, Fitzgerald PJ, Siscovick DS, de Korte CL, Aikawa M, Airaksinen KE, Assmann G, Becker CR, Chesebro JH, Farb A, Galis ZS, Jackson C, Jang IK, Koenig W, Lodder RA, March K, Demirovic J, Navab M, Priori SG, Rekhter MD, Bahr R, Grundy SM, Mehran R, Colombo A, Boerwinkle E, Ballantyne C, Insull Jr W, Schwartz RS, Vogel R, Serruys PW, Hansson GK, Faxon DP, Kaul S, Drexler H, Greenland P, Muller JE, Virmani R, Ridker PM, Zipes DP, Shah PK, Willerson JT. From vulnerable plaque to vulnerable patient: a call for new definitions and risk assessment strategies: part I. Circulation. 2003;108:1664–72.
126. Naghavi M, Libby P, Falk E, Casscells SW, Litovsky S, Rumberger J, Badimon JJ, Stefanadis C, Moreno P, Pasterkamp G, Fayad Z, Stone PH, Waxman S, Raggi P, Madjid M, Zarrabi A, Burke A, Yuan C, Fitzgerald PJ, Siscovick DS, de Korte CL, Aikawa M, Juhani Airaksinen KE, Assmann G, Becker CR, Chesebro JH, Farb A, Galis ZS, Jackson C, Jang IK, Koenig W, Lodder RA, March K, Demirovic J, Navab M, Priori SG, Rekhter MD, Bahr R, Grundy SM, Mehran R, Colombo A, Boerwinkle E, Ballantyne C, Insull Jr W, Schwartz RS, Vogel R, Serruys PW, Hansson GK, Faxon DP, Kaul S, Drexler H, Greenland P, Muller JE, Virmani R, Ridker PM, Zipes DP, Shah PK, Willerson JT. From vulnerable plaque to vulnerable patient: a call for new definitions and risk assessment strategies: part II. Circulation. 2003;108:1772–8.
127. Rudd JH, Myers KS, Bansilal S, Machac J, Pinto CA, Tong C, Rafique A, Hargeaves R, Farkouh M, Fuster V, Fayad ZA. Atherosclerosis inflammation imaging with 18F-FDG PET: carotid, iliac, and femoral uptake reproducibility, quantification methods, and recommendations. J Nucl Med. 2008;49:871–8.
128. Tawakol A, Migrino RQ, Bashian GG, Bedri S, Vermylen D, Cury RC, Yates D, LaMuraglia GM, Furie K, Houser S, Gewirtz H, Muller JE, Brady TJ, Fischman AJ. In vivo 18F-fluorodeoxyglucose positron emission tomography imaging provides a noninvasive measure of carotid plaque inflammation in patients. J Am Coll Cardiol. 2006;48:1818–24.
129. Tahara N, Kai H, Ishibashi M, Nakaura H, Kaida H, Baba K, Hayabuchi N, Imaizumi T. Simvastatin attenuates plaque inflammation: evaluation by fluorodeoxyglucose positron emission tomography. J Am Coll Cardiol. 2006;48:1825–31.
130. Kooi ME, Cappendijk VC, Cleutjens KB, Kessels AG, Kitslaar PJ, Borgers M, Frederik PM, Daemen MJ, van Engelshoven JM. Accumulation of ultrasmall superparamagnetic particles of iron oxide in human atherosclerotic plaques can be detected by in vivo magnetic resonance imaging. Circulation. 2003;107:2453–8.

131. Nahrendorf M, Keliher E, Marinelli B, Leuschner F, Robbins CS, Gerszten RE, Pittet MJ, Swirski FK, Weissleder R. Detection of macrophages in aortic aneurysms by nanoparticle positron emission tomography-computed tomography. Arterioscler Thromb Vasc Biol. 2011;31:750–7.
132. Amirbekian V, Lipinski MJ, Briley-Saebo KC, Amirbekian S, Aguinaldo JG, Weinreb DB, Vucic E, Frias JC, Hyafil F, Mani V, Fisher EA, Fayad ZA. Detecting and assessing macrophages in vivo to evaluate atherosclerosis noninvasively using molecular MRI. Proc Natl Acad Sci USA. 2007;104: 961–6.
133. Mulder WJ, Strijkers GJ, Briley-Saboe KC, Frias JC, Aguinaldo JG, Vucic E, Amirbekian V, Tang C, Chin PT, Nicolay K, Fayad ZA. Molecular imaging of macrophages in atherosclerotic plaques using bimodal PEG-micelles. Magn Reson Med. 2007;58:1164–70.
134. Jaffer FA, Kim DE, Quinti L, Tung CH, Aikawa E, Pande AN, Kohler RH, Shi GP, Libby P, Weissleder R. Optical visualization of cathepsin K activity in atherosclerosis with a novel, protease-activatable fluorescence sensor. Circulation. 2007;115:2292–8.
135. Galis ZS, Khatri JJ. Matrix metalloproteinases in vascular remodeling and atherogenesis: the good, the bad, and the ugly. Circ Res. 2002;90:251–62.
136. Wagner S, Breyholz HJ, Höltke C, Faust A, Schober O, Schäfers M, Kopka K. A new 18F-labelled derivative of the MMP inhibitor CGS 27023A for PET: radiosynthesis and initial small-animal PET studies. Appl Radiat Isot. 2009;67:606–10.
137. Breyholz HJ, Wagner S, Levkau B, Schober O, Schäfers M, Kopka K. A 18F-radiolabeled analogue of CGS 27023A as a potential agent for assessment of matrix-metalloproteinase activity in vivo. Q J Nucl Med Mol Imaging. 2007;51:24–32.
138. Fujimoto S, Hartung D, Ohshima S, Edwards DS, Zhou J, Yalamanchili P, Azure M, Fujimoto A, Isobe S, Matsumoto Y, Boersma H, Wong N, Yamazaki J, Narula N, Petrov A, Narula J. Molecular imaging of matrix metalloproteinase in atherosclerotic lesions: resolution with dietary modification and statin therapy. J Am Coll Cardiol. 2008;52:1847–57.
139. Lancelot E, Amirbekian V, Brigger I, Raynaud JS, Ballet S, David C, Rousseaux O, Le Greneur S, Port M, Lijnen HR, Bruneval P, Michel JB, Ouimet T, Roques B, Amirbekian S, Hyafil F, Vucic E, Aguinaldo JG, Corot C, Fayad ZA. Evaluation of matrix metalloproteinases in atherosclerosis using a novel noninvasive imaging approach. Arterioscler Thromb Vasc Biol. 2008;28:425–32.
140. Johnson LL, Schofield L, Donahay T, Narula N, Narula J. 99mTc-annexin V imaging for in vivo detection of atherosclerotic lesions in porcine coronary arteries. J Nucl Med. 2005;46:1186–93.
141. Kietselaer BL, Reutelingsperger CP, Heidendal GA, Daemen MJ, Mess WH, Hofstra L, Narula J. Noninvasive detection of plaque instability with use of radiolabeled annexin A5 in patients with carotid-artery atherosclerosis. N Engl J Med. 2004; 350:1472–3.
142. Winter PM, Morawski AM, Caruthers SD, Fuhrhop RW, Zhang H, Williams TA, Allen JS, Lacy EK, Robertson JD, Lanza GM, Wickline SA. Molecular imaging of angiogenesis in early-stage atherosclerosis with alpha(v)beta3-integrin-targeted nanoparticles. Circulation. 2003;108:2270–4.
143. Waldeck J, Hager F, Holtke C, Lanckohr C, von Wallbrunn A, Torsello G, Heindel W, Theilmeier G, Schäfers M, Bremer C. Fluorescence reflectance imaging of macrophage-rich atherosclerotic plaques using an falphagvfbetag3 integrin-targeted fluorochrome. J Nucl Med. 2008;49:1845–51.
144. Saraste A, Laitinen I, Poethko T, Weber AW. Ho ¨lzlwimmer G, Reder S, Nekolla SG, Ylä-Herttuala S, Wester H, Knuuti J, Schwaiger M. Evaluation of [18F]-Galacto-RGD, a PET tracer for imaging alpha(v)beta3 integrin, for detection of atherosclerotic plaques in mouse model. Eur J Nucl Med Mol Imaging. 2008;35S:131.
145. Kunsch C, Medford RM. Oxidative stress as a regulator of gene expression in the vasculature. Circ Res. 1999;85:753–66.
146. Ronald JA, Chen JW, Chen Y, Hamilton AM, Rodriguez E, Reynolds F, Hegele RA, Rogers KA, Querol M, Bogdanov A, Weissleder R, Rutt BK. Enzyme-sensitive magnetic resonance imaging targeting myeloperoxidase identifies active inflammation in experimental rabbit atherosclerotic plaques. Circulation. 2009;120:592–9.
147. Shepherd J, Hilderbrand SA, Waterman P, Heinecke JW, Weissleder R, Libby P. A fluorescent probe for the detection of myeloperoxidase activity in atherosclerosis-associated macrophages. Chem Biol. 2007;14:1221–31.

Advanced Coronary Imaging

2

Femi Philip and Samir R. Kapadia

Introduction

Coronary artery disease remains the leading cause of death in the United States and an estimated 1.4 million Americans have a heart attack every year [1]. Coronary atherosclerosis starts at a young age but the initial plaque does not encroach on the lumen but remodeling of the vessel wall occurs by expansion of the external elastic lamina—a phenomenon described by Glagov as positive remodeling [2]. Coronary angiography visualizes the vessel lumen but does not provide any information about the individual components of the vessel wall. Despite this limitation, coronary angiography is the most common method used to delineate the extent and severity of atherosclerotic narrowing of coronary arteries. This modality provides a two dimensional rendering of a three dimensional structure and is dependent on angle of visualization and morphology of lesions visualized. Intravascular techniques using intravascular ultrasound (IVUS) and optical coherence tomography (OCT) provide information complementary to that provided by conventional coronary angiography. This chapter will discuss the technical aspects of these imaging techniques and provide some insights in their clinical applications.

F. Philip, MD • S.R. Kapadia, MD (✉)
Department of Cardiovascular Medicine, Cleveland Clinic, 9500 Euclid Avenue, Cleveland, OH 44195, USA
e-mail: kapadia@ccf.org

Normal arterial walls consist of an inner layer called the intima, a middle muscular layer called the media and an outermost layer called the adventitia. The intima is the inner most lining of the vessel wall and is in direct contact with components of blood and is normally 1–2 layers thick (varies with the extent of atherosclerotic plaque) and is separated from the media by an inner elastic lamina. The media is the middle layer of the arterial wall and consists predominantly of smooth muscle cells and is separated from the adventitia by an external elastic lamina. The adventitia surrounds the media and is composed of fibrous connective tissue and provides the majority of the external support for the vessel.

Intravascular Ultrasound

IVUS allows visualization of the coronary arterial wall by utilizing a miniature transducer mounted on a flexible catheter that transmits ultrasound in the 10–40 megahertz (MHz) range [3]. Currently, IVUS transducers are oriented at 90° to the length of the catheter to produce a cross-sectional view of the coronary artery. There are currently two types of IVUS catheters in use today: mechanical and phased array.

- Mechanical catheters utilize a single mechanical transducer mounted on a catheter tip that rotates to visualize the entire vessel wall in cross-section. The design is simple with a high signal to power output and produces excellent overall resolution of up to 100–150

S.J. Nicholls and T. Crowe (eds.), *Imaging Coronary Atherosclerosis*, Contemporary Cardiology,
DOI 10.1007/978-1-4939-0572-0_2, © Springer Science+Business Media New York 2014

micrometers (μm). The images are dependent upon uniform rotation of the transducer and are difficult to use in tortuous vessels.

- Phased array catheters use multiple transducer elements that are mounted on the circumference of the catheter tip. Each of these elements sends and receives ultrasounds from a sector that corresponds to a portion of the vessel wall. When these images are incorporated, they produce a cross-sectional image of the vessel wall. Image resolution is somewhat less than mechanical catheters especially close to the transducer, but the ease of use of these catheters has made them very popular.

Components of the IVUS Image

The cross-sectional image of the arterial wall that is obtained occurs as a result of differential tissue acoustic impedance to ultrasound. The IVUS catheter emits ultrasound waves from the catheter tip and these waves will be reflected back as it encounters an interface of different acoustic impedance. Acoustic impedance is primarily dependent upon the density of the tissue. Therefore, ultrasound will traverse blood with minimal refection and be highly reflected as it encounters the intima. These reflected ultrasound waves would be displayed as a single concentric echo. Some of the ultrasound will not be reflected and will penetrate into the media. Since the media is composed of smooth muscle cells, ultrasound will pass through with minimal reflection and will appear as a dark zone. The remainder of the ultrasound waves will penetrate and encounter the adventitia and will be highly reflected due to the presence of dense collagen fibers. In essence the normal arterial wall will consist of a series of alternating bright and dark echoes called the normal "three layer appearance" of the coronary artery [4–6]. This is not strictly correct since IVUS resolution is approximately ~120 μm and is not able to detect a truly normal endothelial layer (thickness of 50 μm) seen in Fig. 2.3. However, this inner layer becomes quite well visualized in the presence of atherosclerotic disease. Therefore, IVUS images are able to delineate the extent, morphology, and distribution of atherosclerotic plaque (concentric versus eccentric plaque distribution). This makes IVUS uniquely suited for determining severity of an eccentric plaque over conventional angiography where this can be more challenging as shown in Fig. 2.1. In addition, due to the high resolution of IVUS, vessel wall and plaque size can be more precisely quantified. While angiography allows measurement of luminal diameters in 2 or 3 orthogonal views, IVUS extends this by providing a 360° tomographic view allowing a precise assessment of vessel size. The true maximal and minimal luminal diameter (MLD) can be obtained by IVUS with cross-sectional area measurements of both the lumen and the vessel [6–10].

Information regarding plaque composition is also available with the use of IVUS, as different plaque compositions will reflect ultrasound differently. The characteristic architecture of a thin-cap fibroatheromas (TCFA) overlying a lipid pool has prompted enhancements in IVUS, including backscatter-intravascular ultrasound (BS-IVUS), virtual histology-intravascular ultrasound (VH-IVUS), IVUS elastography, and palpography. Conventional gray-scale angiography is limited in its ability to characterize plaque components. Automatic processing uses the amplitude of the backscattered echo signal to differentiate highly echogenic components (calcium and fibrous tissues) from echolucent ones (lipid and necrotic cores) but it is not able to accurately distinguish between fibrous from fatty plaques [11]. Virtual histology IVUS uses an autoregression model to generate multiple spectral parameters of the backscattered ultrasound signal. These parameters are used in classification of trees to generate a tissue map of the plaque components: fibrous (dark green), fibrofatty (yellow-green), necrotic core (red), and dense calcium (white). The VH-IVUS has been validated in histopathology of autopsy specimens and found to have an accuracy of 79.7, 81.2, and 92.8 % in detecting fibrous, necrotic cores, and calcium, respectively [12, 13]. Backscatter IVUS uses fast Fourier transformation to extract buried frequency components in the original IVUS signal. In autopsy-based studies, the sensitivity of

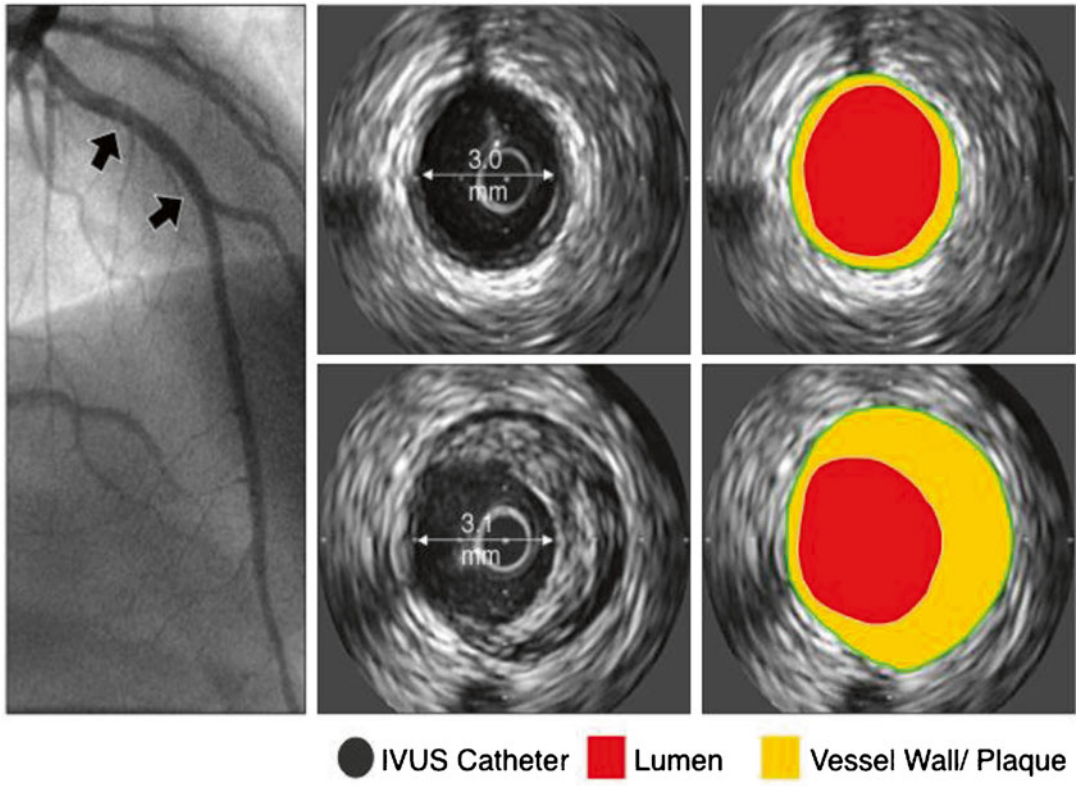

Fig. 2.1 Intravascular ultrasound image of mid-segment of the left anterior descending artery. The *top arrow* coincides with the top two IVUS images and the *lower arrow* with the lower two IVUS images. The atherosclerotic plaques are shown in *yellow*, vessel lumen in *red* and IVUS catheter in gray. In comparison to the accompanying angiogram, the IVUS images show almost half of the vessel area filled by atherosclerotic plaque. The plaque is not associated with luminal stenosis, because it has expanded the vessel size at the lesion site

IB-IVUS for calcification, fibrous and lipid-rich plaque was 100 %, 94 %, and 84 %, respectively, which compares favorably with OCT (100 %, 98 %, and 95 %, respectively) and when compared to "VH-IVUS" there is higher diagnostic accuracy with histological assessments [14]. Intravascular elastography and palpography are methods to assess the strain properties of atherosclerotic coronary arteries using tissue characteristics to determine the degree of deformation of vessel walls [15, 16]. Additional information provided by IVUS has improved our understanding in several areas for example gender-specific differences in atherosclerosis. The coronary vessels in women tend to have a smaller lumen and external elastic lamina in comparison to men [17]. Interestingly these vessel dimensions change in heart transplantation when a donor female heart is transplanted into a male recipient suggesting some direct hormonal influence. In addition, the extent of atherosclerotic calcification is higher in men than in women suggesting an earlier onset of atherosclerosis with potentially different pathophysiology to injury [18]. These differences may help to understand differences in outcomes of percutaneous coronary intervention (PCI) in women compared to men. In some situations IVUS provides more precise quantification of plaque morphology over conventional coronary angiography. Coronary angiography provides an imprecise measure of lumen morphology and size especially when there is haziness noted in the vessel [19, 20]. This can be due to the presence of irregular plaque, dissection, thrombus, or calcified plaque. IVUS can help to distinguish between these and can often reclassify "angiographically" normal vessels into those with diffuse disease [21].

IVUS provides visualization of vessel wall which is critical to study of plaque and arterial remodeling. The coronary arteries are living structures that can adapt and change with atherosclerosis. Coronary arteries will initially enlarge over time to accommodate focal plaque deposition in an attempt to preserve luminal integrity. This compensatory enlargement to preserve luminal diameter will not be seen on conventional angiography [22–24].

Clinical Applications of IVUS

Anatomically Ambiguous Lesions

IVUS is useful in characterizing angiographically ambiguous lesions including intermediate lesions, ostial stenosis at branch vessels, sites with dissections, and plaque rupture [25]. However, specific threshold criteria for intervention derived by IVUS have not been prospectively validated with noninvasive assessments of myocardial ischemia. Functional lesion assessment using a coronary pressure wire has been prospectively validated and some studies have provided concordance between IVUS characteristics and functional flow reserve (FFR) of <0.75 [26]. The most consistent IVUS cutoff value for major epicardial coronary arteries (excluding the left main) with moderate correlation with an FFR < 0.75 are minimal luminal area (MLA) in the range of 3–4 mm [2]. Furthermore, an MLA of >4 mm [2] is associated with a good clinical outcome but has a low FFR-based specificity. While a combination of an MLA <1.8 mm and angiographic area stenosis of >70 % has a better sensitivity (100 %) [27]. Taken together, these modalities are synergistic and may lead to a reduction of many unnecessary revascularization procedures for intermediate lesions.

Left Main Lesions

The correlation between IVUS measurements and FFR within the epicardial tree is modest. The left main trunk is uniquely suited given the large vessel size and variable length allows a greater degree of concordance between these two modalities. The MLA of the LMCA on IVUS was a strong predictor of the rate of major adverse cardiac events [28]. Furthermore, several outcome-based studies have addressed the IVUS criteria that correlates with FFR and major adverse cardiovascular events (MACE) but an MLD of 2.8 mm [2] was found to have the highest sensitivity and specificity (93 % and 95 %, respectively) for defining true functional significance of the ULMA stenosis. In the absence of corresponding physiological measurements, IVUS-based criteria of LM compromise have been successfully used to solely guide clinical decision making. While several values have been studied, an MLA of <6 mm [2] has been used as a binary cutoff to defer those who can be managed with revascularization versus medical therapy [29].

Percutaneous Coronary Intervention

The use of IVUS in PCI helps in planning a pre-intervention strategy based on vessel morphology, the presence of calcium, and the burden of thrombus in the vessel and is supported by the American Heart Association (ACC/AHA) PCI guidelines [30]. Adequacy of stent deployment can be very effectively studied with IVUS. Several IVUS characteristics have been associated with increased adverse events after PCI with bare-metal stents (BMS), including smaller minimal stent area (MSA), stent underexpansion, persistent edge dissections, incomplete stent apposition (ISA), and incomplete lesion coverage [31–36]. Smaller MSA has been most commonly associated with target vessel failure at follow-up with rates of restenosis reduced by 19 % per 1 mm [2] increase in MSA [37]. The main clinical benefit of an IVUS-guided BMS PCI strategy is driven by a reduction in restenosis rate and target vessel revascularization (TLR) [38].

There is increasing evidence for utility of an IVUS-directed approach in drug-eluting stenting (DES) [39]. Most of the evidence is however retrospective. Although the randomized trials including HOME-DES (Long-Term Health

Outcome and Mortality Evaluation After Invasive Coronary Treatment Using Drug-Eluting Stents with or without IVUS Guidance) and AVIO (Angiography versus IVUS Optimization) did not demonstrate lower rates of TLR or improved clinical outcomes, IVUS provides important clinical information in many patients to justify its widespread use [40, 41]. There is some evidence for benefit with IVUS-directed DES placement with a reduction in the incidence of stent thrombosis [42], detection of high-grade edge dissections [43] and stent underexpansion [44]. IVUS may also have a role in the treatment of long lesions (>20 mm) which was studied in the TULIP study when at 12 months the use of IVUS guidance was associated with a significant reduction in angiographic restenosis (23 % versus 45 %) and TLR (10 % versus 23 %) [45]. In unprotected left main PCI, the adverse effects of suboptimal stenting are more dramatic and in this subset IVUS guidance is of particular use. This was studied in the MAIN-COMPARE (Revascularization for Unprotected Left Main Coronary Artery Stenosis: Comparison between Percutaneous Coronary Angioplasty Versus Surgical Revascularization) trial. In this analysis, there was a trend toward lower 3-year mortality in the IVUS-guided strategy versus angiography alone group (6.0 % versus 13 % $P=0.0063$) and this was significant in the subgroup receiving DES (4.7 % versus 16 %, $P=0.048$) [40]. IVUS is also advocated by the ACC/AHA PCI guidelines in assisting in the treatment of in-stent restenosis (ISR) [30]. In these cases, IVUS can assist in differentiating between restenosis due to intimal hyperplasia versus that due to mechanical complications such as strut fracture or stent underexpansion.

Allograft Coronary Vasculopathy

Since the intimal and medial layers of the arterial wall have differing acoustical densities, IVUS can distinguish these layers and thereby detect abnormal thickening of the intima. IVUS detects intimal thickening in more than 80 % of patients as early as one year after transplantation. The most rapid rate of intimal thickening occurs in the first year after transplantation, followed by a slower rate of thickening. This process is diffuse and circumferential, many patients with moderate to severe intimal thickening on IVUS. These changes are not detectable on coronary angiography. The proximal segments of the transplanted coronary arteries have focal and eccentric pattern (similar to that seen in native coronary arteries) while the mid and distal segments of the vessels have diffuse and circumferential disease. This suggests at least two etiologies for the vascular lesions: proximal disease that may be donor-transmitted; and distal disease that may be the result of acquired immune-mediated vessel injury exacerbated by significant metabolic perturbations that occur after transplant. The only possible way to distinguish between donor-transmitted disease and de novo allograft vasculopathy is by performing serial IVUS studies starting with a baseline imaging early after transplant. The identification of allograft vasculopathy has prognostic importance. It has been noted that the absence of angiographic coronary disease was a significant predictor of survival without adverse cardiac events at 2 years [46]. Worsening global TIMI frame count (the mean TIMI FC for the three coronary arteries) from baseline to one year was associated with increased mortality rate during mean 4.3-year follow-up [47–51]. Abnormalities detected by IVUS are predictive of cardiac events and death. In a multicenter study of 125 patients, the change in maximal intimal thickness (MIT) from baseline to 1 year was compared at several matched sites in the same coronary artery. An increase in MIT of ≥0.5 mm was present in 24 patients (19 %). At 5-year follow-up, these 24 patients had more frequent death or graft loss (20.8 versus 5.9 % in those with an MIT increase <0.5 mm) [46]. Similar findings were noted in a series of 143 patients in which MIT on IVUS was measured at baseline and 1 year; rapidly progressive vasculopathy was again defined as an increase in MIT of ≥0.5 mm [50]. Rapid progression by IVUS was noted in 54 patients (37 %) at 1 year after transplant. At 5.9-year follow-up, patients with rapid progression at 1 year had significantly higher rates of mortality (26 versus 11 % in those with an MIT increase of

less than 0.5 mm), the combined endpoint of death or myocardial infarction (51 versus 16 %), as well as angiographic disease (22 and 2 %).

These data have led to use of IVUS as a surrogate endpoint in clinical trials of new immunosuppressive and other agents known to affect intimal proliferation. Given the cost, small risk and the time-consuming nature of the procedure. The ISHLT consensus statement recommends against use as routine surveillance outside of clinical trials [52]. In addition to its value in research, IVUS may be of clinical value in selected patients in identifying the cause of unexplained graft failure (i.e., in the absence of rejection) patients with normal coronary arteriography.

Preventative Strategies on Coronary Artery Atherosclerotic Plaque Dimensions and Composition

Coronary artery disease continues to be the most common cause of mortality and morbidity worldwide and preventative strategies only reduce cardiovascular risk by 30–40 %. Germane to further reduction in cardiovascular risk are therapies directed at prevention of atherosclerotic disease. As described above, IVUS is able to detect the contours of the leading edge of the lumen and the media–adventitia interface and so permits direct measurements of the lumen and the total vessel cross-sectional area and absolute and percent plaque volume. While the relationship between low-density lipoprotein (LDL) cholesterol levels and coronary atherosclerosis was established in postmortem studies. The linear relationship between the LDL cholesterol levels and the atheroma plaque progression was first noted using IVUS [53, 54]. There have now been many studies that have studied the progression or regression of coronary atherosclerosis using IVUS. The REVERSAL (Reversal of Atherosclerosis with Aggressive Lipid Lowering) trial tested in a prospective, randomized manner the effect of 18 months of intensive versus moderate intensity lipid-lowering therapy on coronary artery plaque progression [55]. The intensive lipid-lowering arm reduced the LDL cholesterol levels to 78 mg/dL and stopped progression of atherosclerosis. The ASTERIOD (Study to Evaluate the Effect of Rosuvastatin on Intravascular Ultrasound-Derived Coronary Atheroma Burden) trial extended this observation by showing regression of atherosclerotic plaque volume with the use of high-intensity statin therapy [56]. Besides statins, other novel agents including inhibitors of acyl-coenzyme-A cholesterol acyltransferase (ACAT) and cholesterol ester transfer protein have been studied and these have shown no change in coronary plaque progression [57, 58].

Optical Coherence Tomography

OCT is a light-based imaging modality that generated high-resolution cross-sectional image of tissue microstructure [59]. Thus, the principle of OCT is similar to the use of ultrasound in IVUS. In essence, by measurement of the time delay of the optical echoes obtained due to reflection or backscatter from biological tissues, structural information as a function of depth can be obtained.

OCT light is in the near-infrared (NIR) range with wavelengths in the 1.3 μm. Both the bandwidth of the infrared light used and the wave velocity are orders of magnitude higher than in medical ultrasound. Like IVUS, the OCT image quality is dependent on the spatial resolution (distance between two points that are detectable by the imaging modality). This is measured as the degree of axial (line parallel to the light beam) or lateral resolution (perpendicular to the light beam) and is dependent on the spectral wavelength. Near the tip of the catheter, light is focused and directed at the vessel wall and as such the lateral resolution is best at its area. The resulting resolution is one order of magnitude larger than that of IVUS: the axial resolution of OCT is about 15 μm; the lateral resolution is approximately 25 μm seen in Fig. 2.1 and Table 2.1. However, the imaging depth of approximately 1.0–1.5 mm within the coronary artery wall is less than that of IVUS.

OCT measures the time delay of light reflected or backscattered from tissue using interferometry. Light from the OCT system is split into a sample (going to the patient) and reference (going to a predetermined reference distance) segment.

Table 2.1 A comparison of FD-OCT and IVUS

Variables	IVUS	FD-OCT
Wavelength	1.3μ	20–40 MHz
Resolution	12–15 μm (axial)	35–80 μm
	20–40 μm (lateral)	100–200 μm (axial)
		200–300 μm (lateral)
Frame rate	100 frames/s	30 frames/s
Pullback rate	20 mm/s	0.5–1 mm/s
Max. scan diameter	9.7 mm	15 mm
Tissue penetration	1.0–2.5 mm	10 mm

When light is reflected back from tissue, it is collected by the catheter, and combined. The distances between the sample and reference light transferred and detected generates a pattern of high and low intensities known as interference. The OCT system is able to interpret this pattern and determine the degree of backscatter in relation to depth. When the optics are rotated in the catheter around a 360° plane, the result is a cross-sectional image of the vessel wall.

There are two types of OCT systems: earlier time-domain OCT (TD-OCT) and recent Fourier-domain OCT (FD-OCT). In the FD-OCT system, the depth profile can be constructed by the Fourier transform. Most signals can be thought of as a summation of sine waves with different frequencies. The Fourier transform extracts those frequencies, and their relative weights, from the signal. The source wavelength in Fourier-domain OCT can be swept at a much higher rate than the position scan of the reference arm mirror in a time-domain OCT system. This development has led to faster image acquisition speeds, with greater penetration depth, without loss of vital detail or resolution, and represents a great advancement on current conventional OCT systems [60]. Coronary arteries can be imaged with high OCT catheter pullback speeds within seconds, which allows for widespread clinical use in a broad range of patients and lesions.

Optical Coherence Tomography: Imaging Catheters and Imaging Procedures

OCT imaging catheters have an imaging core at the distal tip that is oriented at 90° to the length of the catheter as shown in Fig. 2.2. When these catheters are rotated along the long axis of the vessel a cross-

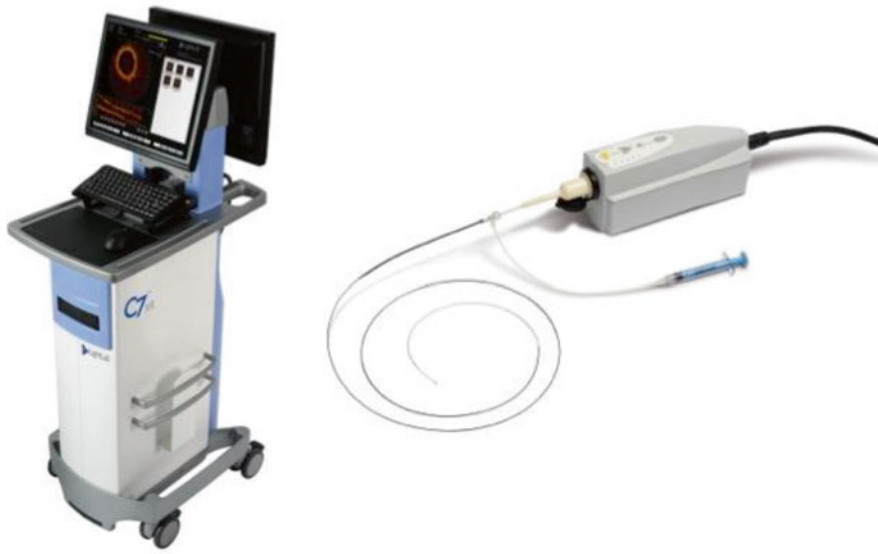

Fig. 2.2 Optical coherence tomography system (C7-XR) showing the image display on the *left* and the Dragonfly imaging catheter on the *right*. The Dragonfly catheter has an insertable length of 135 cm with a 2.7 Fr tip and a 0.014 in. wire lumen and is able to produce images at 30 cm/s with a maximal length per run of 54 mm

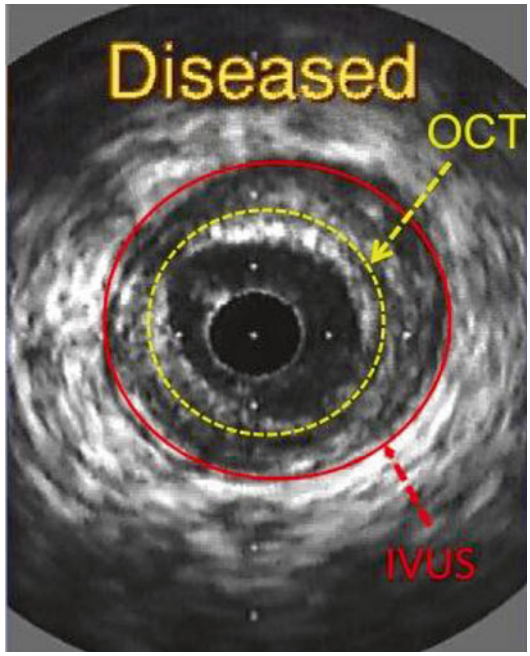

Fig. 2.3 Intravascular ultrasound (IVUS) cross-sectional image of a coronary arterial wall showing the imaging depth obtained by both modalities. *OCT* optical coherence tomography

sectional view of the coronary artery is obtained allowing the user to get a high-resolution image of the coronary artery. When performing an intracoronary OCT, the imaging catheter (2.7 Fr) is introduced over a guidewire (0.014 in.) into the distal coronary artery. A motorized pullback is performed to scan the coronary artery segment. The pullback speed is typically 20 mm/s with a frame rate of 100 frames per second or higher. Since blood scatters the OCT signal, it is temporarily cleared by an injection of X-ray contrast medium during the duration of the OCT pullback (typical flush rate 3.0 mL/s). A variety of solutions, warmed to 37 °C have been used alternatively as flush medium, including Lactated Ringer's, viscous iso-osmolar contrast media, and mixtures of lactated Ringer's and contrast media or low molecular weight dextrose. The time needed to image a 50 mm artery segment is typically 3 s with a total volume of X-ray contrast of 10–12 ml, which is comparable to the amount of X-ray contrast needed for a single angiographic run.

Like IVUS, current practice requires that patients be anticoagulated, typically with heparin, before insertion of the guidewire into the coronary artery. The image acquisition should be performed only after the administration of intracoronary nitroglycerin. In patients with severe left ventricular dysfunction, single remaining coronary vessel, renal dysfunction, and compromised hemodynamics, OCT should be performed with caution. In lesions with coexisting rich collateral blood flow or when coaxial positioning of the guiding catheter is not feasible, OCT imaging can be difficult due to the inability of blood clearance. In these cases, wire-based OCT can be used with a proximal balloon occlusion to facilitate blood clearance. If there are near complete stenosis or complete total occlusions of vessels, then OCT cannot be performed until there is antegrade restoration of blood flow.

OCT is a safe procedure with little applied energy (output power 5–8 mW) and is not thought to cause any functional or structural damage to tissue. The principle safety considerations relate to the possible induction of ischemia due to the need of blood displacement for image acquisition. This was more so with the TD-OCT systems where there was transient T-wave inversion or ST segment depression in 44–46 %, 1.1 % incidence of ventricular fibrillation, and 0.2 % risk of vessel dissection. Current OCT systems allow for very fast data within a few seconds and therefore are unlikely to lead to significant ischemia. In preliminary registries of patients imaged with FD-OCT, the most frequent event was transient T-wave inversion or ST segment depression (10 %) but there were no complications within a 24-h period [61, 62].

Components of the OCT Image

The normal vessel wall is characterized by layered architecture, comprising highly backscattered (signal-rich) intima (appears bright), followed by low backscattered (signal-poor media) and then heterogeneous but highly backscattered (signal-rich) adventitia as shown in Fig. 2.4. Light is highly reflected by the elastic membranes and this serves to distinguish between the three concentric layers with the innermost signal-rich layer reflects the internal elastic membrane and the

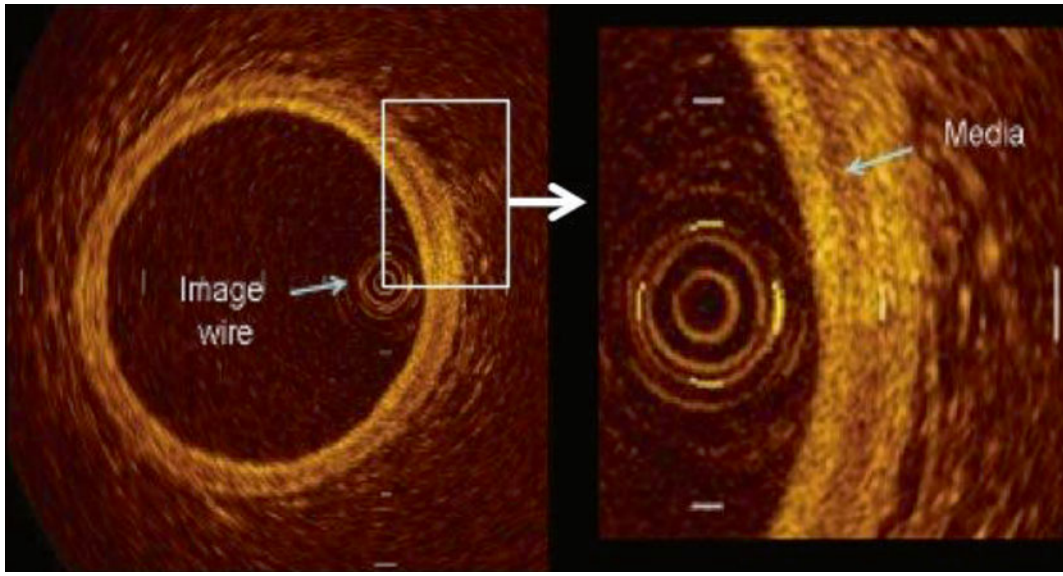

Fig. 2.4 Optical coherence tomographic image of a normal coronary artery showing the cross-sectional anatomy. The normal vessel wall is characterized by layered architecture, comprising highly backscattered (signal-rich) intima (appears bright), followed by low backscattered (signal-poor media) and then heterogeneous but highly backscattered (signal-rich) adventitia

outer, signal-rich layer representing the external elastic lamina. It must be noted that the normal three-layer appearance by OCT is not synonymous to the three-layer appearance by IVUS. IVUS cannot visualize the architecture of a normal coronary vessel due to its resolution of 120 μm while OCT is able to do so (resolution of 10 μm) as seen in Fig. 2.1.

IVUS and OCT images are fundamentally different from histology. However, owing to the high, 10 μm resolution of OCT, images do appear similar to histological sections. There may be some capacity to detect and quantify specific contents of vessel walls analogous to histological features. Caution must be used as not all features can be identified and the extent to which OCT can describe pathology is still unknown.

Qualitative Description of Atherosclerosis

As various components of atherosclerotic plaques have different optical properties, OCT makes it possible to differentiate between them. The identification of plaque components by OCT depends on the degree of vessel wall penetration by the incident light beam. The depth of penetration is highest in fibrous tissues but least in thrombi with calcium and lipid tissue having intermediate values. There are distinct morphological characteristics that have been found when assessing atherosclerotic plaque.

– TCFA is a delineated necrotic core with an overlying fibrous cap where the minimal thickness of the fibrous cap is less than 65 μm (defined by histology) shown in Fig. 2.5. Thin fibrous cap atheromas are considered the most important morphologic substrate for a plaque at high risk to rupture and causing acute coronary syndrome. OCT allows the diagnosis of thin fibrous cap atheroma with a sensitivity of 90 % and a specificity of 79 % when compared to histopathology and for accurate measurement of the fibrous cap thickness with low variability [63]. Ongoing research suggests that the ability of OCT to measure changes in the fibrous cap thickness could be used to monitor the effect of therapeutic agents aiming at plaque stabilization although this is still extremely controversial.

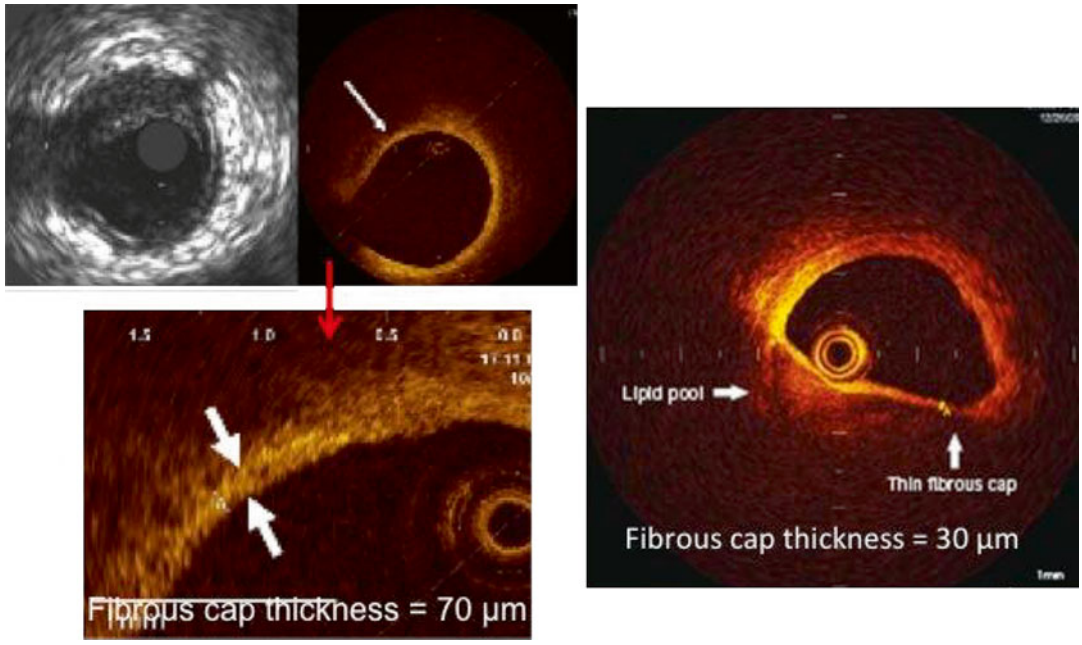

Fig. 2.5 Optical coherence tomographic images showing precise measurement of the fibrous cap thickness. The OCT image on the right shows a fibrous cap thickness of <65 µm with a large lipid pool and is called a thin-cap fibroatheroma (TCFA)

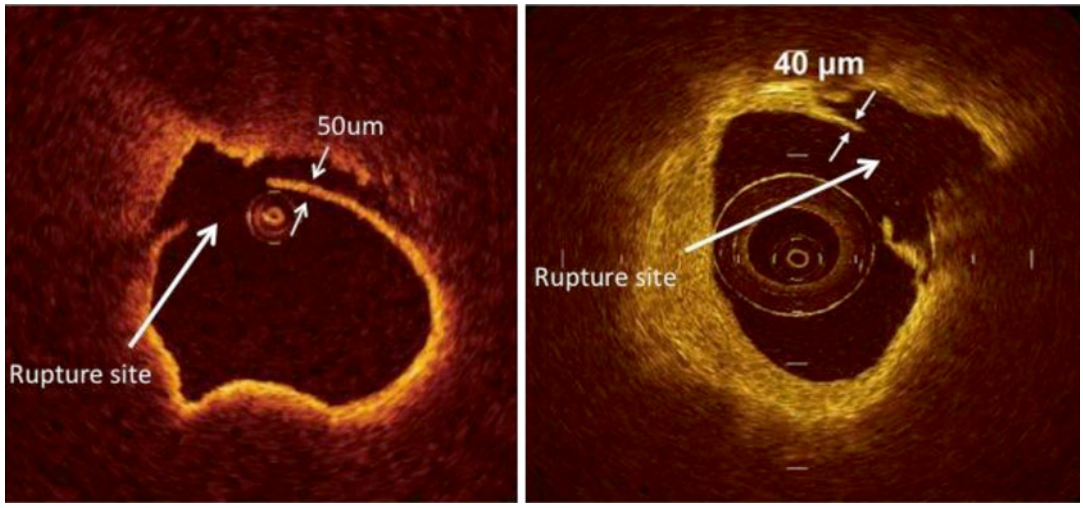

Fig. 2.6 Optical coherence tomographic image showing discontinuity of the fibrous cap with cavity formation in the plaque consistent with plaque rupture

- Atherosclerotic plaque (atheroma), which is a mass lesion (focal thickening) or loss of the layer structure of the vessel wall.
- Fibrous plaques have high backscattering with relatively homogenous signal due to the rich collagen or smooth muscle cells present in Fig. 2.6. Calcifications within plaques are identified by the presence of well delineated, low backscattering, signal-poor heterogeneous regions.
- A necrotic core is a signal-poor region within an atherosclerotic plaque and has poorly defined borders often with overlying signal-rich bands, corresponding to fibrous caps. The necrotic core may also contain cholesterol

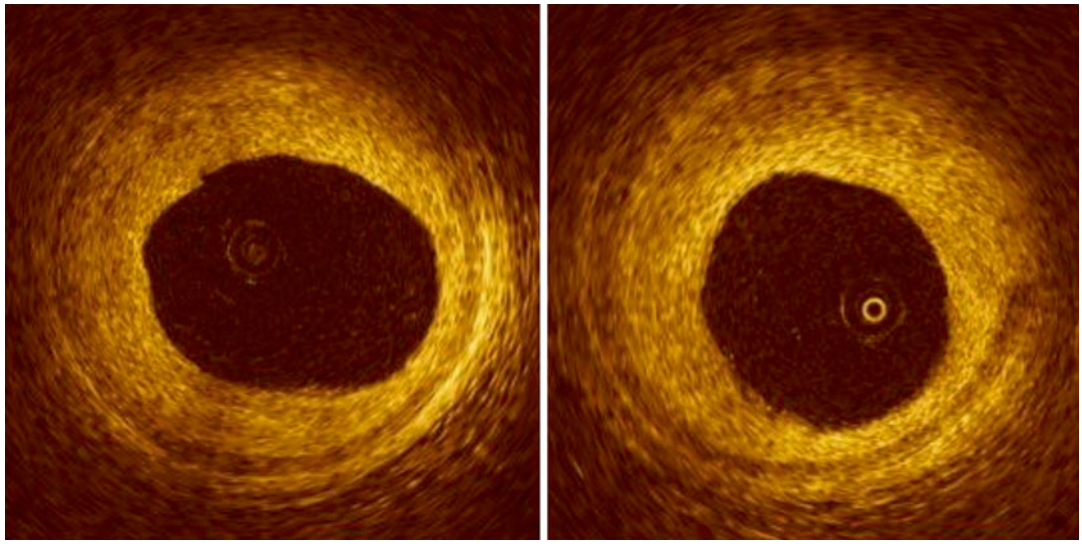

Fig. 2.7 Optical coherence tomographic image showing lipid plaque which is characterized by the regions of low reflectivity, diffuse margins, and high attenuation that appear homogenous

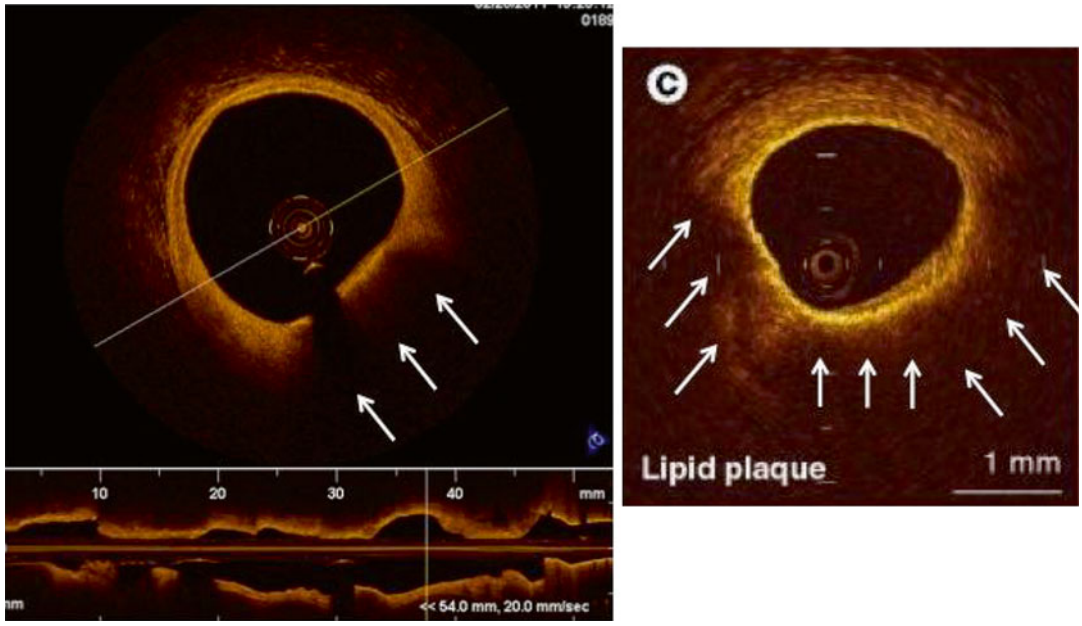

Fig. 2.8 Optical coherence tomographic image showing calcified plaque which is characterized by the regions of low reflectivity, sharp margins, and low attenuation that appear heterogenous

crystals (these appear as thin, linear region of high intensity). It is important to distinguish between the signal-poor regions noted due to the presence of calcium as shown in Fig. 2.7, which have sharply delineated signal-poor regions, as opposed to signal-poor regions of necrotic core, which are undefined or poorly defined as shown in Fig. 2.8. The superiority of OCT for lipid-rich plaque detection has been confirmed in other studies comparing OCT-, IVUS-, and IVUS-derived techniques for plaque composition analysis

– Thrombi are identified as masses protruding into the vessel lumen discontinuous from the

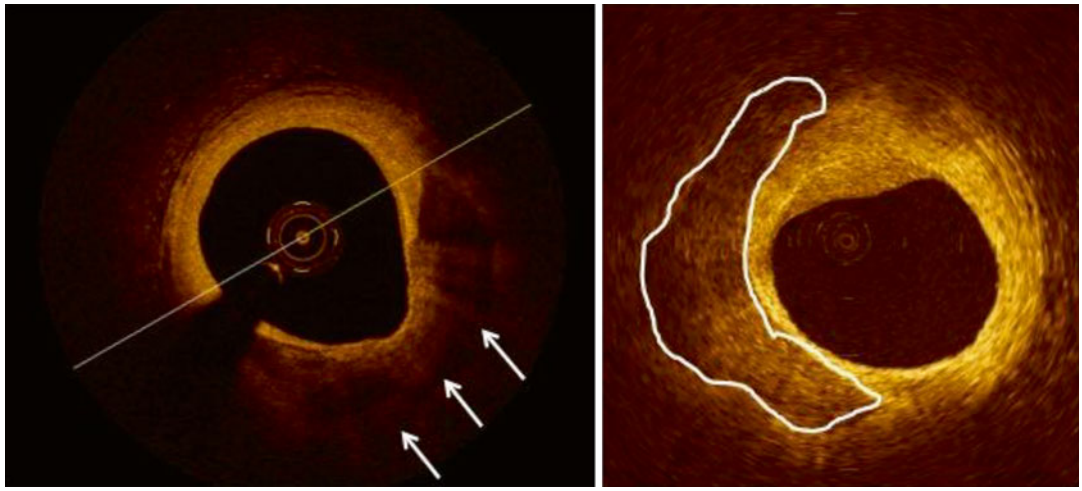

Fig. 2.9 Optical coherence tomographic image showing intracoronary thrombus. Red thrombi consist mainly of red blood cells; relevant OCT images are characterized as high-backscattering protrusions with signal-free shadowing (seen on the *left*). White thrombi consist mainly of platelets and white blood cells and are characterized by a signal-rich, low-backscattering billowing projections protruding into the lumen (seen on the *right*)

surface of the vessel wall. Red thrombi consist mainly of red blood cells; relevant OCT images are characterized as high-backscattering protrusions with signal-free shadowing. White thrombi consist mainly of platelets and white blood cells and are characterized by a signal-rich, low-backscattering billowing projections protruding into the lumen as shown in Figs. 2.9 and 2.10. OCT is highly sensitive in diagnosing intracoronary thrombi, as the high contrast between the lumen and the surrounding structures facilitate the diagnosis. This is in contrast to IVUS were it is often difficult to differentiate thrombi from the blood-filled lumen or at times from soft plaque [64].

– Macrophage accumulation and intimal vasculature characterization have been described but are currently under investigation [65].

OCT in Plaque Rupture and Intracoronary Thrombosis

Acute coronary syndromes occur due to rupture of a coronary plaque triggering intracoronary thrombosis. Detecting lesions that are at high risk for rupture may play a role in the prevention of future acute coronary syndromes. OCT has a unique role in the identification of lesions in unstable angina and specifically locates TCFAs, which have ruptured or ulcerated. OCT allows for the diagnosis of TCFA with a sensitivity of 90 % and a specificity of 79 % when compared to histopathology [66]. In a study comparing OCT to IVUS and angioscopy in patients with myocardial infarction, OCT was able to estimate fibrous cap thickness [67]. Given the near-field resolution, OCT is well suited for in vivo detection of TCFA, follow the phenotype and assess for rupture. These applications provide the opportunity to assess the dynamic nature of atherosclerotic plaque and note changes over time. In fact, polarization-sensitive OCT (PS-OCT) is a new technology that can enhance OCT imaging using tissue birefringence allowing for the presence of collagen in vessel walls. This can be used to assess for the amount of collagen present in the TCFA allowing for an assessment of mechanical stability [68]. OCT is also ideally suited for the visualization of vessel morphology in the context of plaque rupture as the intima can be interrogated for an intimal tear, erosion, ulceration, or dissection of the TCFA and thrombus.

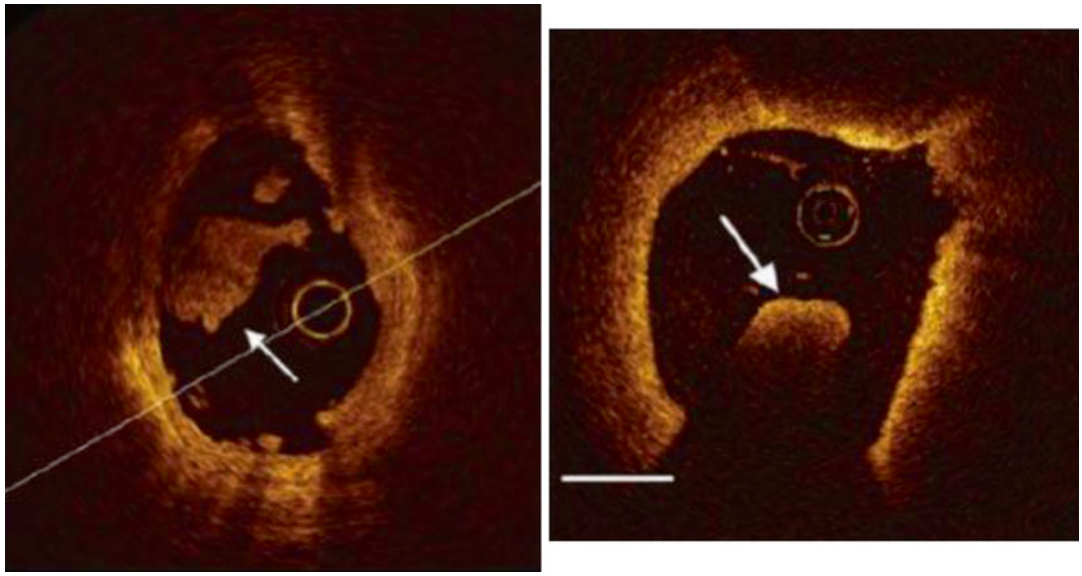

Fig. 2.10 Optical coherence tomographic image showing a fibrous plaque which is homogenous with high reflectivity, diffuse margins with less attenuation

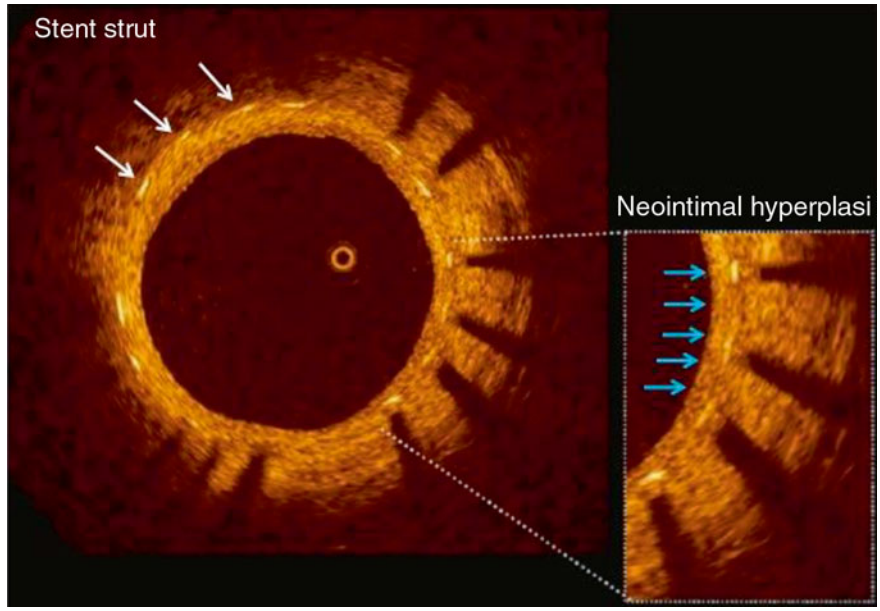

Fig. 2.11 Optical coherence tomographic image of neointimal coverage of a stent strut

OCT and the Assessment of Coronary Stents

IVUS has been used to assess the acute result following coronary stent implantation to assess for adequate stent expansion and apposition against the wall seen in Fig. 2.11. The high-resolution capabilities of OCT and its diminished susceptibility to artifacts at the stent-strut surface compared to IVUS make it capable of visualizing tissue overlying the struts. These allow for precise determination if the struts are *covered* (tissue identified above the struts) or *uncovered*

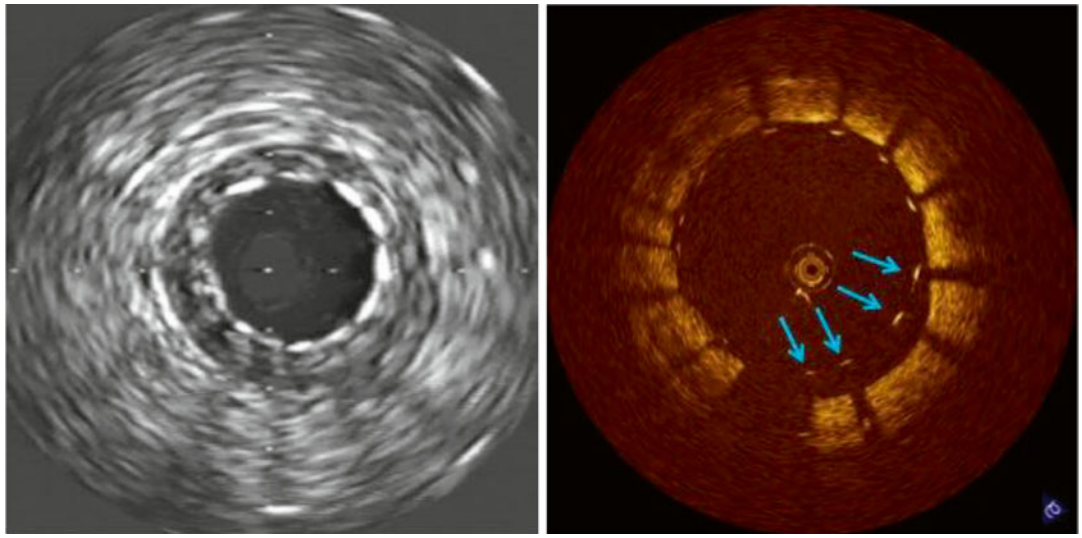

Fig. 2.12 A side by side comparison of an intravascular ultrasound image and optical coherence tomographic image of an intracoronary stent showing the superior resolution at detecting stent malapposition

(intervening space between the struts and the vessel wall) shown in Fig. 2.12. From a clinical viewpoint, a stent should be expanded with all struts apposed to the vessel wall (*covered*) in order to allow for optimal blood flow. IVUS studies have suggested that stent-strut malapposition is a relatively uncommon finding, observed in about 7 % of cases, and it does not increase the incidence of MACE [69, 70]. In contrast, OCT studies have demonstrated a high degree of struts (9.1 ± 7.4 % per lesion) that are not opposed to the wall and this is related to the strut thickness, closed cell design, overlapping nature of the stents, and acute stent recoil [66]. In cases of malapposition of stents, a high pressure deployment is performed but this can result in peri-procedural vessel damage. OCT is able to determine the degree of vessel damage and also characterize the presence and nature of disease in the segments proximal and distal to the stented segments [67]. Plaque type (TCFA versus fibrous) at the proximal and distal edge of the stents are important determinants of the incidence of edge dissection [71]. While the observations are useful for better design and deployment of stents, the clinical relevance is currently unknown.

Long-term stent-strut/vessel wall interaction is of interest to both researchers and clinicians. The stability of the acute result, the identification of complex anatomy that is not accessible by angiography or IVUS, and the understanding of reasons for stent failures, when they do occur, are example of information that is of interest. In contrast to IVUS, OCT can reliably detect and quantify early and very thin layers of tissue coverage on stent struts [72–74], even in DES with very thin layers of neointima, often below 80 μm in thickness, with high reliability.

OCT has been employed in prospective clinical trials to compare the long-term outcome of various stents:

- The LEADERS randomized trial was a comparison of a biolimus-eluting stent (BES) with biodegradable polymer with sirolimus-eluting stent using a durable polymer. Fifty-six consecutive patients underwent OCT during angiographic follow-up at 9 months. Strut coverage at an average follow-up of 9 months was significantly more complete in patients allocated to BES when compared to those with SES [weighted difference −1.4 %, 95 % CI, −3.7 to 0.0] [75]
- In the Harmonizing Outcomes with Revascularization and Stents in Acute Myocardial Infarction (HORIZONS-AMI) trial, patients with STEMI were randomized to

paclitaxel-eluting stent (PES) or BMS implantation. The OCT substudy revealed that implantation of PES as compared with BMS significantly reduced neointimal hyperplasia but resulted in higher rates of uncovered and malapposed stent struts at 13-month follow-up (1.1 ± 2.5 % in BMS lesions versus 5.7 ± 7.0 % in PES lesions) [76].

- OCT was employed to study tissue coverage at follow-up in bioresorbable scaffolds. OCT was able to visualize the particular structure of the scaffold struts, the tissue coverage over time, as well as the changes in the optical properties of the vascular tissue during the bioresorption process [77].

While these observations are important to understand differences in-stent design, further studies are required to determine the clinical significance of these findings. Today, no threshold for coverage is established. Pathological data in humans suggest that neointimal coverage of stent struts could be used as a surrogate for endothelialization due to the good correlation between strut coverage and thrombus formation. However, OCT data must be interpreted with caution as OCT resolution will still miss a single layer of endothelial cells over struts and the presence of an OCT detectable endothelial layer does not imply a functional endothelium. Despite these limitations, OCT is the only imaging modality to date that offers the possibility to understand tissue coverage and neointimal formation in intracoronary stents.

Other Clinical Applications of OCT

Today, no clinical indications for OCT imaging are established. There are no randomized data supporting a prognostic role for OCT in catheter-based intervention. However, there is broad expert agreement that the detailed, easy accessible and interpretable information of OCT on the presence of atherosclerosis, its extent, lumen narrowing as well as on the result of any interventional measure can be of clinical value, at least in individual patients and in specific clinical scenarios

Conclusion

Intracoronary imaging has resulted in significant gains in our understanding of the nature of atherosclerosis and vessel biology. OCT has added to this by the generation of unprecedented image resolution and its application for the visualization of atherosclerotic plaques, stents, and the stent–vessel interaction is an exciting area of current investigation.

References

1. Brown MS, Goldstein JL. Heart attacks: gone with the century? Science. 1996;272:629.
2. Glagov S, Weisenberg E, Zarins CK. Compensatory Enlargement of Human Atherosclerotic Coronary Arteries. N Engl J Med. 1987;316:1371–5.
3. von Birgelen C, Slager CJ, Di Mario C, de Feyter PJ, Serruys PW. Volumetric intracoronary ultrasound: a new maximum confidence approach for the quantitative assessment of progression-regression of atherosclerosis? Atherosclerosis. 1995;118(Suppl):S103–13.
4. Böse D, von Birgelen C, Erbel R. Intravascular ultrasound for the evaluation of therapies targeting coronary atherosclerosis. J Am Coll Cardiol. 2007;49:925–32.
5. Mintz GS, Nissen SE, Anderson WD, Bailey SR, Erbel R, Fitzgerald PJ, et al. American College of Cardiology clinical expert consensus document on standards for acquisition, measurement and reporting of intravascular ultrasound studies. J Am Coll Cardiol. 2001;37:1478–92.
6. Di Mario C, Görge G, Peters R, Kearney P, Pinto F, Hausmann D, et al. Clinical application and image interpretation in intracoronary ultrasound. Eur Heart J. 1998;19:207–29.
7. von Birgelen C, de Very EA, Mintz GS, Nicosia A, Bruining N, Li W, et al. ECG-gated three-dimensional intravascular ultrasound: feasibility and reproducibility of the automated analysis of coronary lumen and atherosclerotic plaque dimensions in humans. Circulation. 1997;96:2944–52.
8. Jensen LO, Thayssen P, Pedersen KE, Stender S, Haghfelt T. Low variation and high reproducibility in plaque volume with intravascular ultrasound. Int J Cardiol. 2004;97:463–9.
9. Kastelein JJ, de Groot E. Ultrasound imaging techniques for the evaluation of cardiovascular therapies. Eur Heart J. 2008;29:849–58.
10. Lindsay AC, Choudhury RP. Form to function: current and future roles for atherosclerosis imaging in drug development. Nat Rev Drug Discov. 2008;7:517–29.

11. Low AF, Kawase Y, Chan YH, Tearney GJ. In vivo characterization of coronary plaques with conventional grey-scale intravascular ultrasound: correlation with optical coherence tomography. EuroIntervention. 2009;4:626–32.
12. Okubo M, Kawasaki M, Ishihara Y. Tissue characterization of coronary plaques: comparison of integrated backscatter intravascular ultrasound with virtual histology intravascular ultrasound. Circulation. 2008;72:1631–9.
13. Nair A, Kuban BD, Tuzcu EM. Coronary plaque classification with intravascular ultrasound radiofrequency data analysis. Circulation. 2002;106:2200–6.
14. Kawasaki M, Bouma BE, Bresser J. Diagnostic accuracy of optical coherence tomography and integrated backscatter intravascular ultrasound images for tissue characterization of human coronary plaques. J Am Coll Cardiol. 2006;45:1946–53.
15. Cespedes EI, de Korte CL, van der Steen AF. Intraluminal ultrasonic palpation: assessment of local and cross-sectional tissue stiffness. Ultrasound Med Biol. 2000;26:385–96.
16. Doyley MM, Mastik F, de Korte CL. Advancing intravascular ultrasonic palpation towards clinical applications. Ultrasound Med Biol. 2001;27:1471–80.
17. Sheifer SE, Canos MR, Weinfurt KP. Sex differences in coronary artery size assessed by intravascular ultrasound. Am Heart J. 2000;139:649.
18. Herity NA, Lo S, Lee DP. Effect of a change in gender on coronary arterial size: a longitudinal ultrasound study in transplanted hearts. J Am Coll Cardiol. 2003;41:1539.
19. Mintz GS, Popma JJ, Pichard AD. Limitations of angiography in the assessment of plaque distribution in coronary artery disease: a systemic study of target lesion eccentricity in 1446 lesions. Circulation. 1996;93:924.
20. Ziada KM, Tuzcu EM, De Franco AC. Intravascular ultrasound assessment of the prevalence and causes of angiographic "haziness" following high-pressure coronary stenting. Am J Cardiol. 1997;80:116.
21. Mintz GS, Painter JA, Pichard AD, et al. Atherosclerosis in angiographically "normal" coronary artery reference segments: an intravascular ultrasound study with clinical correlations. J Am Coll Cardiol. 1995;25:1479.
22. St Goar FG, Pinto FJ, Alderman EL, et al. Intravascular ultrasound imaging of angiographically normal coronary arteries: an in vivo comparison with quantitative angiography. J Am Coll Cardiol. 1991;18:952.
23. Glagov S, Weisenberg E, Zarins CK, et al. Compensatory enlargement of human atherosclerotic coronary arteries. N Engl J Med. 1987;316:1371.
24. Ziada KM, Tuzcu EM, De Franco AC. Intravascular ultrasound assessment of the prevalence and causes of angiographic "haziness" following high-pressure coronary stenting. Am J Cardiol. 1997;80:116–21.
25. Bech GL, De Bruyne B, Pijls NH. Fractional flow reserve to determine the appropriateness of angioplasty in moderate coronary stenosis: a randomized trial. Circulation. 2001;103:2928–34.
26. Briguori C, Anzuini A, Airoldi F. Intravascular ultrasound criteria for the assessment of functional significance of intermediate coronary artery stenosis and comparison with functional flow reserve. Am J Cardiol. 2001;87:136–41.
27. Ricciardi MJ, Meyers S, Choi K, Pang J. Angiographically silent left main disease detected by intravascular ultrasound: a marker for future adverse cardiac events. Am Heart J. 2003;146:507–12.
28. Kang SJ, Lee JY, Ahn JM. Intravascular ultrasound derived predictors for fractional flow reserve in intermediate left main disease. J Am Coll Cardiol Intv. 2011;4:1168–74.
29. Timmis SB, Burns WJ, Hermiller JB, et al. Influence of coronary atherosclerotic remodeling on the mechanism of balloon angioplasty. Am Heart J. 1997;134:1099.
30. Smith Jr SC, Feldman TE, Hirshfeld Jr JW, et al. ACC/AHA/SCAI 2005 guideline update for percutaneous coronary intervention—summary article: a report of the American College of Cardiology/American Heart Association Task Force on Practice Guidelines (ACC/AHA/SCAI Writing Committee to Update 2001 Guidelines for Percutaneous Coronary Intervention). J Am Coll Cardiol. 2006;47:216–35.
31. Cutlip DE, Baim DS, Ho KK, et al. Stent thrombosis in the modern era: a pooled analysis of multicenter coronary stent clinical trials. Circulation. 2001;103:1967–71.
32. Cheneau E, Leborgne L, Mintz GS, et al. Predictors of subacute stent thrombosis: results of a systematic intravascular ultrasound study. Circulation. 2003;108:43–7.
33. Fitzgerald PJ, Oshima A, Hayase M, et al. Final results of the Can Routine Ultrasound Influence Stent Expansion (CRUISE) study. Circulation. 2000;102:523–30.
34. Uren NG, Schwarzacher SP, Metz JA, et al. for the POST Registry Investigators. Predictors and outcomes of stent thrombosis: an intra- vascular ultrasound registry. Eur Heart J. 2002;23:124–32.
35. Doi H, Maehara A, Mintz GS, et al. Impact of postintervention minimal stent area on 9-month follow-up patency of paclitaxel-eluting stents: an integrated intravascular ultrasound analysis from the TAXUS IV, V, and VI and TAXUS ATLAS Workhorse, Long Lesion, and Direct Stent Trials. J Am Coll Cardiol Intv. 2009;2:1269–75, 27.
36. Eshtehardi P, Samady H. Intravascular ultrasound for assessment of coronary drug-eluting stent deployment: an evolving field in need of new criteria. J Am Coll Cardiol Intv. 2010;3:364.
37. Kasaoka S, Tobis JM, Akiyama T, et al. Angiographic and intravascular ultrasound predictors of in-stent restenosis. J Am Coll Cardiol. 1998;32:1630–5.
38. Parise H, Maehara A, Stone GW, Leon MB, Mintz GS. Meta- analysis of randomized studies comparing intravascular ultrasound versus angiographic guidance of percutaneous coronary intervention in pre-drug-eluting stent era. Am J Cardiol. 2011;107:374–82.

39. Park SM, Kim JS, Ko YG, et al. Angiographic and intravascular ultrasound follow up of paclitaxel- and sirolimus-eluting stent after poststent high-pressure balloon dilation: from the poststent optimal stent expansion trial. Catheter Cardiovasc Interv. 2011; 77:15–21.
40. Jakabcin J, Spacek R, Bystron M, et al. Long-term health outcome and mortality evaluation after invasive coronary treatment using drug eluting stents with or without the IVUS guidance. Randomized control trial. HOME DES IVUS. Catheter Cardiovasc Interv. 2010;75:578–83.
41. Colombo A, Caussin C, Presbitero P, et al. AVIO: A prospective, randomized trial of intravascular-ultrasound guided compared to angiography guided stent implantation in complex coronary lesions (abstr). J Am Coll Cardiol 2010;56:Suppl B:xvii.
42. Roy P, Steinberg DH, Sushinsky SJ, et al. The potential clinical utility of intravascular ultrasound guidance in patients undergoing percutaneous coronary intervention with drug-eluting stents. Eur Heart J. 2008;29:1851–7.
43. Choi SY, Witzenbichler B, Maehara A, et al. Intravascular ultrasound findings of early stent thrombosis after primary percutaneous intervention in acute myocardial infarction: a Harmonizing Outcomes with Revascularization and Stents in Acute Myocardial Infarction (HORIZONS-AMI) substudy. Circ Cardiovasc Interv. 2011;4:239–47.
44. Oemrawsingh PV, Mintz GS, Schalij MJ, et al. Intravascular ultrasound guidance improves angiographic and clinical outcome of stent implantation for long coronary artery stenoses: final results of a randomized comparison with angiographic guidance (TULIP Study). Circulation. 2003;107:62.
45. Park SJ, Kim YH, Park DW. Impact of intravascular ultrasound guidance on long-term mortality in stenting fro unprotected left main coronary artery stenosis. Circ Cardiovasc Interv. 2009;28:1304–9.
46. Tuzcu EM, Kapadia SR, Sachar R, et al. Intravascular ultrasound evidence of angiographically silent progression in coronary atherosclerosis predicts long-term morbidity and mortality after cardiac transplantation. J Am Coll Cardiol. 2005;45:1538.
47. Mehra MR, Ventura HO, Stapleton DD, et al. Presence of severe intimal thickening by intravascular ultrasonography predicts cardiac events in cardiac allograft vasculopathy. J Heart Lung Transplant. 1995;14:632.
48. Kapadia SR, Nissen SE, Ziada KM, et al. Development of transplantation vasculopathy and progression of donor-transmitted atherosclerosis: comparison by serial intravascular ultrasound imaging. Circulation. 1998;98:2672.
49. Barbir M, Lazem F, Banner N, et al. The prognostic significance of non-invasive cardiac tests in heart transplant recipients. Eur Heart J. 1997;18:692.
50. Kobashigawa JA, Tobis JM, Starling RC, et al. Multicenter intravascular ultrasound validation study among heart transplant recipients: outcomes after five years. J Am Coll Cardiol. 2005;45:1532.
51. Ramasubbu K, Schoenhagen P, Balghith MA, et al. Repeated intravascular ultrasound imaging in cardiac transplant recipients does not accelerate transplant coronary artery disease. J Am Coll Cardiol. 2003;41:1739.
52. Mehra MR, Crespo-Leiro MG, Dipchand A, et al. International Society for Heart and Lung Transplantation working formulation of a standardized nomenclature for cardiac allograft vasculopathy-2010. J Heart Lung Transplant. 2010;29:717.
53. von Birgelen C, Hartmann M, Mintz GS, Baumgart D, Schmermund A, Erbel R. Relation between progression and regression of atherosclerotic left main coronary artery disease and serum cholesterol levels as assessed with serial long-term (≥12 months) follow-up intravascular ultrasound. Circulation. 2003;108:2757–62.
54. Hartmann M, von Birgelen C, Mintz GS, van Houwelingen GK, Eggebrecht H. Bo¨se D et al. Relation between plaque progression and low-density lipoprotein cholesterol during aging as assessed with serial long-term (≥12 months) follow-up intravascular ultrasound of the left main coronary artery. Am J Cardiol. 2006;98:1419–23.
55. Nissen SE, Tuzcu EM, Schoenhagen P, Brown BG, Ganz P, Vogel RA, et al. Effect of intensive compared with moderate lipid-lowering therapy on progression of coronary atherosclerosis: a randomized controlled trial. JAMA. 2004;291:1071–80.
56. Nissen SE, Nicholls SJ, Sipahi I, Libby P, Raichlen JS, Ballantyne CM, et al. Effect of very high-intensity statin therapy on regression of coronary atherosclerosis: the ASTEROID trial. JAMA. 2006;295: 1556–65.
57. Nissen SE, Tuzcu EM, Brewer HB, Sipahi I, Nicholls SJ, Ganz P, et al. Effect of ACAT inhibition on the progression of coronary atherosclerosis. N Engl J Med. 2006;354:1253–63.
58. Nissen SE, Tardif JC, Nicholls SJ, Revkin JH, Shear CL, Duggan WT, et al. Effect of torcetrapib on the progression of coronary atherosclerosis. N Engl J Med. 2007;356:1304–16.
59. Haung D, Swanson EA, Lin CP. Optical coherence tomography. Science. 1991;254:1178–81.
60. Takarada S, Imanishi T, Liu Y. Advantage of next-generation frequency-domain optical coherence tomography compared to conventional time-domain system in the assessment of coronary lesion. Catheter Cardiovasc Interv. 2010;75:202–6.
61. Barlis P, Gonzalo N, Di Mario C. A multicenter evaluation of the safety of intracoronary optical coherence tomography. EuroIntervention. 2009;5:90–5.
62. Imola F, Mallus MT, Ramazzotti V. Safety and feasibility of frequency domain optical coherence tomography to guide decision making in percutaneous coronary intervention. EuroIntervention. 2010;6:575–81.
63. Virmani R, Bruke AP, Farb A. Pathology of the vulnerable plaque. J Am Coll Cardiol. 2006;47:C13–8.
64. Kume T, Akasaka T, Kawamoto T. Assessment of coronary arterial thrombus by optical coherence tomography. Am J Cardiol. 2006;97:1713–7.

65. Tearney GJ, Yabushita H, Houser SL, et al. Quantification of macrophage content in atherosclerotic plaques by optical coherence tomography. Circulation. 2003;107:113–9.
66. Kume T, Okura H, Yamada R, et al. Frequency and spatial distribution of thin-cap fibroatheroma assessed by 3-vessel intravascular ultrasound and optical coherence tomography: an ex vivo validation and an initial in vivo feasibility study. Circ J. 2009;73:1086–91.
67. Barlis P, Serruys PW, Gonzalo N, et al. Assessment of culprit and remote coronary narrowings using optical coherence tomography with long- term outcomes. Am J Cardiol. 2008;102:391–5.
68. Nadkarni SK, Pierce MC, Park BH, et al. Measurement of collagen and smooth muscle cell content in atherosclerotic plaques using polarization-sensitive optical coherence tomography. J Am Coll Cardiol. 2007;49:1474–81.
69. Hong MK, Mintz GS, Lee CW, et al. Late stent malapposition after drug-eluting stent implantation: an intravascular ultrasound analysis with long-term follow-up. Circulation. 2006;113:414–9.
70. Tanabe K, Serruys PW, Degertekin M, et al. Incomplete stent apposition after implantation of paclitaxel-eluting stents or bare metal stents: in- sights from the randomized TAXUS II trial. Circulation. 2005;111:900–5.
71. Bouma BE, Tearney GJ, Yabushita H, et al. Evaluation of intracoronary stenting by intra- vascular optical coherence tomography. Heart. 2003;89:317–20.
72. Tanigawa J, Barlis P, Dimopoulos K, Di Mario C. Optical coherence tomography to assess malapposition in overlapping drug-eluting stents. EuroIntervention. 2008;3:580–3.
73. Gonzalo N, Serruys PW, Okamura T, et al. Optical coherence tomography assessment of the acute effects of stent implantation on the vessel wall: a systematic quantitative approach. Heart. 2009;95:1913–9.
74. Tanimoto S, Rodriguez-Granillo G, Barlis P, et al. A novel approach for quantitative analysis of intracoronary optical coherence tomography: high inter-observer agreement with computer-assisted contour detection. Catheter Cardiovasc Interv. 2008;72: 228–35.
75. Barlis P, Regar E, Serruys PW, et al. An optical coherence tomography study of a biodegradable vs. durable polymer-coated limus-eluting stent: a LEADERS trial sub-study. Eur Heart J. 2010;31:165–76.
76. Guagliumi G, Costa MA, Sirbu V, et al. Strut coverage and late malapposition with paclitaxel- eluting stents compared with bare metal stents in acute myocardial infarction: optical coherence tomography substudy of the Harmonizing Out- comes with Revascularization and Stents in Acute Myocardial Infarction (HORIZONS-AMI) Trial. Circulation. 2011;123:274–81.
77. van Beusekom HM, Serruys PW. Drug-eluting stent endothelium: presence or dysfunction. JACC Cardiovasc Interv. 2011;3:76–7.

Evaluation of Medical Therapies and Intravascular Devices with Quantitative Coronary Angiography

3

Sorin J. Brener

Introduction

Coronary artery disease (CAD) remains the entity responsible for most non-accidental deaths in the world [1]. Despite significant progress in understanding the pathophysiology of this condition and in treating its acute presentations, there is currently no cure for CAD and there is no consistent therapy for slowing its progression. Hence, considerable interest exists in developing reliable technologies to assess the effect of new medical and interventional therapies on the rate of progression of CAD and on the factors responsible for its destabilization. The matter is further complicated by the fact that CAD is a process that predominantly affects the vessel wall, such that the early phases of the disease are not at all manifested by impingement on the lumen of the epicardial coronary arteries and their branches, which are visualized during invasive coronary angiography [2–4]. As early as the second decade of life, changes in endothelial function caused by exposure to adverse metabolic or hemodynamic conditions lead to penetration of lipid moieties in the coronary vessel wall. An inflammatory reaction ensues, marked by accumulation of macrophages and oxidation of low-density lipoprotein. A fatty plaque is formed, and it is this precursor of CAD which progresses slowly over decades until it becomes clinically active. The early and intermediate stages of this process are almost entirely invisible to imaging of the lumen of the coronary artery, particularly when visual estimates are used, because of the compensatory expansion of the vessel outward [5].

For over 50 years, invasive coronary angiography with contrast media has been the mainstay for evaluation of CAD and accompanied all the major therapeutic breakthroughs in this field. The first two decades of the technology were dedicated to perfecting the techniques for imaging the coronary arteries and for storing this information on transferable media. Even before the advent of digital storage of images, considerable interest developed in the quantitative aspects of coronary angiography (QCA), particularly in order to measure and compare the effects of medical and interventional therapies on the progression of CAD.

In this chapter we will review the main principles of QCA and assess its utility for quantification of CAD progression or response to intravascular devices.

Principles of Quantitative Coronary Angiography

Thirty years ago, Brown and colleagues introduced the first quantitative assessment of coronary arteries by magnifying 35 mm cine angiograms

S.J. Brener, MD (✉)
Department of Medicine, New york Methodist Hospital, 506 6th Street, Brooklyn, NY 11215, USA
e-mail: sjb9005@nyp.org

S.J. Nicholls and T. Crowe (eds.), *Imaging Coronary Atherosclerosis*, Contemporary Cardiology,
DOI 10.1007/978-1-4939-0572-0_3,

and tracing the contour of the arteries on a large screen [6, 7]. Early computer software corrected for pincushion distortion (created by the magnification process and leading to "pinching" of the artery in the middle of the segment) and tracings were then digitized and reconstructed into a three dimensional rendering of the coronary arteries, assuming elliptical geometry. This early prototype served as the basis for the automated contour detection software used routinely in QCA today. As digital acquisition of images became the standard in invasive cardiology, the need for digitization of the cine angiograms disappeared. The images, acquired in a DICOM (Digital Imaging and Communications in Medicine) format with 2:1 JPEG lossless compression, are then calibrated using the dye-filled injection catheter's known dimensions as the reference. A calibration factor (mm per pixel) allows the measurement of various aspects of the vessel. Each such study occupies ~500 MB of storage. The most basic measurements include reference vessel diameter (RVD), minimal lumen diameter (MLD), and percent diameter stenosis (DS). RVD determination is particularly important as it is the basis for derivation of many of the other parameters. Typically the interpolation method is used by the software algorithm to approximate the normal decrease in vessel diameter as it progresses distally. The lesion length (LL), defined from shoulder-to-shoulder (where DS is at least 50 % of RVD), can also be measured. In every angiography core laboratory (ACL), inter- and intra-observer variability is measured frequently to ensure consistency of film review. In general, the inter-observer variability is <0.25 mm for most automated software. Considering coronary vessels of 3–4 mm in diameter, this translates in ~5 % variability. Beyond the variability caused by observer, biological factors play an important role in our ability to perform adequate QCA. Acquisition of images is affected significantly by the quality of the camera, by the consistency of the acquisition (respiratory variation, quantum mottling or nonuniform film density, foreshortening, and out-of-plane magnification), and by the skill of the angiographer. Inadequate filling of the artery (streaming), lack of separation of branches, different angles (important for follow-up studies), and vasomotor tone can all influence the precision of QCA. The two most commonly used systems for QCA are discussed briefly below.

The Cardiovascular Angiography Analysis System (CAAS, Pie Medical Data, The Netherlands) is an online and off-line analysis system. It has pincushion distortion correction and a weighted (50 %) sum of the first two derivatives of the mean pixel density. It provides an interpolated RVD and has subsegmental and specialty modules for bifurcation lesions, three-dimensional reconstruction, and stent analysis.

The Coronary Measurement System (CMS, MEDIS, The Netherlands) uses similar technology but also has a two-point user-defined centerline identification for catheter calibration and vessel contour.

Beyond RVD, DS, and MLD, typical QCA parameters used in clinical trials include late lumen loss (LLL, defined as the difference between MLD at baseline minus MLD at follow-up), late loss index (defined as LLL divided by initial MLD gain), and binary angiographic restenosis (BAS, defined as DS > 50 % at follow-up). In addition to these classical parameters of percutaneous coronary intervention (PCI) and atherosclerosis studies, semiquantitative and quantitative indices have been devised to describe coronary perfusion at the epicardial and myocardial (tissue) level. These include TIMI (thrombolysis in myocardial infarction) flow grade (0—no flow, to 3—normal flow), TIMI frame counts (number of frames needed for contrast to traverse a defined segment of the coronary tree), and myocardial blush grade (MBG, defined as the penetration of contrast in the microcirculation supplied by the vessel undergoing PCI). These three indices are particularly relevant to patients undergoing reperfusion therapy with fibrinolytic therapy or primary PCI for ST-elevation myocardial infarction.

QCA in Studies of Medical Treatment of Atherosclerosis

In reviewing this topic, the most important element to understand is the underlying mechanisms of CAD. As briefly mentioned above, coronary atherosclerosis develops predominantly

in the vessel wall before it extends into the lumen. The coronary artery remodels and expands outwardly to accommodate this increased volume of tissue in its media. As such, coronary angiography has limited ability to evaluate changes related to progression or regression of atherosclerosis, except when the process is sufficiently advanced to affect lumen size. Furthermore, changes in plaque size, or lumen size can be very modest and yet coexist with dramatic reduction in clinical events. This important observation reflects the ability of plaque-modifying agents, such as statins, to reduce the propensity for plaque rupture or disruption leading to acute coronary syndromes. Thus, much more relevant information has been obtained in this area by studies utilizing intravascular ultrasound (IVUS) to detect small changes in plaque area and volume, including that residing in the vessel wall. Yet, the beginnings of the science of atherosclerosis regression date back to a time when IVUS was not yet available and QCA was the best tool available to assess these changes.

One of the first trials to illustrate the paradox of minimal changes in MLD and large reductions in clinical events was HATS (HDL Atherosclerosis Treatment Study) [8]. Among 146 randomized men who had apolipoprotein B levels ≥125 mg/dL, documented CAD, 120 completed the study, including baseline and follow-up angiography. Patients were given dietary counseling and were randomly assigned to one of the three treatments: lovastatin (20 mg twice a day) and colestipol (10 g three times a day); niacin (1 g four times a day) and colestipol (10 g three times a day); or conventional therapy with placebo (or colestipol if the LDL level was elevated). Coronary events were reduced by 66 % by the combination therapy (6.5 % vs. 19.2 % for placebo) after 2.5 years of therapy. This dramatic effect was achieved despite very modest changes in angiographic parameters: among 1,316 baseline lesions, DS increased by 2.1 % in the conventional therapy group and decreased by 0.7 % in the combination therapy arm ($P=0.003$), with more effect in lesions with DS ≥ 50 % at baseline. MLD decreased by 0.05 mm in the conventional therapy group and increased by 0.012 mm in the combination therapy group among the proximal segment lesions ($P=0.01$). In a similar study—REGRESS (Regression Growth Evaluation Statin Study), treatment with pravastatin, compared with placebo, resulted in less progression of atherosclerosis (change in mean lumen diameter 0.06 mm vs. 0.10 mm, $P=0.02$, change in MLD 0.03 mm vs. 0.09 mm, $P=0.001$) and fewer cardiovascular events (11 % vs. 19 %, $P=0.002$) [9]. Reduction in coronary events with statin therapy has been most pronounced in patients with established coronary disease (secondary prevention) but also occurs in those without it (primary prevention). The benefit of aggressive lipid-lowering therapy with statins in the former category was indexed directly to the on-treatment LDL level. When LDL falls below 100 mg/dL, the rate of CAD events is below 10 % and reaches as low as 5 % with the recommended target for LDL in high-risk patients (70 mg/dL) [10, 11]. For the latter, Brugts et al. compiled data from ten randomized clinical trials encompassing nearly 70,000 patients. All-cause mortality was reduced by 12 % with statins, major coronary events—by 30 % and cerebrovascular events—by 19 % [12]. There was no heterogeneity in response based on gender, age, or the presence of diabetes mellitus.

When angiography was performed at baseline and after treatment in studies of primary and secondary prevention, the changes in angiographic parameters were consistent with data from HATS and REGRESS. Gotto performed a systematic analysis of such trials and showed that while there was a statistically significant correlation between change in MLD and on-treatment LDL ($R^2=0.61$, $P=0.001$), absolute changes in MLD varied between −0.01 mm (progression of atherosclerosis) and 0.05 mm (regression) [13]. Brown et al. examined the ability of experienced operators to distinguish in serial studies between lesions that definitely changed in severity, those that possibly changed and those that did not. In FATS (Familial Atherosclerosis Treatment Study) 120 patients were randomized to three lipid-lowering strategies. In 81 % of lesions scored as "definitely" changed by operators, there was more than 10 % change in DS, as measured by QCA. It appeared that the threshold for visual classification of definite changes was 9.3 % [14].

Lipid lowering may be only one paradigm for atherosclerosis regression. Correction of other risk factors for CAD, such as hypertension, may have a similar effect on atherosclerosis progression. Amlodipine, a long-acting calcium channel blocker used to treat hypertension, was found to have antioxidant effects and to prevent the abnormal accumulation of calcium induced by cholesterol in smooth muscle cells in animals [15]. In one trial, amlodipine reduced progression of atherosclerosis in carotid arteries, but not in coronary arteries [16]. The NORMALISE (Norvasc for Regression of Manifest Atherosclerotic Lesions by Intravascular Sonographic Evaluation) trial compared the effects of amlodipine, enalapril, and placebo among 431 normotensive patients followed for 2 years with coronary angiography and IVUS at baseline and at the end of study, as part of the larger CAMELOT (Comparison of Amlodipine versus Enalapril to Limit Occurrences of Thrombosis) study [17]. Only 69 % of patients completed the follow-up angiographic study. The mean change in MLD was -0.02 ± 0.13 for amlodipine, -0.03 ± 0.12 for enalapril, and -0.03 ± 0.17 mm for placebo ($P = 0.40$). There were no significant correlations between changes in MLD and blood pressure reduction, age, gender, or the presence of diabetes mellitus [18]. An ischemic event, as defined in the primary endpoint, occurred in 20.2, 24.0, and 25.2 % of the amlodipine, enalapril, and placebo groups, respectively ($P = 0.68$). The change in MLD in patients with and without cardiovascular events (cardiovascular death, nonfatal MI, resuscitated cardiac arrest, coronary revascularization, angina or heart failure requiring hospitalization, ischemic stroke or transient ischemic attack, or a new diagnosis of peripheral arterial disease), regardless of treatment assignment, was -0.05 ± 0.20 mm and -0.02 ± 0.13 mm, respectively ($P = 0.48$). Thus, there was neither a significant change in atherosclerosis burden nor a reduction in cardiovascular events, regardless of antihypertensive agent used in this trial.

In summarizing the utility of QCA in assessing the effects of medical treatment of CAD, we can state that there is considerable dissociation between the angiographic changes induced by statin therapy and their clinical effects, suggesting that pleiotropic effects of statins are very important [19]. These include the prevention of white blood cells attachment to the endothelial cells, attenuation of platelet reactivity, and reduction in secretion of CD40 ligand from platelets and anti-inflammatory effects. In general, changes in lumen dimensions are very modest and reflect the fact that most of the atherosclerotic plaque in patients with less than critical CAD resides in the vessel wall, and cannot be reliably imaged with coronary angiography. While this statement reflects our current understanding of CAD pathophysiology, it is notable that even IVUS cannot detect major changes in plaque volume after treatment with statins. For example, in ASTEROID (A Study to Evaluate the Effect of Rosuvastatin on Intravascular Ultrasound-Derived Coronary Atheroma Burden), rosuvastatin lowered LDL from 130 to 60 mg/dL (53 %, $P < 0.001$). Yet mean percent atheroma volume (PAV), the primary endpoint, decreased by only 0.98 % ($P < 0.001$) [20]. The totality of these data suggests that the effect of statins in the medical therapy of CAD is exerted via stabilization of plaque and not via significant change in atherosclerosis burden.

QCA in Studies of Intravascular Devices

Ever since PCI became available more than 30 years ago, procedural success was defined by two important criteria—adequacy of flow in the treated artery (TIMI flow grade) and residual diameter stenosis. Furthermore, the long-term success of the procedure has been defined by the maintenance of vessel patency at the treated site, expressed as DS at a follow-up angiogram. Interventional cardiologists are quite adept at assessing DS, particularly when classifying it in major categories based on clinical significance. Gottsauner-Wolf et al. compared visual estimate of DS with QCA in 30 patients and found excellent correlation, supported by functional assessment with dipyridamole stress test, for stenoses >50 and >75 % [21].

The most important contribution of QCA to the field of interventional cardiology is the ability to consistently and systematically evaluate early and late results of PCI. LLL has become a surrogate endpoint for the efficacy of new interventional devices and was accepted by regulatory agencies as an important endpoint in clinical trials. The introduction of bare-metal stents (BMS) in the late 1980s and drug-eluting stents (DES) in the early 2000s was made possible by this process. Compared with balloon angioplasty (PTCA) alone, stenting with BMS has reduced significantly LLL and the incidence of restenosis (BAR). In the landmark BENESTENT study, 520 patients were assigned to PTCA or BMS. Repeat angiography was performed in 93 % of the eligible patients and the primary angiographic endpoint was MLD at follow-up. MLD at follow-up was 1.73 mm vs. 1.82 mm, respectively, $P=0.09$ but restenosis decreased from 32 % for PTCA to 22 % with BMS, $P=0.02$. The study elegantly demonstrated the principle that BMS achieves a larger initial lumen after procedure than PTCA (2.48 mm vs. 2.05 mm, $P<0.001$) but there is greater late loss in follow-up (0.65 mm vs. 0.32 mm, $P<0.001$), resulting ultimately in a larger MLD at follow-up. The concept was compared by Kuntz et al. to a "higher tax paid on a higher income," resulting eventually in a larger net income [22]. In a similarly designed study, the STRESS (STent REstenosis Study) Investigators randomized 410 patients to PTCA or BMS, with 6 month follow-up angiography, which was performed in 88 % of eligible patients. The primary endpoint was BAR. Patients assigned to BMS had larger acute gain (1.72 vs. 1.23 mm, $P<0.001$), larger late loss (0.74 mm vs. 0.38 mm, $P<0.001$) and larger net gain (0.98 mm vs. 0.80 mm, $P=0.01$), compared with PTCA patients. Restenosis occurred in 31.6 % and 42.1 % of the groups, respectively, $P=0.046$.

Many subsequent analyses have confirmed that BMS results in LLL of 0.7–1.0 mm. DES revolutionized interventional cardiology because of their ability to reduce neointimal proliferation and restenosis. In a meta-analysis of 29 trials comparing various DES with nearly 9,000 patients undergoing follow-up, protocol-mandated angiography, LLL proved to be an excellent indicator of BAR ($R^2=0.5301$; $P<0.0001$) and target vessel revascularization (TVR–$R^2=0.4604$; $P<0.0001$) [23]. These data extended across five major platforms of DES (Figs. 3.1 and 3.2) and showed LLL of 0.13–0.56 mm. DES containing sirolimus or its analogues had TVR as low as 2.8 % (Table 3.1). Importantly, there was no threshold in this relationship, meaning that the lower LLL was, the lower the probability for revascularization was as well. Nearly 75 % of patients with angiographic restenosis needed TVR.

Beyond measurements of lumen size and evaluation of restenosis, QCA provides important insight into the process of reperfusion in patients with ST-elevation myocardial infarction (STEMI). Grading of flow in the infarct-related artery (IRA) after treatment with fibrinolytic therapy or with primary PCI provides critical prognostic information regarding survival. Using the TIMI classification [24], it was shown convincingly that patients with TIMI 3 flow in the IRA have better survival than those with lesser grades. In an analysis of two large STEMI trials with over 5,000 patients, final TIMI 3 flow increased survival at 1 year threefold, compared with TIMI 0–2 (HR = 3.67 [2.45, 5.48], $P<0.001$) [25]. Because TIMI flow classification is semiquantitative, a fully quantitative evaluation of flow—corrected TIMI frame count (cTFC)—was developed by Gibson et al. [26]. They showed that flow was disturbed not only in IRA, but also in non-culprit arteries, compared with normal arteries in patients without STEMI (39.2 ± 20.0 vs. 25.5 ± 9.8 vs. 21.0 ± 3.1, $P<0.001$), reflecting the heightened platelet reactivity and vascular tone in the former group. The same group extended these observations in patients treated with fibrinolytic therapy for STEMI and showed that cTFC was an independent predictor of survival at 2 years ($P=0.01$), after adjusting for important baseline characteristics and revascularization [27].

Even more important than epicardial flow is the tissue myocardial perfusion after STEMI. Ito et al. were among the first to demonstrate that nearly 40 % of patients with successful reperfusion of the IRA have no-reflow at the myocyte

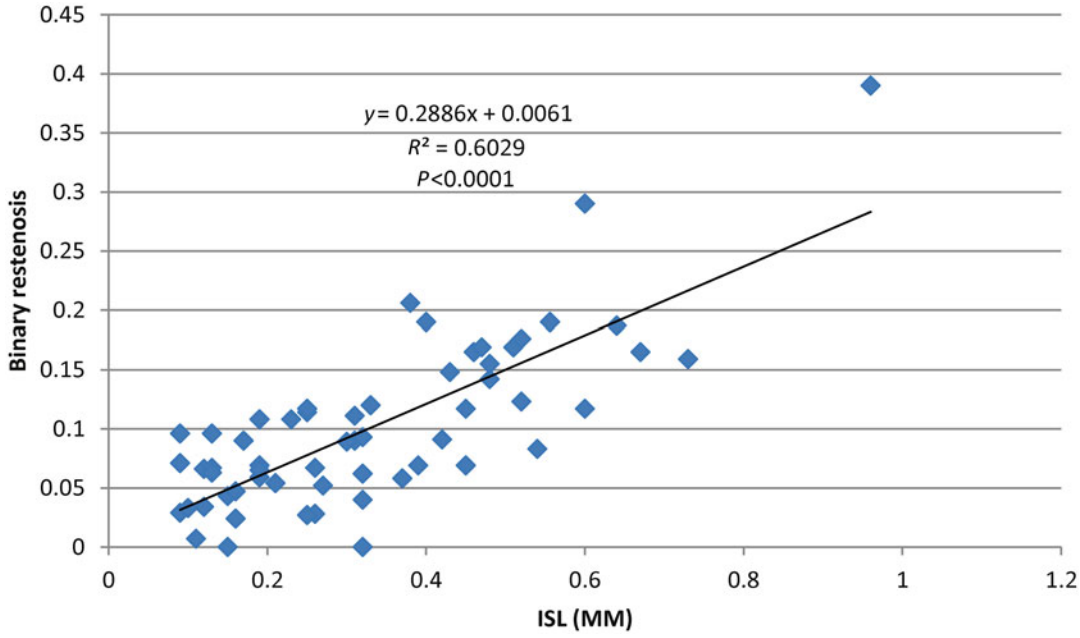

Fig. 3.1 Relationship between in-stent loss (ISL) and binary angiographic restenosis (Adapted from Brener SJ, Prasad AJ, Khan Z, Sacchi TJ. The relationship between late lumen loss and restenosis among various drug-eluting stents: a systematic review and meta-regression analysis of randomized clinical trials. Atherosclerosis. 2011; 214(1):158–62. With permission from Elsevier)

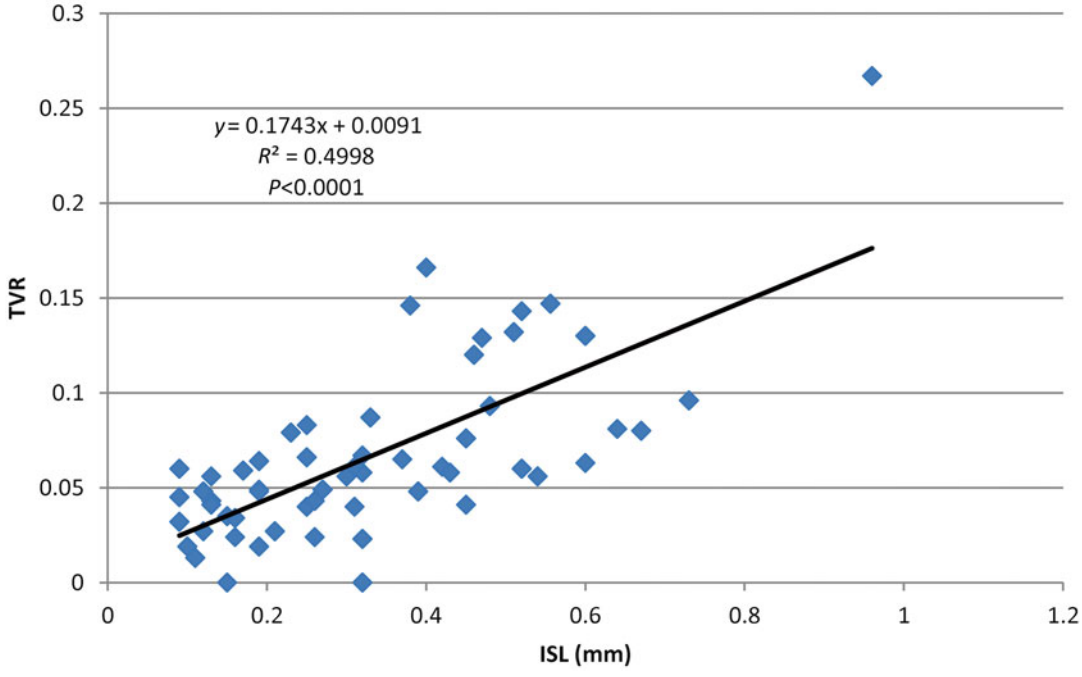

Fig. 3.2 Relationship between in-stent loss (ISL) and target vessel revascularization (TVR) (Adapted from Brener SJ, Prasad AJ, Khan Z, Sacchi TJ. The relationship between late lumen loss and restenosis among various drug-eluting stents: a systematic review and meta-regression analysis of randomized clinical trials. Atherosclerosis. 2011;214(1):158–62. With permission from Elsevier)

Table 3.1 Relationship between late lumen loss and angiographic or clinical restenosis

Drug	ISLLL (mm)	BAR (%)	TVR (%)
SES	0.17	8.0	5.7
PES	0.40	13.1	8.4
EES	0.15	4.7	3.5
ZES	0.56	12.0	6.8
Other platforms	0.44	15.1	11.3

Adapted from Brener SJ, Prasad AJ, Khan Z, Sacchi TJ. The relationship between late lumen loss and restenosis among various drug-eluting stents: a systematic review and meta-regression analysis of randomized clinical trials. Atherosclerosis. 2011;214(1):158–62. With permission from Elsevier

ISLLL in-stent late lumen loss, *BAR* binary angiographic restenosis, *TVR* target vessel revascularization, *SES* sirolimus-eluting stent, *PES* paclitaxel-eluting stent, *EES* everolimus-eluting stent, *ZES* zotarolimus-eluting stent (ENDEAVOR platform)

level, using myocardial contrast echocardiography. Patients with no-reflow had adverse ventricular remodeling, more heart failure, and other adverse outcomes [28]. Thus, accurate evaluation of myocardial reperfusion after primary PCI may help the operator tailor therapy, in the angiography suite and after the procedure, to the risk for adverse events. Myocardial reperfusion, or "blush score," can be assessed using two paradigms. The dynamic method (TIMI myocardial perfusion grade—TMPG) assesses the entry and exit of contrast from the myocardium distal to initial IRA lesion [29]. The densitometric method (myocardial blush grade—MBG) compares the density of contrast opacification of the IRA territory to a reference territory [30]. Assessment of MBG can be computerized [31]. Both scales use grades from 0 to 3 and grades 2 or 3 indicate an open microcirculation [32]. In the HORIZONS AMI (Harmonizing Outcomes with Revascularization and Stents in AMI), myocardial reperfusion was assessed independently by both methods. Both TMPG 2 or 3 (HR = 0.53 [0.38, 0.73], $P < 0.0001$) and MBG 2 or 3 (HR = 0.54 [0.40, 0.75], $P < 0.0001$) were significant independent predictor survival at 3 years, even after adjusting for TIMI flow grade in IRA [33].

The principal limitation of QCA is its insensitivity to the functional significance of coronary stenoses. Recent advances in CT imaging promise to resolve this deficiency [34].

In summary, QCA plays a critical role in assessing the efficacy of intravascular devices and procedures. There is a robust correlation between measures of lumen loss and angiographic and clinical restenosis, which lead to TVR. QCA can reliably differentiate between the antiproliferative effects of various DES platforms and serves as an excellent surrogate endpoint for stent-vs.-stent comparisons. QCA-derived parameters of reperfusion are powerful predictors of survival and freedom from adverse events after STEMI.

Conclusions

Systematic and consistent evaluation of angiographic parameters has contributed significantly to improvements in CAD therapy, both for pharmacological interventions and for intravascular devices and procedures. Accurate measurement of changes in lumen and plaque size has highlighted the important dissociation between atherosclerosis regression and prevention of ischemic cardiac events. Changes in lumen size and even in plaque volume are small, yet they are associated with an important reduction in clinical events, suggesting that plaque modification and stabilization is more important than the change in size, particularly in earlier stages of the disease. Technologies geared at assessing plaque composition and vulnerability are much more critical to this field than QCA.

In contrast, the development and approval of intravascular devices is critically linked to QCA. Surrogate endpoints of most clinical trials incorporate angiographic parameters. QCA has proven able to differentiate between devices with reliability and accuracy. There is robust correlation between angiographic endpoints of lumen size and reperfusion and clinical endpoints.

References

1. Roger VL, Go AS, Lloyd-Jones DM, Adams RJ, Berry JD, Brown TM, et al. Heart Disease and Stroke Statistics–2011 Update: A report from the American

Heart Association. Circulation. 2011;123(4):e18–209. Epub 2010/12/17.
2. Libby P. Changing concepts of atherogenesis. J Intern Med. 2000;247(3):349–58.
3. Libby P, Ridker PM, Maseri A. Inflammation and Atherosclerosis. Circulation. 2002;105(9):1135–43.
4. Libby P, Theroux P. Pathophysiology of Coronary Artery Disease. Circulation. 2005;111(25):3481–8.
5. Glagov S, Weisenberg E, Zarins CK, Stankunavicius R, Kolettis GJ. Compensatory enlargement of human atherosclerotic coronary arteries. N Engl J Med. 1987;316(22):1371–5.
6. Brown B, Bolson E, Frimer M, Dodge H. Quantitative coronary arteriography. Estimation of dimensions, hemodynamic resistance, and atheroma mass of coronary artery lesions using the arteriogram and digital computation. Circulation. 1977;55:329–37.
7. Brown B, Bolson E, Dodge H. Quantitative computer techniques for analyzing coronary arteriograms. Prog Cardiovasc Dis. 1986;28:403–18.
8. Brown G, Albers JJ, Fisher LD, Schaefer SM, Lin JT, Kaplan C, et al. Regression of coronary artery disease as a result of intensive lipid-lowering therapy in men with high levels of apolipoprotein B. N Engl J Med. 1990;323(19):1289–98.
9. Jukema JW, Bruschke AV, van Boven AJ, Reiber JH, Bal ET, Zwinderman AH, et al. Effects of lipid lowering by pravastatin on progression and regression of coronary artery disease in symptomatic men with normal to moderately elevated serum cholesterol levels. The Regression Growth Evaluation Statin Study (REGRESS). Circulation. 1995;91(10):2528–40.
10. O'Keefe Jr JH, Cordain L, Harris WH, Moe RM, Vogel R. Optimal low-density lipoprotein is 50 to 70 mg/dl: lower is better and physiologically normal. J Am Coll Cardiol. 2004;43(11):2142–6. Epub 2004/06/03.
11. Robinson JG, Smith B, Maheshwari N, Schrott H. Pleiotropic effects of statins: benefit beyond cholesterol reduction?: A meta-regression analysis. J Am Coll Cardiol. 2005;46(10):1855–62.
12. Brugts JJ, Yetgin T, Hoeks SE, Gotto AM, Shepherd J, Westendorp RG, et al. The benefits of statins in people without established cardiovascular disease but with cardiovascular risk factors: meta-analysis of randomised controlled trials. BMJ. 2009;338:b2376.
13. Gotto Jr AM. Review of primary and secondary prevention trials with lovastatin, pravastatin, and simvastatin. Am J Cardiol. 2005;96(5A):34F–8. Epub 2005/08/30.
14. Brown BG, Hillger LA, Lewis C, Zhao XQ, Sacco D, Bisson B, et al. A maximum confidence approach for measuring progression and regression of coronary artery disease in clinical trials. Circulation. 1993;87(3 Suppl):II66–73.
15. Tulenko TN, Brown J, Laury-Kleintop L, Khan M, Walter MF, Mason RP. Atheroprotection with amlodipine: cells to lesions and the PREVENT trial. Prospective Randomized Evaluation of the Vascular Effects of Norvasc Trial. J Cardiovasc Pharmacol. 1999;33 Suppl 2:S17–22.
16. Pitt B, Byington RP, Furberg CD, Hunninghake DB, Mancini GB, Miller ME, et al. Effect of amlodipine on the progression of atherosclerosis and the occurrence of clinical events. PREVENT Investigators. Circulation. 2000;102(13):1503–10. Epub 2000/09/27.
17. Nissen SE, Tuzcu EM, Libby P, Thompson PD, Ghali M, Garza D, et al. Effect of antihypertensive agents on cardiovascular events in patients with coronary disease and normal blood pressure: the CAMELOT study: a randomized controlled trial. JAMA. 2004; 292(18):2217–25.
18. Brener SJ, Ivanc TB, Poliszczuk R, Chen M, Tuzcu EM, Hu T, et al. Antihypertensive therapy and regression of coronary artery disease: insights from the Comparison of Amlodipine versus Enalapril to Limit Occurrences of Thrombosis (CAMELOT) and Norvasc for Regression of Manifest Atherosclerotic Lesions by Intravascular Sonographic Evaluation (NORMALISE) trials. Am Heart J. 2006;152(6):1059–63. Epub 2006/12/13.
19. Ray KK, Cannon CP. The potential relevance of the multiple lipid-independent (Pleiotropic) effects of statins in the management of acute coronary syndromes. J Am Coll Cardiol. 2005;46(8):1425–33.
20. Nissen SE, Nicholls SJ, Sipahi I, Libby P, Raichlen JS, Ballantyne CM, et al. Effect of very high-intensity statin therapy on regression of coronary atherosclerosis: the ASTEROID trial. JAMA. 2006;295(13): 1556–65.
21. Gottsauner-Wolf M, Sochor H, Moertl D, Gwechenberger M, Stockenhuber F, Probst P. Assessing coronary stenosis. Quantitative coronary angiography versus visual estimation from cine-film or pharmacological stress perfusion images. Eur Heart J. 1996;17(8):1167–74. Epub 1996/08/01.
22. Kuntz RE, Gibson CM, Nobuyoshi M, Baim DS. Generalized model of restenosis after conventional balloon angioplasty, stenting and directional atherectomy. J Am Coll Cardiol. 1993;21(1):15–25. Epub 1993/01/01.
23. Brener SJ, Prasad AJ, Khan Z, Sacchi TJ. The relationship between late lumen loss and restenosis among various drug-eluting stents: a systematic review and meta-regression analysis of randomized clinical trials. Atherosclerosis. 2011;214(1):158–62. Epub 2010/12/03.
24. The Thrombolysis in Myocardial Infarction (TIMI) trial. Phase I findings. TIMI Study Group. N Engl J Med. 1985;312(14):932–6.
25. Brener SJ, Mehran R, Brodie BR, Guagliumi G, Witzenbichler B, Cristea E, et al. Predictors and implications of coronary infarct artery patency at initial angiography in patients with acute myocardial infarction (from the CADILLAC and HORIZONS-AMI Trials). Am J Cardiol. 2011;108(7):918–23. Epub 2011/07/19.
26. Gibson CM, Cannon CP, Daley WL, Dodge Jr JT, Alexander Jr B, Marble SJ, et al. TIMI frame count: a quantitative method of assessing coronary artery flow. Circulation. 1996;93(5):879–88.

27. Gibson CM, Cannon CP, Murphy SA, Marble SJ, Barron HV, Braunwald E. Relationship of the TIMI myocardial perfusion grades, flow grades, frame count, and percutaneous coronary intervention to long-term outcomes after thrombolytic administration in acute myocardial infarction. Circulation. 2002; 105(16):1909–13.
28. Ito H, Maruyama A, Iwakura K, Takiuchi S, Masuyama T, Hori M, et al. Clinical implications of the 'no reflow' phenomenon. A predictor of complications and left ventricular remodeling in reperfused anterior wall myocardial infarction. Circulation. 1996;93(2):223–8.
29. Gibson CM, Cannon CP, Murphy SA, Ryan KA, Mesley R, Marble SJ, et al. Relationship of TIMI myocardial perfusion grade to mortality after administration of thrombolytic drugs. Circulation. 2000; 101(2):125–30.
30. van't Hof AW, Liem A, Suryapranata H, Hoorntje JC, de Boer MJ, Zijlstra F. Angiographic assessment of myocardial reperfusion in patients treated with primary angioplasty for acute myocardial infarction: myocardial blush grade. Zwolle Myocardial Infarction Study Group. Circulation. 1998;97(23):2302–6.
31. Vogelzang M, Vlaar PJ, Svilaas T, Amo D, Nijsten MW, Zijlstra F. Computer-assisted myocardial blush quantification after percutaneous coronary angioplasty for acute myocardial infarction: a substudy from the TAPAS trial. Eur Heart J. 2009;30(5): 594–9.
32. Poli A, Fetiveau R, Vandoni P, del Rosso G, D'Urbano M, Seveso G, et al. Integrated analysis of myocardial blush and ST-segment elevation recovery after successful primary angioplasty: Real-time grading of microvascular reperfusion and prediction of early and late recovery of left ventricular function. Circulation. 2002;106(3):313–8. Epub 2002/07/18.
33. Brener SJ, Cristea E, Mehran R, Dressler O, Lansky AJ, Stone GW. Relationship between angiographic dynamic and densitometric assessment of myocardial reperfusion and survival in patients with acute myocardial infarction treated with primary percutaneous coronary intervention: The Harmonizing Outcomes with Revascularization and Stents in AMI (HORIZONS-AMI) trial. Am Heart J. 2011;162(6): 1044–51. Epub 2011/12/06.
34. Ko BS, Cameron JD, Meredith IT, Leung M, Antonis PR, Nasis A, et al. Computed tomography stress myocardial perfusion imaging in patients considered for revascularization: a comparison with fractional flow reserve. Eur Heart J. 2012;33(1):67–77. Epub 2011/08/04.

Use of Intravascular Ultrasound in Interventional Cardiology

4

Samuel L. Sidharta, Matthew Worthley, and Stephen Worthley

Introduction

Since Mason Sones performed the world's first diagnostic coronary angiography in 1958, coronary angiography has been widely used as the standard clinical imaging to identify the significance of coronary arterial narrowing and to guide catheter based and surgical revascularisation strategy [1, 2]. However, despite its excellent ability to visualise the contour of the vascular lumen, coronary angiography has some inherent inadequacies and limitations. Among others, coronary angiography provides little insight regarding tissue composition, atheroma plaque characteristics, as well as its extent and distribution [3, 4]. This is not entirely surprising given angiography merely produces a two-dimensional silhouette of the contrast filled lumen and does not visualise vessel wall, the site in which plaque accumulates. Moreover, coronary angiography is subject to significant intraobserver and interobserver variability, raising the issue regarding its accuracy and reproducibility in assessing the extent of coronary artery disease [2, 5–7]. In fact, major discrepancies between angiographic visual estimation of lesion severity and post-mortem examination had been reported previously [2, 8, 9]. The use of intravascular imaging technique with intravascular ultrasound (IVUS) provides a meticulous characterisation of vessel wall as well as information regarding the extent and distribution of atherosclerotic plaque [10]. IVUS has also demonstrated the ubiquitous presence of plaque in the region which appears normal when assessed with coronary angiography [3]. Thus, IVUS provides a unique opportunity to examine the natural history of atherosclerosis in vivo, the impact of medical therapies on changes in plaque burden, and to guide revascularisation strategy with percutaneous coronary intervention (PCI).

History of IVUS

The first real-time catheter ultrasound system designed for intracardiac imaging was introduced by Bom et al. in the late 1960s [11, 12]. The transducer for this system was a 32 barium titanate piezoelectric (pressure-electric) element circular array mounted at the tip of a 3 mm (9 Fr) catheter. Clear images were obtainable with this system; however, limitation with image quality and ring down artefact led a number of groups to develop mechanical catheter imaging systems [12–14]. Hodgson et al. [15] then performed the first in vivo IVUS study on 20 patients during cardiac catheterisation by inserting a 20 MHz transducer over

S.L. Sidharta, MBBS, BMedSc (✉)
Department of Medicine, Cardiovascular Research Centre, University of Adelaide,
North Terrace, Adelaide, SA 5000, Australia
e-mail: samuel.sidharta@adelaide.edu.au

M. Worthley, MBBS, PhD, FRACP, FCSANZ, FACC
S. Worthley, MBBS, PhD
Department of Cardiology, Royal Adelaide Hospital, Adelaide, SA, Australia

S.J. Nicholls and T. Crowe (eds.), *Imaging Coronary Atherosclerosis*, Contemporary Cardiology,
DOI 10.1007/978-1-4939-0572-0_4, © Springer Science+Business Media New York 2014

a 0.014″ floppy guidewire. Since then, IVUS has made a major leap in coronary imaging for both clinical and research indications. Technological advances in IVUS, including reduction in ultrasound transducer size (0.87–1.17 mm) and increasing ultrasound frequency (30–45 MHz) permit the placement of the ultrasound transducer on the end of low profile catheters in close proximity to the endothelial surface [16]. The result is a high resolution, cross sectional, tomographic image of the entire vessel wall resembling histology cross sectional specimen.

Principles of IVUS

Medical ultrasound images are produced by passing an electrical current through a miniaturised crystal that expands and contracts to produce sound waves. The generated sound waves then propagate through the different tissue and subsequently reflected according to the acoustic properties of the tissue it travels through [17, 18]. The final image created is a three-layered appearance of the coronary artery in alternating bright and dark echoes: a bright echo from the intima, a dark zone from the media, and a bright echo from the adventitia [14, 19, 20] (Fig. 4.1). For the usual IVUS transducers (20–40 MHz), the axial resolution is approximately 150–200 μm and the lateral resolution is 200–250 μm with >5 mm depth penetration [21].

There are two different types of IVUS transducer: mechanical single element rotating transducer and the solid state electronic phased array transducer [17, 18, 21, 22]. The mechanical system utilises a single rotating transducer which is driven by a flexible drive cable at 1800 rotations per minute to sweep a beam almost perpendicular to the catheter. It offers a greater resolution owing to its higher frequency system and also a more uniform pullback. This system is available commercially as the 40 MHz iCross or Atlantis SR Pro catheters (Boston Scientific, Santa Clara, CA), the Revolution 45 MHz catheter (Volcano Corp, Rancho Cordova, CA), and the 40 MHz Lipiscan IVUS (InfraReDx, Burlington, MA). The electronic phased array system, on the other hand, uses multiple transducer elements which are arranged in an annular array and sequentially activated to generate an image. Commercially, it is available as 5 Fr 20 MHz Eagle Eye catheter (Volcano Corp). Benefits of this system include enhanced trackability and lack of non-uniform rotational distortion artefacts. The latter is unique to mechanical system and due to mechanical binding of the drive cable [23].

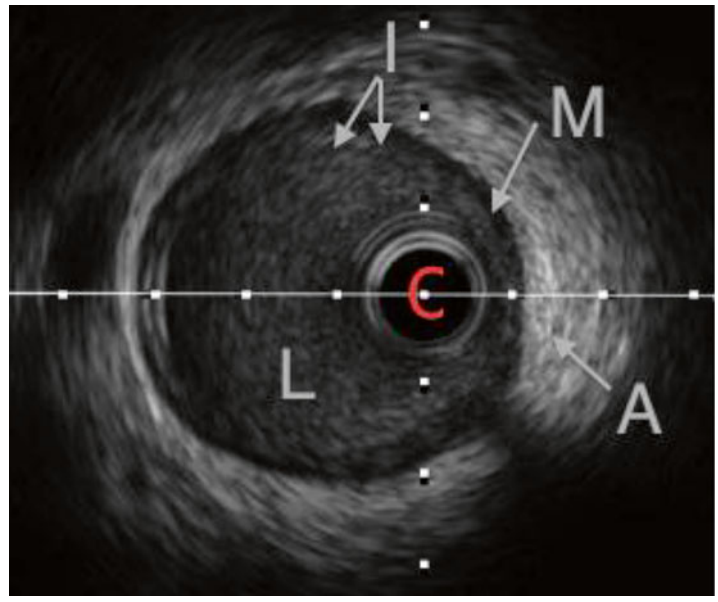

Fig. 4.1 The three-layered appearance of a cross sectional coronary artery as assessed by IVUS. *I* intima, *M* media, *A* adventitia, *L* lumen, *C* IVUS catheter

Clinical Application

Evaluation of Ambiguous Lesions in Non-Left Main Coronary Artery

Assessment and management of angiographic intermediate lesion (50–70 % stenosis) is one of the clinical dilemmas that is faced by an interventional cardiologist especially when the patient's symptomatology is difficult to ascertain. This issue is further compounded by various angiographic limiting aspects, such as lesion eccentricity, vessel overlapping and tortuosity, degree of calcification, and diffuse reference vessel disease [24]. In this context, IVUS has the ability to provide complementary information to coronary angiography. In fact, the use of pre-intervention IVUS in coronary artery disease management has been reported to result in redirection of therapy in up to 40 % of patients [25].

Although fractional flow reserve (FFR) is currently being preferred as the investigational tool to assess the functional significance of an intermediate lesion [26–28], IVUS has an advantage in permitting precise quantification of anatomical distribution and morphology of a lesion; an important consideration in devising procedural strategy and device selection. Several studies have also reported reasonable correlation between structural data derived from IVUS with physiological parameters from FFR [29–34]. For example, earlier studies have identified IVUS-derived minimum lumen area (MLA) <4 mm^2 as being haemodynamically significant when compared with FFR and SPECT imaging [29, 30]. Furthermore, using this MLA cut off, a long-term follow-up study reported a low event rate among patients who had their intervention deferred for an MLA ≥ 4 mm^2 [31]. The latter studies, however, suggest a lower MLA cut-off value of 2.4–3.6 mm^2 as being haemodynamically significant as compared with FFR [32–34]. This apparent discrepancy is not entirely surprising given a single MLA value is significantly influenced by multiple factors including involved vessel and its size, lesion location, and length, and the presence of plaque rupture [33]. Therefore a combination of IVUS-derived parameters, such as plaque burden, area stenosis, and lesion length also needs to be taken into consideration when assessing an intermediate lesion [22, 24, 35]. Illustration of basic IVUS measurement can be seen in Fig. 4.2.

Evaluations and Management of Left Main Coronary Artery Disease

Evaluation of Left Main Disease Severity

It has been well documented that quantifying angiographic left main disease severity especially that which involves the proximal segment is particularly challenging and is subject to significant interobserver variability [36, 37]. Three major anatomical factors which impair left main evaluation include aortic cusp opacification, short length of vessel trunk, and the presence of bifurcation or trifurcation at the distal segment [21]. Contrast streaming in the aortic cusp can obscure the ostium of the left main making angiographic evaluation problematic. On the other hand, the short segment of the left main shaft leaves little reference site for comparison. Also, the bifurcation into sub-branches at the distal end potentially conceals the distal left main. IVUS, in contrast, suffers not from the aforementioned limitation making it an investigation of choice when assessing left main lesion (Fig. 4.3).

In the case of angiographic intermediate left main stenosis, an IVUS minimum lumen diameter (MLD) of <2.8 mm or an MLA <6 mm^2 suggest a physiologically significant stenosis and thus merits revascularisation [24, 26]. A study of 55 patients with moderate left main disease demonstrates that these cut-off values correlate well with physiologically significant lesion as assessed by FFR with a sensitivity of 93 % and a specificity of 98 % [38]. Additionally, a recent multicentre, prospective study showed that deferral of revascularisation among patients with left main MLA ≥ 6 mm^2 carried a similar outcome with the revascularised group who has left main MLA < 6mm^2 during long-term follow-up [39]. Another comparative study used an MLA cut-off value of 7.5 mm^2 to

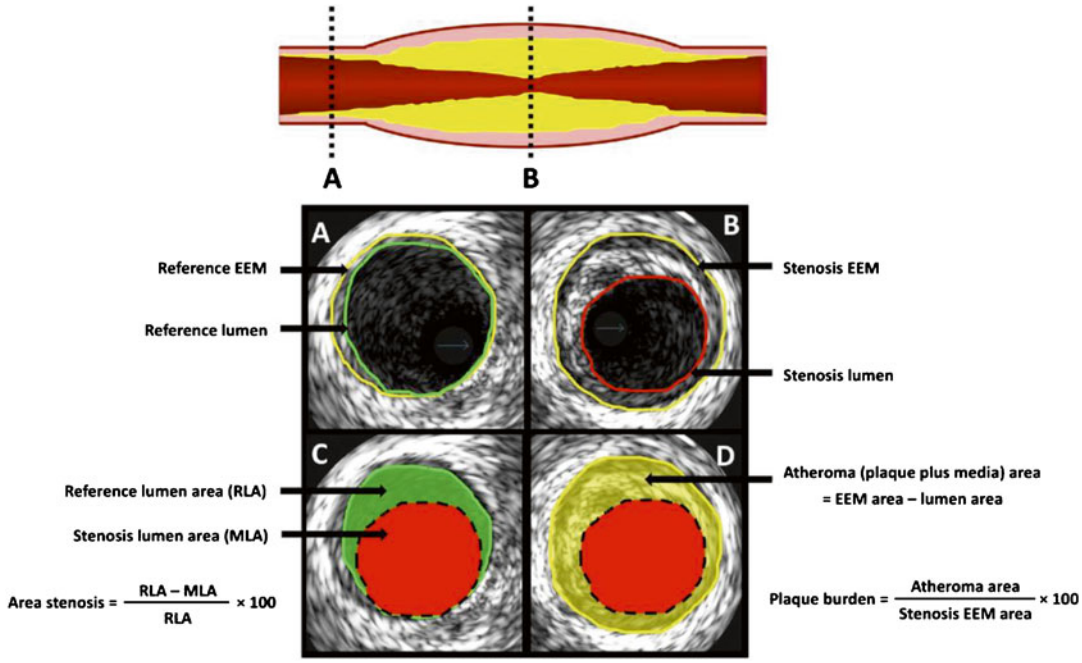

Fig. 4.2 Basic IVUS measurement. (**a**) The proximal reference segment. (**b**) Cross sectional image taken from the most stenotic segment. (**c**) The calculation of the area stenosis. (**d**) The IVUS quantification of plaque burden. Area stenosis is a measure of luminal stenosis relative to the normal reference segment. In contrast, plaque burden refers to the area within the EEM (external elastic membrane) which is occupied by atheroma (Reprinted from McDaniel, M.C., et al., Contemporary clinical applications of coronary intravascular ultrasound. JACC. Cardiovascular Interventions, 2011. 4(11): p. 1155–67. With permission from Elsevier)

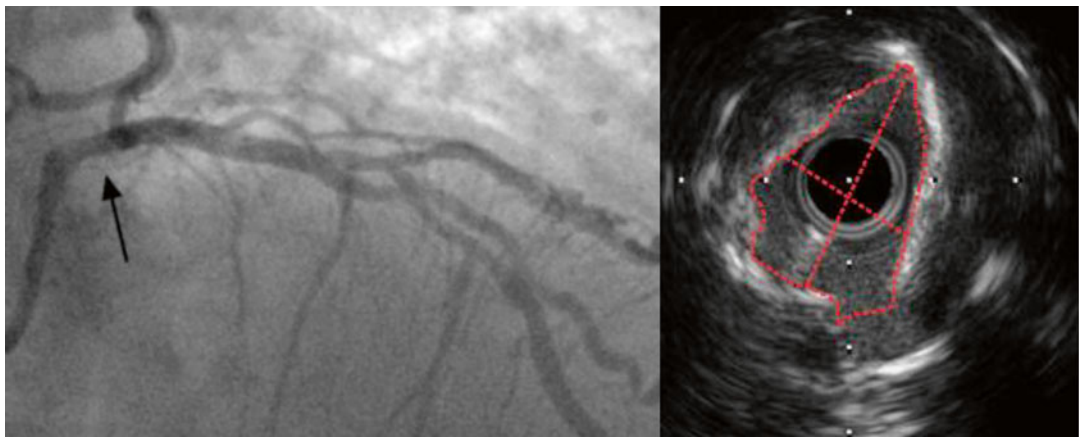

Fig. 4.3 Indeterminant ostial left main stenosis. This is the coronary angiogram picture taken from an 82-year-old man who presents with chest pain and strongly positive stress test (*left*). *Black arrow* demonstrates area of haziness involving the ostium of the left main coronary artery. This segment correlates with the IVUS image on the *right* which shows an eccentric, calcified left main lesion, with minimum lumen area (MLA) of 3.9 mm^2. The patient was revascularised percutaneously and had a good outcome

determine whether a patient should undergo revascularisation or to have a deferral strategy [40]. It concluded that during the mean follow-up of 3.3 ± 2 years, there was no difference in major adverse cardiac event (MACE) between the two cohorts. Altogether, in conjunction with clinical information, it is reasonably safe to defer revascularisation in patients with MLA ≥ 7.5 mm^2 and to consider revascularisation in patients with MLA < 6mm^2. Patients with intermediate MLA value (6–7.5 mm^2) would require further physiological assessment, for example with FFR [27]. Based on the available evidence, IVUS was given a class IIA indication for the assessment of angiographically indeterminant left main coronary artery disease by the recent joint American College of Cardiology/American Heart Association/Society for Cardiovascular Angiography and Interventions (ACC/AHA/SCAI) guideline [41].

IVUS-Guided PCI for Unprotected Left Main Disease

Aside from its ability to provide further stratification of left main disease severity, IVUS also made a major contribution in the area of unprotected left main PCI. Patients with significant left main disease (≥50% stenosis) carry a high-risk mortality and morbidity from cardiovascular events considering the area of myocardium at risk should the flow in this vessel becomes compromised. To date, coronary artery bypass surgery remains the "gold standard" treatment for majority of significant left main disease especially in those with multivessel involvement. Nevertheless, the introduction of drug-eluting stent (DES) has ushered a new era of complex PCI, such as unprotected left main coronary artery disease and bifurcation lesion PCI due to its low rate of restenosis [42]. The use of pre-intervention IVUS in the left main PCI permits a detailed assessment of the vessel anatomy, the size of the vessel, and to determine the extent of ostial involvement at the daughter sub-branches [26, 43]. This information helps the operator to optimise stent selection and provide complete disease coverage. IVUS also assists in ensuring adequate stent expansion and apposition; important risk factors for restenosis and stent thrombosis [44–46]. Finally, IVUS also reveals the extent of calcification. This information will be useful in deciding whether to employ debulking strategy with rotational atherectomy to facilitate the stent placement [47–49].

The role of IVUS-guided strategy for unprotected left main PCI, however, remains a controversial issue given the conflicting data in the literature [46]. Nonetheless, several recent reports provide clinical data favouring its routine use. In a large Korean registry study [50], the use of IVUS-guided left main PCI was associated with a 3 year reduction in mortality when compared with angiographic guidance PCI. This benefit is particularly observed among the 145 matched pairs of patients who receive DES (4.7 % vs. 16 %, $p = 0.048$). Moreover, a prospective, randomised, non-inferior study comparing PCI vs. CABG for left main disease (PRECOMBAT trial) reported a low event rate in the PCI group and comparable outcome with the CABG group (8.7 % vs. 6.7 %, $p = 0.02$ for non-inferiority) [51]. In this multicentre trial, IVUS was extensively used. Some of this clinical benefit may be derived from IVUS ability to determine the extent of disease burden and lesion complexity thus assisting the operator with the appropriate procedure strategy. For instance, the MLA of the confluent zone between the distal segment of left main coronary artery and its daughter branches has been shown to be an accurate indicator of bifurcation left main disease severity and a predictor of post-stent underexpansion and clinical outcome [43, 52]. Another study then demonstrated that among patients who undergo bifurcation left main PCI, those with post-stenting underexpansion have significantly lower MACE-free survival rate in 2 years when compared with their counterpart [53]. Taken together, IVUS should be considered to guide unprotected left main PCI especially when it involves the bifurcation point.

IVUS and PCI

Refinement of PCI Technique and Practice

IVUS has been instrumental in helping us to understand the arterial responses to different coronary interventional modality [54–57] and has assisted in the improvement of technical

details of the devices application and their manufacturing. For instance, IVUS has given a significant insight into the different mechanism of restenosis post-intervention. It discovers that whilst a combination of elastic recoil and concentric remodelling and to a lesser role, local intimal hyperplasia account for the mechanism of restenosis in post-balloon angioplasty [58–60], neointimal hyperplasia is the sole mechanism of late lumen loss in the stented artery receiving bare metal stent (BMS) [61, 62]. These observations were extremely valuable in guiding the development of management strategy for in stent restenosis, which ultimately leads to the development of DES. IVUS has also revolutionised the technique of stent deployment and post-stent medication regime as it is practised today. Following the enthusiasm with the introduction of stents, clinicians began to notice the issue with stent implantation in the form of subacute thrombosis [63]. This issue was further compounded by major bleeding issue due to intensive use of oral anticoagulation regime in order to reduce the incidence of stent thrombosis. IVUS then began to identify the association between subacute stent thrombosis and stent deployment issue, such as inadequate stent expansion and incomplete stent apposition (ISA) [64]. Inadequate stent expansion occurs when part of the stent is insufficiently expanded when compared to the proximal and distal reference site. Incomplete stent apposition, in contrast, refers to a lack of contact between the stent struts and the underlying arterial wall. Based on this observation, Colombo et al. developed post-stent deployment high pressure technique [65]. This strategy not only led to the reduction of stent thrombosis incidence but also allowed oral anticoagulation to be replaced with dual antiplatelet therapy thus reducing the length of hospital stay and vascular complication rate.

IVUS and Bare Metal Stent PCI

The benefit of IVUS in coronary intervention was initially demonstrated in the era of balloon angioplasty. Randomised and non-randomised IVUS trials demonstrated that IVUS-guided strategy resulted in the improvement of final lumen diameter and caused significant reduction in clinically driven reintervention rate when compared with the angiography group [66, 67]. Another randomised trial of 254 patients (BEST trial) then reported a similar clinical outcome between IVUS-guided balloon angioplasty (with provisional stenting) vs. routine angiography-guided stenting [68]. It is however worth noting that in this trial, there is a high crossover rate (44 %) in the balloon angioplasty group to stenting. Taken together, the use of IVUS is effective in optimising final balloon angiographic and clinical outcome. This approach, however, was viewed as time consuming and cost-ineffective especially as the stent profile continued to improve and its price continued to decline. Thus, routine stenting now is the preferred strategy above balloon angioplasty with provisional stenting [63].

The benefit of IVUS-guided strategy in BMS PCI has been examined in both observational [69–71] and randomised trials [72–75]. IVUS can be used to perform pre-interventional evaluation of the extent of lumen obstruction and the mechanism of obstruction (e.g. thrombus or calcification). This in turn allows for each management strategy to be individualised and tailored according to patient's clinical baseline status. Post-intervention, IVUS may assist with optimising procedural outcome, such as assessment of stent expansion and stent strut apposition, detection of PCI complication (e,g., dissection, plaque shift), and identification of residual stenosis and stent fracture. Of these, inadequate stent expansion has been associated consistently with target vessel failure resulting from either in stent restenosis [71, 76–78] or stent thrombosis [79, 80]. Despite its practical use and demonstrable benefit by case control studies, the data regarding IVUS clinical benefit from randomised trials are conflicting. The TULIP study, a randomised controlled trial involving 144 patients with long disease segment (>20 mm) demonstrated a significant improvement in both angiographic and clinical end points in the IVUS-guided group when compared to the angiographic directed group [74]. Another trial, AVID, however reported a slight different outcome.

AVID randomised 800 patients into IVUS vs. angiography-guided intervention with total follow-up of 12 months. Indeed, AVID is the largest randomised trial evaluating the benefit of IVUS in BMS PCI. In this trial, IVUS-guided strategy resulted in the improvement of post-procedural minimum stent area (a marker of adequate stent expansion) but did not result in the reduction of clinical end point (death/myocardial infarction/target lesion revascularisation) except in the subgroup with moderate size vessel (2.5–3.5 mm) and in saphenous vein graft PCI [72]. In this subgroup, the reduction in clinical end point is mainly driven by target lesion revascularisation. Thus the main clinical benefit of IVUS, based on these trials is the reduction of target vessel failure without added mortality benefit. These findings were further replicated in a meta-analysis from seven randomised trials involving 2,193 patients [81]. It concludes that IVUS guidance was associated with a significantly larger post-procedure angiographic MLD, lower rate of 6-month angiographic restenosis, a reduction in the revascularisation rate, and overall MACEs. However, no significant effect was seen for myocardial infarction or mortality. Overall, the efficacy of IVUS in optimising procedural outcome and reducing restenosis rate in BMS PCI is unquestionable, nonetheless its routine use in clinical practice still needs to be weighed against a number of factors, including cost, time, availability, and the operators skill, to accurately acquire and interpret the images.

IVUS and Drug-Eluting Stent PCI

The arrival of DES opened a new chapter in the world of interventional cardiology. DES had been shown to significantly reduce the risk of restenosis to less than 10 % [44, 82–85] when compared to BMS. It does this by inhibiting neointimal proliferation through its drug coating [86, 87]. As a result, operators began to put less attention on achieving optimal final procedural outcome as in the days of BMS [65]. However, the discovery of increasing incidence of stent thrombosis, especially very late stent thrombosis in the patients receiving DES has resulted in renewed interest in the use of IVUS to direct therapy.

Stent thrombosis, despite its rare occurrence (annual risk ~0.5%), carries a significant mortality and morbidity [88]. The overall prognosis is poor with 10–30% mortality rate. Several precipitating factors have been implicated to cause stent thrombosis and these essentially can be categorised as patient factors, lesion characteristics, device factors, and procedural factors. IVUS has provided significant insights into the morphologic pattern and possible causes of stent thrombosis following DES implantation, specifically stent underexpansion and incomplete stent apposition. Fuji et al. conducted a retrospective analysis on 15 patients who developed stent thrombosis following successful DES implantation [89]. They reported that lesions leading to stent thrombosis had more stent underexpansion, smaller minimum stent area, and residual edge stenosis. The strong association between IVUS detected stent underexpansion and stent thrombosis was also observed and well established in various other DES trials [90–95] and BMS trials [79, 80]. The role of incomplete stent apposition in causing stent thrombosis, on the other hand, is still controversial. Firstly, incomplete stent apposition is common, occurring in 10–20% of DES and can be acute or late [96]. Whilst acute ISA is procedural related, late ISA may be due to a combination of positive vessel remodelling (i.e. vessel expansion), intimal hyperplasia, or dissolved thrombus or plaque which led to a gap between vessel wall and stent [97]. Secondly, there is a discrepancy of observation among various trials regarding the link between ISA and stent thrombosis. In a case control study by Cook et al., a significantly high rate of ISA was noted in the very late stent thrombosis patients as compared to the DES control group [98]. This association was observed in another observational study [99] but not identified in follow-up studies of large randomised DES trials [83, 100–103]. In a recent sub-analysis of a randomised DES trial, Cook et al. reported that very late stent thrombosis and MACE occurs more frequently in patients with ISA than without ISA [104]. In this study, there was no difference in mortality observed.

Based on these IVUS observations, several trials have been conducted to assess the clinical

benefit of IVUS-directed therapy in DES PCI. A study by Roy et al. compared 1-year clinical outcomes in 884 patients who underwent IVUS-guided PCI with a propensity-matched cohort of angiographically guided patients [105]. IVUS-directed therapy was found to be associated with lower incidence of stent thrombosis at 30 days (0.5% vs. 1.4%, $p=0.05$) and 1 year (0.7% vs. 2.0%, $p=0.01$) with no difference in the rates of myocardial infarction or death. Claessen et al. subsequently reported that IVUS guidance strategy resulted in significant reduction of early, medium-term, and long-term clinical outcome in a large registry study [106]. This benefit is mostly driven by reduction in the numbers of myocardial infarction. In another large observational study involving 8,371 patients, IVUS-guided DES PCI was also found to be associated with a 3-year reduction in mortality (HR 0.46; 95% CI 0.33–0.66, $p<0.001$) [107]. Despite all these demonstrable benefits, to date there is still a lack of information regarding clinical outcome from IVUS-randomised trials. Indeed, there is only one randomised trial assessing the efficacy of IVUS use in DES implantation. AVIO trial randomised 284 patients with complex lesion (e.g. small and diffuse vessel disease, bifurcation lesion, chronic total occlusion) into IVUS-guided or angiography-guided arms [108]. Optimal stent expansion is defined as achieving ≥70% of the cross sectional area of the post-dilation balloon. The preliminary data from 9-month follow-up indicated that IVUS-guided strategy resulted in larger post-procedural MLD but no difference was observed in the rate of MACE. On balance, there is no strong recommendation for routine IVUS-guided PCI at this stage. However, IVUS use should be considered in patients with high risk of stent thrombosis or in patients whereby the consequence of stent thrombosis is fatal, such as left main coronary artery disease. IVUS should also be considered for evaluation of in stent restenosis or stent thrombosis, especially when it is a recurring event.

Safety

Despite its clinical advantages over coronary angiogram, the widespread use of IVUS has been somewhat limited by its invasive nature. The safety of IVUS has been investigated extensively and yields low overall rate of complication [109–111]. The most common complication recorded is transient vessel spasm, which occurs in the order of 2% of IVUS procedure. Major IVUS complications, such as dissection and abrupt vessel closure are quite rare with <0.5% of all procedures [111]. This mainly occurs in the vessel that undergoes simultaneous PCI or in ACS patients as supposed to patients who just undergo diagnostic imaging. Importantly, IVUS has not been shown to result in accelerating disease progression [112, 113].

Imaging Atherosclerosis

The Quest of Vulnerable Plaque

In the last decade, IVUS technology has been constantly used in the research arena in an attempt to identify vulnerable plaque, which is the major substrate of acute coronary syndrome. Vulnerable plaque or thin-capped fibroatheroma (TCFA) is defined histologically as a plaque with thin fibrous cap (<65 μm) which is associated with a large necrotic core (often containing haemorrhage or calcification), reduced smooth muscle content, and a large number of infiltrative inflammatory cells, such as macrophages and activated T cells [114]. Several other pathological features have also been observed to be present in TCFA, such as positive remodelling (expansion of the external elastic membrane in response to plaque accumulation) [115] and abundant intraplaque vasa vasorum, indicating neoangiogenesis and active inflammation [116, 117]. Some of these TCFA features like positive

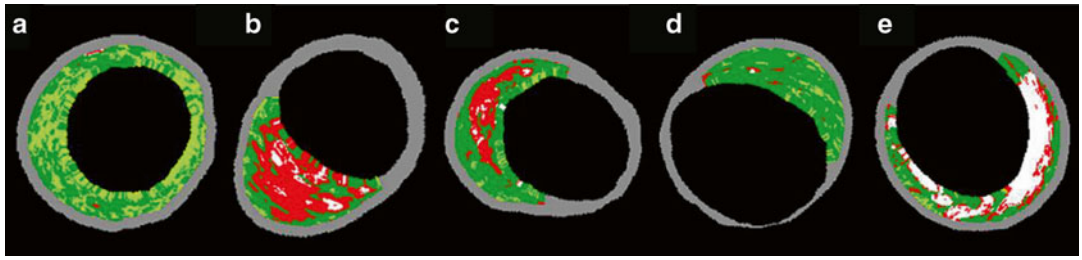

Fig. 4.4 Lesion type classification by VH-IVUS. Based on the VH-IVUS algorithm, coronary lesion, or plaque can be characterised according to the combination of different tissue colour map (fibrous, *green*; fibrofatty, *yellow green*; necrotic core, *red*; dense calcium, *white*). (**a**) Pathological intimal thickening. (**b**) VH-IVUS-derived thin-capped fibroatheroma. (**c**) Thick-capped fibroatheroma. (**d**) Fibrotic plaque. (**e**) Fibrocalcific plaque (Reprinted from Kubo, T., et al., The dynamic nature of coronary artery lesion morphology assessed by serial virtual histology intravascular ultrasound tissue characterisation. Journal of the American College of Cardiology, 2010. 55(15): p. 1590–7. With permission from Elsevier)

remodelling are discoverable by standard greyscale IVUS; however, it falls short in its capability to characterise plaque composition which determine vulnerability. Greyscale IVUS is also limited due to its considerable post-processing to produce an image and reliance on visual inspection of acoustic reflections to determine plaque component.

In an effort to improve the detection of plaque composition, an IVUS capability called virtual histology-IVUS (VH-IVUS) was developed. VH-IVUS uses mathematical autoregressive spectral analysis of the radiofrequency backscatter data to generate a tissue map of the four plaque components: fibrous (green), fibrofatty (yellow green), necrotic core (red), and dense calcium (white) [118] (Fig. 4.4). An alternative algorithm to characterise plaque composition called integrated backscatter-IVUS (IB-IVUS) has also been developed. This algorithm uses fast Fourier transform analysis of the backscatter signal of a tissue volume to generate tissue colour map [119, 120]. VH-IVUS accuracy in detecting these plaque types has been validated in vivo with a predictive accuracy of 87.1, 87.1, 88.3, and 96.5 % for fibrous, fibrofatty, necrotic core, and dense calcium respectively [121]. VH-IVUS, however, is limited in its ability to visualise thrombus and may misclassify it as fibrous or fibrofatty plaque. Owing to its axial resolution (200 μm), VH-IVUS is also unable to identify the fibrous cap thickness of TCFA, which is <65 μm. As a result, VH-IVUS-derived TCFA (VH-TCFA) has been defined as confluent necrotic core-rich plaque (>10%) without evidence of overlying fibrous tissue on three consecutive frames with the arc of the necrotic core in contact with the lumen for 36° along lumen circumference [122]. It also must have percent atheroma of ≥40% [123]. Based on these criteria, investigators have found that VH-TCFA is more prevalent in the patients with acute coronary syndrome than in patients with chronic stable angina, making it a reasonable surrogate for vulnerable plaque [124, 125].

Information derived from both IVUS and VH-IVUS have been critical in providing us with information to help predicting individual future coronary event. Yamagishi et al. analysed 106 patients with angiographic minimal coronary artery disease with baseline conventional IVUS [126]. At follow-up, plaques that resulted in acute coronary syndrome were found to exhibit higher baseline plaque volume, eccentric in its distribution, and manifest echolucent zone characteristics. Another study which analysed the impact of baseline plaque composition on future coronary event is PROSPECT trial (Providing Regional Observations to Study Predictors of Events in the Coronary Tree) [127]. PROSPECT is the first prospective study utilising three imaging modality: coronary angiogram, conventional IVUS, and VH-IVUS to assess the natural history of vulnerable plaque. In this study, 697 patients with acute coronary syndrome underwent three vessel IVUS and VH-IVUS post-PCI with primary end point of MACE (death/cardiac arrest/myocardial

infarction/rehospitalisation). After a median follow-up of 3.4 years, 20.4 % of patients experience MACE. Events were adjudicated to be related to culprit lesions in 12.9 % of patients and to non-culprit lesions in 11.6 %. Predictors for MACE in non-culprit lesion were identified to be diabetes, IVUS plaque burden ≥70%, MLA ≤ 4mm^2, and the presence of VH-TCFA. In the absence of VH-TCFA, the event rate in the non-culprit lesion was reduced to 1.3–1.9% in 3 years depending on the presence of other risk factors. In another serial VH-IVUS study by Kubo et al., VH-TCFA may stabilise, remain unchanged, or even evolve in a new territory suggesting that the natural history of vulnerable plaque is a dynamic process [128]. Altogether, the combination of conventional IVUS and VH-IVUS could potentially provide a prognostic tool to predict a lesion with potential for coronary event, even in artery with angiographically minimal disease.

Besides VH-IVUS, there are several other IVUS-based technologies that have been developed in order to identify certain pathological features associated with vulnerable plaque. Some examples include IVUS elastography/palpography [129–131] and contrast-enhanced IVUS (CE-IVUS) [132–134]. The former attempts to identify the plaque vulnerability by analysing the mechanical strain property of the arterial wall [135]. The differences in tissue deformity potentially allow differentiation of various plaque components. On the other hand, CE-IVUS uses microbubble contrast agent in order to quantify vasa vasorum density and plaque perfusion, a feature of inflammation, which is one of the signatures of vulnerable plaque [134, 136]. This technology, however, remains an experimental tool at this stage and has not been established as a valid surrogate clinical end point.

Evaluation of Atherosclerotic Plaque Progression/Regression

Plaque progression, as measured by serial IVUS has been associated with an increased risk of future cardiac event [137, 138]. As a result, IVUS-measured atheroma change has been used extensively in randomised clinical trials as a surrogate clinical end point of various novel [139–144] or existing cardiovascular medication [145–151]. The use of IVUS as a surrogate end point allows trials to be conducted in a shorter time frame with smaller number of participants thus expediting the process of drug development. Among these trials, IVUS has provided especially a significant insight into the impact of statin therapy on the natural history of atheroma. The use of intensive statin therapy is not only shown to halt disease progression but also causes disease regression [145, 148]. Furthermore, VH-IVUS has extended this observation by demonstrating that statin therapy also results in the change of plaque composition [150, 152]. Altogether, these trials demonstrate that pharmacological therapy has the potentials to halt, reverse, and alter the course of the natural history of atheroma progression.

Future Perspectives

IVUS has made a major leap in imaging atherosclerosis with the continual expansion of its new capabilities. In the near future, we will see a more IVUS synergism with other imaging modality to improve tissue characterisation and arterial imaging. A co-registration with optical coherence tomography (OCT), for example is already on the horizon [153]. OCT has a much higher spatial resolution (10–20 μm) compared to conventional IVUS [154]. Owing to this, OCT is excellent in visualising the thin cap of TCFA and stent strut coverage. Some of its tissue characterisation includes red blood cell-rich thrombus, platelet-rich thrombus, and macrophages infiltration [155].

Recently, a combination catheter of IVUS and near-infrared spectroscopic (NIRS) imaging was developed and performed in vivo [156, 157]. NIRS provides information of plaque composition by analysing the pattern of near-infrared light absorbance by different tissue [158]. It is superior to IVUS in terms of its ability to detect the presence of cholesterol crystals which is abundant in the necrotic cores [159]. It, however, does not provide structural information. Thus the combination of these two imaging modalities

would provide a superior, structural, and compositional information. Ultimately, the optimum intravascular imaging of coronary artery would combine the spectroscopic capabilities of NIRS, the near-field resolution of OCT, and the tissue penetration ability of IVUS.

Another exciting area from IVUS research is the use of IVUS to assess the relationship between segmental coronary endothelial function and regional plaque burden. It has been well established that endothelial dysfunction, as assessed by the vasodilator responses to different endothelial-dependent stimuli is associated with an increased risk of future cardiovascular event [160–162]. Recently, we published a data from our sets of experiment that looked at the relationship between plaque burden and endothelial function as a plausible explanation for the association of this phenomenon with adverse clinical events [163]. We utilised IVUS to evaluate the vasodilator properties of the study artery to the endothelial-dependent stimulus, intracoronary salbutamol. The study showed a strong relationship between in vivo segmental human coronary endothelial-dependent macrovascular and microvascular function with associated underlying atheroma burden. We have also undertaken a program to evaluate the impact of this dynamic process on atherosclerotic plaque progression (http://www.anzctr.org.au/ACTRN12612000594820.aspx). The impact of this dynamic process and its relationship to plaque burden and/or progression on clinical outcome is yet to be defined.

Summary

The role of IVUS in the world of interventional cardiology continues to evolve in parallel with the refinement of PCI technique, devices, and approach. IVUS has played an important role in helping us to understand the different arterial response to various interventional approaches as well as guiding the clinician with the device selection and strategy. Its role is even more paramount in the area of complex PCI, such as left main or bifurcation disease, whereby the consequences of complication could be severe. Advances in IVUS, such as VH-IVUS and IVUS with NIRS capability, also permit a more optimal characterisation of atherosclerosis plaque. This provides not only a significant insight into the natural history of atherosclerosis but also an opportunity to evaluate the impact of different pharmacological therapy on modifying the disease progression. Finally, large prospective clinical trials are needed to assess the clinical benefit of emerging novel IVUS technology.

References

1. Mueller RL, Sanborn TA. The history of interventional cardiology: cardiac catheterization, angioplasty, and related interventions. Am Heart J. 1995;129(1):146–72.
2. Topol EJ, Nissen SE. Our preoccupation with coronary luminology. The dissociation between clinical and angiographic findings in ischemic heart disease. Circulation. 1995;92(8):2333–42.
3. Nissen S. Coronary angiography and intravascular ultrasound. Am J Cardiol. 2001;87(4A):15A–20.
4. Nicholls SJ, Nissen SE. Invasive imaging modalities and atherosclerosis: the role of intravascular ultrasound. In: Ballantyne CM, editor. Clinical lipidology: a companion to Braunwald's heart disease. Philadelphia, PA: Saunders Elsevier; 2009. p. 410–9.
5. Zir LM, et al. Interobserver variability in coronary angiography. Circulation. 1976;53(4):627–32.
6. Murphy ML, Galbraith JE, de Soyza N. The reliability of coronary angiogram interpretation: an angiographic-pathologic correlation with a comparison of radiographic views. Am Heart J. 1979;97(5):578–84.
7. Galbraith JE, Murphy ML, de Soyza N. Coronary angiogram interpretation. Interobserver variability. JAMA. 1978;240(19):2053–6.
8. Roberts WC, Jones AA. Quantitation of coronary arterial narrowing at necropsy in sudden coronary death: analysis of 31 patients and comparison with 25 control subjects. Am J Cardiol. 1979;44(1):39–45.
9. Arnett EN, et al. Coronary artery narrowing in coronary heart disease: comparison of cineangiographic and necropsy findings. Ann Intern Med. 1979;91(3):350–6.
10. Puri R, Worthley MI, Nicholls SJ. Intravascular imaging of vulnerable coronary plaque: current and future concepts. Nat Rev Cardiol. 2011;8(3):131–9.
11. Bom N, Lancee CT, Van Egmond FC. An ultrasonic intracardiac scanner. Ultrasonics. 1972;10(2):72–6.
12. Yock PG, Linker DT, Angelsen BA. Two-dimensional intravascular ultrasound: technical development and initial clinical experience. J Am Soc Echocardiogr. 1989;2(4):296–304.
13. Roelandt JR, et al. Intravascular real-time, two-dimensional echocardiography. Int J Card Imaging. 1989;4(1):63–7.

14. Pandian NG, et al. Ultrasound angioscopy: real-time, two-dimensional, intraluminal ultrasound imaging of blood vessels. Am J Cardiol. 1988;62(7):493–4.
15. Hodgson JM, et al. Clinical percutaneous imaging of coronary anatomy using an over-the-wire ultrasound catheter system. Int J Card Imaging. 1989;4(2–4): 187–93.
16. Nicholls SJ, Andrews J, Moon KW. Exploring the natural history of atherosclerosis with intravascular ultrasound. Expert Rev Cardiovasc Ther. 2007; 5(2):295–306.
17. Mintz GS, et al. American College of Cardiology Clinical Expert Consensus Document on Standards for Acquisition, Measurement and Reporting of Intravascular Ultrasound Studies (IVUS). A report of the American College of Cardiology Task Force on Clinical Expert Consensus Documents. J Am Coll Cardiol. 2001;37(5):1478–92.
18. Garcia-Garcia HM, et al. IVUS-based imaging modalities for tissue characterization: similarities and differences. Int J Cardiovasc Imaging. 2011; 27(2):215–24.
19. Gussenhoven WJ, et al. Intravascular echographic assessment of vessel wall characteristics: a correlation with histology. Int J Card Imaging. 1989; 4(2–4):105–16.
20. Nishimura RA, et al. Intravascular ultrasound imaging: in vitro validation and pathologic correlation. J Am Coll Cardiol. 1990;16(1):145–54.
21. Nissen SE, Yock P. Intravascular ultrasound: novel pathophysiological insights and current clinical applications. Circulation. 2001;103(4):604–16.
22. McDaniel MC, et al. Contemporary clinical applications of coronary intravascular ultrasound. JACC Cardiovasc Interv. 2011;4(11):1155–67.
23. ten Hoff H, et al. Imaging artifacts in mechanically driven ultrasound catheters. Int J Card Imaging. 1989;4(2–4):195–9.
24. Sipahi I, Nicholls SJ, Tuzcu EM. Intravascular ultrasound in the current percutaneous coronary intervention era. Cardiol Clin. 2006;24(2):163–73. v.
25. Mintz GS, et al. Impact of preintervention intravascular ultrasound imaging on transcatheter treatment strategies in coronary artery disease. Am J Cardiol. 1994;73(7):423–30.
26. Tobis J, Azarbal B, Slavin L. Assessment of intermediate severity coronary lesions in the catheterization laboratory. J Am Coll Cardiol. 2007;49(8): 839–48.
27. Kern MJ, Samady H. Current concepts of integrated coronary physiology in the catheterization laboratory. J Am Coll Cardiol. 2010;55(3):173–85.
28. Kern MJ, et al. Physiological assessment of coronary artery disease in the cardiac catheterization laboratory: a scientific statement from the American Heart Association Committee on Diagnostic and Interventional Cardiac Catheterization, Council on Clinical Cardiology. Circulation. 2006;114(12): 1321–41.
29. Abizaid A, et al. Clinical, intravascular ultrasound, and quantitative angiographic determinants of the coronary flow reserve before and after percutaneous transluminal coronary angioplasty. Am J Cardiol. 1998;82(4):423–8.
30. Nishioka T, et al. Clinical validation of intravascular ultrasound imaging for assessment of coronary stenosis severity: comparison with stress myocardial perfusion imaging. J Am Coll Cardiol. 1999;33(7):1870–8.
31. Abizaid AS, et al. Long-term follow-up after percutaneous transluminal coronary angioplasty was not performed based on intravascular ultrasound findings: importance of lumen dimensions. Circulation. 1999;100(3):256–61.
32. Koo BK, et al. Optimal intravascular ultrasound criteria and their accuracy for defining the functional significance of intermediate coronary stenoses of different locations. JACC Cardiovasc Interv. 2011; 4(7):803–11.
33. Kang SJ, et al. Usefulness of minimal luminal coronary area determined by intravascular ultrasound to predict functional significance in stable and unstable angina pectoris. Am J Cardiol. 2012;109(7):947–53.
34. Ben-Dor I, et al. Intravascular ultrasound lumen area parameters for assessment of physiological ischemia by fractional flow reserve in intermediate coronary artery stenosis. Cardiovasc Revasc Med. 2012;13(3):177–82.
35. Lee CH. Intravascular ultrasound guided percutaneous coronary intervention: a practical approach. J Interv Cardiol. 2012;25(1):86–94.
36. Fisher LD, et al. Reproducibility of coronary arteriographic reading in the coronary artery surgery study (CASS). Cathet Cardiovasc Diagn. 1982;8(6): 565–75.
37. Isner JM, et al. Accuracy of angiographic determination of left main coronary arterial narrowing. Angiographic–histologic correlative analysis in 28 patients. Circulation. 1981;63(5):1056–64.
38. Jasti V, et al. Correlations between fractional flow reserve and intravascular ultrasound in patients with an ambiguous left main coronary artery stenosis. Circulation. 2004;110(18):2831–6.
39. de la Torre Hernandez JM, et al. Prospective application of pre-defined intravascular ultrasound criteria for assessment of intermediate left main coronary artery lesions results from the multicenter LITRO study. J Am Coll Cardiol. 2011;58(4):351–8.
40. Fassa AA, et al. Intravascular ultrasound-guided treatment for angiographically indeterminate left main coronary artery disease: a long-term follow-up study. J Am Coll Cardiol. 2005;45(2):204–11.
41. Levine GN, et al. ACCF/AHA/SCAI Guideline for Percutaneous Coronary Intervention. A report of the American College of Cardiology Foundation/ American Heart Association Task Force on Practice Guidelines and the Society for Cardiovascular Angiography and Interventions. J Am Coll Cardiol. 2011;58(24):e44–122.

42. Garg S, Serruys PW. Coronary stents: current status. J Am Coll Cardiol. 2010;56(10 Suppl):S1–42.
43. Kang SJ, et al. Intravascular ultrasound assessment of distal left main bifurcation disease: The importance of the polygon of confluence of the left main, left anterior descending, and left circumflex arteries. Catheter Cardiovasc Interv. 2013;82(5):737–45.
44. Sonoda S, et al. Impact of final stent dimensions on long-term results following sirolimus-eluting stent implantation: serial intravascular ultrasound analysis from the sirius trial. J Am Coll Cardiol. 2004; 43(11):1959–63.
45. Sakurai R, et al. Predictors of edge stenosis following sirolimus-eluting stent deployment (a quantitative intravascular ultrasound analysis from the SIRIUS trial). Am J Cardiol. 2005;96(9):1251–3.
46. Palmerini T, et al. Percutaneous revascularization of left main: role of imaging, techniques, and adjunct pharmacology. Catheter Cardiovasc Interv. 2012; 79(6):990–9.
47. Park SJ, et al. Elective stenting of unprotected left main coronary artery stenosis: effect of debulking before stenting and intravascular ultrasound guidance. J Am Coll Cardiol. 2001;38(4):1054–60.
48. Takagi T, et al. Results and long-term predictors of adverse clinical events after elective percutaneous interventions on unprotected left main coronary artery. Circulation. 2002;106(6):698–702.
49. Anderson HV, et al. A contemporary overview of percutaneous coronary interventions. The American College of Cardiology-National Cardiovascular Data Registry (ACC-NCDR). J Am Coll Cardiol. 2002;39(7):1096–103.
50. Park SJ, et al. Impact of intravascular ultrasound guidance on long-term mortality in stenting for unprotected left main coronary artery stenosis. Circ Cardiovasc Interv. 2009;2(3):167–77.
51. Park SJ, et al. Randomized trial of stents versus bypass surgery for left main coronary artery disease. N Engl J Med. 2011;364(18):1718–27.
52. Kang SJ, et al. Effect of intravascular ultrasound findings on long-term repeat revascularization in patients undergoing drug-eluting stent implantation for severe unprotected left main bifurcation narrowing. Am J Cardiol. 2011;107(3):367–73.
53. Kang SJ, et al. Comprehensive intravascular ultrasound assessment of stent area and its impact on restenosis and adverse cardiac events in 403 patients with unprotected left main disease. Circ Cardiovasc Interv. 2011;4(6):562–9.
54. Laskey WK, et al. Intravascular ultrasonographic assessment of the results of coronary artery stenting. Am Heart J. 1993;125(6):1576–83.
55. Mintz GS, et al. Intravascular ultrasound evaluation of the effect of rotational atherectomy in obstructive atherosclerotic coronary artery disease. Circulation. 1992;86(5):1383–93.
56. Potkin BN, et al. Arterial responses to balloon coronary angioplasty: an intravascular ultrasound study. J Am Coll Cardiol. 1992;20(4):942–51.
57. de Lezo Suarez J, et al. Intracoronary ultrasound assessment of directional coronary atherectomy: immediate and follow-up findings. J Am Coll Cardiol. 1993;21(2):298–307.
58. Costa MA, et al. Three dimensional intravascular ultrasonic assessment of the local mechanism of restenosis after balloon angioplasty. Heart. 2001;85(1):73–9.
59. Fuessl RT, Hoepp HW, Sechtem U. Intravascular ultrasonography in the evaluation of results of coronary angioplasty and stenting. Curr Opin Cardiol. 1999;14(6):471–9.
60. Costa MA, Simon DI. Molecular basis of restenosis and drug-eluting stents. Circulation. 2005;111(17): 2257–73.
61. Hoffmann R, et al. Patterns and mechanisms of in-stent restenosis. A serial intravascular ultrasound study. Circulation. 1996;94(6):1247–54.
62. Mintz GS, et al. Intravascular ultrasound to discern device-specific effects and mechanisms of restenosis. Am J Cardiol. 1996;78(3A):18–22.
63. Orford JL, Lerman A, Holmes DR. Routine intravascular ultrasound guidance of percutaneous coronary intervention: a critical reappraisal. J Am Coll Cardiol. 2004;43(8):1335–42.
64. Nakamura S, et al. Intracoronary ultrasound observations during stent implantation. Circulation. 1994; 89(5):2026–34.
65. Colombo A, et al. Intracoronary stenting without anticoagulation accomplished with intravascular ultrasound guidance. Circulation. 1995;91(6):1676–88.
66. Stone GW, et al. Improved procedural results of coronary angioplasty with intravascular ultrasound-guided balloon sizing: the CLOUT Pilot Trial. Clinical Outcomes With Ultrasound Trial (CLOUT) Investigators. Circulation. 1997;95(8):2044–52.
67. Frey AW, et al. Ultrasound-guided strategy for provisional stenting with focal balloon combination catheter: results from the randomized Strategy for Intracoronary Ultrasound-guided PTCA and Stenting (SIPS) trial. Circulation. 2000;102(20):2497–502.
68. Schiele F, et al. Intravascular ultrasound-guided balloon angioplasty compared with stent: immediate and 6-month results of the multicenter, randomized Balloon Equivalent to Stent Study (BEST). Circulation. 2003;107(4):545–51.
69. de Jaegere P, et al. Intravascular ultrasound-guided optimized stent deployment. Immediate and 6 months clinical and angiographic results from the Multicenter Ultrasound Stenting in Coronaries Study (MUSIC Study). Eur Heart J. 1998;19(8):1214–23.
70. Fitzgerald PJ, et al. Final results of the Can Routine Ultrasound Influence Stent Expansion (CRUISE) study. Circulation. 2000;102(5):523–30.
71. Kasaoka S, et al. Angiographic and intravascular ultrasound predictors of in-stent restenosis. J Am Coll Cardiol. 1998;32(6):1630–5.
72. Russo RJ, et al. A randomized controlled trial of angiography versus intravascular ultrasound-directed bare-metal coronary stent placement (the AVID Trial). Circ Cardiovasc Interv. 2009;2(2):113–23.

73. Mudra H, et al. Randomized comparison of coronary stent implantation under ultrasound or angiographic guidance to reduce stent restenosis (OPTICUS Study). Circulation. 2001;104(12):1343–9.
74. Oemrawsingh PV, et al. Intravascular ultrasound guidance improves angiographic and clinical outcome of stent implantation for long coronary artery stenoses: final results of a randomized comparison with angiographic guidance (TULIP Study). Circulation. 2003;107(1):62–7.
75. Schiele F, et al. Impact of intravascular ultrasound guidance in stent deployment on 6-month restenosis rate: a multicenter, randomized study comparing two strategies—with and without intravascular ultrasound guidance. RESIST Study Group. REStenosis after Ivus guided STentin. J Am Coll Cardiol. 1998;32(2):320–8.
76. Moussa I, et al. Does the specific intravascular ultrasound criterion used to optimize stent expansion have an impact on the probability of stent restenosis? Am J Cardiol. 1999;83(7):1012–7.
77. Hoffmann R, et al. Intravascular ultrasound predictors of angiographic restenosis in lesions treated with Palmaz-Schatz stents. J Am Coll Cardiol. 1998;31(1):43–9.
78. de Feyter PJ, et al. Reference chart derived from post-stent-implantation intravascular ultrasound predictors of 6-month expected restenosis on quantitative coronary angiography. Circulation. 1999; 100(17):1777–83.
79. Uren NG, et al. Predictors and outcomes of stent thrombosis: an intravascular ultrasound registry. Eur Heart J. 2002;23(2):124–32.
80. Moussa I, et al. Subacute stent thrombosis in the era of intravascular ultrasound-guided coronary stenting without anticoagulation: frequency, predictors and clinical outcome. J Am Coll Cardiol. 1997;29(1):6–12.
81. Parise H, et al. Meta-analysis of randomized studies comparing intravascular ultrasound versus angiographic guidance of percutaneous coronary intervention in pre-drug-eluting stent era. Am J Cardiol. 2011;107(3):374–82.
82. Abizaid A, et al. Sirolimus-eluting stents inhibit neointimal hyperplasia in diabetic patients. Insights from the RAVEL Trial. Eur Heart J. 2004;25(2): 107–12.
83. Colombo A, et al. Randomized study to assess the effectiveness of slow- and moderate-release polymer-based paclitaxel-eluting stents for coronary artery lesions. Circulation. 2003;108(7):788–94.
84. Serruys PW, et al. Intravascular ultrasound findings in the multicenter, randomized, double-blind RAVEL (RAndomized study with the sirolimus-eluting VElocity balloon-expandable stent in the treatment of patients with de novo native coronary artery Lesions) trial. Circulation. 2002;106(7):798–803.
85. Silber S, et al. Final 5-year results of the TAXUS II trial: a randomized study to assess the effectiveness of slow- and moderate-release polymer-based paclitaxel-eluting stents for de novo coronary artery lesions. Circulation. 2009;120(15):1498–504.
86. Burke SE, et al. Neointimal formation after balloon-induced vascular injury in Yucatan minipigs is reduced by oral rapamycin. J Cardiovasc Pharmacol. 1999;33(6):829–35.
87. Poon M, et al. Rapamycin inhibits vascular smooth muscle cell migration. J Clin Invest. 1996;98(10): 2277–83.
88. Serruys PW, Daemen J. Are drug-eluting stents associated with a higher rate of late thrombosis than bare metal stents? Late stent thrombosis: a nuisance in both bare metal and drug-eluting stents. Circulation. 2007;115(11):1433–9. discussion 1439.
89. Fujii K, et al. Stent underexpansion and residual reference segment stenosis are related to stent thrombosis after sirolimus-eluting stent implantation: an intravascular ultrasound study. J Am Coll Cardiol. 2005;45(7):995–8.
90. Liu X, et al. A volumetric intravascular ultrasound comparison of early drug-eluting stent thrombosis versus restenosis. JACC Cardiovasc Interv. 2009; 2(5):428–34.
91. Okabe T, et al. Intravascular ultrasound parameters associated with stent thrombosis after drug-eluting stent deployment. Am J Cardiol. 2007;100(4):615–20.
92. Alfonso F, et al. Intravascular ultrasound findings during episodes of drug-eluting stent thrombosis. J Am Coll Cardiol. 2007;50(21):2095–7.
93. Takebayashi H, et al. Intravascular ultrasound assessment of lesions with target vessel failure after sirolimus-eluting stent implantation. Am J Cardiol. 2005;95(4):498–502.
94. Vautrin E, et al. Very late stent thrombosis after drug eluting stent: management therapy guided by intravascular ultrasound imaging. Int J Cardiol. 2012; 154(3):349–51.
95. Cheneau E, et al. Predictors of subacute stent thrombosis: results of a systematic intravascular ultrasound study. Circulation. 2003;108(1):43–7.
96. Mintz GS. Features and parameters of drug-eluting stent deployment discoverable by intravascular ultrasound. Am J Cardiol. 2007;100(8B):26M–35.
97. Mintz GS. What to do about late incomplete stent apposition? Circulation. 2007;115(18):2379–81.
98. Cook S, et al. Incomplete stent apposition and very late stent thrombosis after drug-eluting stent implantation. Circulation. 2007;115(18):2426–34.
99. Siqueira DA, et al. Late incomplete apposition after drug-eluting stent implantation: incidence and potential for adverse clinical outcomes. Eur Heart J. 2007;28(11):1304–9.
100. Jimenez-Quevedo P, et al. Vascular effects of sirolimus-eluting versus bare-metal stents in diabetic patients: three-dimensional ultrasound results of the Diabetes and Sirolimus-Eluting Stent (DIABETES) Trial. J Am Coll Cardiol. 2006;47(11):2172–9.
101. Ako J, et al. Late incomplete stent apposition after sirolimus-eluting stent implantation: a serial intravascular ultrasound analysis. J Am Coll Cardiol. 2005;46(6):1002–5.
102. Kimura M, et al. Outcome after acute incomplete sirolimus-eluting stent apposition as assessed by

serial intravascular ultrasound. Am J Cardiol. 2006; 98(4):436–42.
103. Degertekin M, et al. Long-term follow-up of incomplete stent apposition in patients who received sirolimus-eluting stent for de novo coronary lesions: an intravascular ultrasound analysis. Circulation. 2003;108(22):2747–50.
104. Cook S, et al. Impact of incomplete stent apposition on long-term clinical outcome after drug-eluting stent implantation. Eur Heart J. 2012;33(11):1334–43.
105. Roy P, et al. The potential clinical utility of intravascular ultrasound guidance in patients undergoing percutaneous coronary intervention with drug-eluting stents. Eur Heart J. 2008;29(15):1851–7.
106. Claessen BE, et al. Impact of intravascular ultrasound imaging on early and late clinical outcomes following percutaneous coronary intervention with drug-eluting stents. JACC Cardiovasc Interv. 2011; 4(9):974–81.
107. Hur SH, et al. Impact of intravascular ultrasound-guided percutaneous coronary intervention on long-term clinical outcomes in a real world population. Catheter Cardiovasc Interv. 2013;81(3):407–16.
108. Colombo A. AVIO: a prospective, randomized trial of intravascular-ultrasound guided compared to angiography guided stent implantation in complex coronary lesions. in transcatheter cardiovascular therapeutics. 2010. Washington DC, USA.
109. Hausmann D, et al. The safety of intracoronary ultrasound. A multicenter survey of 2207 examinations. Circulation. 1995;91(3):623–30.
110. Batkoff BW, Linker DT. Safety of intracoronary ultrasound: data from a Multicenter European Registry. Cathet Cardiovasc Diagn. 1996;38(3):238–41.
111. Bose D, von Birgelen C, Erbel R. Intravascular ultrasound for the evaluation of therapies targeting coronary atherosclerosis. J Am Coll Cardiol. 2007; 49(9):925–32.
112. Ramasubbu K, et al. Repeated intravascular ultrasound imaging in cardiac transplant recipients does not accelerate transplant coronary artery disease. J Am Coll Cardiol. 2003;41(10):1739–43.
113. Guedes A, et al. Long-term safety of intravascular ultrasound in nontransplant, nonintervened, atherosclerotic coronary arteries. J Am Coll Cardiol. 2005; 45(4):559–64.
114. Friedewald VE, et al. The editor's roundtable: atherosclerosis regression. Am J Cardiol. 2008;101(7): 967–74.
115. Varnava AM, Mills PG, Davies MJ. Relationship between coronary artery remodeling and plaque vulnerability. Circulation. 2002;105(8):939–43.
116. Kolodgie FD, et al. Intraplaque hemorrhage and progression of coronary atheroma. N Engl J Med. 2003;349(24):2316–25.
117. Galis ZS, Lessner SM. Will the real plaque vasculature please stand up? Why we need to distinguish the vasa plaquorum from the vasa vasorum. Trends Cardiovasc Med. 2009;19(3):87–94.
118. Nair A, et al. Coronary plaque classification with intravascular ultrasound radiofrequency data analysis. Circulation. 2002;106(17):2200–6.
119. Kawasaki M, et al. In vivo quantitative tissue characterization of human coronary arterial plaques by use of integrated backscatter intravascular ultrasound and comparison with angioscopic findings. Circulation. 2002;105(21):2487–92.
120. Kawasaki M, et al. Noninvasive quantitative tissue characterization and two-dimensional color-coded map of human atherosclerotic lesions using ultrasound integrated backscatter: comparison between histology and integrated backscatter images. J Am Coll Cardiol. 2001;38(2):486–92.
121. Nasu K, et al. Accuracy of in vivo coronary plaque morphology assessment: a validation study of in vivo virtual histology compared with in vitro histopathology. J Am Coll Cardiol. 2006;47(12):2405–12.
122. Garcia-Garcia HM, et al. Tissue characterisation using intravascular radiofrequency data analysis: recommendations for acquisition, analysis, interpretation and reporting. EuroIntervention. 2009;5(2):177–89.
123. Rodriguez-Granillo GA, et al. In vivo intravascular ultrasound-derived thin-cap fibroatheroma detection using ultrasound radiofrequency data analysis. J Am Coll Cardiol. 2005;46(11):2038–42.
124. Hong MK, et al. Comparison of virtual histology to intravascular ultrasound of culprit coronary lesions in acute coronary syndrome and target coronary lesions in stable angina pectoris. Am J Cardiol. 2007;100(6):953–9.
125. Nakamura T, et al. Plaque characteristics of the coronary segment proximal to the culprit lesion in stable and unstable patients. Clin Cardiol. 2009;32(8):E9–12.
126. Yamagishi M, et al. Morphology of vulnerable coronary plaque: insights from follow-up of patients examined by intravascular ultrasound before an acute coronary syndrome. J Am Coll Cardiol. 2000; 35(1):106–11.
127. Stone GW, et al. A prospective natural-history study of coronary atherosclerosis. N Engl J Med. 2011;364(3):226–35.
128. Kubo T, et al. The dynamic nature of coronary artery lesion morphology assessed by serial virtual histology intravascular ultrasound tissue characterization. J Am Coll Cardiol. 2010;55(15):1590–7.
129. Choi SH, et al. Emerging approaches for imaging vulnerable plaques in patients. Curr Opin Biotechnol. 2007;18(1):73–82.
130. Carlier SG, et al. Imaging of atherosclerosis. Elastography. J Cardiovasc Risk. 2002;9(5):237–45.
131. Suh WM, et al. Intravascular detection of the vulnerable plaque. Circ Cardiovasc Imaging. 2011;4(2): 169–78.
132. Vavuranakis M, et al. A new method for assessment of plaque vulnerability based on vasa vasorum imaging, by using contrast-enhanced intravascular ultrasound and differential image analysis. Int J Cardiol. 2008;130(1):23–9.

133. Vavuranakis M, et al. Contrast-enhanced intravascular ultrasound: combining morphology with activity-based assessment of plaque vulnerability. Expert Rev Cardiovasc Ther. 2007;5(5):917–25.
134. Carlier S, et al. Vasa vasorum imaging: a new window to the clinical detection of vulnerable atherosclerotic plaques. Curr Atheroscler Rep. 2005;7(2):164–9.
135. Doyley MM, et al. Advancing intravascular ultrasonic palpation toward clinical applications. Ultrasound Med Biol. 2001;27(11):1471–80.
136. Staub D, et al. Contrast-enhanced ultrasound imaging of the vasa vasorum: from early atherosclerosis to the identification of unstable plaques. JACC Cardiovasc Imaging. 2010;3(7):761–71.
137. von Birgelen C, et al. Relationship between cardiovascular risk as predicted by established risk scores versus plaque progression as measured by serial intravascular ultrasound in left main coronary arteries. Circulation. 2004;110(12):1579–85.
138. Nicholls SJ, et al. Intravascular ultrasound-derived measures of coronary atherosclerotic plaque burden and clinical outcome. J Am Coll Cardiol. 2010; 55(21):2399–407.
139. Tardif JC, et al. Effects of the acyl coenzyme A:cholesterol acyltransferase inhibitor avasimibe on human atherosclerotic lesions. Circulation. 2004; 110(21):3372–7.
140. Serruys PW, et al. Effects of the direct lipoprotein-associated phospholipase A(2) inhibitor darapladib on human coronary atherosclerotic plaque. Circulation. 2008;118(11):1172–82.
141. Nissen SE, et al. Effect of rimonabant on progression of atherosclerosis in patients with abdominal obesity and coronary artery disease: the STRADIVARIUS randomized controlled trial. JAMA. 2008;299(13): 1547–60.
142. Nissen SE, et al. Effect of torcetrapib on the progression of coronary atherosclerosis. N Engl J Med. 2007;356(13):1304–16.
143. Nissen SE, et al. Effect of recombinant ApoA-I Milano on coronary atherosclerosis in patients with acute coronary syndromes: a randomized controlled trial. JAMA. 2003;290(17):2292–300.
144. Nissen SE, et al. Effect of ACAT inhibition on the progression of coronary atherosclerosis. N Engl J Med. 2006;354(12):1253–63.
145. Nissen SE, et al. Effect of very high-intensity statin therapy on regression of coronary atherosclerosis: the ASTEROID trial. JAMA. 2006;295(13):1556–65.
146. Nissen SE, et al. Comparison of pioglitazone vs glimepiride on progression of coronary atherosclerosis in patients with type 2 diabetes: the PERISCOPE randomized controlled trial. JAMA. 2008;299(13): 1561–73.
147. Nissen SE, et al. Effect of intensive compared with moderate lipid-lowering therapy on progression of coronary atherosclerosis: a randomized controlled trial. JAMA. 2004;291(9):1071–80.
148. Nicholls SJ, et al. Effect of two intensive statin regimens on progression of coronary disease. N Engl J Med. 2011;365(22):2078–87.
149. Nissen SE, et al. Effect of antihypertensive agents on cardiovascular events in patients with coronary disease and normal blood pressure: the CAMELOT study: a randomized controlled trial. JAMA. 2004;292(18):2217–25.
150. Nasu K, et al. Effect of fluvastatin on progression of coronary atherosclerotic plaque evaluated by virtual histology intravascular ultrasound. JACC Cardiovasc Interv. 2009;2(7):689–96.
151. Hirohata A, et al. Impact of olmesartan on progression of coronary atherosclerosis a serial volumetric intravascular ultrasound analysis from the OLIVUS (impact of OLmesarten on progression of coronary atherosclerosis: evaluation by intravascular ultrasound) trial. J Am Coll Cardiol. 2010;55(10):976–82.
152. Nozue T, et al. Statin treatment for coronary artery plaque composition based on intravascular ultrasound radiofrequency data analysis. Am Heart J. 2012;163(2):191–9e1.
153. Li X, et al. High-resolution coregistered intravascular imaging with integrated ultrasound and optical coherence tomography probe. Appl Phys Lett. 2010; 97(13):133702.
154. Maehara A, Mintz GS, Weissman NJ. Advances in intravascular imaging. Circ Cardiovasc Interv. 2009; 2(5):482–90.
155. Bezerra HG, et al. Intracoronary optical coherence tomography: a comprehensive review clinical and research applications. JACC Cardiovasc Interv. 2009;2(11):1035–46.
156. Garg S, et al. First use in patients of a combined near infra-red spectroscopy and intra-vascular ultrasound catheter to identify composition and structure of coronary plaque. EuroIntervention. 2010;5(6):755–6.
157. Schultz CJ, et al. First-in-man clinical use of combined near-infrared spectroscopy and intravascular ultrasound: a potential key to predict distal embolization and no-reflow? J Am Coll Cardiol. 2010; 56(4):314.
158. Gardner CM, et al. Detection of lipid core coronary plaques in autopsy specimens with a novel catheter-based near-infrared spectroscopy system. JACC Cardiovasc Imaging. 2008;1(5):638–48.
159. Moreno PR, et al. Detection of lipid pool, thin fibrous cap, and inflammatory cells in human aortic atherosclerotic plaques by near-infrared spectroscopy. Circulation. 2002;105(8):923–7.
160. Halcox JP, et al. Prognostic value of coronary vascular endothelial dysfunction. Circulation. 2002;106(6): 653–8.
161. Schachinger V, Britten MB, Zeiher AM. Prognostic impact of coronary vasodilator dysfunction on adverse long-term outcome of coronary heart disease. Circulation. 2000;101(16):1899–906.
162. Al Suwaidi J, et al. Association between obesity and coronary atherosclerosis and vascular remodeling. Am J Cardiol. 2001;88(11):1300–3.
163. Puri R, et al. Coronary beta2-adrenoreceptors mediate endothelium-dependent vasoreactivity in humans: novel insights from an in vivo intravascular ultrasound study. Eur Heart J. 2012;33(4):495–504.

5 Monitoring the Progression and Regression of Coronary Atherosclerosis with Intravascular Ultrasound

Rishi Puri and Stephen J. Nicholls

Introduction

Atherosclerosis and its thrombotic complications remains the commonest cause of death in western societies [1]. This pattern of disease is soon to be replicated worldwide [2], due in part to the obesity epidemic and its related metabolic disorders [3]. HMG-CoA reductase inhibitors, or statins, remain the backbone of our treatment for atherosclerosis, with major benefits observed across many clinical trials powered for hard clinical endpoints and burden of disease [4, 5]. Statins were introduced into clinical practice in the 1980s, and since then, a number of experimental anti-atherosclerotic compounds have reached phase 1–4 clinical trial evaluation in humans. Most, if not all of these compounds have either failed due to futility or toxicity. Hence, there remains a large unmet clinical need for the development of novel anti-atherosclerotic compounds to combat the residual risk of cardiovascular events observed despite statin therapy. In addition, current risk prediction algorithms are somewhat limited in their ability to deal with fluctuating, or modifiable risk factors, as well as novel and emerging biomarkers of risk. As such, considerable attention has focused on direct atherosclerosis imaging, as a complementary means of evaluating cardiovascular risk. This rationale stems from necropsy studies and a variety of vascular imaging modalities that show a strong, consistent association between a greater burden of atherosclerosis in those individuals succumbing to a cardiovascular event [6–11].

The last decade has been witness to the pertinent role of atherosclerosis imaging for providing mechanistic insights into the natural history of the disease process, as well as the utility of serial plaque quantification for measuring the efficacy of novel anti-atherosclerotic compounds. Intravascular ultrasound (IVUS), in particular, has evolved as an imaging modality that generates high-resolution, precise volumetric quantification of epicardial coronary atherosclerosis, the vascular bed responsible for a majority of the morbidity and mortality arising from atherosclerosis. By measuring the change in coronary atheroma volume over time, IVUS can evaluate the potential anti-atherosclerotic efficacy of interventions on plaque development. Clinical trials of this nature have served as gatekeepers, with the findings of plaque progression (or lack of regression) providing important information

R. Puri, MBBS, FRACP (✉)
Department of Cardiovascular Medicine,
CS Research Cleveland Clinic, 9500 Euclid Avenue,
Mail Code JJ65, Cleveland, OH 44195, USA

University of Adelaide, Adelaide, SA, Australia
e-mail: rishi_puri@hotmail.com; purir@ccf.org

S.J. Nicholls, MBBS, PhD, FRACP, FACC, FESC, FAHA, FCSANZ
South Australian Health and Medical Research Institute, Adelaide, SA, Australia

University of Adelaide, Adelaide, SA, Australia

Royal Adelaide Hospital, Adelaide, SA, Australia
e-mail: stephen.nicholls@sahmri.com

S.J. Nicholls and T. Crowe (eds.), *Imaging Coronary Atherosclerosis*, Contemporary Cardiology,
DOI 10.1007/978-1-4939-0572-0_5, © Springer Science+Business Media New York 2014

regarding mechanistic efficacy of the studied compound. Lack of efficacy observed in such imaging trials, allows the drug-developer to halt the development program of the studied compound, not only saving millions of dollars, but most importantly, preventing the public from being exposed to a futile or unsafe compound. On the other hand, proof of a compounds mechanistic efficacy and safety provides a supportive signal to further invest in a large-scale clinical trial to test the clinical efficacy of a compound. With ongoing technological advancements in plaque imaging, there remains significant interest in the role that IVUS and affiliated intravascular imaging technologies will play in drug development programs, as well as improving our understanding of the serial behavior of potential high-risk, unstable plaques in at-risk patients.

Angiographic Plaque Imaging

For over 50 years, angiography has been the preferred imaging modality for the detection of atherosclerosis within the coronary vasculature. It remains fundamental for clinical decision making and guiding PCI within patients with symptomatic coronary artery disease. Coronary angiography has provided us with important insights into the temporal behavior of complex coronary lesions identified during acute infarct angioplasty [12]. Earlier studies also showed that the number of diseased vessels on angiography predicted clinical outcome [13]. However, the angiographic severity of lesions detected via coronary angiography has not been shown to be an accurate predictor of future ischemic coronary events [14, 15]. Angiography is simply a 2-dimensional (2D) lumen-based imaging modality that fails to directly image plaque. Given that angiography detects luminal encroachment of plaque (percent stenosis) expressed in proportion to the lumen diameter of an apparently normal reference segment (which itself may contain a substantial amount of plaque), angiography typically underestimates the true amount of plaque present [16]. Although angiography has been utilized in clinical trials to evaluate the effects of medical therapies, its indirect approach to atherosclerosis imaging has limited the justification to use this modality for quantifying changes in disease burden [17].

Intravascular Ultrasound

IVUS is a high-frequency imaging modality that provides high-resolution, cross-sectional, topographic images of the vascular lumen and each component of the vessel wall. IVUS has provided a unique insight into the burden and distribution of atherosclerotic plaque, allowing for a comprehensive characterization of the vessel wall, demonstrating the ubiquitous presence of plaque in regions that appear normal on angiography [18] (Fig. 5.1). This phenomenon has been explained by the ability of the artery (as determined by IVUS) to adapt to plaque accumulation within the vessel wall in order to preserve lumen encroachment—which is termed "adaptive" or "positive" remodeling [19]. Originally described by Glagov and colleagues following analysis of arterial necropsy specimens [20], IVUS has accurately characterized patterns of coronary arterial remodeling in vivo. Luminal dimensions are typically preserved via the expansion of the external elastic membrane (EEM) in response to atheroma formation within the arterial wall. As a result, a significant amount of atheroma can accumulate within the arterial wall without angiographic evidence of a significant stenosis. Angiographic-detected stenoses (lumen constriction) typically appear once a substantial amount of atheroma has accumulated within the arterial wall. In addition, the EEM can constrict in response to atheroma accumulation, further compromising luminal dimensions. This response has been termed negative (or "constrictive") remodeling. Indeed, the dynamic nature of the arterial wall in response to atheroma burden may play an important role in the propensity of particular plaque segments to undergo biological transformations that result in a corresponding clinical syndrome [21].

The high-resolution images attained from IVUS allow for the accurate identification of the lumen–plaque (or lumen–intima) interface, as

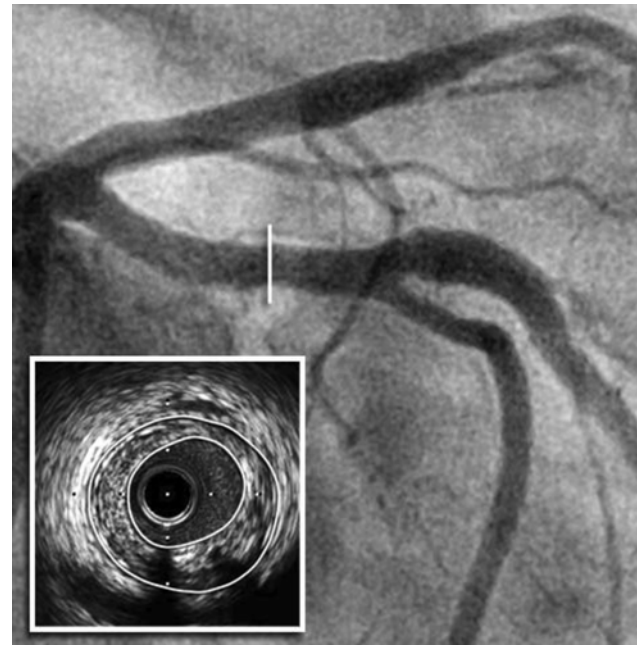

Fig. 5.1 IVUS-derived plaque evident in angiographically normal segments. A coronary angiogram showing minimal atherosclerotic disease within the mid portion of the left circumflex artery. *Inset* shows the corresponding IVUS cross-sectional view highlighting significant plaque burden (Adapted from Puri R, Tuzcua EM, Nissen SE, et al. Exploring coronary atherosclerosis with intravascular imaging. Int J Cardiol. 2013. doi.org/10.1016/j.ijcard.2013.03.024. With permission from Elsevier)

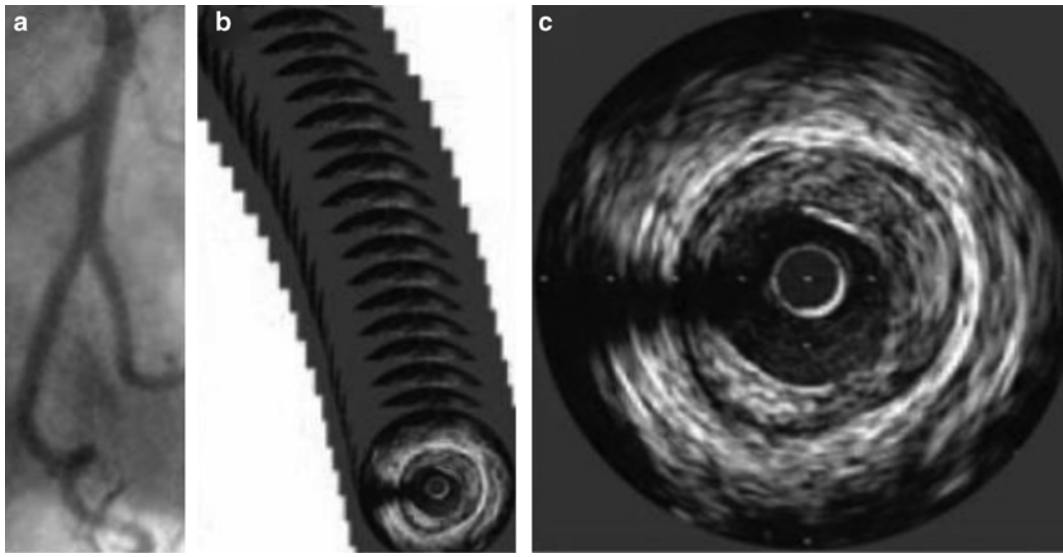

Fig. 5.2 Generation of images by intravascular ultrasound. Pullback of the ultrasound transducer through the artery (**a**) generates a series of tomographic images (**b**). Images separated by 1-mm intervals are then used for measurements (**c**) (Adapted from Nicholls SJ, Sipahi I, Schoenhagen P, et al. Application of intravascular ultrasound in anti-atherosclerotic drug development. Nat Rev Drug Discov. 2006;5(6):485–92. With permission from Nature Publishing Group)

well as the EEM. Allowing for the negligible thickness of the media, guidelines issued by the American College of Cardiology and European Society of Cardiology have endorsed the calculation of the area between the EEM and lumen edges as being the area occupied by plaque [22]. A constant automated transducer pull-back speed permits the volumetric quantification of atheroma burden with IVUS (Figs. 5.2 and 5.3). The ability to image anatomically matched arterial

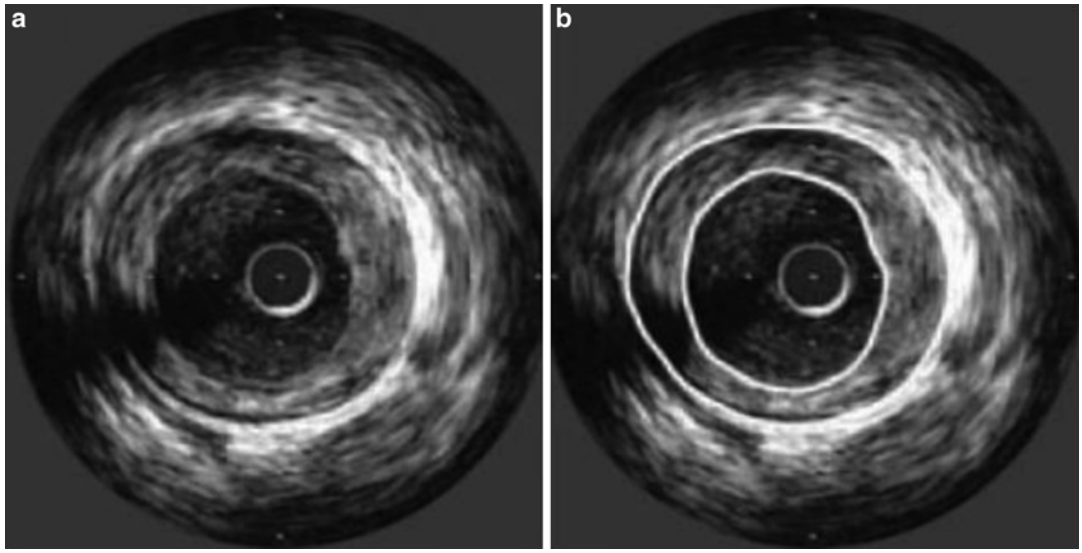

Fig. 5.3 Images from intravascular ultrasound. (**a**) Representative example of a cross-sectional tomographic image of a coronary artery acquired by intravascular ultrasound. (**b**) The panel illustrates the standard measurements that are made by manual planimetry of the leading edges of the external elastic membrane (*outer circle*) and lumen (*inner circle*). The area between these leading edges represents the plaque area (Adapted from Nicholls SJ, Sipahi I, Schoenhagen P, et al. Application of intravascular ultrasound in anti-atherosclerotic drug development. Nat Rev Drug Discov. 2006;5(6):485–92. With permission from Nature Publishing Group)

segments at different time points also provided the opportunity to accurately measure the effect of various therapeutic strategies on disease progression (Fig. 5.4).

A number of experimental models and serial imaging studies in humans had previously suggested that atherosclerosis is a potentially reversible disease. In turn, numerous studies have been designed to assess the impact of favorably modifying one or more of the known traditional cardiovascular risk factors and the resulting influence upon the natural history of coronary atherosclerotic plaque. As a result, several drug classes have been tested in large-scale trials to determine whether they can halt the progression of atherosclerosis. A number of these trials have employed IVUS to detect changes in atheroma burden.

Low-Density Lipoprotein Cholesterol and Atherosclerosis Progression

Lowering serum low-density lipoprotein cholesterol (LDL-C) levels with statins has known anti-atherosclerotic effects, demonstrated in large-scale atherosclerosis imaging trials [5, 23–25], which support the consistent findings of reductions in hard clinical endpoints in both primary [26–28] and secondary disease prevention [29–33]. Most notably, these clinical benefits appear most pronounced in the setting of intensive LDL-C lowering [4]. However the precise mechanism(s) as to how statin therapy contributes to these benefits remains unclear. The degree of atheroma regression appears more modest than the magnitude of clinical benefit accrued from statins, as well as the residual burden of disease that persists during therapy. Prior angiographic studies had not shown consistent atherosclerosis regression with statin monotherapy to corroborate the profound impact that statin therapy had shown upon clinical event rates. With the known limitations of angiography in mind, trials were designed to test the hypothesis that intensive LDL-C lowering with statins would significantly alter the rate of coronary atheroma progression evaluated with serial IVUS.

A consistent observation in IVUS trials is the linear relationship between mean LDL-C levels achieved on statin therapy and the median

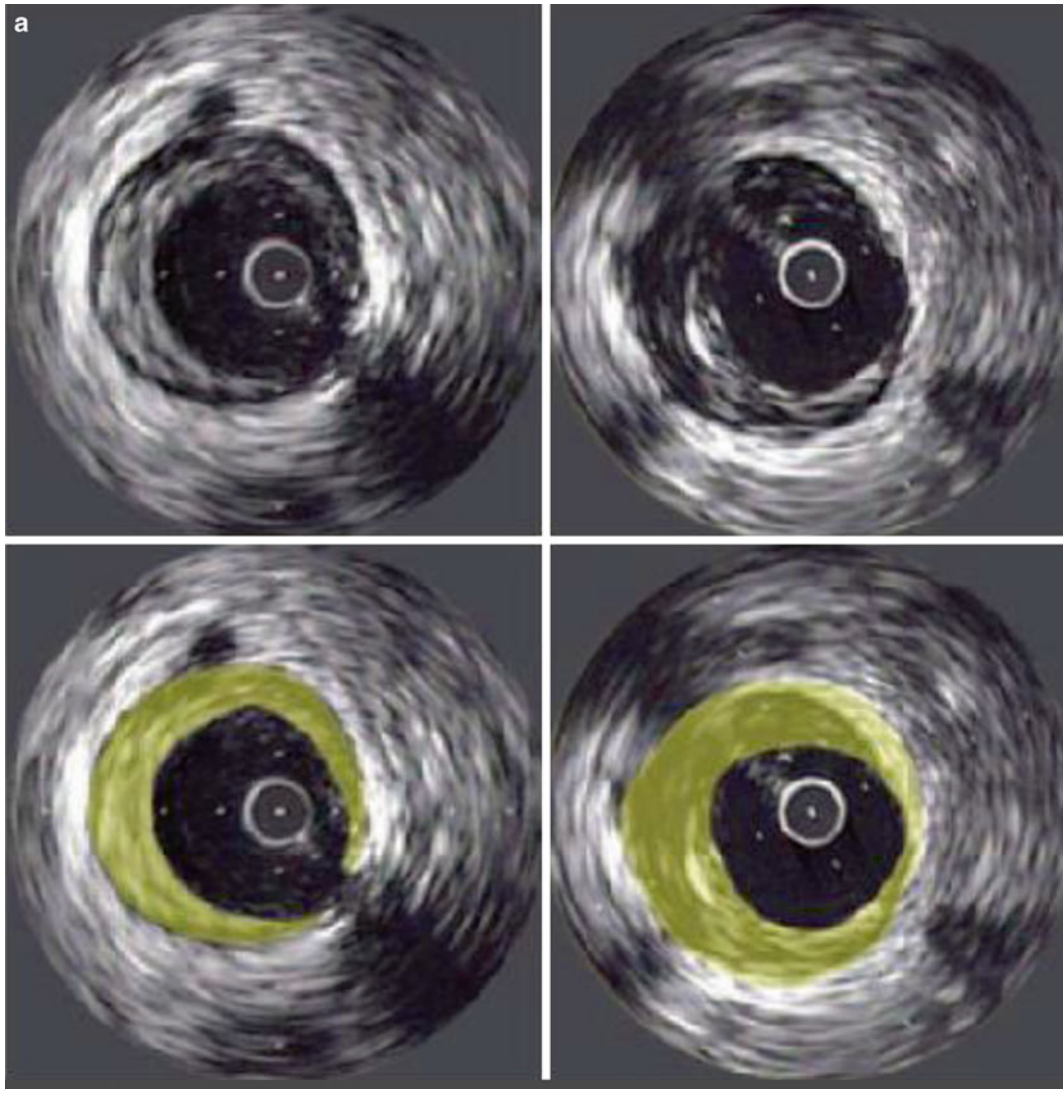

Fig. 5.4 Plaque progression and regression assessed by intravascular ultrasound. (**a**) Illustrative example of plaque progression at a matched site from IVUS studies performed in the same arterial segment a baseline (*left panels*) and follow-up (*right panels*).(**b**) Illustrative example of plaque regression at a matched site from IVUS studies performed in the same arterial segment at baseline (*left panels*) and follow-up (*right panels*). The shading in the *lower panels* highlights the plaque area at each time point (Adapted from Nicholls SJ, Sipahi I, Schoenhagen P, et al. Application of intravascular ultrasound in anti-atherosclerotic drug development. Nat Rev Drug Discov. 2006;5(6):485–92. With permission from Nature Publishing Group)

progression–regression rate of atherosclerosis (Fig. 5.5). In the Reversing Atherosclerosis with Aggressive Lipid Lowering (REVERSAL) trial, 18 months of moderate LDL-C reduction (pravastatin 40 mg) resulting in a mean on-treatment LDL-C level of 110 mg/dL associated with significant disease progression [23]. Intensive LDL-C lowering (atorvastatin 80 mg) on the other hand, resulted in a mean on-treatment LDL-C level of 79 mg/dL, halting the natural progression of disease. Interestingly, despite there being a direct relationship between LDL-C lowering and slowing of disease progression, C-reactive protein lowering, a marker of systemic

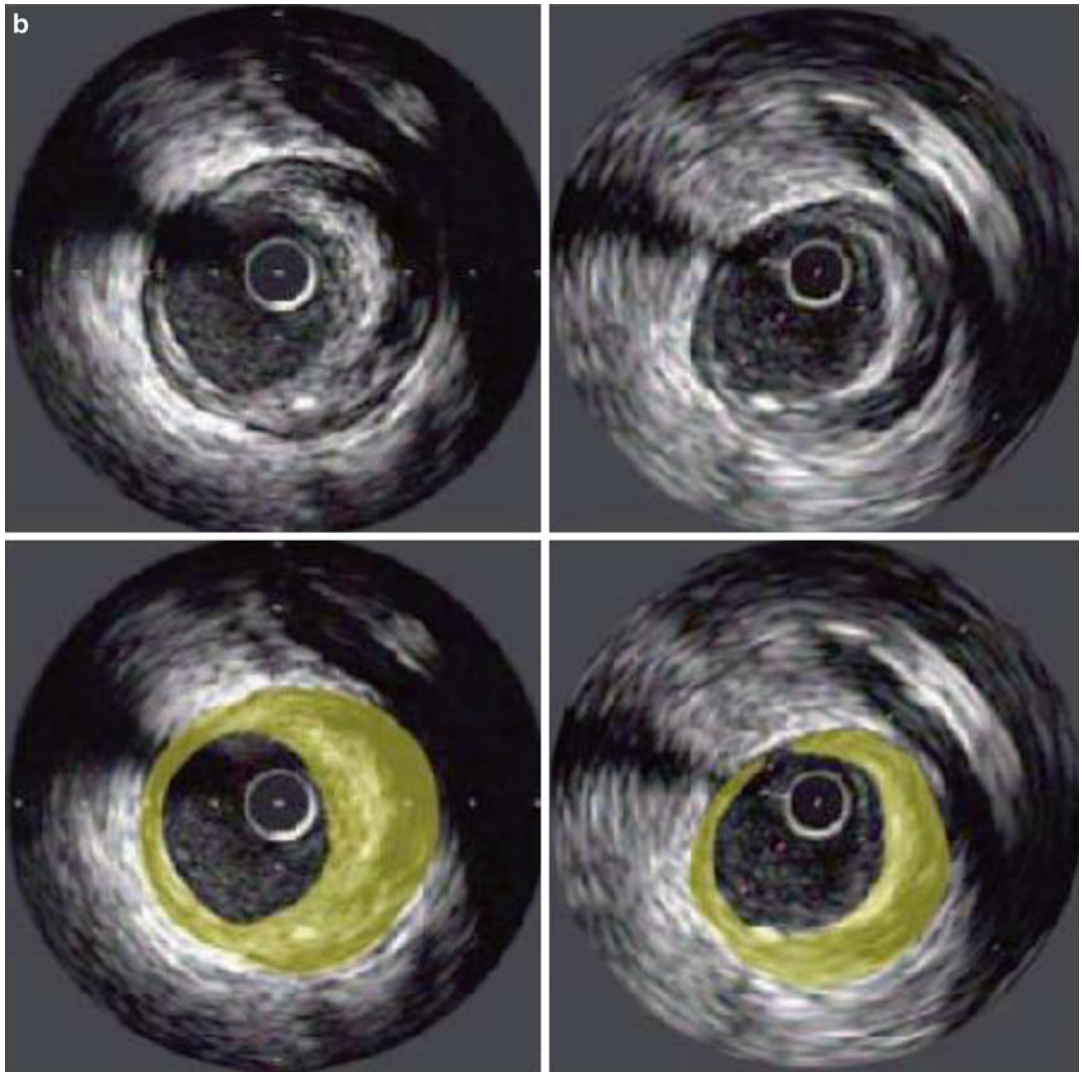

Fig.5.4 (continued)

inflammation, also independently associated with less disease progression [34]. This suggests that non-cholesterol mediated, or pleiotropic effects of statins, are likely to be important in mediating the progression of disease.

The ASTEROID (A study to evaluate the effect of rosuvastatin on IVUS-derived coronary atheroma burden) trial was designed to test the hypothesis that lowering LDL-C levels to below those achieved in REVERSAL might regress plaque. Unequivocal LDL-C reductions to a mean on-treatment level of 61 mg/dL were achieved with rosuvastatin 40 mg daily for 24 months. As predicted by the regression line, this degree of LDL-C lowering associated with significant plaque regression [24]. On the basis of these findings, SATURN (Study of Coronary Atheroma by Intravascular Ultrasound: Effect of Rosuvastatin Versus Atorvastatin) was performed to directly compare the anti-atherosclerotic efficacy of rosuvastatin 40 mg daily and atorvastatin 80 mg daily for 24 months [5]. Marked regression of coronary atherosclerosis was evident in each treatment group, following the

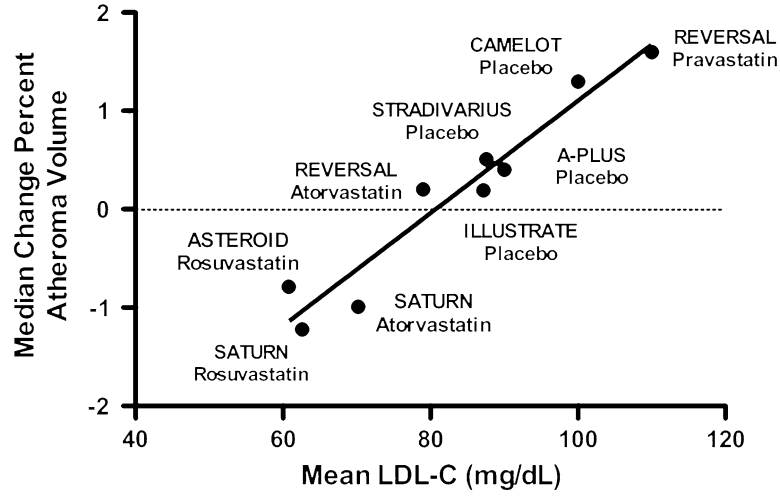

Fig. 5.5 The relationship between plaque regression and achieved LDL-C levels in clinical trials. Line of regression highlighting the relationship between on-treatment mean LDL-C vs. median change in atheroma volume (Adapted from Nicholls SJ, Ballantyne CM, Barter PJ, et al. Effect of Two Intensive Statin Regimens on Progression of Coronary Disease. N Eng J Med 2011;365:2078–87. With permission from Massachusetts Medical Society)

achievement of very low on-treatment LDL-C levels (62 mg/dL vs. 70 mg/dL) in the rosuvastatin and atorvastatin arms, respectively, with two-thirds of the SATURN population demonstrating disease regression. These findings highlight the benefit of high-intensity statin therapy in patients with coronary artery disease, particularly when achieved LDL-C levels are consistent with or lower than those recommended by current treatment guidelines [35, 36]. It remains to be seen however, whether a ceiling effect of the magnitude of plaque regression exists, or whether further degrees of regression are achievable when on-treatment LDL-C levels are driven below those achieved in SATURN. Clinical trials are currently underway to test this hypothesis. The finding that a proportion of individuals continue to demonstrate disease progression despite significant LDL-C lowering with high-intensity statin therapy also highlights the multifactorial nature of the disease process [37], the need to globally intensify risk-factor control in these patients, as well as the importance of identifying novel anti-atherosclerotic strategies to tackle the residual risk and disease burden following statin therapy.

High-Density Lipoprotein Cholesterol and Atherosclerosis Progression

A number of animal and population-based studies have demonstrated the protective effects of high-density lipoprotein cholesterol (HDL-C) [38, 39]. The inverse relationship between HDL-C levels and cardiovascular risk holds true even in the setting of very low LDL-C [40]. A meta-analysis of several trials that employed serial IVUS measures of coronary atheroma volume identified that plaque regression was most likely to occur in patients who, despite achieve LDL-C levels below 87.5 mg/dL, also experienced an increase in HDL-C from baseline of at least 7.5 % [41]. As a result, considerable attention has focused upon developing biological strategies of elevating HDL-C levels and/or promoting HDL particle functionality.

IVUS-based trials, that have tested the anti-atherosclerotic efficacy of direct HDL infusions in humans, have collectively demonstrated safety and potential benefit. Rapid and large amounts of coronary atheroma regression was demonstrated

in relatively few patients afflicted with acute coronary syndrome who underwent weekly intravenous infusions of reconstituted HDL, vs. placebo infusion, over a 5-week period [42]. Further analysis revealed that this degree of plaque regression occurred in concert with preservation of lumen size [43], indicative of reverse remodeling of the coronary arterial wall, most likely a result of rapid plaque delipidation. Similar, beneficial effects have been observed following infusion of apoA-1 particles or autologous, delipidated HDL particles [44, 45]. Whether these favorable effects upon the arterial wall will translate into clinical benefit, remains to be investigated.

The ability to substantially raise HDL-C levels stimulated enthusiasm for the development of cholesteryl ester transfer protein (CETP) inhibitors. This enzyme is responsible for the transfer of esterified cholesterol from HDL-C to atherogenic LDL-C particles in exchange for triglyceride [46]. This pathway seemed an attractive target, as inhibition of CETP would not only result in preventing the cholesterol enrichment of atherogenic lipoproteins, but also substantially raise HDL-C levels, with concomitant modest LDL-C lowering. To add support to this hypothesis, lower cardiovascular event rates have been observed in populations with a genetic predisposition for CETP inhibition, and elevated CETP levels associated with increasing risk of cardiovascular events [47, 48]. However, the first tested CETP inhibitor, torcetrapib, failed to alter the natural progression of coronary atherosclerosis [49], and a parallel run large-scale phase 4 clinical trial was prematurely terminated due to molecule-specific toxicity related to torcetrapib's activation of the renin–angiotensin–aldosterone system [50]. A post hoc analysis however, revealed that those with the highest achieved HDL-C levels demonstrated atheroma regression, indicative of intact HDL functionality in mobilizing lipid from the coronary arterial wall in such patients [51]. Next-generation CETP inhibitors are subsequently under clinical investigation.

Another therapeutic approach involving HDL is to promote the generation of functional HDL particles in vivo, via the up-regulation of endogenous hepatic ApoA-1 synthesis. The theory being that this would result in the generation of nascent HDL particles that would have the ability to undertake the variety of known anti-atherosclerotic functions of HDL, such as reverse cholesterol transport and anti-inflammatory effects. The implications of an oral ApoA-1 inducer (RVX-208) upon the progression of coronary plaque is currently being tested in a serial IVUS study called ASSURE (ApoA-1 Synthesis Stimulation and Intravascular Ultrasound for Coronary Atheroma Regression Evaluation) [52].

Blood Pressure

Little is known about the direct anti-atherosclerotic effects of systemic blood pressure lowering, with a study employing serial carotid intima-medial thickening measurements demonstrating attenuation of disease progression following commencement of antihypertensive therapy [53]. Contrary to current national blood pressure lowering guidelines, it remains unclear as to what the optimal or target blood pressure should be in patients afflicted with coronary artery disease. The Comparison of Amlodipine vs. Enalapril to Limit Occurrences of Thrombosis (CAMELOT) trial was designed to assess the effect of blood pressure reduction with amlodipine or enalapril (compared to placebo) in patients with coronary artery disease [54]. An embedded IVUS substudy within CAMELOT demonstrated that blood pressure lowering with amlodipine of the magnitude of 5/3 mmHg corroborated a halting of atheroma progression, compared with the placebo group whose atheroma burden progressed significantly. A further analyses revealed a direct relationship between the degree of systolic blood pressure lowering and plaque volume, with a trend towards plaque regression in patients with a systolic BP < 120 mmHg [55]. A post hoc analysis examined the effect of intensive control of both LDL and blood pressure upon atheroma progression in coronary artery disease patients. Patients with on-treatment serum LDL levels $\leq$70 mg/dL and systolic blood pressure $\leq$120 mmHg experienced less disease progression and more frequent atheroma regression [56]. These findings suggest

the need for such patients to have their blood pressure lowered to levels below those endorsed by current national blood pressure guidelines. As such, there is currently no consensus of the optimal blood pressure target in patients with demonstrable coronary disease, particularly when guidelines currently recommend a treatment goal of systolic blood pressure of <140 mmHg.

Diabetes and Obesity

As the incidence of diabetes mellitus continues to rise, parallel increases in the rates of diabetic atherosclerotic vascular disease are projected to impart major health and socioeconomic challenges for authorities worldwide. Atherosclerosis is the predominant disease phenotype in diabetic individuals, particularly within the coronary, cerebrovascular, and peripheral arterial territories. Diabetic individuals display progressive coronary atherosclerosis, despite LDL-C lowering [57], emphasizing the importance of evaluating novel therapies that reduce the burden and progression of diabetic atherosclerosis. Whilst controversy exists regarding the safety of rosiglitazone [58], IVUS has yielded important mechanistic insights into the anti-atherogenic effects of the PPAR-γ agonist pioglitazone in diabetic patients with coronary artery disease. PERISCOPE (Pioglitazone Effect on Regression of Intravascular Sonographic Coronary Obstruction Prospective Evaluation) was a trial that compared the effects of pioglitazone to the insulin secretagogue, glimepiride, upon atherosclerosis progression. The pioglitazone group demonstrated a significantly lower rate of plaque progression when compared to the glimepiride group, who demonstrated plaque progression. These results were supported by the clinical results from the PROACTIVE (Prospective Pioglitazone Clinical Trial In Macrovascular Events), a trial that demonstrated a reduction in hard clinical endpoints with pioglitazone [59].

The increasing prevalence of abdominal obesity is a major factor for the worldwide increase in metabolic syndrome, insulin resistance, and atherosclerotic cardiovascular disease. The Strategy To Reduce Atherosclerosis Development Involving Administration of Rimonabont—the Intravascular Ultrasound Study (STRADIVARIUS) tested the hypothesis that a medication that selectively antagonized the cannabinoid type 1 receptor over an 18-month period might reduce the progression of coronary artery disease in abdominally obese individuals with metabolic syndrome [60]. Rimonabant, however, had no significant effect upon the primary endpoint of change in percent atheroma volume (PAV) from baseline, but had a significant effect on the secondary endpoint, reduction of total atheroma volume (TAV). More frequent psychiatric adverse effects were also reported in the rimonabont group, despite more favorable changes in HDL-C and triglyceride levels, weight loss, and waist circumference reduction compared to the placebo group. Nevertheless, the lack of an overt anti-atherosclerotic effect from rimonabont led to cessation of development of this compound.

Non-Lipid Plaque-Modifying Therapies

IVUS has also been instrumental in outlining the effects of non-lipid modifying compounds on plaque. Inhibition of acyl-coenzyme A:cholesterol acyltransferase (ACAT) promised to be an exciting therapeutic target. The lack of a direct effect on serum LDL-C or HDL-C concentrations made the dose-finding exercise of the potential anti-atherosclerotic effects of this class of compound difficult. Imaging endpoints were thus considered the most appropriate technique for demonstration of mechanistic efficacy. Despite demonstrative anti-atherosclerotic properties of ACAT inhibitors in animal models of disease, the failure to observe disease regression on serial IVUS with ACAT inhibition in two separate clinical trials resulted in halting the development programs of ACAT inhibitors [61, 62].

The mechanical strain of the arterial wall, coupled with local tissue deformation can be determined by the cross-correlation analysis of the radiofrequency IVUS signal, to derive localized strain maps of the arterial wall. The imputed

degree of radial strain can be incorporated within the plaque area to determine the local elastography of the segment, or upon the luminal boundary (to a depth of 450 μm) to determine the local palpography of the respective plaque segment. As such, these elastic properties of the coronary arterial wall have been proposed to predict plaque vulnerability [63]. Subsequently, the Integrated Biomarker and Imaging (IBIS-2) trial was designed to assess for changes in plaque deformability (utilizing IVUS-palpography) in response to the lipoprotein-associated phospholipase A2 inhibitor, darapladib [64]. This was the first drug-intervention trial designed to explore if a therapeutic intervention could modulate plaque composition, and subsequent plaque phenotype. Although it was postulated that darapladib would lower the deformability/strain of coronary atherosclerotic plaques, the results of this trial failed to show any overall significant effect of darapladib upon plaque mechanical strain, despite changes in atheroma composition, which was an exploratory endpoint. The total atheroma burden in the treatment group also remained unchanged, questioning the anti-atherosclerotic potential of this compound, although further clinical trials are currently underway to assess the anti-atherosclerotic and clinical efficacy of this compound.

Cardiac Allograft Vasculopathy

IVUS has also yielded significant insights into the pathogenesis and modulation of cardiac allograft vasculopathy, the single greatest determinant of allograft failure and overall mortality within this patient group. Moreover, serial IVUS imaging has been employed to assess the progression of cardiac allograft vasculopathy [65]. Everolimus-based immunosuppressive therapy following cardiac transplantation was demonstrated to show a beneficial impact upon the rate of progression of intimal thickening within cardiac allograft recipients [66]. Moreover, this was associated with fewer episodes of rejection and the need for repeat transplantation when compared to a standard azathioprine-based immunosuppressive regimen. A separate study identified the rate of intimal thickening seen on IVUS at the 1-year mark following cardiac transplantation to predict 5-year mortality [67].

Clinical Implications of the Burden and Plaque Progression–Regression on IVUS

Although IVUS has been instrumental in enabling us to determine the efficacy of anti-atherosclerotic strategies, the clinical relevance of such an approach lies in the ability to demonstrate an association between the burden of atherosclerotic disease, its rate of progression and subsequent clinical outcomes. A number of studies employing IVUS, that have either measured plaque burden of defined lesions in a non-volumetric fashion [68, 69], or via a volumetric analysis of whole vessel segments [10, 70], have described an association between IVUS-derived plaque burden and incident clinical events, driven largely by an increased risk of coronary revascularization. In addition, a pooled analysis revealed that the rate of progression of IVUS-derived plaque volume independently associated with the composite risk of death, myocardial infarction, and coronary revascularization [10]. Further studies, with larger numbers of enrolled patients, with longer duration of clinical follow-up, will be required to confirm these associations in a single trial.

Conclusions

IVUS-derived plaque burden and its rate of change are well-established imaging biomarkers used in clinical trials to test the efficacy of currently utilized and experimental anti-atherosclerotic therapies. Indeed, changes in plaque volume have been largely congruent to the clinical findings of experimental agents, such that IVUS-based trial results have been fundamental in determining the fate of these compounds. Serial coronary imaging with IVUS however, has affirmed the importance of stringent and global atherosclerosis risk-factor modification in order

to attenuate, and even regress the disease process. Further refinements in ultrasound technologies will enable enhanced plaque characterization, which will continue to promote the role of direct coronary imaging for not only future drug development programs, but also to better risk-stratify individuals. Whether this information will be strong enough to alter clinical practice remains to be seen.

References

1. Roger VL, Go AS, Lloyd-Jones DM, et al. Heart disease and stroke statistics–2012 update: a report from the American Heart Association. Circulation. 2012;125:e2–220.
2. Yusuf S, Reddy S, Ounpuu S, Anand S. Global burden of cardiovascular diseases: Part II: variations in cardiovascular disease by specific ethnic groups and geographic regions and prevention strategies. Circulation. 2001;104:2855–64.
3. Bandyopadhyay P. Cardiovascular diseases and diabetes mellitus. Drug News Perspect. 2006;19:369–75.
4. Baigent C, Blackwell L, Emberson J, et al. Efficacy and safety of more intensive lowering of LDL cholesterol: a meta-analysis of data from 170,000 participants in 26 randomised trials. Lancet. 2010;376: 1670–81.
5. Nicholls SJ, Ballantyne CM, Barter PJ, et al. Effect of two intensive statin regimens on progression of coronary disease. N Engl J Med. 2011;365:2078–87.
6. Cliff WJ, Heathcote CR, Moss NS, Reichenbach DD. The coronary arteries in cases of cardiac and noncardiac sudden death. Am J Pathol. 1988;132:319–29.
7. Dalager S, Falk E, Kristensen IB, Paaske WP. Plaque in superficial femoral arteries indicates generalized atherosclerosis and vulnerability to coronary death: an autopsy study. J Vasc Surg. 2008;47:296–302.
8. Ringqvist I, Fisher LD, Mock M, et al. Prognostic value of angiographic indices of coronary artery disease from the Coronary Artery Surgery Study (CASS). J Clin Invest. 1983;71:1854–66.
9. Lorenz MW, Markus HS, Bots ML, Rosvall M, Sitzer M. Prediction of clinical cardiovascular events with carotid intima-media thickness: a systematic review and meta-analysis. Circulation. 2007;115:459–67.
10. Nicholls SJ, Hsu A, Wolski K, et al. Intravascular ultrasound-derived measures of coronary atherosclerotic plaque burden and clinical outcome. J Am Coll Cardiol. 2010;55:2399–407.
11. Lin FY, Shaw LJ, Dunning AM, et al. Mortality risk in symptomatic patients with nonobstructive coronary artery disease: a prospective 2-center study of 2,583 patients undergoing 64-detector row coronary computed tomographic angiography. J Am Coll Cardiol. 2011;58:510–9.
12. Goldstein JA, Demetriou D, Grines CL, Pica M, Shoukfeh M, O'Neill WW. Multiple complex coronary plaques in patients with acute myocardial infarction. N Engl J Med. 2000;343:915–22.
13. Coronary artery surgery study (CASS): a randomized trial of coronary artery bypass surgery. Survival data. Circulation 1983;68:939–50.
14. Falk E, Shah PK, Fuster V. Coronary plaque disruption. Circulation. 1995;92:657–71.
15. Naghavi M, Libby P, Falk E, et al. From vulnerable plaque to vulnerable patient: a call for new definitions and risk assessment strategies: Part I. Circulation. 2003;108:1664–72.
16. Topol EJ, Nissen SE. Our preoccupation with coronary luminology. The dissociation between clinical and angiographic findings in ischemic heart disease. Circulation. 1995;92:2333–42.
17. Ballantyne CM. Clinical trial endpoints: angiograms, events, and plaque instability. Am J Cardiol. 1998;82: 5M–11.
18. Mintz GS, Painter JA, Pichard AD, et al. Atherosclerosis in angiographically "normal" coronary artery reference segments: an intravascular ultrasound study with clinical correlations. J Am Coll Cardiol. 1995;25:1479–85.
19. Schoenhagen P, Ziada KM, Vince DG, Nissen SE, Tuzcu EM. Arterial remodeling and coronary artery disease: the concept of "dilated" versus "obstructive" coronary atherosclerosis. J Am Coll Cardiol. 2001;38: 297–306.
20. Glagov S, Weisenberg E, Zarins CK, Stankunavicius R, Kolettis GJ. Compensatory enlargement of human atherosclerotic coronary arteries. N Engl J Med. 1987;316:1371–5.
21. Schoenhagen P, Ziada KM, Kapadia SR, Crowe TD, Nissen SE, Tuzcu EM. Extent and direction of arterial remodeling in stable versus unstable coronary syndromes : an intravascular ultrasound study. Circulation. 2000;101:598–603.
22. Mintz GS, Nissen SE, Anderson WD, et al. American College of Cardiology Clinical Expert Consensus Document on Standards for Acquisition, Measurement and Reporting of Intravascular Ultrasound Studies (IVUS). A report of the American College of Cardiology Task Force on Clinical Expert Consensus Documents. J Am Coll Cardiol. 2001;37:1478–92.
23. Nissen SE, Tuzcu EM, Schoenhagen P, et al. Effect of intensive compared with moderate lipid-lowering therapy on progression of coronary atherosclerosis: a randomized controlled trial. JAMA. 2004;291: 1071–80.
24. Nissen SE, Nicholls SJ, Sipahi I, et al. Effect of very high-intensity statin therapy on regression of coronary atherosclerosis: the ASTEROID trial. JAMA. 2006;295:1556–65.
25. Crouse 3rd JR, Raichlen JS, Riley WA, et al. Effect of rosuvastatin on progression of carotid intima-media thickness in low-risk individuals with subclinical atherosclerosis: the METEOR Trial. JAMA. 2007; 297:1344–53.

26. Shepherd J, Cobbe SM, Ford I, et al. Prevention of coronary heart disease with pravastatin in men with hypercholesterolemia. West of Scotland Coronary Prevention Study Group. N Engl J Med. 1995; 333:1301–7.
27. Ford I, Murray H, Packard CJ, Shepherd J, Macfarlane PW, Cobbe SM. Long-term follow-up of the West of Scotland Coronary Prevention Study. N Engl J Med. 2007;357:1477–86.
28. Ridker PM, Danielson E, Fonseca FA, et al. Rosuvastatin to prevent vascular events in men and women with elevated C-reactive protein. N Engl J Med. 2008;359:2195–207.
29. Randomised trial of cholesterol lowering in 4444 patients with coronary heart disease: the Scandinavian Simvastatin Survival Study (4S). Lancet 1994;344: 1383–9.
30. Prevention of cardiovascular events and death with pravastatin in patients with coronary heart disease and a broad range of initial cholesterol levels. The Long-Term Intervention with Pravastatin in Ischaemic Disease (LIPID) Study Group. N Engl J Med 1998; 339:1349–57.
31. MRC/BHF Heart Protection Study of cholesterol lowering with simvastatin in 20,536 high-risk individuals: a randomised placebo-controlled trial. Lancet 2002;360:7–22.
32. Sacks FM, Pfeffer MA, Moye LA, et al. The effect of pravastatin on coronary events after myocardial infarction in patients with average cholesterol levels. Cholesterol and Recurrent Events Trial investigators. N Engl J Med. 1996;335:1001–9.
33. LaRosa JC, Grundy SM, Waters DD, et al. Intensive lipid lowering with atorvastatin in patients with stable coronary disease. N Engl J Med. 2005;352:1425–35.
34. Nissen SE, Tuzcu EM, Schoenhagen P, et al. Statin therapy, LDL cholesterol, C-reactive protein, and coronary artery disease. N Engl J Med. 2005;352: 29–38.
35. Grundy SM, Cleeman JI, Merz CN, et al. Implications of recent clinical trials for the National Cholesterol Education Program Adult Treatment Panel III guidelines. Circulation. 2004;110:227–39.
36. Smith Jr SC, Benjamin EJ, Bonow RO, et al. AHA/ACCF secondary prevention and risk reduction therapy for patients with coronary and other atherosclerotic vascular disease: 2011 update: a guideline from the American Heart Association and American College of Cardiology Foundation endorsed by the World Heart Federation and the Preventive Cardiovascular Nurses Association. J Am Coll Cardiol. 2011;58:2432–46.
37. Bayturan O, Kapadia S, Nicholls SJ, et al. Clinical predictors of plaque progression despite very low levels of low-density lipoprotein cholesterol. J Am Coll Cardiol. 2010;55:2736–42.
38. Gordon DJ, Probstfield JL, Garrison RJ, et al. High-density lipoprotein cholesterol and cardiovascular disease. Four prospective American studies. Circulation. 1989;79:8–15.
39. Barter PJ, Nicholls S, Rye KA, Anantharamaiah GM, Navab M, Fogelman AM. Antiinflammatory properties of HDL. Circ Res. 2004;95:764–72.
40. Barter P, Gotto AM, LaRosa JC, et al. HDL cholesterol, very low levels of LDL cholesterol, and cardiovascular events. N Engl J Med. 2007;357:1301–10.
41. Nicholls SJ, Tuzcu EM, Sipahi I, et al. Statins, high-density lipoprotein cholesterol, and regression of coronary atherosclerosis. JAMA. 2007;297:499–508.
42. Nissen SE, Tsunoda T, Tuzcu EM, et al. Effect of recombinant ApoA-I Milano on coronary atherosclerosis in patients with acute coronary syndromes: a randomized controlled trial. JAMA. 2003;290:2292–300.
43. Nicholls SJ, Tuzcu EM, Sipahi I, et al. Relationship between atheroma regression and change in lumen size after infusion of apolipoprotein A-I Milano. J Am Coll Cardiol. 2006;47:992–7.
44. Tardif JC, Gregoire J, L'Allier PL, et al. Effects of reconstituted high-density lipoprotein infusions on coronary atherosclerosis: a randomized controlled trial. JAMA. 2007;297:1675–82.
45. Waksman R, Torguson R, Kent KM, et al. A first-in-man, randomized, placebo-controlled study to evaluate the safety and feasibility of autologous delipidated high-density lipoprotein plasma infusions in patients with acute coronary syndrome. J Am Coll Cardiol. 2010;55:2727–35.
46. Barter PJ, Brewer Jr HB, Chapman MJ, Hennekens CH, Rader DJ, Tall AR. Cholesteryl ester transfer protein: a novel target for raising HDL and inhibiting atherosclerosis. Arterioscler Thromb Vasc Biol. 2003;23:160–7.
47. Boekholdt SM, Kuivenhoven JA, Wareham NJ, et al. Plasma levels of cholesteryl ester transfer protein and the risk of future coronary artery disease in apparently healthy men and women: the prospective EPIC (European Prospective Investigation into Cancer and nutrition)-Norfolk population study. Circulation. 2004;110:1418–23.
48. Johannsen TH, Frikke-Schmidt R, Schou J, Nordestgaard BG, Tybjaerg-Hansen A. Genetic inhibition of CETP, ischemic vascular disease and mortality, and possible adverse effects. J Am Coll Cardiol. 2012;60:2041–8.
49. Nissen SE, Tardif JC, Nicholls SJ, et al. Effect of torcetrapib on the progression of coronary atherosclerosis. N Engl J Med. 2007;356:1304–16.
50. Barter PJ, Caulfield M, Eriksson M, et al. Effects of torcetrapib in patients at high risk for coronary events. N Engl J Med. 2007;357:2109–22.
51. Nicholls SJ, Tuzcu EM, Brennan DM, Tardif JC, Nissen SE. Cholesteryl ester transfer protein inhibition, high-density lipoprotein raising, and progression of coronary atherosclerosis: insights from ILLUSTRATE (Investigation of Lipid Level Management Using Coronary Ultrasound to Assess Reduction of Atherosclerosis by CETP Inhibition and HDL Elevation). Circulation. 2008;118:2506–14.
52. ApoA-I Synthesis Stimulation and Intravascular Ultrasound for Coronary Atheroma Regression

Evaluation (ASSURE I). http://clinicaltrials.gov/ct2/show/NCT01067820?term=ASSURE&rank=4 2011. Last accessed on July 5th, 2013.
53. Zanchetti A. Antiatherosclerotic effects of antihypertensive drugs: recent evidence and ongoing trials. Clin Exp Hypertens. 1996;18:489–99.
54. Nissen SE, Tuzcu EM, Libby P, et al. Effect of antihypertensive agents on cardiovascular events in patients with coronary disease and normal blood pressure: the CAMELOT study: a randomized controlled trial. JAMA. 2004;292:2217–25.
55. Sipahi I, Tuzcu EM, Schoenhagen P, et al. Effects of normal, pre-hypertensive, and hypertensive blood pressure levels on progression of coronary atherosclerosis. J Am Coll Cardiol. 2006;48:833–8.
56. Chhatriwalla AK, Nicholls SJ, Wang TH, et al. Low levels of low-density lipoprotein cholesterol and blood pressure and progression of coronary atherosclerosis. J Am Coll Cardiol. 2009;53:1110–5.
57. Nicholls SJ, Tuzcu EM, Kalidindi S, et al. Effect of diabetes on progression of coronary atherosclerosis and arterial remodeling: a pooled analysis of 5 intravascular ultrasound trials. J Am Coll Cardiol. 2008; 52:255–62.
58. Nissen SE, Wolski K. Effect of rosiglitazone on the risk of myocardial infarction and death from cardiovascular causes. N Engl J Med. 2007;356:2457–71.
59. Dormandy JA, Charbonnel B, Eckland DJ, et al. Secondary prevention of macrovascular events in patients with type 2 diabetes in the PROactive Study (PROspective pioglitAzone Clinical Trial In macroVascular Events): a randomised controlled trial. Lancet. 2005;366:1279–89.
60. Nissen SE, Nicholls SJ, Wolski K, et al. Effect of rimonabant on progression of atherosclerosis in patients with abdominal obesity and coronary artery disease: the STRADIVARIUS randomized controlled trial. JAMA. 2008;299:1547–60.
61. Nissen SE, Tuzcu EM, Brewer HB, et al. Effect of ACAT inhibition on the progression of coronary atherosclerosis. N Engl J Med. 2006;354:1253–63.
62. Tardif JC, Gregoire J, L'Allier PL, et al. Effects of the acyl coenzyme A: cholesterol acyltransferase inhibitor avasimibe on human atherosclerotic lesions. Circulation. 2004;110:3372–7.
63. de Korte CL, van der Steen AF, Cespedes EI, Pasterkamp G. Intravascular ultrasound elastography in human arteries: initial experience in vitro. Ultrasound Med Biol. 1998;24:401–8.
64. Serruys PW, Garcia-Garcia HM, Buszman P, et al. Effects of the direct lipoprotein-associated phospholipase A(2) inhibitor darapladib on human coronary atherosclerotic plaque. Circulation. 2008;118:1172–82.
65. Kapadia SR, Nissen SE, Tuzcu EM. Impact of intravascular ultrasound in understanding transplant coronary artery disease. Curr Opin Cardiol. 1999;14:140–50.
66. Eisen HJ, Tuzcu EM, Dorent R, et al. Everolimus for the prevention of allograft rejection and vasculopathy in cardiac-transplant recipients. N Engl J Med. 2003; 349:847–58.
67. Kobashigawa JA, Tobis JM, Starling RC, et al. Multicenter intravascular ultrasound validation study among heart transplant recipients: outcomes after five years. J Am Coll Cardiol. 2005;45:1532–7.
68. Stone GW, Maehara A, Lansky AJ, et al. A prospective natural-history study of coronary atherosclerosis. N Engl J Med. 2011;364:226–35.
69. Stone PH, Saito S, Takahashi S, et al. Prediction of progression of coronary artery disease and clinical outcomes using vascular profiling of endothelial shear stress and arterial plaque characteristics: the PREDICTION Study. Circulation. 2012;126:172–81.
70. Puri R, Wolski K, Uno K, et al. Left main coronary atherosclerosis progression, constrictive remodeling, and clinical events. JACC Cardiovasc Interv. 2013;6: 29–35.

6 Evaluation of Cardiac Allograft Vasculopathy: From Angiography to Intravascular Ultrasound and Beyond

Olcay Aksoy and E. Murat Tuzcu

Heart transplantation has emerged as the definitive treatment for patients with end-stage cardiac disease with more than 5,000 heart transplants performed annually worldwide [1]. The overall survival of heart transplant recipients has improved in the recent decades primarily due to the development of immunosuppressive agents. While rejection remains the most common mode of organ failure up to 1 year, cardiac allograft vasculopathy (CAV) has proven to be the major cause of long-term morbidity and mortality [1]. As opposed to atherosclerosis, CAV is characterized by intimal hyperplasia that is associated with a diffuse, pan-arterial process and accounts for 32 % of all deaths 5 years post-transplant. Angiographic evidence of CAV is present in approximately 50 % of transplanted hearts at 5 years and if diagnosed within 1 year after the transplant, it is an independent predictor of mortality at 5 years [1–3].

There are two distinct forms of coronary lesions in the transplanted heart [4–8]: (1) Coronary atherosclerosis that is already present in the donor heart at the time of the transplant has the composition of the typical atherosclerotic plaque and is more likely to present as focal and eccentric stenosis. (2) CAV, which results from complex interplay of immune and nonimmune factors, in the long run leads to diffuse intimal hyperplasia of the coronary vasculature. It is this diffuse type of vasculopathy that leads to adverse outcomes in patients with heart transplants [7, 8].

Pathophysiology

While atherosclerotic coronary disease is characterized by focal, eccentric stenosis of the epicardial vasculature, CAV, although intimal thickening starts focally, has a more diffuse distribution throughout the coronary tree with involvement of epicardial and the smaller distal vessels [2, 8]. Although lesions associated with CAV exhibit similarities to the typical atherosclerotic plaque (i.e., leukocyte infiltration, lipid accumulation, intimal smooth muscle proliferation, and endothelial dysfunction), these disease entities are distinct from each other due to the underlying immunological changes that occur in the setting of the transplant [4, 5]. Histopathology studies have shown fibroelastic proliferation of the intima following endothelial injury that arises from immunological and non-immunological factors [9, 10]. These changes in the intima begin as early as 3 months after transplantation with patchy thickening in the vessel. As the disease progresses, all segments of the artery get involved with continuous inflammation and remodeling with diffuse, concentric, and longitudinal intimal hyperplasia. Several risk factors for CAV have been described including cytomegalovirus (CMV) infection, hypertension, hypercholesterolemia,

O. Aksoy, MD • E.M. Tuzcu, MD (✉)
Department of Cardiovascular Medicine, Cleveland Clinic, 9500 Euclid Avenue, Cleveland, OH 44195, USA
e-mail: tuzcue@ccf.org

S.J. Nicholls and T. Crowe (eds.), *Imaging Coronary Atherosclerosis*, Contemporary Cardiology,
DOI 10.1007/978-1-4939-0572-0_6,

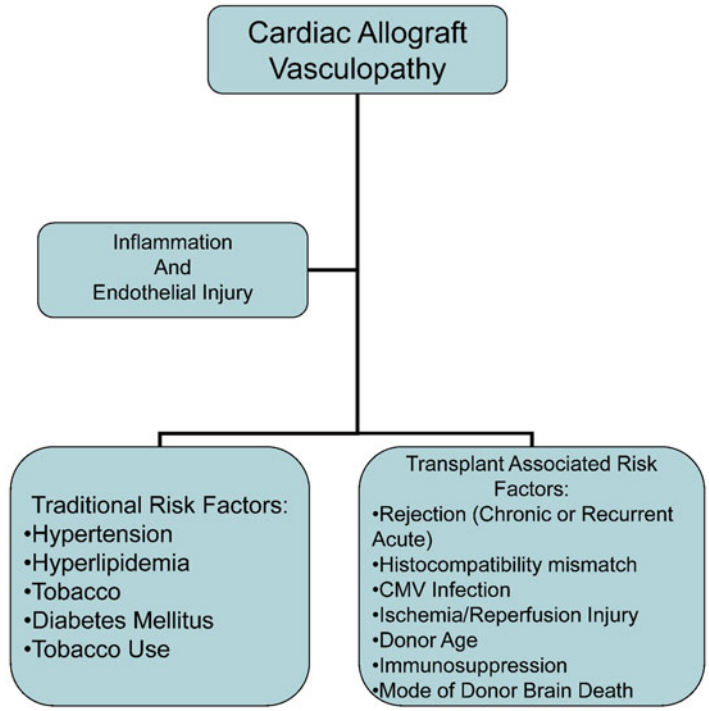

Fig. 6.1 Several traditional and nontraditional factors are associated with the development of cardiac allograft vasculopathy

diabetes mellitus, histocompatibility mismatch, ischemia reperfusion, organ preservation, and donor brain death [9–12] (Fig. 6.1).

Evaluation

The clinical evaluation for CAV is challenging as the development and progression of disease is clinically silent due to the denervation of the transplanted heart. Even in the more advanced stages of disease, patients' symptoms might be limited to dyspnea and exercise intolerance. Classic anginal symptoms might not be present making the clinical syndrome difficult to define [12, 13]. While clinical syndrome has proven to be elusive, the presence of even mild to moderate disease found on angiography has been associated with very poor outcomes with 17 % survival at 5 years [14]. Furthermore, if there is multi-vessel disease on angiography, the survival is abysmal at 13 % at 2 years [14]. Therefore, it's imperative to have a low threshold to evaluate patients for ischemia early after the transplant as early aggressive medical management might alter the rate of progression of CAV.

Several imaging modalities might be helpful in establishing the diagnosis of disease early in its course. Noninvasive testing modalities including exercise electrocardiography, echocardiography, thallium scintigraphy, and exercise radionuclide ventriculography provide reasonable sensitivity and specificity in the diagnosis of CAV [15–19]. These imaging modalities do not yield the requisite accuracy in the diagnosis of CAV, however, as they cannot identify mild to moderate disease in the absence of hemodynamically significant lesions, that is, until late in the course of disease. Therefore, these tests lead to underdiagnosis in the early stages of disease and might be associated with undertreatment of CAV if used as the only diagnostic modality. Coronary multi-detector CT has a higher sensitivity due to visualization of the luminal and extraluminal characteristics of the vasculature and its role is yet to be defined in the transplanted patient cohort [20, 21].

Given the inherent limitations of the noninvasive methods and considering the morbidity and mortality associated with CAV in transplant recipients, surveillance coronary angiography is recommended (Class I, Level of Evidence C

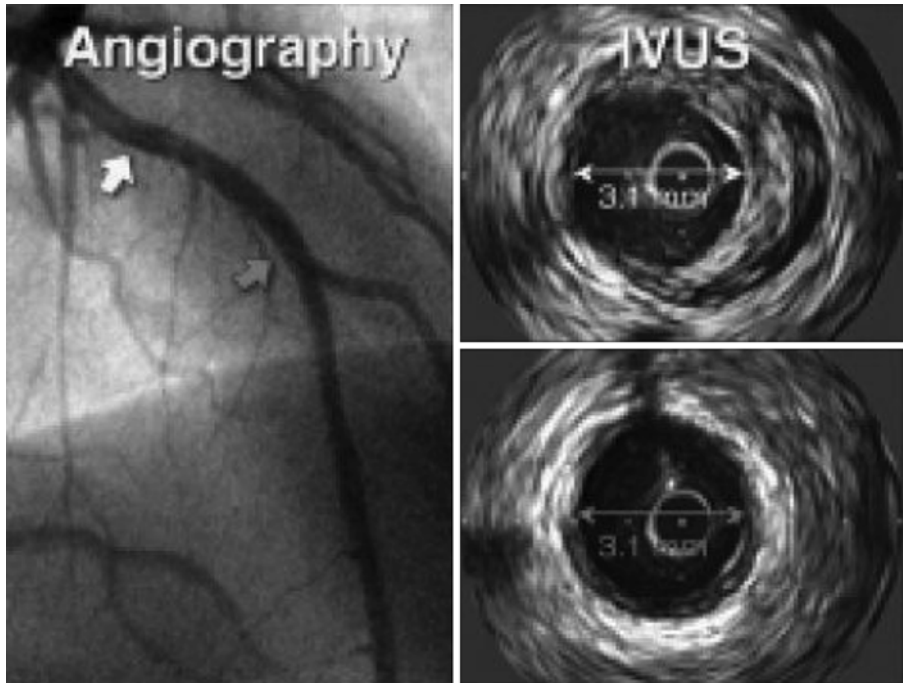

Fig. 6.2 Use of intravascular ultrasound leads to improved diagnostic accuracy as compared to coronary angiography. In this case, while coronary angiography shows similar luminal diameter in two areas of the vessel, IVUS shows that the more proximal segment has significant intimal hyperplasia whereas the distal segment has minimal disease. This case demonstrates the potential shortcomings of luminal angiographic assessment only

as per ISHLT) starting shortly after the transplant and annually thereafter. Routine angiography identifies focal and stenotic disease in 10 % of patients at 1 year and 50 % by 5 years [22]. Once mild disease is recognized by angiography, the likelihood of progression to severe disease is increased several fold [23]. While the gold standard in the diagnosis of coronary artery disease, coronary angiography has several limitations. Early in the course of CAV, there is no compromise in the luminal diameter of the vessels due to positive remodeling. Given that the angiogram essentially provides a luminographic assessment of the vasculature, its sensitivity is limited and leads to significant underdiagnosis of CAV [3, 24–26]. Furthermore, one of the strengths of angiography is its ability for the clinician to compare the abnormal segments with the normal segments—which is problematic in CAV as the disease process is diffuse and that there is no truly normal segment. Several studies have shown that coronary angiography alone has limited positive predictive value in the 40–50 % range [26, 27]. Using the angiogram, a TIMI frame count and myocardial blush grade may also help with identification of CAV; however, flow is usually normal in the early stages of disease and these techniques are of limited value [28].

Intravascular ultrasound (IVUS) allows for high-resolution cross-sectional imaging of the vessel and provides not only accurate information about the vessel size but also the morphology of the vessel wall, thickening, and plaque composition. It is used widely during coronary interventions as it provides tomographic pictures of the wall as well as the lumen of the coronary artery. Given the information that IVUS can provide over and beyond coronary angiography, it has emerged as the optimal diagnostic tool for early detection of disease in native atherosclerotic disease. In the cardiac transplant patient cohort, IVUS is considered as a valuable adjunct in the early diagnosis of intimal thickening and arteriopathy (Fig. 6.2).

Several studies have shown that where coronary angiography identifies 10–20 % of heart transplant patients to have CAV, IVUS detects intimal thickening in approximately 50 % of the patients at 1 year [3, 29]. Early diagnosis of allograft vasculopathy allows the clinician to be more aggressive about the early treatment of CAV.

What Have We Learned About Cardiac Allograft Vasculopathy with IVUS?

Serial IVUS studies have led to further understanding of the progression of CAV (Fig. 6.3). These studies have shown that coronary artery narrowing is influenced not only by progressive intimal hyperplasia but by the remodeling as well. A 5-year serial IVUS study has shown that most of the intimal thickening occurs during the first year after the transplantation. Intimal thickening is followed by an expansion of the external elastic membrane that preserves the lumen diameter as the vessel remodels. In later stages of disease, there is lumen loss as the negative remodeling occurs with constriction of the lumen area [30–32].

Serial IVUS studies have been instrumental in determining the risk of progression as well. Traditionally, CAV is diagnosed when intimal thickness is >0.3 mm. Rapidly progressive CAV is defined as an increase of ≥0.5 mm in the first year of transplantation and has been associated with adverse outcomes correlating highly with angiographic development of disease [33–36]. Those with >0.6 mm intimal thickening even in the absence of angiographically visible disease are at significantly increased risk for cardiac events [35]. In contrast, those patients who receive donor-transmitted lesions do not have worse outcomes as compared to those associated with CAV—arguing for differences in pathophysiology and progression of these two distinct entities.

Given the usefulness of quantitative analysis of the intimal thickness, the Stanford scale has been developed to classify the lesions associated with CAV (Table 6.1). Case series have shown that in patients, where Stanford Grade 0–1 were found, CAV did not develop during follow-up whereas those with higher grade lesions are at higher risk of development of significant CAV [37].

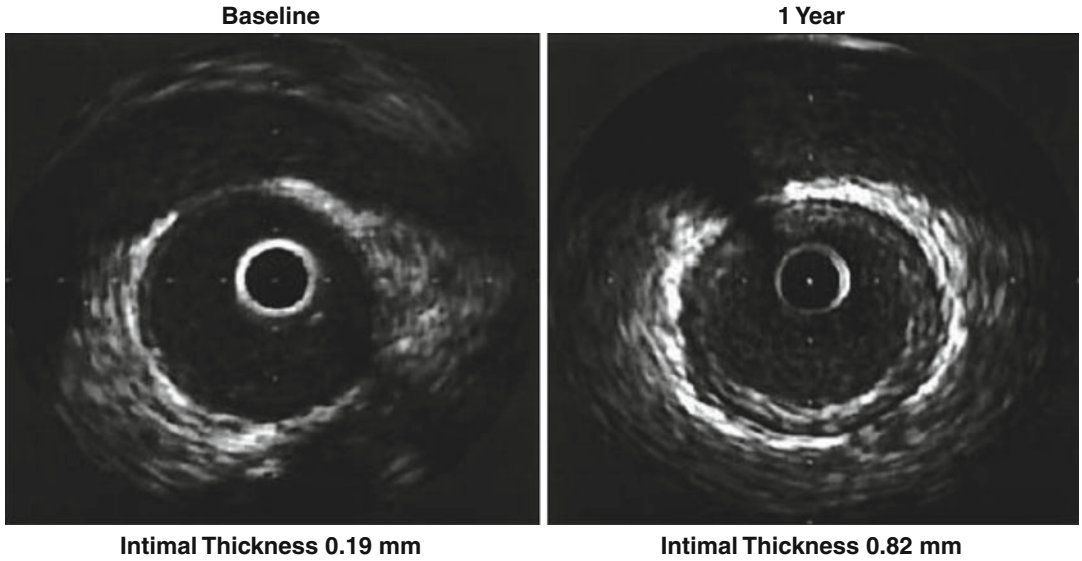

Fig. 6.3 Progression of disease can be monitored by serial IVUS imaging in patients with cardiac allograft vasculopathy as demonstrated below

Table 6.1 Maximal intimal thickness (MIT) and circumference involvement as defined for every measured segment using the Stanford classification

Stanford Grade	Definition
Grade 0	No evidence of an intimal layer
Grade 1	Intimal layer <0.3 mm involving <180° of vessel circumference
Grade 2	Intimal layer <0.3 mm involving ≥180° of circumference, or 0.3–0.5 mm with <180° of vessel circumference
Grade 3	Intimal layer 0.3–0.5 mm involving ≥180° of circumference, or 0.5–1.0 mm with <180° of vessel circumference
Grade 4	Intimal layer >0.5 mm involving ≥180° of vessel circumference, or >1 mm

There are emerging data for the use of virtual histology-IVUS (VH-IVUS) where plaque composition can be studied. With this technology, plaque can be distinguished into four major components: necrotic core, calcium, fibrous, and fibrofatty. Studies have shown significant correlation between the VH-IVUS-derived plaque characteristics with the presence of diabetes mellitus, age of the donor, and male recipients. These studies have shown that in the first stages of intimal thickening, fibrous and fibrofatty components dominate, whereas necrotic core and calcification becomes more prominent at long term. The presence of necrotic core in males, older donors, and patients with diabetes mellitus especially with volume >2.01 mm^3 is associated with the need for revascularization during follow-up. Furthermore, when plaque is characterized as inflammatory (necrotic core and dense calcium ≥30 %) and noninflammatory (necrotic core and dense calcium <30 %), those with inflammatory plaque were found to have higher risk of progression of CAV and early recurrent rejection. These findings are consistent with initial fibrous proliferation in the vasculature with CAV. Serial VH-IVUS studies have shown however that during long-term follow-up, the extent of necrotic core and calcification increase arguing for the dynamic process involved in the development of CAV [38–40].

Limitations and Safety of Intravascular Ultrasound

There are several limitations of IVUS imaging. Due to the size of the IVUS catheter, only proximal to mid epicardial vessels can be imaged leaving secondary and tertiary vessels unassessed. Furthermore, usual practice is to image only one coronary artery (usually the LAD) which further diminishes the sensitivity of the IVUS assessment. In a study, CAV was diagnosed in 58 % of patients where all 3 vessels were imaged at 1 year as opposed to 27 % seen in single-vessel imaging [41].

Safety of IVUS interrogation of the coronary tree has been well established. The rate of transient spasm varies from 1 to 3 % with vessel dissection or closure in 0.5 % of the cases. There had been some concern whether repeated IVUS assessment would accelerate CAV by causing endothelial injury; however, a serial longitudinal study has shown that IVUS is safe and does not contribute to progression of disease [42].

How Can the Information be Used in Patient Management?

Early diagnosis of CAV is of paramount value as adjustments in antirejection regimen and management of atherosclerotic risk factors might be organ- and life-saving. Several medications have been associated with improved outcomes when utilized in patients with CAV.

The use of rapamycin (sirolimus) in the immunomodulatory regimen has been associated with slowing the progression of CAV in several case series and is now widely accepted as the medication of choice in patients with CAV [43, 44]. Another immunosuppressive agent, mycophenolate mofetil (MMF) when compared to azathioprine has also been shown to reduce progression of intimal thickening [45]. Both rapamycin and MMF exert their action by inhibiting growth and activation of B and T cells, with

proposed effect of slowing the degree of inflammation in the vessel wall leading to retardation of progression of CAV.

Several other drug categories have been associated with improved outcomes. Statins, via their pleiotropic effects, have been associated with slower progression of CAV [46, 47]. There are also data suggesting that combination therapy of angiotensin-converting enzyme (ACE) inhibitors and calcium channel blockers can attenuate the process of CAV [48, 49]. Interestingly, the treatment of CMV infection with ganciclovir can also slow the progression of CAV most likely by protecting the endothelium; which are otherwise targets for CMV infection [50]. Further therapeutic options for CAV include mechanical treatment of the coronary stenosis (percutaneous intervention) and coronary artery bypass grafting (CABG). Drug-eluting stents have been associated with lower restenosis rates as compared to bare metal stents in CAV consistent with treatment effects found with atherosclerotic disease [51]. Outcomes described with CABG have generally been poor, however, with high perioperative and 1-year mortality rates [52, 53].

Importantly, when assessing the impact of above therapies on the coronary vasculature in patients with CAV, IVUS has played an instrumental role in determining the progression of disease during longitudinal follow-up. This imaging modality has been used as the diagnostic outcome imaging of choice in assessing the effects of therapy.

When severe CAV is present and revascularization options are exhausted, retransplantation is the only effective therapy with survival rates in the 70–80 % range at 12–24 months [54]. Given the scarcity of donor organs however, retransplantation in this setting needs to be carefully assessed.

Conclusions

CAV, once present, is a major source of morbidity and mortality. Several treatment options are present, yet outcomes are poor unless the disease is detected early and aggressively treated. The use of highly sensitive techniques such as IVUS has enabled early diagnosis of disease with early aggressive treatment leading to improved outcomes.

References

1. Taylor DO, Stehlik J, Edwards LB, et al. Registry of the International Society for Heart and Lung Transplantation: Twenty-sixth Official Adult Heart Transplant Report-2009. J Heart Lung Transplant. 2009;28:1007–22.
2. Robbins RC, Barlow CW, Oyer PE, et al. Thirty years of cardiac transplantation at Stanford university. J Thorac Cardiovasc Surg. 1999;117:939–51.
3. Tuzcu EM, Kapadia SR, Tutar E, et al. High prevalence of coronary atherosclerosis in asymptomatic teenagers and young adults: evidence from intravascular ultrasound. Circulation. 2001;103:2705–10.
4. Rahmani M, Cruz RP, Granville DJ, McManus BM. Allograft vasculopathy versus atherosclerosis. Circ Res. 2006;99:801–15.
5. Ramzy D, Rao V, Brahm J, Miriuka S, Delgado D, Ross HJ. Cardiac allograft vasculopathy: a review. Can J Surg. 2005;48:319–27.
6. Jimenez J, Kapadia SR, Yamani MH, et al. Cellular rejection and rate of progression of transplant vasculopathy: a 3-year serial intravascular ultrasound study. J Heart Lung Transplant. 2001;20:393–8.
7. Billingham ME. Histopathology of graft coronary disease. J Heart Lung Transplant. 1992;11:S38–44.
8. Tuzcu EM, De Franco AC, Goormastic M, et al. Dichotomous pattern of coronary atherosclerosis 1 to 9 years after transplantation: insights from systematic intravascular ultrasound imaging. J Am Coll Cardiol. 1996;27:839–46.
9. Labarrere CA, Nelson DR, Faulk WP. Endothelial activation and development of coronary artery disease in transplanted human hearts. JAMA. 1997;278:1169–75.
10. Valantine HA. Cardiac allograft vasculopathy: central role of endothelial injury leading to transplant "atheroma". Transplantation. 2003;76:891–9.
11. Suciu-Foca N, Ciubotariu R, Liu Z, Ho E, Rose EA, Cortesini R. Persistent allopeptide reactivity and epitope spreading in chronic rejection. Transplant Proc. 1998;30:2136–7.
12. Colvin-Adams M, Agnihotri A. Cardiac allograft vasculopathy: current knowledge and future direction. Clin Transplant. 2011;25:175–84.
13. Weis M, von Scheidt W. Cardiac allograft vasculopathy: a review. Circulation. 1997;96:2069–77.
14. Keogh AM, Valantine HA, Hunt SA, et al. Impact of proximal or midvessel discrete coronary artery stenoses on survival after heart transplantation. J Heart Lung Transplant. 1992;11:892–901.

15. Fang JC, Rocco T, Jarcho J, Ganz P, Mudge GH. Noninvasive assessment of transplant-associated arteriosclerosis. Am Heart J. 1998;135:980–7.
16. Akosah KO, Mohanty PK, Funai JT, et al. Noninvasive detection of transplant coronary artery disease by dobutamine stress echocardiography. J Heart Lung Transplant. 1994;13:1024–38.
17. Spes CH, Klauss V, Mudra H, et al. Diagnostic and prognostic value of serial dobutamine stress echocardiography for noninvasive assessment of cardiac allograft vasculopathy: a comparison with coronary angiography and intravascular ultrasound. Circulation. 1999;100:509–15.
18. Elhendy A, van Domburg RT, Vantrimpont P, et al. Prediction of mortality in heart transplant recipients by stress technetium-99 m tetrofosmin myocardial perfusion imaging. Am J Cardiol. 2002;89:964–8.
19. Hacker M, Tausig A, Romuller B, et al. Dobutamine myocardial scintigraphy for the prediction of cardiac events after heart transplantation. Nucl Med Commun. 2005;26:607–12.
20. Wu YW, Yen RF, Lee CM, et al. Diagnostic and prognostic value of dobutamine thallium-201 single-photon emission computed tomography after heart transplantation. J Heart Lung Transplant. 2005;24: 544–50.
21. Sigurdsson G, Carrascosa P, Yamani MH, et al. Detection of transplant coronary artery disease using multidetector computed tomography with adaptative multisegment reconstruction. J Am Coll Cardiol. 2006;48:772–8.
22. Pflugfelder PW, Boughner DR, Rudas L, Kostuk WJ. Enhanced detection of cardiac allograft arterial disease with intracoronary ultrasonographic imaging. Am Heart J. 1993;125:1583–91.
23. Costanzo MR, Naftel DC, Pritzker MR, et al. Heart transplant coronary artery disease detected by coronary angiography: a multiinstitutional study of preoperative donor and recipient risk factors. Cardiac Transplant Research Database. J Heart Lung Transplant. 1998;17:744–53.
24. Rickenbacher PR, Pinto FJ, Chenzbraun A, et al. Incidence and severity of transplant coronary artery disease early and up to 15 years after transplantation as detected by intravascular ultrasound. J Am Coll Cardiol. 1995;25:171–7.
25. Johnson DE, Alderman EL, Schroeder JS, et al. Transplant coronary artery disease: histopathologic correlations with angiographic morphology. J Am Coll Cardiol. 1991;17:449–57.
26. Spes CH, Klauss V, Rieber J, et al. Functional and morphological findings in heart transplant recipients with a normal coronary angiogram: an analysis by dobutamine stress echocardiography, intracoronary Doppler and intravascular ultrasound. J Heart Lung Transplant. 1999;18:391–8.
27. St Goar FG, Pinto FJ, Alderman EL, et al. Intracoronary ultrasound in cardiac transplant recipients. In vivo evidence of "angiographically silent" intimal thickening. Circulation. 1992;85:979–87.
28. Fang JC, Kinlay S, Wexberg P, et al. Use of the thrombolysis in myocardial infarction frame count for the quantitative assessment of transplant-associated arteriosclerosis. Am J Cardiol. 2000;86:890–2.
29. Yeung AC, Davis SF, Hauptman PJ, et al. Incidence and progression of transplant coronary artery disease over 1 year: results of a multicenter trial with use of intravascular ultrasound. Multicenter Intravascular Ultrasound Transplant Study Group. J Heart Lung Transplant. 1995;14:S215–20.
30. Tsutsui H, Ziada KM, Schoenhagen P, et al. Lumen loss in transplant coronary artery disease is a biphasic process involving early intimal thickening and late constrictive remodeling: results from a 5-year serial intravascular ultrasound study. Circulation. 2001;104:653–7.
31. Li H, Tanaka K, Oeser B, Kobashigawa JA, Tobis JM. Vascular remodelling after cardiac transplantation: a 3-year serial intravascular ultrasound study. Eur Heart J. 2006;27:1671–7.
32. Lim TT, Liang DH, Botas J, Schroeder JS, Oesterle SN, Yeung AC. Role of compensatory enlargement and shrinkage in transplant coronary artery disease. Serial intravascular ultrasound study. Circulation. 1997;95:855–9.
33. Rickenbacher PR, Pinto FJ, Lewis NP, et al. Prognostic importance of intimal thickness as measured by intracoronary ultrasound after cardiac transplantation. Circulation. 1995;92:3445–52.
34. Tuzcu EM, Kapadia SR, Sachar R, et al. Intravascular ultrasound evidence of angiographically silent progression in coronary atherosclerosis predicts long-term morbidity and mortality after cardiac transplantation. J Am Coll Cardiol. 2005;45:1538–42.
35. Mehra MR, Ventura HO, Stapleton DD, Smart FW, Collins TC, Ramee SR. Presence of severe intimal thickening by intravascular ultrasonography predicts cardiac events in cardiac allograft vasculopathy. J Heart Lung Transplant. 1995;14:632–9.
36. Kobashigawa JA, Tobis JM, Starling RC, et al. Multicenter intravascular ultrasound validation study among heart transplant recipients: outcomes after five years. J Am Coll Cardiol. 2005;45:1532–7.
37. Zakliczynski M, Swierad M, Zakliczynska H, Maruszewski M, Buszman P, Zembala M. Usefulness of Stanford scale of intimal hyperplasia assessed by intravascular ultrasound to predict time of onset and severity of cardiac allograft vasculopathy. Transplant Proc. 2005;37:1343–5.
38. Hernandez JM, de Prada JA, Burgos V, et al. Virtual histology intravascular ultrasound assessment of cardiac allograft vasculopathy from 1 to 20 years after heart transplantation. J Heart Lung Transplant. 2009;28:156–62.
39. Konig A, Kilian E, Sohn HY, et al. Assessment and characterization of time-related differences in plaque composition by intravascular ultrasound-derived radiofrequency analysis in heart transplant recipients. J Heart Lung Transplant. 2008;27:302–9.
40. Raichlin E, Bae JH, Kushwaha SS, et al. Inflammatory burden of cardiac allograft coronary atherosclerotic

plaque is associated with early recurrent cellular rejection and predicts a higher risk of vasculopathy progression. J Am Coll Cardiol. 2009;53:1279–86.
41. Kapadia SR, Ziada KM, L'Allier PL, et al. Intravascular ultrasound imaging after cardiac transplantation: advantage of multi-vessel imaging. J Heart Lung Transplant. 2000;19:167–72.
42. Ramasubbu K, Schoenhagen P, Balghith MA, et al. Repeated intravascular ultrasound imaging in cardiac transplant recipients does not accelerate transplant coronary artery disease. J Am Coll Cardiol. 2003;41:1739–43.
43. Keogh A, Richardson M, Ruygrok P, et al. Sirolimus in de novo heart transplant recipients reduces acute rejection and prevents coronary artery disease at 2 years: a randomized clinical trial. Circulation. 2004;110:2694–700.
44. Mancini D, Pinney S, Burkhoff D, et al. Use of rapamycin slows progression of cardiac transplantation vasculopathy. Circulation. 2003;108:48–53.
45. Kobashigawa JA, Tobis JM, Mentzer RM, et al. Mycophenolate mofetil reduces intimal thickness by intravascular ultrasound after heart transplant: reanalysis of the multicenter trial. Am J Transplant. 2006;6:993–7.
46. Kobashigawa JA, Moriguchi JD, Laks H, et al. Ten-year follow-up of a randomized trial of pravastatin in heart transplant patients. J Heart Lung Transplant. 2005;24:1736–40.
47. Kobashigawa JA, Katznelson S, Laks H, et al. Effect of pravastatin on outcomes after cardiac transplantation. N Engl J Med. 1995;333:621–7.
48. Schroeder JS, Gao SZ, Alderman EL, et al. A preliminary study of diltiazem in the prevention of coronary artery disease in heart-transplant recipients. N Engl J Med. 1993;328:164–70.
49. Mehra MR, Ventura HO, Smart FW, Collins TJ, Ramee SR, Stapleton DD. An intravascular ultrasound study of the influence of angiotensin-converting enzyme inhibitors and calcium entry blockers on the development of cardiac allograft vasculopathy. Am J Cardiol. 1995;75:853–4.
50. Bonaros NE, Kocher A, Dunkler D, et al. Comparison of combined prophylaxis of cytomegalovirus hyperimmune globulin plus ganciclovir versus cytomegalovirus hyperimmune globulin alone in high-risk heart transplant recipients. Transplantation. 2004;77:890–7.
51. Bader FM, Kfoury AG, Gilbert EM, et al. Percutaneous coronary interventions with stents in cardiac transplant recipients. J Heart Lung Transplant. 2006; 25:298–301.
52. Halle 3rd AA, Disciascio G, Massin EK, et al. Coronary angioplasty, atherectomy and bypass surgery in cardiac transplant recipients. J Am Coll Cardiol. 1995;26:120–8.
53. Musci M, Loebe M, Wellnhofer E, et al. Coronary angioplasty, bypass surgery, and retransplantation in cardiac transplant patients with graft coronary disease. Thorac Cardiovasc Surg. 1998;46:268–74.
54. Boucek MM, Faro A, Novick RJ, Bennett LE, Keck BM, Hosenpud JD. The Registry of the International Society for Heart and Lung Transplantation: Fourth Official Pediatric Report—2000. J Heart Lung Transplant. 2001;20:39–52.

Assessment of Plaque Composition by Intravascular Ultrasound

7

Salvatore Brugaletta and Hector M. Garcia-Garcia

Introduction

Acute coronary syndromes are often the first manifestation of coronary atherosclerosis and the possibility to identify plaques at high risk of complication would represent an important strategy to reduce casualties associated with atherosclerosis. Our current understanding of plaque biology suggests that ~60 % of clinically evident plaque rupture originates within an inflamed thin-capped fibroatheroma (TCFA), characterized by a large necrotic core and containing numerous cholesterol clefts, cellular debris, and micro-calcifications. The overlying fibrous cap is thin and rich in inflammatory cells, macrophages, and T lymphocytes with few smooth muscle cells [1, 2]. Pathological studies demonstrated that these plaques are mainly located in the proximal portions of the left anterior descending and circumflex arteries, and are more disperse in the right coronary artery [3]. This tendency to develop preferentially in these locations has been explained by the low shear stress conditions generated in areas with tortuosity or many branches: low shear stress may induce the migration of lipid and monocytes into the vessel wall leading to the progression of the lesion toward a plaque with high risk of rupture [4].

Coronary angiography has been for many years the only imaging modality available to detect atherosclerosis. However it does not visualize the vessel wall, but depicts artery as a planar silhouette of the contrast-filled lumen. For this reason, it is not suitable for complete assessment of atherosclerosis [5]. On the contrary, intracoronary-imaging techniques have been established as the gold standard for in vivo imaging of the vessel wall of the coronary arteries [5, 6]. Grayscale intravascular ultrasound (IVUS) represents the first of these techniques in chronological order. However, it has a limited resolution, which makes difficult, if not impossible, to identify qualitatively (e.g., visually) the plaque morphology similar as that of histopathology, the gold standard to characterize and quantify coronary plaque tissue components [7].

For these reasons, during the last years new imaging techniques have been developed based on the interpretation of ultrasound radiofrequency backscattering.

Characterization of Atherosclerosis

Atheroma

Although a detailed description of atherosclerosis development and composition is beyond the scope of this chapter, some important concepts

S. Brugaletta, MD, PhD
Department of Cardiology, Hospital Clinic, Thorax Institute, Barcelona, Spain

H.M. Garcia-Garcia, MD, PhD (✉)
Department of Interventional Cardiology, Thoraxcenter, Erasmus Medical Center, Thoraxcenter—Erasmus University, z120 Erasmus MC, Dr. Molewaterplein 40, Rotterdam, The Netherlands, 3015 GD
e-mail: h.garciagarcia@erasmusmc.nl

S.J. Nicholls and T. Crowe (eds.), *Imaging Coronary Atherosclerosis*, Contemporary Cardiology,
DOI 10.1007/978-1-4939-0572-0_7,

are important to support the use of tissue characterization imaging modalities for plaque characterization.

In brief, an atheroma is formed by an intricate sequence of events, not necessarily in a linear chronologic order, that involves extracellular lipid accumulation, endothelial dysfunction, leukocyte recruitment, intracellular lipid accumulation (foam cells), smooth muscle cell migration and proliferation, expansion of extracellular matrix, neo-angiogenesis, tissue necrosis, and mineralization at later stages [8, 9]. The ultimate characteristic of an atherosclerotic plaque at any given time depends on the relative contribution of each of these features [8]. Thus, in histological cross-sections, the pathologic intimal thickening is rich in proteoglycans and lipid pools, but no trace of necrotic core is seen. Conversely, the necrotic core appears in the fibroatheroma (FA), that is, the precursor lesion of symptomatic heart disease. TCFA is a lesion characterized by a large necrotic core containing numerous cholesterol clefts, cellular debris, and micro-calcifications. The overlying fibrous cap is thin and rich in inflammatory cells, macrophages, and T lymphocytes with a few smooth muscle cells. On the basis of tissue echogenicity (i.e., their appearance), not necessarily histological composition, atheromas have been classified in four categories by grayscale IVUS: (1) soft plaque (lesion echogenicity less than the surrounding adventitia), (2) fibrous plaque [intermediate echogenicity between soft (echolucent) atheromas and highly echogenic calcified plaques], (3) calcified plaque (echogenicity higher than the adventitia with acoustic shadowing), and (4) mixed plaques (no single acoustical subtype represents >80 % of the plaque) [6].

Detection of Calcification

The presence, depth, and circumferential distribution of calcification are important factors not only for selecting the type of interventional device and estimating the risk of vessel dissection and perforation during PCI, but also in designing and conducting studies on progression/regression of coronary atheroma. Plaques with moderate to severe calcification showed no change or progression of atheroma size [10]. Thus careful selection of coronary segments to evaluate the effect of drug on coronary atherosclerosis should be considered.

On IVUS, calcium appears as bright echoes that obstruct the penetration of ultrasound (acoustic shadowing). Therefore, IVUS detects only the leading edge of calcium and cannot determine its thickness. Using grayscale IVUS, a three-dimensional and quantitative analysis of atherosclerotic plaque composition by automated differential echogenicity has been developed to facilitate automatic detection of calcified areas [11]. Virtual histology, in comparison with histology, has a predictive accuracy of 96.7 % for detection of dense calcium [12].

Coronary Remodeling

Arterial remodeling refers to a continuous process involving changes in vessel size measured by the external elastic membrane (EEM) cross-sectional area (also called vessel cross-sectional area, CSA). “Positive remodeling” occurs when there is an outward increase in EEM, conversely “negative remodeling” when the EEM decreases in size (shrinkage of the vessel) [6]. The magnitude and direction of remodeling can be expressed by the following index: EEM cross-sectional area at the plaque site divided by EEM CSA at the reference “non-diseased” vessel. Positive remodeling will demonstrate an index >1.0, while negative remodeling has an index <1.0. Direct evidence of remodeling can only be demonstrated in serial studies showing changes in the EEM CSA over time, since remodeling may also be encountered at the “normal-appearing” reference coronary segment [13].

The limitation of angiography in determining disease burden and stenosis severity is largely due to vessel remodeling. Detection of remodeling is extremely important during PCI to define plaque burden and appropriate size of devices. Pathological studies have also suggested a relationship between positive vessel remodeling and plaque vulnerability. Vessel with positive remodeling showed increased inflammatory

marker concentrations, larger lipid cores, paucity of smooth muscle cells, and medial thinning [14, 15]. Several IVUS studies have also linked positive vessel remodeling with culprit [16] and ruptured coronary plaques [17, 18]. Positive remodeling has been observed more often in patients with acute coronary syndromes than in those with stable coronary artery disease [19], and has been identified as an independent predictor of major adverse cardiac events in patients with unstable angina [20]. Plaques exhibiting positive remodeling also had more often thrombus and signs of rupture [21]. Pattern of remodeling has also been correlated with plaque composition: soft plaques are associated with positive remodeling while fibrocalcific plaques more often have negative or constrictive remodeling [22]. Similar findings have been observed in studies utilizing IVUS radiofrequency data analysis: positive remodeling was directly correlated with the presence and size of necrotic core, and inversely associated with fibrotic tissue [23].

Ruptured Plaques and Trombi

Plaque ruptures occur at sites of significant plaque accumulation, but are often not highly stenotic by coronary angiography due to positive vascular remodeling [17, 18, 24]. The transition to plaque rupture has been characterized by the presence of active inflammation (monocyte/macrophage infiltration), thinning of the fibrous cap (<65 mm), development of a large lipid necrotic core, endothelial denudation with superficial platelet aggregation, and intraplaque hemorrhage [25].

Ruptured plaques may have a variable appearance on IVUS. The American College of Cardiology clinical expert consensus document recommended use of the following definitions: (1) *Plaque ulceration*: A recess in the plaque beginning at the luminal–intimal border, typically without enlargement of the EEM compared with the reference segment. (2) *Plaque rupture*: plaque ulceration with a tear detected in a fibrous cap. Contrast injections may be used to prove and define the communication point [6]. The tear of the rupture (identified in ~60 %) occurs more often at the shoulder of the plaque than in the center [10, 26]. IVUS features of ruptured plaques are as follows: large in volume, eccentric, have mixed or soft composition and irregular surface, and are associated with positive vessel remodeling [17, 18]. Ruptured plaques have less calcium, especially superficial calcium, but a larger number of small (<90° arc) calcium deposits, particularly deep calcium deposits [27].

IVUS has also been used to assess the natural evolution of ruptured plaques. Up to 50 % of the ruptured plaques detected in the first ACS event heal with medical therapy, without significant change in plaque size [28]. Another study revealed complete healing of plaque rupture in 29 % of the patients treated with statins and incomplete healing in untreated patients [29].

Thrombus represents the ultimate pathological feature leading to ACS. Thrombus is usually recognized as an echolucent intraluminal mass, often with a layered or pedunculated appearance by IVUS [6]. Fresh or acute thrombus may appear as an echodense intraluminal tissue, which does not follow the circular appearance of the vessel wall, while an older, more organized thrombus has a darker ultrasound appearance. However, none of these IVUS features are a hallmark for thrombus, and one should consider slow flow (fresh thrombus), air, stagnant contrast or black hole, an echolucent neointimal tissue observed after drug-eluting stent (DES) and radiation therapy, as differential diagnoses [6]. In addition, IVUS resolution is limited to precisely characterize thrombus. In a study in patients with acute myocardial infarction, intracoronary thrombus was observed in all cases by optical coherence tomography (OCT) and angioscopy but was identified in only 33 % by IVUS [30].

Intravascular Ultrasound

Imaging Formation and Catheter Designs

The IVUS image is the result of reflected ultrasound waves that are converted to electrical signals and sent to an external processing system for amplification, filtering, and scan conversion.

Grayscale IVUS imaging is formed by the envelope (amplitude) of the radiofrequency signal. More recently, autoregressive spectral analysis of IVUS-backscattered data has been incorporated into conventional IVUS systems to facilitate image interpretation of different tissue components and strain values (Fig. 7.1).

Grayscale IVUS provides a limited insight into atheroma composition. Soft (echolucent) plaques have been related either to high lipid content [31, 32] or the presence of smooth muscle cells [11]. While fibrous plaques usually have an intermediate echogenicity, but sometimes very dense fibrous plaques can also appear as calcified lesions [6]. Traditionally, acoustic shadowing has been considered as a sign of calcification, but necrotic tissue can also cause shadowing [11]. In addition, the interobserver variability in the plaque type assessment by grayscale IVUS reported in the literature varies considerably, with percentages of concordance between observers ranging from 88 % to only 47 % [13, 33, 34].

Tissue Characterization Using Virtual Histology IVUS or iMAP-IVUS

Two softwares for ultrasound backscattering tissue characterization are currently available in clinical practice (Fig. 7.2). The first commercial available radiofrequency (RF) signal-based tissue composition analysis tool was the so-called virtual histology (VH-IVUS, Volcano Therapeutics, Rancho Cordova, CA, USA) software [12, 35, 36]. It uses in-depth analysis of the backscattered RF signal in order to provide a more detailed description of the atheromatous plaque composition and is performed with either a 20 MHz, 2.9 Fr phased array transducer catheter (Eagle Eye™ Gold, Volcano Therapeutics) or 45 MHz 3.2 Fr rotational catheter (Revolution, Volcano Therapeutics) that acquires IVUS data electrocardiogram gated [36]. The main principle of this technique is that it uses not only the envelope amplitude of the reflected RF signals (as grayscale IVUS does), but also the underlying frequency content to analyze the tissue components present in coronary plaques. This combined information is processed using autoregressive models and thereafter in a classification tree that determines four basic color-coded plaque tissue components [1, 35]: fibrous tissue (dark green) [2], fibrofatty tissue (light green) [3], necrotic core (red), and [4] dense calcium (white). The current software version assumes the presence of a media layer, which is artificially added, positioned just at the inside of the outer vessel contour. This technique has been compared in several studies against histology in humans and other species [12, 35, 37].

Recently, another RF-based processing method has become commercially available for coronary plaque tissue characterization and it is called iMAP-IVUS (Boston Scientific, Santa Clara, CA, USA) [38, 39]. In principle this software is comparable, from methodological point of view, to the IVUS-VH. However, by design, these two IVUS catheters have different capabilities for tissue characterization. Unlike VH, iMap uses a 40 MHz single rotational transducer on a drive shaft and can acquire radiofrequency data continuously, while VH uses similar catheter and additionally is also available in the electronic catheter (20 MHz). iMap and VH (40 MHz vs. 45/20 MHz) have relative advantages and disadvantages in displaying grayscale images. iMap has higher resolution, but displays specific artifacts such as nonuniform rotational distortion, because it is a rotational catheter. In addition, far-field imaging can be more problematic with high frequency catheters due to amplified attenuation and enhanced blood backscatter. Whereas VH feeds the spectra that are obtained from the radiofrequency data using autoregressive models into a classification tree that has reported diagnostic accuracies of over 90 % each plaque components as compared to histology [12], iMap uses a pattern recognition algorithm on the spectra that were obtained from a fast Fourier transformation and a histology-derived database [38]. The color code for tissue types is also different: iMap depicts fibrotic (light green), lipidic (yellow), necrotic (pink), and

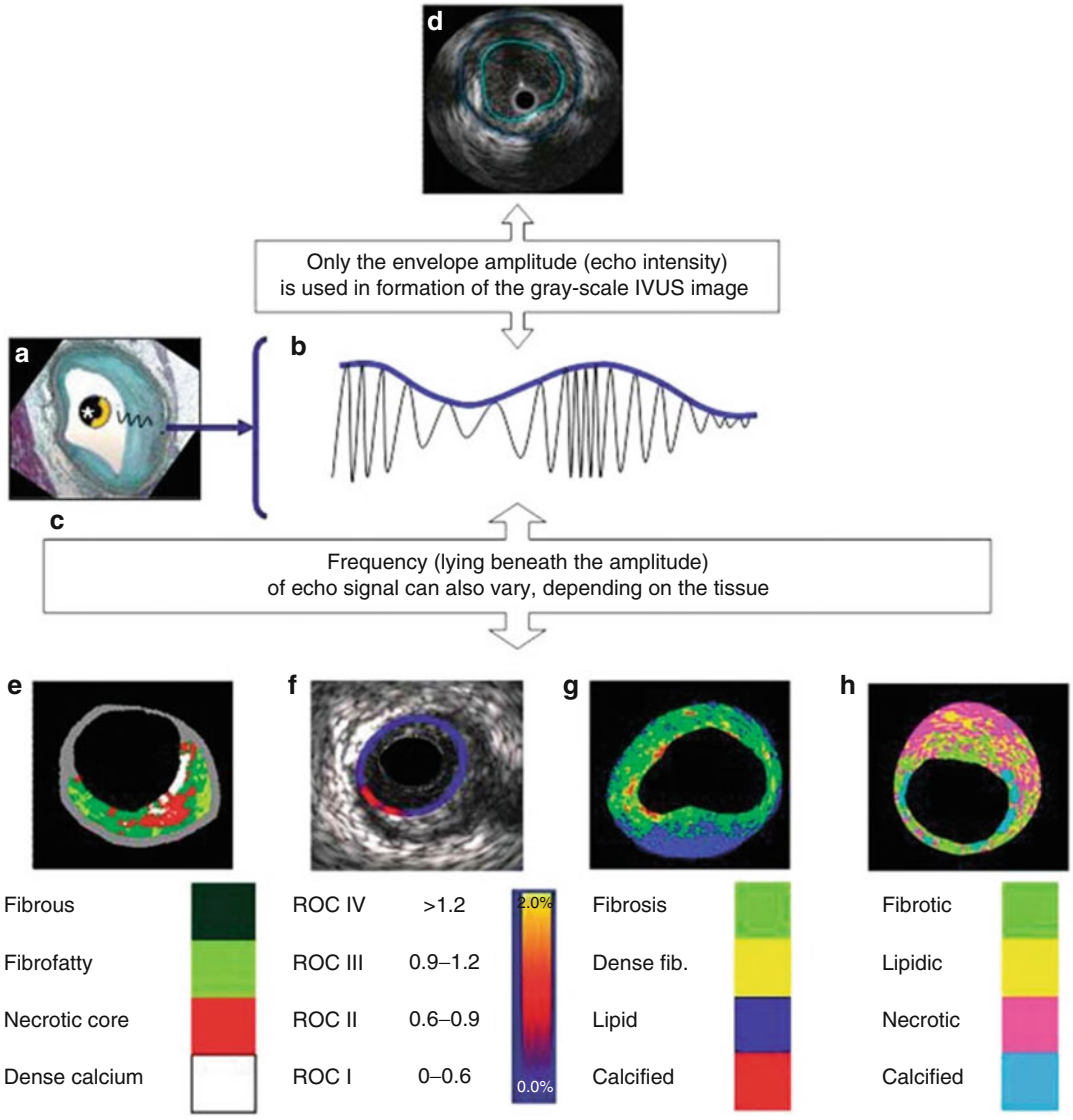

Fig. 7.1 Intravascular ultrasound signal is obtained from the vessel wall (**a**). Grayscale intravascular ultrasound imaging is formed by the envelope (amplitude) (**b**) of the radiofrequency signal (**c**). By grayscale, atherosclerotic plaque can be classified into four categories: soft, fibrotic, calcified, and mixed plaques. (**d**) shows a cross-sectional view of a grayscale image. The *blue lines* limit the actual atheroma. The frequency and power of the signal commonly differ between tissues, regardless of similarities in the amplitude. From the backscatter radiofrequency data different types of information can be retrieved: virtual histology (**e**), palpography (**f**), integrated backscattered intravascular ultrasound (**g**), and iMAP (**h**). Virtual histology is able to detect four tissue types: necrotic core, fibrous, fibrofatty, and dense calcium. Plaque deformability at palpography is reported in strain values, which are subsequently categorized into four grades according to the Rotterdam Classification (ROC). The tissues characterized by integrated backscattered intravascular ultrasound are lipidic, fibrous, and calcified; iMAP detects fibrotic, lipidic, necrotic, and calcified (Reprinted from Garcia-Garcia HM, Costa MA, Serruys PW. Imaging of coronary atherosclerosis: intravascular ultrasound. Eur Heart J 2010;31:2456-69. With permission from Oxford University Press)

	IVUS	VH	i-MAP
	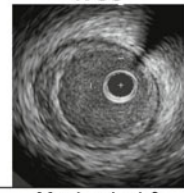	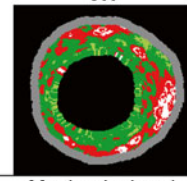	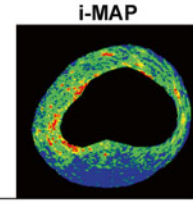
Type of device	Mechanical & electrical	Mechanical and Electrical	Mechanical
Transducer Frequency	20-40 MHz	20-45 MHz	40MHz
Color code	Gray-scale	Fibrous: Green Necrotic Core: Red Calcium: White Fibrofatty: Light green	Fibrous: Light green Necrotic Core: Pink Calcium: Blue Fibrofatty: Yellow
Backscatter Radiofrequency signal analysis	Amplitude (dB)	Autoregressive model	Fast Fourier Transformation

Fig. 7.2 Similarities and differences of IVUS and IVUS-based imaging modalities

calcified tissue (blue), while VH depicts fibrous (green), fibrofatty (yellow green), necrotic core (red), and dense calcium (white), respectively. Taken together, it is possible that these distinctive features may lead to differences in the tissue characteristics of the images of coronary plaque obtained.

Shin et al. compared in vivo findings of this two IVUS-based tissue characterization system, showing a significant and systematic variability in plaque composition estimates [39]. iMap classified plaque as necrotic tissue in poor signal areas, such as guidewire artifact or acoustic shadowing, while VH displays fibrofatty. VH showed EEM as a gray medial stripe, while iMap always provided plaque composition results even for very thin plaques. VH tends to overestimate metallic stent struts, and iMap shows thinner stent thickness than VH. Also, in the VH there is peri-stent dense calcium with necrotic core halo, not seen in the iMap (Fig. 7.3).

Plaque Type Characterization by IVUS-VH

Using IVUS-VH, the various stages of atherosclerosis can be defined (Fig. 7.4). The definition of an IVUS-derived TCFA, for example, is a lesion fulfilling the following criteria in at least three consecutive frames [1]: plaque burden ≥40 % [2]; confluent necrotic core ≥10 % in direct contact with the lumen (i.e., no visible overlying tissue) [40]. Using this definition of IVUS-derived TCFA, in patients with ACS who underwent IVUS of all three epicardial coronaries there were, on average, two IVUS-derived TCFAs per patient with half of them showing outward remodeling [40]. The potential value of these IVUS-VH-derived plaque types in the prediction of adverse coronary events was evaluated in an international multicentre prospective study, the Providing Regional Observations to Study Predictors of Events in the Coronary Tree study (PROSPECT study) [41]. The PROSPECT trial was a multicenter, natural history study of acute coronary syndrome patients: all patients underwent PCI in their culprit lesion at baseline, followed by an angiogram and IVUS virtual histology analyses of the three major coronary arteries. The longitudinal distribution of atherosclerotic plaque burden, virtual histology-IVUS characterized necrotic core content, and VH-TCFA was as follows: there was a gradient in plaque burden from the proximal (42.4 %) to mid (37.6 %) to distal (32.6 %) 30-mm-long segments ($p < 0.0001$). Overall, 67.4 % of proximal, 41.0 % of mid, and 29.7 % of distal 30-mm-long

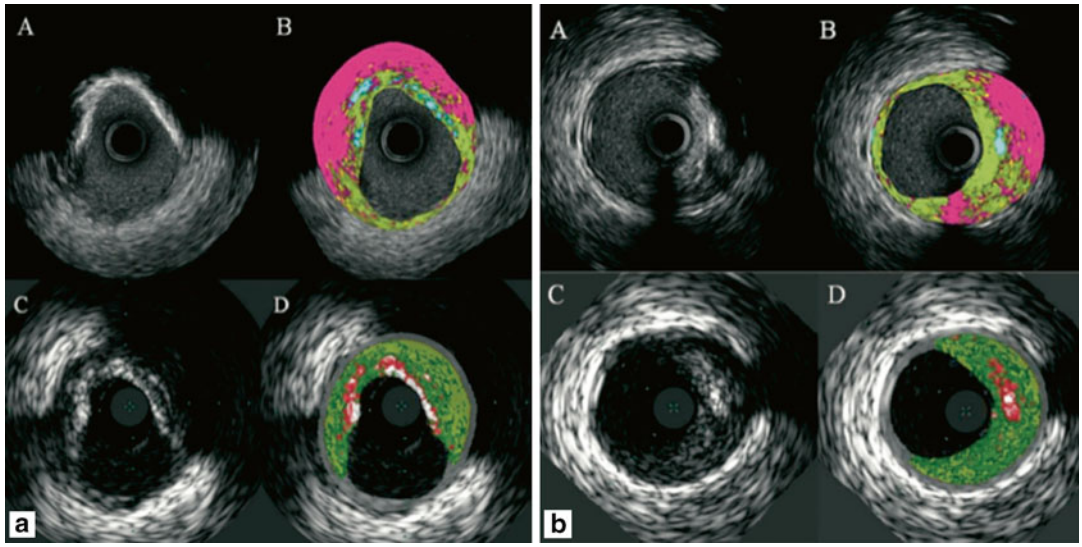

Fig. 7.3 Corresponding cross-section of iMap (*top*) and VH images (*bottom*). iMap shows large amounts of necrotic tissue behind calcium , while with VH the same area is reported as fibrous or fibrofatty tissue. In panel B, iMAP shows necrotic tissue because also of the wire artifact (Reprinted from EuroIntervention 6 [7] Shin E, García-García HM, Ligthart J, et al. In vivo findings of tissue characteristics using iMap™ IVUS and Virtual Histology™ IVUS. EuroIntervention:1017-1019; ©2011. With permission from Europa Digital and Publishing)

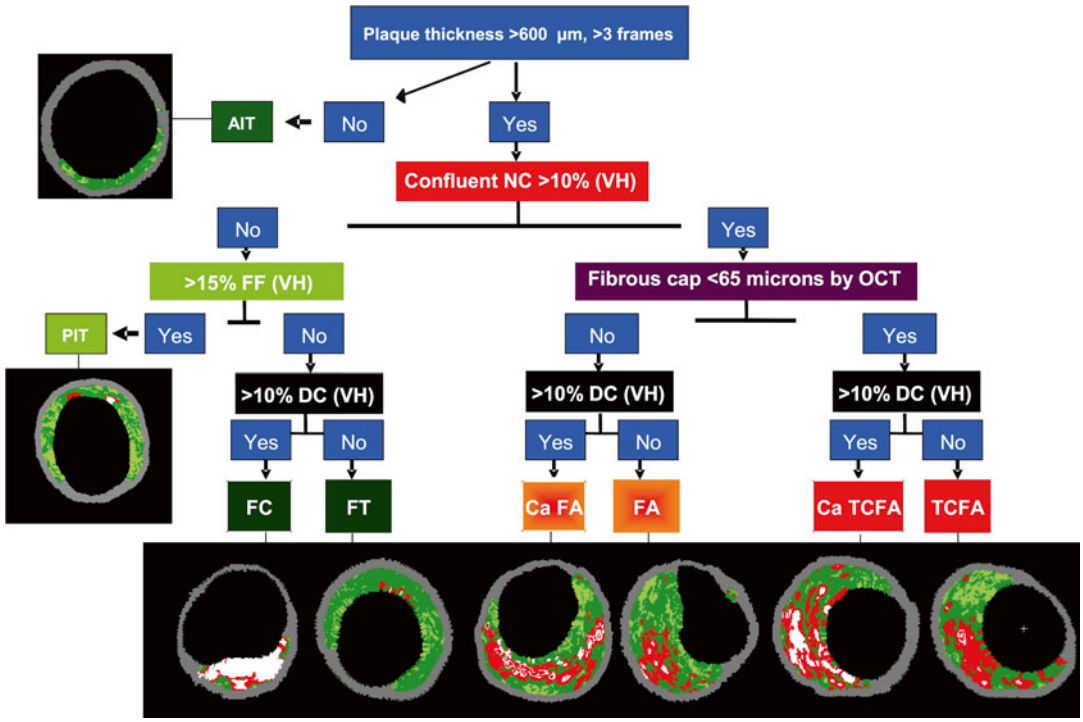

Fig. 7.4 Flow chart for VH classification of coronary plaque. *AIT* adaptive intima thickness, *PIT* pathological intima thickness, *FC* fibrocalcific plaque, *FT* fibrotic plaque, *CaFa* calcified fibroatheroma, *FA* fibroatheroma, *CaTCFA* calcified thin-cap fibroatheroma, *TCFA* thin-cap fibroatheroma, *NC* necrotic core, *FF* fibrofatty, *DC* dense calcium, *OCT* optical coherence tomography

segments contained at least 1 lesion (plaque burden >40 %). Proportion of NC, however, was similar in the proximal and mid 30-mm-long segments of all arteries (10.3 % [interquartile range (IQR): 4.8–16.7 %] vs. 10.6 % [IQR: 5.0–18.1 %], $p=0.25$), but less in the distal 30-mm-long segment (9.1 % [IQR: 3.7–17.8 %], $p=0.03$ compared with the proximal segment and $p=0.003$ compared with the mid segment). Overall, 17.3 % of proximal, 11.5 % of mid, and 9.1 % of distal 30-mm-long segments had at least one lesion that was classified as VH-TCFA ($p<0.0001$). Comparing the LMCA with the combined cohort of proximal left anterior descending, left circumflex, and right coronary artery 30-mm-long segments: (1) plaque burden was less (35.4 % [IQR: 28.8–43.5 %] vs. 40.9 % [IQR: 33.3–48.0 %], $p<0.0001$); (2) fewer LMCAs contained at least 1 lesion (17.5 %, $p<0.0001$); (3) there was less NC (6.5 % [IQR: 2.9–12.2 %] vs. 9.3 % [IQR: 4.3–15.9 %], $p<0.0001$); and (4) LMCAs rarely contained a VH-TCFA (1.8 %, $p<0.0001$). Authors concluded that lesions that are responsible for acute coronary events (large, plaque burden-rich in NC) are somewhat more likely to be present in the proximal than the distal coronary tree, except for the LMCA [42].

A TCFA with a minimum lumen area of ≤ 4 mm^2 and a large plaque burden (≥ 70 %) had a 17.2 % likelihood of causing an event within 3 years. Interestingly, the anticipated high frequency of acute thrombotic cardiovascular events did not occur, with only a 1 % rate of myocardial infarction and no deaths directly attributable to non-culprit vessels over 3 years of follow-up. These results suggest that non-culprit, yet obstructive coronary plaques are most likely to be associated with increasing symptoms rather than thrombotic acute events, with 8.5 % of patients presenting with worsening angina and 3.3 % with unstable angina. The PROSPECT findings were recently confirmed by the VIVA study [43].

Although plaque characteristics (i.e., tissue characterization) do not yet influence current therapeutic guidelines, the available IVUS-based tissue characterization techniques have the ability to identify some of the pathological atheroma features described above and could help us to advance further our understanding on atherosclerosis.

Assessment of Drug Effect on Atherosclerosis by IVUS-VH

IVUS-VH has been so far used in various studies in order to show serial changes of plaque composition in patients treated with various statin treatments (Table 7.1).

In one of them, patients with stable angina pectoris ($n=80$) treated with fluvastatin for 1 year had significant regression of the plaque volume, and changes in the atherosclerotic plaque composition with a significant reduction of the fibrofatty volume ($p<0.0001$). These changes in the fibrofatty volume had a significant correlation with changes in the LDL-cholesterol level ($r=0.703$, $p<0.0001$) and in the hs-C reactive protein level ($r=0.357$, $p=0.006$) [44]. Of note, the necrotic core did not change significantly.

In a second study, Hong et al. randomized 100 patients with stable angina and ACS to either rosuvastatin 10 mg or simvastatin 20 mg for 1 year. The overall necrotic core volume significantly decreased ($p=0.010$) and the fibrofatty plaque volume increased ($p=0.006$) after statin treatments. Particularly, there was a significant decrease in the necrotic core volume ($p=0.015$) in the rosuvastatin-treated subgroup. By multiple stepwise logistic regression analysis, they showed that the only independent clinical predictor of decrease in the necrotic core volume was the baseline HDL-cholesterol level ($p=0.040$, OR: 1.044, 95 % CI 1.002–1089) [45].

The IBIS 2 study compared the effects of 12 months of treatment with darapladib (oral Lp-PLA2 inhibitor, 160 mg daily) or placebo in 330 patients [46]. Endpoints included changes in necrotic core size (IVUS-VH) and atheroma size (IVUS-grayscale). Background therapy was comparable between groups, with no difference in LDL-cholesterol at 12 months (placebo: 88 ± 34 and darapladib: 84 ± 31 mg/dL, $p=0.37$). In the placebo-treated group, however, necrotic

Table 7.1 IVUS-based tissue characterization studies

Yokoyama [63]	RCT	2005	Atorvastatin	25	6 months	Overall plaque size and tissue characterization by IB IVUS	Atorvastatin reduced plaque size and changed plaque composition
			Control	25			
Kawasaki [64]	RCT	2005	Pravastatin,	17	6 months	Overall tissue characterization by IB IVUS	Statins reduced lipid without changes in plaque size
			Atorvastatin	18			
			Diet	17			
IBIS 2 [46]	RCT	2008	Darapladib	175	12 months	Necrotic core volume by IVUS-VH	Darapladib significantly reduced necrotic core
			Placebo	155			
Nasu [44]	Observational	2009	Fluvastatin	40	12 months	Overall tissue characterization by IVUS-VH	Fluvastatin reduced plaque and fibrofatty volume
			Control	40			
Hong [45]	RCT	2009	Simvastatin	50	12 months	Overall tissue characterization by IVUS-VH	Both reduced necrotic core and increased fibrofatty volume
			Rosuvastatin	50			
Toi [65]	RCT	2009	Atorvastatin	80	2–3 weeks	Overall tissue characterization by IVUS-VH	Pitavastatin reduced plaque volume and fibrofatty
			Pivastatin	80			
Miyagi [66]	Observational	2009	Statin (pravastatin, pitavastatin, atorvastatin, fluvastatin, simvastatin)	44	6 months	Overall tissue characterization by IB IVUS	Statins reduced lipid and increased fibrous
			Non statin	56			

RCT randomized controlled trial, *PAV* percent atheroma volume, *IVUS* intravascular ultrasound, *IB* integrated backscatter, *VH* virtual histology
*$p<0.05$ between groups ‡$p<0.05$ vs. Baseline
[a]%Change in plaque volume = [Total plaque volume$_{\text{Follow-up}}$ − Total plaque volume$_{\text{Baseline}}$]/[Total plaque volume$_{\text{Baseline}}$] × 100
Total plaque volume = [External elastic membrane (EEM)$_{\text{Cross-sectional area (CSA)}}$] − [Lumen$_{\text{CSA}}$]
PAV = (EEM$_{\text{CSA}}$ − Lumen$_{\text{CSA}}$)/(EEM$_{\text{CSA}}$) × 100

core volume increased significantly, whereas darapladib halted this increase, resulting in a significant treatment difference of −5.2 mm^3 ($p=0.012$). These intraplaque compositional changes occurred without a significant treatment difference in total atheroma volume. Indeed, in a detailed report on the predictors of change either in percentage of necrotic core (PNC) or percentage of atheroma volume (PAV) were the variables associated with a decrease in PNC from baseline were darapladib, ACS, and a large content of NC at baseline, while variables associated with an increase in PNC were previous stroke and percentage diameter stenosis at baseline. Those variables associated with a decrease in PAV from baseline were waist circumference, statin use, CD40L, and baseline PAV, while the only variable associated with an increase in PAV was baseline diastolic blood pressure [47].

Despite all these studies, there is no a single report describing a clear direct association between reduction in the plaque size and/or the plaque composition with reduction in clinical events. The best attempt was a pooled analysis of 4,137 patients from 6 clinical trials that used serial IVUS: the relationship between baseline and change in PAV with incident major adverse cardiovascular events (MACE) was investigated. Each standard deviation increase in PAV was associated with a 1.32-fold (95 % CI: 1.22–1.42; $p<0.001$) greater likelihood of experiencing a MACE [48].

Assessment of Stent by IVUS-VH

Polymeric Scaffolds

Kim et al. have previously shown that metallic stents eluting sirolimus and paclitaxel introduce artifacts in IVUS-VH images that interfere with the classification of plaque behind the struts [49]. Normally struts of DES appear as dense calcium, surrounded by a red halo. Although the ABSORB scaffold is made of nonmetallic materials, it is also recognized by IVUS-VH software as dense calcium and necrotic core. Moreover the presence of "pseudo" dense calcium and necrotic core could be used as quantitative surrogate for the presence of the polymeric material of the scaffold and may help to evaluate the bioresorption process during follow-up [50–53]. Garcia-Garcia et al. have already shown in a sub-study of ABSORB cohort A trial that polymeric struts are identified with radiofrequency backscattering signal as calcific structures and that the ability of IVUS-VH to recognize polymeric struts is important not only to study imaging of the ABSORB post-implantation, but also to potentially follow the mechanical support or bioresorption process [51] (Fig. 7.5). The absence of validation to recognize polymeric material by VH should be, however, acknowledged.

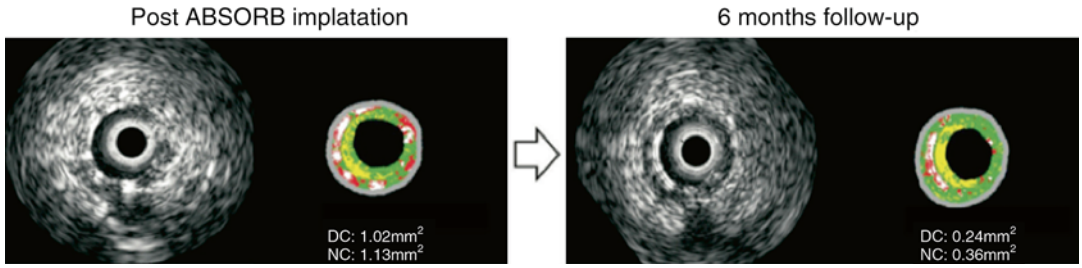

Fig. 7.5 IVUS-VH recognizes the polymeric struts of the ABSORB scaffold as dense calcium (DC), surrounded by a *red* halo of necrotic core (NC). At follow-up, a reduction in DC and NC can be appreciated. In order to pick up all the struts, the lumen contour has been drawn surrounding the catheter, according to the Shin's method

Analysis of Changes in Scaffolded Plaque Composition

IVUS-VH can also be used to analyze the changes in composition of the plaque scaffolded by a metallic or a bioresorbable scaffold. Kubo et al., analyzing the long-term effects of DES and of BMS on coronary arterial wall morphology by IVUS-VH, have shown that DES-treated lesions had a greater frequency of unstable lesion morphometry at follow-up compared to BMS [54]. In particular assessing the total amount of the four color-VH components including also the contribution of the stent, they found that DES-treated lesions showed, at follow-up, a significantly higher incidence of necrotic core abutting the lumen compared to BMS-treated lesions, although there was not a significant difference in necrotic core mean area between the two groups. This was due to a suppression of the protective neointimal hyperplasia layer in DES compared with BMS.

Aoki et al. have demonstrated in vivo that plaque volume behind the metallic stent eluting sirolimus increases slightly at 4 months follow-up and then significantly decreases at 4 years follow-up compared to post-implantation and that change in echogenicity is suggestive of a change in plaque composition [55]. He also documented a significant increase of plaque area outside metallic stent eluting paclitaxel at 6 months, with its regression at 2 years [56]. In these situations, it would be interesting to know what type of tissue is contributed to this process and, from a quantitative point, to develop a third (stent) contour in the VH software in order to characterize selectively intimal hyperplasia and peri-stent tissue. The potential lack of validation of VH in the assessment of in-stent restenosis should be, however, acknowledged.

Sarno et al. analyzing IVUS-VH plaque characterization behind the first-generation ABSORB scaffold found a reduction in necrotic core component between 6-month and 2 years follow-up, probably related to a synergistic effect of the bioresorption process and the anti-inflammatory action of everolimus [52].

Nevertheless, it should be keep in mind that, since the stent's struts are recognized by IVUS-VH as dense calcium and necrotic core, careful evaluation of exclusively the plaque behind the stent should be done to avoid any misclassification of the actual tissue [49, 52]. Recently a customized software has been developed and used to introduce in a semiautomatic way a third contour behind the stent, allowing then to focus the analysis on only the plaque behind the struts [57].

Stent Thrombosis

Another possible application of IVUS-VH for stent evaluation is about stent thrombosis mechanisms. It is known that one of the proposed pathological mechanisms of coronary stent thrombosis is stenting of necrotic core-rich plaques with extensive tissue prolapse and plaque disruption in the proximity of the stented arterial segment [12, 58, 59]. Thus, pre-stenting imaging using IVUS-VH can give us an insight not only into the extent of plaque, but also on the extent of necrotic core within and beyond the intended stenting segment. In this context, studying 24 patients in whom 26 stented segments using IVUS-VH were assessed, no stent thrombosis was observed, where necrotic core-rich areas were left unstented [59]. Ramcharitar et al. presented the first clinical case of a patient with a no-culprit IVUS-VH-derived TCFA, successfully treated with PCI, with a good 6-month angiographic follow-up [60]. A large trial in which patients are randomized to IVUS-VH or angiography-guided optimal coronary stenting is required to draw firm conclusions.

Edge Effects Assessed by IVUS-VH

The concept of edge vascular response was firstly introduced in the era of endovascular brachytherapy utilizing radioactive stents of various activity levels. Although endovascular brachytherapy reduced intrastent neointimal hyperplasia and thereby the incidence of in-stent restenosis in

a dose-dependent manner, tissue proliferation at the non-irradiated proximal and distal edges resulted in the failure of this invasive treatment. The advent of the first- and second-generation DES reduced in-stent restenosis to approximately 5–10 % dependent on the lesion subset and type of DES. When in-segment restenosis (stent and 5 mm proximal and distal margins) occurred, this was most commonly focal and located at the proximal edge. In addition stent thrombosis, the other main contributing factor for DES failure, appeared in part to be directly related to the presence of residual plaque and the underlying tissue composition at the landing zone of the implanted device, particularly if implanted in a necrotic core-rich milieu. More recently the introduction of bioresorbable scaffolds for the treatment of coronary artery disease has prompted the reevaluation of the EVR. The transient scaffolding properties of the bioresorbable scaffolds may potentially eliminate the long-term EVR pitfalls, namely in segment restenosis and device thrombosis.

Based on previous pathological studies, we hypothesized that the tissue associated with an increase of plaque at the edges of the paclitaxel stent is mainly fibrofatty tissue as assessed by IVUS-VH. Fibrofatty, in IVUS-VH, has been described as loosely packed bundles of collagen fibers with regions of lipid deposition and extracellular matrix without necrotic areas [12].

In the BETAX study [61], 24 patients (26 paclitaxel-eluting stents) were studied. Serial expansive vascular remodeling was observed at the proximal and distal edges of the stent to accommodate fibrofatty and fibrous tissue growth. More specifically, proximal and distal segments were divided into five subsegments of 1-mm. In the first two subsegments adjacent to the proximal edge of the stent, the vessel wall grew to compensate the plaque growth without affecting the lumen size. In the following three subsegments, overcompensation (vessel wall increased more than plaque size) was observed. Consequently, the lumen size increased. At the distal edge, overcompensation was observed in all five subsegments, followed by an increase in lumen size. In summary, proximal and distal growth patterns were characterized by an increase in fibrofatty tissue ($p<0.001$ and $p<0.001$, respectively), a decrease in necrotic core ($p=0.014$ and $p<0.001$, respectively), and a decrease in dense calcium content ($p<0.001$ and $p<0.001$, respectively).

The ABSORB bioresorbable vascular scaffold (BVS) (Abbott Vascular, Santa Clara, CA) has been evaluated with the ABSORB Cohort A trial (A Clinical Evaluation of the Bioabsorbable Vascular Solutions Everolimus Eluting Coronary Stent System in the Treatment of Patients With Single de Novo Native Coronary Artery Lesions) up to 5 years and the ABSORB Cohort B up to 2 years. The EVR was assessed non-serially up to 1 year (Cohort B1, $n=45$ and B2, $n=56$) and serially (Cohort B1) up to 2 years. The non-serial evaluation demonstrated some degree of constrictive remodeling at the proximal edge of: Δ EEM: −1.80 % [−3.18; 1.30], ($p<0.05$) similar to that previously seen with metallic stents at the same time point; however, this response was less evident at 1 year: Δ EEM: −1.53 % [−7.74; 2.48], ($p=0.06$) [62].

The serial evaluation at 2 years (post-procedure to 2 years) revealed a lumen loss of: Δ−6.68 % [−17.33; 2.08], ($p=0.027$) with a trend toward plaque area increase of: Δ+7.55 % [−4.68; 27.11], ($p=0.06$) at the proximal edge and distal edge tissue composition changes with a significant increase of the fibrofatty tissue component (from 6 months to 2 years) from 0.09 mm^2 [0.04; 0.22] mm^2 to 0.22 mm^2 [0.14; 0.51], respectively, translated to a percentage increase of: Δ+68.37 % [17.82; 171.17], ($p=0.013$) (personal communication at EuroPCR 2012). In summary the EVR up to 2 years with a fully bioresorbable device demonstrates proximal edge effect with tissue composition changes at the distal edge.

Conclusions

During the last 10 years, IVUS and IVUS-VH have been widely applied to study the natural history of coronary plaques “in vivo” and to assess the efficacy of new drug or new devices.

A lot of achievements have been reached: (1) VH-derived TCFAs were strongly correlated to future coronary events; (2) VH showed the pharmacological or mechanical treatment of coronary atherosclerosis may positively modify plaque composition; (3) in addition it can be used to explore causes of DES pitfalls and it can be applied in the field of the new polymeric intracoronary devices.

Despite the clear potential of the technology in these areas, its role in daily clinical practice has still to be defined. It is, in fact, unknown if we should screen for VH-TCFA presence and if we should treat them in order to prevent future adverse events. In case of treatment, efficacious pharmacological or mechanical treatment would be needed. Randomized trials to address these issues would be difficult and costly.

References

1. Virmani R, Burke AP, Farb A, Kolodgie FD. Pathology of the vulnerable plaque. J Am Coll Cardiol. 2006; 47:C13–8.
2. Schaar JA, Muller JE, Falk E, et al. Terminology for high-risk and vulnerable coronary artery plaques. Report of a meeting on the vulnerable plaque, June 17 and 18, 2003, Santorini, Greece. Eur Heart J. 2004; 25:1077–82.
3. Cheruvu PK, Finn AV, Gardner C, et al. Frequency and distribution of thin-cap fibroatheroma and ruptured plaques in human coronary arteries: a pathologic study. J Am Coll Cardiol. 2007;50:940–9.
4. Cunningham KS, Gotlieb AI. The role of shear stress in the pathogenesis of atherosclerosis. Lab Invest. 2005;85:9–23.
5. Garcia-Garcia HM, Costa MA, Serruys PW. Imaging of coronary atherosclerosis: intravascular ultrasound. Eur Heart J. 2010;31:2456–69.
6. Mintz GS, Nissen SE, Anderson WD, et al. American College of Cardiology Clinical Expert Consensus Document on Standards for Acquisition, Measurement and Reporting of Intravascular Ultrasound Studies (IVUS). A report of the American College of Cardiology Task Force on Clinical Expert Consensus Documents. J Am Coll Cardiol. 2001;37:1478–92.
7. Garcia-Garcia HM, Gogas BD, Serruys PW, Bruining N. IVUS-based imaging modalities for tissue characterization: similarities and differences. Int J Cardiovasc Imaging. 2011;27:215–24.
8. Virmani R, Kolodgie FD, Burke AP, Farb A, Schwartz SM. Lessons from sudden coronary death: a comprehensive morphological classification scheme for atherosclerotic lesions. Arterioscler Thromb Vasc Biol. 2000;20:1262–75.
9. Ross R. Atherosclerosis—an inflammatory disease. N Engl J Med. 1999;340:115–26.
10. Bruining N, de Winter S, Roelandt JR, et al. Coronary calcium significantly affects quantitative analysis of coronary ultrasound: importance for atherosclerosis progression/regression studies. Coron Artery Dis. 2009;20:409–14.
11. Bruining N, Verheye S, Knaapen M, et al. Three-dimensional and quantitative analysis of atherosclerotic plaque composition by automated differential echogenicity. Catheter Cardiovasc Interv. 2007;70: 968–78.
12. Nair A, Margolis MP, Kuban BD, Vince DG. Automated coronary plaque characterisation with intravascular ultrasound backscatter: ex vivo validation. EuroIntervention. 2007;3:113–20.
13. Palmer ND, Northridge D, Lessells A, McDicken WN, Fox KA. In vitro analysis of coronary atheromatous lesions by intravascular ultrasound; reproducibility and histological correlation of lesion morphology. Eur Heart J. 1999;20:1701–6.
14. Pasterkamp G, Schoneveld AH, van der Wal AC, et al. Relation of arterial geometry to luminal narrowing and histologic markers for plaque vulnerability: the remodeling paradox. J Am Coll Cardiol. 1998;32: 655–62.
15. Burke AP, Kolodgie FD, Farb A, Weber D, Virmani R. Morphological predictors of arterial remodeling in coronary atherosclerosis. Circulation. 2002;105: 297–303.
16. Kotani J, Mintz GS, Castagna MT, et al. Intravascular ultrasound analysis of infarct-related and non-infarct-related arteries in patients who presented with an acute myocardial infarction. Circulation. 2003;107: 2889–93.
17. Maehara A, Mintz GS, Bui AB, et al. Morphologic and angiographic features of coronary plaque rupture detected by intravascular ultrasound. J Am Coll Cardiol. 2002;40:904–10.
18. von Birgelen C, Klinkhart W, Mintz GS, et al. Plaque distribution and vascular remodeling of ruptured and nonruptured coronary plaques in the same vessel: an intravascular ultrasound study in vivo. J Am Coll Cardiol. 2001;37:1864–70.
19. Nakamura M, Nishikawa H, Mukai S, et al. Impact of coronary artery remodeling on clinical presentation of coronary artery disease: an intravascular ultrasound study. J Am Coll Cardiol. 2001;37:63–9.
20. Gyongyosi M, Yang P, Hassan A, et al. Intravascular ultrasound predictors of major adverse cardiac events in patients with unstable angina. Clin Cardiol. 2000; 23:507–15.
21. Gyongyosi M, Yang P, Hassan A, et al. Arterial remodelling of native human coronary arteries in patients with unstable angina pectoris: a prospective intravascular ultrasound study. Heart. 1999;82: 68–74.

22. Tauth J, Pinnow E, Sullebarger JT, et al. Predictors of coronary arterial remodeling patterns in patients with myocardial ischemia. Am J Cardiol. 1997;80: 1352–5.
23. Rodriguez-Granillo GA, Serruys PW, Garcia-Garcia HM, et al. Coronary artery remodelling is related to plaque composition. Heart. 2006;92:388–91.
24. Fujii K, Mintz GS, Carlier SG, et al. Intravascular ultrasound profile analysis of ruptured coronary plaques. Am J Cardiol. 2006;98:429–35.
25. Kolodgie FD, Gold HK, Burke AP, et al. Intraplaque hemorrhage and progression of coronary atheroma. N Engl J Med. 2003;349:2316–25.
26. Jensen LO, Mintz GS, Carlier SG, et al. Intravascular ultrasound assessment of fibrous cap remnants after coronary plaque rupture. Am Heart J. 2006;152: 327–32.
27. Fujii K, Carlier SG, Mintz GS, et al. Intravascular ultrasound study of patterns of calcium in ruptured coronary plaques. Am J Cardiol. 2005;96:352–7.
28. Rioufol G, Gilard M, Finet G, Ginon I, Boschat J, Andre-Fouet X. Evolution of spontaneous atherosclerotic plaque rupture with medical therapy: long-term follow-up with intravascular ultrasound. Circulation. 2004;110:2875–80.
29. Hong MK, Mintz GS, Lee CW, et al. Serial intravascular ultrasound evidence of both plaque stabilization and lesion progression in patients with ruptured coronary plaques: effects of statin therapy on ruptured coronary plaque. Atherosclerosis. 2007;191:107–14.
30. Kubo T, Imanishi T, Takarada S, et al. Assessment of culprit lesion morphology in acute myocardial infarction: ability of optical coherence tomography compared with intravascular ultrasound and coronary angioscopy. J Am Coll Cardiol. 2007;50:933–9.
31. Honda O, Sugiyama S, Kugiyama K, et al. Echolucent carotid plaques predict future coronary events in patients with coronary artery disease. J Am Coll Cardiol. 2004;43:1177–84.
32. Gronholdt ML, Nordestgaard BG, Schroeder TV, Vorstrup S, Sillesen H. Ultrasonic echolucent carotid plaques predict future strokes. Circulation. 2001;104: 68–73.
33. Hiro T, Leung CY, Russo RJ, et al. Variability in tissue characterization of atherosclerotic plaque by intravascular ultrasound: a comparison of four intravascular ultrasound systems. Am J Card Imaging. 1996;10: 209–18.
34. Hodgson JM, Reddy KG, Suneja R, Nair RN, Lesnefsky EJ, Sheehan HM. Intracoronary ultrasound imaging: correlation of plaque morphology with angiography, clinical syndrome and procedural results in patients undergoing coronary angioplasty. J Am Coll Cardiol. 1993;21:35–44.
35. Nair A, Kuban BD, Tuzcu EM, Schoenhagen P, Nissen SE, Vince DG. Coronary plaque classification with intravascular ultrasound radiofrequency data analysis. Circulation. 2002;106:2200–6.
36. Garcia-Garcia HM, Mintz GS, Lerman A, et al. Tissue characterisation using intravascular radiofrequency data analysis: recommendations for acquisition, analysis, interpretation and reporting. EuroIntervention. 2009;5:177–89.
37. Granada JF, Wallace-Bradley D, Win HK, et al. In vivo plaque characterization using intravascular ultrasound-virtual histology in a porcine model of complex coronary lesions. Arterioscler Thromb Vasc Biol. 2007;27:387–93.
38. Sathyanarayana S, Carlier S, Li W, Thomas L. Characterisation of atherosclerotic plaque by spectral similarity of radiofrequency intravascular ultrasound signals. EuroIntervention. 2009;5:133–9.
39. Shin ES, Garcia-Garcia HM, Ligthart JM, et al. In vivo findings of tissue characteristics using iMap IVUS and Virtual Histology IVUS. EuroIntervention. 2011;6:1017–9.
40. Garcia-Garcia HM, Goedhart D, Schuurbiers JC, et al. Virtual histology and remodeling index allow in vivo identification of allegedly high risk coronary plaques in patients with acute coronary syndromes: a three vessel intravascular ultrasound radiofrequency data analysis. EuroIntervention. 2006;2:338–44.
41. Stone GW, Maehara A, Lansky AJ, et al. A prospective natural-history study of coronary atherosclerosis. N Engl J Med. 2011;364:226–35.
42. Wykrzykowska JJ, Mintz GS, Garcia-Garcia HM, et al. Longitudinal distribution of plaque burden and necrotic core-rich plaques in nonculprit lesions of patients presenting with acute coronary syndromes. JACC Cardiovasc Imaging. 2012;5:S10–8.
43. Calvert PA, Obaid DR, O'Sullivan M, et al. Association between IVUS findings and adverse outcomes in patients with coronary artery disease: the VIVA (VH-IVUS in Vulnerable Atherosclerosis) Study. JACC Cardiovasc Imaging. 2011;4:894–901.
44. Nasu K, Tsuchikane E, Katoh O, et al. Effect of fluvastatin on progression of coronary atherosclerotic plaque evaluated by virtual histology intravascular ultrasound. JACC Cardiovasc Interv. 2009;2:689–96.
45. Hong MK, Park DW, Lee CW, et al. Effects of statin treatments on coronary plaques assessed by volumetric virtual histology intravascular ultrasound analysis. JACC Cardiovasc Interv. 2009;2:679–88.
46. Serruys PW, Garcia-Garcia HM, Buszman P, et al. Effects of the direct lipoprotein-associated phospholipase A(2) inhibitor darapladib on human coronary atherosclerotic plaque. Circulation. 2008;118:1172–82.
47. Garcia-Garcia HM, Klauss V, Gonzalo N, et al. Relationship between cardiovascular risk factors and biomarkers with necrotic core and atheroma size: a serial intravascular ultrasound radiofrequency data analysis. Int J Cardiovasc Imaging. 2012;28(4):695–703.
48. Nicholls SJ, Hsu A, Wolski K, et al. Intravascular ultrasound-derived measures of coronary atherosclerotic plaque burden and clinical outcome. J Am Coll Cardiol. 2010;55:2399–407.

49. Kim SW, Mintz GS, Hong YJ, et al. The virtual histology intravascular ultrasound appearance of newly placed drug-eluting stents. Am J Cardiol. 2008;102: 1182–6.
50. Serruys PW, Ormiston JA, Onuma Y, et al. A bioabsorbable everolimus-eluting coronary stent system (ABSORB): 2-year outcomes and results from multiple imaging methods. Lancet. 2009;373:897–910.
51. Garcia-Garcia HM, Gonzalo N, Pawar R, et al. Assessment of the absorption process following bioabsorbable everolimus-eluting stent implantation: temporal changes in strain values and tissue composition using intravascular ultrasound radiofrequency data analysis. A substudy of the ABSORB clinical trial. EuroIntervention. 2009;4:443–8.
52. Sarno G, Onuma Y, Garcia Garcia HM, et al. IVUS radiofrequency analysis in the evaluation of the polymeric struts of the bioabsorbable everolimus-eluting device during the bioabsorption process. Catheter Cardiovasc Interv. 2010;75:914–8.
53. Ormiston JA, Serruys PW, Regar E, et al. A bioabsorbable everolimus-eluting coronary stent system for patients with single de-novo coronary artery lesions (ABSORB): a prospective open-label trial. Lancet. 2008;371:899–907.
54. Kubo T, Maehara A, Mintz GS, et al. Analysis of the long-term effects of drug-eluting stents on coronary arterial wall morphology as assessed by virtual histology intravascular ultrasound. Am Heart J. 2010; 159:271–7.
55. Aoki J, Abizaid AC, Serruys PW, et al. Evaluation of four-year coronary artery response after sirolimus-eluting stent implantation using serial quantitative intravascular ultrasound and computer-assisted gray-scale value analysis for plaque composition in event-free patients. J Am Coll Cardiol. 2005;46:1670–6.
56. Aoki J, Colombo A, Dudek D, et al. Peristent remodeling and neointimal suppression 2 years after polymer-based, paclitaxel-eluting stent implantation: insights from serial intravascular ultrasound analysis in the TAXUS II study. Circulation. 2005;112: 3876–83.
57. Brugaletta S, Garcia-Garcia HM, Garg S, et al. Temporal changes of coronary artery plaque located behind the struts of the everolimus eluting bioresorbable vascular scaffold. Int J Cardiovasc Imaging. 2011;27(6):859–66; Epub ahead of print.
58. Farb A, Burke AP, Kolodgie FD, Virmani R. Pathological mechanisms of fatal late coronary stent thrombosis in humans. Circulation. 2003;108:1701–6.
59. Garcia-Garcia HM, Goedhart D, Serruys PW. Relation of plaque size to necrotic core in the three major coronary arteries in patients with acute coronary syndrome as determined by intravascular ultrasonic imaging radiofrequency. Am J Cardiol. 2007;99:790–2.
60. Ramcharitar S, Gonzalo N, van Geuns RJ, et al. First case of stenting of a vulnerable plaque in the SECRITT I trial-the dawn of a new era? Nat Rev Cardiol. 2009;6:374–8.
61. Garcia-Garcia HM, Gonzalo N, Tanimoto S, Meliga E, de Jaegere P, Serruys PW. Characterization of edge effects with paclitaxel-eluting stents using serial intravascular ultrasound radiofrequency data analysis: the BETAX (BEside TAXus) Study. Rev Esp Cardiol. 2008;61:1013–9.
62. Gogas BD, Serruys PW, Diletti R, et al. Vascular response of the segments adjacent to the proximal and distal edges of the ABSORB everolimus-eluting bioresorbable vascular scaffold: 6-month and 1-year follow-up assessment: a virtual histology intravascular ultrasound study from the first-in-man ABSORB cohort B trial. JACC Cardiovasc Interv. 2012;5: 656–65.
63. Yokoyama M, Komiyama N, Courtney BK, et al. Plasma low-density lipoprotein reduction and structural effects on coronary atherosclerotic plaques by atorvastatin as clinically assessed with intravascular ultrasound radio-frequency signal analysis: a randomized prospective study. Am Heart J. 2005;150:287.
64. Kawasaki M, Sano K, Okubo M, et al. Volumetric quantitative analysis of tissue characteristics of coronary plaques after statin therapy using three-dimensional integrated backscatter intravascular ultrasound. J Am Coll Cardiol. 2005;45:1946–53.
65. Toi T, Taguchi I, Yoneda S, et al. Early effect of lipid-lowering therapy with pitavastatin on regression of coronary atherosclerotic plaque. Comparison with atorvastatin. Circ J. 2009;73:1466–72.
66. Miyagi M, Ishii H, Murakami R, et al. Impact of long-term statin treatment on coronary plaque composition at angiographically severe lesions: a nonrandomized study of the history of long-term statin treatment before coronary angioplasty. Clin Ther. 2009;31: 64–73.

Optical Coherence Tomography of Coronary Atherosclerosis

8

Manabu Kashiwagi, Hironori Kitabata,
Takashi Akasaka, and Guillermo J. Tearney

Introduction

Intravascular optical coherence tomography (IVOCT) is an invasive, catheter-based, cross-sectional microscopic imaging technology that employs near-infrared light and provides a depth-dependent resolution of approximately 10 μm and a lateral resolution of about 30 μm [1]. The resolution of IVOCT makes it possible to characterize the detailed structure of the superficial artery wall. IVOCT has been shown to be capable of classifying coronary plaque and various components related to atherosclerosis in vivo, which may provide an improved understanding of atherosclerosis and acute coronary syndrome (ACS) [2–6]. IVOCT may also enable the detection of certain types of "vulnerable plaque" in vivo as well as their clinical features and prognosis [7]. With respect to coronary intervention, IVOCT trials have revealed the association between IVOCT morphological information and adverse cardiac events [8]. It is expected that this improved level of detailed information will help cardiologists make more informed decisions, which will in turn improve patient interventional outcomes. In this chapter, we will provide an introduction to IVOCT imaging, including a brief description of the technology, image interpretation, and areas of further research.

M. Kashiwagi, MD
Wellman Center for Photomedicine, Massachusetts General Hospital, 40 Blossome Street, RSH 160, Boston, MA 02114, USA
e-mail: mkashiwagi2@partners.org

H. Kitabata, MD, PhD • T. Akasaka, MD, PhD
Department of Cardiovascular Medicine, Medical University, 811-1, Kimiidera, Wakayama 641-8509, Japan
e-mail: miu1205@hotmail.co.jp; akasat@wakayama-med.ac.jp

G.J. Tearney, MD, PhD (✉)
Department of Pathology, Massachusetts General Hospital, 40 Parkman Street, RSL 160, Boston, MA 02114, USA
e-mail: gtearney@partners.org

Optical Coherence Tomography

IVOCT is an interferometric imaging technology that uses near-infrared light to obtain information as a function of depth from the luminal surface. IVOCT can provide an axial (depth) resolution of approximately 10 μm and a transverse resolution that ranges between 20 and 40 μm. To obtain optical coherence tomography (OCT) images from vessels such as in the coronary artery, blood needs to be removed from the field of view because near-infrared light is attenuated by the presence of red blood cells. With the first-generation form of IVOCT, termed time-domain OCT (TD-OCT), two methods were used for image acquisition: a balloon occlusion method and a continuous flushing method [6, 9]. However, images were obtained at a slow rate and patients could be exposed to temporary myocardial ischemia to obtain clear images using these flushing methods.

S.J. Nicholls and T. Crowe (eds.), *Imaging Coronary Atherosclerosis*, Contemporary Cardiology,
DOI 10.1007/978-1-4939-0572-0_8,

FD-OCT and OFDI

Frequency domain OCT (FD-OCT) or optical frequency domain imaging (OFDI) is the second-generation form of OCT that is able to acquire images at frame rates that are more than an order magnitude higher than those of TD-OCT [10]. Due to high-speed image acquisition of these technologies, three-dimensional comprehensive volumetric microscopy of long arterial segments can be obtained using an 8–10 cm^3 radiocontrast or saline flush and helically scanning the catheter's optics [11].

Ex Vivo Studies

Normal Vessels

The normal vessel wall is composed of three layers: intima, media, and adventitia. While intravascular ultrasound (IVUS) cannot completely distinguish the boundary of intima and media if the thickness of intima is less than 180 μm [12], IVOCT is capable of detecting intimal thicknesses that are much smaller. In an OCT image, the normal vessel wall is characterized by a layered architecture, comprising a highly backscattering or signal-rich intima, a media that frequently has low backscattering or is signal poor, and heterogeneous and frequently highly backscattering adventitia (Fig. 8.1 and Table 8.1). On occasion, the internal elastic membrane and external elastic membrane are visualized as highly backscattering thin structures that flank the media [7].

Plaque Characterization

Criteria for OCT plaque characterization have been previously established by investigating 357 specimens (162 aortas, 105 carotid bulbs, and 90 coronary arteries) from 90 cadavers [8]. Fibrous plaques were characterized by high scattering and homogeneous signal, fibrocalcific plaque as a signal-poor lesion or heterogeneous region with a

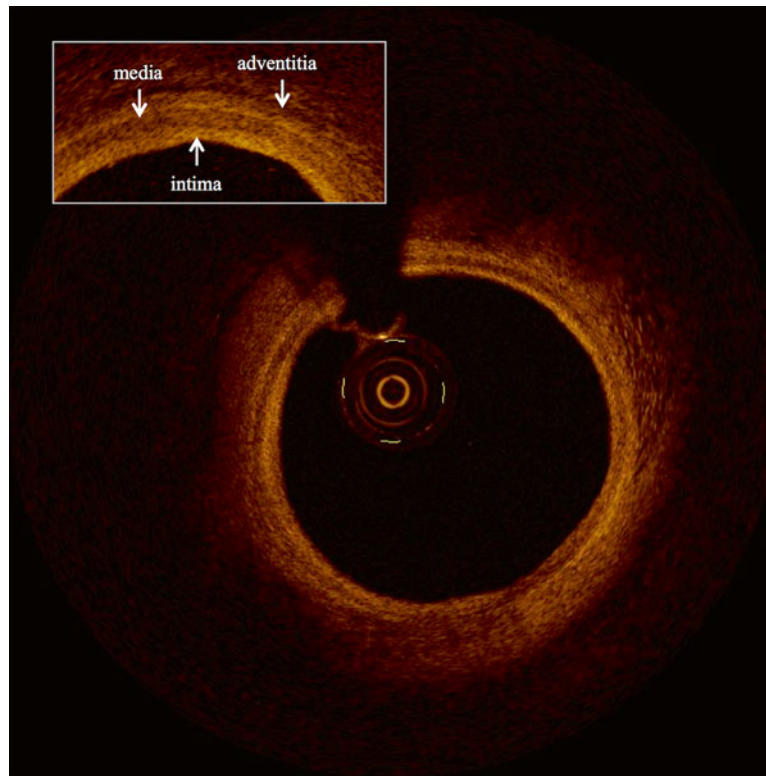

Fig. 8.1 Normal artery wall. Normal artery wall shows a three-layered architecture, comprising a high backscattering, thin intima, a low backscattering media, and a heterogeneous and/or high backscattering adventitia (Courtesy of Wakayama Medical University)

Table 8.1 OCT image features of vessel wall

Histology	OCT
Intima	Signal-rich layer nearest lumen
Media	Signal-poor middle layer
Adventitia	Signal-rich heterogeneous outer lumen
Internal elastic lamina (IEL)	Signal-rich band between intima and media
External elastic lamina (EEL)	Signal-rich band between media and adventitia

Reprinted from Jang IK, Bouma BE, Kang DH, Park SJ, Park SW, Seung KB, et al. Visualization of coronary atherosclerotic plaques in patients using optical coherence tomography: comparison with intravascular ultrasound. J Am Coll Cardiol. 2002;39(4):604–9. With permission from Elsevier

sharply delineated border, and lipid-rich plaques by signal-poor area with diffuse borders (Figs. 8.2 and 8.3). These criteria demonstrated a sensitivity and specificity of 71–79 % and 97–98 % for fibrous plaques, 95–96 % and 97 % for fibrocalcific plaques, and 90–94 % and 90–92 % for lipid-rich plaques, respectively [8]. These results were also confirmed in other ex vivo studies, which showed even higher accuracy of evaluation for lipid-rich plaque compared to IVUS [13].

Macrophages

Macrophages play a key role in all phases of coronary artery atherosclerosis. It has been hypothesized that macrophages show high backscattering because they contain lipid and other cellular debris (Fig. 8.4). In a one study of 27 cadaver necrotic core fibroatheromas, OCT images were acquired and quantified using the "Normalized Standard Deviation" (NSD) parameter that measures local OCT image heterogeneity. NSD was compared to registered histologic slides that were immunohistochemically stained by CD68 [3]. A positive correlation between OCT and histologic measurement of CD68 was found ($r=0.84$, $p<0.00001$); a range of NSD thresholds (6.15–6.35 %) demonstrated 100 % sensitivity and specificity for differentiating caps containing >10 % CD68 staining [3].

Thrombi

OCT can distinguish two major types of thrombi: red and white (Fig. 8.5). The red thrombus shows high backscattering and high attenuation. In contrast, the white thrombus shows less backscattering, low attenuation, and a homogeneous signal [4]. The appearance of mixed and organized thrombi by OCT is hypothesized to be heterogeneous, but the image characteristics of organized thrombi are not well understood or validated.

Cholesterol Crystals

Cholesterol crystals can be seen by IVOCT within atheromatous plaque, usually in combination with lipid. Cholesterol crystals appear as needle-shaped clefts on pathology and OCT demonstrates similarly shaped, linear highly scattering signals [5] (Fig. 8.6). Some investigators have suggested that cholesterol crystal might have the potential to injure the fibrous cap, leading to ACS, but to date, there are no in vivo OCT examinations or trials that test this hypothesis [14].

Neovascularization

Vulnerable plaque is pathologically defined as a plaque with a thin fibrous cap, necrotic core, and macrophage infiltration within a fibrous cap. In addition, neovascularization in atheromatous plaque, called "vasa vasorum," may also be related to plaque vulnerability [15]. Neovascularization is identified as regions with little or no IVOCT backscattering and are frequently observed over several frames [16] (Fig. 8.7). Although there is little histopathologic validation of IVOCT for neovascularization, a clinical OCT study demonstrates that these regions in coronary plaques correlate with the presence of thin-cap fibroatheromas (TCFA) and positive arterial remodeling [17]. More recently, it has been reported that neovascularization seen by IVOCT is strongly associated with the progression of coronary artery plaques [18].

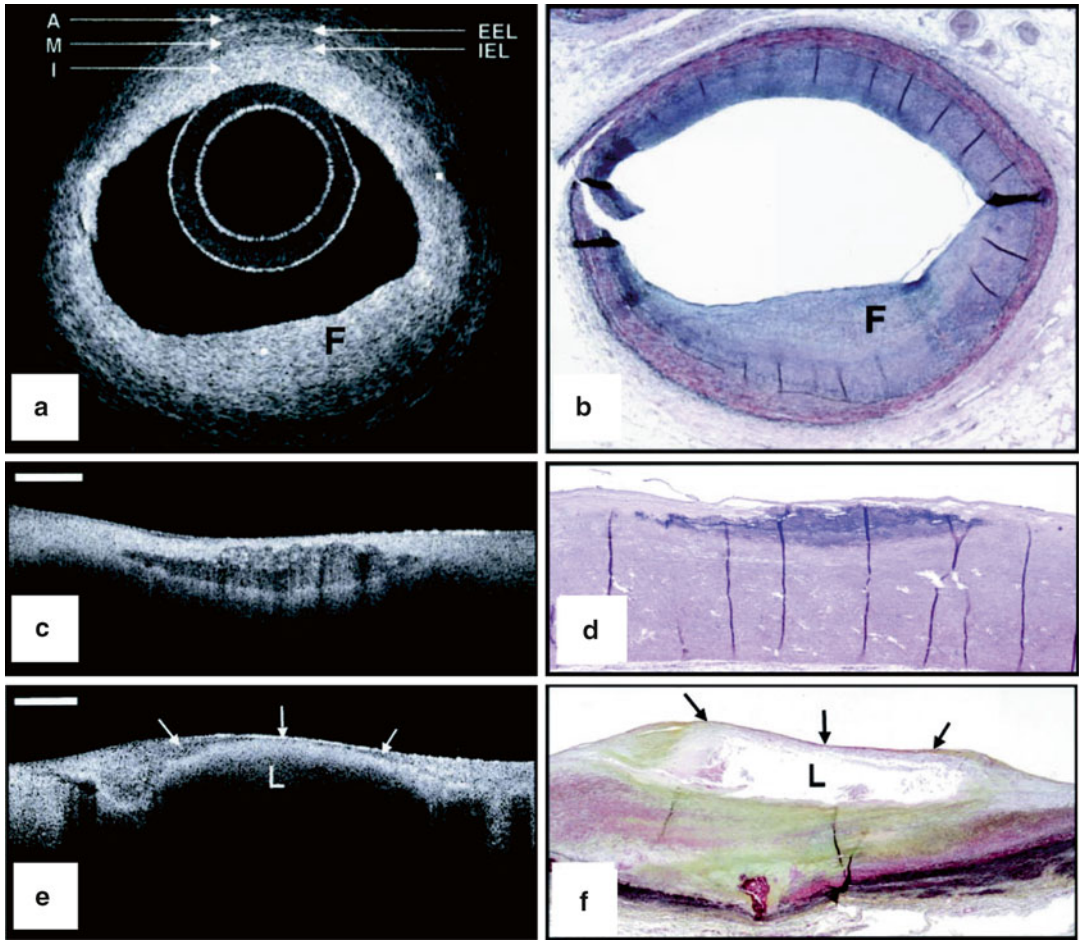

Fig. 8.2 Ex vivo OCT images of human plaques. (**a**) OCT image of a fibrous coronary plaque showing a homogeneous, signal-rich interior (F). An area of intimal hyperplasia is seen opposite fibrous lesion, demonstrating intima (I, with intimal hyperplasia), internal elastic lamina (IEL), media (M), external elastic lamina (EEL), and adventitia (A). (**b**) Corresponding histology (Movat's pentachrome; magnification ×40). (**c**) OCT image of a fibrocalcific aortic plaque showing a sharply delineated region with a signal-poor interior. Bar = 500 μm. (**d**) Corresponding histology (H&E; magnification ×40). (**e**) OCT image of a lipid-rich carotid plaque showing a signal-poor lipid pool (L) with poorly delineated borders beneath a thin homogeneous band, corresponding to fibrous cap (*arrows*). Bar = 500 μm. (**f**) Corresponding histology (Movat's pentachrome; magnification ×20) (Reprinted from Yabushita H, Bouma BE, Houser SL, Aretz HT, Jang IK, Schlendorf KH, et al. Characterization of human atherosclerosis by optical coherence tomography. Circulation. 2002;106(13):1640–5. With permission from Wolters Kluwer Health)

Fig. 8.4 Ex vivo OCT image of macrophages. Raw (**a**) and logarithm base 10 (**b**) OCT images of a fibroatheroma with a low density of macrophages within the fibrous cap. (**c**) Corresponding histology for (**a**) and (**b**) (CD68 immunoperoxidase; original magnification ×100). Raw (**d**) and logarithm base 10 (**e**) OCT images of a fibroatheroma with a high density of macrophages within the fibrous cap. (**f**) Corresponding histology for (**d**) and (**e**) (CD68 immunoperoxidase; original magnification ×100) (Reprinted from Tearney GJ, Yabushita H, Houser SL, Aretz HT, Jang IK, Schlendorf KH, Kauffman CR, Shishkov M, Halpern EF, Bouma BE. Quantification of macrophage content in atherosclerotic plaques by optical coherence tomography. Circulation. 2003;107(1):113–9. With permission from Wolters Kluwer Health)

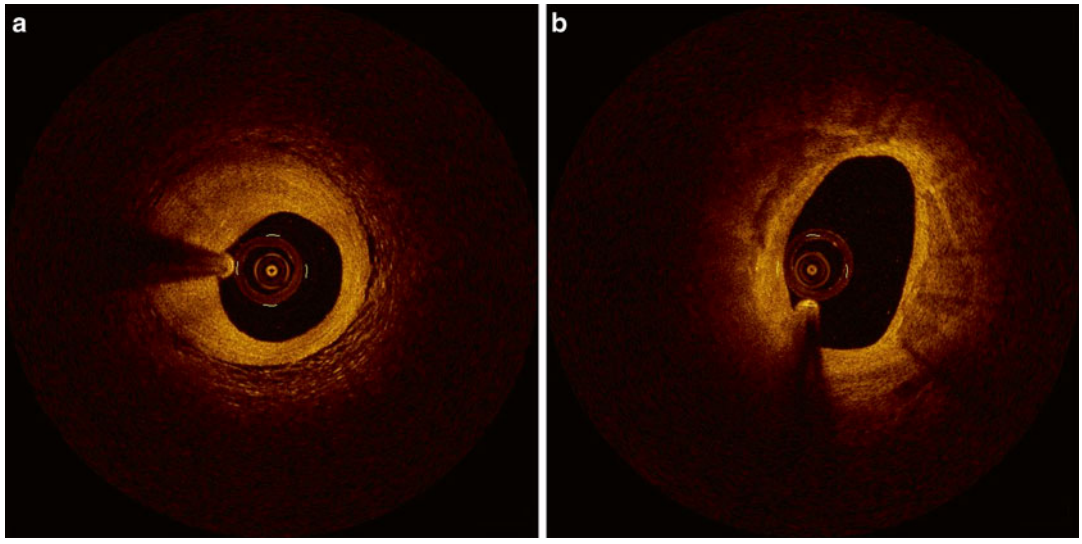

Fig. 8.3 In vivo coronary artery plaques. (**a**) Fibrous plaque. High scattering and homogeneous signal is observed. (**b**) Fibrocalcified plaque. Signal-poor heterogeneous region on both sides with well-delineated borders (Courtesy of Wakayama Medical University)

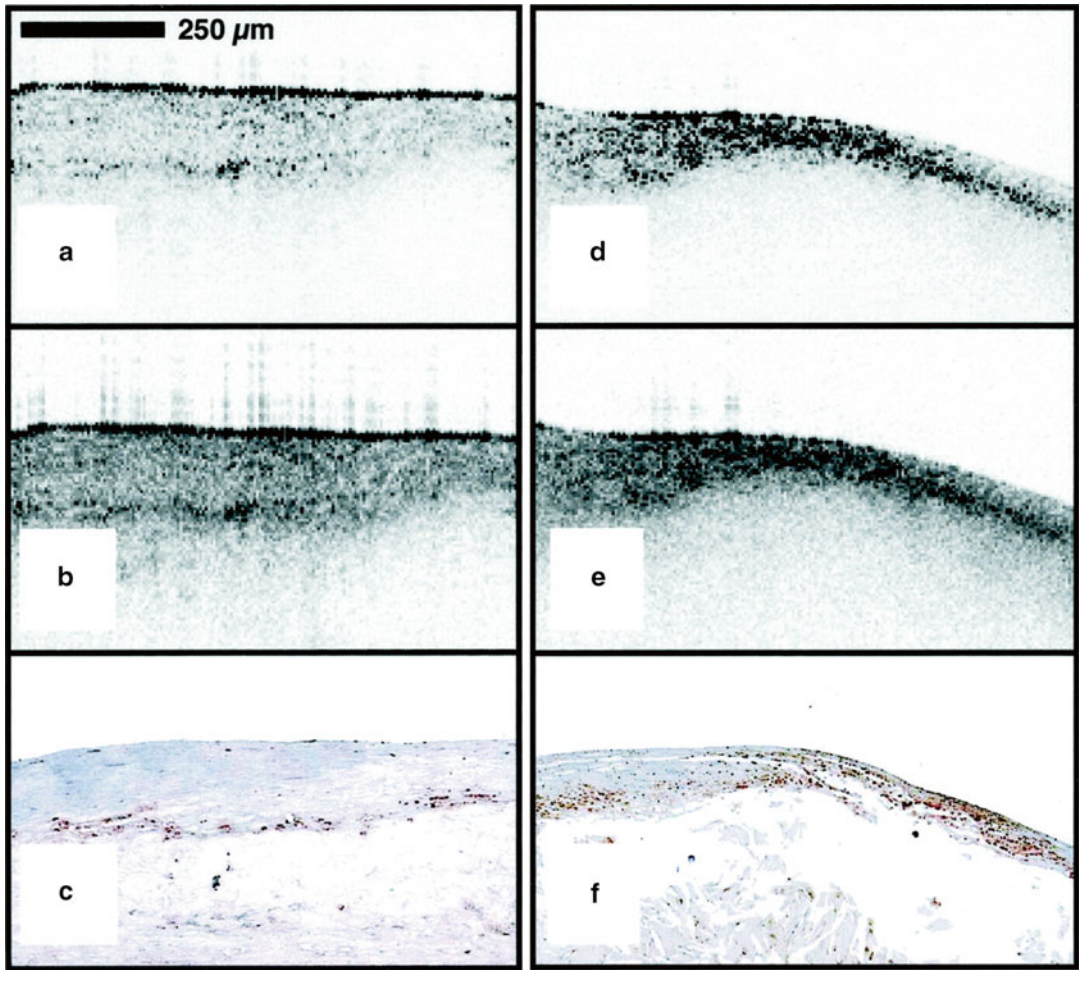

Fig. 8.4 (continued)

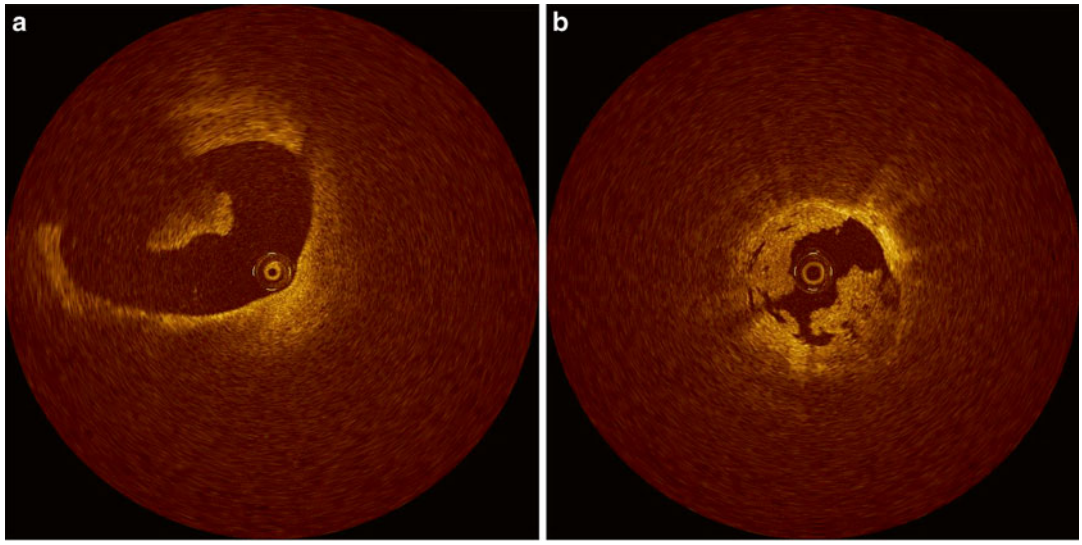

Fig. 8.5 Thrombi. (**a**) Red thrombus. A red thrombus with high IVOCT backscattering and attenuation is floating in the coronary artery. (**b**) White thrombus. White thrombus with homogeneous backscattering and low attenuation attached to coronary artery wall (Courtesy of Wakayama Medical University)

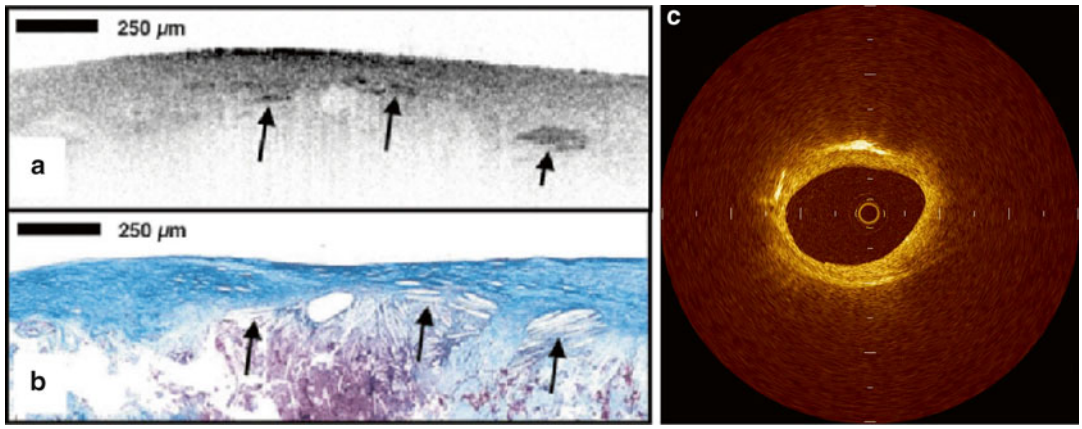

Fig. 8.6 Cholesterol crystal. OCT image (**a**) demonstrates oriented, linear, highly reflecting structures near the fibrous cap-lipid pool junction (*arrows*). Corresponding histology (**b**, Masson's trichrome; original magnification ×40) demonstrated the presence of cholesterol crystals (*arrows*). Cholesterol crystals in vivo OCT image (**c**) appears as linear, highly backscattering structures within in the plaque (Reprinted from Tearney GJ, Jang IK, Bouma BE. Evidence of Cholesterol Crystals in Atherosclerotic Plaque by Optical Coherence Tomographic (OCT) Imaging. Eur. Heart J. 2003:23;1462. With permission from Oxford University Press)

In Vivo Studies

Detection of Vulnerable Plaques

For cardiologists, the detection of vulnerable plaques, the most common of which is the TCFA, is a key goal for predicting and preventing the course of ACS. On IVOCT assessment, TCFA has been defined by some as a plaque with ≥2 quadrants of lipid and the thinnest part of a fibrous cap measuring <65 μm. In one study, 57 patients who underwent successful percutaneous coronary intervention (PCI) were divided into three groups: acute myocardial infarction (AMI) ($n = 20$), ACS ($n = 20$), and stable angina pectoris (SAP) ($n = 17$). Patients with AMI and ACS demonstrated higher incidence of TCFA

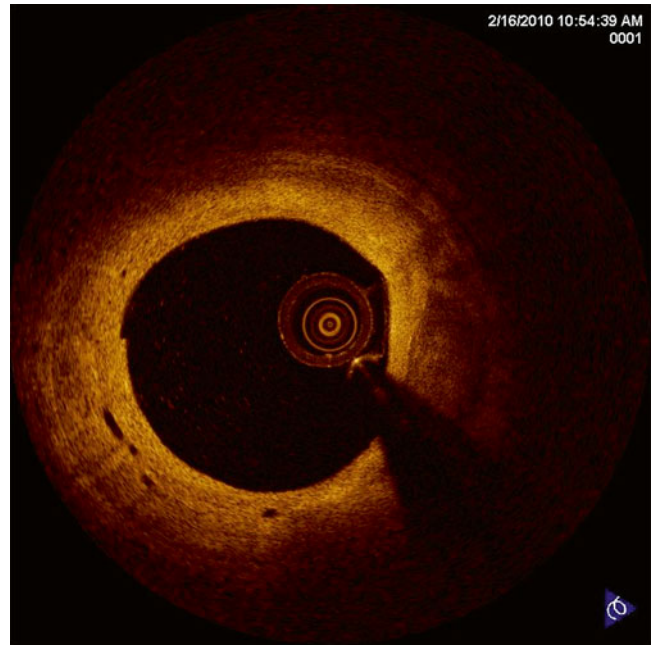

Fig. 8.7 Neovascularization. Intimal vessels are well-delineated regions or voids with low OCT backscattering (Courtesy of Wakayama Medical University)

and thinner fibrous cap thickness compared with SAP [19].

Frequency and distribution of TCFA were also examined, and pathology reports that indicated TCFA defined by OCT were dominant in the proximal left anterior descending artery, whereas TCFA in the left circumflex artery and the right coronary artery were equally distributed [20, 21]. As with culprit lesions, TCFA in non-culprit lesions were more frequent in patients with ACS than SAP [22].

The alternative criteria of TCFA recently have been proposed by OCT consensus document [23]. An OCT-TCFA is defined as an IVOCT-delineated necrotic core with an overlying fibrous cap in which the minimum thickness of the fibrous cap is less than a predetermined threshold. The clinical significance of lipid arc dimensions was determined to be unknown and remains an area of future investigation [23].

Macrophages In Vivo

Macrophage content was investigated in vivo in a study that enrolled 49 patients undergoing PCI [24] where again patients were divided into three groups: ST-elevation myocardial infarction (STEMI) ($n = 19$), ACS ($n = 19$), and SAP ($n = 11$). Macrophages were measured in the caps of IVOCT-determined fibroatheroma. NSD values showed a relationship between macrophage concentrations and the various clinical presentations. Patients with unstable clinical presentation had higher concentrations of macrophages and macrophage densities correlated with white blood count, the thickness of the fibrous cap, and arterial remodeling [25, 26]. Further, macrophage density was found to be higher at cap rupture sites of culprit lesions than at non-rupture sites (Fig. 8.8). Even though these results have showed interesting relationships between macrophages and other clinical and microstructural findings, the clinical implication of NSD measurements by OCT, especially prognostic value, remains unknown.

Acute Coronary Syndrome

New findings from clinical studies have elucidated some of the intricacies of ACS [27–30]. For example, IVOCT demonstrated that the morphologies of exertion-triggered and rest-onset ruptured plaques differ in ACS patients,

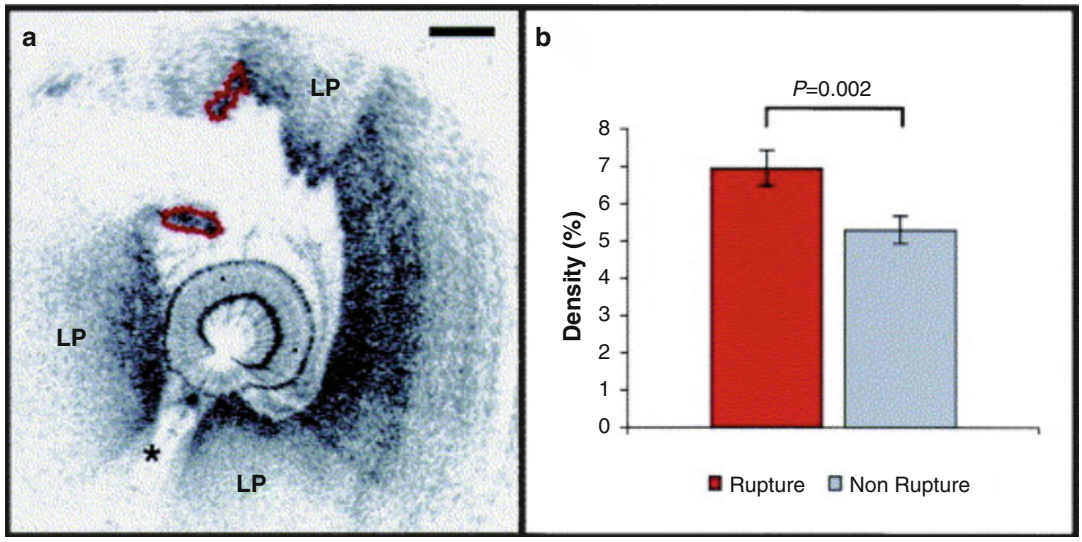

Fig. 8.8 Intracoronary OCT macrophage imaging. (**a**) Optical coherence tomography (OCT) image of a rupture site (outlined in *red*) overlying a lipid-rich plaque (LP). The *asterisk* symbol represents guide wire shadow. A 500 **μ**m scale bar is seen in the *top right-hand corner*. (**b**) Bar graph representing mean macrophage density at sites of rupture, corresponding to outlined segment in panel (**a**), compared with the rest of the plaque. Standard error bars are represented. (Reprinted from MacNeill BD, Jang IK, Bouma BE, Iftimia N, Takano M, Yabushita H, et al. Focal and multifocal plaque macrophage distributions in patients with acute and stable presentations of coronary artery disease. J Am Coll Cardiol. 2004;44(5):972–9. With permission from Elsevier)

and that some plaque ruptures may occur in thick fibrous caps, up to 140 μm, depending on exertion levels [27] (Fig. 8.9). Another IVOCT trial reported the differences in culprit lesion morphology between STEMI and non-ST-segment elevation acute coronary syndrome (NSTEACS). As a result, culprit lesions in STEMI showed higher incidence of plaque rupture, TCFA, and red thrombus than those in NSTEACS [28]. Patients with STEMI also had greater plaque disruption and smaller minimal lumen area than patients with NSTEM [29]. These results suggest that the indicate that morphological features at culprit lesions could relate to the clinical presentation in patients with acute coronary disease. Moreover, IVOCT revealed a relationship between lesion morphology on OCT and Braunwald classification of unstable angina pectoris (UAP). Patients with class II UAP more frequently showed plaque rupture and thrombosis formation [30]. These findings suggest that IVOCT may provide a novel means for exploring the pathophysiology of ACS in vivo.

Prognosis

IVOCT has also revealed findings regarding the natural history of coronary artery disease. In one recent clinical study, the percent changes in fibrous cap thickness assessed by OCT correlated with the percent changes in external elastic membrane cross-sectional area within a time frame of 6 months [31]. In another study, the change in high-sensitivity C-reactive protein was also found to be significantly correlated with changes in fibrous cap thickness [32]. OCT studies have revealed certain aspects about the effects of medical therapy on the coronary artery. Statin therapies have been found to be related to increased fibrous cap thickness, reduced plaque volume, and overall a more stable coronary structural phenotype [33, 34]. One IVOCT trial revealed that TCFA and neovascularization are independent predictors of luminal progression [18]. These results support the notion that TCFA leads to plaque progression in vivo. Nevertheless, the question of whether or not

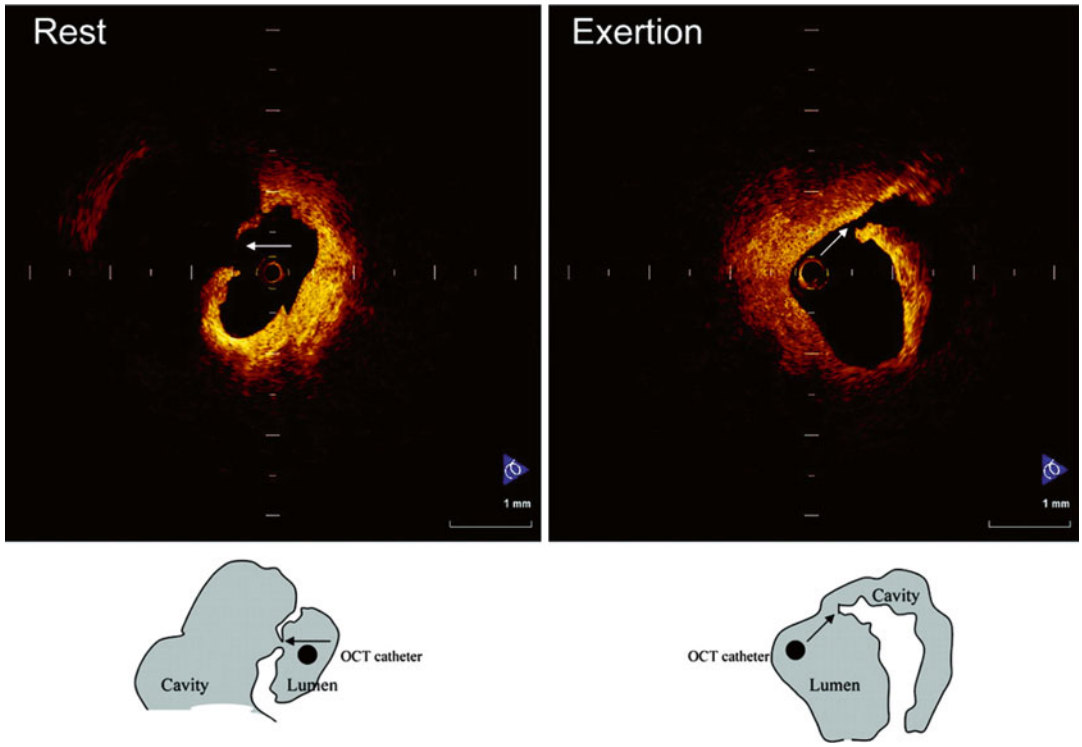

Fig. 8.9 Representative cases of plaque rupture occurring at rest or with exertion. (*Left*) Plaque rupture that occurred at rest. Fibrous cap was broken at the midportion, and a thin fibrous cap could be observed. (*Right*) Plaque rupture that occurred during heavy farm work. Thick fibrous cap was broken at shoulder of plaque (Reprinted from Tanaka A, Imanishi T, Kitabata H, Kubo T, Takarada S, Tanimoto T, et al. Morphology of exertion-triggered plaque rupture in patients with acute coronary syndrome: an optical coherence tomography study. Circulation. 2008;118:2368–73. With permission from Wolters Kluwer Health)

OCT-derived TCFA leads to ACS in real-world scenarios still remains.

Neoatherosclerosis in Stented Lesions

A recent pathological study showed that neoatherosclerosis and consequent plaque vulnerability can occur in previously stented lesions 5 years after bare-metal stent (BMS) placement [35]. An in vivo OCT observational study revealed that late-phase BMS (>5 years) showed higher incidence of vulnerable atherosclerotic changes, including lipid-laden intima, intimal disruption, and thrombus, than early-phase BMS (<6 months) [36]. In some cases, neoatherosclerosis in BMS eventually led to plaque rupture and secondary thrombus formation, resulting in ACS [37] (Fig. 8.10). Also in drug-eluting stents (DES), neoatherosclerosis is a frequent finding and pathologically can occur earlier than in BMS, potentially due to more pronounced inflammation related to drug and durable polymer [38]. In vivo OCT examination revealed that late-phase DES (>20 months) had a higher incidence of TCFA-containing neointima and red thrombus [39]. Even though DES has been reported to greatly reduce restenosis and offer an effective approach to coronary artery disease, 0.4–0.6 % annual incidences of late stent thrombosis (LST) occurs rarely. Neoatherosclerosis and subsequent plaque rupture in DES are considered to be one of the potential causes of LST [40].

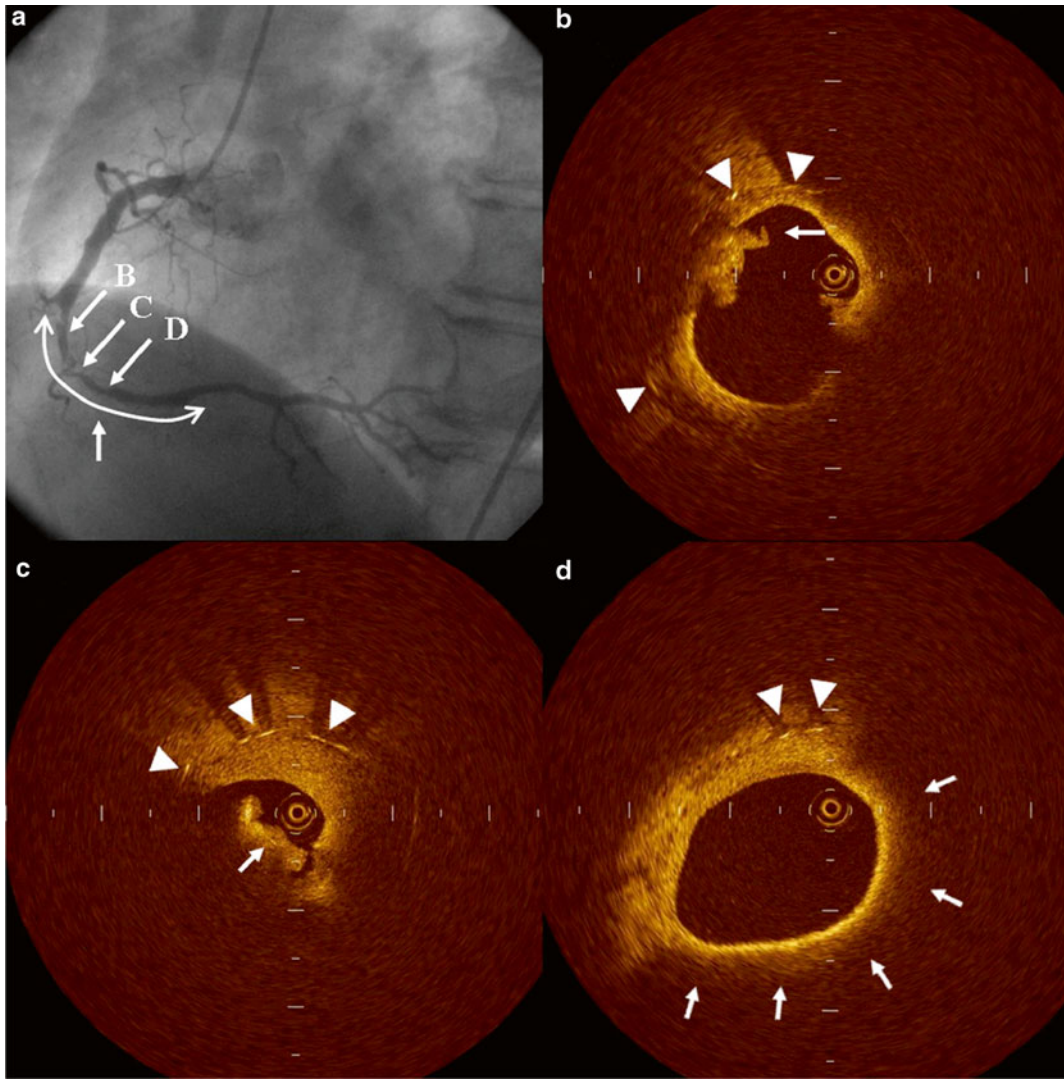

Fig. 8.10 Neoatherosclerosis and acute event at late phase BMS. An emergent coronary angiogram showed severe in-stent stenosis in the previously stented segment (**a**). OCT examination demonstrated plaque rupture in the stented segment (**b**). The thickness of broken fibrous cap was 40 μm. Intracoronary thrombus was also visualized as a mass protruding into the vessel lumen (**c**). Lipid-rich plaque (*arrow*) covered by thin fibrous cap (60 μm) was imaged and determined as a thin-cap fibroatheroma (**d**). *Arrow head* indicates stent strut (Reprinted from Kashiwagi M, Kitabata H, Tanaka A, Okochi K, Ishibashi K, Komukai K, et al. Very late clinical cardiac event after BMS implantation: in vivo optical coherence tomography examination. JACC Cardiovasc Imaging. 2010;3(5):525–7. With permission from Elsevier)

Percutaneous Coronary Intervention

Like IVUS-guided PCI, IVOCT-guided intervention is still a concept under investigation [41–46]. IVOCT-derived lipid plaque is considered as a predictor for no-reflow phenomenon and post-PCI creatine kinase elevation [8, 47]. Moreover, as compared to IVUS, OCT can potentially more accurately detect adverse events after stenting, including stent-edge dissection, tissue protrusion, and malapposition [48]. Regarding OCT-guided intervention, Imola et al. conducted a single-center registry to evaluate the safety and feasibility of OCT-guided PCI and they con-

cluded FD-OCT has potential to become a safety guidance tool for PCI [49]. In another retrospective trial, IVOCT demonstrated adverse features requiring further intervention in 34.7 % patients and OCT-guided intervention provided a significantly lower risk of cardiac death or myocardial infarction event compared to angiography-guided intervention [50]. However, because evidence about OCT-guided intervention is not fully elucidated, this issue needs to be investigated in further outcome-based studies that reveal which information extracted from IVOCT images can be used during intervention to improve patient outcome.

Future Developments

A newer OCT technology, termed "micro OCT" (μOCT), has ten times greater resolution (approximately 1 μm) than conventional IVOCT [51]. The higher resolution of μOCT makes it possible to image cellular and subcellular morphologic features associated with atherogenesis, thrombosis, and responses to interventional therapy. In the first study to demonstrate this technology ex vivo, macrophage foam cells and cholesterol crystals were clearly visualized. μOCT also enabled the detection of DES polymer in cadaver specimens, which is difficult to appreciate in currently available IVOCT systems. Another technological advancement is the combination of IVOCT with other imaging technologies. Recently, a dual-modality, catheter-based combination of IVOCT and near-infrared fluorescence (NIRF) imaging [52] has been shown and demonstrated in rabbits in vivo. This multimodality technology simultaneously provides images of colocalized molecular and microstructural information [52]. This technology has the potential to enable the detection of fibrin over stents, which could in the future be used to inform decisions regarding antiplatelet therapy [52]. It furthermore can assess enzymatic activity in the context of the microstructure of the plaque [52]. The unique capabilities of NIRF-OFDI may make it a valuable tool for assessing atherosclerosis and stent healing at both the molecular and microstructural levels.

Conclusion

IVOCT has been demonstrated to clearly enable the visualization of microstructural features of the superficial coronary wall. The advent of second-generation forms of IVOCT has made it practical to use this technology in the cardiovascular catheterization lab. While this technology is very promising for investigating plaque structure, composition, and the stent healing process, much needs to be learned regarding its ability to be used to guide intervention and improve patient outcomes. Future generation IVOCT technologies offer the promise of imaging cells and subcellular structures in the coronary wall and simultaneously obtaining molecular and microstructural information. The promise of today's IVOCT and future iterations of this technology makes this field a very interesting area for research and clinical application development.

Acknowledgements We gratefully acknowledge Takashi Akasaka, MD and Hironori Kitabata, MD for providing clinical in vivo OCT images.

Disclosure: Massachusetts General Hospital has a licensing arrangement with Terumo Corporation regarding IVOCT technology. Dr. Tearney has the right to receive royalties as part of this licensing arrangement. Dr. Tearney receives sponsored research from Canon Corporation.

References

1. Bouma BE, Tearney GJ. Power-efficient nonreciprocal interferometer and linear-scanning fiber-optic catheter for optical coherence tomography. Opt Lett. 1999;24(8):531–3.
2. Yabushita H, Bouma BE, Houser SL, Aretz HT, Jang IK, Schlendorf KH, et al. Characterization of human atherosclerosis by optical coherence tomography. Circulation. 2002;106(13):1640–5.
3. Tearney GJ, Yabushita H, Houser SL, Aretz HT, Jang IK, Schlendorf KH, et al. Quantification of macrophage content in atherosclerotic plaques by optical coherence tomography. Circulation. 2003;107(1):113–9.
4. Kume T, Akasaka T, Kawamoto T, Ogasawara Y, Watanabe N, Toyota E, et al. Assessment of coronary arterial thrombus by optical coherence tomography. Am J Cardiol. 2006;97(12):1713–7.
5. Tearney GJ, Jang IK, Bouma BE. Evidence of cholesterol crystals in atherosclerotic plaque by optical coherence tomographic (OCT) imaging. Eur Heart J. 2003;23:1462.

6. Prati F, Regar E, Mintz GS, Arbustini E, Di Mario C, Jang IK, et al. Expert review document on methodology, terminology, and clinical applications of optical coherence tomography: physical principles, methodology of image acquisition, and clinical application for assessment of coronary arteries and atherosclerosis. Eur Heart J. 2010;31:401–15.
7. Jang IK, Bouma BE, Kang DH, Park SJ, Park SW, Seung KB, et al. Visualization of coronary atherosclerotic plaques in patients using optical coherence tomography: comparison with intravascular ultrasound. J Am Coll Cardiol. 2002;39(4):604–9.
8. Tanaka A, Imanishi T, Kitabata H, Kubo T, Takarada S, Tanimoto T, et al. Lipid-rich plaque and myocardial perfusion after successful stenting in patients with non-ST-segment elevation acute coronary syndrome: an optical coherence tomography study. Eur Heart J. 2009;30:1348–55.
9. Kataiwa H, Tanaka A, Kitabata H, Matsumoto H, Kashiwagi M, Kuroi A, et al. Head to head comparison between the conventional balloon occlusion method and the non-occlusion method for optical coherence tomography. Int J Cardiol. 2011;146(2): 186–90.
10. Yun SH, Tearney GJ, Vakoc BJ, Shishkov M, Oh WY, Desjardins AE, et al. Comprehensive volumetric optical microscopy in vivo. Nat Med. 2006;12(12): 1429–33.
11. Tearney GJ, Waxman S, Shishkov M, Vakoc BJ, Suter MJ, Freilich MI, et al. Three-dimensional coronary artery microscopy by intracoronary optical frequency domain imaging. JACC Cardiovasc Imaging. 2008; 1(6):752–61.
12. Fitzgerald PJ, St Goar FG, Connolly AJ, Pinto FJ, Billingham ME, Popp RL, et al. Intravascular ultrasound imaging of coronary arteries. Is three layers the norm? Circulation. 1992;86(1):154–8.
13. Kume T, Akasaka T, Kawamoto T, Watanabe N, Toyota E, Neishi Y, et al. Assessment of coronary arterial plaque by optical coherence tomography. Am J Cardiol. 2006;97(8):1172–5.
14. Abela GS, Aziz K, Vedre A, Pathak DR, Talbott JD, Dejong J. Effect of cholesterol crystals on plaques and intima in arteries of patients with acute coronary and cerebrovascular syndromes. Am J Cardiol. 2009; 103(7):959–68.
15. Moreno PR, Purushothaman KR, Fuster V, Echeverri D, Truszczynska H, Sharma SK, et al. Plaque neovascularization is increased in ruptured atherosclerotic lesions of human aorta: implications for plaque vulnerability. Circulation. 2004;110:2032–8.
16. Vorpahl M, Nakano M, Virmani R. Small black holes in optical frequency domain imaging matches intravascular neoangiogenesis formation in histology. Eur Heart J. 2010;31(15):1889.
17. Kitabata H, Tanaka A, Kubo T, Takarada S, Kashiwagi M, Tsujioka H, et al. Relation of microchannel structure identified by optical coherence tomography to plaque vulnerability in patients with coronary artery disease. Am J Cardiol. 2010;105(12):1673–8.
18. Uemura S, Ishigami K, Soeda T, Okayama S, Sung JH, Nakagawa H, et al. Thin-cap fibroatheroma and microchannel findings in optical coherence tomography correlate with subsequent progression of coronary atheromatous plaques. Eur Heart J. 2012; 33(1):78–85.
19. Jang IK, Tearney GJ, MacNeill B, Takano M, Moselewski F, Iftima N, et al. In vivo characterization of coronary atherosclerotic plaque by use of optical coherence tomography. Circulation. 2005;111(12): 1551–5.
20. Tanaka A, Imanishi T, Kitabata H, Kubo T, Takarada S, Kataiwa H, et al. Distribution and frequency of thin-capped fibroatheromas and ruptured plaques in the entire culprit coronary artery in patients with acute coronary syndrome as determined by optical coherence tomography. Am J Cardiol. 2008;102(8):975–9.
21. Fujii K, Kawasaki D, Masutani M, Okumura T, Akagami T, Sakoda T, et al. OCT assessment of thin-cap fibroatheroma distribution in native coronary arteries. JACC Cardiovasc Imaging. 2010;3(2): 168–75.
22. Kubo T, Imanishi T, Kashiwagi M, Ikejima H, Tsujioka H, Kuroi A, et al. Multiple coronary lesion instability in patients with acute myocardial infarction as determined by optical coherence tomography. Am J Cardiol. 2010;105(3):318–22.
23. MacNeill BD, Jang IK, Bouma BE, Iftimia N, Takano M, Yabushita H, et al. Focal and multi-focal plaque macrophage distributions in patients with acute and stable presentations of coronary artery disease. J Am Coll Cardiol. 2004;44(5):972–9.
24. Tearney GJ, Regar E, Akasaka T, Adriaenssens T, Barlis P, Bezerra HG, et al. Consensus standards for acquisition, measurement, and reporting of intravascular optical coherence tomography studies: a report from the International Working Group for Intravascular Optical Coherence Tomography Standardization and Validation. J Am Coll Cardiol. 2012;59:1058–72.
25. Raffel OC, Tearney GJ, Gauthier DD, Halpern EF, Bouma BE, Jang IK. Relationship between a systemic inflammatory marker, plaque inflammation, and plaque characteristics determined by intravascular optical coherence tomography. Arterioscler Thromb Vasc Biol. 2007;27(8):1820–7.
26. Raffel OC, Merchant FM, Tearney GJ, Chia S, Gauthier DD, Pomerantsev E, et al. In vivo association between positive coronary artery remodelling and coronary plaque characteristics assessed by intravascular optical coherence tomography. Eur Heart J. 2008;29(14):1721–8.
27. Tanaka A, Imanishi T, Kitabata H, Kubo T, Takarada S, Tanimoto T, et al. Morphology of exertion-triggered plaque rupture in patients with acute coronary syndrome: an optical coherence tomography study. Circulation. 2008;118:2368–73.

28. Ino Y, Kubo T, Tanaka A, Kuroi A, Tsujioka H, Ikejima H, et al. Difference of culprit lesion morphologies between ST-segment elevation myocardial infarction and non-ST-segment elevation acute coronary syndrome: an optical coherence tomography study. JACC Cardiovasc Interv. 2011;4(1):76–82.
29. Toutouzas K, Karanasos A, Tsiamis E, Riga M, Drakopoulou M, Synetos A, et al. New insights by optical coherence tomography into the differences and similarities of culprit ruptured plaque morphology in non-ST-elevation myocardial infarction and ST-elevation myocardial infarction. Am Heart J. 2011;161(6):1192–9.
30. Mizukoshi M, Imanishi T, Tanaka A, Kubo T, Liu Y, Takarada S, et al. Clinical classification and plaque morphology determined by optical coherence tomography in unstable angina pectoris. Am J Cardiol. 2010;106(3):323–8.
31. Yamada R, Okura H, Kume T, Saito K, Miyamoto Y, Imai K, et al. Relationship between arterial and fibrous cap remodeling: a serial three-vessel intravascular ultrasound and optical coherence tomography study. Circ Cardiovasc Interv. 2010;3(5):484–90.
32. Takarada S, Imanishi T, Ishibashi K, Tanimoto T, Komukai K, Ino Y, et al. The effect of lipid and inflammatory profiles on the morphological changes of lipid-rich plaques in patients with non-ST-segment elevated acute coronary syndrome: follow-up study by optical coherence tomography and intravascular ultrasound. JACC Cardiovasc Interv. 2010;3(7): 766–72.
33. Hattori K, Ozaki Y, Ismail TF, Okumura M, Naruse H, Kan S, et al. Impact of statin therapy on plaque characteristics as assessed by serial OCT, grayscale and integrated backscatter-IVUS. JACC Cardiovasc Imaging. 2012;5(2):169–77.
34. Takarada S, Imanishi T, Kubo T, Tanimoto T, Kitabata H, Nakamura N, et al. Effect of statin therapy on coronary fibrous-cap thickness in patients with acute coronary syndrome: assessment by optical coherence tomography study. Atherosclerosis. 2009;202(2): 491–7.
35. Inoue K, Abe K, Ando K, Shirai S, Nishiyama K, Nakanishi M, et al. Pathological analyses of long-term intracoronary Palmaz-Schatz stenting; Is its efficacy permanent? Cardiovasc Pathol. 2004;13:109–15.
36. Takano M, Yamamoto M, Inami S, Murakami D, Ohba T, Seino Y, et al. Appearance of lipid-laden intima and neovascularization after implantation of bare-metal stents extended late-phase observation by intracoronary optical coherence tomography. J Am Coll Cardiol. 2009;55(1):26–32.
37. Kashiwagi M, Kitabata H, Tanaka A, Okochi K, Ishibashi K, Komukai K, et al. Very late clinical cardiac event after BMS implantation: in vivo optical coherence tomography examination. JACC Cardiovasc Imaging. 2010;3(5):525–7.
38. Nakazawa G, Otsuka F, Nakano M, Vorpahl M, Yazdani SK, Ladich E, et al. The pathology of neoatherosclerosis in human coronary implants bare-metal and drug-eluting stents. J Am Coll Cardiol. 2011; 57(11):1314–22.
39. Kang SJ, Mintz GS, Akasaka T, Park DW, Lee JY, Kim WJ, et al. Optical coherence tomographic analysis of in-stent neoatherosclerosis after drug-eluting stent implantation. Circulation. 2011;123(25):2954–63.
40. Guagliumi G, Sirbu V, Musumeci G, Gerber R, Biondi-Zoccai G, Ikejima H, et al. Examination of the in vivo mechanisms of late drug-eluting stent thrombosis: findings from optical coherence tomography and intravascular ultrasound imaging. JACC Cardiovasc Interv. 2012;5(1):12–20.
41. Schiele F, Meneveau N, Vuillemenot A, Zhang DD, Gupta S, Mercier M, et al. Impact of intravascular ultrasound guidance in stent deployment on 6-month restenosis rate: a multicenter, randomized study comparing two strategies–with and without intravascular ultrasound guidance. RESIST Study Group. REStenosis after Ivus guided STenting. J Am Coll Cardiol. 1998;32:320–8.
42. Fitzgerald PJ, Oshima A, Hayase M, Metz JA, Bailey SR, Baim DS, et al. Final results of the Can Routine Ultrasound Influence Stent Expansion (CRUISE) study. Circulation. 2000;120:523–30.
43. Mudra H, di Mario C, de Jaegere P, Figulla HR, Macaya C, Zahn R, et al. Randomized comparison of coronary stent implantation under ultrasound or angiographic guidance to reduce stent restenosis (OPTICUS study). Circulation. 2001;104:1343–9.
44. Russo RJ, Silva PD, Teirstein PS, Attubato MJ, Davidson CJ, DeFranco AC, et al. A randomized controlled trial of angiography versus intravascular ultrasound-directed bare-metal coronary stent placement (The AVID Trial). Circ Cardiovasc Interv. 2009;2:113–23.
45. Roy P, Steinberg DH, Sushinsky SJ, Okabe T, Pinto Slottow TL, Kaneshige K, et al. The potential clinical utility of intravascular ultrasound guidance in patients undergoing percutaneous coronary intervention with drug-eluting stents. Eur Heart J. 2008;29:1851–7.
46. Claessen BE, Mehran R, Mintz GS, Weisz G, Leon MB, Dogan O, et al. Impact of intravascular ultrasound imaging on early and late clinical outcomes following percutaneous coronary intervention with drug-eluting stents. J Am Coll Cardiol Intv. 2011; 4:974–81.
47. Yonetsu T, Kakuta T, Lee T, Takahashi K, Yamamoto G, Iesaka Y, et al. Impact of plaque morphology on creatine kinase-MB elevation in patients with elective stent implantation. Int J Cardiol. 2011;146:180–5.
48. Kubo T, Imanishi T, Kitabata H, Kuroi A, Ueno S, Yamano T, et al. Comparison of vascular response after sirolimus-eluting stent implantation between unstable angina pectoris and stable angina pectoris: a serial optical coherence tomography study. J Am Coll Cardiol Img. 2008;1:475–84.
49. Imola F, Mallus MT, Ramazzotti V, Manzoli A, Pappalardo A, Di Giorgio A, et al. Safety and feasibil-

ity of frequency domain optical coherence tomography to guide decision making in percutaneous coronary intervention. EuroIntervention. 2010;6:575–81.
50. Prati F, Di Vito L, Biondi-Zoccai G, Occhipinti M, La Manna A, Tamburino C, et al. Angiography alone versus angiography plus optical coherence tomography to guide decision-making during percutaneous coronary intervention: the Centro per la Lotta contro l'Infarto-Optimisation of Percutaneous Coronary Intervention (CLI-OPCI) study. EuroIntervention. 2012;8:823–9.
51. Liu L, Gardecki JA, Nadkarni SK, Toussaint JD, Yagi Y, Bouma BE, et al. Imaging the subcellular structure of human coronary atherosclerosis using micro-optical coherence tomography. Nat Med. 2011;17(8):1010–4.
52. Yoo H, Kim JW, Shishkov M, Namati E, Morse T, Shubochkin R, et al. Intra-arterial catheter for simultaneous microstructural and molecular imaging in vivo. Nat Med. 2011;17(12):1680–4.

Finding the Hot Plaque: Intravascular Thermography

9

Konstantinos Toutouzas, Archontoula Michelongona, Maria Drakopoulou, and Christodoulos Stefanadis

Introduction

Atherosclerosis and its cardiovascular complications remain the leading cause of death in developed countries [1]. According to the World Health Organization, 17.5 million people die every year from cardiovascular diseases and it is estimated that this number will approach 20 million by 2015.

Atherosclerosis consists a systemic disease, which may lead—through a continuous process—to plaque rupture and, consequently, to acute coronary syndromes (ACS). During the last two decades, enormous progress has been made in current imaging modalities in order to identify high-risk patients for a future acute coronary event. However, the prediction of plaque rupture in a patient, vessel or plaque level analysis is still inevitable, as these events may occur subclinically, or as the first manifestation of coronary atherosclerosis in previously apparently asymptomatic individuals with non-flow-limiting plaques [2]. Despite our vast knowledge of the underlying molecular and cellular events in atherosclerosis, it remains uncertain why all atherosclerotic lesions do not progress uniformly even in the same patient [3–6].

Histopathological studies in patients with sudden death revealed that the culprit atherosclerotic plaques seem to be non-flow-limiting, and thereby cannot be identified solely by angiography. These plaques are described as *vulnerable*, unstable, or "high-risk" and are often quiescent. The VPs are characterized by several pathologic features: (1) a large lipid core (≥40 % plaque volume) composed of free cholesterol crystals, cholesterol esters, and oxidized lipids impregnated with tissue factor, (2) a thin fibrous cap (<65 μm), (3) an expansive (positive) remodeling, (4) inflammatory cell infiltration of fibrous cap and adventitia (monocyte-macrophages, activated T cells and mast cells), and (5) increased neovascularization [7].

There are no imaging or functional methods providing all these information in vivo in subjects with multiple prognostic factors of coronary artery disease or in patients with established

K. Toutouzas, MD (✉)
First Department of Cardiology, Athens Medical School, Hippokration Hospital, 24, Karaoli and Dimitriou Street, Holargos, Athens 15562, Greece
e-mail: ktoutouz@gmail.com

A. Michelongona, MD
First Department of Cardiology, Athens Medical School, Hippokration Hospital, 7, Tainarou Street, Peiraeus 18453, Greece
e-mail: amichelongona@yahoo.gr

M. Drakopoulou, MD
First Department of Cardiology, Athens Medical School, Hippokration Hospital, 4, Amiklon Street, Halandri 15231, Greece
e-mail: mdrakopoulou@hotmail.com

C. Stefanadis, MD
First Department of Cardiology, Athens Medical School, Hippokration Hospital, 9 Tepeleniou Street, Paleo Psychico 15454, Greece
e-mail: chstefan@med.uoa.gr

S.J. Nicholls and T. Crowe (eds.), *Imaging Coronary Atherosclerosis*, Contemporary Cardiology,
DOI 10.1007/978-1-4939-0572-0_9,

disease. Thus, each method can utilize distinct high-risk features of atheromatic plaques that can be identified directly or indirectly. Limited data have been provided regarding the prognostic value of these methods for predicting cardiovascular events. The first prospective trial using multimodality imaging to characterize the coronary tree (Providing Regional Observations to Study Predictors of Events Coronary Tree Trial—PROSPECT) showed that most non-culprit plaques which become symptomatic have a large plaque burden, a large lipid core, and a small lumen area [8].

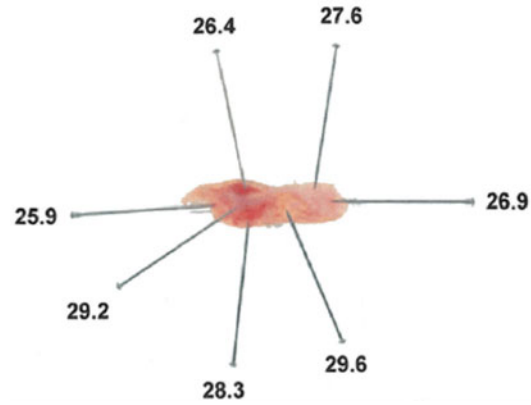

Fig. 9.1 Endarterectomized carotid plaques show temperature heterogeneity

Mechanisms of Heat Production in Atherosclerotic Plaques

One of the major pathophysiological substrate in the process of atheromatosis and plaque destabilization is the inflammatory activation. Inflammation constitutes an integral part of VP development and progression and heat is an established feature of inflammation. Intravascular thermography (IVT) has been introduced as a promising method for the identification of the VP. Inflammation plays a crucial role in all stages of the atherosclerotic disease, from the initiation of the fatty streak to the final stage of plaque rupture. The three mechanisms involved in plaque thermogenesis include the high metabolic rate of inflammatory cell infiltration, the increased neoangiogenesis, and the ineffective thermogenesis. In specific, the intense inflammatory response manifested by the local invasion of macrophages and lymphocytes and the activation of matrix metalloproteinases have been shown to degrade the supporting collagen and promote plaque fragility [3, 9]. By the time the inflammatory cells exhaust their supply of oxygen, anaerobic metabolism ensues, leading to local acidosis [10]. Apart from the central role of inflammation in VP, studies have shown that remarkable high rate of neoangiogenesis in VP also results in increased blood flow inside plaques and higher temperatures [11, 12] (Fig. 9.1). In addition, many areas of atherosclerotic plaques are known to be ischemic, and the lack of oxygen can lead to increased metabolic rate of nutrients and greater loss of energy in the form of heat instead of Adenosine triphosphate production [13, 14]. The increased heat production from unstable plaques has been confirmed in several ex vivo human studies, in experimental models, and in human in vivo studies.

Human Ex Vivo Thermography Studies

The hypothesis that plaque temperature is a marker of local inflammation was originally proposed on the basis of observations from human ex vivo carotid endarterectomy specimens. Casscells et al. measured the intimal surface temperature of 20 sites of 50 samples of carotid plaques taken during surgical endarterectomy, using a sensitive needle thermistor. The measurements revealed several regions in which the surface temperatures varied from 0.2 to 0.3 °C, but 37 % of plaques had points not distinguished by naked eye, with substantially different temperatures (0.4–2.2 °C). These results were reproducible, while thermal heterogeneity (ΔT) could also be confirmed using an infrared camera in vivo. Furthermore, plaque temperature was directly correlated with inflammatory cell density ($r=0.68$, $p=0.0001$) and inversely proportional to the distance of the cell clusters from the luminal surface ($r=-0.38$, $p=0.0006$). This was the first study demonstrating that localized heat is generated from inflamed atherosclerotic plaques in humans [15].

These observations were also confirmed in preliminary clinical studies. A correlation between the serum matrix metalloproteinase −1, −3, and −9 concentration with temperature difference in samples obtained through direct coronary atherectomy in eight patients has been reported [16]. In another study, in order to assess the possible contribution of infections to generation of heat in atherosclerotic plaques, the genus-specific monoclonal antibody CF-2 against Chlamydia pneumonia was used. Incubation of hot plaques with indomethacin showed a gradual decrease in plaque heat production over 5 h, suggesting an inflammatory origin of heat production in atherosclerotic plaques. However, no significant association between ΔT and Chlamydia pneumonia was found [17].

In pH readings in VP of human carotid endarterectomy specimens and atherosclerotic rabbit aortas, lower pH was associated with a higher temperature ($r=0.7$; $p<0.01$). Lipid-rich areas had a lower pH and a higher temperature, whereas calcified areas showed a higher pH and a lower temperature. Temperature and pH were significantly inversely correlated ($r=0.94$; $p<0.01$). This finding was in accordance with the assumption that lipid-rich vulnerable areas may have a more acidic environment [18].

Animal IVT Studies

Intravascular Thermography has been applied by several investigators in the past for the assessment of ΔT in animal models, validating the feasibility of this method in vivo. Naghavi et al. developed a contact-based "thermobasket" catheter for measuring in vivo the temperature at several points on the vessel wall in the presence of blood flow [19]. This catheter is equipped with four small, flexible wires with built-in thermocouples and a thermal sensor in its central wire for simultaneous monitoring of the blood temperature. The technical characteristics of the device are thermal resolution of 0.02 °C, thermal accuracy of 0.02 °C with a sampling rate of 20 temperature readings per second, and 7 sensors. The system was applied in a canine and a rabbit model of atherosclerosis. This catheter could detect ΔT over the atherosclerotic plaques in the femoral arteries of inbred atherosclerotic dogs and the aortas of Watanabe rabbits. In inbred cholesterol-fed dogs with femoral atherosclerosis, marked ΔT was measured on the atherosclerotic regions but not on disease-free regions ($p<0.05$) (Fig. 9.2). Marked ΔT was also observed in the aortas of atherosclerotic rabbits but not in normal ones. The specific catheter showed satisfactory accuracy, reproducibility, and safety.

Another over-the-wire thermography catheter with 4 thermistors was used in thermographic assessment of 20 rabbits: 10 in a normal diet and 10 after 6 months of cholesterol-rich diet. Marked ΔT (up to 1 °C) was detected in hypercholesterolemic rabbits at sites of thick plaques, as assessed by intravascular ultrasound (IVUS). In these same sites, histology showed a high macrophage density, but ΔT was absent at sites of plaques with a low macrophage density. The temperature heterogeneity detected in hypercholesterolemic rabbits was reduced significantly after 3 months of cholesterol lowering, while plaque histology showed a marked loss of macrophages but lack of changes in the plaque thickness [20]. In another study where rabbit atheromatic model was used, in vivo temperature measurements showed increased ΔT in plaques that contained higher density of macrophages, less smooth muscle cell concentration, and higher metalloproteinase-9 activity [21].

Human In Vivo IVT Studies

Many different types of intracoronary thermography catheters have been designed and important pathophysiological insights in the development of the unstable plaque have been obtained (Fig. 9.3). Intravascular Thermography had promising results as a method of assessment of plaque vulnerabilities, especially in specific group of patients, as well as in risk stratification and in evaluation of treatment (Table 9.1).

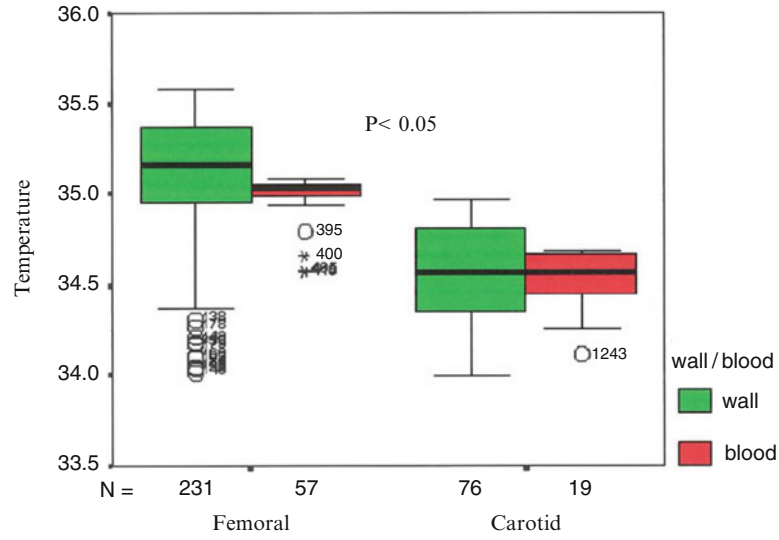

Fig. 9.2 The thermography basket catheter showed higher absolute temperatures as well as temperature heterogeneity on atherosclerotic lesions compared to lesion-free segments

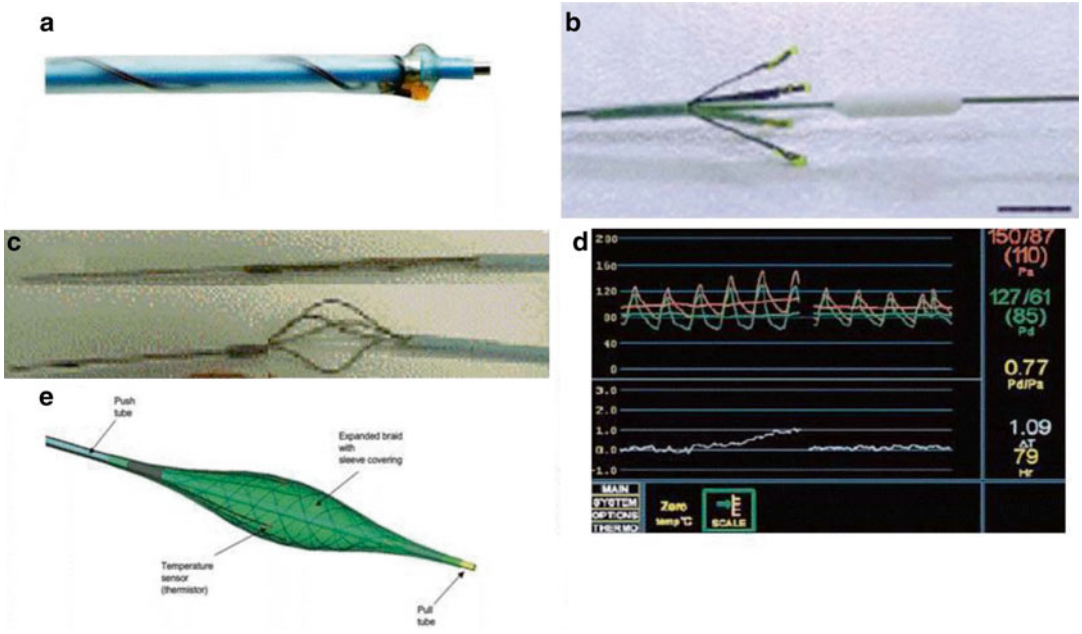

Fig. 9.3 (**a**) Epiphany thermography system (Epiphany, Medispes S.W., Zug, Switzerland). A monorail system containing two lumens with a temperature accuracy of 0.05 °C and a time constant of 300 ms. (**b**) Thermocore thermography system with a functional probe containing four thermistors with an accuracy of 0.01 °C. Epiphany coronary thermography system. (**c**) Volcano non-occluding thermography catheter (Volcano Therapeutics, Orange County, CA) with a self-expanding basket, five nitinol arms at its tip, with one thermocouple on each arm and another one on the central wire, allowing for real-time, cross-sectional thermal mapping of the arterial wall. (**d**) Radi PressureWire® (Radi Medical Systems, Inc., Uppsala, Sweden): a 0.014-in. wire that contains a high-sensitivity thermistor of 0.1 °C. (**e**) Accumed Systems, Inc. (Ann Arbor, MI, USA): A blood-flow-occluding feature with a temperature sensing structure at its distal end and a proximal end including a manually operated expansion control

Table 9.1 Human in vivo thermography studies

Author	Year	Main finding	Type of catheter
Stefanadis et al. [22]	1999	Temperature differences between atherosclerotic plaque and healthy vessel wall increased through the clinical spectrum	Epiphany catheter: single-channel, thermistor-based
Stefanadis et al. [31]	2000	Positive correlation of C-reactive protein and serum amyloid A with the temperature difference of the plaque	Epiphany catheter: single-channel, thermistor-based
Stefanadis et al. [28]	2001	Increased local temperature in atherosclerotic plaques is strong predictor of an unfavorable clinical outcome in patients with coronary artery disease undergoing percutaneous interventions	Epiphany catheter: single-channel, thermistor-based
Stefanadis et al. [30]	2002	Statin intake showed a favorable effect on heat release from atherosclerotic plaques	Epiphany catheter: single-channel, thermistor-based
Webster et al. [42]	2002	Increased thermal heterogeneity detected in atherosclerotic plaques. No correlation with C-reactive protein was found	RADI PressureWire high-sensitivity thermistor
Stefanadis et al. [35]	2003	Thermal heterogeneity was underestimated in atherosclerotic plaques due to the "cooling effect" of coronary blood flow	Epiphany catheter: single-channel, thermistor-based
Stefanadis et al. [39]	2003	In vivo atherosclerotic plaque temperature recording was feasible with the new balloon-thermography catheter. Higher temperature difference was found after complete interruption of blood flow by inflation of the balloon	A balloon-thermography catheter designed for temperature measurements during coronary flow interruption. The thermistor probe is positioned at the distal segment of the catheter with a balloon at the opposite site. By inflation of the balloon, coronary flow is interrupted
Schmermund et al. [24]	2003	Increased thermal heterogeneity in atherosclerotic plaques of patients with stable or unstable angina	Volcano catheter: self-expanding basket with five nitinol arms, one on each arm and one on the central wire
Stefanadis et al. [43]	2004	Coronary sinus temperature was increased in patients with coronary artery disease and was found to be a prognostic factor for mid-term clinical outcome	A 7 Fr thermographic catheter possessing a steering arm at the proximal part of the catheter and a thermistor probe at the catheter tip. Manipulation of the steering arm proximally enables the distal end of the catheter to be curved (0–180°)
Toutouzas et al. [23]	2004	Increased plaque temperature was observed for an extended period after myocardial infarction. Statins intake showed a beneficial effect after myocardial infarction on plaque temperature	Epiphany catheter: single-channel, thermistor-based
Dudek et al. [44]	2005	Thermography was unable to differentiate between lesions at risk, despite a selection of lesions that should appear most distinct to differentiate	Volcano catheter

(continued)

Table 9.1 (continued)

Author	Year	Main finding	Type of catheter
Toutouzas et al. [45]	2005	Systemic inflammation correlated with coronary sinus temperature independently of the extent of coronary artery disease	A 7 Fr thermographic catheter possessing a steering arm at the proximal part of the catheter and a thermistor probe at the catheter tip. Manipulation of the steering arm proximally enables the distal end of the catheter to be curved (0–180°).
Toutouzas et al. [27]	2005	Patients with diabetes mellitus had increased temperature difference compared to patients without. Statin intake showed beneficial effect on plaque temperature	Epiphany catheter: single-channel, thermistor-based
Toutouzas et al. [46]	2006	Heat was generated in non-culprit lesions progressively increasing from patients with acute coronary syndrome to patients with stable angina	Epiphany catheter: single-channel, thermistor-based
Rzeszutko et al. [47]	2006	Intracoronary thermography was safe and feasible. No ability to differentiate between lesions at risk, despite a selection of lesions that should appear most distinct to differentiate	Volcano catheter
Worthley et al. [38]	2006	No significant temperature increase in patients with acute coronary syndrome, compared to baseline temperature	RADI PressureWire high-sensitivity thermistor
Wainstein et al. [33]	2007	Intracoronary thermography detected vulnerable plaques, as these were assessed by intravascular ultrasound and atherectomy tissue histology	ThermoCoil guidewire
Toutouzas et al. [34]	2007	Local inflammatory activation in non-culprit lesions correlated with systemic inflammation. Statins showed a beneficial effect on non-culprit lesion heat production	Epiphany catheter: single-channel, thermistor-based
Toutouzas et al. [34]	2007	Culprit lesions with plaque rupture and positive arterial remodeling had increased thermal heterogeneity	Epiphany catheter: single-channel, thermistor-based
Takumi et al. [48]	2007	Thermography showed accurate identification of the culprit lesion in patients with acute myocardial infarction and coronary total occlusion	RADI PressureWire high-sensitivity thermistor
Cuisset et al. [32]	2009	Temperature increase across the lesion correlated with the pressure drop across the stenosis ($R=0.72$, $p<0.001$)	RADI PressureWire high-sensitivity thermistor

Spectrum of ACS: First Clinical Study

The first clinical study with in vivo IVT performed by Stefanadis et al. in 1999 included 90 patients. The intracoronary thermography catheter utilized uses a thermistor-based sensor that contains two lumens (Epiphany; Medispes S. W., Zug, Switzerland). The first one runs through the distal 20 cm of the device and is used for the insertion of a guidewire (0.014-in.) that serves as a monorail provision system. The thermistor is positioned at the distal part of the thermography catheter of the second lumen. This catheter is 3, 3.5, or 4 F in diameter, depending on the size of the vessel, while the technical characteristics of this particular polyamide thermistor are: (1) temperature accuracy of 0.05 °C; (2) time constant of 300 ms; (3) spatial resolution of 0.5 mm; and (4) linear correlation of resistance vs. temperature over the range of 33–43 °C. The ΔT between atherosclerotic plaques and adjacent healthy segments increased progressively from control subjects through the ACS spectrum, from stable angina to acute myocardial infarction patients. Plaque ΔT was present in 20 %, 40 %, and 67 % of the patients with stable angina, unstable angina, and acute myocardial infarction, respectively, and did not correlate with the degree of stenosis. Temperature was constant within the arteries of the control subjects, whereas most atherosclerotic plaques showed higher temperature difference compared with healthy vessel wall [22]. Moreover, in another study including 55 patients, increased plaque temperature was observed for an extended period after myocardial infarction, indicating that the inflammatory process is sustained after plaque rupture. In patients with recent myocardial infarction ΔT was 0.19 ± 0.18 °C, while in patients with stable angina ΔT was 0.10 ± 0.08 °C ($p = 0.03$) [23]. Scmermund et al. observed ΔT in 50 % of patients with unstable angina and in 27 % of patients with stable angina. The range of difference was 0.14–0.36 °C. Although this study showed a difference between the two groups, there was still a considerable overlap [24].

IVT in Patients with Diabetes Mellitus

Inflammation of atherosclerotic lesions seems to be even more significant in diabetic patients. In a study including 45 patients with diabetes mellitus and 63 patients without, patients with *diabetes mellitus* had increased temperature difference compared to the control group. Patients with diabetes mellitus suffering from coronary artery disease showed increased local inflammatory involvement compared to patients without diabetes mellitus. This finding is in accordance with previous observations that patients with diabetes mellitus have more severe inflammation in their coronary atherosclerotic plaques, suggesting that diabetes mellitus has a strong impact on plaque destabilization via inflammatory activation. The inflammatory activation in patients with diabetes mellitus could be the explanation for the lack of favorable outcomes of trials in cardiovascular events, even in patients with intensive treatment to control blood glucose levels. Thus, the strict control of glucose levels with stabilization of local inflammatory involvement could potentially reduce the cardiovascular mortality in this high-risk group [25–27].

Risk Stratification

The impact of IVT on risk stratification of patients undergoing percutaneous coronary intervention has also been investigated. The association of temperature differences between the atherosclerotic plaque and the healthy vessel wall with the event-free survival has been studied in 86 patients after successful percutaneous coronary intervention with bare metal stents at the culprit lesion. The patients that were enrolled had stable angina (34.5 %), unstable angina (34.5 %), or acute myocardial infarction (30 %). Temperature difference increased progressively from stable angina to acute myocardial infarction, while after a median clinical follow-up period of 17.88 ± 7.16 months thermal heterogeneity was greater in patients with adverse cardiac events

than in patients without events ($p<0.0001$). In addition, temperature difference was found to be a strong predictor of adverse cardiac events during the follow-up period (OR = 2.14, $p=0.043$). However, the impact of local inflammatory activation on (1) restenosis in the era of drug-eluting stents, and (2) on the progression of non-culprit lesions remains to be determined in large prospective studies [28].

Effect of Statins on Local Inflammatory Activity

The anti-inflammatory effect of statins is already a field of increased interest, as they reduce the number of macrophages while increasing the collagen content in atherosclerotic plaques, hence stabilizing the plaque [29]. We investigated a possible stabilizing effect of statin on hot plaques in a study including 72 patients; 37 patients receiving statins for more than 4 weeks and 35 not receiving statins [30]. Thermal heterogeneity of the culprit lesion was lower in patients treated with statins, independently of the clinical syndrome under expression and of the serum cholesterol level at hospital admission. In this study, patients with diabetes mellitus under treatment with statins showed decreased temperature difference compared with untreated patients, suggesting that statins have a favorable effect in patients with diabetes mellitus and coronary artery disease [27]. These findings indicate that aggressive treatment with statins may be essential for the stabilization of the vulnerable atherosclerotic plaque in patients with coronary artery disease, including those planned for percutaneous coronary intervention, as it has been observed that patients with increased culprit plaque temperature at the time of intervention have poor prognosis. Moreover, the effect of statins on non-culprit lesion inflammation has been recently investigated. Temperature difference was less in patients treated with statin in both clinical groups. This is likely secondary to the proven anti-inflammatory "pleiotropic" vascular effects of statins. Intracoronary thermography remains the only method demonstrating the effect of statin treatment on in vivo local inflammatory status.

Systemic Inflammation

Several studies have demonstrated a correlation between systemic inflammation determined by elevated levels of serum biomarkers, such as C-reactive protein, and local plaque temperature. A strong correlation between C-reactive protein and serum amyloid A levels, with detected differences in temperature was the outcome of the study of 60 patients with coronary artery disease (20 with stable angina, 20 with unstable angina, and 20 with acute myocardial infarction) and 20 sex- and age-matched controls without coronary artery disease [31]. An apparently higher mean C-reactive protein level has been demonstrated in patients with higher temperature heterogeneity compared to those without elevated temperature (14.0 vs. 6.2 mg/L) [32].

IVT and IVUS

Thirteen patients presenting with either acute or chronic coronary syndromes as indications for percutaneous coronary intervention were evaluated by three interventional methods: *intracoronary thermography (ThermoCoil Guidewire), IVUS, and angiography*. In two of these patients, directional atherectomy was performed and tissue was histologically analyzed. Intra-arterial temperature between 0.1 °C and 0.3 °C was noted in four subjects. Intravascular ultrasound findings and atherectomy tissue histology indicated correlation of plaque vulnerability and elevated temperature [33]. In a study where IVUS and endovascular thermography were performed in 81 consecutive patients (48 with ACS and 33 with stable angina), *a strong positive correlation between coronary remodeling index* (defined as the ratio of the external elastic membrane area of the lesion, to that at the proximal site) and temperature difference between the atherosclerotic plaque and healthy vascular wall was found in patients with ACS. More specific, patients with ACS had greater remodeling index than patients with stable angina (1.15 ± 0.18 °C vs. 0.90 ± 0.12 °C; $p<0.01$), as well as increased temperature difference (0.08 ± 0.03 °C vs. 0.04 ± 0.02 °C; $p<0.01$). Moreover, patients with

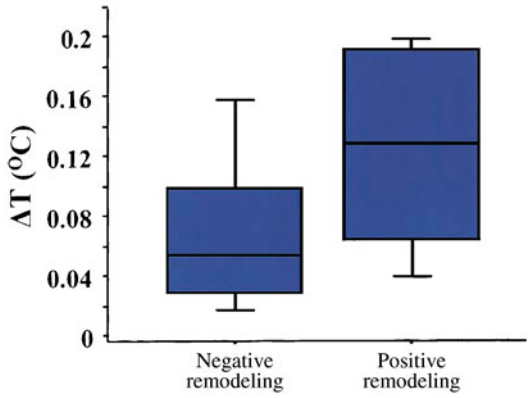

Fig. 9.4 Difference in atherosclerotic plaque temperature from background temperature (ΔT) between patients with negative remodeling and those with positive remodeling

positive remodeling had higher thermal heterogeneity than patients with negative remodeling (0.07 ± 0.03 °C vs. 0.04 ± 0.02 °C; $p < 0.001$) (Fig. 9.4). Patients with plaque rupture had increased temperature difference compared to patients without rupture (0.09 ± 0.03 °C vs. 0.05 ± 0.02 °C; $p < 0.01$). Although culprit lesions with plaque rupture and positive arterial remodeling have increased thermal heterogeneity, in certain patients a discrepancy between morphologic and functional characteristics was observed [34].

The "Cooling Effect"

In the majority of the studies with IVT, a discrepancy was observed between the in vivo and ex vivo temperature measurements. The major factor for this difference was the "cooling effect" of coronary blood flow on measured temperature, as complete obstruction of blood flow proved to increase the degree of detected temperature heterogeneity by 60–76 % [35]. Likewise, in 5 out of 20 lesions evaluated before and after the interruption of blood flow with the use of an occluding thermographic catheter, an elevation of 0.3 °C was recorded [36]. In a stimulation model of a coronary artery segment containing a heat source, various types of catheter material, diameter, and location with respect to the plaque were studied in both flow and no-flow situations. Occlusion of blood flow increased ΔT values in all cases [37]. Worthley et al. measured a mean temperature difference of 0.02 ± 0.01 °C in the culprit lesion, which was below the resolution of the thermistor (the 0.014-in. Radi PressureWire XT) and not significantly different from the baseline temperature difference of 0.00 ± 0.01 °C [32]. Using the same system, Cuisset et al. assessed intracoronary pressure and temperature variations in 18 patients with acute myocardial infarction. In this study, when the sensor was advanced across the lesion, an increase in the temperature signal (average 0.059 ± 0.028 °C) was uniformly observed in all patients. However, the increase in the temperature signal was proportional to the pressure drop across the stenosis ($R = 0.72$, $p < 0.001$) [38]. This study suggested that the measurements obtained so far in patients with acute coronary syndromes may be affected by pressure and flow. Both studies, however, may have been limited by the fact that the Radi wire is not designed for measuring the coronary plaque temperature, but rather for measuring the blood temperature within the lumen. To eliminate this shortcoming, new catheter designs were introduced, but still remains to be investigated in a large number of patients [36, 39].

Future Perspectives

Although intracoronary thermography has proven a feasible and safe method detecting functional characteristics of the VP, several technical limitations have arisen. Apart from the "cooling effect" that we already have described as a factor of underestimation of temperature measurements, the accurate assessment of thermal heterogeneity presupposes the direct contact of the thermistor with the vessel wall. Therefore, the correct interpretation of intravascular thermographic measurements and the definition of a cut-off value for the presence of VP might require knowledge of data with respect to flow and morphological characteristics of the atherosclerotic plaque that are not readily available at this stage.

Intravascular Thermography does not provide any information for morphological features of

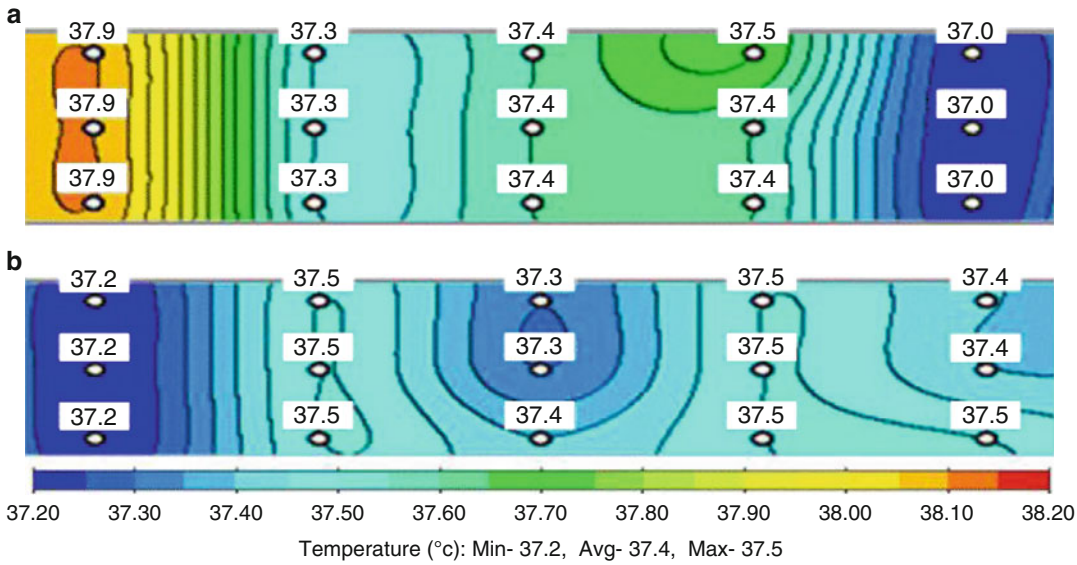

Fig. 9.5 Thermal mapping of the abdominal aorta of the rabbits with the use of the microwave radiometry. (**a**) A representative temperature difference of 0.9 °C measured at the aorta of a hypercholesterolemic rabbit. (**b**) A representative temperature field of the aorta of a control rabbit showing equally distributed temperatures with ΔT of 0.3 °C. Each temperature corresponds to a specific color and the scale is depicted in the bottom of the temperature fields

the VP, as the lipid pool, the thickness of the fibrous cap, or the degree of positive remodeling. The combination of this method with other imaging modalities giving information for the structure of the plaque, such as IVUS and optical coherence tomography (OCT), could enhance the diagnostic capabilities for the detection of VP.

Moreover, newer noninvasive imaging modalities are required to distinguish stable and vulnerable plaques, especially in primary prevention. Microwave radiometry (RTM-01-RES system, MR) is a new promising method for the noninvasive functional assessment of the atherosclerotic plaque, already applied in oncology. The probe of the system, in contact with the skin surface, detects noninvasively natural electromagnetic radiation produced by internal tissues, and provides accurate temperature measurements depicted on a thermal mapping. In an experimental model, 24 New Zealand rabbits were randomized to either a normal ($n=12$) or cholesterol-rich (0.3 %) diet ($n=12$) for 6 months. Temperature measurements of the abdominal aorta were performed both noninvasively by MR and invasively by IVT and temperature differences of atherosclerotic aortic segments were significantly higher compared to temperature differences of the controls ($p<0.001$) (Fig. 9.5). The measurements with both techniques were correlated positively ($p<0.001$, $R=0.94$), and following assessment of the aortic segments by histology confirmed the thermal heterogeneity detected. In specific, segments with higher thermal heterogeneity measured by both methods had also higher inflammatory cell density (lymphocytes and mast cells), while histological analysis showed good correlation between temperature differences and plaque thickness (MR: $R=0.60$, $p<0.001$, IVT: $R=0.41$, $p=0.004$) (Fig. 9.6) [40]. In first in vivo application of MR in human carotids, 43 patients undergoing carotid endarterectomy and control volunteers were estimated by ultrasound and MR. In addition, specimens of the group of patients were histologically studied. Thermal heterogeneity was higher in atherosclerotic carotid arteries compared with the carotid arteries of controls ($p<0.01$). As far as concerned correlation of ultrasound findings with MR measurements, fatty plaques had higher ΔT compared with mixed and calcified plaques ($p<0.01$), while plaques with ulcerated surface

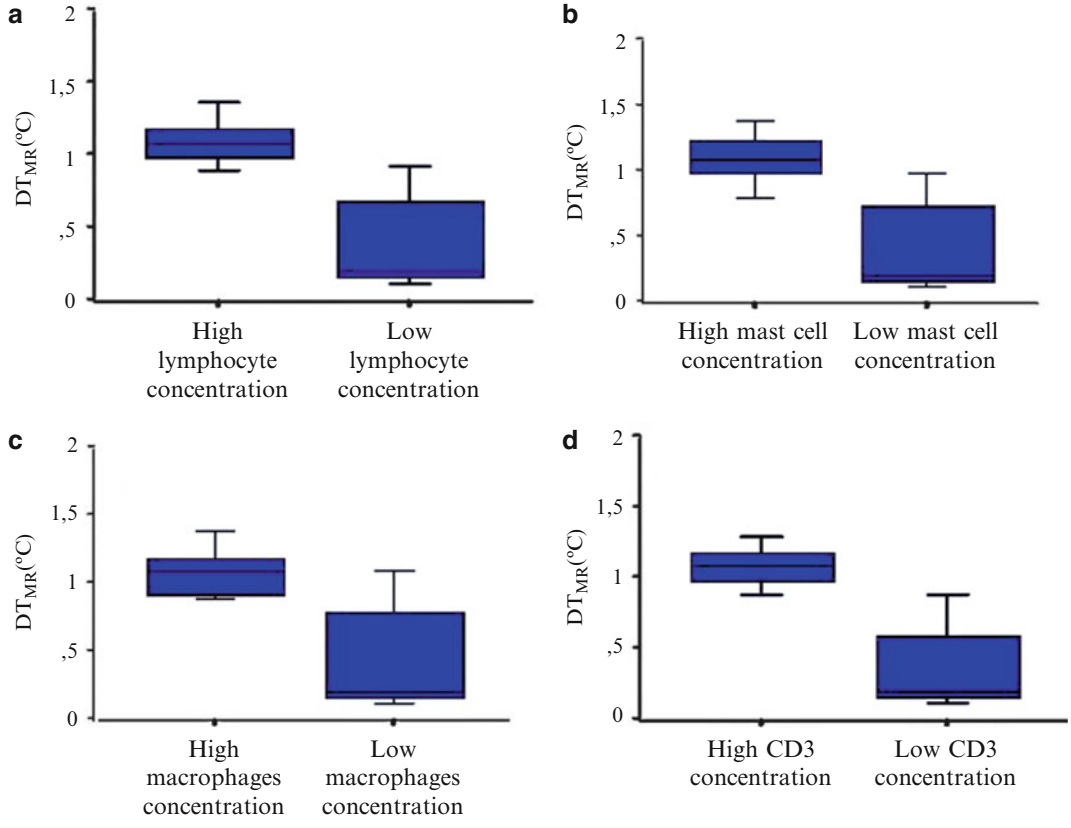

Fig. 9.6 Temperature differences by microwave radiometry (ΔT MR (°C)) in segments with intense vs. low expression of inflammatory indexes. (**a**) Intense vs. low expression of lymphocyte concentration. (**b**) Intense vs. low expression of mast cell concentration. (**c**) Intense vs. low expression of macrophage concentration (CD68). (**d**) Intense vs. low expression of CD3

had higher ΔT compared with plaques with irregular and regular surface ($p<0.01$). Heterogeneous plaques had higher ΔT compared with homogenous ($p<0.01$). In histological study, specimens with thin fibrous cap and intense expression of CD3, CD68, and vascular endothelial growth factor (VEGF) had higher ΔT compared with specimens with thick cap and low expression of CD3, CD68, and VEGF ($p<0.01$) [41].

Conclusions

Despite advances in current imaging modalities, the ability to identify patients of high risk for a future acute coronary event is still limited. The progress in the identification of vulnerable plaques is dependent on a greater understanding of the mechanisms of atherosclerotic plaque progression, including inflammation. Intravascular Thermography, a method for the functional characterization of vulnerable plaque that has been introduced into clinical practice, provides important information regarding the local inflammatory activity which is definitely increased in special clinical syndromes. There are no prospective data however for the predictive value of IVT, as the current technology of invasive catheters cannot overcome certain limitations. The combination of current technology of IVT catheters with methods providing structural details could increase the prognostic value and needs to be prospectively investigated. Moreover, new noninvasive much promising techniques, like microwave radiometry, remain to be further assessed in clinical trials.

References

1. Rosamond W, Flegal K, Furie K, Go A, Greenlund K, Haase N, Hailpern SM, Ho M, Howard V, Kissela B, Kittner S, Lloyd-Jones D, McDermott M, Meigs J, Moy C, Nichol G, O'Donnell C, Roger V, Sorlie P, Steinberger J, Thom T, Wilson M, Hong Y. Heart disease and stroke statistics–2008 update: a report from the American Heart Association Statistics Committee and Stroke Statistics Subcommittee. Circulation. 2008;117(4):e25–146.
2. Honda Y, Fitzgerald PJ. Frontiers in intravascular imaging technologies. Circulation. 2008;117(15): 2024–37.
3. Ross R. Atherosclerosis–an inflammatory disease. N Engl J Med. 1999;340(2):115–26.
4. Libby P, Ridker PM, Hansson GK. Inflammation in atherosclerosis: from pathophysiology to practice. J Am Coll Cardiol. 2009;54(23):2129–38.
5. Libby P, Ridker PM, Maseri A. Inflammation and atherosclerosis. Circulation. 2002;105(9):1135–43.
6. Schoenhagen P. Plaque temperature, arterial remodeling, and inflammation: understanding "hot-spots" in the coronary arteries. J Am Coll Cardiol. 2007; 49(23):2272–3.
7. Naghavi M, Falk E, Hecht HS, Jamieson MJ, Kaul S, Berman D, Fayad Z, Budoff MJ, Rumberger J, Naqvi TZ, Shaw LJ, Faergeman O, Cohn J, Bahr R, Koenig W, Demirovic J, Arking D, Herrera VL, Badimon J, Goldstein JA, Rudy Y, Airaksinen J, Schwartz RS, Riley WA, Mendes RA, Douglas P, Shah PK. From vulnerable plaque to vulnerable patient–Part III: executive summary of the Screening for Heart Attack Prevention and Education (SHAPE) Task Force report. Am J Cardiol. 2006;98(2A):2H–15.
8. Stone GW, Maehara A, Lansky AJ, de Bruyne B, Cristea E, Mintz GS, Mehran R, McPherson J, Farhat N, Marso SP, Parise H, Templin B, White R, Zhang Z, Serruys PW. A prospective natural-history study of coronary atherosclerosis. N Engl J Med. 2011; 364(3):226–35.
9. Toutouzas K, Synetos A, Nikolaou C, Tsiamis E, Tousoulis D, Stefanadis C. Matrix metalloproteinases and vulnerable atheromatous plaque. Curr Top Med Chem. 2012;12(10):1166–80.
10. Heinle H. Metabolite concentration gradients in the arterial wall of experimental atherosclerosis. Exp Mol Pathol. 1987;46(3):312–20.
11. Tenaglia AN, Peters KG, Sketch Jr MH, Annex BH. Neovascularization in atherectomy specimens from patients with unstable angina: implications for pathogenesis of unstable angina. Am Heart J. 1998;135(1): 10–4.
12. Madjid M, Willerson JT, Casscells SW. Intracoronary thermography for detection of high-risk vulnerable plaques. J Am Coll Cardiol. 2006;47(8 suppl):C80–5.
13. Kockx MM, Seye C, De Meyer GR, Knaapen MW. Decreased apoptosis and tissue factor expression after lipid lowering. Circulation. 2000;102(13):E99.
14. Kockx MM, De Meyer GR, Buyssens N, Knaapen MW, Bult H, Herman AG. Cell composition, replication, and apoptosis in atherosclerotic plaques after 6 months of cholesterol withdrawal. Circ Res. 1998;83(4):378–87.
15. Casscells W, Hathorn B, David M, Krabach T, Vaughn WK, McAllister HA, Bearman G, Willerson JT. Thermal detection of cellular infiltrates in living atherosclerotic plaques: possible implications for plaque rupture and thrombosis. Lancet. 1996;347(9013):1447–51.
16. Toutouzas K, Spanos V, Ribichini F. A correlation of coronary plaque temperature with inflammatory markers obtained from atherectomy specimens in humans. Am J Cardiol. 2003;92:476.
17. Madjid M, Naghavi M, Malik BA, Litovsky S, Willerson JT, Casscells W. Thermal detection of vulnerable plaque. Am J Cardiol. 2002;90(10C):36L–9L.
18. Naghavi M, John R, Naguib S, Siadaty MS, Grasu R, Kurian KC, van Winkle WB, Soller B, Litovsky S, Madjid M, Willerson JT, Casscells W. pH Heterogeneity of human and rabbit atherosclerotic plaques; a new insight into detection of vulnerable plaque. Atherosclerosis. 2002;164(1):27–35.
19. Naghavi M, Madjid M, Gul K, Siadaty MS, Litovsky S, Willerson JT, Casscells SW. Thermography basket catheter: in vivo measurement of the temperature of atherosclerotic plaques for detection of vulnerable plaques. Catheter Cardiovasc Interv. 2003;59(1): 52–9.
20. Verheye S, De Meyer GR, Van Langenhove G, Knaapen MW, Kockx MM. In vivo temperature heterogeneity of atherosclerotic plaques is determined by plaque composition. Circulation. 2002;105(13): 1596–601.
21. Krams R, Verheye S, van Damme LC, Tempel D, Mousavi Gourabi B, Boersma E, Kockx MM, Knaapen MW, Strijder C, van Langenhove G, Pasterkamp G, van der Steen AF, Serruys PW. In vivo temperature heterogeneity is associated with plaque regions of increased MMP-9 activity. Eur Heart J. 2005;26(20):2200–5.
22. Stefanadis C, Diamantopoulos L, Vlachopoulos C, Tsiamis E, Dernellis J, Toutouzas K, Stefanadi E, Toutouzas P. Thermal heterogeneity within human atherosclerotic coronary arteries detected in vivo: a new method of detection by application of a special thermography catheter. Circulation. 1999;99(15): 1965–71.
23. Toutouzas K, Vaina S, Tsiamis E, Vavuranakis M, Mitropoulos J, Bosinakou E, Toutouzas P, Stefanadis C. Detection of increased temperature of the culprit lesion after recent myocardial infarction: the favorable effect of statins. Am Heart J. 2004;148(5):783–8.
24. Schmermund A, Rodermann J, Erbel R. Intracoronary thermography. Herz. 2003;28(6):505–12.

25. Toutouzas K, Markou V, Drakopoulou M, Mitropoulos I, Tsiamis E, Vavuranakis M, Vaina S, Stefanadis C. Increased heat generation from atherosclerotic plaques in patients with type 2 diabetes: an increased local inflammatory activation. Diabetes Care. 2005; 28(7):1656–61.
26. Toutouzas K, Tsiamis E, Drakopoulou M, Synetos A, Karampelas J, Riga M, Tsioufis C, Tousoulis D, Stefanadi E, Vlasis C, Stefanadis C. Impact of type 2 diabetes mellitus on diffuse inflammatory activation of de novo atheromatous lesions: implications for systemic inflammation. Diabetes Metab. 2009;35(4):299–304.
27. Toutouzas K, Markou V, Drakopoulou M, Mitropoulos I, Tsiamis E, Stefanadis C. Patients with type two diabetes mellitus: increased local inflammatory activation in culprit atheromatous plaques. Hellenic J Cardiol. 2005;46(4):283–8.
28. Stefanadis C, Toutouzas K, Tsiamis E, Stratos C, Vavuranakis M, Kallikazaros I, Panagiotakos D, Toutouzas P. Increased local temperature in human coronary atherosclerotic plaques: an independent predictor of clinical outcome in patients undergoing a percutaneous coronary intervention. J Am Coll Cardiol. 2001;37(5):1277–83.
29. Libby P. Lipid-lowering therapy stabilizes plaque, reduces events by limiting inflammation. Am J Manag Care. 2002;Suppl 1:4.
30. Stefanadis C, Toutouzas K, Vavuranakis M, Tsiamis E, Tousoulis D, Panagiotakos DB, Vaina S, Pitsavos C, Toutouzas P. Statin treatment is associated with reduced thermal heterogeneity in human atherosclerotic plaques. Eur Heart J. 2002;23(21):1664–9.
31. Stefanadis C, Diamantopoulos L, Dernellis J, Economou E, Tsiamis E, Toutouzas K, Vlachopoulos C, Toutouzas P. Heat production of atherosclerotic plaques and inflammation assessed by the acute phase proteins in acute coronary syndromes. J Mol Cell Cardiol. 2000;32(1):43–52.
32. Cuisset T, Beauloye C, Melikian N, Hamilos M, Sarma J, Sarno G, Naslund M, Smith L, Van de Vosse F, Pijls NH, De Bruyne B. In vitro and in vivo studies on thermistor-based intracoronary temperature measurements: effect of pressure and flow. Catheter Cardiovasc Interv. 2009;73(2):224–30.
33. Wainstein M, Costa M, Ribeiro J, Zago A, Rogers C. Vulnerable plaque detection by temperature heterogeneity measured with a guidewire system: clinical, intravascular ultrasound and histopathologic correlates. J Invasive Cardiol. 2007;19(2):49–54.
34. Toutouzas K, Synetos A, Stefanadi E, Vaina S, Markou V, Vavuranakis M, Tsiamis E, Tousoulis D, Stefanadis C. Correlation between morphologic characteristics and local temperature differences in culprit lesions of patients with symptomatic coronary artery disease. J Am Coll Cardiol. 2007;49(23):2264–71.
35. Stefanadis C, Toutouzas K, Tsiamis E, Mitropoulos I, Tsioufis C, Kallikazaros I, Pitsavos C, Toutouzas P. Thermal heterogeneity in stable human coronary atherosclerotic plaques is underestimated in vivo: the "cooling effect" of blood flow. J Am Coll Cardiol. 2003;41(3):403–8.
36. Belardi JA, Albertal M, Cura FA, Mendiz O, Balino PP, Padilla LT, Lauer M, Korotko J, O'Neill W. Intravascular thermographic assessment in human coronary atherosclerotic plaques by a novel flow-occluding sensing catheter: a safety and feasibility study. J Invasive Cardiol. 2005;17(12):663–6.
37. ten Have AG, Draaijers EB, Gijsen FJ, Wentzel JJ, Slager CJ, Serruys PW, van der Steen AF. Influence of catheter design on lumen wall temperature distribution in intracoronary thermography. J Biomech. 2007;40(2):281–8.
38. Worthley S, Farouque MO, Worthley M, Baldi M, Chew D, Meredith I. The RADI PressureWire high-sensitivity thermistor and culprit lesion temperature in patients with acute coronary syndromes. J Invasive Cardiol. 2006;18(11):528–31.
39. Stefanadis C, Toutouzas K, Vavuranakis M, Tsiamis E, Vaina S, Toutouzas P. New balloon-thermography catheter for in vivo temperature measurements in human coronary atherosclerotic plaques: a novel approach for thermography? Catheter Cardiovasc Interv. 2003;58(3):344–50.
40. Toutouzas K, Grassos H, Synetos A, Drakopoulou M, Tsiamis E, Moldovan C, Agrogiannis G, Patsouris E, Siores E, Stefanadis C. A new non-invasive method for detection of local inflammation in atherosclerotic plaques: experimental application of microwave radiometry. Atherosclerosis. 2011;215(1):82–9.
41. Toutouzas K, Grassos C, Drakopoulou M, Synetos A, Tsiamis E, Aggeli C, Stathogiannis K, Klettas D, Kavantzas N, Agrogiannis G, Patsouris E, Klonaris C, Liasis N, Tousoulis D, Siores E, Stefanadis C. First in vivo application of microwave radiometry in human carotids: a new noninvasive method for detection of local inflammatory activation. J Am Coll Cardiol. 2012;59(18):1645–53.
42. Webster M, Stewart J, Ruygrok P. Intracoronary thermography with a multiple thermocouple catheter: initial human experience. Am J Cardiol. 2002;90:24H.
43. Stefanadis C, Tsiamis E, Vaina S, Toutouzas K, Boudoulas H, Gialafos J, Toutouzas P. Temperature of blood in the coronary sinus and right atrium in patients with and without coronary artery disease. Am J Cardiol. 2004;93(2):207–10.
44. Dudek D, Rzeszutko L, Legutko J, Wizimirski M, Chyrchel M, Witanek B, Dubiel JS. High-risk coronary artery plaques diagnosed by intracoronary thermography. Kardiol Pol. 2005;62(4):383–9.
45. Toutouzas K, Drakopoulou M, Markou V, Stougianos P, Tsiamis E, Tousoulis D, Stefanadis C. Increased coronary sinus blood temperature: correlation with systemic inflammation. Eur J Clin Invest. 2006; 36(4):218–23.

46. Toutouzas K, Drakopoulou M, Mitropoulos J, Tsiamis E, Vaina S, Vavuranakis M, Markou V, Bosinakou E, Stefanadis C. Elevated plaque temperature in non-culprit de novo atheromatous lesions of patients with acute coronary syndromes. J Am Coll Cardiol. 2006;47(2):301–6.
47. Rzeszutko L, Legutko J, Kaluza GL, Wizimirski M, Richter A, Chyrchel M, Heba G, Dubiel JS, Dudek D. Assessment of culprit plaque temperature by intracoronary thermography appears inconclusive in patients with acute coronary syndromes. Arterioscler Thromb Vasc Biol. 2006;26(8):1889–94.
48. Takumi T, Lee S, Hamasaki S, Toyonaga K, Kanda D, Kusumoto K, Toda H, Takenaka T, Miyata M, Anan R, Otsuji Y, Tei C. Limitation of angiography to identify the culprit plaque in acute myocardial infarction with coronary total occlusion utility of coronary plaque temperature measurement to identify the culprit plaque. J Am Coll Cardiol. 2007;50(23): 2197–203.

Chemical Fingerprinting of Plaque: Spectroscopic Techniques

10

Emmanouil S. Brilakis, Subhash Banerjee, Zhihua He, Stephen T. Sum, Sean Madden, and James Muller

Near-infrared spectroscopy (NIRS) is a novel coronary imaging technology that analyzes the light reflected in a range of wavelengths to determine the chemical composition of tissue, including lipids such as cholesterol and cholesteryl esters. This chapter presents the basic principles of NIRS, describes the equipment and interpretation of NIRS findings, presents the studies that validated the ability of NIRS to detect lipid core plaques (LCPs), and discusses its clinical and research applications.

Principles of Diffuse Reflectance NIRS

In diffuse reflectance NIRS, light from the near-infrared region of the electromagnetic spectrum (approximately 800–2,500 nm) is directed to a sample and the diffusely reflected light is collected. The proportion of light returned from the sample is dependent on wavelength and is dependent on loss of light in the tissue due to scattering and absorption. Scattering occurs when light is randomly reflected by cellular and extracellular structures in the sample, while absorption results from the transformation of light into molecular energy primarily in the form of molecular vibrations of atoms about their chemical bonds.

NIRS allows direct and rapid measurements for qualitative and quantitative compositional analysis in an array of applications with little to no sample preparation. As a result, NIRS has been widely adopted in many different areas including agriculture, food, petroleum, astronomy, pharmaceuticals, and medicine [1, 2].

Interpretation of the NIRS spectra of complex, multi-constituent samples is difficult and requires multivariate methods of analysis. This is accomplished by mathematical modeling using calibration samples whose chemical and physical properties span the expected range of future samples. Reference values for the target components in these samples are obtained by an independent method (e.g., histology). Models constructed from the calibration samples compare the measured NIRS signals with the reference values, allowing qualitative or quantitative determination of unknown samples based on their NIRS spectra [3].

Validation of LCP Detection by NIRS

Early studies demonstrated that NIRS can detect cholesterol and collagen in rabbit and human aortic tissue and in human carotid and coronary tissue

E.S. Brilakis, MD, PhD (✉) • S. Banerjee, MD
Department of Cardiovascular Diseases,
VA North Texas Health Care System,
University of Texas Southwestern Medical School,
4500 S. Lancaster Road (111A), Dallas,
TX 75216, USA
e-mail: esbrilakis@gmail.com; subhash.banerjee@va.gov

Z. He, PhD • S.T. Sum, PhD • S. Madden, PhD,
J. Muller, MD
Infaredx, Inc., 34 Third Ave.,
Burlington, MA 01803, USA
e-mail: vhe@infraredx.com; ssum@infraredx.com;
smadden@infraredx.com; jmuller@infraredx.com

S.J. Nicholls and T. Crowe (eds.), *Imaging Coronary Atherosclerosis*, Contemporary Cardiology,
DOI 10.1007/978-1-4939-0572-0_10,

ex vivo [4–6]. Subsequently, NIRS intravascular diagnostic systems were developed to detect lipid-rich plaque through blood [7–10].

The detection of LCP by NIRS was validated in a large study of human coronary autopsy specimens [11]. Arterial segments were first scanned during pulsatile coronary artery perfusion using blood and then cut into 2-mm thick cross-sectional blocks for histopathological analysis. A total of 84 autopsy hearts and 216 segments were used to build and validate an algorithm capable of automatically recognizing the NIRS spectral signals associated with LCP. For the purpose of this study, LCP was defined as a fibroatheroma containing a necrotic core at least 200 μm thick with a circumferential span of at least 60° on cross-section. The primary endpoint of the algorithm validation was the accuracy of detecting LCP meeting this definition. The algorithm was prospectively validated for detection of LCP in nearly 2,000 individual blocks from 51 hearts achieving an area under the receiver operating characteristic (ROC) curve (AUC) of 0.80 for lumen diameters of up to 3.0 mm.

A concurrent in vivo study called SPECTroscopic Assessment of Coronary Lipid (SPECTACL) showed prospectively that the spectral features of coronary arteries in patients were similar to those obtained from autopsy specimens [12]. The spectral similarity between NIRS measurements collected in vivo and ex vivo demonstrated the applicability of the autopsy tissue-based LCP detection algorithm to patients.

Fig. 10.1 TVC imaging system, which is a combination NIRS and IVUS system. (**a**) The console includes two touch-screen monitors displaying the NIRS chemogram and IVUS images (transverse and longitudinal). (**b**) The catheter contains fiber optics and mirrors for near-infrared light, as well as a coax cable and a transducer for ultrasound

Design of the Near-Infrared: Intravascular Ultrasound Combination System and Interpretation of its Findings

Currently coronary NIRS is available as a combined NIRS and intravascular ultrasound (IVUS) system (TVC Imaging System, InfraReDx, Inc., Burlington, MA) [13]. The system consists of a console, a pullback and rotation device (PBR), and an intravascular catheter [14] (Fig. 10.1). The system console contains a near-infrared scanning laser, computer, power system, and two monitors. The PBR houses the electronic, optical and mechanical components for delivering and detecting ultrasound and near-infrared light signals, and for translating and rotating the imaging core of the catheter. The catheter is 3.2-Fr, rapid exchange catheter consisting of a tip with a 40 MHz ultrasound transducer and two mirrors, a core with two optical fibers and a coax cable inside a drive cable. The delivery and collection

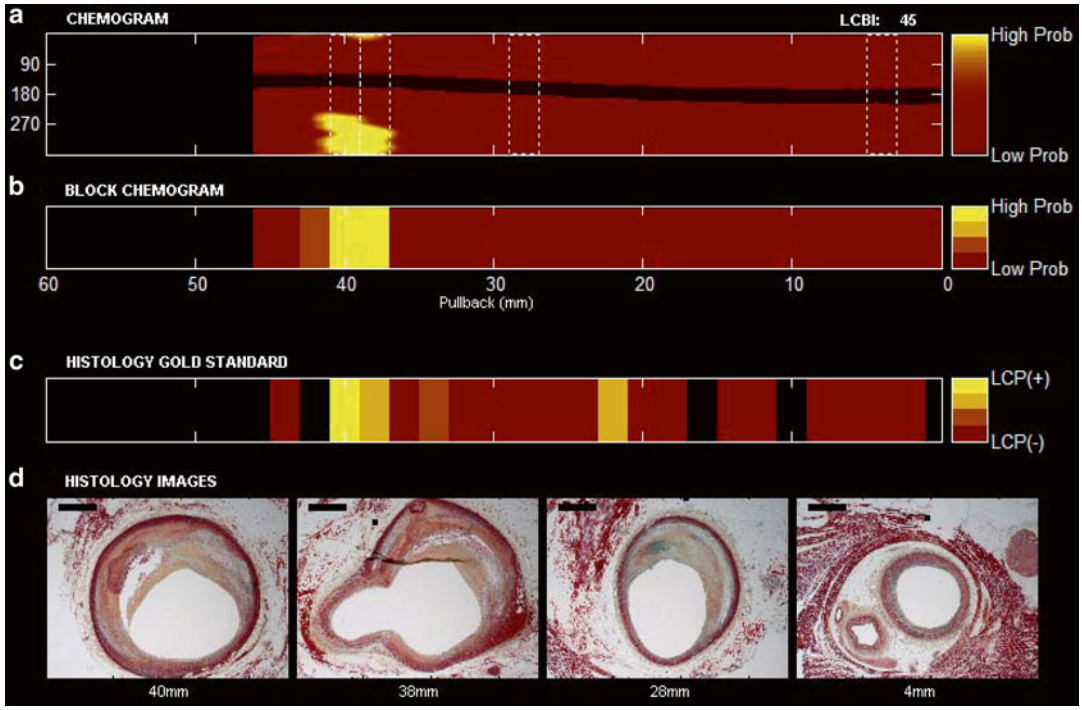

Fig. 10.2 NIRS pullback and selected histologic findings from a human coronary artery segment. (**a**) Chemogram image indicating LCP content by NIRS (*x*-axis = pullback distance in mm, *y*-axis = rotation angle in degrees). Pixel colors range from *red* for low probability to *yellow* for high probability of LCP. The contiguous black region is the guide wire. (**b**) Block chemogram image indicating summary metric of the presence of LCP at 2-mm intervals in four probability categories. (**c**) Diagram demonstrating the presence of LCP by histologic evaluation. (**d**) Movat cross-sections from locations along the artery indicated by *dotted boxes* in the chemogram. *Image interpretation*: The chemogram shows large LCP signals from 36 to 42 mm. The block chemogram indicates that there is the region of the strongest signal. Histology (panel **c** and **d**) confirms the presence of fibroatheroma at this location

fibers in the core are terminated by mirrors embedded in the tip for sending incident light through blood onto the artery wall and collecting the diffusely reflected light. The coax cable transmits and receives the electrical signal to and from the ultrasound transducer. The catheter imaging core rotates at 960 rpm with automated pullback at a rate of 0.5 mm/s, interrogating tissue in a helical pattern.

In the NIRS modality, the resulting spectra are processed and interpreted by the LCP detection algorithm to generate a longitudinal image (called a chemogram) of the scanned artery segment (Fig. 10.2). Each spectral measurement is assigned a probability of LCP by the detection algorithm and displayed in a false color map (Fig. 10.3) with colors ranging from red (low probability of LCP) to yellow (high probability of LCP). From the chemogram, a summary metric of the probability that an LCP is present in a 2-mm interval of the pullback is computed and displayed in a supplementary false color map called a block chemogram (Fig. 10.2b). Blocks correspond to one of four discrete categories, each represented by a distinct color (red, orange, tan, and yellow, in increasing order of LCP probability).

An additional metric, the lipid core burden index (LCBI), is used to quantify the amount of LCP in a scanned artery segment. The LCBI is defined as the fraction of yellow pixels in the chemogram multiplied by 1,000 (0–1,000 scale). Figure 10.3 illustrates the computation of the LCBI.

The transverse IVUS image is overlaid with a chemogram ring taken from the corresponding longitudinal location in the chemogram, and the

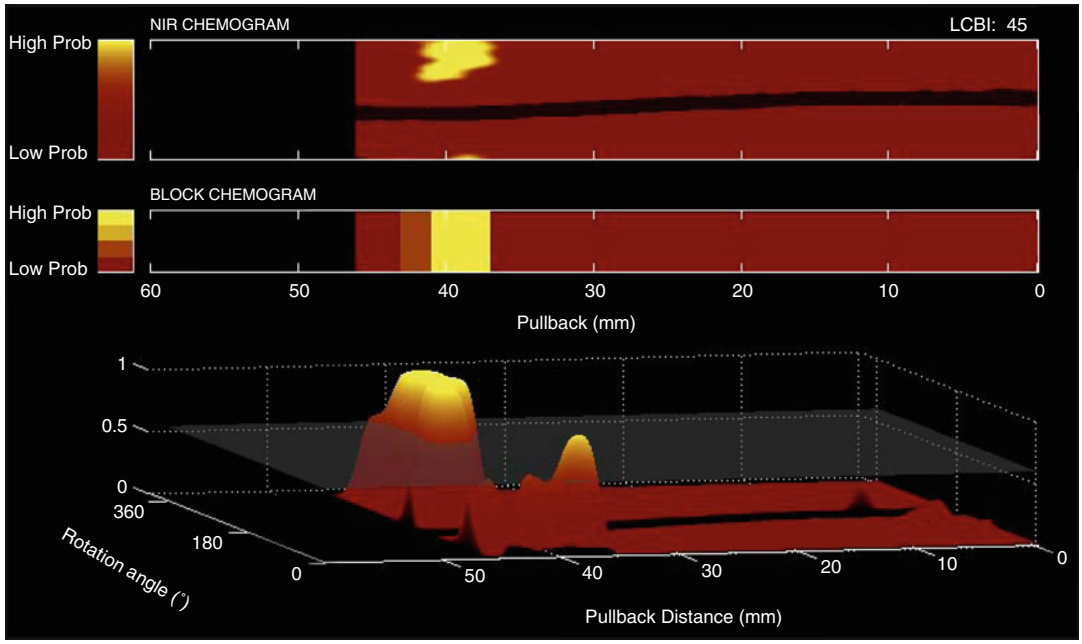

Fig. 10.3 Illustration of the lipid core burden index (LCBI). The LCBI (*top right*) shows the proportion of lipid in a scanned artery on a 0–1,000 scale. The LCBI is calculated as the fraction of valid pixels in the chemogram that are *yellow*, multiplied by a factor of 1,000. *Yellow* pixels are those whose values (probability of LCP) exceed a specified threshold, as indicated by the horizontal plane in the *bottom panel*

block chemogram color is displayed in the catheter artifact. In addition, the longitudinal IVUS image is aligned with the chemogram and block chemogram.

Research and Clinical Utility of the NIRS and IVUS Catheter

In April 2008, the US Food and Drug Administration (FDA) cleared coronary NIRS for clinical use in the USA [15]. The clearance was based on the autopsy validation data [11] and the demonstration of similarity between clinical and autopsy spectra [12]. NIRS was approved for the detection of lipid core containing plaques of interest and the assessment of lipid core burden in coronary arteries. In June 2010 the FDA approved the combination NIRS-IVUS catheter.

Potential clinical applications of NIRS include: (1) improving the safety of percutaneous coronary interventions (PCIs), (2) identifying coronary lesions at risk for causing subsequent clinical events and selecting an optimal medical management, and (3) evaluating novel anti-atherosclerotic therapies. All these applications are currently undergoing extensive clinical evaluation.

PCI Outcome Optimization

In spite of the rapid evolution of PCI techniques, complications such as peri-procedural myocardial infarction (MI) [16] distal embolization and acute stent thrombosis [17] continue to occur. NIRS imaging can improve the safety of PCI by enabling rapid, easy, and accurate prediction of the risk of peri-procedural complications, such as no-reflow and peri-procedural acute myocardial infarction and, as a result, providing guidance for the use of clinical measures to prevent such complications.

NIRS for Predicting Peri-procedural Myocardial Infarction

PCI of a large LCP, as detected by NIRS, has been associated with high risk for distal embolization, no-reflow, and post-PCI myocardial infarction [18–23]. Four published case reports and two case

Table 10.1 Published studies evaluating the association between NIRS findings and post-percutaneous coronary intervention myocardial infarction and no-reflow

Author	Year	*n*	Near-infrared spectroscopy finding	Outcomes
Case reports				
Goldstein et al. [18]	2009	4	Large LCP by NIRS was found in 3 cases	No-reflow occurred in two cases—one case was an autopsy case in which thrombus was formed at LCP site
Saeed et al. [19]	2010	1	Large circumferential LCP	Slow flow post-LAD stenting
Schultz et al. [20]	2010	1	Large, near-circumferential LCP	Transient chest discomfort post-stenting and post-PCI MI
Fernandez-Friera et al. [23]	2010	1	Large circumferential LCP	PCI complicated by transient no-reflow and a periprocedural MI (peak troponin, 8.1 ng/mL)
Case series	Year	*n*	Large LCP definition	Post PCI MI definition
Raghunathan et al. [21]	2011	30	Two or more yellow blocks on block chemogram	Several thresholds were used (CK-MB increase >1×, 2×, and 3× ULN)
Goldstein et al. [22]	2011	62	maxLCBI4 mm ≥500	CK-MB or troponin increase >3× ULN

LCP lipid core plaque, *NIRS* near-infrared spectroscopy, *LAD* left anterior descending artery, *PCI* percutaneous coronary intervention, *MI* myocardial infarction, *LCBI* lipid core burden index, *CK-MB* creatine kinase MB fraction, *ULN* upper limit of normal

series have described an association of large LCP by NIRS with no-reflow and with post-PCI myocardial infarction (MI) (Table 10.1). Goldstein et al. [18], Saeed et al. [19], and Fernandez-Friera et al. [23] presented case reports of no-reflow, whereas Schultz et al. [20] presented a case of transient chest pain and post-PCI MI after stenting of lesions containing large LCPs.

Raghunathan et al. evaluated the association between the presence and extent of coronary LCPs detected by NIRS performed prior to PCI with post-procedural myocardial infarction [21] using various LCP and MI definitions. Compared to patients who did not have post-PCI MI, those who experienced post-PCI MI had similar clinical characteristics but received more stents and had more yellow blocks within the stented lesion. CK-MB level elevation >3× the upper limit of normal was observed in 27 % of patients with two or more yellow block vs. in none of the patients with 0–1 yellow blocks within the stented lesion ($p=0.02$).

Goldstein et al. studied 62 patients undergoing PCI from the COLOR registry [22]. The extent of LCP in the treatment zone was calculated as the maximal LCBI measured by NIRS for each of the 4-mm longitudinal segments in the treatment zone. Peri-procedural MI occurred in nine patients (14.5 %). Seven of 14 patients (50 %) with a maxLCBI4mm of ≥500 had post-PCI MI compared to 2 of 48 patients (4.2 %) with maxLCBI4mm <500 ($p=0.0002$).

Several other studies using various intracoronary imaging modalities have demonstrated that the presence of LCP (thin-cap fibroatheroma, as assessed by OCT [24], necrotic core, as assessed by IVUS-VH [25], and attenuated plaque [26], as assessed by IVUS) are associated with higher incidence of no-reflow and post-PCI MI. Therefore, LCP-containing lesions are at increased risk for causing complications and could form the target for preventive and therapeutic interventions. Although patients with acute coronary syndromes are more likely to have LCPs, approximately half of patients with stable angina also had LCPs [27] within their culprit lesions, suggesting that some stable angina patients may also be at increased risk for post-PCI complications.

Whether NIRS can help identify saphenous vein graft (SVG) lesions at high risk of distal

embolization is under investigation; however, Wood et al. recently demonstrated that ostial SVG lesions were less likely to have LCPs, as detected by NIRS, compared to body lesions [28]. This lower frequency of LCP in the ostial and anastomotic lesions might explain the lower likelihood of post-PCI myocardial infarction in these lesions compared to SVG body lesions [29, 30].

NIRS-Based Insights into the Mechanism of Peri-procedural Myocardial Infarction

Whether distal embolization, thrombosis, or side-branch occlusion is the main cause of post-PCI MI remains under evaluation. Selvanaygam et al. described two patterns of myocardial injury post-PCI: one adjacent to the area of stent, presumably due to epicardial side branch occlusion and one involving the distal myocardial segment supplied by the target coronary artery, likely due to distal embolization [31].

Two pilot NIRS-based studies have provided insights on the mechanism of post-PCI MI. In the first study, an embolic protection device (EPD) was used in nine patients with large LCPs undergoing PCI [32] (Fig. 10.4). EPD use resulted in capture of embolized material in eight of the nine lesions: the captured material mainly consisted of fibrin and platelet aggregates, suggesting that a major mechanism of peri-stenting infarction might be distal embolization of thrombi associated with exposure of blood to LCP in the lesion. Post-PCI MI occurred in two patients (22 %), in one of whom two filters were required because of significant debris distal embolization causing "clogging" of the filter. The role of distal embolization in post-PCI MI is further supported by several studies showing a significant decrease in LCBI post-stenting [32, 33].

Papayannis et al. extended the above observation by describing that stenting of large LCPs (defined as at least three 2-mm yellow blocks on the NIRS block chemogram with >200° angular extent) was more likely to lead to in-stent thrombus formation (as detected by optical coherence tomography) compared to stenting coronary lesions without large LCP [34]. Two of three patients with a large LCP (67 %) developed intrastent thrombus post-stent implantation (Fig. 10.5) compared to none of six patients without large LCPs (0 %, $p=0.02$). This may be due to the high thrombogenicity of the lipid core with direct activation of platelets by the oxidized lipids, but also to the high content of active tissue factor in the lipid core, that can trigger the extrinsic clotting cascade [35]. As noted above, it is possible that the thrombus formed within the stent subsequently embolizes and EPD use may prevent embolization not only of the LCP but also of the platelet or fibrin thrombus. Interestingly, similar observations were made in an intravascular imaging study that used optical coherence tomography: Porto et al. analyzed 50 patients undergoing PCI and found three predictors or post-PCI MI: thin-cap fibroatheroma (OR 29.7, 95 % CI 1.4–32.1), intrastent thrombus (OR 5.5, 95 % CI 1.2–24.9), and intrastent dissection (OR 5.3, 95 % CI 1.2–24.3) [24].

Given the above observations, although the optimal strategy for preventing post-PCI MI in high-risk lesions remains to be determined, it is likely that a combination strategy of an EPD and aggressive antiplatelet/anticoagulant therapy may be needed to prevent both distal embolization and the accelerated formation of intrastent thrombus that could subsequently embolize.

Several ongoing studies are evaluating the mechanism of post-PCI MI and potential preventive strategies. The Lipid Core Shift Study (NCT00905671) is examining whether PCI of large LCP lesions may cause plaque shift and side branch occlusion. The CANARY (Coronary Assessment by Near-infrared of Atherosclerotic Rupture-prone Yellow, NCT01268319) trial is a prospective randomized-controlled trial that is randomizing patients with large LCPs in native coronary arteries undergoing clinically indicated PCI to use a Filterwire (Boston Scientific, Natick, MA) or standard of care without EPD. The use of EPDs is currently only approved in the USA for SVG lesions [36].

NIRS and Stent Length Selection

Stenting from "normal" proximal to "normal" distal reference segment is usually performed

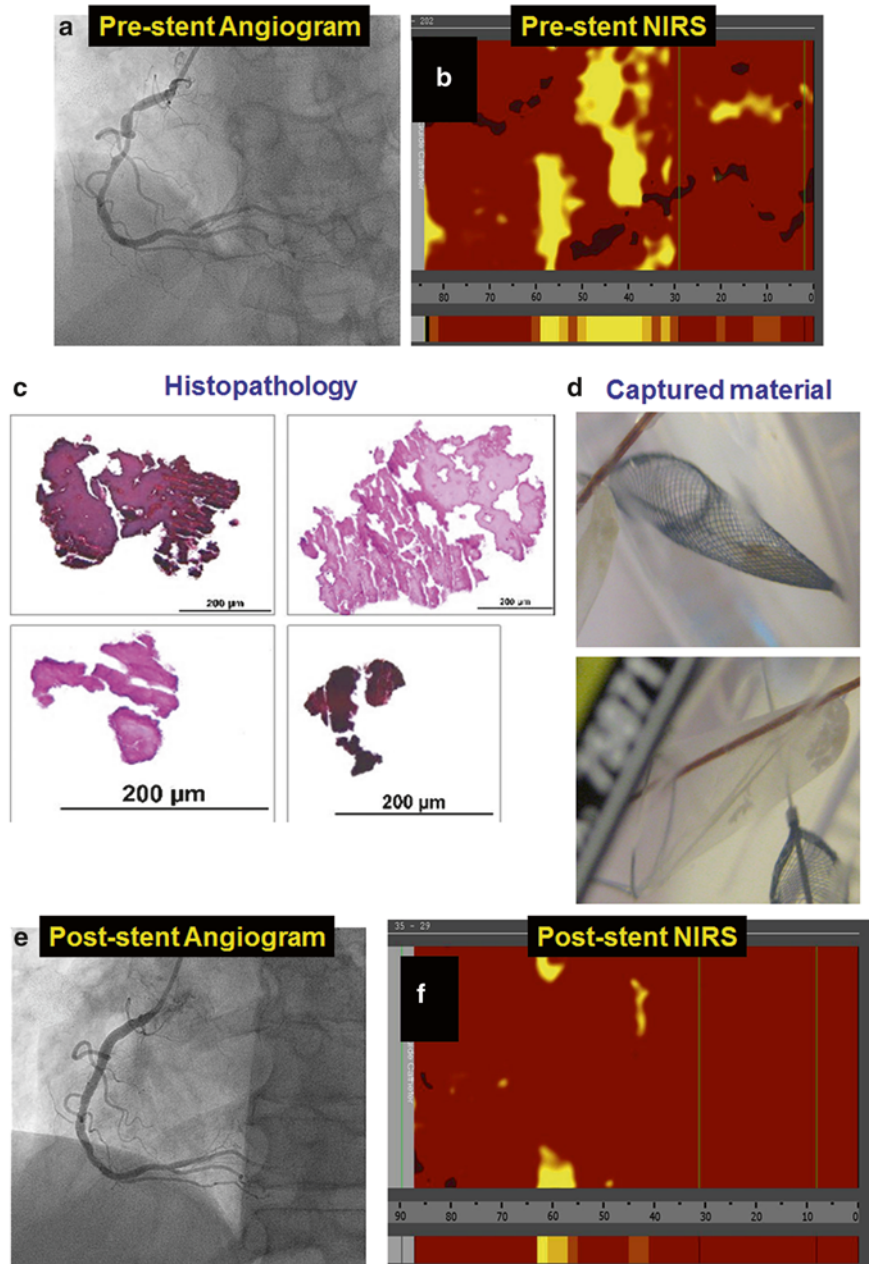

Fig. 10.4 Example of distal embolization and thrombus formation in a patient undergoing percutaneous coronary intervention. Coronary angiography demonstrating diffuse right coronary artery obstructive disease (panel **a**) with large lipid core plaque (LCP) by near-infrared spectroscopy (panel **b**). Stenting of the right coronary artery was performed using a filter for embolic protection. Fibrin and platelet aggregates (panel **c**) were retrieved in the filter (panel **d**) post-PCI. An excellent angiographic result as obtained (panel **e**) along with reduction of the LCP size (panel **f**)

when drug-eluting stents (DES) are used for PCI. However, occasionally these angiographically "normal" sites may contain LCP that does not narrow the lumen due to positive remodeling. Dixon et al. analyzed 50 LCP-containing lesions and found that in eight of those lesions (16 %) LCP extended beyond the angiographic margins of the lesion [37].

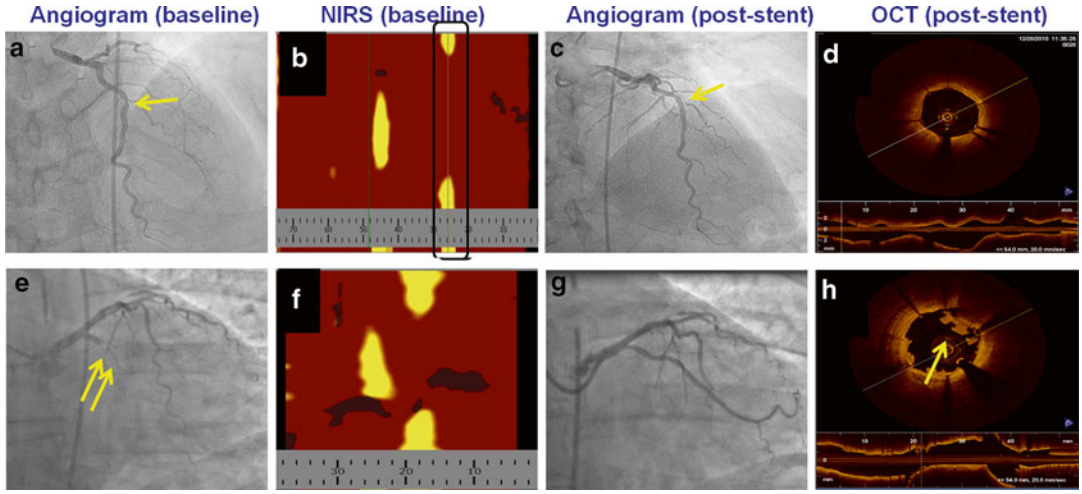

Fig. 10.5 Example of in-stent thrombus formation post-stenting of a large LCP. A patient underwent stenting of a lesion in the mid left anterior descending artery that contained a small LCP (panel **b**) with an excellent angiographic result (panel **c**) and no in-stent thrombus formation (panel **d**). Another patient underwent stenting of a circumflex lesion (panel **e**) that contained a large LCP (panel **f**), and although a good angiographic result was achieved (panel **g**) intrastent thrombus formed post-deployment (panel **h**)

Disruption or incomplete coverage of such lesions might result in stent thrombosis or restenosis [38, 39]. Sakhuja et al. reported acute stent thrombosis in a patient who underwent right coronary stenting, in whom a large LCP extended proximal to the proximal stent edge [39]. Use of coronary NIRS could, therefore, aid selection of the appropriate length of artery to stent based on the length of the lesion as determined by angiography and NIR and the presence or absence of adjacent LCP.

Identification of High-Risk Coronary Lesions and Optimization of Medical Management

The identification of non-obstructive coronary lesions that are at high risk for causing subsequent adverse clinical events and demonstrating that early treatment improves clinical outcomes remains an important goal of plaque imaging [40–42]. The only group of intermediate lesions in which prophylactic stenting has been shown to be beneficial is SVG lesions. In the VELETI (Moderate VEin Graft LEsion Stenting With the Taxus Stent and IVUS) trial prophylactic stenting of intermediate SVG lesions with a paclitaxel-eluting stent improved outcomes compared to medical therapy alone [43].

The largest natural history study of non-obstructive native coronary artery lesions is the Providing Regional Observations to Study Predictors of Events in the Coronary Tree (PROSPECT) study [36]. PROSPECT followed 697 patients with acute coronary syndromes who underwent three-vessel coronary angiography and gray-scale and radiofrequency intravascular ultrasonographic imaging after PCI of the culprit lesion [44]. After a median follow-up time of 3.4 years, the rate of major adverse cardiovascular events due to initially untreated lesions was 11.6 %. Most of those lesions were either thin-cap fibroatheromas, as determined by virtual histology IVUS (VH-IVUS) or were characterized by a large plaque burden, a small luminal area, or some combination of these characteristics, as determined by gray-scale and radiofrequency intravascular ultrasonography [44]. Only 17.2 % of the highest risk lesions caused symptoms during follow-up, making preemptive lesion treatment impractical.

Although theoretically attractive, whether NIRS-based LCP detection may provide better

prediction of future cardiovascular events compared to gray-scale and radiofrequency IVUS remains to be determined [45]. Brugaletta et al. demonstrated that the presence and extent of necrotic core by NIRS has only a weak association with percent necrotic core, as detected by radiofrequency IVUS [46]. Pu et al. demonstrated a weak positive relationship between radiofrequency ultrasound detected percent necrotic core and NIRS-derived LCBI in selected sets of very large non-calcified plaques, but not in calcified plaques [26]. In early analyses from the COLOR registry moderate lesions without LCP were unlikely to progress. NIRS may provide prognostic information that is not provided by traditional cardiovascular risk score systems: no correlation was found between the Framingham risk score and LCBI of a non-culprit coronary vessel among 208 patients undergoing PCI [47]. Similarly, no correlation was found between LCBI and creatinine clearance [48] and with the SYNTAX score [49].

Apart from mechanical treatments, patients with extensive LCPs might benefit from aggressive pharmacologic therapies, such an intensive antithrombotic regimen, aggressive low-density lipoprotein cholesterol lowering, high-density lipoprotein infusion, low-density lipoprotein apheresis, or with medications such as niacin, fibrates, or in the future with novel compounds that are currently under clinical trial evaluation [50]. The NIRS-IVUS coronary imaging could also serve as a marker of high coronary risk that could motivate patients to comply with the prescribed medical treatments and to adopt beneficial lifestyle changes.

Evaluation of Novel Anti-atherosclerotic Treatments

Most past and ongoing studies utilizing intracoronary imaging to assess changes in the coronary artery as a result of various treatments have used as primary endpoint the change in volume of a mildly or moderately diseased segment of the coronary artery wall (usually measured by IVUS as percent or total atheroma volume) [51]. However, many anti-atherosclerotic therapies, especially those that target serum lipoproteins, would be more likely to affect LCP—rather than non-LCP-containing lesions. Hence, use of NIRS would be expected to provide a more sensitive endpoint in plaque regression studies. Use of NIRS in longitudinal studies is feasible given its excellent intra- and inter-catheter reproducibility [33, 52].

To date, only one study has utilized NIRS to longitudinally assess coronary lesions, the Reduction in YELlow Plaque by Aggressive Lipid-LOWering Therapy (YELLOW) Trial (presented at the 2012 American College of Cardiology annual scientific sessions in Chicago, Illinois). The YELLOW trial randomized 87 patients with multivessel coronary artery disease who were scheduled to undergo staged PCI. During the initial catheterization, all patients underwent FFR, IVUS, and NIRS of the nontarget lesion and if the lesion was hemodynamically significant (as assessed by fractional flow reserve) they were randomized to standard of care vs. rosuvastatin 40 mg daily for 6–8 weeks. They then underwent repeat coronary angiography and imaging of the nontarget lesion. In spite of the limited duration of treatment, a significant reduction in the lesion LCBI was observed (Fig. 10.6).

The Atherosclerosis Lesion Progression Intervention using Niacin Extended Release in Saphenous Vein Grafts (ALPINE-SVG) Pilot Trial is using imaging with IVUS, NIRS-IVUS, and optical coherence tomography to assess the impact of extended-release niacin in intermediate SVG lesions treated for 12 months (NCT01221402). Similarly, the Prasugrel for Prevention of Early Saphenous Vein Graft Thrombosis study (NCT01560780) is assessing the effect of prasugrel within the first year after coronary bypass graft surgery in SVGs using imaging with IVUS, NIRS-IVUS, and optical coherence tomography. Several other prospective coronary atherosclerosis studies are currently utilizing coronary NIRS as an endpoint, such as the AtheroREMO and the IBIS-3 trial. Finally, COLOR (Chemometric Observations of Lipid Core Containing Plaques of Interest in

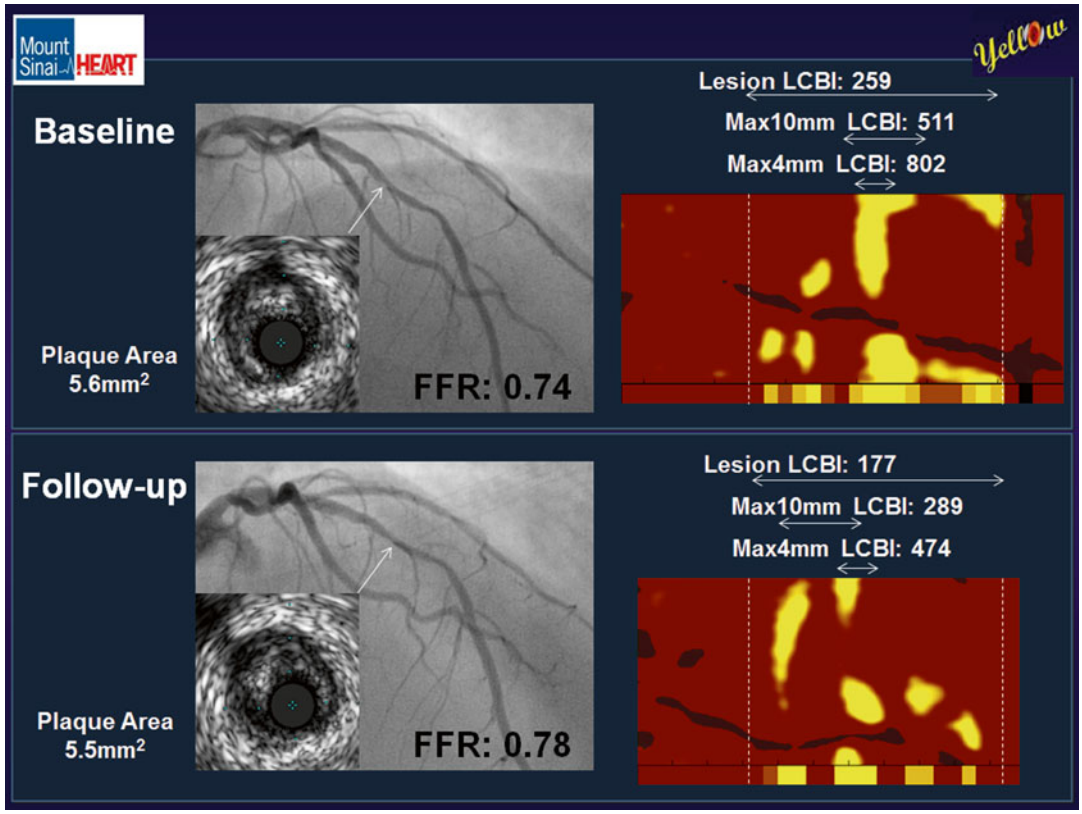

Fig. 10.6 Example of LCP regression after 2 months of intensive lipid-lowering therapy (rosuvastatin 40 mg daily) from a patient participating in the YELLOW trial (Courtesy of Dr. Anapoorna Kini and Dr. Samin Sharma (Mount Sinai School of Medicine, New York, NY))

Native Coronary Arteries, NCT00831116) is an ongoing observational registry of coronary NIRS use in the USA that is providing valuable insights on the clinical use and utility of NIRS [22]. Over 1,100 patients are currently under observation in COLOR.

In summary, coronary NIRS is novel imaging modality for the in vivo detection of LCPs. It has undergone extensive development and validation and is currently being utilized to assist with clinical decision making in the cardiac catheterization laboratory and with evaluation of novel anti-atherosclerotic treatments.

Conflicts of interest: Z.H., S.T.S., S.P.M., and J.E.M. are employees of InfraReDx, Inc.

References

1. Williams P, Norris K. Near-infrared technology in the agriculture and food industries. St. Paul, MN: American Association of Cereal Chemists; 2001.
2. Ciurczak EW, Drennen JK. Pharmaceutical and medical applications of near-infrared spectroscopy. New York, NY: Marcel Dekker; 2002.
3. Lavine B, Workman J. Chemometrics. Anal Chem. 2008;80:4519–31.
4. Lodder RA, Cassis L, Ciurczak EW. Arterial analysis with a novel near-IR fiber-optic probe. Spectroscopy. 1990;5:12–7.
5. Lilledahl MB, Haugen OA, Barkost M, Svaasand LO. Reflection spectroscopy of atherosclerotic plaque. J Biomed Opt. 2006;11:021005.
6. Dempsey RJ, Davis DG, Buice RG, Lodder RA. Biological and medical applications of near-infrared spectrometry. Appl Spectrosc. 1996;50:18A–34A.

7. Marshik B, Tan H, Tang J. Discrimination of lipid-rich plaques in human aorta specimens with NIR spectroscopy through whole blood. Am J Cardiol. 2002;90(Suppl 6A):129H.
8. Marshik B, Tan H, Tang J. Detection of thin-capped fibroatheromas in human aorta tissue with near infrared spectroscopy through blood. J Am Coll Cardiol. 2003;41(Suppl 1).
9. Waxman S, Tang J, Marshik BJ. In vivo detection of a coronary artificial target with a near infrared spectroscopy catheter. Am J Cardiol. 2004;94(Suppl 6A):141E.
10. Caplan JD, Waxman S, Nesto RW, Muller JE. Near-infrared spectroscopy for the detection of vulnerable coronary artery plaques. J Am Coll Cardiol. 2006; 47:C92–6.
11. Gardner CM, Tan H, Hull EL, et al. Detection of lipid core coronary plaques in autopsy specimens with a novel catheter-based near-infrared spectroscopy system. JACC Cardiovasc Imaging. 2008;1:638–48.
12. Waxman S, Dixon SR, L'Allier P, et al. In vivo validation of a catheter-based near-infrared spectroscopy system for detection of lipid core coronary plaques: initial results of the SPECTACL study. JACC Cardiovasc Imaging. 2009;2:858–68.
13. Madder RD, Steinberg DH, Anderson RD. Multimodality direct coronary imaging with combined near-infrared spectroscopy and intravascular ultrasound: initial US experience. Catheter Cardiovasc Interv. 2013;81(3):551–7.
14. Garg S, Serruys PW, van der Ent M, et al. First use in patients of a combined near infra-red spectroscopy and intra-vascular ultrasound catheter to identify composition and structure of coronary plaque. EuroIntervention. 2010;5:755–6.
15. U.S. Food and Drug Administration. Coronary artery plaque imaging device cleared by FDA. Press Announcements. 29 April 2008. http://www.fda.gov/NewsEvents/Newsroom/PressAnnouncements/2008/ucm116888.htm. Accessed 8 July 2013.
16. Prasad A, Herrmann J. Myocardial infarction due to percutaneous coronary intervention. N Engl J Med. 2011;364:453–64.
17. Prasad A, Rihal CS, Lennon RJ, Wiste HJ, Singh M, Holmes Jr DR. Trends in outcomes after percutaneous coronary intervention for chronic total occlusions: a 25-year experience from the Mayo Clinic. J Am Coll Cardiol. 2007;49:1611–8.
18. Goldstein JA, Grines C, Fischell T, et al. Coronary embolization following balloon dilation of lipid-core plaques. JACC Cardiovasc Imaging. 2009;2:1420–4.
19. Saeed B, Banerjee S, Brilakis ES. Slow flow after stenting of a coronary lesion with a large lipid core plaque detected by near-infrared spectroscopy. EuroIntervention. 2010;6:545.
20. Schultz C, Serruys P, van der Ent M, et al. Prospective identification of a large lipid core coronary plaque with a novel near-infrared spectroscopy and intravascular ultrasound (NIR-IVUS) catheter: infarction following stenting possibly due to distal embolization of plaque contents. J Am Coll Cardiol. 2010;56:314.
21. Raghunathan D, Abdel-Karim AR, Papayannis AC, et al. Relation between the presence and extent of coronary lipid core plaques detected by near-infrared spectroscopy with postpercutaneous coronary intervention myocardial infarction. Am J Cardiol. 2011;107:1613–8.
22. Goldstein JA, Maini B, Dixon SR, et al. Detection of lipid-core plaques by intracoronary near-infrared spectroscopy identifies high risk of periprocedural myocardial infarction. Circ Cardiovasc Interv. 2011;4:429–37.
23. Fernandez-Friera L, Garcia-Alvarez A, Romero A, et al. Lipid-rich obstructive coronary lesions is plaque characterization any important? JACC Cardiovasc Imaging. 2010;3:893–5.
24. Porto I, Di Vito L, Burzotta F, et al. Predictors of periprocedural (Type IVa) myocardial infarction, as assessed by frequency-domain optical coherence tomography. Circ Cardiovasc Interv. 2012;5:89–96.
25. Hong YJ, Jeong MH, Choi YH, et al. Impact of plaque components on no-reflow phenomenon after stent deployment in patients with acute coronary syndrome: a virtual histology-intravascular ultrasound analysis. Eur Heart J. 2011;32:2059–66.
26. Pu J, Mintz GS, Brilakis ES, et al. In vivo characterization of coronary plaques: novel findings from comparing greyscale and virtual histology intravascular ultrasound and near-infrared spectroscopy. Eur Heart J. 2012;33:372–83.
27. Madder RD, Smith JL, Dixon SR, Goldstein JA. Composition of target lesions by near-infrared spectroscopy in patients with acute coronary syndrome versus stable angina. Circ Cardiovasc Interv. 2012; 5:55–61.
28. Wood FO, Badhey N, Garcia B, et al. Analysis of saphenous vein graft lesion composition using near-infrared spectroscopy and intravascular ultrasonography with virtual histology. Atherosclerosis. 2010;212:528–33.
29. Hong MK, Mehran R, Dangas G, et al. Creatine kinase-MB enzyme elevation following successful saphenous vein graft intervention is associated with late mortality. Circulation. 1999;100:2400–5.
30. Sdringola S, Assali AR, Ghani M, et al. Risk assessment of slow or no-reflow phenomenon in aortocoronary vein graft percutaneous intervention. Catheter Cardiovasc Interv. 2001;54:318–24.
31. Selvanayagam JB, Porto I, Channon K, et al. Troponin elevation after percutaneous coronary intervention directly represents the extent of irreversible myocardial injury: insights from cardiovascular magnetic resonance imaging. Circulation. 2005;111:1027–32.
32. Brilakis ES, Abdel-Karim AR, Papayannis AC, et al. Embolic protection device utilization during stenting of native coronary artery lesions with large lipid core plaques as detected by near-infrared spectroscopy. Catheter Cardiovasc Interv. 2012;80(7):1157–62.
33. Garcia BA, Wood F, Cipher D, Banerjee S, Brilakis ES. Reproducibility of near-infrared spectroscopy for the detection of lipid core coronary plaques and

observed changes after coronary stent implantation. Catheter Cardiovasc Interv. 2010;76:359–65.
34. Papayannis AC, Abdel-Karim AR, Mahmood A, Michael TT, Banerjee S, Brilakis ES. Association of coronary lipid core plaque with intra-stent thrombus formation: a near-infrared spectroscopy and optical coherence tomography study. Catheter Cardiovasc Interv. 2013;81(3):488–93.
35. Reininger AJ, Bernlochner I, Penz SM, et al. A 2-step mechanism of arterial thrombus formation induced by human atherosclerotic plaques. J Am Coll Cardiol. 2010;55:1147–58.
36. Banerjee S, Brilakis ES. Embolic protection during saphenous vein graft interventions. J Invasive Cardiol. 2009;21:415–7.
37. Dixon SR, Grines CL, Munir A, et al. Analysis of target lesion length before coronary artery stenting using angiography and near-infrared spectroscopy versus angiography alone. Am J Cardiol. 2012;109:60–6.
38. Farb A, Burke AP, Kolodgie FD, Virmani R. Pathological mechanisms of fatal late coronary stent thrombosis in humans. Circulation. 2003;108:1701–6.
39. Sakhuja R, Suh WM, Jaffer FA, Jang IK. Residual thrombogenic substrate after rupture of a lipid-rich plaque: possible mechanism of acute stent thrombosis? Circulation. 2010;122:2349–50.
40. Muller JE, Abela GS, Nesto RW, Tofler GH. Triggers, acute risk factors and vulnerable plaques: the lexicon of a new frontier. J Am Coll Cardiol. 1994;23:809–13.
41. Naghavi M, Libby P, Falk E, et al. From vulnerable plaque to vulnerable patient: a call for new definitions and risk assessment strategies: Part II. Circulation. 2003;108:1772–8.
42. Naghavi M, Libby P, Falk E, et al. From vulnerable plaque to vulnerable patient: a call for new definitions and risk assessment strategies: Part I. Circulation. 2003;108:1664–72.
43. Rodes-Cabau J, Bertrand OF, Larose E, et al. Comparison of plaque sealing with paclitaxel-eluting stents versus medical therapy for the treatment of moderate nonsignificant saphenous vein graft lesions. the moderate vein graft lesion stenting with the taxus stent and intravascular ultrasound (VELETI) pilot trial. Circulation. 2009;120:1978–86.
44. Stone GW, Maehara A, Lansky AJ, et al. A prospective natural-history study of coronary atherosclerosis. N Engl J Med. 2011;364:226–35.
45. Muller JE, Tawakol A, Kathiresan S, Narula J. New opportunities for identification and reduction of coronary risk: treatment of vulnerable patients, arteries, and plaques. J Am Coll Cardiol. 2006;47:C2–6.
46. Brugaletta S, Garcia-Garcia HM, Serruys PW, et al. NIRS and IVUS for characterization of atherosclerosis in patients undergoing coronary angiography. JACC Cardiovasc Imaging. 2011;4:647–55.
47. Heo JH, Garcia-Garcia HM, Brugaletta S, et al. Lipid core burden index and Framingham score: can a Systemic Risk Score predict lipid core burden in non-culprit coronary artery? Int J Cardiol. 2012;156:211–3.
48. Simsek C, Garcia-Garcia HM, Brugaletta S, et al. Correlation between kidney function and near-infrared spectroscopy derived lipid-core burden index score of a non-intervened coronary artery segment. Int J Cardiol. 2012;156:226–8.
49. Zynda TK, Thompson CD, Seto AH, et al. Evaluation of Coronary Arterial Lipid Content with Angiographic Complexity: Comparison of Near-Infrared Spectroscopy and SYNTAX Score. Catheter Cardiovasc Interv. 2011;77:S1–110.
50. Sacks FM, Rudel LL, Conner A, et al. Selective delipidation of plasma HDL enhances reverse cholesterol transport in vivo. J Lipid Res. 2009;50:894–907.
51. Bose D, von Birgelen C, Erbel R. Intravascular ultrasound for the evaluation of therapies targeting coronary atherosclerosis. J Am Coll Cardiol. 2007;49:925–32.
52. Abdel-Karim AR, Rangan BV, Banerjee S, Brilakis ES. Intercatheter reproducibility of near-infrared spectroscopy for the in vivo detection of coronary lipid core plaques. Catheter Cardiovasc Interv. 2011; 77:657–61.

Coronary Calcification: Roles in Risk Prediction and Monitoring Therapies

11

Irfan Zeb and Matthew J. Budoff

Introduction

Coronary artery calcium (CAC) represents calcified atherosclerosis in the coronary arteries which is believed to represent a dynamic marker of coronary risk assessment subject to influence by environmental factors and therapeutic interventions. The traditional cardiovascular risk assessment may underestimate the prediction of cardiovascular disease (CVD) risk and many individuals still suffer events in the absence of established risk factors for atherosclerosis [1]. CAC has been shown to be the strongest independent predictor of future adverse cardiovascular events and also provides incremental information to the traditional cardiovascular risk factors assessment. It can be used to risk stratify asymptomatic individuals, improve the risk prediction provided by Framingham risk score (FRS), and follow the effect of various therapeutic interventions on coronary atherosclerosis.

I. Zeb, MD (✉) • M.J. Budoff, MD, FACC, FAHA
Department of Medicine/Cardiology, Los Angeles Biomedical Research Institute at Harbor-UCLA Medical Center, 1124 West Carson Street, Torrance, CA 90502, USA
e-mail: irfanzeb82@yahoo.com

CAC as a Risk Stratification Tool

There is tremendous evidence available that supports the role of CAC as the best risk stratifier for asymptomatic individuals. Based on literature evidence, CAC has been incorporated into the ACC/AHA guidelines for screening of asymptomatic individuals for CVD. CAC has been advocated as a screening tool for risk assessment of asymptomatic adults at intermediate risk (10–20 % 10-year risk), low to intermediate risk (6–10 % 10-year risk), and patients with diabetes [2]. CAC has been persistently shown to have superior independent and incremental predictor of CVD compared with traditional risk factors [3–13]. The Multi-Ethnic Study of Atherosclerosis (MESA) sponsored by the National Heart, Lung, and Blood Institute was a prospective population based study of four different ethnic groups (whites, Hispanics, Asians, and African Americans) which provided a detailed insight into the role of CAC in risk assessment. Detrano et al. [4] showed that adjusted risk for coronary events increased by a factor of 7.73 among subjects with CAC scores between 101 and 300 and by a factor of 9.67 with CAC score above 300 when compared with CAC score 0 in 6,772 MESA participants. Across four ethnic groups, a doubling of CAC increased the risk of major coronary event by 15–35 % and the risk of any coronary event by 18–39 %. CAC provided an incremental value for prediction of major coronary events when added to the standard risk factors (0.79 vs. 0.83 area

S.J. Nicholls and T. Crowe (eds.), *Imaging Coronary Atherosclerosis*, Contemporary Cardiology,
DOI 10.1007/978-1-4939-0572-0_11, © Springer Science+Business Media New York 2014

under the curve for risk factors alone vs. risk factors plus CAC, $p=0.006$). Budoff et al. [5] showed CAC to be an independent predictor of mortality after controlling for age, gender, ethnicity, and cardiac risk factors (model chi-square=2,017, $p<0.0001$), in a registry of 25,253 asymptomatic individuals. CAC was shown to have significant incremental value compared with risk factors resulting in a higher concordance index (0.61 vs. 0.81; $p<0.0001$). Risk-adjusted relative risk ratios for CAC scores 11–100, 101–299, 300–399, 400–699, 700–999, and >1,000 were 2.2-, 4.5-, 6.4-, 9.2-, 10.4-, and 12.5-fold when compared with CAC score 0, respectively ($p<0.0001$). Greenland et al. [6] performed a prospective observational population-based study on 1,461 asymptomatic adults with coronary risk factors who underwent CAC score and followed prospectively for up to 8.5 years for nonfatal myocardial infarctions or coronary heart disease (CHD) deaths. Compared with CAC score of zero, a CAC score of more than 300 was significant predictor (hazard ratio HR, 3.9; 95 % confidence interval (CI) 2.1–7.3; $p<0.001$) of nonfatal myocardial infarctions or CHD deaths. Across FRS categories (0–9 %, 10–15 %, 16–20 %, and ≥21 %), CACS was predictive of risk among patients with an FRS higher than 10 % ($p<0.001$) but not with an FRS less than 10 %. FRS plus CAC resulted in a significantly greater mean area under the curve for the receiver operating characteristics curve compared with FRS alone (0.68 vs. 0.63; $p<0.001$). Similarly, data from ACC/AHA clinical consensus document comprising 27,622 asymptomatic subjects showed that patients with CAC scores between 400–1,000 and >1,000 had 3–5 year rates of cardiac deaths or myocardial infarctions of 4.6 and 7.1 % resulting in a relative risk ratios of 7.2 (95 % CI: 5.2–9.9; $p<0.001$) and 10.8 (95 % CI: 4.2–27.7; $p<0.0001$) compared with patients with CAC score 0 [14].

Pencina et al. [15] introduced the concept of net reclassification improvement (NRI) which measures the extent to which people with and without events are appropriately reclassified into clinically accepted higher or lower risk categories with the addition of a new marker. CAC has been shown to reclassify the risk assessment based on FRS and National Cholesterol Education Adult Treatment Panel (ATP) III guidelines into either higher or lower risk categories based on CAC score information [13, 16–18]. Erbel et al. performed a prospective population-based study on 4,129 subjects without overt CAD at baseline and followed them for 5 years. Risk reclassification into to either low-risk category or high-risk category using CAC <100 and CAC ≥400 yielded an NRI of 21.7 % ($p=0.0002$) and 30.6 % ($p<0.0001$) for the FRS, respectively. Integrated discrimination improvement using FRS variables and CAC was 1.52 % ($p<0.0001$). There was significant improvement in the area under the curve from 0.681 to 0.749 ($p<0.003$) and from 0.653 to 0.755 ($p=0.0001$) by adding CAC scores to the FRS and National Cholesterol Education Panel ATP III categories, respectively. Polonsky et al. [16] showed that a model involving CAC in addition to traditional risk factors (age, gender, tobacco use, systolic blood pressure, antihypertensive medication use, total and high-density lipoprotein cholesterol, and race/ethnicity) resulted in significant improvement in risk prediction compared to traditional risk factors alone (NRI=0.25, 95 % CI: 10.16–0.34, $p<0.001$). A model involving CAC classified 77 % of the cohort into lowest or highest risk categories compared with 69 % without CAC.

Blaha et al. [19] used the entry criteria for JUPITER trial [20] (low-density lipoprotein (LDL) <130 mg/dL) and highly sensitive C-reactive protein (hsCRP) concentration ≥2 mg/L in MESA population (950 subjects) to compare the risk prediction value of CAC across ranges of low- and high hsCRP values and calculated 5-year number needed to treat by applying the benefit recorded in JUPITER trial to the events within each CAC strata. For CHD, the predicted 5-year number needed to treat were 549 for CAC score 0, 94 for scores 1–100, and 24 for scores greater than 100. For CVD, the number needed to treat was 124, 54, and 19, respectively. hsCRP was not associated with either disease after multivariable adjustment. For rosuvastatin, the number needed to treat to prevent the occurrence of adverse cardiovascular event for an average 5-year treatment period is 25 [20, 21].

CAC can also be used to estimate an arterial age in adults [22]. Estimated arterial age is obtained as a simple linear function of log-transformed CAC. Framingham risk calculated using arterial age is more predictive of short-term incident coronary events than Framingham risk based on observed age (area under the ROC curve 0.75 for Framingham risk based on observed age, 0.79 using arterial age, $p = 0.006$).

The risk for future adverse cardiovascular events increases with increasing CAC scores; however, the absence of CAC presents a very unique situation which is associated with very low-risk status for the individual (10 year event rate of ~1 %) [11, 12]. Blaha et al. [11] showed that there were 104 deaths (0.52 % event rate) among patients with CAC score zero (19,898 patients) compared with patients with CAC score >10 (3.96 % event rate). The annualized all-cause mortality rates for CAC score zero and CAC >10 were 0.87 and 7.48 deaths/1,000 person-years. CAC score of zero separates the very low-risk group from subjects that are at relatively higher risk for future adverse cardiovascular events whether the amount of CAC is minimal or significant. Budoff et al. [23] performed an analysis in a multiethnic population of MESA study where they showed that the CAC score of zero (3,415 individuals) was associated with 17 CHD events (0.5 %) compared with 11 in those with CAC of 1–10 (2 % event rate). In age- and gender-adjusted analysis, the presence of minimal CAC (1–10) was associated with an estimated three-fold higher risk of a hard CHD event (HR: 3.23; 95 % CI: 1.17–8.95) which remained robust even after adjustment for traditional cardiovascular risk factors and carotid intima-media thickness. Raggi et al. [24] followed 632 patients for a mean of 32 ± 7 months for the development of acute myocardial infarction or cardiac death. The annualized event rate in patients with CAC score 0 was 0.11 % compared with 4.8 % in patients with CAC score >400. Greenland et al. [14] showed that asymptomatic patients with CAC score zero had a low event rate (0.4 %) over the 3–5 years period in ACC/AHA clinical consensus document. Similarly, in MESA study, subjects with CAC score 0 had an exceptionally low CVD event rate in an ethnically diverse subject population [4]. Due to extremely low event rate in subjects with CAC score of zero, it is being used to exclude CAD as the cause of chest pain in low-risk patients in NICE clinical guidelines in Britain [25].

Traditional risk factor assessment has been shown to underestimate coronary risk in certain population groups especially women and young adults [26–28]. As a result, many of these patients may not receive aggressive medical management for their coronary risk factors. CAC may help to refine the risk stratification and treatment strategies of these patient populations who are otherwise categorized as low risk based on FRS categorization. Among 3,601 women in MESA study [29], 90 % of women were in the low-risk category according to FRS categorization after excluding women with diabetes and older than 79 years of age. In this group, >30 % of women were found to have CAC score >0 whereas the prevalence of significant CAC (≥300) was 4 %. The hazard ratio of CHD in women with CAC score >0 was 6.5 (95 % CI: 2.6–16.4) compared with women with CAC score of zero. Berry et al. studied incidence and progression of subclinical atherosclerosis in young adults ≤50 years of age in subjects enrolled in Coronary Artery Risk Development in Young Adults (CARDIA) and MESA study [30]. They divided the patients into groups based on their 10 year and lifelong risk for CVD into low 10-year (<10 %)/low lifetime risk (<39 %), low 10-year (<10 %)/high lifetime risk (≥39 %), and high 10-year risk (≥10 %) or diagnosed diabetes. They found that individuals with low 10-year but high lifetime risk have a greater subclinical atherosclerotic burden on carotid IMT and CAC and greater incidence of atherosclerotic progression compared to individuals with low 10-year and low lifetime risk. In light of these and other data, current practice guidelines suggest physicians consider current risk factor burden within the context of long-term or lifetime risk for CVD [31–33].

CAC has also been shown to have superior predictive value compared to other markers of coronary risk assessment such as carotid intima-media thickness and C-reactive protein [3, 34].

MESA study showed that the hazard of CVD increased 2.1-fold for log-transformed CAC vs. 1.3-fold for maximum IMT for each standard deviation increment of log-transformed CAC and maximum IMT. An ROC analysis showed CAC to be a better predictor of incident CVD than IMT [34]. Similarly, CAC has been shown to perform better than C-reactive protein and highly correlate to future CVD in a population-based study of 4,903 asymptomatic individuals [3].

CAC is a noninvasive measure of atherosclerosis; however, its use is associated with certain radiation exposure and medical cost. Rozanski et al. [35] studied the direct impact of CAC on future CAD risk and downstream medical cost compared to that of the conventional medical practice. They performed a prospective randomized trial on 2,137 volunteers that either undergo CAC scanning or did not undergo CAC scanning before risk factor counseling. The primary end point of the trial was 4-year change in CAD risk factors and FRS. Compared with no scan group, the scan group showed a net favorable change in systolic blood pressure ($p=0.02$), LDL cholesterol ($p=0.04$), waist circumference for those with increased abdominal girth ($p=0.01$), and tendency to weight loss among overweight subjects ($p=0.07$). FRS remained static in the scan group compared with no scan group (0.002 ± 4.9 vs. 0.7 ± 5.1, $p=0.003$). Within the scan group, increasing baseline CAC score was associated with a dose–response improvement in systolic and diastolic blood pressure ($p<0.001$), total cholesterol ($p<0.001$), LDL cholesterol ($p<0.001$), triglycerides ($p<0.001$), weight ($p<0.001$), and FRS ($p=0.003$). Downstream medical testing and costs in the scan group were comparable to those of the no-scan group; however, it was dependent on the level of CAC score. Shaw et al. prospectively evaluated the procedural cost and resource consumption patterns in the EISNER study (Early Identification of Subclinical Atherosclerosis by Noninvasive Imaging Research) study after CAC measurement during the 4-year follow-up period using Medicare reimbursement rates. They showed that downstream frequency of medical tests and costs was markedly differential, rising progressively with increasing CAC scores which represented only a small proportion of the study (8.2 % having CAC scores ≥400). The radiation exposure associated with CAC scans has been significantly reduced, now comparable to 1–2 mammograms (~1 mSv) [36, 37] while providing important information about the subject coronary risk and cardiac anatomy.

Predictive Value of Serial CAC Score Progression

Atherosclerosis is a dynamic process which may be affected by traditional risk factors, environmental factors, and therapeutic interventions. Baseline CAC represents as a single point in time on atherosclerosis time curve, whereas progression presents the slope of that curve. CAC progression may provide insight into ongoing atherosclerotic disease activity. Therefore, CAC progression might represent a better marker of disease activity, a better predictor of future adverse cardiovascular events and can be used to evaluate the effect of various therapeutic interventions. However, there are certain inherent limitations to the use of CAC progression before it can be used as a clinical measure for risk assessment and evaluating therapeutic efficacy. This may be due to the method of measurement (Agatston scoring may not represent true change in coronary plaque due to its stepwise nature of the density factor), interscan variability, and the method to determine CAC progression (absolute change, percent change, or mathematical transformation of CAC scores). Measurement of CAC progression highly depends on accurate reproducibility of CAC scores [38, 39]. In general, interscan variability increases as the level of baseline CAC increases and can introduce a bias in the evaluation of CAC progression [40]. Thus, high baseline CAC can introduce overestimation of the actual progression of atherosclerosis measured as a change in absolute CAC compared with those with low baseline CAC. Hokanson et al. [40] suggested that using a progression of square root-transformed calcium volume score ≥2.5 mm [3] (the SQRT method) can show a significant change in CAC progression. The SQRT method corrects for the bias in the progression of

CAC introduced by high levels of baseline CAC and provides a stable estimate of interscan variability across the ranges of coronary calcium. Budoff et al. showed that CAC progression was significantly associated with mortality even after adjusting for baseline CAC, age, sex, time between scans, hypertension, hypercholesterolemia, diabetes, family history, and smoking (hazard ratio = 3.32, 95 % CI: 2.62–4.20, $p < 0.0001$) in 4,609 consecutive asymptomatic individuals undergoing two scans. Adjusted models showed that the presence of CAC at baseline and associated significant progression of CAC was a significant predictor of future mortality (HR: 5.33, 95 % CI: 3.74–7.60, $p < 0.0001$) [41]. This study also evaluated various methods of CAC progression estimation and their performance in predicting future mortality [absolute score difference, percent annualized difference between baseline and follow-up scans, and the difference between square root of baseline and square root of follow-up CAC score >2.5 (the SQRT method)]. The SQRT method was found superior followed by a percent increase in CAC score (>15 % yearly increase) in predicting mortality. Berry et al. [30] showed that among 2,988 study participants in CARDIA study with low 10-year risk of a cardiac event, those with a high lifetime risk had significantly greater annual CAC progression (22.3 % vs. 15.4 % in men; 8.7 % vs. 5.3 % in women) compared with those with a low lifetime risk. Similar results were observed in the 1,076 MESA participants in this study. Raggi et al. [42] in an observational study related the occurrence of acute myocardial infarction to CAC progression in 817 asymptomatic individuals referred for sequential electron beam tomographic imaging (average interval 2.2 ± 1.3 years). The yearly mean absolute calcium volume score change in 45 patients who had myocardial infarction was 147 compared with 63 patients without events. In another study with 495 asymptomatic subjects undergoing sequential CAC scans and statin therapy after the initial scan, Raggi et al. showed that subjects having myocardial infarction had a greater annual change of CAC scores compared with those who did not have an event (42 ± 23 % vs. 17 ± 25 %, $p = 0.0001$), respectively [43]. Relative risk of having myocardial infarction in the presence of CAC progression was 17.2-fold (95 % CI: 4.1–71.2) higher than without CAC progression ($p < 0.0001$). The follow-up CAC score ($p = 0.034$) as well as a score change >15 % per year ($p < 0.001$) were shown to be independent predictors of time to MI. The St. Francis Heart Study [3] prospectively evaluated the prognostic accuracy of CAC progression in the prediction of cardiac events in 4,613 adults between 50 and 70 years of age. Follow-up was over 4.3 years, and events occurred in 119 subjects (2.6 %). The median increase in CAC score was significantly higher in those with cardiac events compared with those without events (247 vs. 4) respectively.

CAC progression has been shown to correlate with all the traditional risk factors; however, the association is not consistent across studies. This may be due to the differences in baseline cohort demographics or the measure of CAC progression utilized [44–53]. Kronmal et al. [44] showed that most traditional cardiovascular risk factors were associated with the risk of developing new incident CAC and an increase in existing calcification in a multiethnic population of 5,756 participants in the MESA study. The incidence of newly detectable CAC averaged 6.6 % per year. There were few factors that were associated with only incident CAC risk such as low- and high-density lipoprotein cholesterol and creatinine. Diabetic patients are more likely to develop CHD and tend to have greater plaque burden than patients without diabetes [54, 55]. Diabetes mellitus was found to have the strongest association of CAC progression for blacks and weakest for Hispanic, with intermediate association for whites and Chinese in the MESA study [44].

Role of CAC in Guiding Therapeutic Interventions

CAC represents the culmination of various processes going on in the body that result in the formation of coronary atherosclerotic plaque. Atherosclerosis is a dynamic process undergoing both progression and regression. It is possible to alter the progression of atherosclerosis by modifying risk factors, lifestyle changes, and therapeutic

interventions. On the other hand, CAC can also be used to follow the effect of various therapeutic regimens for coronary artery risk reduction. However, the literature evidence is not consistent for the role of CAC as a primary end point for preventive therapeutic regimens. Arad et al. [56] performed a double-blinded, placebo-controlled randomized clinical trial of atorvastatin 20 mg daily, vitamin C 1 g daily, and vitamin E (alpha-tocopherol) 1,000 U daily, vs. matching placebos in 1,005 asymptomatic, apparently healthy men and women age 50–70 years with coronary calcium scores at or above the 80th percentile for age and gender and followed them for 4.3 years for occurrence of cardiac events. Despite the significant reduction in LDL, there was no significant effect on CAC progression and failed to significantly reduce the primary end point, a composite of all atherosclerotic CVD events. However, events rate was reduced in patients with CAC >400 (8.7 % vs. 15.0 %, $p=0.046$). Houslay et al. [57] performed a double blind randomized controlled trial with 48 patients receiving atorvastatin and 54 to placebo and a median follow-up of 24 months. Despite reduction in LDL and C-reactive protein concentrations, there was a significant increase in CAC scores in atorvastatin group compared with the placebo group (26 % vs. 18 %) respectively. Similarly, Terry et al. [58] performed a randomized trial with participants receiving simvastatin 80 mg or matching placebo for 12 months. Despite significant reduction in LDL, total CAC volume increased in the treatment group compared with placebo (9 % vs. 5 %), respectively. Schmermund et al. [59] performed a multicenter randomized clinical trial to evaluate the effect of intensive vs. standard lipid-lowering therapy (80 vs. 10 mg atorvastatin) on CAC progression over 12 months period. The mean progression of CAC volume score was nonsignificantly different between two groups [27 % (95 % CI: 20.8–33.1) in 80 mg atorvastatin group vs. 25 % (95 % CI: 19.1–30.8) in 10 mg atorvastatin group, $p=0.65$]. Similarly, in another randomized clinical trial involving postmenopausal women randomized to aggressive (atorvastatin 80 mg/day) vs. moderate (pravastatin 40 mg/day) lipid-lowering therapy. After 12 months of treatment, the median percent increase in total CAC volume score change was similar among women receiving atorvastatin and those receiving pravastatin (15.1 % vs. 14.3 %, $p=0.64$), respectively [60].

The failure of statins to reduce CAC progression may be due to the fact that statins have been shown to promote micro-calcifications [61, 62] which might lead to an increase in CAC scores even when the total atherosclerosis is reduced on statin therapy [63]. Although statins lead to an increase in CAC progression over time, majority of the trials performed had a limited follow-up time. It may be possible that statin treatment may need longer time to affect the CAC deposition process resulting in the formation of stabilized atherosclerotic plaque with associated lower adverse cardiovascular events. Another possibility is that risk factor modification may lead to significant decline in CAC progression compared with statins. Motro et al. [64] performed a study to compare the effect of nifedipine once daily to co-amilozide diuretic treatment of high-risk hypertensive patients on progression of CAC over 3-year time interval. Treatment with nifedipine once daily was associated with significant slower progression of CAC in hypertensive patients compared with co-amilozide over 3 years (40 % vs. 78 %, $p=0.02$), respectively. Aged garlic extract and supplements have also been shown to reduce the progression of CAC over 1 year compared with placebo in a double blind randomized clinical trial [65]. In another study, Budoff et al. [66] showed that women taking unopposed estrogen replacement had significantly less CAC progression compared with estrogen plus progestin and placebo (9 ± 22 %, 24 ± 23 % and 22.3 ± 32 %, respectively). Shea et al. [67] showed that phylloquinone supplementation slows the progression of CAC in healthy older adults with preexisting CAC, independent of its effect on total Matrix G1a protein concentration which is a vitamin K-dependent calcification inhibitor.

Baseline CAC score may also provide a useful option to strategize preventive therapeutic and aggressive treatment strategies due to its ability to reclassify low-risk populations as determined by the traditional risk assessment tools. In MESA study, 23 % of those who experienced events

were reclassified to high risk, and 13 % without events were reclassified to low risk using CAC in addition to traditional risk factors [16]. Also, 90 % of women in MESA study were found to be at low risk. In this group, >30 % of women were found to have CAC score >0 whereas the prevalence of significant CAC (≥300) was 4 % [29]. These subjects would have not received preventive therapeutic treatments based on traditional risk factor assessment alone. However, the use of CAC in these populations may be helpful to identify individuals who are in need of these therapeutic treatments.

Studies are also looking at the effect of novel cardiac risk factors on progression of CAC such as C-reactive protein, cystatin-C, and microalbuminuria [44, 68, 69].

Conclusion

CAC has been shown to have superior predictive and incremental value in risk stratification of asymptomatic individuals. It has been suggested for use in risk stratification of intermediate risk, low to intermediate risk, and diabetic individuals in recent AHA/ACC guidelines. Serial measurement of CAC over time also provides useful information about the coronary risk of that individual. However, due to the intricacies in having a unified definition regarding CAC progression and interscan variability issues, the use of CAC progression may still be an issue in clinical practice use. CAC may be helpful in reclassifying the risk for certain population groups and help better strategize the treatment options. The use of CAC to follow the effect of statin treatment may not be the right choice due to propensity of statins to cause micro-calcifications.

References

1. Raggi P. Coronary-calcium screening to improve risk stratification in primary prevention. J La State Med Soc. 2002;154(6):314–8.
2. Greenland P, Alpert JS, Beller GA, et al. 2010 ACCF/AHA guideline for assessment of cardiovascular risk in asymptomatic adults: a report of the American College of Cardiology Foundation/American Heart Association Task Force on Practice Guidelines. Circulation. 2010;122(25):e584–636.
3. Arad Y, Goodman KJ, Roth M, Newstein D, Guerci AD. Coronary calcification, coronary disease risk factors, C-reactive protein, and atherosclerotic cardiovascular disease events: the St. Francis Heart Study. J Am Coll Cardiol. 2005;46(1):158–65.
4. Detrano R, Guerci AD, Carr JJ, et al. Coronary calcium as a predictor of coronary events in four racial or ethnic groups. N Engl J Med. 2008;358(13):1336–45.
5. Budoff MJ, Shaw LJ, Liu ST, et al. Long-term prognosis associated with coronary calcification: observations from a registry of 25,253 patients. J Am Coll Cardiol. 2007;49(18):1860–70.
6. Greenland P, LaBree L, Azen SP, Doherty TM, Detrano RC. Coronary artery calcium score combined with Framingham score for risk prediction in asymptomatic individuals. JAMA. 2004;291(2):210–5.
7. Kondos GT, Hoff JA, Sevrukov A, et al. Electron-beam tomography coronary artery calcium and cardiac events: a 37-month follow-up of 5635 initially asymptomatic low- to intermediate-risk adults. Circulation. 2003;107(20):2571–6.
8. Shaw LJ, Raggi P, Schisterman E, Berman DS, Callister TQ. Prognostic value of cardiac risk factors and coronary artery calcium screening for all-cause mortality. Radiology. 2003;228(3):826–33.
9. Taylor AJ, Bindeman J, Feuerstein I, Cao F, Brazaitis M, O'Malley PG. Coronary calcium independently predicts incident premature coronary heart disease over measured cardiovascular risk factors: mean three-year outcomes in the Prospective Army Coronary Calcium (PACC) project. J Am Coll Cardiol. 2005;46(5):807–14.
10. Becker A, Leber A, Becker C, Knez A. Predictive value of coronary calcifications for future cardiac events in asymptomatic individuals. Am Heart J. 2008;155(1):154–60.
11. Blaha M, Budoff MJ, Shaw LJ, et al. Absence of coronary artery calcification and all-cause mortality. JACC Cardiovasc Imaging. 2009;2(6):692–700.
12. Shareghi S, Ahmadi N, Young E, Gopal A, Liu ST, Budoff MJ. Prognostic significance of zero coronary calcium scores on cardiac computed tomography. J Cardiovasc Comput Tomogr. 2007;1(3):155–9.
13. Erbel R, Mohlenkamp S, Moebus S, et al. Coronary risk stratification, discrimination, and reclassification improvement based on quantification of subclinical coronary atherosclerosis: the Heinz Nixdorf Recall study. J Am Coll Cardiol. 2010;56(17):1397–406.
14. Greenland P, Bonow RO, Brundage BH, et al. ACCF/AHA 2007 clinical expert consensus document on coronary artery calcium scoring by computed tomography in global cardiovascular risk assessment and in evaluation of patients with chest pain: a report of the American College of Cardiology Foundation Clinical Expert Consensus Task Force (ACCF/AHA Writing

Committee to Update the 2000 Expert Consensus Document on Electron Beam Computed Tomography) developed in collaboration with the Society of Atherosclerosis Imaging and Prevention and the Society of Cardiovascular Computed Tomography. J Am Coll Cardiol. 2007;49(3):378–402.
15. Pencina MJ, D'Agostino Sr RB, D'Agostino Jr RB, Vasan RS. Evaluating the added predictive ability of a new marker: from area under the ROC curve to reclassification and beyond. Stat Med. 2008;27(2):157–72. Discussion 207–112.
16. Polonsky TS, McClelland RL, Jorgensen NW, et al. Coronary artery calcium score and risk classification for coronary heart disease prediction. JAMA. 2010;303(16):1610–6.
17. Elias-Smale SE, Proenca RV, Koller MT, et al. Coronary calcium score improves classification of coronary heart disease risk in the elderly: the Rotterdam study. J Am Coll Cardiol. 2010;56(17):1407–14.
18. Preis SR, Hwang SJ, Fox CS, et al. Eligibility of individuals with subclinical coronary artery calcium and intermediate coronary heart disease risk for reclassification (from the Framingham Heart Study). Am J Cardiol. 2009;103(12):1710–5.
19. Blaha MJ, Budoff MJ, DeFilippis AP, et al. Associations between C-reactive protein, coronary artery calcium, and cardiovascular events: implications for the JUPITER population from MESA, a population-based cohort study. Lancet. 2011;378(9792):684–92.
20. Ridker PM, Danielson E, Fonseca FA, et al. Rosuvastatin to prevent vascular events in men and women with elevated C-reactive protein. N Engl J Med. 2008;359(21):2195–207.
21. Ridker PM, MacFadyen JG, Fonseca FA, et al. Number needed to treat with rosuvastatin to prevent first cardiovascular events and death among men and women with low low-density lipoprotein cholesterol and elevated high-sensitivity C-reactive protein: justification for the use of statins in prevention: an intervention trial evaluating rosuvastatin (JUPITER). Circ Cardiovasc Qual Outcomes. 2009;2(6):616–23.
22. McClelland RL, Nasir K, Budoff M, Blumenthal RS, Kronmal RA. Arterial age as a function of coronary artery calcium (from the Multi-Ethnic Study of Atherosclerosis [MESA]). Am J Cardiol. 2009;103(1):59–63.
23. Budoff MJ, McClelland RL, Nasir K, et al. Cardiovascular events with absent or minimal coronary calcification: the Multi-Ethnic Study of Atherosclerosis (MESA). Am Heart J. 2009;158(4):554–61.
24. Raggi P, Callister TQ, Cooil B, et al. Identification of patients at increased risk of first unheralded acute myocardial infarction by electron-beam computed tomography. Circulation. 2000;101(8):850–5.
25. NICE clinical guideline 95-Chest pain of recent onset: assessment and diagnosis of recent onset chest pain or discomfort of suspected cardiac origin. 2010. http://www.nice.org.uk/nicemedia/live/12947/47938/47938.pdf. Accessed 24 Apr 2012.
26. Ford ES, Giles WH, Mokdad AH. The distribution of 10-Year risk for coronary heart disease among US adults: findings from the National Health and Nutrition Examination Survey III. J Am Coll Cardiol. 2004;43(10):1791–6.
27. Berry JD, Lloyd-Jones DM, Garside DB, Greenland P. Framingham risk score and prediction of coronary heart disease death in young men. Am Heart J. 2007;154(1):80–6.
28. Akosah KO, Schaper A, Cogbill C, Schoenfeld P. Preventing myocardial infarction in the young adult in the first place: how do the National Cholesterol Education Panel III guidelines perform? J Am Coll Cardiol. 2003;41(9):1475–9.
29. Lakoski SG, Greenland P, Wong ND, et al. Coronary artery calcium scores and risk for cardiovascular events in women classified as "low risk" based on Framingham risk score: the multi-ethnic study of atherosclerosis (MESA). Arch Intern Med. 2007;167(22):2437–42.
30. Berry JD, Liu K, Folsom AR, et al. Prevalence and progression of subclinical atherosclerosis in younger adults with low short-term but high lifetime estimated risk for cardiovascular disease: the coronary artery risk development in young adults study and multi-ethnic study of atherosclerosis. Circulation. 2009;119(3):382–9.
31. Third Report of the National Cholesterol Education Program (NCEP) Expert Panel on Detection, Evaluation, and Treatment of High Blood Cholesterol in Adults (Adult Treatment Panel III) final report. Circulation. 2002;106(25):3143–421.
32. McPherson R, Frohlich J, Fodor G, Genest J, Canadian CS. Canadian Cardiovascular Society position statement–recommendations for the diagnosis and treatment of dyslipidemia and prevention of cardiovascular disease. Can J Cardiol. 2006;22(11):913–27.
33. Mosca L, Banka CL, Benjamin EJ, et al. Evidence-based guidelines for cardiovascular disease prevention in women: 2007 update. Circulation. 2007;115(11):1481–501.
34. Folsom AR, Kronmal RA, Detrano RC, et al. Coronary artery calcification compared with carotid intima-media thickness in the prediction of cardiovascular disease incidence: the Multi-Ethnic Study of Atherosclerosis (MESA). Arch Intern Med. 2008;168(12):1333–9.
35. Rozanski A, Gransar H, Shaw LJ, et al. Impact of coronary artery calcium scanning on coronary risk factors and downstream testing the EISNER (Early Identification of Subclinical Atherosclerosis by Noninvasive Imaging Research) prospective randomized trial. J Am Coll Cardiol. 2011;57(15):1622–32.
36. Budoff MJ, Achenbach S, Blumenthal RS, et al. Assessment of coronary artery disease by cardiac computed tomography: a scientific statement from the American Heart Association Committee on Cardiovascular Imaging and Intervention, Council on Cardiovascular Radiology and Intervention, and Committee on Cardiac Imaging, Council on Clinical Cardiology. Circulation. 2006;114(16):1761–91.
37. Parker MS, Hui FK, Camacho MA, Chung JK, Broga DW, Sethi NN. Female breast radiation exposure during CT pulmonary angiography. AJR Am J Roentgenol. 2005;185(5):1228–33.
38. Callister TQ, Cooil B, Raya SP, Lippolis NJ, Russo DJ, Raggi P. Coronary artery disease: improved

reproducibility of calcium scoring with an electron-beam CT volumetric method. Radiology. 1998; 208(3):807–14.
39. Hong C, Bae KT, Pilgram TK. Coronary artery calcium: accuracy and reproducibility of measurements with multi-detector row CT–assessment of effects of different thresholds and quantification methods. Radiology. 2003;227(3):795–801.
40. Hokanson JE, MacKenzie T, Kinney G, et al. Evaluating changes in coronary artery calcium: an analytic method that accounts for interscan variability. AJR Am J Roentgenol. 2004;182(5):1327–32.
41. Budoff MJ, Hokanson JE, Nasir K, et al. Progression of coronary artery calcium predicts all-cause mortality. JACC Cardiovasc Imaging. 2010;3(12):1229–36.
42. Raggi P, Cooil B, Shaw LJ, et al. Progression of coronary calcium on serial electron beam tomographic scanning is greater in patients with future myocardial infarction. Am J Cardiol. 2003;92(7):827–9.
43. Raggi P, Callister TQ, Shaw LJ. Progression of coronary artery calcium and risk of first myocardial infarction in patients receiving cholesterol-lowering therapy. Arterioscler Thromb Vasc Biol. 2004;24(7):1272–7.
44. Kronmal RA, McClelland RL, Detrano R, et al. Risk factors for the progression of coronary artery calcification in asymptomatic subjects: results from the Multi-Ethnic Study of Atherosclerosis (MESA). Circulation. 2007;115(21):2722–30.
45. Horton KM, Post WS, Blumenthal RS, Fishman EK. Prevalence of significant noncardiac findings on electron-beam computed tomography coronary artery calcium screening examinations. Circulation. 2002;106(5):532–4.
46. Kramer CK, von Muhlen D, Gross JL, Barrett-Connor E. A prospective study of abdominal obesity and coronary artery calcium progression in older adults. J Clin Endocrinol Metab. 2009;94(12):5039–44.
47. Cassidy-Bushrow AE, Bielak LF, Sheedy 2nd PF, et al. Coronary artery calcification progression is heritable. Circulation. 2007;116(1):25–31.
48. Kramer CK, von Muhlen D, Gross JL, Laughlin GA, Barrett-Connor E. Blood pressure and fasting plasma glucose rather than metabolic syndrome predict coronary artery calcium progression: the Rancho Bernardo Study. Diabetes Care. 2009;32(1):141–6.
49. Lee KK, Fortmann SP, Fair JM, et al. Insulin resistance independently predicts the progression of coronary artery calcification. Am Heart J. 2009;157(5):939–45.
50. Costacou T, Edmundowicz D, Prince C, Conway B, Orchard TJ. Progression of coronary artery calcium in type 1 diabetes mellitus. Am J Cardiol. 2007;100(10): 1543–7.
51. Anand DV, Lim E, Darko D, et al. Determinants of progression of coronary artery calcification in type 2 diabetes role of glycemic control and inflammatory/vascular calcification markers. J Am Coll Cardiol. 2007;50(23):2218–25.
52. Elkeles RS, Godsland IF, Rubens MB, Feher MD, Nugara F, Flather MD. The progress of coronary heart disease in Type 2 diabetes as measured by coronary calcium score from electron beam computed tomography (EBCT): the PREDICT study. Atherosclerosis. 2008;197(2):777–83.
53. Kawakubo M, LaBree L, Xiang M, et al. Race-ethnic differences in the extent, prevalence, and progression of coronary calcium. Ethn Dis. 2005;15(2):198–204.
54. Pundziute G, Schuijf JD, Jukema JW, et al. Type 2 diabetes is associated with more advanced coronary atherosclerosis on multislice computed tomography and virtual histology intravascular ultrasound. J Nucl Cardiol. 2009;16(3):376–83.
55. Raggi P, Shaw LJ, Berman DS, Callister TQ. Prognostic value of coronary artery calcium screening in subjects with and without diabetes. J Am Coll Cardiol. 2004;43(9):1663–9.
56. Arad Y, Spadaro LA, Roth M, Newstein D, Guerci AD. Treatment of asymptomatic adults with elevated coronary calcium scores with atorvastatin, vitamin C, and vitamin E: the St. Francis Heart Study randomized clinical trial. J Am Coll Cardiol. 2005;46(1):166–72.
57. Houslay ES, Cowell SJ, Prescott RJ, et al. Progressive coronary calcification despite intensive lipid-lowering treatment: a randomised controlled trial. Heart. 2006;92(9):1207–12.
58. Terry JG, Carr JJ, Kouba EO, et al. Effect of simvastatin (80 mg) on coronary and abdominal aortic arterial calcium (from the coronary artery calcification treatment with zocor [CATZ] study). Am J Cardiol. 2007;99(12):1714–7.
59. Schmermund A, Achenbach S, Budde T, et al. Effect of intensive versus standard lipid-lowering treatment with atorvastatin on the progression of calcified coronary atherosclerosis over 12 months: a multicenter, randomized, double-blind trial. Circulation. 2006;113(3):427–37.
60. Raggi P, Davidson M, Callister TQ, et al. Aggressive versus moderate lipid-lowering therapy in hypercholesterolemic postmenopausal women: Beyond Endorsed Lipid Lowering with EBT Scanning (BELLES). Circulation. 2005;112(4):563–71.
61. Stary HC. The development of calcium deposits in atherosclerotic lesions and their persistence after lipid regression. Am J Cardiol. 2001;88(2A):16E–9.
62. Wu B, Elmariah S, Kaplan FS, Cheng G, Mohler 3rd ER. Paradoxical effects of statins on aortic valve myofibroblasts and osteoblasts: implications for end-stage valvular heart disease. Arterioscler Thromb Vasc Biol. 2005;25(3):592–7.
63. Burgstahler C, Reimann A, Beck T, et al. Influence of a lipid-lowering therapy on calcified and noncalcified coronary plaques monitored by multislice detector computed tomography: results of the New Age II Pilot Study. Invest Radiol. 2007;42(3):189–95.
64. Motro M, Shemesh J. Calcium channel blocker nifedipine slows down progression of coronary calcification in hypertensive patients compared with diuretics. Hypertension. 2001;37(6):1410–3.
65. Budoff MJ, Ahmadi N, Gul KM, et al. Aged garlic extract supplemented with B vitamins, folic acid and L-arginine retards the progression of subclinical atherosclerosis: a randomized clinical trial. Prev Med. 2009;49(2–3):101–7.

66. Budoff MJ, Chen GP, Hunter CJ, et al. Effects of hormone replacement on progression of coronary calcium as measured by electron beam tomography. J Womens Health (Larchmt). 2005;14(5):410–7.
67. Shea MK, O'Donnell CJ, Hoffmann U, et al. Vitamin K supplementation and progression of coronary artery calcium in older men and women. Am J Clin Nutr. 2009;89(6):1799–807.
68. Maahs DM, Ogden LG, Kretowski A, et al. Serum cystatin C predicts progression of subclinical coronary atherosclerosis in individuals with type 1 diabetes. Diabetes. 2007;56(11):2774–9.
69. DeFilippis AP, Kramer HJ, Katz R, et al. Association between coronary artery calcification progression and microalbuminuria: the MESA study. JACC Cardiovasc Imaging. 2010;3(6):595–604.

12 Emerging Role of Computed Tomography Angiography in the Evaluation of Coronary Atherosclerosis

Brian S.H. Ko, Sujith K. Seneviratne, and Dennis T.L. Wong

Introduction

Coronary artery disease (CAD) results in more than half of all cardiovascular deaths in the United States and remains the leading cause of morbidity and mortality worldwide [1]. Based on clinical pathological observations, the natural history of CAD is characterised by the silent accumulation of atherosclerotic plaque in the wall of the coronary arteries, progression onto obstructive disease as excess plaque accumulates beyond maladaptive positive remodelling, the development of stress-induced ischaemia as a result of luminal encroachment and ultimate plaque rupture resulting in unstable angina, myocardial infarction and sudden cardiac death due to atherothrombosis and abrupt coronary artery occlusion [2].

Before the advent of coronary computed tomographic angiography (CCTA), plaque characterisation and assessment could only be achieved by catheter-based procedures including invasive coronary angiography (ICA), intravascular ultrasound (IVUS) and few other invasive imaging techniques. These techniques are typically performed in patients with established CAD or after an adverse cardiac event. Notably in patients with preclinical or suspected CAD, the invasive approach is not routinely applicable and risk stratification of patients to predict obstructive coronary atherosclerosis are based on clinical risk factors and results of non-invasive stress testing which has varied accuracy.

Over the past decade, CCTA has broadened the diagnostic ability of physicians by providing the means of directly imaging coronary atherosclerosis non-invasively. It currently provides a robust and accurate method for high resolution assessment of coronary atherosclerosis, the overall plaque burden, distribution, morphology and extent of associated luminal stenosis. Importantly it has provided the potential of revealing preclinical stages of the atherosclerotic disease which may have important value to improve risk stratification and to monitor the progressive course of the disease. In addition to its current established role in detection of plaque and associated stenosis, the use of CCTA is being rapidly extended to assess the entire spectrum of patients with CAD as it is refined to assess the haemodynamic significance of atherosclerotic plaque, associated myocardial ischaemia and to predict

B.S.H. Ko, BSc (Med), MBBS (Hons), PhD, FRACP
S.K. Seneviratne, MBBS, FRACP
Monash Cardiovascular Research Centre, Department of Medicine, Monash University and Monash Heart, Southern Health, 246 Clayton Road, Clayton, VIC 3168, Australia
e-mail: brianshiuhangko@gmail.com; Sujith.seneviratne@southernhealth.org.au

D.T.L. Wong, BSc (Med), MBBS (Hons), PhD, FRACP (✉)
Monash Cardiovascular Research Centre, Department of Medicine, Monash University, Monash Heart, South Australian Health & Medical Research Institute (SAHMRI), 246 Clayton Road, Clayton, VIC 3168, Australia

Discipline of Medicine, University of Adelaide, Adelaide, SA, Australia
e-mail: drdenniswong@yahoo.com.au

S.J. Nicholls and T. Crowe (eds.), *Imaging Coronary Atherosclerosis*, Contemporary Cardiology,
DOI 10.1007/978-1-4939-0572-0_12, © Springer Science+Business Media New York 2014

clinical outcomes. This chapter reviews the established role and methodology of CCTA to assess atherosclerotic plaque, to predict clinical outcomes and its potential role in assessing the haemodynamic significance of CAD.

Methodology of Coronary CT Angiography

Image Acquisition

Coronary CT angiography is typically performed using multidetector CT scanners, which consist of a mechanically rotating gantry equipped with a radiation source that emits a fan-shaped radiation beam which passes through the patient and is detected by multiple detector rows on the opposite side. Image acquisition is performed upon administration of intravenous iodinated contrast (50–100 mL, typically at rates of 4–6 mL/s) when the coronary arteries are maximally opacified.

Currently, 64-detector row CT is regarded as the minimum required technical standard for robust clinical applications of CCTA [3], based on several multicentre trials which have demonstrated the accuracy of 64-detector CCTA using retrospectively ECG-gated spiral or helical acquisition [4–6]. However limitations do remain. One factor is the limited temporal resolution as compared with the rapid motion of the heart and coronary arteries especially in patients with a heart rate of more than 60 beats per minute. Another potential problem is caused by the fact that image acquisition requires several heart beats, which makes the technique vulnerable to breathing artefacts in patients who are not fully cooperative and to the occurrence of arrhythmias or ectopic beats, which may render retrospectively ECG-gated image reconstruction inaccurate [7].

To address this, manufacturers have chosen different strategies to improve future scanners beyond 64-detector technology (Fig. 12.1). Firstly newer generation scanners are equipped with an increasing number of detector rows from 64, 128, 256 to 320 detector rows. This has resulted in a dramatic decrease in scan acquisition time from 5 to 10 s using narrow detector CT to <1 s using wide-detector CT and minimises the time required for patients to breath hold from 8–10 s to 1–2 s, respectively. Secondly the width of individual detector rows has decreased from 1.25 mm in 4-detector row CT to 0.5–0.625 mm, with a resultant interpolated spatial resolution of 0.24–0.4 mm in all imaging planes. The spatial resolution of latest generation CT scanners is marginally lower than the 0.1 mm and 0.2 mm afforded by IVUS and ICA, respectively. Lastly to optimise the ability to acquire motion free images, modern single source scanners are equipped with faster gantry rotation speeds. Alternatively manufacturers have designed scanners with a gantry system which is equipped with two radiation sources and detectors arranged in a 90° angulation (dual source CT).

	Year	Detector	Spatial Resolution (mm)	Temporal Resolution (ms)
4-MDCT	2000	4	1.25	165-330
16-MDCT	2002	16	0.75	105-210
64-MDCT	2004	64	0.5-0.6	82-165
64-DSCT	2006	2x64	0.6	42-84
320-MDCT	2008	320	0.5	175
HDCT	2008	64	0.23	175
128 –DSCT	2009	2x128	0.6	75
320 2nd gen	2012	320	0.5	135

Fig. 12.1 Advances in CT scanners

This has improved the temporal resolution by a factor of 2 and shortens the time required to acquire a single transaxial image which permits scan acquisition at higher patient heart rates. Compared with the high temporal resolution of 330 ms using 4-detector CT, the latest generation single and dual source CT have a temporal resolution of 135 and 75 ms, respectively.

Patient Preparation

Image quality is optimised by patient preparation prior to image acquisition. Oral or intravenous beta blockers are administered to reduce heart rate to minimise cardiac motion during scan acquisition. Scan acquisition is routinely performed at heart rates ≤65 beats per minute and during mid to late diastole (75–90 % of the R–R interval) when the coronary arteries are most still. Sublingual nitroglycerin is administered immediately prior to scan acquisition to achieve coronary vasodilatation and has been demonstrated to improve image quality [8].

Radiation Exposure

Retrospectively ECG-gated 64-detector CCTA requires an effective radiation exposure of 7–21 millisieverts (mSv) [4]. Advances in imaging techniques have resulted in a much lower currently required radiation dose. Firstly the use of lower tube potential from the standard 120–100 kV in subjects less than 90 kg has markedly reduced radiation exposure by 30–50 % [9]. Secondly, scan acquisitions are now routinely performed using prospective ECG gating, during which radiation exposure occurs only during late systole or diastole, in preference to retrospective ECG gating, during which scan acquisition occurs throughout the entire R–R interval. This has reduced the effective radiation dose by >50 % [10]. Thirdly the use of new scanner technology including wide-detector array and high pitch dual source spiral "flash" scanning has extensively shortened scan acquisition time to within a single heart beat in the majority of patients. Both technologies require excellent heart rate control to achieve maximal radiation minimisation and has resulted in the ability to perform scans with <1 mSv radiation exposure [11, 12]. Lastly the methods of image reconstruction using CT have also evolved from the conventional process of filtered back projection, a rapidly applicable technique which does not make full use of the information contained in the X-ray data acquired to iterative reconstruction which is computationally more elaborate but makes more effective use of the acquired X-ray information. Currently these methods have been applied not so much to improve the image quality of existing scan protocols but to reduce the noise level of low-dose acquisitions and hence permit CCTA with reduced radiation exposure. Clinical trials thus far have demonstrated the ability to lower the dose using this method by up to 44 % [13].

Coronary Plaque and Stenosis Assessment

Qualitative Assessment

Method

CT coronary images are typically interpreted in axial or multiplanar reformatted planes as well as in curved multiplanar reformats. By visual inspection, atherosclerotic plaques can be identified in each of the 17 coronary segments and classified based on stenosis severity which can be graded as normal, minimal plaque with <25 % diameter lumen stenosis, mild: 25–49 % stenosis, moderate: 50–69 % stenosis, severe: 70–99 % stenosis and occluded [14]. Furthermore plaque can be classified based on its morphology based on the presence and relative amount of calcification: non-calcified plaque in which the entire plaque contains no calcium density; calcified plaque in which the plaque appears completely calcified and mixed plaque in which the plaque contains both calcified and non-calcified plaque (Fig. 12.2). Non-calcified plaque can be further subdivided into low-density and high-density non-calcified plaque, based on different attenuation thresholds.

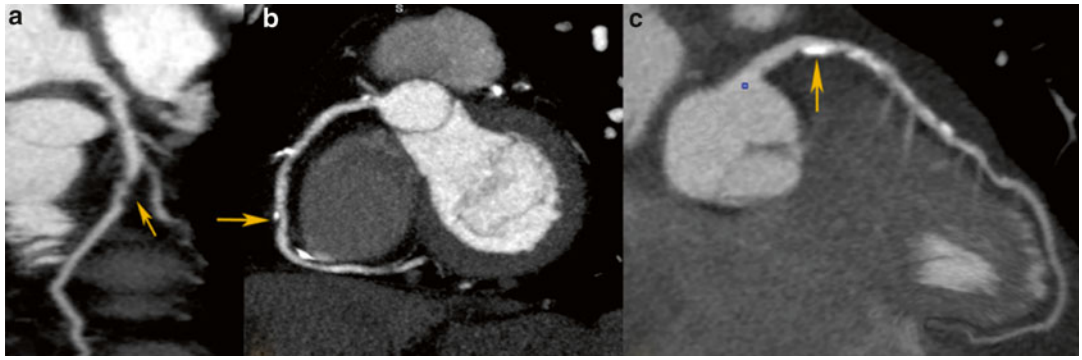

Fig. 12.2 Different types of coronary plaques based on composition. (**a**) Non-calcified plaque, (**b**) mixed plaque, (**c**) calcified plaque

Accuracy

The diagnostic accuracy of qualitative assessment using CCTA has been compared to invasive angiography in a large number of single and multicentre studies based on visual assessment using a binary approach in classifying lumen stenosis as <50 or ≥50 %. In 2008, three large multicentre studies demonstrated in patients with low to intermediate risk of CAD that 64-detector CCTA identified significant coronary artery stenosis with a sensitivity of 85–99 %, specificity of 64–90 % and a negative predictive value of 83–99 % [4–6]. In a recent meta-analysis including 89 studies comprising 7,516 patients with suspected and known CAD, the per-patient sensitivity and specificity for >16 slice CCTA was 98 % and 89 %, respectively [15]. This demonstrates the robustness and accuracy of CCTA to provide coronary assessment in a manner which most closely resembles invasive angiography among all other non-invasive imaging modalities particularly in patients with low to intermediate risk of CAD. Accordingly current European and the US guidelines advocate the use of CT in this population with a Class IIa and Class IIb indication [16, 17]. In addition, since 2010, the ACC/AHA appropriate use criterion has been recommended that it is appropriate to use CCTA as an upfront investigation in this population [18].

Reproducibility

The reproducibility of qualitative stenosis and plaque assessment is optimised in studies performed on patient subsets identified to have excellent image quality. A significantly increased interobserver variability is found in cases with poor image quality [19]. Rinehart reported in a high quality image cohort of 186 coronary segments, an excellent intraobserver agreement for both stenosis rating ($K=0.96$) and plaque classification ($K=0.96$) [20]. Furthermore interobserver agreement was excellent both for the degree of stenosis ($K=0.90$) and for plaque composition ($K=0.88$). Similarly Lehman et al. demonstrated that in a subset of 15 patients (4,057 cross sections) with acute chest pain without acute coronary syndrome (ACS) [21], the intraobserver and interobserver agreement for the detection of any plaque per cross section was excellent ($K=0.95$ and $K=0.93$, respectively). The corresponding agreement was excellent for detection of calcified plaque ($K=0.96$; $K=0.97$) and very good for detection of non-calcified plaque ($K=0.76$ and $K=0.73$).

Quantitative Assessment

Method

Coronary CTA may also provide a quantitative three-dimensional assessment of plaque burden and vessel lumen geometry which had previously only been obtained on IVUS. Using dedicated computed software, geometric parameters including minimal luminal area, minimal luminal diameter, diameter stenosis and area stenosis can be quantified (Fig. 12.3). Furthermore, the total volume of plaque can be determined using a

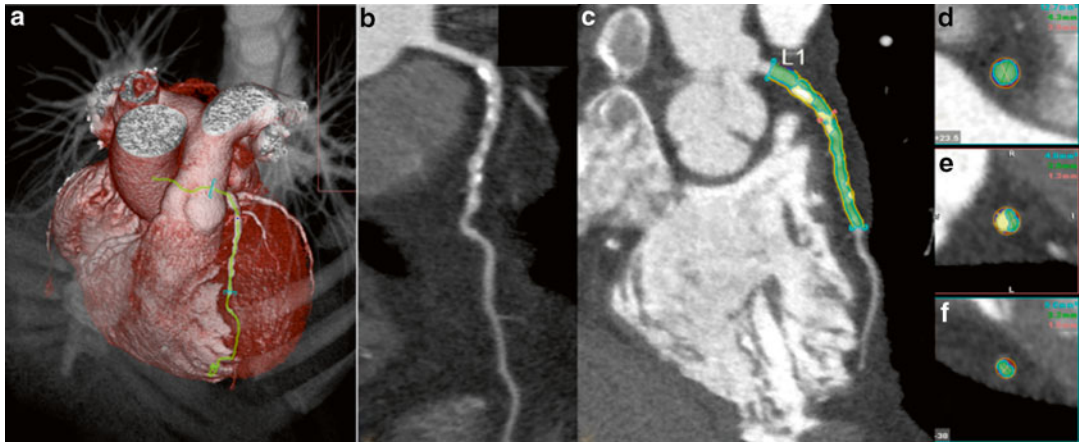

Fig. 12.3 Quantitative plaque assessment using CTA. (**a**) Volume-rendered image, (**b**) multiplanar reconstruction showing diffuse severe mixed plaque in left anterior descending artery, (**c**) quantitative assessment with *blue lines* indicating proximal and distal reference segment, *red line* indicating lesion. (**d**) Cross-sectional image of proximal reference segment, (**e**) cross-sectional image at lesion, (**f**) cross-sectional image of distal reference segment

semi-automated method based on software detection of the inner and outer vessel walls over a length of the coronary artery (Fig. 12.4). Plaque volume is defined as the volume between the inner and outer vessel wall within a defined coronary segment. Using this approach, the volume of calcified and non-calcified plaque based on relative CT densities can also be derived and cross-sectional plaque area or burden, defined as [vessel area—lumen area]/vessel area, can be quantified.

Accuracy

Numerous studies have evaluated the accuracy and reproducibility of quantitative CT assessment using IVUS as reference standard. These studies have typically been performed by expert readers using selected high quality CTA datasets, after exclusion of significantly calcified or non-interpretable segments.

In a recent meta-analysis, Voros et al. identified 33 studies published between 2001 and 2010, including a cohort of 946 patients, in which the accuracy of 64-detector CCTA to qualitatively and quantitatively assess atherosclerotic plaque was compared with IVUS [22]. CCTA was demonstrated to have an excellent sensitivity (94 %) and specificity (92 %) to qualitatively detect atherosclerotic plaque (Fig. 12.5). Notably 22 of the included studies directly compared CT quantified vessel lumen area, plaque area, area stenosis and plaque volume against corresponding IVUS measurements. CCTA was found to slightly overestimate luminal area (0.46 mm^2 or by 6.7 %; $p=0.005$), while there was no significant differences in plaque area (0.09 mm^2; $p=0.88$), volume (5.3 mm^3; $p=0.21$) and percent area stenosis (−1.81 %; $p=0.12$) (Fig. 12.6).

A number of studies have specifically evaluated the accuracy of CCTA to quantify the volume of calcified and non-calcified plaque using IVUS as the reference standard. Otsuka et al. demonstrated that in 76 plaques, CCTA marginally and non-significantly overestimated plaque volume in calcified and mixed plaques ($p=0.20$) with a relative difference of 3 ± 17 % but significantly underestimated plaque volume in non-calcified plaques ($p<0.01$) with a relative difference of 17 ± 19 % [23]. Voros et al. demonstrated in a 60-patient cohort identified to have intermediate stenoses that CTA overestimated plaque volume in calcified plaque with a relative difference of 64 ± 137 %, presumably as a result of blooming artefacts, and underestimated plaque volume in non-calcified plaque with a relative difference of 22 ± 47 % [24].

Reproducibility

The reproducibility of quantitative measurements of geometrical and compositional plaque volume remains an important requirement of any robust method to image atherosclerosis.

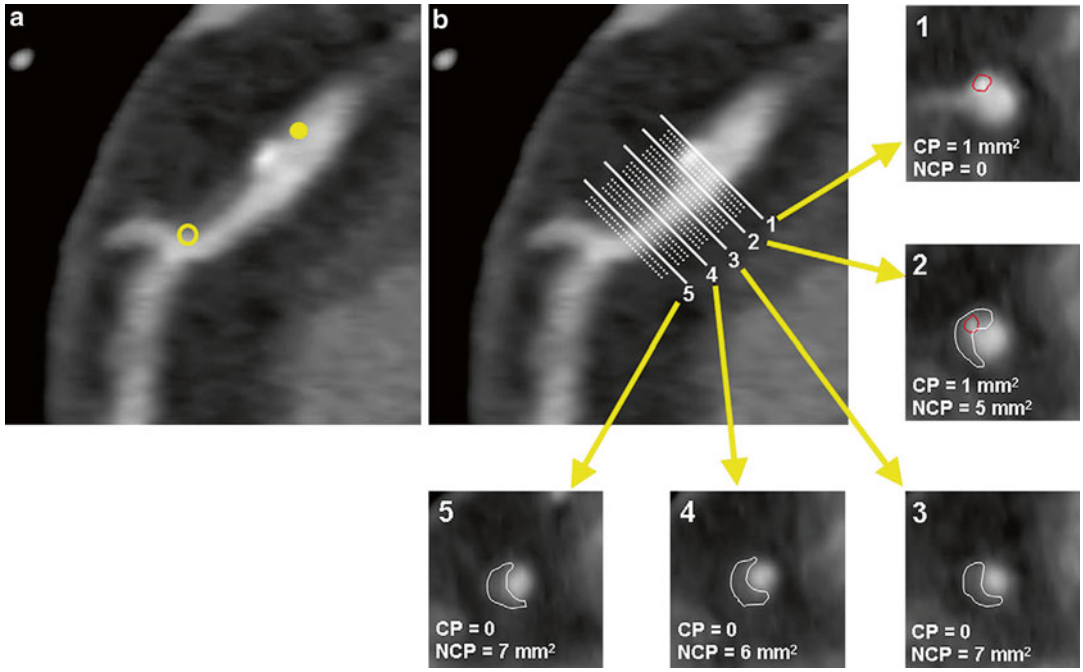

Fig. 12.4 Plaque volume quantification. The length of the plaque is first determined (**a**). Cross-sectional tracing is then performed at each step increment along the longitudinal axis of the plaque to obtain plaque area (**b**). Calcified and non-calcified plaques are traced separately. (**b1**–**5**) Corresponding plaque volumes are calculated by multiplying sums of plaque areas by the step increment (Adapted from Cheng VY, Nakazato R, Dey D et al. Reproducibility of coronary artery plaque volume and composition quantification by 64-detector row coronary computed tomographic angiography: an intraobserver, interobserver, and interscan variability study. J Cardiovasc Comput Tomogr 2009;3(5):312–20. With permission from Elsevier)

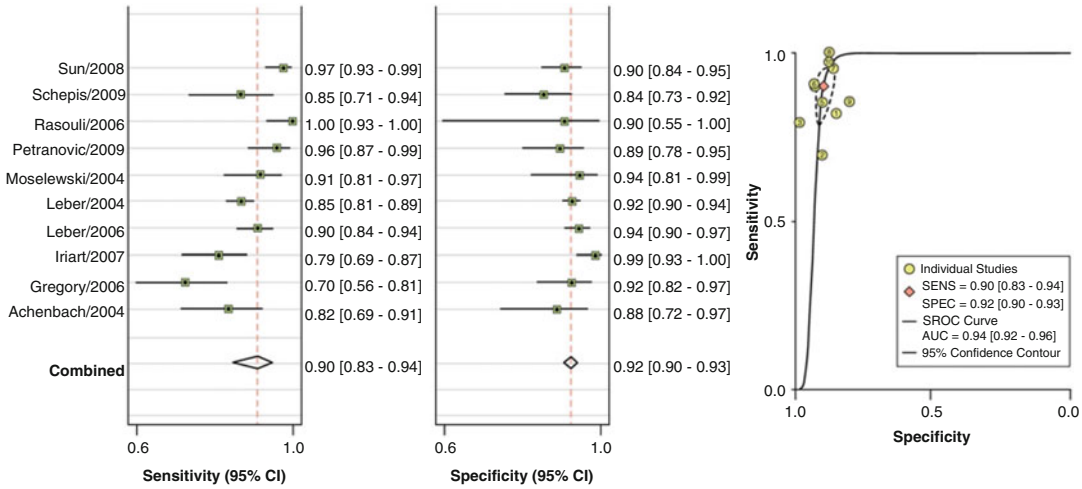

Fig. 12.5 Pooled sensitivity and specificity for coronary CTA vs. IVUS (Adapted from Voros S, Rinehart S, Qian Z et al. Coronary atherosclerosis imaging by coronary CT angiography: current status, correlation with intravascular interrogation and meta-analysis. JACC Cardiovasc Imaging 2011;4:537–48. With permission from Elsevier)

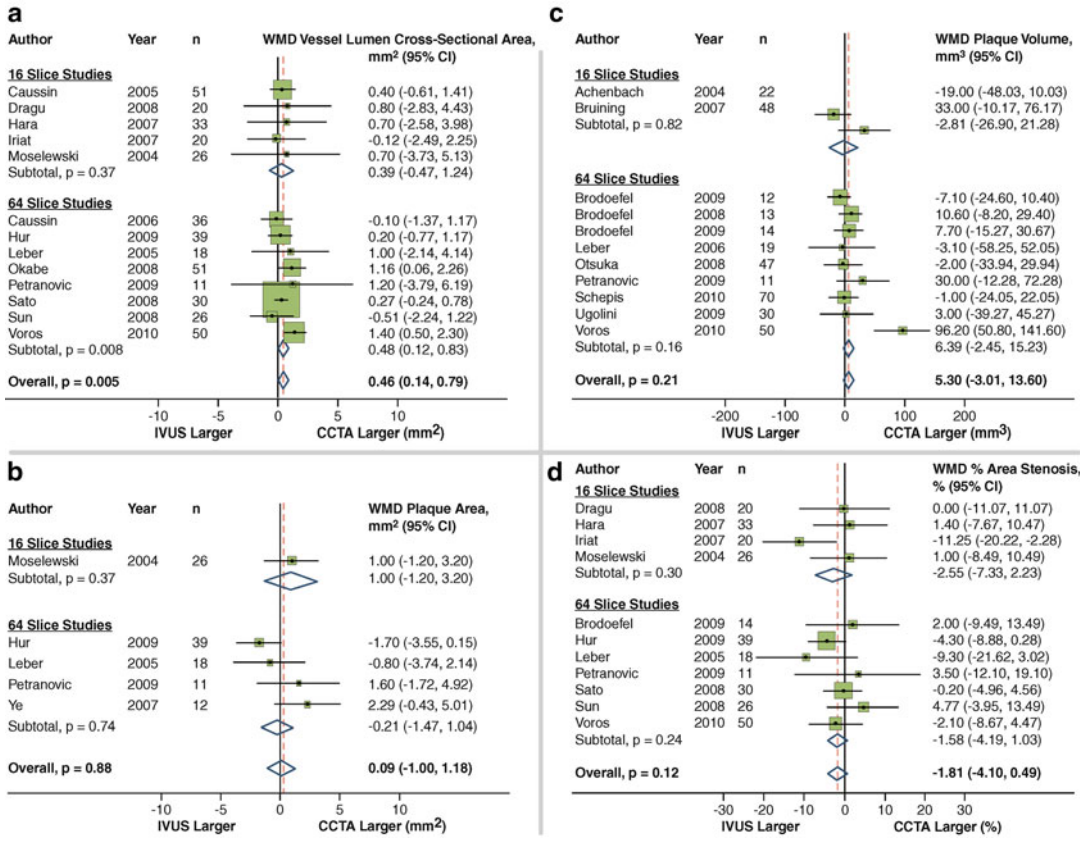

Fig. 12.6 Coronary CTA vs. IVUS to compare vessel lumen area (**a**), plaque area (**b**), plaque volume (**c**) and percent area stenosis (**d**) (Adapted from Voros S, Rinehart S, Qian Z et al. Coronary atherosclerosis imaging by coronary CT angiography: current status, correlation with intravascular interrogation and meta-analysis. JACC Cardiovasc Imaging 2011;4:537–48. With permission from Elsevier)

Geometric Measurements

Rinehart et al. demonstrated that the mean difference in quantifying minimal luminal diameter and minimal luminal area between two experienced observers were small (0.45 % and 0.43 %, respectively, with corresponding limits of agreement of ±11.8 % and ±18.5 %) [20] (Fig. 12.7). Similarly in a more recent publication, Nakazato et al. reported the mean difference in diameter and area stenosis between two observers were small (−2.6 % and −4.1 %, respectively, with limits of agreement of −25.3 to 20.1 % and −28.9 to 20.7 %, respectively) [25].

Quantification of Plaque Volume

Cheng et al. examined the interobserver, intraobserver and interscan variability of calcified and non-calcified plaque volume in a subset of 30 consecutive patients who had undergone two coronary CT angiograms within 200 days on two separate CT scanners [26]. The interobserver correlation was excellent with r values ranging between 0.83 and 0.99 although the limits of agreement were wide ranging from 87 to 226 %. Otzuka et al. demonstrated that reproducibility may be optimised using a dataset which excluded images with heavy calcification and image blurring [23].

Parameter	CCC	95% CI	CTA		Mean difference, absolute	Mean difference, %	Limits of agreement, absolute	Limits of agreement, %
			Reader 1, mean ± SD	Reader 2, mean ± SD				
Length, mm	0.99	0.99-1.00	32.19 ± 32.09	39.45 ± 32.12	−0.26	−0.66	±4.3	±10.9
MLD, mm	0.98	0.98-0.99	2.21 ± 0.74	2.20 ± 0.73	0.01	0.45	±0.26	±11.8
MLA, mm^2	0.99	0.98-0.99	7.02 ± 3.70	6.99 ± 3.63	0.03	0.43	±1.3	±18.5
%AS	0.92	0.90-0.93	35.07 ± 21.40	34.86 ± 20.97	0.21	0.60	±16.7	±47.8
%DS	0.94	0.93-0.95	29.39 ± 16.71	29.30 ± 16.60	0.09	0.31	±11.0	±37.5
RI	0.86	0.83-0.88	79.27 ± 21.52	79.00 ± 20.89	0.26	0.33	±22.1	±27.9
LD-NCP-V, mm^3	0.98	0.98-0.99	24.18 ± 22.79	24.36 ± 22.98	−0.18	−0.74	±5.2	±21.4
HD-NCP-V, mm^3	0.99	0.99-0.99	198.6 ± 176.2	200.3 ± 176.8	−1.6	−0.80	±24.8	±12.4
NCP-V, mm^3	0.99	0.98-0.99	223.0 ± 197.8	224.7 ± 198.3	−1.7	−0.76	±25.7	±11.5
CAP-V, mm^3	0.99	0.99-0.99	39.01 ± 42.28	39.30 ± 42.08	−0.29	−0.74	±9.2	±23.5
%LD-NCP	0.90	0.87-0.91	9.21 ± 3.43	9.13 ± 3.24	0.08	0.11	±3.0	±32.8
%HD-NCP	0.98	0.97-0.98	74.76 ± 11.53	74.77 ± 11.37	−0.01	−0.01	±4.7	±6.3
%NCP	0.99	0.98-0.99	84.01 ± 12.93	83.90 ± 12.80	0.11	0.13	±4.0	±4.8
%CAP	0.99	0.98-0.99	15.98 ± 12.94	16.09 ± 12.80	−0.11	−0.69	±4.1	±25.6

CCC, concordance correlation coefficient; 95% CI, 95% confidence interval; MLD, minimal lumen diameter; MLA, minimal lumen area; RI,remodeling index; CAP, calcified plaque volume; %CAP, percentage of CAP; NCP, noncalcified plaque; %NCP, percentage of NCP; HD-NCP-V, high-density NCP volume; %HD-NCP, percentage of HD-NCP; LD-NCP-V, low-density NCP volume; %LD-NCP, percentage of low-density NCP; %AS, percentage of area stenosis; %DS, percentage of diameter stenosis].

Fig. 12.7 Interobserver agreement for geometric and compositional parameters on a per-coronary segment basis (Adapted from Rinehart S, Vazquez G, Qian Z, Murrieta L, Christian K, Voros S. Quantitative measurements of coronary arterial stenosis, plaque geometry, and composition are highly reproducible with a standardized coronary arterial computed tomographic approach in high-quality CT datasets. J Cardiovasc Comput Tomogr 2011;5:35–43. With permission from Elsevier)

Upon exclusion, the mean intraobserver and interobserver variability to quantify plaque burden was demonstrated to be 0 ± 16 % and 4 ± 24 %, respectively. Similarly Rinehart demonstrated that upon the use of standardised automated software and meticulous expert reader measurements in selected high quality coronary CTA datasets [22], the reported mean difference in calcified and non-calcified plaque volume was −0.74 % and −0.76 % with corresponding limits of agreement of ±23.5 % and ±11.5 %, respectively (Figs. 12.7 and 12.8).

Prediction of Clinical Outcomes Using Cardiac CT

In addition to plaque and stenosis assessment, multiple studies have demonstrated that the burden of CAD visualised on CCTA predicts future adverse events. CCTA meets three fundamental criteria as a good prognostic test: (1) it identifies patients at very low risk for events (2) it provides definition of clear gradations of risk based on tests results and (3) it enables the concentration risk in patients with abnormal tests [27].

Presence of Obstructive Disease on CTA Predicts Prognosis

Min et al. demonstrated in a single-centre consecutive cohort of 1,127 symptomatic patients that all-cause mortality was predicted by a number of angiographic features as assessed on CCTA including the presence of moderate (≥50 %) or severe (≥70 %) coronary stenosis in any coronary artery ($p = 0.007$ and $p < 0.001$, respectively) (Fig. 12.9), the presence of a severe stenosis in any proximal segment of a major epicardial vessel ($p = 0.001$) and the presence of obstructive left main or left anterior descending artery stenosis ($p = 0.001$) [28]. This study also demonstrated that CCTA-derived Duke prognostic CAD index, clinical coronary artery plaque score including a segment stenosis score and segment involvement score were significant predictors of all-cause mortality ($p < 0.001$) [28].

In a pooled analysis of 18 coronary CCTA prognostic studies involving 9,592 symptomatic patients with predominantly suspected CAD [29], Hulten et al. demonstrated that the annual event rates for combined major cardiac events (including death, myocardial infarction and

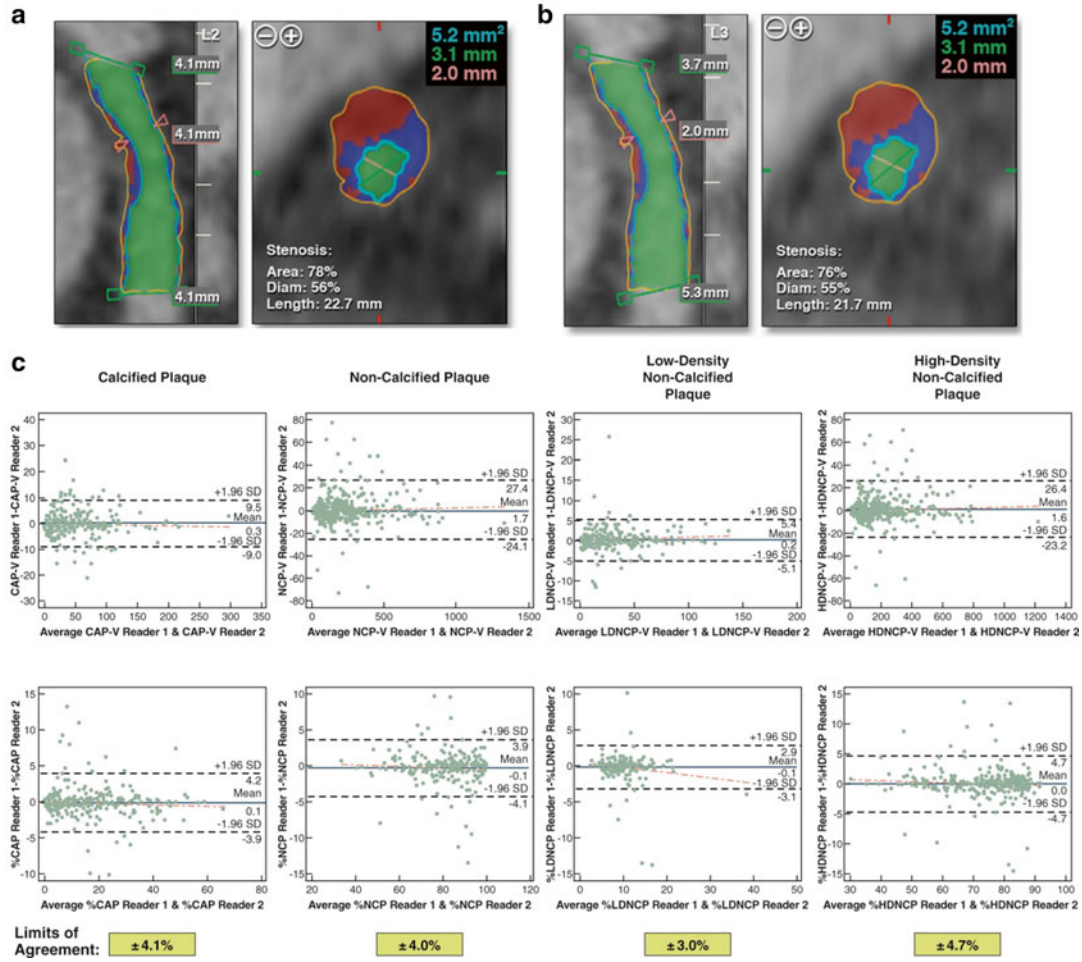

Fig. 12.8 Interobserver variability for calcified, non-calcified, low-density non-calcified and high-density non-calcified plaque (Adapted from Voros S, Rinehart S, Qian Z et al. Coronary atherosclerosis imaging by coronary CT angiography: current status, correlation with intravascular interrogation and meta-analysis. JACC Cardiovasc Imaging 2011;4:537–48. With permission from Elsevier)

revascularisation) and death in patients with obstructive coronary disease defined as the presence of any lesion with ≥50 % stenosis was 8.8 and 2.2 % (Fig. 12.10), which was significantly higher ($p<0.005$) than patients with non-obstructive disease (1.4 and 0.74 %) and normal coronary arteries on CCTA (0.17 and 0.15 %), respectively.

Similar findings were demonstrated using data from a large international multicentre registry (CONFIRM Registry) which included 24,775 patients at a mean follow-up of 2.3 years. It demonstrated that the presence of obstructive disease on CCTA not only risk stratified patients into clinically important risk tertiles [30], but was also a significant predictor of all-cause mortality and provided significant incremental value to LVEF and clinical variables with a net reclassification index of 17.8 % ($p<0.001$) [31]. Furthermore using data from the same registry, Hadamitzky described the novel use of an optimised score which accounted for the number of proximal segments with a stenosis >50 % or with mixed or calcified plaque [32]. The use of this CCTA-based scoring system was demonstrated to significantly improve overall risk prediction beyond the National Cholesterol Education Program Expert Panel on Detection, Evaluation and

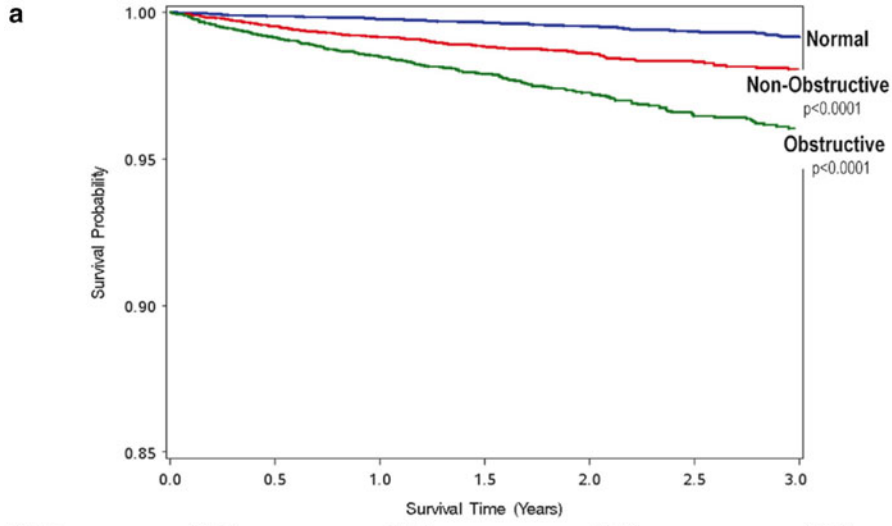

At Risk	Year 0	Year 1	Year 2	Year 3
Normal	10146	9357	5800	2907
Non-Obstructive (1-49%)	8114	7437	4081	1930
Obstructive (≥50%)	5594	5135	3153	1430

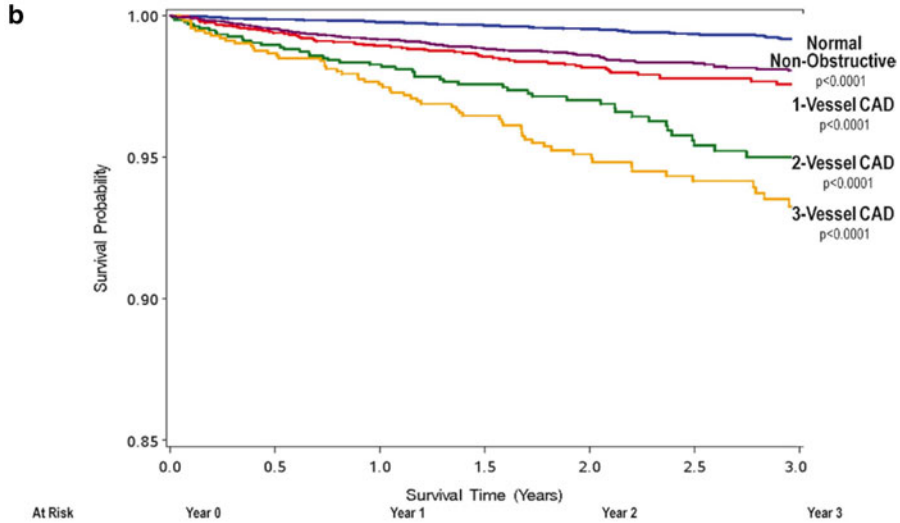

At Risk	Year 0	Year 1	Year 2	Year 3
Normal	10146	9357	5800	2907
Non-Obstructive	8114	7437	4081	1930
1-Vessel	3118	2873	1747	782
2-Vessel	1346	1228	742	324
3-Vessel/Left Main	1130	1034	664	324

Fig. 12.9 Cumulative survival in patients with severe plaque. (**a**) 3-year Kaplan Meier Survival by the maximal per-patient presence of none, nonobstructive and obstructive CAD. (**b**) 3-year Kaplan Meier Survival by the presence, extent and severity of CAD by CCTA (Adapted from Min JK, Dunning A, Lin FY et al. Age- and sex-related differences in all-cause mortality risk based on coronary computed tomography angiography findings results from the International Multicenter CONFIRM (Coronary CT Angiography Evaluation for Clinical Outcomes: An International Multicenter Registry) of 23,854 patients without known coronary artery disease. J Am Coll Cardiol 2011;58:849–60. With permission from Elsevier)

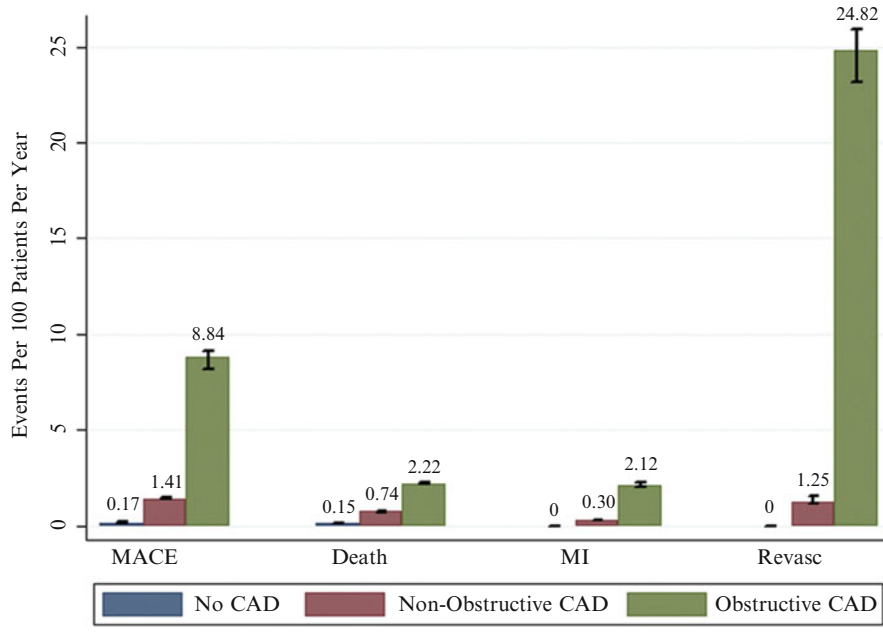

Fig. 12.10 Annual event rates stratified by CTA result (Adapted from Hulten EA, Carbonaro S, Petrillo SP, Mitchell JD, Villines TC. Prognostic value of cardiac computed tomography angiography: a systematic review and meta-analysis. J Am Coll Cardiol 2011;57:1237–47. With permission from Elsevier)

Treatment of High Blood Cholesterol in Adults (ATP III) score [32].

Lastly normal findings on CCTA was found to be associated with very low event rates [28–31] which is comparable to the background event rate among healthy low-risk individuals (<1 %) [33] and is similar to that reported in patients with normal stress testing evaluated on echocardiography or nuclear myocardial perfusion imaging [34].

Presence of Non-obstructive Disease on CCTA Predicts Prognosis

Recently, in a cohort of 2,583 symptomatic patients identified to have non-obstructive coronary artery stenosis (<50 %) on CCTA and mean of 3.1 years follow-up, Lin et al. demonstrated that the presence of non-obstructive plaque was associated with higher mortality (hazard ratio (HR) 1.98, $p=0.03$) when compared with normal findings, with the highest risk among patients who had non-obstructive CAD in three epicardial vessels (HR 4.75, $p=0.0002$) and ≥5 coronary segments (HR 5.12, $p=0.0002$) [35]. Importantly a higher mortality for non-obstructive disease was observed even among patients with low 10-year Framingham risk (3.4 %, $p<0.0001$), as well as those with no traditional, medically treatable cardiovascular risk factors including diabetes mellitus, hypertension and dyslipidemia (5.7 %, $p<0.0001$).

Predicting Acute Coronary Syndrome

CT Plaque Quantification

Verteylen et al. demonstrated that the use of a semi-automated plaque quantification algorithm may provide additional prognostic value in prediction of future ACS beyond conventional CT assessment of stenosis alone [36]. At a mean 26 ± 10 months, patients with ACS were found to have higher total plaque volume (94 vs. 29 mm^3,

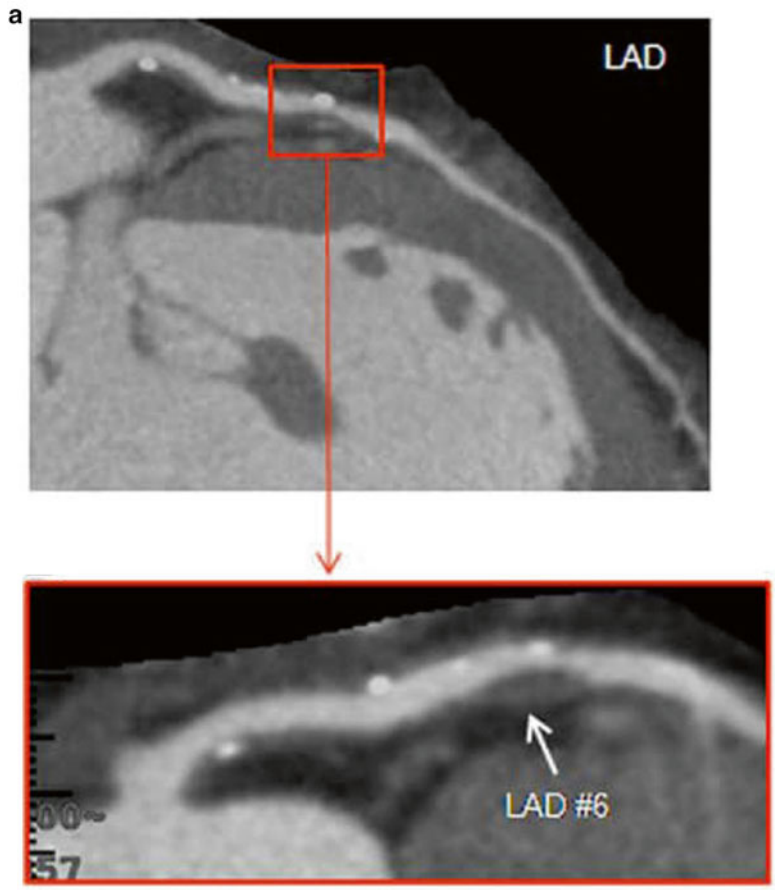

Fig. 12.11 Vulnerable plaque characteristics. Features of vulnerable plaque including the presence of low attenuation plaque, positive remodelling, spotty calcification (**a**), ring-like sign (**b**) and plaque ulceration with intraplaque contrast penetration (**c**). (**a**) Adapted from Motoyama S, Sarai M, Harigaya H et al. Computed tomographic angiography characteristics of atherosclerotic plaques subsequently resulting in acute coronary syndrome. J Am Coll Cardiol 2009;54: 49–57. With permission from Elsevier. (**b**) Adapted from Kashiwagi M, Tanaka A, Kitabata H et al. Feasibility of noninvasive assessment of thin-cap fibroatheroma by multidetector computed tomography. JACC Cardiovasc Imaging 2009;2:1412–9. With permission from Elsevier. (**c**) Adapted from Madder RD, Chinnaiyan KM, Marandici AM, Goldstein JA. Features of disrupted plaques by coronary computed tomographic angiography: correlates with invasively proven complex lesions. Circ Cardiovasc Imaging 2011;4:105–13. With permission from Wolters Kluwer Health

$p<0.001$), non-calcified plaque volume (28 vs. 4 mm^3, $p<0.001$) and plaque burden (57 % vs. 36 %, $p<0.01$). Based on a receiver-operating characteristic model which incorporated semi-automated plaque quantification predicted ACS with an area under the curve of 0.79 which was significantly higher than the use of conventional CCTA reading and Framingham risk scores (0.64, $p<0.05$).

CT Plaque Characteristics Predict Future ACS

Retrospective observational studies have identified a number of CT-based coronary plaque characteristics to be associated with culprit lesions for future ACS (Fig. 12.11). These include the higher frequency of non-calcified plaque [37], higher frequency of lipid-rich plaque subtype [38] or low attenuation plaque (LAP) (<30 HU) [39], larger

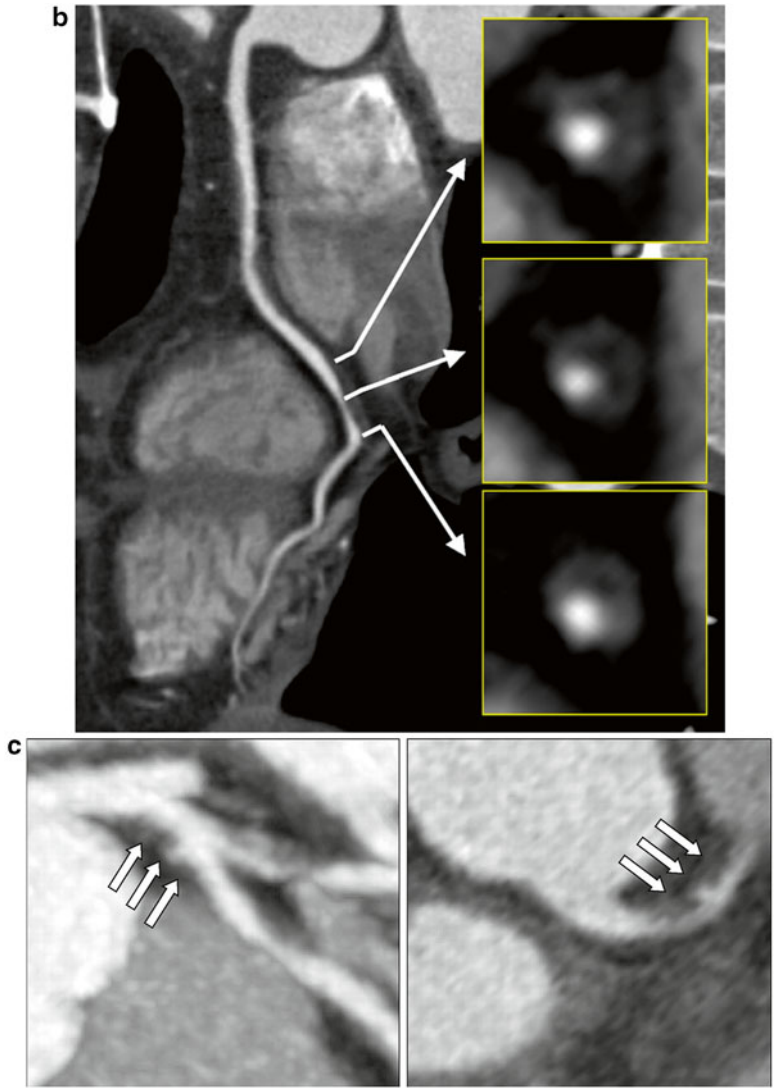

Fig. 12.11 (continued)

plaque volume [40], positive remodelling [38–41], a pattern of spotty calcification [39, 40] and a napkin ring sign which is characterised by a peripheral rim of contrast surrounding the outskirt of plaque [40, 42]. The ring-like sign is speculated to either represent highly active vasa vasorum neovascularisation in the adventitia which surrounds the rupture prone plaque [42], intramural thrombus [43] or a large central lipid core surrounded by fibrous plaque tissue [43]. Lastly in patients with unstable angina CT features of plaque disruption including plaque ulceration and intraplaque dye penetration have been described to be modestly sensitive (53–81 %) and highly specific (82–95 %) for plaque erosion and or intraplaque haemorrhage as demonstrated on invasive angiography [44] (Fig. 12.12).

Motoyama et al. demonstrated that in a large prospective study with a cohort of 1,059 patients, two CT angiographic features, LAP and positive remodelling, were associated with subsequent development of acute coronary events [45]. In this study, there were 45 patients who showed these two features, ACS developed in 10 (22 %),

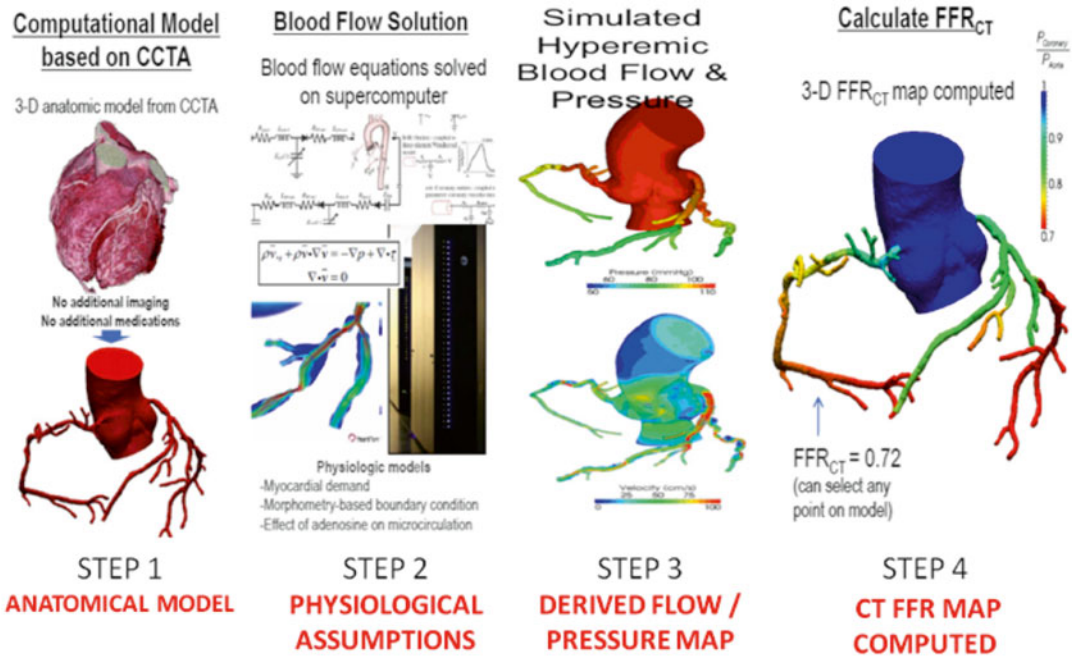

Fig. 12.12 Technique in derivation of CT FFR—Step 1: A three-dimensional model of the aortic root and coronary lumen is constructed using CTA images. Step 2: Assumptions are made regarding the properties of blood, basal total coronary flow, mean aortic pressure and total resistance coronary resistance. Step 3: Using a supercomputer, three dimensional models throughout the cardiac cycle representing the pressure and flow along all points of the arteries are generated during rest and simulated maximal hyperaemic conditions. Step 4: Based on the approximated pressure measurements, a non-invasive FFR based on CT is derived. (Adapted from [59] and [61])

compared with 4 (0.5 %) of the 820 patients without positive remodelling or LAP. None of the 167 patients with normal angiograms sustained acute events ($p<0.001$). Both features were independent predictors of acute coronary events (hazard ratio = 23, 95 % confidence interval 7–75, $p<0.001$). Furthermore analyses of more than 10,000 coronary segments demonstrated significantly greater LAP volume (3.2 ± 0.5 mm^3 vs. 0.5 ± 0.2 mm^3, $p<0.001$) and percent LAP/total plaque area (21.4 ± 3.7 % vs. 7.7 ± 1.5 %, $p<0.001$) in eventful plaques compared with those not associated with future ACS. Importantly the plaques associated with early ACS (0–12 months) when compared with late ACS (12–24 months) had larger LAP volume (4.7 ± 0.51 mm^3 vs. 2.0 ± 0.6 mm^3, $p<0.001$) and percent LAP/total plaque area (31.5 ± 4.5 % vs. 8.1 ± 5.2 %, $p<0.001$).

Rupture prone atherosclerotic plaques have histologically been described as thin-cap fibroatheroma (TCFA). These are distinguished by a large necrotic core with an overlying thin intact fibrous cap, macrophage infiltration and often increased number of intraplaque vasa vasorum [46]. Kashiwagi et al. compared optimal coherence tomography (OCT) and CT angiographic findings and proposed that a ring-like attenuation in a CT angiographic cross section may be a surrogate marker of TCFAs [43]. In this study of 100 patients presenting with either acute coronary event or stable angina, the coronary lesions were divided into a TCFA and a non-TCFA group based on OCT findings. CCTA-verified positive remodelling was observed more frequently in the TCFA (75 %) than in the non-TCFA group (30 %, $p<0.001$). The TCFA group also demonstrated LAP more frequently; CT attenuation value in the TCFA group (35 ± 32 HU) was significantly lower than the non-TCFA group (62 ± 34 HU, $p<0.001$). Notably a ring-like attenuation in the TCFA group was found to be 11-fold more frequent than in the non-TCFA group (44 % vs. 4 %, $p<0.001$).

CT to Monitor Plaque Progression

Schmid et al. studied non-calcified plaque progression in the left main and proximal left anterior descending arteries in 50 patients over 17 ± 6 months and demonstrated a significant increase in the amount of non-calcified plaque volume (91 ± 81 mm^3 to 115 ± 110 mm^3, with an annualised increase of 22 %), while statin use was not shown to significantly influence the mean annualised progression (20 ± 18 % with statins vs. 23.2 ± 28 % without statins, $p = 0.6$) [47]. Similarly Hamirani et al. found in a cohort of 60 patients a 3.7 ± 35 % reduction in non-calcified plaque, 4.8 ± 31.5 % decrease in mixed plaque while on statin therapy [48].

One study has evaluated utilisation of MDCT in detecting plaque progression in patients on statins. Brugstahler et al. in the New Age II pilot study demonstrated, following the commencement of lipid-lowering therapy over 1 year in men without established CAD, a significant decrease in mean non-calcified plaque volume from 42 ± 29 mm^3 to 30 ± 14 mm^3 (24 %, $p < 0.05$) [49]. These studies, while small in number, support the potential feasibility in the use of CT coronary angiography to measure coronary plaque progression and regression.

Assessment of the Haemodynamic Significance of Coronary Atherosclerosis

While CCTA accurately assesses coronary plaque and stenosis, in its current form, it remains limited in assessing the haemodynamic significance of coronary stenosis when compared with nuclear stress myocardial perfusion imaging [50] or the gold standard reference for vessel-specific ischaemia-fractional flow reserve (FFR) (Fig. 12.13) [51, 52]. Notably CCTA lacks specificity and positive predictive value for vessel-specific ischaemia which has been described to range from 48 to 78 % and 46 to 77 %. This is particularly important in the management of stable CAD as the functional significance of coronary stenoses determines clinical prognosis and need for revascularisation [53–55].

Recently three novel techniques have been demonstrated to accurately detect vessel-specific ischaemia using the gold standard reference of invasive FFR, which may broaden the future use of CT to assess both coronary anatomy and ischaemia in a single examination [56–59]. These techniques include (1) the prediction of a non-invasive fractional flow reserve (CT FFR) upon

Author	Yr	N	Per vessel prevalence (%)	Sensitivity (%)	Specificity (%)	PPV (%)	NPV (%)
Meijboom et al (51)	'08	79	18	94	48	49	93
Sarno et al (52)	'09	81	31	79	64	46	88
Koo et al (59)	'11	103	37	91	40	47	89
Bamberg et al (67)	'11	33	30	100	51	47	100
Ko et al (56)	'12	42	51	93	60	68	90
Ko et al (66)	'12	40	33	95	68	77	93
Wong et al (58)	13	53	38	94	66	64	94
Bettencourt et al (57)	'13	101	24	95	67	48	97

Fig. 12.13 Per-vessel diagnostic accuracy of CCTA to detect vessel-specific ischaemia using FFR as reference standard (*PPV* positive predictive value, *NPV* negative predictive value)

applying computational fluid dynamics on CCTA images, (2) the assessment of the transluminal attenuation gradient (TAG) across coronary lesions and (3) the use of CT myocardial perfusion imaging (CTP) acquired during vasodilator stress. The first two techniques can be conveniently applied on resting CCTA images, while CTP requires a separate CT scan in addition to resting CCTA which would require added radiation exposure and contrast usage.

CT FFR

CT FFR or non-invasive FFR is derived by applying computational fluid dynamics to CCTA vessel data (Fig. 12.12) [60, 61]. A three-dimensional model of the aortic root and coronary lumen is first constructed using CTA images. Assumptions are made regarding the properties of blood assuming a constant viscosity, basal total coronary flow based on the total myocardial mass derived on CT, mean aortic pressure which matches the mean brachial pressure and total resistance coronary resistance which is inversely related to the luminal diameter [60]. Using a supercomputer, three dimensional models throughout the cardiac cycle representing the pressure and flow along all points of the arteries are generated during rest and simulated maximal hyperaemic conditions. Based on the approximated pressure measurements, a non-invasive FFR based on CT is derived. Its major advantage is that it can be performed without additional image reconstruction, acquisition or administration of medications. Currently the technique requires 5 h of processing time.

In a multicentre, prospective cohort of 159 vessels in 103 patients, Koo et al. demonstrated that CT FFR, using a threshold of ≤0.8, detected FFR-significant (≤0.8) stenoses with a sensitivity of 84 % and specificity of 82 % [59]. Overall there was a good correlation between CT FFR and FFR ($r=0.72$, $p<0.001$) and the area under the ROC curve (AUC) was 0.90, which was significantly higher than CTA alone (0.70, $p<0.0001$) (Fig. 12.14). A similar improvement in ROC curve was reported when the same investigators repeated the study in a larger multicentre

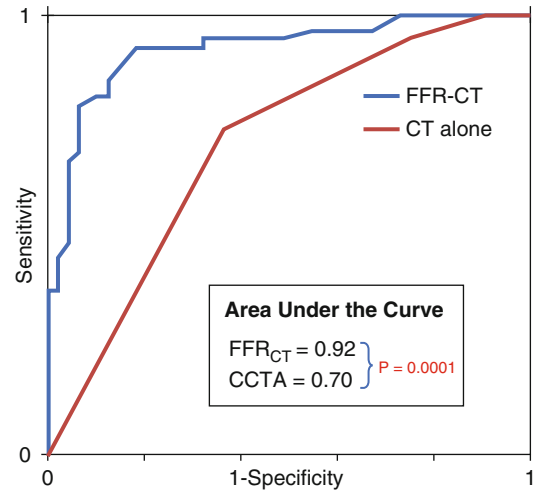

Fig. 12.14 Per-patient diagnostic accuracy of CT FFR compared with CCTA alone (Adapted from Koo BK, Erglis A, Doh JH et al. Diagnosis of ischemia-causing coronary stenoses by noninvasive fractional flow reserve computed from coronary computed tomographic angiograms. Results from the prospective multicenter DISCOVER-FLOW (Diagnosis of Ischemia-Causing Stenoses Obtained Via Noninvasive Fractional Flow Reserve) study. J Am Coll Cardiol 2011;58:1989–97. With permission from Elsevier)

prospective cohort of 285 patients (CTA AUC = 0.68 vs. FFR CT AUC = 0.81, $p<0.001$). The technique was found to have 90 % sensitivity and 54 % specificity for FFR ≤0.8, with an overall accuracy of 67 % [62].

Transluminal Attenuation Gradient

TAG is defined as the linear regression coefficient between intraluminal attenuation (Hounsfeld units) and axial distance. TAG evaluates the slope of decline in intraluminal contrast attenuation from the ostium to the distal coronary vessel (Fig. 12.15). Choi et al. demonstrated that in a cohort of 127 patients (370 vessels) with multivessel disease, TAG performed on resting CTA was significantly lower in occluded vessels compared to those with lesions of 0–49 % stenosis on QCA (−13.46 ± 9.59 HU/10 mm vs. −2.37 ± 4.67 HU/10 mm, $p<0.001$) [63]. The addition of TAG to the interpretation of CTA improved diagnostic accuracy for anatomical

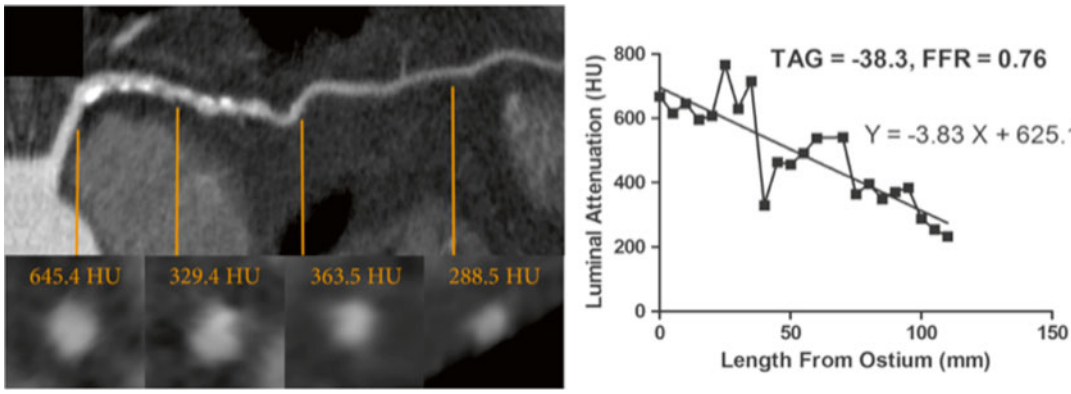

Fig. 12.15 Transluminal attenuation gradient. Left anterior descending artery with significant obstructive plaque burden imaged by CCTA. Axial and representative cross-sectional views with corresponding luminal attenuation (HU) of CCTA. *Black square dots* represent 5 mm intervals at which intraluminal attenuation (HU) was measured. TAG was −38.3, and the FFR was 0.76 (Adapted from Wong DT, Ko BS, Cameron JD et al. Transluminal Attenuation Gradient in Coronary Computed Tomography Angiography Is a Novel Noninvasive Approach to the Identification of Functionally Significant Coronary Artery Stenosis: A Comparison With Fractional Flow Reserve. Journal of the American College of Cardiology 2013 Mar 26;61(12):1271–9. With permission from Elsevier)

stenosis severity ($p=0.001$), especially in vessels with calcified lesions and provided a net reclassification improvement of 0.095 [63]. As the 320-detector row scanner allows isophasic, single beat imaging of entire coronary tree, it was postulated that it would be the ideal platform for TAG assessment. The accuracy and incremental value of TAG derived using resting CTA images to predict the haemodynamic significance of CAD on a 320-detector row scanner has been evaluated by Wong et al. in a cohort of 53 stable CAD patients who demonstrated that TAG assessed in FFR-significant vessels was significantly lower than that found in FFR non-significant vessels (−21 vs. −11 HU/10 mm, $p<0.001$) [58]. Using a retrospectively determined TAG320 cut-off of −15.1 HU/10 mm, TAG320 was reported to predict FFR ≤ 0.8 with 77 % sensitivity and 74 % specificity. Importantly the AUC for the combined use of TAG320 and CCTA was 0.88.

CT Stress Myocardial Perfusion Imaging

Myocardial perfusion imaging on CT is the acquisition of images during first pass of iodinated contrast from the arteries into the myocardium. This can be performed during rest as well as during vasodilator stress. In the absence of artefacts, hypoattenuated areas in the myocardium on CT represent areas of reduced perfusion (Fig. 12.16).

CT stress perfusion imaging (CTP) has been evaluated in numerous single centre studies to date (Fig. 12.13). The sensitivity ranges from 71 to 100 % and specificity from 72 to 98 % depending on scanner type and studied population when compared with SPECT-MPI, MRI perfusion imaging and invasive FFR. In 2005, Kurata et al. were the first to demonstrate a high agreement (83 %) between rest and stress adenosine CTP and stress thallium SPECT-MPI in 12 patients with suspected CAD using 16-detector helical MDCT and retrospective ECG gating [64]. Subsequently, George et al. reported performance of CTP on 40 patients with a history of abnormal SPECT-MPI who underwent stress CTP, using a 64 ($n=24$)- and 256 ($n=16$)-detector CT [65]. Combined use of rest CTA and stress CTP was found to be 81 % sensitive and 85 % specific for identifying vessels territories with a ≥50 % stenosis on QCA and with an associated perfusion defect on SPECT.

Four studies thus far have compared CTP with FFR, all demonstrating that the use of CTP

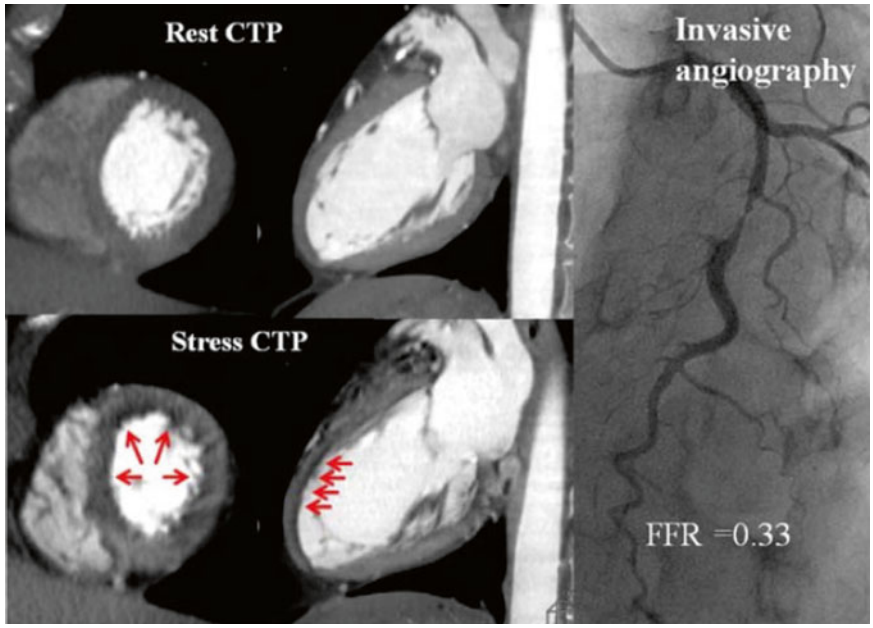

Fig. 12.16 CT perfusion imaging and invasive angiography. Stress perfusion defects are demonstrated on CT in the mid and distal anterior wall corresponding to a severe stenosis in the mid LAD associated with an FFR of 0.33 (Adapted from Ko BS, Cameron JD, Meredith IT et al. Computed tomography stress myocardial perfusion imaging in patients considered for revascularization: a comparison with fractional flow reserve. Eur Heart J 2012;33:67–77. With permission from Oxford University Press)

provided incremental diagnostic accuracy when added to CCTA alone by increasing the specificity and positive predictive value for FFR-significant stenoses [56, 57, 66, 67]. This may be achieved using narrow detector scanners (64 MDCT) [57], wide-detector scanners [56, 66] and dual source multidetector CT [67].

Recently we demonstrated in a prospective cohort of 40 patients including 120 vessels with suspected CAD who were evaluated using 320-detector CT that CTA detected FFR-significant stenoses (≤0.8) with 95 % sensitivity and 78 % specificity [66]. The additional use of CTP increased the per-vessel specificity to 95 % while sensitivity was maintained at 87 %. The combined use of CTA and CTP was associated with an increase in the ROC AUC from 0.93 vs. 0.85 using CTA alone ($p = 0.0003$). Similarly Bettencourt et al. demonstrate that this may be achieved using 64-detector CT [57]. In a cohort of 101 patients with suspected CAD, the combined protocol improved diagnostic accuracy for FFR ≤ 0.8 from 78 % using CCTA alone to 85 %, which was non-inferior to the accuracy of MR perfusion imaging of 88 % which was performed on the same cohort (Fig. 12.17).

Concluding Remarks

Coronary CT offers a robust and non-invasive method to qualitatively and quantitatively assess coronary atherosclerosis with high reproducibility and accuracy. Over the past decade, the advances in scanner technology, image acquisition and reconstruction techniques have resulted in much lower radiation and facilitated a broader use of coronary CT from assessment of the anatomical sequelae of atherosclerotic plaque to assessment of the haemodynamic significance of atherosclerotic plaque and the prediction of clinical outcomes based on CT-derived plaque morphology, characteristics and burden.

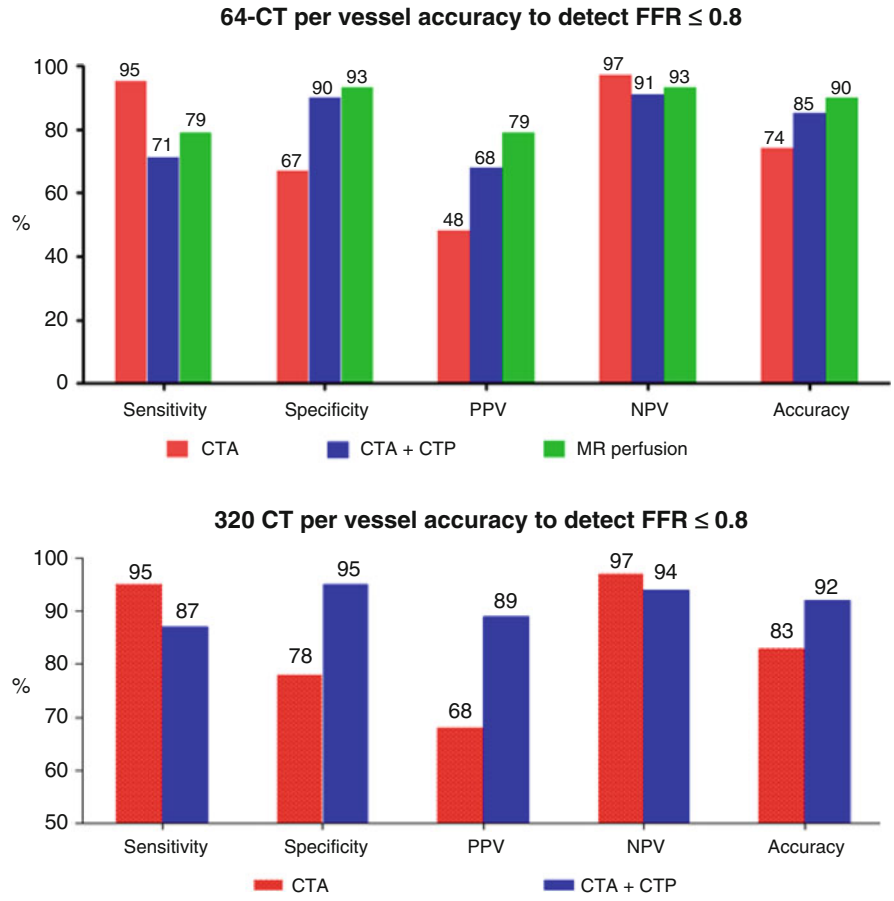

Fig. 12.17 Per-vessel diagnostic accuracy of 64- and 320-detector CCTA, CCTA + CTP and MR perfusion using fractional flow reserve as reference standard (Adapted from [57] and [66])

References

1. Roger VL, Go AS, Lloyd-Jones DM, et al. Heart disease and stroke statistics–2012 update: a report from the American Heart Association. Circulation. 2012; 125:e2–220.
2. Stone GW, Maehara A, Lansky AJ, et al. A prospective natural-history study of coronary atherosclerosis. N Engl J Med. 2011;364:226–35.
3. Abbara S, Arbab-Zadeh A, Callister TQ, et al. SCCT guidelines for performance of coronary computed tomographic angiography: a report of the Society of Cardiovascular Computed Tomography Guidelines Committee. J Cardiovasc Comput Tomogr. 2009;3:1 90–204.
4. Miller JM, Rochitte CE, Dewey M, et al. Diagnostic performance of coronary angiography by 64-row CT. N Engl J Med. 2008;359:2324–36.
5. Meijboom WB, Meijs MF, Schuijf JD, et al. Diagnostic accuracy of 64-slice computed tomography coronary angiography: a prospective, multicenter, multivendor study. J Am Coll Cardiol. 2008;52:2135–44.
6. Budoff MJ, Dowe D, Jollis JG, et al. Diagnostic performance of 64-multidetector row coronary computed tomographic angiography for evaluation of coronary artery stenosis in individuals without known coronary artery disease: results from the prospective multicenter ACCURACY (Assessment by Coronary Computed Tomographic Angiography of Individuals Undergoing Invasive Coronary Angiography) trial. J Am Coll Cardiol. 2008;52: 1724–32.
7. Achenbach S. Cardiac CT: state of the art for the detection of coronary arterial stenosis. J Cardiovasc Comput Tomogr. 2007;1:3–20.
8. Chun EJ, Lee W, Choi YH, et al. Effects of nitroglycerin on the diagnostic accuracy of electrocardiogram-gated coronary computed tomography angiography. J Comput Assist Tomogr. 2008;32:86–92.
9. Bischoff B, Hein F, Meyer T, et al. Impact of a reduced tube voltage on CT angiography and radiation dose:

results of the PROTECTION I study. JACC Cardiovasc Imaging. 2009;2:940–6.
10. Hausleiter J, Meyer T, Hermann F, et al. Estimated radiation dose associated with cardiac CT angiography. JAMA. 2009;301:500–7.
11. Chen MY, Shanbhag SM, Arai AE. Submillisievert median radiation dose for coronary angiography with a second-generation 320-detector row CT scanner in 107 consecutive patients. Radiology. 2013;267:76–85.
12. Achenbach S, Marwan M, Ropers D, et al. Coronary computed tomography angiography with a consistent dose below 1 mSv using prospectively electrocardiogram-triggered high-pitch spiral acquisition. Eur Heart J. 2010;31:340–6.
13. Leipsic J, Labounty TM, Heilbron B, et al. Estimated radiation dose reduction using adaptive statistical iterative reconstruction in coronary CT angiography: the ERASIR study. AJR Am J Roentgenol. 2010;195: 655–60.
14. Raff GL, Abidov A, Achenbach S, et al. SCCT guidelines for the interpretation and reporting of coronary computed tomographic angiography. J Cardiovasc Comput Tomogr. 2009;3:122–36.
15. Schuetz GM, Zacharopoulou NM, Schlattmann P, Dewey M. Meta-analysis: noninvasive coronary angiography using computed tomography versus magnetic resonance imaging. Ann Intern Med. 2010;152: 167–77.
16. Fihn SD, Gardin JM, Abrams J, et al. 2012 ACCF/AHA/ACP/AATS/PCNA/SCAI/STS Guideline for the diagnosis and management of patients with stable ischemic heart disease: a report of the American College of Cardiology Foundation/American Heart Association Task Force on Practice Guidelines, and the American College of Physicians, American Association for Thoracic Surgery, Preventive Cardiovascular Nurses Association, Society for Cardiovascular Angiography and Interventions, and Society of Thoracic Surgeons. J Am Coll Cardiol. 2012;60:e44–164.
17. Montalescot G, Sechtem U, Achenbach S, et al. ESC guidelines on the management of stable coronary artery disease: The Task Force on the management of stable coronary artery disease of the European Society of Cardiology. Eur Heart J. 2013;2013.
18. Taylor AJ, Cerqueira M, Hodgson JM et al. ACCF/SCCT/ACR/AHA/ASE/ASNC/NASCI/SCAI/SCMR 2010 Appropriate Use Criteria for Cardiac Computed Tomography. A Report of the American College of Cardiology Foundation Appropriate Use Criteria Task Force, the Society of Cardiovascular Computed Tomography, the American College of Radiology, the American Heart Association, the American Society of Echocardiography, the American Society of Nuclear Cardiology, the North American Society for Cardiovascular Imaging, the Society for Cardiovascular Angiography and Interventions, and the Society for Cardiovascular Magnetic Resonance. J Cardiovasc Comput Tomogr. 2010;4:407.e1–33.
19. Pflederer T, Schmid M, Ropers D, et al. Interobserver variability of 64-slice computed tomography for the quantification of non-calcified coronary atherosclerotic plaque. Rofo. 2007;179:953–7.
20. Rinehart S, Vazquez G, Qian Z, Murrieta L, Christian K, Voros S. Quantitative measurements of coronary arterial stenosis, plaque geometry, and composition are highly reproducible with a standardized coronary arterial computed tomographic approach in high-quality CT datasets. J Cardiovasc Comput Tomogr. 2011;5:35–43.
21. Lehman SJ, Schlett CL, Bamberg F, et al. Assessment of coronary plaque progression in coronary computed tomography angiography using a semiquantitative score. JACC Cardiovasc Imaging. 2009;2:1262–70.
22. Voros S, Rinehart S, Qian Z, et al. Coronary atherosclerosis imaging by coronary CT angiography: current status, correlation with intravascular interrogation and meta-analysis. JACC Cardiovasc Imaging. 2011;4:537–48.
23. Otsuka M, Bruining N, Van Pelt NC, et al. Quantification of coronary plaque by 64-slice computed tomography: a comparison with quantitative intracoronary ultrasound. Invest Radiol. 2008;43: 314–21.
24. Voros S, Rinehart S, Qian Z, et al. Prospective validation of standardized, 3-dimensional, quantitative coronary computed tomographic plaque measurements using radiofrequency backscatter intravascular ultrasound as reference standard in intermediate coronary arterial lesions: results from the ATLANTA (assessment of tissue characteristics, lesion morphology, and hemodynamics by angiography with fractional flow reserve, intravascular ultrasound and virtual histology, and noninvasive computed tomography in atherosclerotic plaques) I study. JACC Cardiovasc Interv. 2011; 4:198–208.
25. Nakazato R, Shalev A, Doh JH, et al. Aggregate plaque volume by coronary computed tomography angiography is superior and incremental to luminal narrowing for diagnosis of ischemic lesions of intermediate stenosis severity. J Am Coll Cardiol. 2013; 62:460–7.
26. Cheng VY, Nakazato R, Dey D, et al. Reproducibility of coronary artery plaque volume and composition quantification by 64-detector row coronary computed tomographic angiography: an intraobserver, interobserver, and interscan variability study. J Cardiovasc Comput Tomogr. 2009;3:312–20.
27. Hachamovitch R, Di Carli MF. Methods and limitations of assessing new noninvasive tests: Part II: outcomes-based validation and reliability assessment of noninvasive testing. Circulation. 2008;117:2793–801.
28. Min JK, Shaw LJ, Devereux RB, et al. Prognostic value of multidetector coronary computed tomographic angiography for prediction of all-cause mortality. J Am Coll Cardiol. 2007;50:1161–70.
29. Hulten EA, Carbonaro S, Petrillo SP, Mitchell JD, Villines TC. Prognostic value of cardiac computed

tomography angiography: a systematic review and meta-analysis. J Am Coll Cardiol. 2011;57:1237–47.
30. Min JK, Dunning A, Lin FY, et al. Age- and sex-related differences in all-cause mortality risk based on coronary computed tomography angiography findings results from the International Multicenter CONFIRM (Coronary CT Angiography Evaluation for Clinical Outcomes: An International Multicenter Registry) of 23,854 patients without known coronary artery disease. J Am Coll Cardiol. 2011;58:849–60.
31. Chow BJ, Small G, Yam Y, et al. Incremental prognostic value of cardiac computed tomography in coronary artery disease using CONFIRM: COroNary computed tomography angiography evaluation for clinical outcomes: an InteRnational Multicenter registry. Circ Cardiovasc Imaging. 2011;4:463–72.
32. Hadamitzky M, Achenbach S, Al-Mallah M, et al. Optimized Prognostic Score for Coronary Computed Tomographic Angiography: Results From the CONFIRM Registry (COronary CT Angiography EvaluatioN For Clinical Outcomes: An InteRnational Multicenter Registry). J Am Coll Cardiol. 2013;62: 468–76.
33. Wilson PW, D'Agostino RB, Levy D, Belanger AM, Silbershatz H, Kannel WB. Prediction of coronary heart disease using risk factor categories. Circulation. 1998;97:1837–47.
34. Metz LD, Beattie M, Hom R, Redberg RF, Grady D, Fleischmann KE. The prognostic value of normal exercise myocardial perfusion imaging and exercise echocardiography: a meta-analysis. J Am Coll Cardiol. 2007;49:227–37.
35. Lin FY, Shaw LJ, Dunning AM, et al. Mortality risk in symptomatic patients with nonobstructive coronary artery disease: a prospective 2-center study of 2,583 patients undergoing 64-detector row coronary computed tomographic angiography. J Am Coll Cardiol. 2011;58:510–9.
36. Versteylen MO, Kietselaer BL, Dagnelie PC, et al. Additive value of semiautomated quantification of coronary artery disease using cardiac computed tomographic angiography to predict future acute coronary syndrome. J Am Coll Cardiol. 2013;61:2296–305.
37. Henneman MM, Schuijf JD, Pundziute G, et al. Noninvasive evaluation with multislice computed tomography in suspected acute coronary syndrome: plaque morphology on multislice computed tomography versus coronary calcium score. J Am Coll Cardiol. 2008;52:216–22.
38. Hammer-Hansen S, Kofoed KF, Kelbaek H, et al. Volumetric evaluation of coronary plaque in patients presenting with acute myocardial infarction or stable angina pectoris-a multislice computerized tomography study. Am Heart J. 2009;157:481–7.
39. Motoyama S, Kondo T, Sarai M, et al. Multislice computed tomographic characteristics of coronary lesions in acute coronary syndromes. J Am Coll Cardiol. 2007;50:319–26.
40. Pflederer T, Marwan M, Schepis T, et al. Characterization of culprit lesions in acute coronary syndromes using coronary dual-source CT angiography. Atherosclerosis. 2010;211:437–44.
41. Imazeki T, Sato Y, Inoue F, et al. Evaluation of coronary artery remodeling in patients with acute coronary syndrome and stable angina by multislice computed tomography. Circ J. 2004;68:1045–50.
42. Tanaka A, Shimada K, Yoshida K, et al. Non-invasive assessment of plaque rupture by 64-slice multidetector computed tomography–comparison with intravascular ultrasound. Circ J. 2008;72:1276–81.
43. Kashiwagi M, Tanaka A, Kitabata H, et al. Feasibility of noninvasive assessment of thin-cap fibroatheroma by multidetector computed tomography. JACC Cardiovasc Imaging. 2009;2:1412–9.
44. Madder RD, Chinnaiyan KM, Marandici AM, Goldstein JA. Features of disrupted plaques by coronary computed tomographic angiography: correlates with invasively proven complex lesions. Circ Cardiovasc Imaging. 2011;4:105–13.
45. Motoyama S, Sarai M, Harigaya H, et al. Computed tomographic angiography characteristics of atherosclerotic plaques subsequently resulting in acute coronary syndrome. J Am Coll Cardiol. 2009;54:49–57.
46. Virmani R, Burke AP, Farb A, Kolodgie FD. Pathology of the vulnerable plaque. J Am Coll Cardiol. 2006; 47:C13–8.
47. Schmid M, Achenbach S, Ropers D, et al. Assessment of changes in non-calcified atherosclerotic plaque volume in the left main and left anterior descending coronary arteries over time by 64-slice computed tomography. Am J Cardiol. 2008;101:579–84.
48. Hamirani YS, Kadakia J, Pagali SR, et al. Assessment of progression of coronary atherosclerosis using multidetector computed tomography angiography (MDCT). Int J Cardiol. 2011;149:270–4.
49. Burgstahler C, Reimann A, Beck T, et al. Influence of a lipid-lowering therapy on calcified and noncalcified coronary plaques monitored by multislice detector computed tomography: results of the New Age II Pilot Study. Invest Radiol. 2007;42:189–95.
50. Hachamovitch R, Di Carli MF. Nuclear cardiology will remain the "gatekeeper" over CT angiography. J Nucl Cardiol. 2007;14:634–44.
51. Meijboom WB, Van Mieghem CA, van Pelt N, et al. Comprehensive assessment of coronary artery stenoses: computed tomography coronary angiography versus conventional coronary angiography and correlation with fractional flow reserve in patients with stable angina. J Am Coll Cardiol. 2008;52:636–43.
52. Sarno G, Decraemer I, Vanhoenacker PK, et al. On the inappropriateness of noninvasive multidetector computed tomography coronary angiography to trigger coronary revascularization: a comparison with invasive angiography. JACC Cardiovasc Interv. 2009;2:550–7.
53. Tonino PA, De Bruyne B, Pijls NH, et al. Fractional flow reserve versus angiography for guiding percutaneous coronary intervention. N Engl J Med. 2009; 360:213–24.
54. De Bruyne B, Pijls NH, Kalesan B, et al. Fractional flow reserve-guided PCI versus medical therapy in

stable coronary disease. N Engl J Med. 2012;367: 991–1001.
55. Hachamovitch R, Berman DS, Kiat H, et al. Incremental prognostic value of adenosine stress myocardial perfusion single-photon emission computed tomography and impact on subsequent management in patients with or suspected of having myocardial ischemia. Am J Cardiol. 1997;80:426–33.
56. Ko BS, Cameron JD, Meredith IT, et al. Computed tomography stress myocardial perfusion imaging in patients considered for revascularization: a comparison with fractional flow reserve. Eur Heart J. 2012; 33:67–77.
57. Bettencourt N, Chiribiri A, Schuster A, et al. Direct comparison of cardiac magnetic resonance and multidetector computed tomography stress-rest perfusion imaging for detection of coronary artery disease. J Am Coll Cardiol. 2013;61:1099–107.
58. Wong DT, Ko BS, Cameron JD, et al. Transluminal attenuation gradient in coronary computed tomography angiography is a novel noninvasive approach to the identification of functionally significant coronary artery stenosis: a comparison with fractional flow reserve. J Am Coll Cardiol. 2013;61(12):1271–9.
59. Koo BK, Erglis A, Doh JH, et al. Diagnosis of ischemia-causing coronary stenoses by noninvasive fractional flow reserve computed from coronary computed tomographic angiograms. Results from the prospective multicenter DISCOVER-FLOW (Diagnosis of Ischemia-Causing Stenoses Obtained Via Noninvasive Fractional Flow Reserve) study. J Am Coll Cardiol. 2011;58:1989–97.
60. Taylor CA, Fonte TA, Min JK. Computational fluid dynamics applied to cardiac computed tomography for noninvasive quantification of fractional flow reserve: scientific basis. J Am Coll Cardiol. 2013;61:2233–41.
61. Min JK, Berman DS, Budoff MJ, et al. Rationale and design of the DeFACTO (Determination of Fractional Flow Reserve by Anatomic Computed Tomographic AngiOgraphy) study. J Cardiovasc Comput Tomogr. 2011;5:301–9.
62. Min JK, Leipsic J, Pencina MJ, et al. Diagnostic accuracy of fractional flow reserve from anatomic CT angiography. JAMA. 2012;308(12):1237–45.
63. Choi JH, Min JK, Labounty TM, et al. Intracoronary transluminal attenuation gradient in coronary CT angiography for determining coronary artery stenosis. JACC Cardiovasc Imaging. 2011;4:1149–57.
64. Kurata A, Mochizuki T, Koyama Y, et al. Myocardial perfusion imaging using adenosine triphosphate stress multi-slice spiral computed tomography: alternative to stress myocardial perfusion scintigraphy. Circ J. 2005;69:550–7.
65. George RT, Arbab-Zadeh A, Miller JM, et al. Adenosine stress 64- and 256-row detector computed tomography angiography and perfusion imaging: a pilot study evaluating the transmural extent of perfusion abnormalities to predict atherosclerosis causing myocardial ischemia. Circ Cardiovasc Imaging. 2009; 2:174–82.
66. Ko BS, Cameron JD, Leung M, et al. Combined CT coronary angiography and stress myocardial perfusion imaging for hemodynamically significant stenoses in patients with suspected coronary artery disease: a comparison with fractional flow reserve. JACC Cardiovasc Imaging. 2012;5: 1097–111.
67. Bamberg F, Becker A, Schwarz F, et al. Detection of hemodynamically significant coronary artery stenosis: incremental diagnostic value of dynamic CT-based myocardial perfusion imaging. Radiology. 2011;260: 689–98.

13 Emerging Role of Magnetic Resonance Imaging in the Evaluation of Coronary Atherosclerosis

Govind Srinivasan and Joseph B. Selvanayagam

Introduction

Atherosclerotic coronary artery disease (CAD) is the leading cause of death and disability in the developed world [1]. Since the seminal observation of Mason Sones in 1958 [2], cardiac catheterisation has been the cornerstone of CAD diagnosis. However, X-ray coronary angiography (XCA) is invasive and associated with a small risk of serious cardiac and non-cardiac complications. Moreover, whilst XCA affords high temporal and spatial resolution imaging of luminal narrowing, it is suboptimal at visualising changes in the coronary artery vessel wall, where the *earliest* changes of atherosclerosis takes place [3]. Therefore, a non-invasive alternative to XCA would be preferable to assess the significant number of patients suspected to have CAD. Both coronary computed tomography angiography (CCTA) and magnetic resonance coronary angiography (MRCA) have emerged in recent years as viable non-invasive imaging modalities to visualise the coronary artery lumen and the vessel wall [4]. In this chapter we will focus on the role of MRCA in coronary atherosclerotic assessment.

G. Srinivasan, MBBS, FRACP
Department of Medicine, Flinders University,
Flinders Medical Centre,
No. 1, Flinders Drive, Bedford Park,
Adelaide, SA 5042, Australia

J.B. Selvanayagam, MBBS (Hons), FCACP, FRACP, DPhil, FCSANZ, FESC (✉)
Department of Cardiovascular Medicine,
Flinders University, Flinders Medical Centre,
Flinders Drive, Bedford Park,
Adelaide, SA 5042, Australia
e-mail: joseph.selvanayagam@flinders.edu.au

Atherosclerotic Plaque Characterisation by MR

High-resolution magnetic resonance (MR) has emerged as a leading in vivo modality for atherosclerotic plaque characterisation given the inherent advantages of non-invasiveness and high spatial resolution. MR differentiates plaque components on the basis of biophysical and biochemical parameters such as chemical composition and concentration, water content, physical state, molecular motion, or diffusion.

Since detected MR signals rely on the relaxation times T1 and T2 and on proton density, the MR images can be "weighted" to the T1, T2, or proton density values through adaptation of the imaging parameters (such as repetition time and echo time). For example, in a T1-weighted (T1w) image, tissues with lower T1 values will produce pixels with high signal intensity. Conversely, tissues with a longer T2 relaxation time will appear hyperintense in a T2-weighted (T2w) image. In a proton density-weighted (PDW) image, the contrast relies mainly on the differences in density of water and fat protons within the tissue. This contrast is also referred to as intermediate-weighted, as it represents a combination of T1

S.J. Nicholls and T. Crowe (eds.), *Imaging Coronary Atherosclerosis*, Contemporary Cardiology,
DOI 10.1007/978-1-4939-0572-0_13, © Springer Science+Business Media New York 2014

and T2 contrast. Applying these different "weightings," one can produce maps with varying contrast of the same object [5]. This makes the MR method uniquely suitable for the assessment of the vascular wall [6]. Improvements in MR technology, including the development of high-sensitivity coils and faster imaging protocols, have allowed the study of atherosclerotic plaques using multi-contrast (T1w, T2w, and PDW) MR imaging [7]. MR imaging has been used for the study of atherosclerotic plaque in the human aorta [8], carotid arteries [9, 10], and in peripheral arteries [11]. Successful MR imaging of the coronary artery wall has been performed [12], but is technically demanding due to the small size and highly tortuous course of the coronaries. Additionally, to obtain artefact-free images, cardiac and respiratory motion must be reliably suppressed. Use of navigator echoes accounts for any cardiac or diaphragmatic motion, allows visualisation of the coronary wall in a time-efficient way without the need for breath-holding [13].

MR Coronary Atherosclerosis Imaging: Technical Challenges

Even in the modern era, with fast and powerful gradients and image reconstruction capabilities, accurate and reproducible cardiovascular magnetic resonance (CMR) imaging of coronary arteries can be extremely challenging, requiring significant operator experience and expertise. MR coronary artery imaging requires techniques to ensure high signal-to-noise ratio and superior spatial resolution to delineate between the coronary lumen and surrounding structures. This is difficult to achieve when there is intrinsic cardiac and respiratory motion. Therefore image acquisition has to be electrocardiogram (ECG) triggered to synchronise with the cardiac cycle. The period of minimal cardiac motion is in end systole and mid diastole (immediately before atrial systole). The mid diastolic period has a longer acquisition window of 100–125 ms/cycle and higher blood flow but is limited by its sensitivity to heart rate variability. The resting period can be programmed to heart rate but is very variable in each individual and therefore has to be identified for each patient prior to the coronary scan. To reduce the effect of respiratory motion on the image quality, prospective real-time navigator techniques are employed in current practice. This involves monitoring the movement of the right dome of diaphragm in the cranio-caudal direction. Image data are accepted or rejected depending on the position of the diaphragm within the acceptable window. Reduction in the acceptance window minimises the motion artefact but prolongs the overall scan time. An acceptance window of 5 mm results in an efficiency close to 50 % [14–16].

Using the navigator technique, data can be acquired in free breathing mode and using 3D imaging which requires long acquisition periods. The 3D techniques provide increased signal-to-noise ratio and spatial resolution at the cost of reduced contrast between the blood in the coronary lumen and myocardium. Deploying the steady state free precession (SSFP) sequence improves intrinsic signal-to-noise ratio and the contrast between the blood and the myocardium in the 1.5 Tesla (T) system than in the 3 T magnet [17]. At 3 T and higher magnetic field strengths, it is preferable to use gradient echo techniques. Further enhancement in the contrast between the blood and the surrounding fat and myocardium can be achieved by applying the fat suppression and T2 preparation sequences. As T2 preparation pulse suppresses the signal from the deoxygenated blood imaging, the venous anatomy is not possible with this technique.

Using these sequences, images are acquired either by whole heart imaging or target volume imaging. The former approach images the entire heart in three different planes and allows for a three-dimensional reformatting along the course of the coronary vessels. Consequently the acquisition times are longer. The target volume imaging has shorter acquisition times as imaging is targeted to the left and right coronary arteries individually.

Contrast agents can be used to improve the delineation between the coronary lumen and the surrounding tissues. Contrast agents with weak albumin binding are preferred as they provide coronary imaging and scar imaging due to their

prolonged retention time in the blood [18]. This is important as CMR is expected to provide anatomical and tissue characterisation assessment at the same time. The T1 of the contrast containing blood is significantly lower than the myocardium and therefore a high degree of contrast between them is displayed.

Magnetic Resonance Coronary Angiography

Imaging coronary arteries using magnetic resonance has been reported since the late 1980s and early 1990s, when Edelman and colleagues reported feasibility of coronary imaging with a two-dimensional gradient echo pulse sequence and acquired 4 mm thick section of coronary arteries in a single breath hold [19]. Soon Manning et al. prospectively compared MRCA with XCA in 39 subjects [20]. They employed an ultrafast gradient echo sequence on a 1.5 T system in a single breath hold of up to 18 s. They reported a surprisingly high sensitivity and specificity of 90 % and 92 %, respectively, for identifying a stenosis of ≥50 %. Though sensitivity and specificity for left main coronary artery was excellent, it was lower for the other coronary arteries.

The main limitation was perceived to be the long breath holds and the subsequent development of navigator-corrected acquisitions was to overcome this barrier. This technique enabled respiratory gating by assessing the position of diaphragm and the heart during acquisitions, and enabled measurements during free breathing. High spatial resolution was achieved and acquisition times per cardiac cycle were reduced [14, 21–25]. Two-dimensional techniques are limited by poor overall signal-to-noise ratio and partial volume effects. The development of three-dimensional sequences enabled acquisition of the entire volume in a single breath hold and improved the signal-to-noise ratio as well [26]. To enhance the contrast between the coronary lumen and the surrounding tissues Botnar and colleagues developed T2 preparation pulses to suppress the signal from the myocardium (Figs. 13.1 and 13.2) [27].

The first multicentre prospective study comparing MRCA with XCA was conducted by Kim and colleagues in 1999 [28]. They enrolled 109 patients suspected to have CAD and performed MRCA and XCA. The authors used three-dimensional gradient

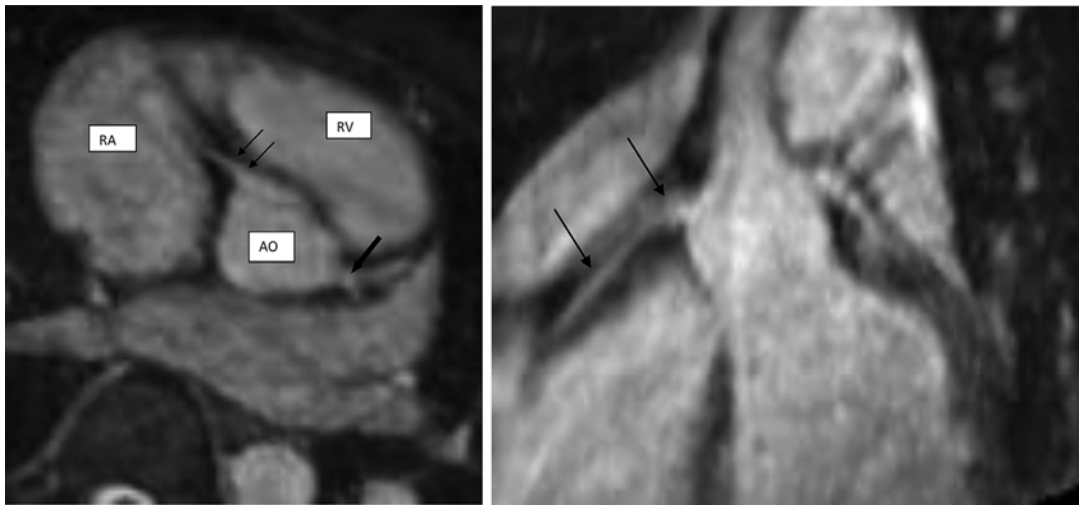

Fig. 13.1 (**a**) Axial view of proximal right coronary artery (*thin arrows*) and left coronary artery (*thick arrows*) acquired on 1.5 T system using the whole heart, navigator technique. *AO* Aorta, *RV* right ventricle, *RA* right atrium. (**b**) Coronal view of proximal right and left coronary arteries acquired on 1.5 T system using the whole heart, navigator technique

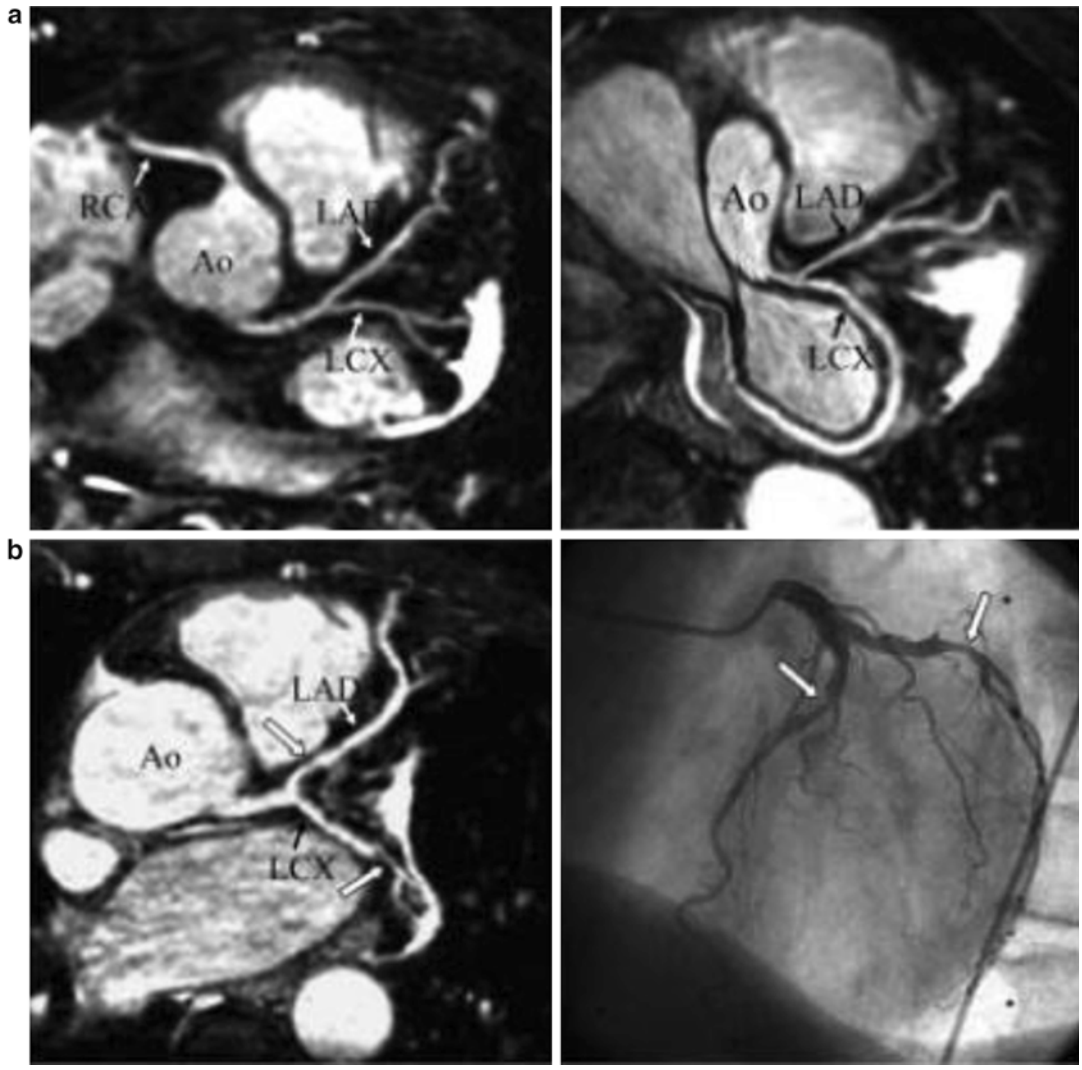

Fig. 13.2 (**a**) Multiplanar reformatted MRCA images of right and left coronary arteries with excellent visualisation of left anterior descending artery (LAD) and left circumflex artery (LCx) with their side branches. *Ao* Aorta, *RCA* right coronary artery (**b**) MRCA of patient with two-vessel disease (*left*) in comparison with X-ray coronary angiography (*right*). *Arrows* point to region of stenosis (Reprinted from Jahnke C, Paetsch I, Nehrke K, et al. Rapid and complete coronary arterial tree visualization with magnetic resonance imaging: feasibility and diagnostic performance. European Heart Journal 2005; 26:2313–2319. With permission from Oxford University Press)

echo sequences during free breathing for 10–15 min and applied the T2-weighted preparation pulse including the frequency selective fat saturation pre pulse. This study demonstrated high sensitivity and specificity for left main coronary disease and three-vessel coronary disease with 87 % accuracy. The specificity for any CAD was low at 42 %. The main limitation of this study was the limited coverage of the coronary system, and the prolonged nature of the examination with a mean scan time of 70 min. Yang and colleagues have reduced the acquisition time to 10 min in their study of 62 patients suspected with CAD. They performed contrast-enhanced whole heart MRCA on the 3 T system in 62 consecutive patients and compared with XCA. The sensitivity, specificity, and accuracy of MRCA for detecting significant stenosis were 94 %, 82 %, and 89 %, respectively [29]. More recently Yoon

and colleagues demonstrated the utility of whole heart MRCA in predicting future risk of cardiac events in patients suspected to have CAD. In their study of 207 patients suspected to have CAD with non-contrast-enhanced free breathing whole heart MRCA on the 1.5 T system, the annual cardiac event rate was 0.3 % in the group without significant stenosis and 6.3 % in the patients with >50 % stenosis on MRCA [30].

The whole heart MRCA approach has increased coverage and greatly reduced imaging time although has not greatly improved diagnostic accuracy. The incorporation of SSFP technique into the whole heart coronary magnetic resonance angiography (MRA) facilitated the visualisation of the middle and distal segments of the coronary arteries [31]. SSFP techniques achieve higher signal- and contrast to noise ratio of the coronary artery lumen against the surrounding myocardium. This sequence is used in most centres currently.

MRCA in Subclinical Coronary Atherosclerosis

Even before reduction in the coronary artery luminal diameter, the artery remodels by increasing wall thickness with preservation of luminal diameter (Glagov remodelling) [3]. This positive remodelling of the vessel wall has been demonstrated on intravascular ultrasound and multidetector computed tomography. Both these modalities have their limitations especially when serial assessment is required. Black blood imaging and improvement in spatial resolution techniques have made it possible to image the coronary artery wall using MR [32]. Fayad et al. were the first to demonstrate the feasibility of black blood fat suppressed magnetic resonance imaging in measuring the coronary wall thickness and visualise the remodelling of the coronary artery wall [12]. Desai and colleagues confirmed reproducibility of this technique and showed that this can be implemented in longitudinal studies of progression and regression of coronary atherosclerosis [33].

The MESA (Multi-Ethnic Study of Atherosclerosis) study assessed the coronary arterial remodelling as a marker of subclinical atherosclerosis using coronary wall MR in asymptomatic population-based cohort [34]. MRCA was performed on 179 subjects using the 3D whole heart navigator, ECG gated, and fat suppressed T2 preparation SSFP sequence in 1.5 T system. They detected positive remodelling in this asymptomatic cohort of men and women. Larger studies are required to assess the therapeutic implications of early detection of coronary atherosclerosis.

MRCA in Plaque Characterisation

Plaque characterisation has been demonstrated using delayed enhancement (DE) CMR imaging using contrast agents (Fig. 13.3). The demonstration of contrast enhancement in coronary atherosclerotic plaques correlated well with increase in severity of plaque calcification as confirmed on multi-slice computed tomography (MSCT) and luminal stenosis seen on coronary angiography, in patients with chronic stable angina [35]. Significant uptake of contrast has been demonstrated in the coronary plaques 6 days post-acute coronary syndrome, which have decreased on 3-month follow-up scans indicating inflammation in the plaque [36].

MRCA in Coronary Revascularisation

The use of intracoronary stents has increased significantly in the last decade. The clinical safety of the stents is well established in the 1.5 T even early after implantation [37–41]. The stents are non-ferromagnetic and are not susceptible to attractive forces or local heating. Though majority of the stents are approved for CMR assessment immediately after implantation their propensity to cause local signal void and susceptibility artefacts results in suboptimal assessment of in-stent disease.

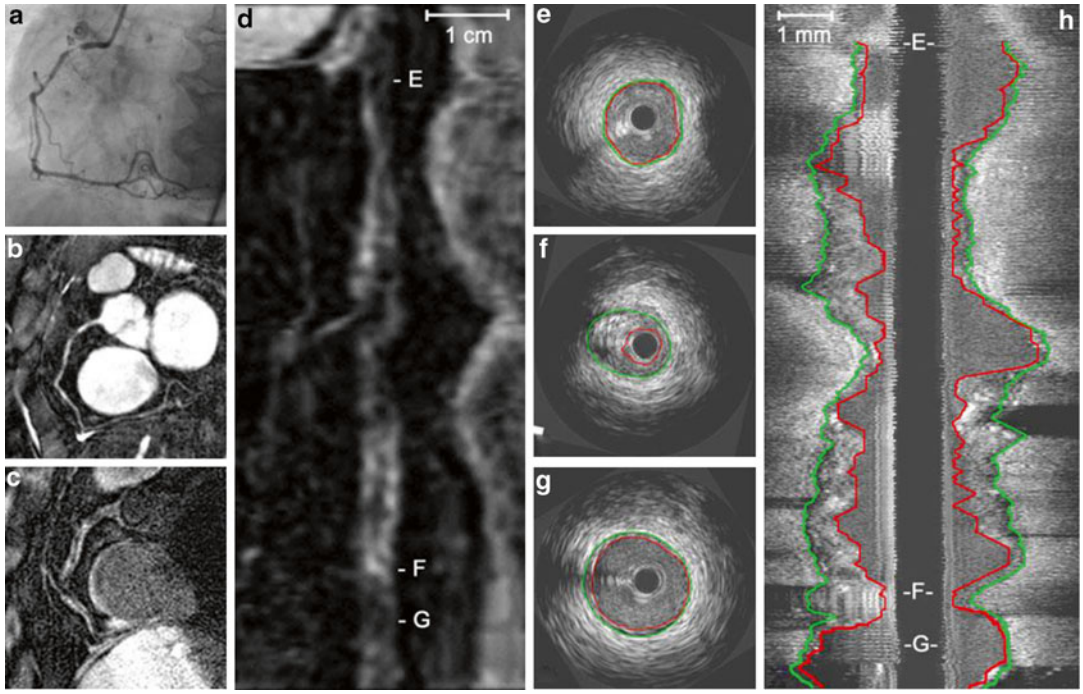

Fig. 13.3 A 61-year-old female patient with stable angina. X-ray angiography (**a**) and coronary MRA (**b**) demonstrate high-grade stenosis in the proximal RCA. (**c**) Corresponding MR vessel wall image demonstrate several areas with vessel wall thickening and high signal intensity. (**e**) (Distal RCA), (**f**) (diseased area) and (**g**) (proximal RCA) are cross-sectional IVUS images and refer to the corresponding areas as shown on stretched multiplanar reformation (MPR) of the vessel wall (**d**: **e**, **f**, **g**) and the longitudinal IVUS reformat (**h**: **e**, **f**, **g**). **f** is the area of maximum stenosis (Reprinted from Gerretsen S. Detection of coronary plaques using MR coronary vessel wall imaging: validation of findings with intravascular ultrasound. European Radiology (2013) 23:115–124. With permission from Springer Science + Business Media)

In contrast, coronary artery bypass grafts (CABG) are large calibre vessels with a predictable course and less influenced by cardiac motion. Therefore they would be ideal to image on MRCA. Langerak and colleagues studied 69 patients awaiting elective coronary angiography for assessment of chest pain post-CABG [42]. They underwent MRCA at baseline and stress flow mapping was performed. When compared to conventional angiography they reported a sensitivity and specificity of 96 and 92 %, respectively, for stenosis in the grafts of ≥70 %. The limitation in imaging the coronary bypass grafts is the susceptibility artefact and signal void created by the metallic clips at anastomotic sites.

Indications for MRCA

Despite advances in imaging techniques and higher field strength scanners, there is a paucity of large multicentre clinical trials in MRCA. Recently, Kato et al. in their 7 centres, Japanese MRCA trial imaged 138 patients with 3D navigator corrected SSFP whole heart MRCA sequence [43]. The average image time was under 10 min. Their results were modest with sensitivity of 88 %, specificity of 72 %, positive predictive value (PPV) of 71 %, and negative predictive value (NPV) of 88 %. Similar to earlier studies, they were able to exclude left main

Table 13.1 Comparison between MRCA and CCTA in the assessment of coronary arteries

MRCA	CCTA
Advantages	
• No exposure to ionising radiation	• Higher accuracy in excluding CAD
• Multi-parametric, functional assessment possible	• More widely available
• No need for oral or intravenous beta blocker	• Easier to perform
• No artefacts with severely calcified plaques	• Shorter scanning times
	• Relatively comfortable for patients
Disadvantages	
• Longer scanning time	• Exposure to radiation
• Restricted availability	• Need for iodinated contrast
• Contraindicated in patients with pacemaker/ intracardiac defibrillators/metallic implants	
Not ideal for claustrophobic patients	

coronary disease and three-vessel coronary disease with NPV of 99 %. When compared to recent multicentre CCTA studies, the NPV in the low pre-test probability of CAD group (<20 %) was similar and therefore may be a safe alternative to CCTA in this group of patients [44, 45]. In the relatively high pre-test probability group, MRCA was able to exclude significant disease in left main coronary artery and three-vessel coronary disease.

In a recent meta-analysis comparing CCTA and MRCA for ruling out clinically significant CAD in adults with suspected or known CAD, 89 and 20 studies, respectively, were eligible for analysis. There were 7,516 patients in the CCTA studies and 989 in the MRCA studies. Bivariate analysis of the data yielded a mean sensitivity and specificity of 97.2 and 87.4 for CCTA and 87.1 and 70.3 % for MRCA [46]. In patients who were suspected to have CAD, CCTA is more accurate in detecting and ruling out clinically relevant CAD (Table 13.1).

The current guidelines recommend MRCA for assessment of coronary anomalies (Class I) and for assessment of aorto CABG (Class II) [47]. MRCA has been proposed in conjunction with DE CMR to rule out ischaemic aetiology in patients with dilated cardiomyopathy [48].

Conclusion

Cardiac MR imaging has evolved significantly in the last two decades and has an established role in the assessment of cardiac anatomy, function, myocardial perfusion, and tissue characterisation. The addition of MRCA to CMR would add to its versatility and provide a safe, non-invasive comprehensive cardiac assessment tool. MRCA is still evolving in the assessment of coronary atherosclerosis and its full potential has not been realised yet. Large multicentre comparative studies and outcome studies in the subclinical detection of coronary atherosclerosis are needed to recommend routine use of this safe, non-invasive imaging modality.

References

1. Ford ES, Ajani UA, Croft JB, Critchley JA, Labarthe DR, Kottke TE, et al. Explaining the decrease in U.S. deaths from coronary disease, 1980–2000. N Engl J Med. 2007;356(23):2388–98.
2. Sones Jr FM. Results of open heart surgery with elective cardiac arrest by potassium citrate in patients with congenital and acquired heart disease. Dis Chest. 1958;34(3):299–316. Epub 1958/09/01.
3. Glagov S, Weisenberg E, Zarins CK, Stankunavicius R, Kolettis GJ. Compensatory enlargement of human

atherosclerotic coronary arteries. N Engl J Med. 1987;316(22):1371–5. Epub 1987/05/28.
4. Spuentrup E, Botnar RM. Coronary magnetic resonance imaging: visualization of the vessel lumen and the vessel wall and molecular imaging of arteriothrombosis. Eur Radiol. 2006;16(1):1–14. Epub 2005/09/01.
5. Fayad ZA, Fuster V. Clinical imaging of the high-risk or vulnerable atherosclerotic plaque. Circ Res. 2001;89(4):305–16.
6. Herfkens RJ, Higgins CB, Hricak H, Lipton MJ, Crooks LE, Sheldon PE, et al. Nuclear magnetic resonance imaging of atherosclerotic disease. Radiology. 1983;148(1):161–6.
7. Fayad ZA, Fuster V. Characterization of atherosclerotic plaques by magnetic resonance imaging. Ann N Y Acad Sci. 2000;902:173–86.
8. Fayad ZA, Nahar T, Fallon JT, Goldman M, Aguinaldo JG, Badimon JJ, et al. In vivo magnetic resonance evaluation of atherosclerotic plaques in the human thoracic aorta: a comparison with transesophageal echocardiography. Circulation. 2000;101(21):2503–9.
9. Yuan C, Beach KW, Smith Jr LH, Hatsukami TS. Measurement of atherosclerotic carotid plaque size in vivo using high resolution magnetic resonance imaging. Circulation. 1998;98(24):2666–71.
10. Wiesmann F, Robson MD, Francis JM, Petersen SE, Leeson CPM, Channon KM, et al. Visualization of the ruptured plaque by magnetic resonance imaging. Circulation. 2003;108:2542.
11. Coulden RA, Moss H, Graves MJ, Lomas DJ, Appleton DS, Weissberg PL. High resolution magnetic resonance imaging of atherosclerosis and the response to balloon angioplasty. Heart. 2000; 83(2):188–91.
12. Fayad ZA, Fuster V, Fallon JT, Jayasundera T, Worthley SG, Helft G, et al. Noninvasive in vivo human coronary artery lumen and wall imaging using black-blood magnetic resonance imaging. Circulation. 2000;102(5):506–10.
13. Botnar RM, Kim WY, Bornert P, Stuber M, Spuentrup E, Manning WJ. 3D coronary vessel wall imaging utilizing a local inversion technique with spiral image acquisition. Magn Reson Med. 2001;46(5):848–54.
14. Danias PG, McConnell MV, Khasgiwala VC, Chuang ML, Edelman RR, Manning WJ. Prospective navigator correction of image position for coronary MR angiography. Radiology. 1997;203(3):733–6. Epub 1997/06/01.
15. Danias PG, Stuber M, Botnar RM, Kissinger KV, Edelman RR, Manning WJ. Relationship between motion of coronary arteries and diaphragm during free breathing: lessons from real-time MR imaging. AJR Am J Roentgenol. 1999;172(4):1061–5. Epub 1999/12/10.
16. Nagel E, Bornstedt A, Schnackenburg B, Hug J, Oswald H, Fleck E. Optimization of realtime adaptive navigator correction for 3D magnetic resonance coronary angiography. Magn Reson Med. 1999;42(2):408–11. Epub 1999/08/10.
17. Deshpande VS, Shea SM, Laub G, Simonetti OP, Finn JP, Li D. 3D magnetization-prepared true-FISP: a new technique for imaging coronary arteries. Magn Reson Med. 2001;46(3):494–502. Epub 2001/09/11.
18. Laurent S, Elst LV, Muller RN. Comparative study of the physicochemical properties of six clinical low molecular weight gadolinium contrast agents. Contrast Media Mol Imaging. 2006;1(3):128–37. Epub 2006/12/29.
19. Edelman RR, Manning WJ, Burstein D, Paulin S. Coronary arteries: breath-hold MR angiography. Radiology. 1991;181(3):641–3. Epub 1991/12/01.
20. Manning WJ, Li W, Edelman RR. A preliminary report comparing magnetic resonance coronary angiography with conventional angiography. N Engl J Med. 1993;328(12):828–32. Epub 1993/03/25.
21. Oshinski JN, Hofland L, Mukundan Jr S, Dixon WT, Parks WJ, Pettigrew RI. Two-dimensional coronary MR angiography without breath holding. Radiology. 1996;201(3):737–43. Epub 1996/12/01.
22. Wang Y, Rossman PJ, Grimm RC, Riederer SJ, Ehman RL. Navigator-echo-based real-time respiratory gating and triggering for reduction of respiration effects in three-dimensional coronary MR angiography. Radiology. 1996;198(1):55–60. Epub 1996/01/01.
23. Li D, Kaushikkar S, Haacke EM, Woodard PK, Dhawale PJ, Kroeker RM, et al. Coronary arteries: three-dimensional MR imaging with retrospective respiratory gating. Radiology. 1996;201(3):857–63. Epub 1996/12/01.
24. McConnell MV, Khasgiwala VC, Savord BJ, Chen MH, Chuang ML, Edelman RR, et al. Comparison of respiratory suppression methods and navigator locations for MR coronary angiography. AJR Am J Roentgenol. 1997;168(5):1369–75. Epub 1997/05/01.
25. Stuber M, Botnar RM, Danias PG, Kissinger KV, Manning WJ. Submillimeter three-dimensional coronary MR angiography with real-time navigator correction: comparison of navigator locations. Radiology. 1999;212(2):579–87. Epub 1999/08/03.
26. Wielopolski PA, van Geuns RJ, de Feyter PJ, Oudkerk M. Breath-hold coronary MR angiography with volume-targeted imaging. Radiology. 1998;209(1): 209–19. Epub 1998/10/14.
27. Botnar RM, Stuber M, Danias PG, Kissinger KV, Manning WJ. Improved coronary artery definition with T2-weighted, free-breathing, three-dimensional coronary MRA. Circulation. 1999;99(24):3139–48. Epub 1999/06/22.
28. Kim WY, Danias PG, Stuber M, Flamm SD, Plein S, Nagel E, et al. Coronary magnetic resonance angiography for the detection of coronary stenoses. N Engl J Med. 2001;345(26):1863–9. Epub 2002/01/05.
29. Yang Q, Li K, Liu X, Bi X, Liu Z, An J, et al. Contrast-enhanced whole-heart coronary magnetic resonance angiography at 3.0-T: a comparative study with X-ray

angiography in a single center. J Am Coll Cardiol. 2009;54(1):69–76.
30. Yoon YE, Kitagawa K, Kato S, Ishida M, Nakajima H, Kurita T, et al. Prognostic value of coronary magnetic resonance angiography for prediction of cardiac events in patients with suspected coronary artery disease. J Am Coll Cardiol. 2012;60(22):2316–22. Epub 2012/11/06.
31. Weber OM, Martin AJ, Higgins CB. Whole-heart steady-state free precession coronary artery magnetic resonance angiography. Magn Reson Med. 2003;50(6):1223–8. Epub 2003/12/04.
32. Edelman RR, Chien D, Kim D. Fast selective black blood MR imaging. Radiology. 1991;181(3):655–60. Epub 1991/12/01.
33. Desai MY, Lai S, Barmet C, Weiss RG, Stuber M. Reproducibility of 3D free-breathing magnetic resonance coronary vessel wall imaging. Eur Heart J. 2005;26(21):2320–4. Epub 2005/06/24.
34. Miao C, Chen S, Macedo R, Lai S, Liu K, Li D, et al. Positive remodeling of the coronary arteries detected by magnetic resonance imaging in an asymptomatic population: MESA (Multi-Ethnic Study of Atherosclerosis). J Am Coll Cardiol. 2009; 53(18):1708–15. Epub 2009/05/02.
35. Yeon SB, Sabir A, Clouse M, Martinezclark PO, Peters DC, Hauser TH, et al. Delayed-enhancement cardiovascular magnetic resonance coronary artery wall imaging: comparison with multislice computed tomography and quantitative coronary angiography. J Am Coll Cardiol. 2007;50(5):441–7. Epub 2007/07/31.
36. Ibrahim T, Makowski MR, Jankauskas A, Maintz D, Karch M, Schachoff S, et al. Serial contrast-enhanced cardiac magnetic resonance imaging demonstrates regression of hyperenhancement within the coronary artery wall in patients after acute myocardial infarction. JACC Cardiovasc Imaging. 2009;2(5):580–8. Epub 2009/05/16.
37. Gerber TC, Fasseas P, Lennon RJ, Valeti VU, Wood CP, Breen JF, et al. Clinical safety of magnetic resonance imaging early after coronary artery stent placement. J Am Coll Cardiol. 2003;42(7):1295–8. Epub 2003/10/03.
38. Kramer CM, Rogers Jr WJ, Pakstis DL. Absence of adverse outcomes after magnetic resonance imaging early after stent placement for acute myocardial infarction: a preliminary study. J Cardiovasc Magn Reson. 2000;2(4):257–61. Epub 2001/09/08.
39. Shellock FG, Shellock VJ. Metallic stents: evaluation of MR imaging safety. AJR Am J Roentgenol. 1999;173(3):543–7. Epub 1999/09/02.
40. Strohm O, Kivelitz D, Gross W, Schulz-Menger J, Liu X, Hamm B, et al. Safety of implantable coronary stents during 1H-magnetic resonance imaging at 1.0 and 1.5 T. J Cardiovasc Magn Reson. 1999; 1(3):239–45.
41. Shellock FG, Forder JR. Drug eluting coronary stent: in vitro evaluation of magnet resonance safety at 3 Tesla. J Cardiovasc Magn Reson. 2005;7(2):415–9. Epub 2005/05/11.
42. Langerak SE, Vliegen HW, Jukema JW, Kunz P, Zwinderman AH, Lamb HJ, et al. Value of magnetic resonance imaging for the noninvasive detection of stenosis in coronary artery bypass grafts and recipient coronary arteries. Circulation. 2003;107(11):1502–8. Epub 2003/03/26.
43. Kato S, Kitagawa K, Ishida N, Ishida M, Nagata M, Ichikawa Y, et al. Assessment of coronary artery disease using magnetic resonance coronary angiography: a national multicenter trial. J Am Coll Cardiol. 2010;56(12):983–91. Epub 2010/09/11.
44. Miller JM, Rochitte CE, Dewey M, Arbab-Zadeh A, Niinuma H, Gottlieb I, et al. Diagnostic performance of coronary angiography by 64-row CT. N Engl J Med. 2008;359(22):2324–36. Epub 2008/11/29.
45. Budoff MJ, Dowe D, Jollis JG, Gitter M, Sutherland J, Halamert E, et al. Diagnostic performance of 64-multidetector row coronary computed tomographic angiography for evaluation of coronary artery stenosis in individuals without known coronary artery disease: results from the prospective multicenter ACCURACY (Assessment by Coronary Computed Tomographic Angiography of Individuals Undergoing Invasive Coronary Angiography) trial. J Am Coll Cardiol. 2008;52(21):1724–32. Epub 2008/11/15.
46. Schuetz GM, Zacharopoulou NM, Schlattmann P, Dewey M. Meta-analysis: noninvasive coronary angiography using computed tomography versus magnetic resonance imaging. Ann Intern Med. 2010; 152(3):167–77. Epub 2010/02/04.
47. Hundley WG, Bluemke DA, Finn JP, Flamm SD, Fogel MA, Friedrich MG, et al. ACCF/ACR/AHA/NASCI/SCMR 2010 expert consensus document on cardiovascular magnetic resonance: a report of the American College of Cardiology Foundation Task Force on Expert Consensus Documents. J Am Coll Cardiol. 2010;55(23):2614–62. Epub 2010/06/02.
48. McCrohon JA, Moon JC, Prasad SK, McKenna WJ, Lorenz CH, Coats AJ, et al. Differentiation of heart failure related to dilated cardiomyopathy and coronary artery disease using gadolinium-enhanced cardiovascular magnetic resonance. Circulation. 2003; 108(1):54–9. Epub 2003/06/25.

Molecular Imaging of Coronary Atherosclerosis

14

Farouc A. Jaffer and Peter Libby

Cardiovascular imaging has traditional roots in the definition of anatomic structure. Imaging of the coronary arteries by contrast angiography provided the basis for assessing the lumen of these vessels, and predominated as a clinical and research tool in cardiac imaging for more than half a century. Both major invasive approaches to the alleviation of coronary artery stenosis—percutaneous intervention and coronary artery bypass surgery—depend on the contrast coronary arteriogram as a guide. Yet, the angiogram per se provides little or no information beyond the arterial lumen, and it imparts almost exclusively anatomical information. Serial coronary arteriograms performed after interventions such as administration of vasodilators or vasoconstrictors opened only a limited window on the function of epicardial coronary arteries [1]. Approaches to the quantitation of contrast "blush" in the myocardium provided limited information regarding myocardial perfusion—as embodied, for example, in the frame count tallied by the Thrombolysis in Myocardial Infarction (TIMI) perfusion score [2].

F.A. Jaffer, MD, PhD
Cardiology Division, Department of Medicine,
Massachusetts General Hospital,
Harvard Medical School, Boston, MA, USA

P. Libby, MD (✉)
Division of Cardiovascular Medicine,
Brigham and Women's Hospital/Harvard
Medical School, 77 Avenue Louis Pasteur, NRB-741,
Boston, MA 02115, USA
e-mail: plibby@partners.org

Ultrasound, in particular the application of intravascular ultrasound (IVUS) to the coronary arteries, helped define the structure of the arterial wall and the intimal lesions of atherosclerosis (see Chaps. 4–7). IVUS in patients permitted reaching beyond the visualization of the lumenal structure furnished by the contrast arteriogram. This approach—and more recently, the use of optical coherence tomographic (OCT; see Chap. 8) interrogation of the coronary arteries—provided increasingly detailed information about the structure of the coronary arterial wall and atherosclerotic plaques. But even in the most advanced, current embodiments, sonographic and OCT approaches yield primarily anatomical information.

Perfusion scanning by nuclear medicine modalities furnishes functional information that complements anatomical information from contrast arteriography or IVUS study of the coronary arteries. In some centers, nuclear techniques serve to evaluate autonomic innervation. Nuclear medicine methods in widespread use today provide little functional information beyond myocardial perfusion.

As anatomical approaches to coronary arterial imaging have evolved to a high level of sophistication and daily clinical utility, the understanding of atherosclerosis at a cellular and molecular level has burgeoned [3]. Work performed around the world over the last quarter century has elucidated many of the cellular and molecular mechanisms that drive atherosclerosis. Moreover, recent research has defined a number of cellular and molecular processes that contribute not only to

S.J. Nicholls and T. Crowe (eds.), *Imaging Coronary Atherosclerosis*, Contemporary Cardiology,
DOI 10.1007/978-1-4939-0572-0_14, © Springer Science+Business Media New York 2014

the formation of lesions and their progression, but also to the thrombotic complications that precipitate acute coronary syndromes [4]. Just as IVUS allowed imaging of the lesion beneath the lumen, the nascent field of molecular imaging aims to reach beyond structural or anatomical information, to visualize biological processes that contribute to coronary atherosclerosis and its most important clinical complications.

This chapter will provide a primer on the field of molecular imaging of atherosclerosis, with particular emphasis on the coronary arteries. It will summarize some of the imaging targets identified by basic research into the biology of atherosclerosis and clinical events. It will deliver a status report on the evolution of clinically applicable modalities for molecular imaging of the coronary arteries. Finally, it will consider the challenges and obstacles to routine clinical adoption of molecular imaging of the coronary arteries, to provide a pathway for future advances.

Fundamental Concepts in Molecular Imaging

Most, but not all, approaches to molecular imaging involve a bifunctional agent—containing a moiety that targets a specific molecular or cellular target, coupled to a moiety that permits visualization by various imaging technologies (Fig. 14.1). The targeting moiety could be an antibody, a peptide, a small molecule complementary to the intended target, or a substrate for a particular enzyme. In the case of agents that target phagocytosis, a nanoparticulate structure rather than a precise complementary targeting moiety promotes uptake of the imaging agent.

Imaging moieties can permit visualization by a number of different modalities that each offer strengths and weaknesses (Table 14.1). These modalities include isotopic approaches that offer great sensitivity or signal-to-background ratio, but generally lack precise localization. Nuclear imaging approaches have the advantage of ready availability, and in the case of clinically used isotopic agents, considerable tissue penetration. Microbubbles used for contrast-enhanced ultrasound, coupled with antibodies or other ligands that serve as targeting moieties, also benefit from a large installed base of ultrasound equipment. Magnetic resonance imaging (MRI) methods that use paramagnetic imaging agents provide favorable contrast-to-noise ratios and good anatomical localization, but have limitations in application to the coronary arteries due to respiratory and cardiac motion during the time span required for optimum image acquisition (see Chap. 13). Optical approaches, such as near-infrared fluorescent (NIRF) technologies, have undergone considerable experimental development for molecular imaging of atherosclerosis. For human coronary artery imaging, however, tissue penetration severely limits external optical imaging. Thus, for coronary arterial applications, NIRF techniques will require intra-arterial approaches,

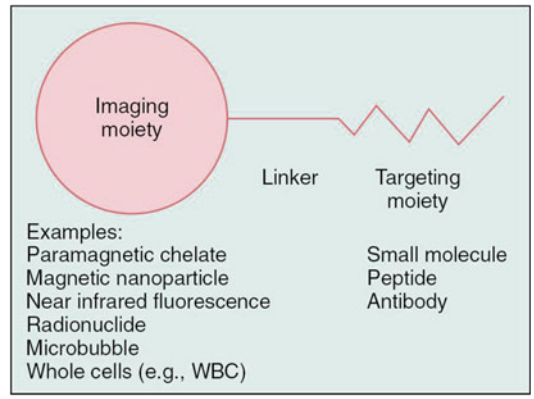

Fig. 14.1 This diagram depicts the typical schematic of a bifunctional molecular imaging agent. The imaging moiety (signal generation molecule) on the *left* connects to a targeting moiety on the *right*. The imaging moiety permits signal detection by a range of modalities including PET, SPECT, MRI, ultrasound, or optical imaging. The targeting moiety provides the "zip code" for delivering the agent to its intended molecular or cellular target. The imaging moiety might consist of a peptide or small molecule, a nanoparticle that can house multiple targeting moieties, and/or a therapeutic payload. The latter class of bifunctional agents, known as theranostic agents, combines a diagnostic imaging agent with targeted delivery of a therapeutic agent (Reprinted from Libby P, Jaffer FA, Weissleder R. Molecular imaging in cardiovascular disease. In: Bonow RO, Mann DL, Zipes DP, Libby P (eds). *Braunwald's Heart Disease: A Textbook of Cardiovascular Medicine, 9th edition.* Philadelphia, PA: Elsevier Saunders; 2011: 448–458. With permission from Elsevier)

Table 14.1 Overview of molecular imaging modalities

Technique	Resolution	Depth	Time	Quantitation	Multichannel imaging	Imaging agents	Target	Cost	Primary small animal use	Clinical use
MR imaging	10–100 μm	No limit	Minutes to hours	Absolute	Multiple	Paramagnetic chelates, magnetic particles	A, P, M	$$$	Versatile imaging modality with high soft tissue contrast	Yes
CT imaging	50 μm	No limit	Minutes	Absolute	Multiple	Iodine	A, P, M[a]	$$	Primarily for vascular, lung, and bone imaging	Yes
Ultrasound imaging	50 μm	Centimeters	Seconds to minutes	Absolute	Multiple	Microbubbles	A, P, M[a]	$$	Vascular and interventional imaging	Yes
PET imaging	1–2 mm	No limit	Minutes to hours	Absolute	No	^{18}F-, ^{64}Cu-, ^{11}C-, and ^{68}Ga- labeled compounds	P, M	$$$	Versatile imaging modality with many different tracers	Yes
SPECT imaging	1–2 mm	No limit	Minutes to hours	Absolute	Two	^{99m}Tc-, ^{111}In-, ^{131}I-labeled compounds; ^{67}Ga, ^{201}Tl	P, M	$$	Commonly used to image labeled antibodies, peptides, or perfusion	Yes
Fluorescence reflectance imaging	1 mm	<1 cm	Seconds to minutes	Relative	Multiple	Photoproteins, fluorochromes	P, M	$	Rapid screening of molecular events in surface-based disease	Yes
Fluorescence-mediated tomography	1 mm	<10 cm	Minutes	Absolute	Multiple	Near-infrared fluorochromes	P, M	$$	Quantitative imaging of targeted or "smart" fluorochrome reporters	In development
Bioluminescence imaging	Several millimeters–centimeters	Centimeters	Minutes	Relative	Multiple	Luciferins, coelenterazines, luminol	M	$$	Gene expression, cell and bacterial tracking, protein processing, and MPO activity	Potentially in development
Intravital microscopy (e.g., confocal, multiphoton)	1 μm	<400–800 μm	Seconds to hours	Relative	Multiple	Photoproteins, fluorochromes	A, P, M	$$$	All of the above at higher resolutions but at limited depths and coverage	In development (endoscopy, skin)

The *Resolution* and *Cost* columns refer to high-resolution, small animal imaging systems and are different for clinical imaging systems. *Quantitation*: absolute and relative refer to techniques that generate signals that are depth independent and depth dependent, respectively. Relative quantitation techniques typically require extensive controls; however, some of them (e.g., multiphoton microscopy) can be used to derive truly quantitative parameters (e.g., cell velocity, interaction time). *Target*: area that a given imaging modality interrogates: A = anatomic; P = physiologic; M = molecular. *Cost of system*: $: <$100,000; $$: $100,000–$300,000; $$$: >$300,000

CT computed tomography, *MR* magnetic resonance, *PET* positron emission tomography, *SPECT* single-photon emission computed tomography

Modified from Weissleder R, Pittet MJ: Imaging in the era of molecular oncology. Nature 2008;452(7187):580–589. With permission from Nature Publishing Group

[a]A limited number of molecularly targeted agents have been described

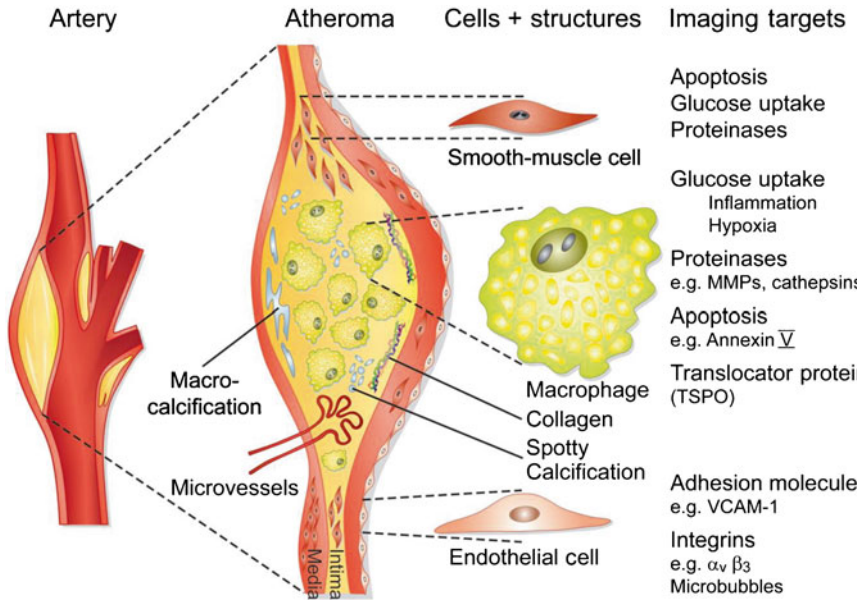

Fig. 14.2 Molecular imaging targets in atherosclerotic plaque. The *left* diagram shows a plaque in the carotid bifurcation. The magnified view of the plaque in the *middle* shows its composition, including a calcified region in *light blue* at the base of the plaque on the *left*, macrophages (*yellow*) in the lipid-rich necrotic core, triple helical collagen fibrils, and smooth-muscle cells within the fibrous cap (*brown*) below the endothelial monolayer. Spotty calcification is shown as *blue dots*. Microvessels may penetrate the plaque's base, starting from the adventitia. Key imaging targets on the major cell types or in the plaque matrix shown are listed on the *right*. *MMPs* matrix metalloproteinases, *VCAM-1* vascular cell adhesion molecule-1 (Reprinted from Camici PG, Rimoldi OE, Gaemperli O, Libby P. Non-invasive anatomic and functional imaging of vascular inflammation and unstable plaque. *Eur Heart J* 2012;33:1309–1317. With permission from Oxford University Press)

as discussed below. Table 14.1 summarizes the strengths and weaknesses of some of the modalities that could serve in molecular imaging of the human coronary arterial tree.

Targets for Molecular Imaging of Coronary Atherosclerosis

Biological investigations of the pathophysiology of atherosclerosis have revealed several potential targets for molecular imaging (Fig. 14.2). The particular biological processes discussed below comprise a partial listing of these processes. The targets detailed here, while not comprehensive, represent those for which exploitation for molecular imaging of atherosclerosis has progressed the most, and that promise the greatest ease of translation to clinical use.

Endothelial Cell Activation

The explosion of understanding of endothelial cell functions during atherogenesis has provided some potential targets for molecular imaging. When the endothelial cells encounter signals implicated in atherogenesis, they augment the expression of several structures, from the usually at low levels in the basal state. Resting endothelial cells, for example, resist prolonged contact with blood leukocytes. When exposed to proinflammatory stimuli implicated in atherogenesis—notably, certain cytokines—endothelial cells display on their surface adhesion molecules that selectively bind various classes of leukocytes. As an iconic example, endothelial cells in normal human arteries have low levels of an adhesion molecule known as vascular cell adhe-

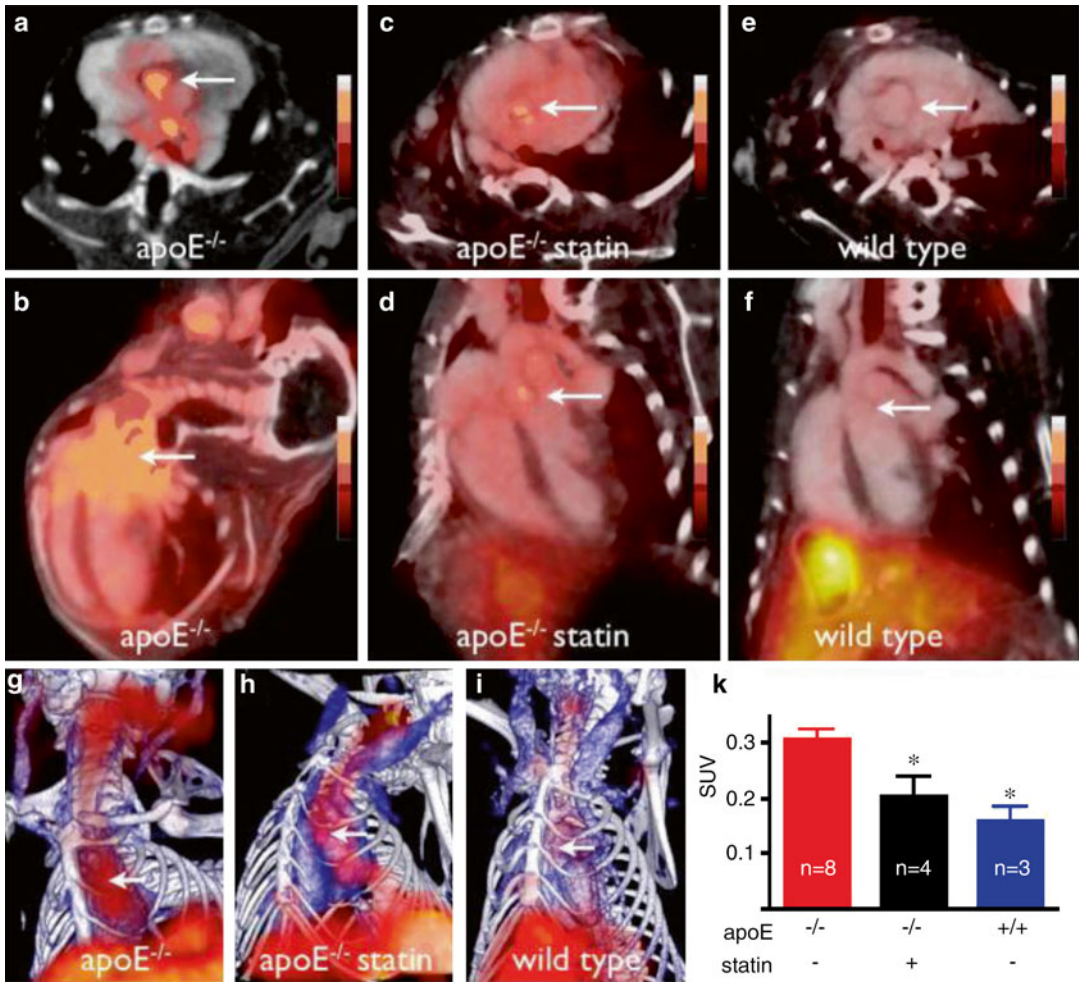

Fig. 14.3 Integrated PET/CT imaging of VCAM-1 expression in apoE$^{-/-}$ mice without and with statin treatment. A tetrameric affinity peptide with high affinity and specificity for VCAM-1 was derivatized with 1,4,7,10-tetraazacyclododecane-1,4,7,10-tetraacetic acid (DOTA) and then ^{18}F labeled and tested in apoE$^{-/-}$ mice, without or with statin treatment. PET detects VCAM-1 expression, and CT provides co-registered anatomical information. (**a**, **c**, **e**) PET-CT short-axis images of the aortic root of apoE$^{-/-}$or wild-type mice (*arrows*). (**b**, **d**, **f**) Long-axis views. (**g**, **h**, **i**) Maximum intensity projection with 3D representation. Bone = *white*; vasculature = *blue*; ^{18}F-4 V = *red*. K: Standard uptake value (SUV) graph of VCAM-1 distribution across the three different groups, $*p < 0.05$ (Reprinted from Nahrendorf M, Keliher E, Panizzi P, et al. ^{18}F-4 V for PET-CT imaging of VCAM-1 expression in inflammatory atherosclerosis. *JACC Cardiovasc Imaging* 2009; 2 (10): 1213–1222. With permission from Elsevier)

sion molecule-1 (VCAM-1), which binds just those types of leukocytes that accumulate in atherosclerotic plaques—most prominently, monocytes/ macrophages and T lymphocytes [5]. In animals that consume an atherogenic diet, or in vitro when stimulated with pro-inflammatory cytokines, endothelial cells express high levels of VCAM-1 [6]. Some approaches to targeting VCAM-1 also have served to target molecular imaging agents—including antibodies bound to microbubbles for contrast-enhanced ultrasonography, and various generations of peptides linked to near-infrared, isotopic, or MRI contrast moieties. Multimodality agents directed at VCAM-1 have successfully imaged atheromata in the aortic root of mice (Fig. 14.3).

Angiogenesis

Hypoxia in evolving atheroma stimulates plaque neovascularization, either from residing endothelial cells (angiogenesis) or from recruited endothelial progenitor cells (vasculogenesis) [7]. Plaque hypoxia accelerates foam cell stress and death, as well as growth and expansion of the necrotic core. While new vessel growth serves to counteract tissue hypoxia, the fragile neovasculature may readily rupture, leading to intraplaque hemorrhage and lesion expansion. Plaque neovessels may also support lesion growth through a nutritive function. Reduction of penetrating vasa vasorum in atheromata thus might reduce intraplaque hemorrhage and lesion growth. In any case, the presence of angiogenesis characterizes advanced, potentially high-risk atheroma and has evolved as a leading molecular imaging target.

Integrins

Integrins mediate many cell–cell and cell–matrix adhesion processes that occur during angiogenesis. In particular, neovessels express abundant integrin alpha-v beta-3 ($\alpha_v\beta_3$), a potentially useful in vivo molecular imaging target. Integrin $\alpha_v\beta_3$ notably binds the tripeptide RGD motif (arginine–glycine–aspartic acid).

Lanza, Wickline, and colleagues first demonstrated imaging integrin $\alpha_v\beta_3$ expression in atheroma in vivo via noninvasive MRI [8]. Utilizing a gadolinium-coated perfluorocarbon nanoscaffold (90,000 gadolinium chelates per scaffold) derivatized with an RGD peptidomimetic, the authors imaged plaque angiogenesis in hyperlipidemic New Zealand white rabbits. Compared to untargeted perfluorocarbon agents, the targeted agents doubled the segmented MRI signal enhancement. Other control groups, including normal rabbits injected with the targeted agent and atheroma-bearing rabbits pre-injected with an unlabeled targeted agent, demonstrated significantly less MRI signal enhancement. Immunostaining of neovessels by integrin $\alpha_v\beta_3$ demonstrated greater expression in atheroma compared to the normal vessel wall.

For near-term clinical translation of angiogenesis molecular imaging, the agent ^{18}F-Galacto-RGD appears intriguing. It has undergone clinical testing in cancer patients [9], providing a precedent for extension to patients with coronary artery disease using integrated positron emission tomography/computed tomography (PET/CT). Of interest, an experimental study imaging mouse atheroma without angiogenesis demonstrated that ^{18}F-Galacto-RGD might colocalize with plaque macrophages [10], and therefore might report on both angiogenic vessels and macrophages in human plaque.

Leukocyte Accumulation

Once attached to the endothelium via interactions with adhesion molecules such as VCAM-1, leukocytes enter the arterial intima. A subset of pro-inflammatory cytokines known as chemokines likely mediates much of this directed migration. Having taken up residence in the arterial plaque, these phagocytes provide a number of targets for molecular imaging. Monocytes that have penetrated into the intima mature into macrophages. They often accumulate lipids and form the foam cells characteristic of atheromatous lesions. Imaging approaches that depend on the phagocytic activity of macrophages are considered below. A subset of macrophages in the atherosclerotic plaque contains the enzyme myeloperoxidase (MPO). This enzyme generates the highly oxidant species, hypochlorous acid (HOCl). Various probes can visualize MPO activity and/or its product, hypochlorite [11, 12].

The mitochondrial membrane in mononuclear phagocytes contains a transporter molecule known as TSPO (translocator protein)—or previously, as the peripheral benzodiazepine receptor. Small molecule ligands that recognize this transporter molecule, coupled to isotopic agents detectable by PET, have served to image inflammation in large arteries in humans [13, 14]. This approach awaits application to smaller arteries, such as those in the coronary tree.

Phagocytic Capacity

Macrophages characteristically exhibit phagocytic activity, allowing them to engulf infectious agents, foreign bodies, and—in the context of atherosclerosis—lipids and various lipoproteins. Some approaches to molecular imaging of atherosclerosis have exploited the phagocytic property of macrophages. Ultrasmall superparamagnetic iron oxide (USPIO) particles can accumulate in macrophages and provide MRI contrast [15]. Experimental studies have demonstrated the feasibility of plaque imaging using this approach. Using suppression of T2-weighted signals, studies have quantitatively correlated macrophage content with such superparamagnetic microparticles in atheromata of a rabbit aorta, a vessel of similar caliber to human coronary arteries (Fig. 14.4) [16].

Proteinase Activity

A plethora of findings, over the last two decades, support the participation of proteinases in arterial remodeling during atherogenesis and the disruption of atherosclerotic plaques [4]. In particular, degradation of interstitial collagen in the plaque's fibrous cap likely renders it susceptible to rupture. Such disruptions of coronary atherosclerotic plaques precipitate a majority of fatal acute myocardial infarctions. The principal collagenolytic enzymes implicated in this process include members of the matrix metalloproteinase (MMP) family. We have shown overexpression of the three principal MMP interstitial collagenases in human atherosclerotic plaques (MMP-1, -8, and -13) [4]. Our extensive gain-of-function and loss-of-function data in atherosclerotic mice, demonstrated directly a role for MMP interstitial collagenases in the economy of collagen in mouse atherosclerotic plaques [4, 17]. Our group has also provided evidence for the involvement of certain potent elastases—including the cysteinyl proteinases cathepsins S, K, and L—in human and experimental atherosclerosis and in experimental and human aneurysmal disease [18].

Several experimental studies have demonstrated the feasibility of imaging these classes of proteinases. NIRF-emitting beacons that assess proteinase activity by liberation of quenched fluorescent moieties following proteolysis, pioneered by the laboratory of Dr. Ralph Weissleder, have proven pivotal in this regard. We visualized the interstitial collagenase MMP-13 in mouse atherosclerotic plaques using this approach [19]. Probes activated by cathepsin K also permit visualization of mouse atheromata [20]. Ex vivo studies of freshly excised human carotid atherosclerotic plaques provide evidence that supports the clinical translatability of such approaches to proteinase imaging. Other laboratories have used radionuclide-labeled proteinase inhibitors to visualize plaque proteolytic enzymes [21]. While the one-to-one stoichiometry of the inhibitor-based approaches does not utilize the catalytic amplification provided by enzymatic activity, the sensitivity and tissue penetration of nuclear approaches might permit external imaging of human atherosclerosis.

Metabolic Activity

Mononuclear phagocytes in the atherosclerotic plaque can exhibit increased glucose uptake. Widespread use of uptake of the glucose analog fluorodeoxyglucose (FdG) in the visualization of tumors led to the exploration of radiolabeled FdG uptake as a marker of macrophage functional status in human atherosclerosis [22]. Experimental studies have correlated macrophage number with FdG signal in atherosclerotic rabbits and in human carotid endarterectomy specimens [23, 24]. Studies have also validated the reproducibility of the measurement of ^{18}F-FdG uptake in human atherosclerotic plaques [22]. These findings have given rise to the concept that increased ^{18}F-FdG signal in human atherosclerotic plaques reports on the inflammatory status of lesions. As inflammation contributes importantly to atherogenesis and its complications, application of this clinically feasible approach has generated considerable enthusiasm. Multiple clinical studies underway

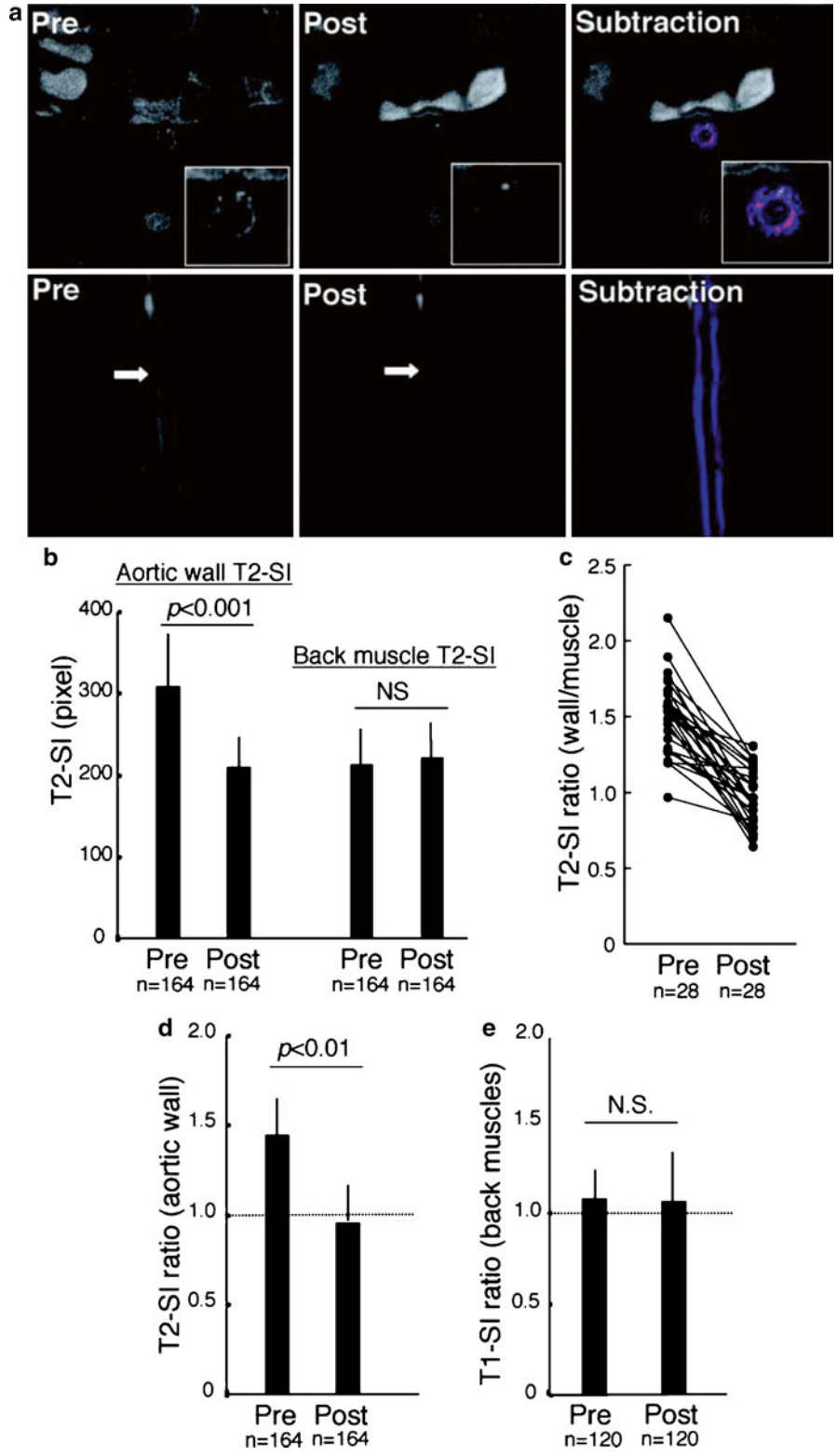

Fig. 14.4 Molecular MRI of plaque macrophages in rabbit aorta using superparamagnetic nanoparticles (MION-47). MION-47 is internalized within plaque macrophages. T2-weighted pulse sequences were used to visualize MION-47-induced MRI signal loss in vivo. (**a**, *top row*) Axial images (pre and post) 72 h after MION-47 injection, with subtraction image (*top right*, pseudocolored) further demonstrating the net effect on the MRI signal.

employ this approach to molecular imaging of atherosclerosis in humans. One large imaging trial will provide data regarding the correlation of clinical events and FdG signal in atherosclerotic plaques.

Our recent *in vitro* experiments have raised the possibility that increased glucose uptake by mononuclear phagocytes in plaques may reflect the hypoxic environment, rather than inflammatory activity [25]. We reasoned that hypoxia in the core of plaques would prompt macrophages to augment anaerobic glycolysis, raising glucose utilization. Hypoxia increases the levels of glucose transporters involved in FdG uptake. Our studies further demonstrated that treatment of human macrophages with statins *in vitro* could reduce the augmented glucose uptake by these cells stimulated by hypoxia. Thus, the conclusion that therapeutic interventions that may lower FdG uptake in atheromata reflect an anti-inflammatory effect requires further validation. This example illustrates how biochemical and molecular rigor help to interpret findings obtained by the application of molecular imaging to atherosclerosis.

Lipid Deposition

Chemical approaches to detect coronary plaque lipids include intracoronary near-infrared spectroscopy (NIRS) and IVUS-virtual histology (VH). These approaches do not specifically interrogate well-defined lipid constituents. Molecular imaging approaches are bridging this knowledge gap.

Oxidized Low-Density Lipoprotein

Following deposition into the artery wall, susceptible moieties on LDL can undergo oxidation. Oxidized LDL (oxLDL) preparations can stimulate inflammation and may augment atherogenesis. Components of oxLDL therefore have emerged as promising targets for molecular imaging of vulnerable plaques.

Extending prior oxLDL-targeted single-photon emission computed tomography (SPECT) imaging reporters [26, 27], Tsimikas, Fayad and colleagues have developed promising oxLDL imaging agents for both MRI and fluorescence imaging—approaches that offer higher-resolution capabilities more suitable to human coronary arteries.

An early effort to develop an oxLDL MRI reporter used antibodies to oxLDL, covalently conjugated to gadolinium-suffused micelles [28]. On T1-weighted MRI at 9.4 T, atheroma-bearing mice demonstrated significant plaque uptake by micelles derivatized with MDA2 (IgG antibody MDA2 targeted to malondialdehyde [MDA]-lysine) or IK17 (human single-chain Fv antibody fragment IK17 targeted to MDA-like epitopes). Enhancement exceeded that of control agents consisting of untargeted micelles or irrelevant antibody conjugated to micelles.

Free gadolinium, however, may dissociate from micelles and thus become toxic to cells. Gadolinium also has relatively modest MRI relaxivity rates, yielding insufficient target-to-background ratios for clinical scanners that operate at 1.5–3.0 T field strength. The same group therefore evaluated the ability to image oxLDL using superparamagnetic iron oxides (SPIOs) as an alternative MRI scaffold [29]. As described above, SPIOs exhibit higher relaxivity

Fig. 14.4 (continued) (*Bottom row*) Coronal view of the same aorta showing diffuse MRI signal loss throughout the aortic wall, with varying magnitudes. *Arrows* indicate the cross section obtained for axial images in the top row. (**b**) MION-47 induced a significant reduction in the aortic T2-signal intensity (SI) ($N=164$ aortic wall levels, $p<0.001$). Of note, T2-SI in muscle was not changed by MION-47. (**c**) Average T2-SI ratio of the aortic wall (T2-SI divided by back muscle T2-SI) of a single representative rabbit, across all aortic sections. (**d**) MION-47 induced a significant reduction in the T2-SI ratio ($p<0.01$, $N=6$ rabbits, 164 cross sections), but not in the T1-SI ratio (120 slices, 6 rabbits), in the aortic wall (Reprinted from Morishige K, Kacher DF, Libby P, et al. High-resolution magnetic resonance imaging enhanced with superparamagnetic nanoparticles measures macrophage burden in atherosclerosis. *Circulation* 2010; 122 (17): 1707–1715. With permission from Wolter Kluwers Health)

rates and can induce substantial MR signal loss on T2-weighted images, resulting in dark/negative contrast. Of note, T2/T2* mediated off-resonance effects can also be imaged with bright/positive contrast using specialized MRI pulse sequences.

To leverage the advantages of iron oxide as a molecular MRI platform, Briley-Saebo et al. conjugated oxLDL-specific antibodies (MDA2, IK17, E06) to either pegylated, lipid-coated SPIOs (LSPIOs) or pegylated, lipid-coated USPIOs (LUSPIOs). After an injection of 3.9 mg Fe/kg into atheroma-bearing mice, in vivo MRI at 9.4 T was performed using both T2-weighted sequences and specialized off-resonance sequences. While LSPIOs did not induce MRI contrast due to their shorter circulating half-life, targeted LUSPIOs significantly enhanced the artery wall compared to control and competitive inhibition groups. Immunohistochemical analyses demonstrated a good correlation between iron oxide (Perls' staining) and MDA-lysine epitopes. Confocal microscopy of rhodamine-conjugated targeted LUSPIOs further demonstrated that the LUSPIOs localized within plaque macrophages, but not within the extracellular matrix. Importantly, non-oxLDL antibody-conjugated LUSPIOs did not localize within plaque macrophages. The U.S. Food and Drug Administration (FDA) has not approved USPIOs for use in humans.

In a very recent advance, Briley-Saebo and colleagues have developed a manganese (Mn(II))-based oxLDL-targeted micelle [30]. Mn concentrates within cells and can induce substantial MRI contrast, a potential advantage over gadolinium-based micelles. To develop Mn-based oxLDL-targeted nanoscaffolds, the authors incorporated Mn and rhodamine into micelles, and then conjugated either MDA2 or IK17 to the micelles. Targeted Mn-micelles (0.05 mmol Mn/kg dose) were compared to untargeted Mn-micelles, as well as MDA2-Gd micelles and IK17-Gd micelles (0.075 mmol Gd/kg). Following injection in apolipoprotein E knockout ($ApoE^{-/-}$) or LDL-receptor knockout ($LDLr^{-/-}$) mice, targeted Mn-micelles produced significant MRI signal enhancement of plaques. Signal enhancement was abolished by competitive pre-injection of targeted unlabeled MDA antibody. Compared to gadolinium-based micelles, Mn-based micelles injected at 1/3 the dose provided similar signal enhancement of plaques on 9.4 T MRI. As the FDA has approved the use of manganese contrast agents in humans, the Mn-based micelle approach offers promise for clinical translation.

Indocyanine Green

We recently demonstrated that the FDA-approved NIRF imaging agent indocyanine green (ICG) targets lipid-rich, inflamed atheroma in vivo [31]. The amphiphilic NIR fluorochrome ICG (excitation/ emission 785/815 nm in aqueous solution, 805/830 nm in blood) has FDA approval for ophthalmologic NIRF imaging. Utilizing the first-generation intravascular coronary artery compatible spectroscopic guidewire [32], we demonstrated that ICG rapidly deposited into aortic plaques of atheroma-bearing rabbits (Fig. 14.5). Good, stable target-to-background ratios were achieved within 20 min of ICG injection, consistent with ICG's short half-life in blood, and a favorable aspect for clinical translation. Detailed histological and fluorescence microscopic studies revealed that ICG colocalized with neutral triglyceride (Oil Red O) and macrophages (RAM-11). Additional studies in ex vivo human carotid specimens reproduced the findings in rabbits, but colocalization was stronger with human macrophages (CD68+) compared to lipid. Due to ICG's ability to target lipid and macrophages, its FDA-approved status, and its rapid targeting capabilities, ICG could enable intravascular NIRF-targeted imaging of high-risk plaques, especially with recent advances in 2D NIRF and NIRF-OFDI (optical frequency domain imagine) catheter technology [33, 34].

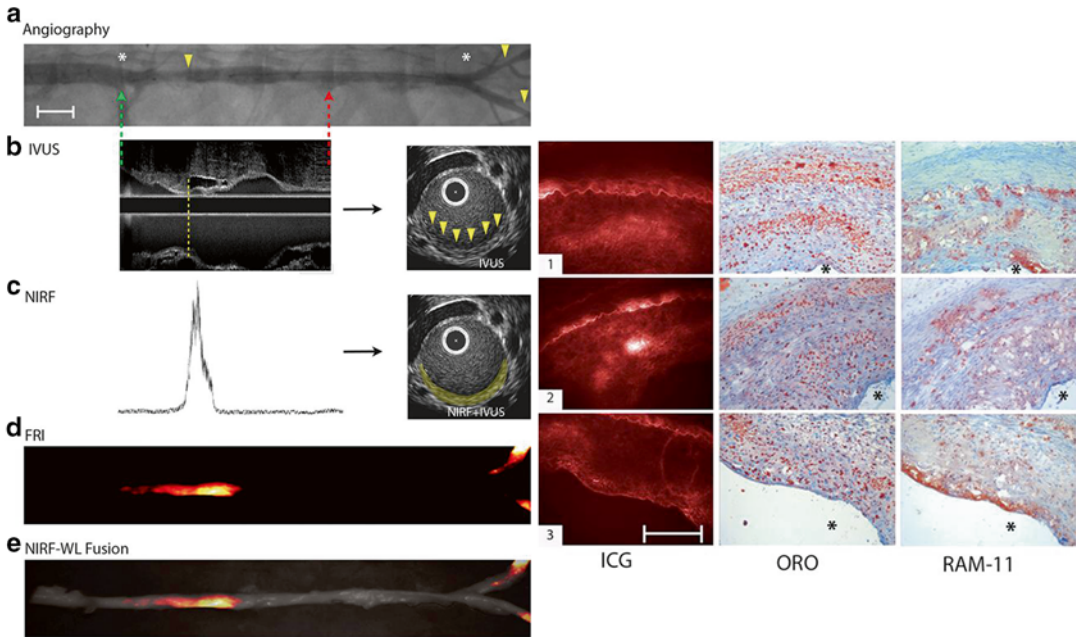

Fig. 14.5 In vivo intravascular NIRF guidewire spectroscopy shows that ICG localizes in atherosclerotic plaques of New Zealand white rabbits (*left panel*). (**a**) X-ray angiography of aortic and iliac plaques (*yellow arrowheads*). The *green* and *red dotted arrows* show the start and end of the guidewire pullbacks, respectively. The *white asterisks* show various arterial branching points. Angiography facilitated co-registration of the NIRF and IVUS datasets. Scale bar, 1 cm. (**b**) IVUS long-axis image of an aortic atheroma-bearing animal (*left*). A small plaque (*dotted yellow line*) is shown in cross section on the corresponding axial image (right side, *yellow arrowheads*). (**c**) Following ICG injection, an NIRF guidewire pullback at 15 min showed focal NIRF signal enhancement (805 nm fluorescence) on automated pullback. The NIRF signal (*right*, *pseudocolored yellow*) was fused on to the IVUS-depicted plaque in the axial slice shown in (**b**). All longitudinal images were similarly scaled. (**d**) Ex vivo fluorescence reflectance images (FRI) show high ICG signal in aortic and iliac plaques. (**e**) Fusion FRI and white light (WL) image. (*Right panel*) Histopathological and fluorescence microscopic deposition of ICG in atheroma sections from three different animals. (*1–3*) From *left* to *right*: ICG fluorescence (845 nm, pseudocolored *red*), ORO staining of neutral lipid, and RAM-11+ macrophages. Within each group, all images are from adjacent sections (6 **μ**m). *Asterisk* (*) denotes lumen. Scale bar, 100 **μ**m (Reprinted from Vinegoni C, Botnaru I, Aikawa E, et al. Indocyanine green enables near-infrared fluorescence imagine of lipid-rich, inflamed atherosclerotic plaques. *Sci Trans Med* 2011; 3 (84): 84ra45. With permission from The American Association for the Advancement of Science)

Apoptosis

Apoptosis of macrophages and smooth muscle cells can modulate atheroma formation and likely contribute to atherothrombotic complications [35]. Apoptotic cells are established targets for molecular imaging of vulnerable plaques. Nearly a decade ago, Kietselaer utilized SPECT imaging of ^{99m}Tc-Annexin V, an agent that binds exposed phosphatidylserine on apoptotic cells, to image carotid plaque apoptosis in human subjects [36]. Subjects ($N=4$) with recent transient ischemic attack or stroke had higher ^{99m}Tc signals compared to asymptomatic patients.

The ability of annexin-based apoptosis imaging agents to also bind viable macrophages, rather than apoptotic cells, presents a challenge [37]. Newer agents that show potential for coronary molecular imaging of apoptosis include annexin-based and caspase enzyme-based reporters for MRI and NIRF imaging [38, 39].

Calcification

Calcification of evolving coronary atheroma occurs frequently. A greater burden of coronary artery calcification portends poorer clinical outcomes. Calcified lesions heighten the complexity of coronary revascularization strategies. While noninvasive CT approaches readily detect advanced calcification in coronary arteries, molecular imaging approaches can provide new insights into the mechanisms of osteogenesis and plaque calcification.

Employing serial intravital fluorescence microscopy technology, Aikawa and colleagues demonstrated that macrophage-rich zones in plaque can temporally evolve to become calcified segments [40]. They detected arterial calcification using an NIR fluorochrome-derivatized bisphosphonate (Fig. 14.6). Further work using in vivo NIRF microscopy has illuminated that arterial calcification occurs at the expense of bone mineralization [41], and depends on cathepsin S protease activity, in mice with chronic kidney disease [42].

Clinical extension of calcium imaging has been demonstrated in human carotid arteries in vivo [43], and more recently in human coronary arteries in vivo using the PET tracer ^{18}F-sodium fluoride [44]. In this latter recent study, Dweck et al. showed that "active" calcium deposition (max TBR > 1.61) detected by ^{18}F-NaF identified

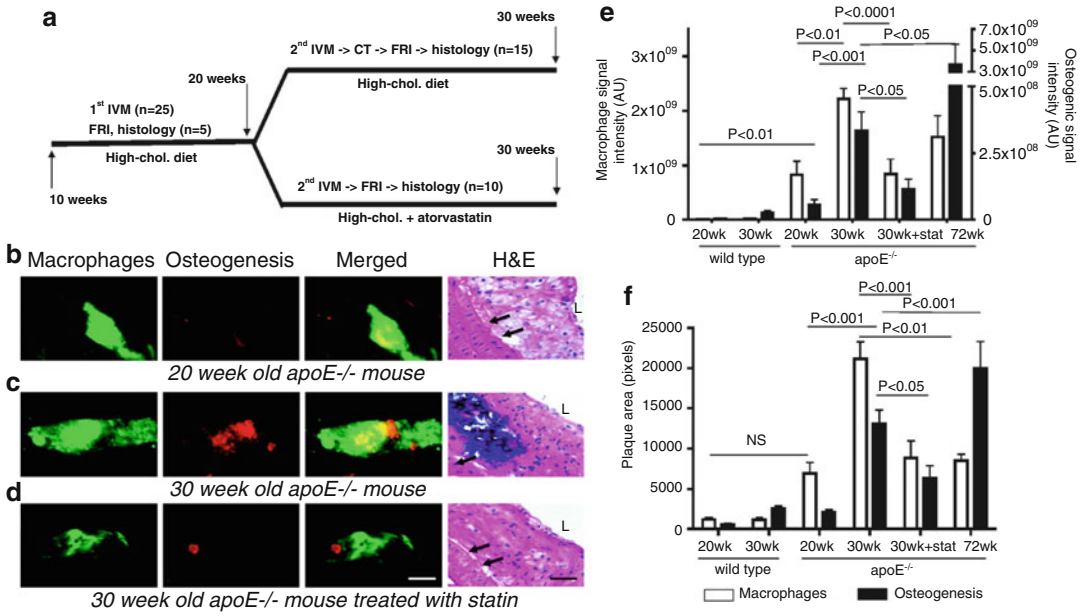

Fig. 14.6 Serial intravital fluorescence microscopy (IVFM) of changes in plaque inflammation and osteogenesis in murine carotid plaques. (**a**) At 20 weeks of age, mice were randomized to continue a high-cholesterol diet (HCD), or HCD admixed with a statin, for 10 more weeks. IVFM was performed serially at 20 weeks (**b**), 30 weeks (**c**), and at 30 weeks on statin diet (**d**). IVFM simultaneously visualized inflammation (*green pseudocolor*, macrophage reporter CLIO-VT680) and osteogenesis (*red pseudocolor*, reporter Osteosense750). Bar = 500 μm. Representative hematoxylin and eosin (H&E) images show correlations of IVFM with histopathology (*right panels*). L = lumen; *arrows* show internal elastic lamina. Bar = 50 μm. (**e**) Quantification of macrophage-derived and osteoblast-derived NIRF signals demonstrated an increase over time, and a decrease with statin treatment. (**f**) Macrophage and calcification content increased from 20 to 30 weeks. Statin therapy reduced both inflammation and calcification after 10 weeks of treatment. At 72 weeks of age, areas of inflammation decreased, but calcification was significantly increased compared to mice at 30 weeks. *AU* arbitrary units, *stat* statin (Reprinted from Aikawa E, Nahrendorf M, Figueiredo JL, et al. Osteogenesis associates with inflammation in early-stage atherosclerosis evaluated by molecular imaging in vivo. Circulation 2007; 116 (24): 2841–2850. With permission from Wolter Kluwers Health)

a subgroup of patients with calcified plaque (on CT) that had higher CV risk. This landmark study was particularly notable for the excellent noninvasive detection of a PET tracer in the coronary arteries, with 83–100 % of coronary segments deemed interpretable. In contrast, the authors also investigated ^{18}F-FdG and found that high myocardial background signal uptake precluded the analysis of 49 % of the territories. Overall, ^{18}F-sodium fluoride appears promising as a noninvasive coronary artery-targeted molecular imaging approach that may indicate high-risk plaques, and warrants further studies.

Translational Challenges

In the last decade, molecular imaging approaches have translated in pilot studies to the clinic for several applications, including myocardial infarction and large-vessel vascular diseases such as aneurysm, arteritis, and carotid atherosclerosis. Application of such approaches to the coronary arteries remains challenging, due to the small volume and complex motion of these vessels. Recently, however, noninvasive approaches to coronary arterial molecular imaging have emerged based on integrated PET/CT, using ^{18}F-based tracers such as ^{18}F-FDG, ^{18}F-TSPO, and ^{18}F-sodium fluoride. Of note, while PET imaging studies are encouraging, quantitation remains difficult due to lower resolution (3–5 mm isotropic). To address this limitation, some intravascular, high-resolution catheter NIRF strategies have emerged utilizing 2D NIRF systems coupled with IVUS, as well as integrated NIRF-OFDI systems. The clinical availability of targeted fluorescence molecular imaging agents (e.g., ICG, folate receptor ligand) may allow progress in high-resolution NIRF coronary molecular imaging to advance rapidly.

The clinical application of many molecular imaging approaches described herein will require overcoming operational obstacles. First, the preparation of imaging probes for clinical use will demand good manufacturing procedures (GMP)—requiring resources beyond those of many of the academic laboratories that have developed these probes. Stable, sterile, and pyrogen-free preparations of imaging agents will require considerable investment. In addition, the clinical use of novel molecular imaging agents will require toxicologic testing—also an undertaking beyond the reach of most academic groups. Overcoming this hurdle might require considerable cooperation between governmental, institutional, and/or private sector resources.

Next steps will require any clinical molecular imaging approach to shift the ROC curve and/or improve the net reclassification index (NRI) beyond conventional risk prediction measures including the Framingham risk score, serum biomarkers, and coronary artery calcification/CT angiography. Thereafter, patients identified as very high risk (i.e., >20 % 10-year risk of death or myocardial infarction) could be rationally and efficiently enrolled in new preventative clinical trials evaluating systemic, local, and regional atherosclerosis therapies.

Molecular imaging of atherosclerosis can also provide an urgently needed tool for the evaluation of novel therapeutics [45]. The very success of contemporary cardiovascular medicine has rendered event rates low enough that clinical trials to show effectiveness of novel therapies require a large number of patients and substantial durations to achieve sufficient power. Yet, we still face an unacceptably high residual burden of events in patients with established coronary atherosclerosis, even on the current standard-of-care regimens. Another challenge in the design of clinical trials of novel agents involves choosing the appropriate dose.

Molecular imaging could address these two issues. By providing a readout that reflects a biological process, molecular imaging biomarkers could serve as an intermediary step in the evaluation of novel therapies. They could test whether an intervention actually targets a functional aspect of the atherosclerotic plaque that might correlate with an improved clinical outcome in a relatively small number of patients, studied over a shorter time period than required by the clinical endpoint trial that would ultimately be required. Molecular imaging could also aid in dose selection by monitoring a biological

process related to the pathophysiology of the plaque, providing a rational basis for the choice of dose to use in a clinical endpoint trial. An approach that visualizes functions of the plaque itself should provide more direct hints regarding efficacy of various doses than the assessment of circulating biomarkers often employed for this purpose.

Despite the considerable challenges, molecular imaging of coronary atherosclerosis promises to extend imaging beyond its traditional province of anatomical structure, to harness the advances in understanding the cellular and molecular biology of atherosclerosis that have accrued over the last decade. Sufficient experimental validation indicates the feasibility of this approach. The road map above provides a pathway to the clinical development of these modalities that may help evaluate novel therapies in humans, and even in clinical practice.

Acknowledgements This work was supported by grants from the Donald W. Reynolds Foundation, from the National Heart, Lung, and Blood Institute (HL-108229, to Dr. Jaffer; HL-80731, HL-80472, to Dr. Libby; HHSN268201000044C, to Dr. R. Weissleder and Dr. Libby), and from the American Heart Association (Scientist Development Grant #0830352N, to Dr. Jaffer) and by a Howard Hughes Medical Institute Early Career Award (to Dr. Jaffer). The authors wish to thank our colleagues Drs. Ralph Weissleder and Matthias Nahrendorf for their support and collaboration.

References

1. Ludmer PL, Selwyn AP, Shook TL, Wayne RR, Mudge GH, Alexander RW, Ganz P. Paradoxical vasoconstriction induced by acetylcholine in atherosclerotic coronary arteries. N Engl J Med. 1986;315: 1046–51.
2. Gibson CM, Murphy SA, Morrow DA, Aroesty JM, Gibbons RJ, Gourlay SG, Barron HV, Giugliano RP, Antman EM, Braunwald E. Angiographic perfusion score: an angiographic variable that integrates both epicardial and tissue level perfusion before and after facilitated percutaneous coronary intervention in acute myocardial infarction. Am Heart J. 2004;148(2): 336–40.
3. Libby P, Ridker PM, Hansson GK. Progress and challenges in translating the biology of atherosclerosis. Nature. 2011;473:317–25.
4. Libby P. Mechanisms of the acute coronary syndromes and their implications for therapy, N Engl J Med. 2013;368:2004–13.
5. Cybulsky MI, Gimbrone Jr MA. Endothelial expression of a mononuclear leukocyte adhesion molecule during atherogenesis. Science. 1991;251:788–91.
6. Li H, Cybulsky MI, Gimbrone Jr MA, Libby P. Inducible expression of vascular cell adhesion molecule-1 (VCAM-1) by vascular smooth muscle cells *in vitro* and within rabbit atheroma. Am J Pathol. 1993;143(12):1551–9.
7. Moreno PR, Sanz J, Fuster V. Promoting mechanisms of vascular health: circulating progenitor cells, angiogenesis, and reverse cholesterol transport. J Am Coll Cardiol. 2009;53(25):2315–23.
8. Winter PM, Morawski AM, Caruthers SD, Fuhrhop RW, Zhang H, Williams TA, Allen JS, Lacy EK, Robertson JD, Lanza GM, Wickline SA. Molecular imaging of angiogenesis in early-stage atherosclerosis with alpha(v)beta3-integrin-targeted nanoparticles. Circulation. 2003;108(18):2270–4.
9. Haubner R, Weber WA, Beer AJ, Vabuliene E, Reim D, Sarbia M, Becker KF, Goebel M, Hein R, Wester HJ, Kessler H, Schwaiger M. Noninvasive visualization of the activated alphavbeta3 integrin in cancer patients by positron emission tomography and [18F] Galacto-RGD. PLoS Med. 2005;2(3):e70.
10. Laitinen I, Saraste A, Weidl E, Poethko T, Weber AW, Nekolla SG, Leppanen P, Yla-Herttuala S, Holzlwimmer G, Walch A, Esposito I, Wester HJ, Knuuti J, Schwaiger M. Evaluation of alphavbeta3 integrin-targeted positron emission tomography tracer 18F-galacto-RGD for imaging of vascular inflammation in atherosclerotic mice. Circ Cardiovasc Imaging. 2009;2(4):331–8.
11. Shepherd J, Hilderbrand SA, Waterman P, Heinecke JW, Weissleder R, Libby P. A fluorescent probe for the detection of myeloperoxidase activity in atherosclerosis-associated macrophages. Chem Biol. 2007;14(11):1221–31.
12. Ronald JA, Chen JW, Chen Y, Hamilton AM, Rodriguez E, Reynolds F, Hegele RA, Rogers KA, Querol M, Bogdanov A, Weissleder R, Rutt BK. Enzyme-sensitive magnetic resonance imaging targeting myeloperoxidase identifies active inflammation in experimental rabbit atherosclerotic plaques. Circulation. 2009;120(7):592–9.
13. Gaemperli O, Boyle JJ, Rimoldi OE, Mason JC, Camici PG. Molecular imaging of vascular inflammation. Eur J Nucl Med Mol Imaging. 2010;37(6):1236.
14. Gaemperli O, Shalhoub J, Owen DR, Lamare F, Johansson S, Fouladi N, Davies AH, Rimoldi OE, Camici PG. Imaging intraplaque inflammation in carotid atherosclerosis with 11C-PK11195 positron emission tomography/computed tomography. Eur Heart J. 2012;33(15):1902–10.
15. Kooi ME, Cappendijk VC, Cleutjens KB, Kessels AG, Kitslaar PJ, Borgers M, Frederik PM, Daemen MJ, van Engelshoven JM. Accumulation of ultrasmall

superparamagnetic particles of iron oxide in human atherosclerotic plaques can be detected by in vivo magnetic resonance imaging. Circulation. 2003; 107(19):2453–8.
16. Morishige K, Kacher DF, Libby P, Josephson L, Ganz P, Weissleder R, Aikawa M. High-resolution MRI enhanced with superparamagnetic nanoparticles measures macrophage burden in atherosclerosis. Circulation. 2010;122:1707–15.
17. Quillard T, Tesmenitsky Y, Croce K, Travers R, Shvartz E, Koskinas KC, Sukhova G, Aikawa E, Aikawa M, Libby P. Selective inhibition of matrix metalloproteinase 13 (MMP-13) increases collagen content of established mouse atheromata. Arterioscler Thromb Vasc Biol. 2011;31(11):2464–72.
18. Liu J, Sukhova GK, Sun JS, Xu WH, Libby P, Shi GP. Lysosomal cysteine proteases in atherosclerosis. Arterioscler Thromb Vasc Biol. 2004;24(8):1359–66.
19. Deguchi J, Aikawa M, Tung C-H, Aikawa E, Kim D-E, Ntziachristos V, Weissleder R, Libby P. Inflammation in atherosclerosis: visualizing matrix metalloproteinase action in macrophages in vivo. Circulation. 2006;114:55–62.
20. Jaffer FA, Kim DE, Quinti L, Tung CH, Aikawa E, Pande AN, Kohler RH, Shi GP, Libby P, Weissleder R. Optical visualization of cathepsin K activity in atherosclerosis with a novel, protease-activatable fluorescence sensor. Circulation. 2007;115(17):2292–8.
21. Razavian M, Tavakoli S, Zhang J, Nie L, Dobrucki LW, Sinusas AJ, Azure M, Robinson S, Sadeghi MM. Atherosclerosis plaque heterogeneity and response to therapy detected by in vivo molecular imaging of matrix metalloproteinase activation. J Nucl Med. 2011;52(11):1795–802.
22. Rudd JH, Myers KS, Bansilal S, Machac J, Pinto CA, Tong C, Rafique A, Hargeaves R, Farkouh M, Fuster V, Fayad ZA. Atherosclerosis inflammation imaging with 18F-FDG PET: carotid, iliac, and femoral uptake reproducibility, quantification methods, and recommendations. J Nucl Med. 2008;49(6):871–8.
23. Tawakol A, Migrino RQ, Hoffmann U, Abbara S, Houser S, Gewirtz H, Muller JE, Brady TJ, Fischman AJ. Noninvasive in vivo measurement of vascular inflammation with F-18 fluorodeoxyglucose positron emission tomography. J Nucl Cardiol. 2005;12(3): 294–301.
24. Tawakol A, Migrino RQ, Bashian GG, Bedri S, Vermylen D, Cury RC, Yates D, LaMuraglia GM, Furie K, Houser S, Gewirtz H, Muller JE, Brady TJ, Fischman AJ. In vivo 18F-fluorodeoxyglucose positron emission tomography imaging provides a noninvasive measure of carotid plaque inflammation in patients. J Am Coll Cardiol. 2006;48(9):1818–24.
25. Folco EJ, Sheikine Y, Rocha VZ, Christen T, Shvartz E, Sukhova GK, Di Carli MF, Libby P. Hypoxia but not inflammation augments glucose uptake in human macrophages. Implications for imaging atherosclerosis with FdG-PET. J Am Coll Cardiol. 2011;58(6): 603–14.
26. Torzewski M, Shaw PX, Han KR, Shortal B, Lackner KJ, Witztum JL, Palinski W, Tsimikas S. Reduced in vivo aortic uptake of radiolabeled oxidation-specific antibodies reflects changes in plaque composition consistent with plaque stabilization. Arterioscler Thromb Vasc Biol. 2004;24(12):2307–12.
27. Li F, Yarnykh VL, Hatsukami TS, Chu B, Balu N, Wang J, Underhill HR, Zhao X, Smith R, Yuan C. Scan-rescan reproducibility of carotid atherosclerotic plaque morphology and tissue composition measurements using multicontrast MRI at 3T. J Magn Reson Imaging. 2010;31(1):168–76.
28. Briley-Saebo KC, Shaw PX, Mulder WJ, Choi SH, Vucic E, Aguinaldo JG, Witztum JL, Fuster V, Tsimikas S, Fayad ZA. Targeted molecular probes for imaging atherosclerotic lesions with magnetic resonance using antibodies that recognize oxidation-specific epitopes. Circulation. 2008;117(25):3206–15.
29. Briley-Saebo KC, Cho YS, Shaw PX, Ryu SK, Mani V, Dickson S, Izadmehr E, Green S, Fayad ZA, Tsimikas S. Targeted iron oxide particles for in vivo magnetic resonance detection of atherosclerotic lesions with antibodies directed to oxidation-specific epitopes. J Am Coll Cardiol. 2011;57(3):337–47.
30. Briley-Saebo KC, Nguyen TH, Saeboe AM, Cho YS, Ryu SK, Volkova ER, Dickson S, Leibundgut G, Wiesner P, Green S, Casanada F, Miller YI, Shaw W, Witztum JL, Fayad ZA, Tsimikas S. In vivo detection of oxidation-specific epitopes in atherosclerotic lesions using biocompatible manganese molecular magnetic imaging probes. J Am Coll Cardiol. 2012; 59(6):616–26.
31. Vinegoni C, Botnaru I, Aikawa E, Calfon MA, Iwamoto Y, Folco EJ, Ntziachristos V, Weissleder R, Libby P, Jaffer FA. Indocyanine green enables near-infrared fluorescence imaging of lipid-rich, inflamed atherosclerotic plaques. Sci Transl Med. 2011;3(84):84ra45.
32. Jaffer FA, Vinegoni C, John MC, Aikawa E, Gold HK, Finn AV, Ntziachristos V, Libby P, Weissleder R. Real-time catheter molecular sensing of inflammation in proteolytically active atherosclerosis. Circulation. 2008;118:1802–9.
33. Jaffer FA, Calfon MA, Rosenthal A, Mallas G, Razansky RN, Mauskapf A, Weissleder R, Libby P, Ntziachristos V. Two-dimensional intravascular near-infrared fluorescence molecular imaging of inflammation in atherosclerosis and stent-induced vascular injury. J Am Coll Cardiol. 2011;57(25):2516–26.
34. Yoo H, Kim JW, Shishkov M, Namati E, Morse T, Shubochkin R, McCarthy JR, Ntziachristos V, Bouma BE, Jaffer FA, Tearney GJ. Intra-arterial catheter for simultaneous microstructural and molecular imaging in vivo. Nat Med. 2011;17(12):1680–4.
35. Geng YJ, Libby P. Progression of atheroma: a struggle between death and procreation. Arterioscler Thromb Vasc Biol. 2002;22(9):1370–80.
36. Kietselaer BL, Reutelingsperger CP, Heidendal GA, Daemen MJ, Mess WH, Hofstra L, Narula J. Noninvasive detection of plaque instability with use of radiolabeled annexin A5 in patients with carotid-artery atherosclerosis. N Engl J Med. 2004;350(14): 1472–3.

37. Laufer EM, Winkens MHM, Narula J, Hofstra L. Molecular imaging of macrophage cell death for the assessment of plaque vulnerability. Arterioscler Thromb Vasc Biol. 2009;29(7):1031–8.
38. Maiseyeu A, Mihai G, Kampfrath T, Simonetti OP, Sen CK, Roy S, Rajagopalan S, Parthasarathy S. Gadolinium-containing phosphatidylserine liposomes for molecular imaging of atherosclerosis. J Lipid Res. 2009;50(11):2157–63.
39. Burtea C, Ballet S, Laurent S, Rousseaux O, Dencausse A, Gonzalez W, Port M, Corot C, Vander Elst L, Muller RN. Development of a magnetic resonance imaging protocol for the characterization of atherosclerotic plaque by using vascular cell adhesion molecule-1 and apoptosis-targeted ultrasmall superparamagnetic iron oxide derivatives. Arterioscler Thromb Vasc Biol. 2012;32(6):e36–48.
40. Aikawa E, Nahrendorf M, Figueiredo JL, Swirski FK, Shtatland T, Kohler RH, Jaffer FA, Aikawa M, Weissleder R. Osteogenesis associates with inflammation in early-stage atherosclerosis evaluated by molecular imaging in vivo. Circulation. 2007;116(24):2841–50.
41. Hjortnaes J, Butcher J, Figueiredo JL, Riccio M, Kohler RH, Kozloff KM, Weissleder R, Aikawa E. Arterial and aortic valve calcification inversely correlates with osteoporotic bone remodelling: a role for inflammation. Eur Heart J. 2010;31(16):1975–84.
42. Aikawa E, Aikawa M, Libby P, Figueiredo J-L, Rusanescu G, Iwamoto Y, Fukuda D, Kohler RH, Shi G-P, Jaffer FA, Weissleder R. Arterial and aortic valve calcification abolished by elastolytic cathepsin S deficiency in chronic renal disease. Circulation. 2009;119(13):1785–894.
43. Derlin T, Wisotzki C, Richter U, Apostolova I, Bannas P, Weber C, Mester J, Klutmann S. In vivo imaging of mineral deposition in carotid plaque using 18F-sodium fluoride PET/CT: correlation with atherogenic risk factors. J Nucl Med. 2011;52(3):362–8.
44. Dweck MR, Chow MW, Joshi NV, Williams MC, Jones C, Fletcher AM, Richardson H, White A, McKillop G, van Beek EJ, Boon NA, Rudd JH, Newby DE. Coronary arterial 18F-sodium fluoride uptake: a novel marker of plaque biology. J Am Coll Cardiol. 2012;59(17):1539–48.
45. Fayad ZA, Mani V, Woodward M, Kallend D, Abt M, Burgess T, Fuster V, Ballantyne CM, Stein EA, Tardif JC, Rudd JH, Farkouh ME, Tawakol A. Safety and efficacy of dalcetrapib on atherosclerotic disease using novel non-invasive multimodality imaging (dal-PLAQUE): a randomised clinical trial. Lancet. 2011;378(9802):1547–59.

Integration of Biomarkers with Plaque Imaging

15

Razvan T. Dadu, Vijay Nambi, and Christie M. Ballantyne

Introduction

Over the last few decades, two key paradigms emerged in the pathophysiology of acute coronary syndromes (ACS): (a) inflammation plays a major role [1, 2] and (b) the majority of ACS result from plaques that were initially associated with a <50 % luminal stenosis [3]. These paradigms led to two important related concepts, the "vulnerable plaque" and the "vulnerable patient." A vulnerable plaque has a high probability of undergoing rapid progression and rupture. Risk factors accumulated since birth promote atherogenesis and lead to plaque rupture, the sentinel event in the pathogenesis of ACS. However, all factors that lead to plaque rupture and then to ACS are not clear. Plaque composition, rather than stenotic severity, appears to play a more important role in determining risk for both plaque rupture and subsequent thrombogenicity. Plaques within the coronary circulation become vulnerable and prone to rupture in response to a wide array of local and systemic factors. Therefore, a combination of risk factors contributes to plaque composition, prothrombotic milieu, and susceptible myocardium, conditions that strongly favor the clinical manifestations of acute cardiovascular disease (CVD) events [4] (Fig. 15.1). Our ability to identify patients at risk for CVD events by using biomarkers is somewhat limited. However, the use of new imaging modalities in combination with newly developed biomarker assessments may increase our understanding of CVD pathophysiology and improve management of patients at risk for CVD in the new millennium.

The concepts of vulnerable patient and vulnerable plaque have helped channel investigative efforts into identifying these phenotypes by using biomarkers, imaging, and a combination of both. In this chapter, we review the potential utility for CVD risk assessment of this integrative approach, focusing on high-sensitivity C-reactive protein (hs-CRP), lipoprotein-associated phospholipase A2 (Lp-PLA2), and myeloperoxidase (MPO) assessed in conjunction with atherosclerotic plaque imaging.

R.T. Dadu, MD
Department of Cardiovascular Medicine, Baylor College of Medicine and Methodist DeBakey Heart and Vascular Center, 6565 Fannin Street, MSA601, Houston, TX 77030, USA
e-mail: dadu@bcm.edu

V. Nambi, MD, PhD
Department of Internal Medicine, Staff Cardiologist Michael E DeBakey Veterans Affairs Hospital, Ben Taub General Hospital, Baylor College of Medicine, Center for Cardiovascular Prevention, Methodist DeBakey Heart and Vascular Center, 2002 Holcombe Blvd, Houston, TX 77030, USA
e-mail: vnambi@bcm.edu

C.M. Ballantyne, MD (✉)
Department of Medicine, Baylor College of Medicine, Methodist DeBakey Heart and Vascular Center, 6565 Fannin, M.S. A-601, Houston, TX 77030, USA
e-mail: cmb@bcm.tmc.edu

S.J. Nicholls and T. Crowe (eds.), *Imaging Coronary Atherosclerosis*, Contemporary Cardiology,
DOI 10.1007/978-1-4939-0572-0_15,

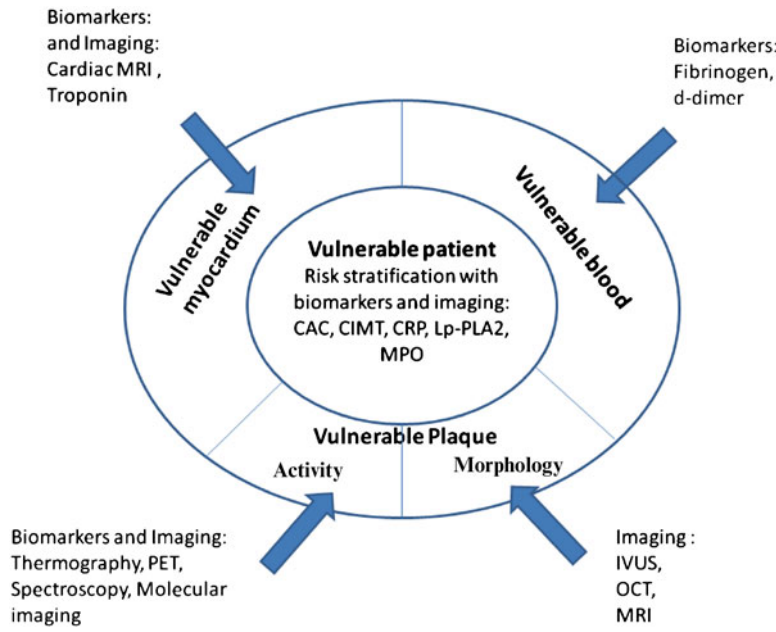

Fig. 15.1 A vulnerable patient, characterized by vulnerable blood, vulnerable myocardium, and vulnerable plaque, may be identified by using risk calculators such as Framingham and Reynolds, which include biomarkers. A combination of biomarkers and imaging may help in further risk stratification and better identification of the vulnerable patient. Combined use of biomarkers and imaging in molecular imaging may help identify not only plaque morphology but also plaque activity, to improve prevention of atherothrombotic events

Biomarkers

A biomarker is a substance that can be measured to evaluate normal biological processes, pathogenic processes, or pharmacological response to a therapeutic intervention [5]. Imaging and genetic testing can be considered biomarkers as well, but for this chapter biomarkers will refer only to blood markers. The desirable characteristics of a biomarker differ with the intended use [6]. Biomarkers may have value in improving global CVD risk assessment, monitoring response to therapy, or as targets for therapy [7]. Biomarkers can be classified as screening biomarkers (screening for subclinical disease), diagnostic biomarkers (recognizing overt disease), staging biomarkers (categorizing disease severity), or prognostic biomarkers (predicting future disease course, including recurrence and response to therapy, and monitoring efficacy of therapy) [8]. For screening biomarkers, features such as high sensitivity, specificity, and predictive values, large likelihood ratios, and low costs are important. For biomarkers to monitor the response to therapy, features such as narrow intraindividual variation and association with disease outcome are critical [8, 9]. A multimarker strategy may help us to understand the pathophysiological mechanisms of CVD and to develop new treatments in atherosclerosis. Inflammatory, hemodynamic, and vascular damage biomarkers are currently available and may be considered for the multimarker approach [5, 10, 11].

Given the complex pathophysiology of CVD, it is unlikely that any single biomarker will be able to serve as a universal surrogate for atherosclerosis. Lipoproteins have been used for a long time as biomarkers in CVD risk assessment and prevention. Biomarkers that can be measured in blood have the advantage of availability, lower cost, and repeatability, and hence they have value in risk stratification but may not prove as sensitive as imaging modalities for the detection or assessment of disease [12]. Although atherosclerosis is a generalized disease that involves most

of the arterial bed, most deaths are caused by thrombotic occlusion secondary to a single plaque rupture. Thus, nonspecific biomarkers for the generalized process of atherosclerosis are less likely to help identify an individual vulnerable plaque in a disease that is often multifocal or even diffuse; however, such biomarkers may help in the identification of a vulnerable patient [13]. Atherosclerotic lesions or vulnerable plaques associated with thrombosis are frequently found to have a thin and/or fissured cap [14]. The risk is also higher if the plaque has a large lipid core, a history of rupture or remodeling, and is associated with inflammation [15, 16]. Soluble biomarkers may help in detecting systemic inflammation. For example, the inflammatory marker CRP is elevated in patients with unstable angina and more so in patients with acute myocardial infarction (MI) [17]. Moreover, CRP levels are predictive of risk for MI in patients with or without prevalent coronary heart disease (CHD) [17]. The caveat is that CRP is not specific for atherosclerosis and as a consequence can be elevated in other conditions, such as renal disease, infection, cancer, autoimmune diseases, liver and kidney disease, and trauma [13]. Other biomarkers for which assessment is currently available are similarly not specific in detecting atherosclerosis.

Plaque Imaging and Biomarkers

Ideally, we would need better approaches or biomarkers that would identify vulnerable plaques before they become culprit plaques. To evaluate plaque vulnerability, a combined approach capable of evaluating structural characteristics (morphology) as well as functional properties (activity) of plaque may be more informative and may provide higher predictive value than a single approach (Fig. 15.1). Many of these features can be detected by imaging modalities such as angiography, computed tomography (CT), magnetic resonance imaging (MRI), intravascular ultrasonography (IVUS), and molecular imaging [12, 18]. However, newer imaging technology may be limited by technical difficulty, availability, and cost. Therefore, a combined approach using both circulating biomarkers and imaging modalities may be more cost-effective. A number of biomarkers have been examined in conjunction with imaging data for noninvasive identification of high-risk atherosclerotic plaques [19, 20]. It should be noted, however, that circulating biomarkers may be weakly correlated with quantifiable imaging parameters, as shown in the Integrated Biomarker and Imaging Study (IBIS) [21]. Table 15.1 shows the applicability of biomarkers and imaging in CVD risk prediction, therapeutic monitoring, and treatment targets.

Table 15.1 Applicability of biomarkers and imaging in CVD risk prediction, monitoring therapy, and treatment targets

	Risk prediction	Monitoring therapy	Treatment targeting
Biomarkers	++	++	++
Imaging	+++	+++	+

C-Reactive Protein

C-reactive protein (CRP) is a nonspecific inflammatory marker that has now been extensively studied in CVD. It is a member of the pentraxin family of innate immune response proteins [22]. CRP is postulated to have a role in atherosclerosis, as it has been shown to enhance expression of endothelial cell surface adhesion molecules, monocyte chemoattractant protein-1, endothelin-1, and endothelial plasminogen activator inhibitor-1 [23]. Many studies have shown that hs-CRP is associated with incident CVD events in healthy individuals as well as in patients with CVD [17, 24]. Inclusion of hs-CRP measurement has also been shown to improve CVD risk prediction as assessed by the area under the receiving operator characteristic curve (AUC), and hs-CRP is used in conjunction with other risk factors for cardiovascular risk prediction in the Reynolds risk score [25].

A number of studies have shown that statin therapy reduces the risk for CVD events in individuals with high concentrations of hs-CRP [26–28]. In the recent Justification for the Use of

Table 15.2 Event rates per 1,000 patient-years by hs-CRP and CAC categories in MESA

CAC	CVD events/1,000 patient-years		CHD events/1,000 patient-years	
category	hs-CRP < 2 mg/L	hs-CRP ≥ 2 mg/L	hs-CRP < 2 mg/L	hs-CRP ≥ 2 mg/L
0	4	4	2	1
1–100	7	8	3	5
>100	24	26	21	20

Reprinted from Blaha MJ, Budoff MJ, DeFilippis AP, Blankstein R, Rivera JJ, Agatston A, et al. Associations between C-reactive protein, coronary artery calcium, and cardiovascular events: implications for the JUPITER population from MESA, a population-based cohort study. Lancet. 2011;378(9792):684–92. With permission from Elsevier

Statins in Primary Prevention: an Intervention Trial Evaluating Rosuvastatin (JUPITER), which enrolled subjects without known CVD who had hs-CRP ≥2 mg/L and low-density lipoprotein cholesterol (LDL-C) <130 mg/dL, CVD event rate was reduced with rosuvastatin versus placebo [26]. Based on the results from JUPITER, rosuvastatin is indicated for primary prevention of CVD in men aged 50 years or older and women aged 60 years or older who have hs-CRP ≥2 mg/L in conjunction with at least one additional cardiovascular risk factor, even without overt hyperlipidemia.

The American College of Cardiology (ACC)/American Heart Association (AHA) risk guideline recommendations include consideration of hs-CRP to inform treatment decisions in individuals whose risk is uncertain based on quantitative risk assessment, with hs-CRP ≥ 2 mg/L supporting increasing estimated risk [29]. In contrast, the US Preventive Task Force (USPTF) concluded that the current evidence is insufficient to assess the balance of benefits and risks of using hs-CRP to screen asymptomatic men and women with no history of CHD to prevent CHD events [30]. Several investigators have compared hs-CRP and plaque imaging data in an effort to assess which is better in identifying vulnerable individuals and whether combining biomarkers and imaging improves risk stratification.

CRP and Coronary Artery Calcium in Risk Prediction

Analyses from the Multi-Ethnic Study of Atherosclerosis (MESA) evaluated hs-CRP and CT assessment of coronary artery calcium (CAC) in 950 participants who met the JUPITER entry criteria [31, 32]. In this study, hs-CRP was not associated with CHD (hazard ratio [HR] 0.98, 95 % confidence interval [CI]: 0.62–1.57) or CVD (HR 1.15, 95 % CI: 0.78–1.68) events after adjustments for age, sex, and race. In the same models, CAC was a strong predictor of both CHD (HR 6.65, 95 % CI: 2.99–14.78) and CVD (3.06, 95 % CI: 1.82–5.13). This association persisted even in the multivariate adjusted models. When the population was divided according to hs-CRP (high versus low), it was noticed that increased CAC burden produced similar increases in CHD and CVD events in both hs-CRP groups. The highest CVD event rates per 1,000 patient-years was recorded in the subgroup with both high hs-CRP and CAC >100 (Table 15.2). In this study, hs-CRP did not help in risk prediction for CVD events; however, CAC helped in risk stratification in patients eligible for JUPITER in both high (≥2 mg/L) and low (<2 mg/L) hs-CRP groups. These results suggest that CAC could be used to target subgroups of patients who are expected to derive the most (hs-CRP ≥ 2 mg/L) and the least (hs-CRP <2 mg/L) absolute benefit from statin treatment [32].

In the St. Francis Heart Study, Arad et al. compared the prognostic accuracy of CAC with that of hs-CRP in a setting of primary prevention after 4.3 years of follow-up in 4,613 patients [33]. In this study, hs-CRP and CAC were weakly correlated ($r = 0.06$, $p = 0.01$). After adjustment for standard risk factors, hs-CRP levels no longer predicted the CAC score. CAC predicted CHD events independently of standard risk factors (chi-square = 6.6, $p = 0.01$) and the combination of standard risk factors and hs-CRP

(chi-square = 6.6, $p = 0.01$). Whereas other studies and meta-analyses found that the relative risk for a CHD event in the highest hs-CRP tertile versus the lowest hs-CRP tertile was <2 [34], the relative risk for a CHD event in the highest CAC tertile versus the lowest CAC tertile was 13.9 (95 % CI: 7.1–27.3) in this study. Moreover, after adjustment for CAC score, hs-CRP failed to predict events ($p = 0.47$). Although these findings do not invalidate hs-CRP as a risk marker, they indicate that CRP, like standard risk factors, is not as powerful a predictor of events as the CAC score [33]. Several other studies that compared the predictive ability of hs-CRP to that of CAC also found that CAC was a better predictor of CVD events than CRP [35–38].

In another comparison of hs-CRP and CAC score, risk stratification of patients at intermediate risk may have benefited from inclusion of both parameters [39]. In this study, the CAC score risk groups were defined by tertiles as low (<3.7), medium (3.7–142.1), and high (>142.1). For hs-CRP, risk groups were defined by the 75th percentile as normal (<4.05 mg/L) and abnormal (≥4.05 mg/L). Compared with participants in the low-risk group for both CAC score and hs-CRP (reference group), risk for MI/coronary events increased with increasing hs-CRP level and increasing calcium score (relative risk ranged from 1.8 to 6.1; $p = 0.003$ for trend across the six risk groups). Although this study suggested that using both tests may improve risk prediction, the values used for the hs-CRP and CAC categories were different from those in previous studies.

The results of these studies suggest that although imaging parameters such as CAC score might be better prediction tools for identifying vulnerable individuals, imaging and hs-CRP appear to be complementary for risk prediction of CVD events in previously asymptomatic adults.

CRP and Carotid Intima-Media Thickness

Other investigators have analyzed the hs-CRP and carotid intima-media thickness (CIMT) in CVD event risk prediction. In the Cardiovascular Health Study, Cao et al. studied the association of hs-CRP and CIMT with incident strokes in 5,417 participants aged 65 years or older without preexisting stroke or chronic atrial fibrillation [40]. In this study, hs-CRP was correlated with CIMT. For each 1-standard deviation (SD) increment in common or internal CIMT, hs-CRP was 0.37 and 0.40 mg/L higher, respectively ($p < 0.001$). The association of hs-CRP with incident stroke differed depending on CIMT; there was no association between hs-CRP and stroke among those in the lowest CIMT tertile (adjusted HR 1.03, 95 % CI: 0.98–1.08), but a significant association was found among those with CIMT in the second and third tertiles (HR 1.07, 95 % CI: 1.02–1.12 for the second tertile and HR 1.07, 95 % CI: 1.02–1.12 for the third tertile). These results suggest that hs-CRP may help improve risk prediction in individuals who have thickened CIMT [40].

CRP and IVUS

Imaging, in conjunction with biomarkers, may also help in monitoring disease progression. Nissen et al. analyzed the combination of hs-CRP and IVUS to monitor the progression of atherosclerosis in 502 statin-treated patients who had IVUS performed at baseline and at 18-month follow-up [41]. This study revealed that the decrease in hs-CRP levels with statin therapy was independently and significantly correlated with the rate of progression of atherosclerosis. Patients with reductions in both LDL-C and hs-CRP that were greater than the median reductions had significantly slower rates of progression of atherosclerosis assessed by IVUS than patients with reductions in both biomarkers that were less than the median ($p = 0.001$) [41]. This study illustrates how imaging and biomarkers may be used in combination to monitor progression of atherosclerotic disease.

CRP and Carotid Magnetic Resonance Imaging

MRI can noninvasively characterize human carotid plaque composition, including the lipid-

rich core. Plaques with lipid-rich cores are more prone to rupture, leading to clinical events [15]. Using carotid MRI, Wasserman et al. explored the associations of cardiovascular risk factors with lipid-rich plaques in the healthy population of MESA and found no association between the presence of a lipid-rich core and hs-CRP [42]. This finding is noteworthy because hs-CRP has been strongly associated with plaque rupture in other studies [43], which suggests that hs-CRP may be a marker of plaque instability independent of the presence of a lipid core.

Lipoprotein-Associated Phospholipase A2

Lp-PLA2 is another biomarker that is currently approved for use in CVD risk prediction. Lp-PLA2 is an enzyme that generates lysophosphatidylcholine and oxidized free fatty acids. Lysophosphatidylcholine in turn suppresses release of nitric oxide and up-regulates CD40 ligand expression in T lymphocytes [44]. Lp-PLA2 is associated with vascular inflammation and has relatively low biologic fluctuations [45]. Several large studies have demonstrated an association between Lp-PLA2 and incident CVD events [46–48], but other studies have shown only a modest increase in AUC when Lp-PLA2 was evaluated in risk prediction models [49, 50].

Lp-PLA2 and CAC

A few studies have been conducted to investigate the association of Lp-PLA2 and CAC measured with CT. In a nested case–control study among young adults participating in the Coronary Artery Risk Development in Young Adults (CARDIA) study, Iribarren et al. examined the association of Lp-PLA2 mass and activity with calcified coronary plaque and found that in age-adjusted logistic regression, the odds ratios of having calcified coronary plaque were 1.40 (95 % CI: 1.17–1.67) per 1-SD increment in Lp-PLA2 mass and 1.39 (95 % CI: 1.14–1.70) per 1-SD increment in Lp-PLA2 activity [51]. After adjusting for multiple covariates, including LDL-C, high-density lipoprotein cholesterol (HDL-C), triglycerides, and hs-CRP, a statistically significant association was found for Lp-PLA2 mass (odds ratio 1.28, 95 % CI: 1.03–1.60) [51]. Kardys et al. found that in the Rotterdam Coronary Calcification Study, Lp-PLA2 activity measured in samples collected 7 years before CAC assessment was moderately associated with coronary calcification after adjustment for age in men but not in women [52]. After additional adjustment for non-HDL-C and HDL-C, the association previously seen in men disappeared. No association was found between Lp-PLA2 activity measured concurrently with CT scanning and CAC [52]. In another small study that investigated the relation of Lp-PLA2 levels with a CAC score >0 in American and Japanese men, no association was found between Lp-PLA2 tertile and CAC >0 in Americans and a negative association was found in Japanese men with LDL-C >130 mg/dL [53]. The above-mentioned studies suggest that Lp-PLA2 measurement has a modest correlation with CAC. To date, no head-to-head comparison or evaluation of the combination of Lp-PLA2 and CAC for CVD risk prediction has been published.

Lp-PLA2 and CIMT

Bartoli et al. reported that circulating Lp-PLA2 was increased in patients with high-grade carotid stenosis and unstable plaque [54]. The relationship of Lp-PLA2 mass with CIMT measured by carotid ultrasonography was investigated in diabetic and nondiabetic subjects by Constantinides et al., who found that in nondiabetic patients, CIMT was correlated positively with Lp-PLA2 mass in univariate correlation analysis ($r=0.325$, $p<0.009$) as well as in multiple linear regression analysis ($\beta=0.192$, $p=0.048$) but found no association between CIMT and Lp-PLA2 in patients with diabetes [55]. Two other population-based studies have found an association between CIMT and Lp-PLA2 mass or activity [56, 57]. Although studies suggest that Lp-PLA2 is correlated with CIMT and that Lp-PLA2 and CIMT predict

future CVD events, no studies comparing the value of Lp-PLA2 and CIMT in CVD risk prediction have been published.

Lp-PLA2 and IVUS

Several studies have shown that Lp-PLA2 is strongly expressed in the necrotic core of atherosclerotic plaque. In a pathologic study of coronary artery segments from 25 sudden coronary death patients, Lp-PLA2 was absent or minimally detected in early plaques, but thin-cap fibroatheromas and ruptured plaques showed intense Lp-PLA2 expression within the necrotic cores and surrounding macrophages including those in the fibrous cap [58]. Consequently, Lp-PLA2 is being investigated as a possible target for therapy. In the Integrated Biomarkers and Imaging Study-2 (IBIS-2), IVUS and hs-CRP were used to monitor the response to therapy with darapladib, an Lp-PLA2 inhibitor [59]. This study compared the effects of 12 months of treatment with darapladib versus placebo on coronary atheroma deformability and plasma hs-CRP level in 330 patients with angiographically documented CHD. Although no difference in palpography, the primary endpoint, was observed between treatment groups, the secondary endpoint of change in necrotic core, a key determinant of plaque vulnerability, as assessed by virtual histology indicated continued expansion of the necrotic core in patients receiving placebo, whereas Lp-PLA2 inhibition with darapladib prevented necrotic core expansion. No significant difference in plasma hs-CRP levels was seen between treatment groups in this study [59]. This study is an example of how biomarkers may be used in combination with plaque imaging for evaluation of new therapies aimed to treat atherosclerosis.

Lp-PLA2 and MRI

Brilakis et al. examined the association of Lp-PLA2 with atherosclerosis characterized by MRI in the Dallas Heart Study. In this study, Lp-PLA2 was not associated with abdominal aortic plaque or aortic wall thickness in men or women [60].

Myeloperoxidase

MPO is another soluble biomarker that is being investigated for possible use in CVD risk prediction. MPO, a protein produced by polymorphonuclear neutrophils and macrophages, is released in inflammatory conditions [61]. MPO is involved in oxidation of lipids contained within LDL and is thought to promote the formation of foam cells in atherosclerotic plaques [62]. Inflammatory cells producing MPO are found more frequently in ruptured plaques of patients with ACS than in patients with stable CHD [63, 64]. Therefore, MPO may be a marker of vulnerable plaque. Although several studies have shown an association of MPO and CVD events in healthy individuals as well as in patients with acute and chronic CVD [65–68], the additional predictive value of MPO levels in the stratification of cardiovascular risk in clinical practice is still not clear. Additional studies are necessary to evaluate the diagnostic and prognostic ability of MPO in the different forms of presentation of CVD.

MPO and CAC

Wong et al. studied the relation of MPO and CAC in CVD event prediction in 1,302 asymptomatic adults [69]. They found that mean MPO levels were greater with increasing CAC categories; however, after adjustment for other risk factors, this relation was attenuated. Although CAC was the main factor associated with increased CVD event rates, MPO level at or above versus below the median level remained an independent predictor of CVD events (HR 1.9, $p=0.04$). For prediction of CVD events, compared with a model with age, sex, and other risk factors alone (AUC = 0.755), AUC was significantly improved in models that added CAC categories (AUC = 0.833, $p=0.005$) and combined MPO and CAC categories (AUC = 0.838, $p=0.0037$) but not in the model that added MPO alone

(AUC = 0.762, $p = 0.59$). No significant improvement in AUC was observed when MPO was added to the model that already included CAC [69]. This study suggests that CAC is superior to MPO in CVD risk prediction and that combining CAC and MPO may not add any benefit in CVD risk prediction.

MPO and MRI

Matijevic et al. examined the relation of circulating blood cellular markers, including MPO, with carotid atherosclerotic plaque size and composition as measured by MRI in the Atherosclerosis Risk in Communities (ARIC) population [70]. In this study, intracellular levels of MPO were inversely associated with total arterial wall volume, which may be explained by the depletion of MPO during monocyte activation when MPO is released into plasma. This possible explanation is supported by reports that plasma MPO levels are increased in CHD and are associated with increased risk for atherosclerotic events [71, 72].

Biomarkers as Imaging Targets in Molecular Imaging

Molecular imaging provides the opportunity to assess entities or processes defined at the molecular level. It can reveal the expression or activity of specific proteins and localize labeled biomolecules, which may uncover specific biological pathways or cellular processes. Thus it is likely to contribute to our understanding of biological processes and disease mechanisms and lead to a better understanding of atherosclerotic plaque activity. This information may also lead to the identification of novel imaging biomarkers [73, 74]. The pathogenesis of atherosclerosis involves a complex interplay of endothelial dysfunction, mononuclear leukocyte adhesion and migration, and uptake of oxidized lipoproteins into monocyte-derived macrophages, leading to the eventual formation of an atheromatous core [75].

One of the molecular imaging targets used to study atherosclerotic plaque is vascular cell adhesion molecule-1 (VCAM-1), which is upregulated in inflamed endothelium and mediates adhesion and transmigration of mononuclear leukocytes [76]. Studies have shown that the information on VCAM-1-targeted antibodies that was obtained from MRI was correlated with VCAM-1 expression as demonstrated by immunohistochemistry in atherosclerotic plaques after atorvastatin treatment, illustrating the potential of molecular imaging for treatment monitoring [20, 73]. Other targets such as macrophages, matrix metalloproteinases, and oxidized LDL have been also used for imaging of the atherosclerotic plaques and show promising results [77–80].

Molecular imaging may enhance our understanding of specific molecular events in the arterial wall that are responsible for rapid lesion progression or plaque rupture. Identification of novel imaging phenotypes through molecular imaging may help in the diagnosis of disease, assessment of disease progression, risk stratification, and monitoring of treatment response. Because molecular imaging reports on cellular processes and the actual mechanism of the disease, it may also facilitate the in vivo evaluation of new drugs in small, rapid trials.

Conclusion

The use of biomarkers and imaging to assess risk for CVD events and response to therapy has the potential to optimize patient care by guiding the intensity of therapy for prevention of atherothrombotic events and evaluating drug efficacy. Although studies indicate that imaging is superior to biomarkers for risk prediction in most instances, the limited data suggest that combining biomarker measurements with imaging parameters may provide an additional small benefit on risk prediction. However, further research is needed to identify more specific biomarkers or panels of biomarkers and improved imaging modalities, including larger prospective studies to determine how information from biomarker and imaging measures can be integrated to optimize clinical care and enhance clinical research.

References

1. Ross R. The pathogenesis of atherosclerosis—an update. N Engl J Med. 1986;314(8):488–500. Epub 1986/02/20.
2. Libby P, Theroux P. Pathophysiology of coronary artery disease. Circulation. 2005;111(25):3481–8. Epub 2005/06/29.
3. Kolodgie FD, Virmani R, Burke AP, Farb A, Weber DK, Kutys R, et al. Pathologic assessment of the vulnerable human coronary plaque. Heart. 2004;90(12): 1385–91. Epub 2004/11/18.
4. Naghavi M, Falk E, Hecht HS, Jamieson MJ, Kaul S, Berman D, et al. From vulnerable plaque to vulnerable patient—Part III: executive summary of the Screening for Heart Attack Prevention and Education (SHAPE) Task Force report. Am J Cardiol. 2006; 98(2A):2H–15. Epub 2006/07/18.
5. Paramo JA, Rodriguez Ja JA, Orbe J. Integrating soluble biomarkers and imaging technologies in the identification of vulnerable atherosclerotic patients. Biomark Insights. 2007;1:165–73. Epub 2007/01/01.
6. LaBaer J. So, you want to look for biomarkers (introduction to the special biomarkers issue). J Proteome Res. 2005;4(4):1053–9. Epub 2005/08/09.
7. Nambi V, Ballantyne CM. Role of biomarkers in developing new therapies for vascular disease. World J Surg. 2007;31(4):676–81. Epub 2007/03/28.
8. Vasan RS. Biomarkers of cardiovascular disease: molecular basis and practical considerations. Circulation. 2006;113(19):2335–62. Epub 2006/05/17.
9. Hlatky MA, Greenland P, Arnett DK, Ballantyne CM, Criqui MH, Elkind MS, et al. Criteria for evaluation of novel markers of cardiovascular risk: a scientific statement from the American Heart Association. Circulation. 2009;119(17):2408–16. Epub 2009/04/15.
10. Muller JE, Tawakol A, Kathiresan S, Narula J. New opportunities for identification and reduction of coronary risk: treatment of vulnerable patients, arteries, and plaques. J Am Coll Cardiol. 2006;47(8 Suppl): C2–6. Epub 2006/04/25.
11. Tardif JC, Heinonen T, Orloff D, Libby P. Vascular biomarkers and surrogates in cardiovascular disease. Circulation. 2006;113(25):2936–42. Epub 2006/06/28.
12. Naghavi M, Libby P, Falk E, Casscells SW, Litovsky S, Rumberger J, et al. From vulnerable plaque to vulnerable patient: a call for new definitions and risk assessment strategies: Part I. Circulation. 2003;108(14):1664–72. Epub 2003/10/08.
13. Madjid M, Zarrabi A, Litovsky S, Willerson JT, Casscells W. Finding vulnerable atherosclerotic plaques: is it worth the effort? Arterioscler Thromb Vasc Biol. 2004;24(10):1775–82. Epub 2004/08/17.
14. Virmani R, Kolodgie FD, Burke AP, Farb A, Schwartz SM. Lessons from sudden coronary death: a comprehensive morphological classification scheme for atherosclerotic lesions. Arterioscler Thromb Vasc Biol. 2000;20(5):1262–75. Epub 2000/05/16.
15. Falk E, Shah PK, Fuster V. Coronary plaque disruption. Circulation. 1995;92(3):657–71. Epub 1995/08/01.
16. Fernandez-Ortiz A, Badimon JJ, Falk E, Fuster V, Meyer B, Mailhac A, et al. Characterization of the relative thrombogenicity of atherosclerotic plaque components: implications for consequences of plaque rupture. J Am Coll Cardiol. 1994;23(7):1562–9. Epub 1994/06/01.
17. Ridker PM, Hennekens CH, Buring JE, Rifai N. C-reactive protein and other markers of inflammation in the prediction of cardiovascular disease in women. N Engl J Med. 2000;342(12):836–43. Epub 2000/03/25.
18. Naghavi M, Madjid M, Khan MR, Mohammadi RM, Willerson JT, Casscells SW. New developments in the detection of vulnerable plaque. Curr Atheroscler Rep. 2001;3(2):125–35. Epub 2001/03/20.
19. Lipinski MJ, Fuster V, Fisher EA, Fayad ZA. Technology insight: targeting of biological molecules for evaluation of high-risk atherosclerotic plaques with magnetic resonance imaging. Nat Clin Pract Cardiovasc Med. 2004;1(1):48–55. Epub 2005/11/03.
20. Nahrendorf M, Jaffer FA, Kelly KA, Sosnovik DE, Aikawa E, Libby P, et al. Noninvasive vascular cell adhesion molecule-1 imaging identifies inflammatory activation of cells in atherosclerosis. Circulation. 2006;114(14):1504–11. Epub 2006/09/27.
21. Van Mieghem CA, McFadden EP, de Feyter PJ, Bruining N, Schaar JA, Mollet NR, et al. Noninvasive detection of subclinical coronary atherosclerosis coupled with assessment of changes in plaque characteristics using novel invasive imaging modalities: the Integrated Biomarker and Imaging Study (IBIS). J Am Coll Cardiol. 2006;47(6):1134–42. Epub 2006/03/21.
22. Bassuk SS, Rifai N, Ridker PM. High-sensitivity C-reactive protein: clinical importance. Curr Probl Cardiol. 2004;29(8):439–93. Epub 2004/07/20.
23. Pasceri V, Willerson JT, Yeh ET. Direct proinflammatory effect of C-reactive protein on human endothelial cells. Circulation. 2000;102(18):2165–8. Epub 2000/11/01.
24. Ridker PM, Cushman M, Stampfer MJ, Tracy RP, Hennekens CH. Inflammation, aspirin, and the risk of cardiovascular disease in apparently healthy men. N Engl J Med. 1997;336(14):973–9. Epub 1997/04/03.
25. Ridker PM, Buring JE, Rifai N, Cook NR. Development and validation of improved algorithms for the assessment of global cardiovascular risk in women: the Reynolds Risk Score. JAMA. 2007; 297(6):611–9. Epub 2007/02/15.
26. Ridker PM, Danielson E, Fonseca FA, Genest J, Gotto Jr AM, Kastelein JJ, et al. Rosuvastatin to prevent vascular events in men and women with elevated C-reactive protein. N Engl J Med. 2008;359(21):2195–207. Epub 2008/11/11.
27. Ridker PM, Rifai N, Pfeffer MA, Sacks FM, Moye LA, Goldman S, et al. Inflammation, pravastatin, and the risk of coronary events after myocardial infarction in

patients with average cholesterol levels. Cholesterol and Recurrent Events (CARE) Investigators. Circulation. 1998;98(9):839–44.
28. Ridker PM, Rifai N, Clearfield M, Downs JR, Weis SE, Miles JS, et al. Measurement of C-reactive protein for the targeting of statin therapy in the primary prevention of acute coronary events. N Engl J Med. 2001;344(26):1959–65. Epub 2001/06/30.
29. Goff DC Jr, Lloyd-Jones DM, Bennett G, Coady S, D'Agostino RB Sr, Gibbons R, et al. ACC/AHA Guideline on the Assessment of Cardiovascular Risk: A Report of the American College of Cardiology/American Heart Association Task Force on Practice Guidelines. J Am Coll Cardiol. 2003. Epub 2013/11/14.
30. Using nontraditional risk factors in coronary heart disease risk assessment: U.S. Preventive Services Task Force recommendation statement. Ann Intern Med. 2009;151(7):474–82. Epub 2009/10/07.
31. Jain A, McClelland RL, Polak JF, Shea S, Burke GL, Bild DE, et al. Cardiovascular imaging for assessing cardiovascular risk in asymptomatic men versus women: the Multi-Ethnic Study of Atherosclerosis (MESA). Circ Cardiovasc Imaging. 2011;4(1):8–15. Epub 2010/11/12.
32. Blaha MJ, Budoff MJ, DeFilippis AP, Blankstein R, Rivera JJ, Agatston A, et al. Associations between C-reactive protein, coronary artery calcium, and cardiovascular events: implications for the JUPITER population from MESA, a population-based cohort study. Lancet. 2011;378(9792):684–92. Epub 2011/08/23.
33. Arad Y, Goodman KJ, Roth M, Newstein D, Guerci AD. Coronary calcification, coronary disease risk factors, C-reactive protein, and atherosclerotic cardiovascular disease events: the St. Francis Heart Study. J Am Coll Cardiol. 2005;46(1):158–65. Epub 2005/07/05.
34. Danesh J, Wheeler JG, Hirschfield GM, Eda S, Eiriksdottir G, Rumley A, et al. C-reactive protein and other circulating markers of inflammation in the prediction of coronary heart disease. N Engl J Med. 2004;350(14):1387–97. Epub 2004/04/09.
35. Patel AA, Budoff MJ. Screening for heart disease: C-reactive protein versus coronary artery calcium. Expert Rev Cardiovasc Ther. 2010;8(1):125–31. Epub 2009/12/18.
36. Vliegenthart R, Oudkerk M, Hofman A, Oei HH, van Dijck W, van Rooij FJ, et al. Coronary calcification improves cardiovascular risk prediction in the elderly. Circulation. 2005;112(4):572–7. Epub 2005/07/13.
37. Taylor AJ, Bindeman J, Feuerstein I, Cao F, Brazaitis M, O'Malley PG. Coronary calcium independently predicts incident premature coronary heart disease over measured cardiovascular risk factors: mean three-year outcomes in the Prospective Army Coronary Calcium (PACC) project. J Am Coll Cardiol. 2005;46(5):807–14. Epub 2005/09/06.
38. Ridker PM, Rifai N, Rose L, Buring JE, Cook NR. Comparison of C-reactive protein and low-density lipoprotein cholesterol levels in the prediction of first cardiovascular events. N Engl J Med. 2002;347(20):1557–65. Epub 2002/11/15.
39. Park R, Detrano R, Xiang M, Fu P, Ibrahim Y, LaBree L, et al. Combined use of computed tomography coronary calcium scores and C-reactive protein levels in predicting cardiovascular events in nondiabetic individuals. Circulation. 2002;106(16):2073–7. Epub 2002/10/16.
40. Cao JJ, Thach C, Manolio TA, Psaty BM, Kuller LH, Chaves PH, et al. C-reactive protein, carotid intima-media thickness, and incidence of ischemic stroke in the elderly: the Cardiovascular Health Study. Circulation. 2003;108(2):166–70. Epub 2003/06/25.
41. Nissen SE, Tuzcu EM, Schoenhagen P, Crowe T, Sasiela WJ, Tsai J, et al. Statin therapy, LDL cholesterol, C-reactive protein, and coronary artery disease. N Engl J Med. 2005;352(1):29–38. Epub 2005/01/07.
42. Wasserman BA, Sharrett AR, Lai S, Gomes AS, Cushman M, Folsom AR, et al. Risk factor associations with the presence of a lipid core in carotid plaque of asymptomatic individuals using high-resolution MRI: the Multi-Ethnic Study of Atherosclerosis (MESA). Stroke. 2008;39(2):329–35. Epub 2008/01/05.
43. Burke AP, Tracy RP, Kolodgie F, Malcom GT, Zieske A, Kutys R, et al. Elevated C-reactive protein values and atherosclerosis in sudden coronary death: association with different pathologies. Circulation. 2002;105(17):2019–23. Epub 2002/05/01.
44. Iribarren C. Lipoprotein-associated phospholipase A2 and cardiovascular risk: state of the evidence and future directions. Arterioscler Thromb Vasc Biol. 2006;26(1):5–6. Epub 2005/12/24.
45. McConnell JP, Hoefner DM. Lipoprotein-associated phospholipase A2. Clin Lab Med. 2006;26(3):679–97. Epub 2006/08/30.
46. Gerber Y, McConnell JP, Jaffe AS, Weston SA, Killian JM, Roger VL. Lipoprotein-associated phospholipase A2 and prognosis after myocardial infarction in the community. Arterioscler Thromb Vasc Biol. 2006;26(11):2517–22. Epub 2006/08/12.
47. Ballantyne CM, Hoogeveen RC, Bang H, Coresh J, Folsom AR, Heiss G, et al. Lipoprotein-associated phospholipase A2, high-sensitivity C-reactive protein, and risk for incident coronary heart disease in middle-aged men and women in the Atherosclerosis Risk in Communities (ARIC) study. Circulation. 2004;109(7):837–42. Epub 2004/02/06.
48. Thompson A, Gao P, Orfei L, Watson S, Di Angelantonio E, Kaptoge S, et al. Lipoprotein-associated phospholipase A_2 and risk of coronary disease, stroke, and mortality: collaborative analysis of 32 prospective studies. Lancet. 2010;375(9725):1536–44. Epub 2010/05/04.
49. Koenig W, Khuseyinova N, Lowel H, Trischler G, Meisinger C. Lipoprotein-associated phospholipase A2 adds to risk prediction of incident coronary events by C-reactive protein in apparently healthy middle-aged men from the general population: results from the 14-year follow-up of a large cohort from southern

Germany. Circulation. 2004;110(14):1903–8. Epub 2004/09/29.
50. Oei HH, van der Meer IM, Hofman A, Koudstaal PJ, Stijnen T, Breteler MM, et al. Lipoprotein-associated phospholipase A2 activity is associated with risk of coronary heart disease and ischemic stroke: the Rotterdam Study. Circulation. 2005;111(5):570–5. Epub 2005/02/09.
51. Iribarren C, Gross MD, Darbinian JA, Jacobs Jr DR, Sidney S, Loria CM. Association of lipoprotein-associated phospholipase A2 mass and activity with calcified coronary plaque in young adults: the CARDIA study. Arterioscler Thromb Vasc Biol. 2005;25(1):216–21. Epub 2004/10/23.
52. Kardys I, Oei HH, Hofman A, Oudkerk M, Witteman JC. Lipoprotein-associated phospholipase A2 and coronary calcification. The Rotterdam Coronary Calcification Study. Atherosclerosis. 2007;191(2): 377–83. Epub 2006/05/09.
53. El-Saed A, Sekikawa A, Zaky RW, Kadowaki T, Takamiya T, Okamura T, et al. Association of lipoprotein-associated phospholipase A2 with coronary calcification among American and Japanese men. J Epidemiol. 2007;17(6):179–85. Epub 2007/12/21.
54. Sarlon-Bartoli G, Boudes A, Buffat C, Bartoli MA, Piercecchi-Marti MD, Sarlon E, et al. Circulating lipoprotein-associated phospholipase A2 in high-grade carotid stenosis: a new biomarker for predicting unstable plaque. Eur J Vasc Endovasc Surg. 2012;43(2):154–9. Epub 2011/11/15.
55. Constantinides A, van Pelt LJ, van Leeuwen JJ, de Vries R, Tio RA, van der Horst IC, et al. Carotid intima media thickness is associated with plasma lipoprotein-associated phospholipase A2 mass in nondiabetic subjects but not in patients with type 2 diabetes. Eur J Clin Invest. 2011;41(8):820–7. Epub 2011/02/02.
56. Persson M, Nilsson JA, Nelson JJ, Hedblad B, Berglund G. The epidemiology of Lp-PLA$_2$: distribution and correlation with cardiovascular risk factors in a population-based cohort. Atherosclerosis. 2007;190(2):388–96. Epub 2006/03/15.
57. Kardys I, Oei HH, van der Meer IM, Hofman A, Breteler MM, Witteman JC. Lipoprotein-associated phospholipase A2 and measures of extracoronary atherosclerosis: the Rotterdam Study. Arterioscler Thromb Vasc Biol. 2006;26(3):631–6. Epub 2005/12/24.
58. Kolodgie FD, Burke AP, Skorija KS, Ladich E, Kutys R, Makuria AT, et al. Lipoprotein-associated phospholipase A2 protein expression in the natural progression of human coronary atherosclerosis. Arterioscler Thromb Vasc Biol. 2006;26(11):2523–9. Epub 2006/09/09.
59. Serruys PW, Garcia-Garcia HM, Buszman P, Erne P, Verheye S, Aschermann M, et al. Effects of the direct lipoprotein-associated phospholipase A_2 inhibitor darapladib on human coronary atherosclerotic plaque. Circulation. 2008;118(11):1172–82. Epub 2008/09/04.
60. Brilakis ES, Khera A, Saeed B, Banerjee S, McGuire DK, Murphy SA, et al. Association of lipoprotein-associated phospholipase A2 mass and activity with coronary and aortic atherosclerosis: findings from the Dallas Heart Study. Clin Chem. 2008;54(12):1975–81. Epub 2008/10/04.
61. Hochholzer W, Morrow DA, Giugliano RP. Novel biomarkers in cardiovascular disease: update 2010. Am Heart J. 2010;160(4):583–94. Epub 2010/10/12.
62. Podrez EA, Schmitt D, Hoff HF, Hazen SL. Myeloperoxidase-generated reactive nitrogen species convert LDL into an atherogenic form in vitro. J Clin Invest. 1999;103(11):1547–60. Epub 1999/06/08.
63. Naruko T, Ueda M, Haze K, van der Wal AC, van der Loos CM, Itoh A, et al. Neutrophil infiltration of culprit lesions in acute coronary syndromes. Circulation. 2002;106(23):2894–900. Epub 2002/12/04.
64. Buffon A, Biasucci LM, Liuzzo G, D'Onofrio G, Crea F, Maseri A. Widespread coronary inflammation in unstable angina. N Engl J Med. 2002;347(1):5–12. Epub 2002/07/05.
65. Zhang R, Brennan ML, Fu X, Aviles RJ, Pearce GL, Penn MS, et al. Association between myeloperoxidase levels and risk of coronary artery disease. JAMA. 2001;286(17):2136–42. Epub 2001/11/22.
66. Meuwese MC, Stroes ES, Hazen SL, van Miert JN, Kuivenhoven JA, Schaub RG, et al. Serum myeloperoxidase levels are associated with the future risk of coronary artery disease in apparently healthy individuals: the EPIC-Norfolk Prospective Population Study. J Am Coll Cardiol. 2007;50(2):159–65. Epub 2007/07/10.
67. Baldus S, Heeschen C, Meinertz T, Zeiher AM, Eiserich JP, Munzel T, et al. Myeloperoxidase serum levels predict risk in patients with acute coronary syndromes. Circulation. 2003;108(12):1440–5. Epub 2003/09/04.
68. Brennan ML, Penn MS, Van Lente F, Nambi V, Shishehbor MH, Aviles RJ, et al. Prognostic value of myeloperoxidase in patients with chest pain. N Engl J Med. 2003;349(17):1595–604. Epub 2003/10/24.
69. Wong ND, Gransar H, Narula J, Shaw L, Moon JH, Miranda-Peats R, et al. Myeloperoxidase, subclinical atherosclerosis, and cardiovascular disease events. JACC Cardiovasc Imaging. 2009;2(9):1093–9. Epub 2009/09/19.
70. Matijevic N, Wu KK, Howard AG, Wasserman B, Wang WY, Folsom AR, et al. Association of blood monocyte and platelet markers with carotid artery characteristics: the Atherosclerosis Risk on Communities Carotid MRI Study. Cerebrovasc Dis. 2011;31(6):552–8. Epub 2011/04/14.
71. Duzguncinar O, Yavuz B, Hazirolan T, Deniz A, Tokgozoglu SL, Akata D, et al. Plasma myeloperoxidase is related to the severity of coronary artery disease. Acta Cardiol. 2008;63(2):147–52. Epub 2008/05/13.
72. Wainstein RV, Wainstein MV, Ribeiro JP, Dornelles LV, Tozzati P, Ashton-Prolla P, et al. Association between myeloperoxidase polymorphisms and its plasma levels with severity of coronary artery disease. Clin Biochem. 2010;43(1–2):57–62. Epub 2009/08/05.
73. Kaufmann BA, Sanders JM, Davis C, Xie A, Aldred P, Sarembock IJ, et al. Molecular imaging of inflammation in atherosclerosis with targeted ultrasound detec-

tion of vascular cell adhesion molecule-1. Circulation. 2007;116(3):276–84. Epub 2007/06/27.
74. Shaw SY. Molecular imaging in cardiovascular disease: targets and opportunities. Nat Rev Cardiol. 2009;6(9):569–79. Epub 2009/07/22.
75. Libby P. Inflammation in atherosclerosis. Nature. 2002;420(6917):868–74. Epub 2002/12/20.
76. Cybulsky MI, Iiyama K, Li H, Zhu S, Chen M, Iiyama M, et al. A major role for VCAM-1, but not ICAM-1, in early atherosclerosis. J Clin Invest. 2001;107(10):1255–62. Epub 2001/05/26.
77. Schafers M, Riemann B, Kopka K, Breyholz HJ, Wagner S, Schafers KP, et al. Scintigraphic imaging of matrix metalloproteinase activity in the arterial wall in vivo. Circulation. 2004;109(21):2554–9. Epub 2004/05/05.
78. Su H, Spinale FG, Dobrucki LW, Song J, Hua J, Sweterlitsch S, et al. Noninvasive targeted imaging of matrix metalloproteinase activation in a murine model of postinfarction remodeling. Circulation. 2005; 112(20):3157–67. Epub 2005/11/09.
79. Breyholz HJ, Wagner S, Levkau B, Schober O, Schafers M, Kopka K. A 18F-radiolabeled analogue of CGS 27023A as a potential agent for assessment of matrix-metalloproteinase activity in vivo. Q J Nucl Med Mol Imaging. 2007;51(1):24–32. Epub 2007/03/21.
80. Lancelot E, Amirbekian V, Brigger I, Raynaud JS, Ballet S, David C, et al. Evaluation of matrix metalloproteinases in atherosclerosis using a novel noninvasive imaging approach. Arterioscler Thromb Vasc Biol. 2008;28(3):425–32. Epub 2008/02/09.

Index

S.J. Nicholls and T. Crowe (eds.), *Imaging Coronary Atherosclerosis*, Contemporary Cardiology,
DOI 10.1007/978-1-4939-0572-0, © Springer Science+Business Media New York 2014

E

F

H